# E3 UBIQUITIN LIGASES: FROM STRUCTURE TO PHYSIOLOGY

EDITED BY: Victor M. Bolanos-Garcia, Julien Licchesi, Heike Laman and Fumiyo Ikeda

PUBLISHED IN: Frontiers in Physiology

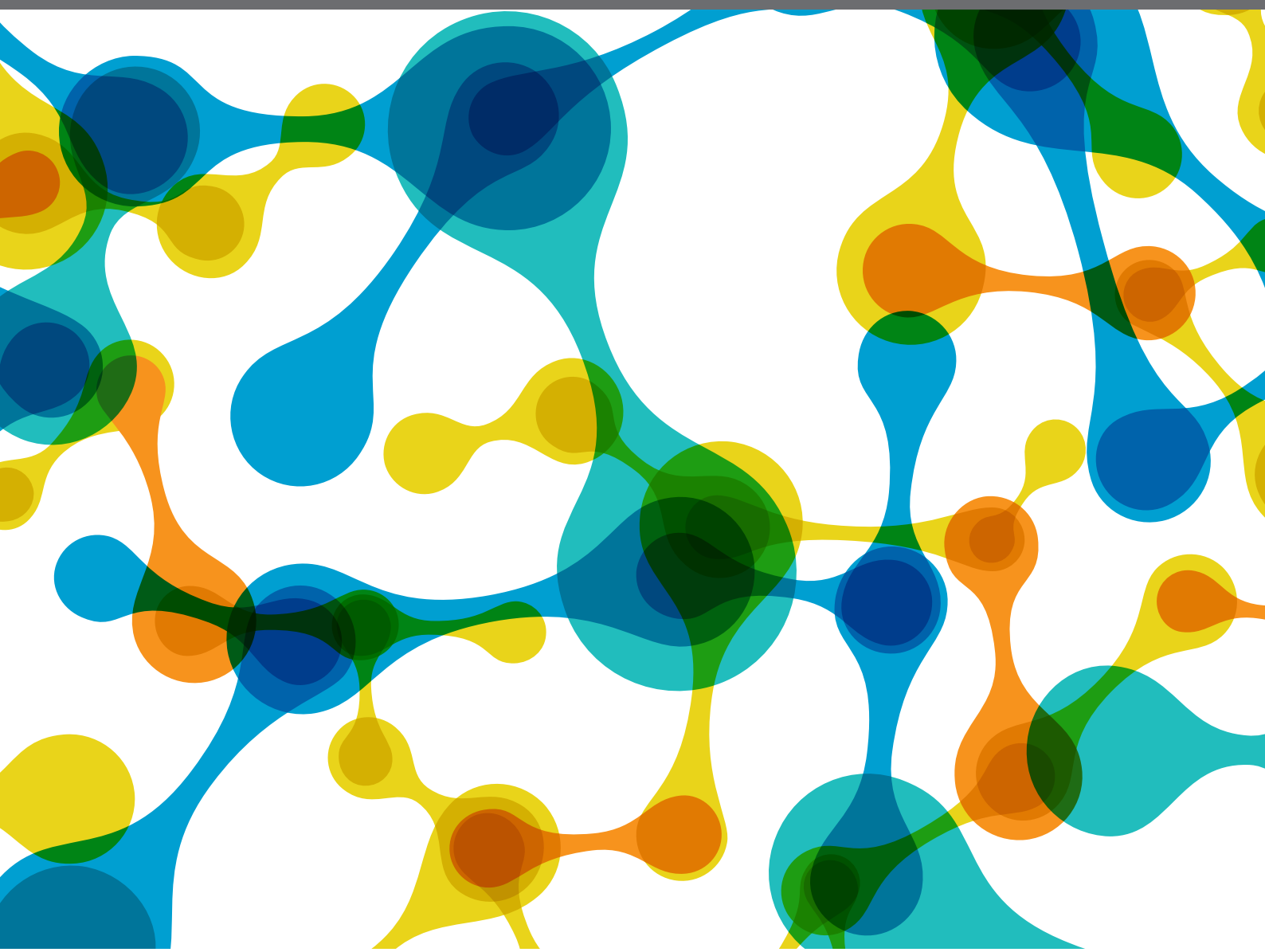

frontiers Research Topics

frontiers



ISSN 1664-8714
ISBN 978-2-88963-883-3
DOI 10.3389/978-2-88963-883-3

## About Frontiers

Frontiers is more than just an open-access publisher of scholarly articles: it is a pioneering approach to the world of academia, radically improving the way scholarly research is managed. The grand vision of Frontiers is a world where all people have an equal opportunity to seek, share and generate knowledge. Frontiers provides immediate and permanent online open access to all its publications, but this alone is not enough to realize our grand goals.

## Frontiers Journal Series

The Frontiers Journal Series is a multi-tier and interdisciplinary set of open-access, online journals, promising a paradigm shift from the current review, selection and dissemination processes in academic publishing. All Frontiers journals are driven by researchers for researchers; therefore, they constitute a service to the scholarly community. At the same time, the Frontiers Journal Series operates on a revolutionary invention, the tiered publishing system, initially addressing specific communities of scholars, and gradually climbing up to broader public understanding, thus serving the interests of the lay society, too.

## Dedication to Quality

Each Frontiers article is a landmark of the highest quality, thanks to genuinely collaborative interactions between authors and review editors, who include some of the world's best academicians. Research must be certified by peers before entering a stream of knowledge that may eventually reach the public - and shape society; therefore, Frontiers only applies the most rigorous and unbiased reviews.
Frontiers revolutionizes research publishing by freely delivering the most outstanding research, evaluated with no bias from both the academic and social point of view. By applying the most advanced information technologies, Frontiers is catapulting scholarly publishing into a new generation.

## What are Frontiers Research Topics?

Frontiers Research Topics are very popular trademarks of the Frontiers Journals Series: they are collections of at least ten articles, all centered on a particular subject. With their unique mix of varied contributions from Original Research to Review Articles, Frontiers Research Topics unify the most influential researchers, the latest key findings and historical advances in a hot research area! Find out more on how to host your own Frontiers Research Topic or contribute to one as an author by contacting the Frontiers Editorial Office: researchtopics@frontiersin.org

# E3 UBIQUITIN LIGASES: FROM STRUCTURE TO PHYSIOLOGY

Topic Editors:
**Victor M. Bolanos-Garcia,** Oxford Brookes University, United Kingdom
**Julien Licchesi,** University of Bath, United Kingdom
**Heike Laman,** University of Cambridge, United Kingdom
**Fumiyo Ikeda,** Austrian Academy of Sciences (OeAW), Austria

**Citation:** Bolanos-Garcia, V. M., Licchesi, J., Laman, H., Ikeda, F., eds. (2021). E3 Ubiquitin Ligases: From Structure to Physiology. Lausanne: Frontiers Media SA. doi: 10.3389/978-2-88963-883-3

# Table of Contents

frontiers in Physiology

EDITORIAL
published: 26 November 2020
doi: 10.3389/fphys.2020.621053

# Editorial: E3 Ubiquitin Ligases: From Structure to Physiology

*Julien D. F. Licchesi*[1], *Heike Laman*[2], *Fumiyo Ikeda*[3] *and Victor M. Bolanos-Garcia*[4*]

[1] Department of Biology and Biochemistry, University of Bath, Bath, United Kingdom, [2] Department of Pathology, University of Cambridge, Cambridge, United Kingdom, [3] Division of Inflammation and Proteostasis, Medical Institute of Bioregulation, Kyushu University, Fukuoka, Japan, [4] Department of Biological and Medical Sciences, Oxford Brookes University, Oxford, United Kingdom

**Keywords: E3 ubiquitin ligases, really interesting new gene (RING), HECTs (Homologous to the E6AP carboxyl terminus), RING-in between-RING (RBR), SCF (Skp1, Cullin, F-box protein), ubiquitin chain assembly, cancer, neurological disorders**

OPEN ACCESS

***Edited and reviewed by:***
*Leonardo Alexandre Peyré-Tartaruga, Federal University of Rio Grande do Sul, Brazil*

***Correspondence:**
*Victor M. Bolanos-Garcia*
*vbolanos-garcia@brookes.ac.uk*

***Specialty section:***
*This article was submitted to Integrative Physiology, a section of the journal Frontiers in Physiology*

***Received:*** *24 October 2020*
***Accepted:*** *02 November 2020*
***Published:*** *26 November 2020*

***Citation:***
*Licchesi JDF, Laman H, Ikeda F and Bolanos-Garcia VM (2020) Editorial: E3 Ubiquitin Ligases: From Structure to Physiology. Front. Physiol. 11:621053. doi: 10.3389/fphys.2020.621053*

## Editorial on the Research Topic

## E3 Ubiquitin Ligases: From Structure to Physiology

Protein ubiquitination has emerged as a central regulatory mechanism of eukaryotic cells that affects multiple cellular processes and is critical for timely protein degradation and signal transduction. The topological nature of the assembled ubiquitin chain largely dictates the function of the ubiquitinated protein and the cellular outcome. The molecules responsible for the post-translational modification of protein substrates with ubiquitin comprise E1 ubiquitin-activating, E2 ubiquitin-conjugating, and E3 ubiquitin ligating enzymes. While deubiquitinating (DUB) enzymes which remove ubiquitin chains have received a lot of attention, especially in the field of drug discovery where some DUB inhibitors are approaching clinical trials, E3 ubiquitin ligases are only recently coming into the limelight.

Despite impressive advances in the structural to physiological understanding of E3 ubiquitin ligases, important aspects of E3s structure to function remain obscure. Undoubtedly, an enhanced knowledge of the conformational dynamics, macromolecular interactions, and functional integration of E3 ligases into cellular pathways will illuminate the precise roles of E3 ligases in aberrant signaling processes. This will pave the way toward rationally manipulating these enzymes for therapeutic intervention in many diseases that represent important health and societal challenges. Targeted protein degradation has emerged as a powerful approach for the removal of proteins driving human diseases. Amongst these, PROTACs, LYTACs, and AUTACs are technologies that harness the endogenous protein ubiquitination machinery and target proteins for degradation by the proteasome, lysosome, or through autophagy (Sakamoto et al., 2001; Takahashi et al., 2019; Banik et al., 2020). Given these recent advances, a more detailed understanding of E3

ubiquitin ligase functions and their modes of action are paramount in order to fully exploit these endogenous cellular waste recycling plants to improve human health.

The contributors to this Topic discuss how the integration of cellular, chemical, biophysical, and structural biology methods with "omics" approaches have clarified important aspects of E3 ubiquitin ligases activity, function, and mode of regulation. Such insights include the mode of cooperation of E3s with other enzymes for ubiquitin chain initiation and elongation, the precise positioning of the donor and acceptor ubiquitin sites, and the principles underpinning substrate-assisted catalysis. The subtle mechanistic and ligand-recognition variations that are inscribed in a spatial and temporal framework, confer these enzymes with great substrate selectivity and specificity. Excitingly, all the families of E3 ubiquitin ligases, including Really interesting Genes (RING), HECTs (Homologous to the E6AP carboxyl terminus), and RING-in between-RING, are represented in this Research Topic. We would also like to bring to the attention of readers, the Frontiers in Chemistry Research Topic on "Probing the Ubiquitin Landscape" which focus on new chemical biology tools and techniques to further dissect the role of protein ubiquitination (Mulder et al., 2020).

Progressing from E3 ligases structure to physiology, Deol et al. summarize our current understanding of the key molecular principles of ubiquitin chain assembly and discuss current evidence that supports two alternative, mechanistic models of polyubiquitylation: a "sequential addition" model wherein one ubiquitin unit is transferred at a time to a growing substrate-linked ubiquitin and an "en bloc" model in which ubiquitin units are assembled prior to their transfer onto a substrate. They also discuss how the weak and dynamic nature of the interactions represents a challenge to establish the trajectory of the functional enzyme-substrate complexes.

Weber et al. review HECT-containing E3 ligases and explain the reasons manipulating their catalytic activity is challenging include their transient interactions and low binding affinities with their substrates, as well as the redundancy among E3 ligases, where depending on the cellular context, a specific substrate may be modulated by several E3s. They argue that although the high conservation of the HECT domain within the HECT family means it may be difficult to develop specific inhibitory compounds, a greater understanding of the structural features and the underlying ubiquitination mechanisms used by different HECT E3 ligases remains an important biological question with the potential to unveil new opportunities for therapeutic intervention. Mayor and collaborators investigate the HECT ubiquitin ligase, UBE3A. Mutations in *Ube3a* cause Angelman and Prader-Willi syndromes (Wheeler et al., 2017; Harris and Stafford, 2020), both of which have no cure. Elu et al. identified the UBE3A-dependent ubiquitination sites and ubiquitin chain types formed on DDI1, a proteasome receptor. This contribution is an important step toward the full characterization of the UBE3A-dependent ubiquitination pathway that provides new insight into the molecular basis of rare neurological disorders. Some of the most poorly understood E3 ligases are the HERCs (homologous to the E6AP carboxyl terminus and regulator of chromosome condensation 1 (RCC1)-like domain-containing proteins), which are divided into large and small subfamilies. García-Cano et al. describe the high structural complexity of large-HERC family members and their important functions in diverse physiological processes, including cell proliferation, neuronal development, DNA repair, and inflammation. They also discuss the ways in which dysregulation of large-HERC ubiquitin ligases can lead to neurological disorders and cancer.

Mdm2 and its homolog MdmX (also known as Mdm4) are two RING E3 ubiquitin ligases that exert oncogenic activity. A precise understanding of the nature of Mdm2-MdmX interactions can be critical to exploiting them as potential therapeutic targets for reactivation of p53 function in tumors. Kosztyu et al. report a systematic mutational analysis of human Mdm2 that included the exchange of segments of its RING domain with the corresponding MdmX regions in order to identify the molecular features that determine their differential ability to forms dimers. Interestingly, the Mdm2 single substitution C449N blocked the ability of this protein to form a heterodimer with MdmX, but it did not disrupt Mdm2 RING self-association to form homodimers. Taken together, the studies suggest that the effect of certain conserved amino acid residues on Mdm2 homodimers and Mdm2-MdmX heterodimers formation is context-specific and possibly not entirely structurally equivalent. In contrast to HECT ligases, RING E3s do not have intrinsic catalytic activity *per se* and instead rely on adaptor molecules for the recruitment of substrate proteins (Deshaies and Joazeiro, 2009). Rathje et al. report an unanticipated function of Fbxo7, the substrate-recognition subunit of an SCF-type ubiquitin E3 ligase complex, in male germ cell cytoplasmic remodeling. They show that Fbxo7-deficient male mice were completely sterile despite successful meiosis, nuclear elongation and exclusion of histones from chromatin. At the same time, Fbxo7 mutant mice exhibited a sterility phenotype that has not been described before, where total death and phagocytosis of all condensing spermatids occurred in the absence of typical hallmarks of spermatid apoptosis. A previous, independent report on the fruit fly Fbxo7 ortholog nutcracker (ntc) shown to cause sterility at a similar stage of germ cell development, indicates a conserved requirement for Fbxo7 across species. The Fbxo7 mutant mice represent a valuable new animal model for the study of late spermiogenic, cell and tissue remodeling, and phagocytic events in germ cell development. Yoshida et al. focus their review on lectin-type F-box proteins, which recognize cytosolic sugar chains as markers of unwanted proteins and organelles that mediate aberrant or harmful signals and trigger ubiquitination, thus ensuring homeostasis. They concluded that elucidation of the molecular mechanisms underlying induction of sugar-recognizing F-box proteins and promotion of SCF complex formation by various stimuli is crucial for a deeper understanding of F-box proteins functions and of cytosolic sugar chains. The RING family of E3 ligases includes over 600 enzymes clustered into TRIM, UBR and cullin-RING ligases. Zanchetta and Meroni discuss MID1 and MID2, two members of the TRIpartite Motif (TRIM) family of RING E3 ligases, the overexpression of which is associated with lung adenocarcinoma, prostate and breast cancer. They review the emerging evidence supporting

the involvement of MID1 and MID2 in the regulation of cytokinesis through MID1/MAD2 dynamic association with the proteins Astrin, BRAF35, and PP2A and how defects in the assembly of these complexes impairs cytokinesis, leading to severe adverse outcomes, including embryo development defects and cancer.

Approximately 50% of cancer patients receive treatment with ionizing radiation (radiotherapy) at some point during their cancer treatment. Fouad et al. present an analysis of how radiotherapy efficacy could be improved in combination with small size drugs that regulate the ubiquitin-proteasome system (UPS), some of which are currently undergoing clinical trials. The cullin family of E3 ligases is involved in several pathways of immune responses which can be exploited to modulate localized radiotherapy to induce out-of-target anti-tumor effects leading to tumor regression at non-irradiated metastatic sites, a phenomenon known as the abscopal effect. Fouad et al. go one step further and discuss the therapeutic approaches to target CRLs that have potential use in the clinic, including proteolysis targeting chimeras (PROTACs) of CRL adaptors that are only activated upon ionizing radiation or under a specific stimulus that mimic the tumor's microenvironment such as hypoxia that ultimately aim to improve patient survival.

Lescouzères and Bomont review the role of the Cullin 3-RING E3 ligase Gigaxonin in neurological diseases. Gigaxonin mutation are most commonly associated with Giant Axonal Neuropathies (GAN), a rare neurodegenerative disease which in the most severe cases has a fatal outcome usually before the third decade. Phenotypically, GAN results in enlarged axons which are filled with abnormal neurofilaments. The authors provide a comprehensive review of the roles and functions of Gigaxonin, including its known substrates, in cytoskeleton architecture, signal transduction through Hedgehog signaling and autophagosome production. The diversity in terms of substrates and cellular processes regulated by Gigaxonin further emphasizes the challenges associated with assigning a specific mechanism as disease-causing which currently limits the development of new therapies.

The RING-in between-RING (RBR) type of E3 ubiquitin ligases ubiquitinate substrates via a RING-HECT hybrid manner, and there are 14 RBR ligases known in humans. Lawrence et al. discuss about one of the RBR ligases, Natural Killer Lytic-Associated Molecule (NKLAM)/RNF19B in the regulation of innate immunity. NKLAM was originally identified by the authors as an IFNβ-induced gene in a human natural killer cell line. NKLAM regulates immune signaling cascades of STAT and NF-κB in immune cells, thus regulating cytokine production. Through its important roles of NKLAM in immunity, NKLAM shows anti-tumor function *in vivo*. More recent studies revealed that NKLAM regulates not only immunity, but also autophagy and responses to ER stress. The role of the ubiquitin ligase activity of NKLAM in innate immunity or other biological functions is yet to be discovered.

Finally, Escobar-Henriques and Joaquim discuss the role of E3 ubiquitin ligases in the regulation of mitochondrial quality control pathways. Mitochondria are highly dynamic organelles that constantly undergo anchoring, fission, transport, and membrane fusion. The latter process involves membrane remodeling in which the highly conserved proteins mitofusins (MFN1 and MFN2 in mammals and Fzo1 in yeast) play a central role. The authors review the ubiquitin E3 ligases that modify mitofusins in response to a variety of cellular inputs. They focus their analysis on the mitochondrial RING E3 ubiquitin ligases March5 and Mul1; Gp78, a ligase associated to the ER; and the cytosolic enzymes the RING MGRN1, the HECT ligase HUWE1 and the RBR E3 Parkin, all of which ubiquitylate mitofusins. The elucidation of molecular details underpinning mitofusins' modifications by E3 ligases should pave the way to develop new therapeutic approaches for the treatment of neurodegenerative, cardiovascular and obesity-associated disorders. The authors also provide novel insights on the roles of ubiquitin-dependent mechanisms in the regulation of inter-organelle membrane contact sites, a field which is revolutionizing our view of organelle biology (Scorrano et al., 2019).

In summary, this Research Topic highlights important discoveries in the structure to physiology understanding of E3 ubiquitin ligases, setting the stage to address important yet unanswered questions in the ubiquitin signaling field. These include the determination of the 3D structure of full length E3 ubiquitin ligases, which is now achievable, as the cryo-EM structure of the HECT ligase HUWE1 has shown (Hunkeler et al., 2020); the definition of the entire human ubiquitome; the mechanisms underlying substrate recognition and processing; the regulation of protein ubiquitination in time and space and tissue; the molecular basis for how deregulation of E3 ubiquitin ligases lead to disease. Addressing these questions will be instrumental in order to develop innovative therapeutics.

## AUTHOR CONTRIBUTIONS

All authors listed have made a substantial, direct and intellectual contribution to the work and approved it for publication.

## FUNDING

Funding to HL was provided by the BBSRC (Grand No. BB/J007846/1) and Parkinson's UK. Funding to FI was provided by JSPS KAKENHI (Grant No. JP18K19959). JL was funded by Ph.D. studentships from Alzheimer's Research UK, the GW4 BioMed MRC Doctoral Training Partnership and the BBSRC South West Biosciences Doctoral Training Partnership. VB-G was funded by CRUK (C5255/A18085) through the CRUK Oxford Centre.

## ACKNOWLEDGMENTS

JL, FI, HL, and VB-G would like to thank all contributing authors and reviewers for their support to the Research Topic.

## REFERENCES

Banik, S. M., Pedram, K., Wisnovsky, S., Ahn, G., Riley, N. M., and Bertozzi, C. R. (2020). Lysosome-targeting chimaeras for degradation of extracellular proteins. *Nature* 584, 291–297. doi: 10.1038/s41586-020-2545-9

Deshaies, R. J., and Joazeiro, C. A. P. (2009). RING domain E3 ubiquitin ligases. *Annu. Rev. Biochem.* 78, 399–434. doi: 10.1146/annurev.biochem.78.101807.093809

Harris, R. M., and Stafford, D. E. J. (2020). Prader Willi syndrome: endocrine updates and new medical therapies. *Curr. Opin. Endocrinol. Diabetes Obes.* 27, 56–62. doi: 10.1097/MED.0000000000000517

Hunkeler, M., Cyrus, J., Ma, M. W., Overwijn, D., Monda, J. K., Bennett, E. J., et al. (2020). Modular HUWE1 architecture serves as hub for degradation of cell-fate decision factors. *bioRxiv [Preprint]*. doi: 10.1101/2020.08.19.257352

Mulder, M. P. C., Zhuang, Z., Liu, L., Kessler, B. M., and Ovaa, H. (2020). Editorial: probing the ubiquitin landscape. *Front. Chem.* 8:449. doi: 10.3389/fchem.2020.00449

Sakamoto, K. M., Kim, K. B., Kumagai, A., Mercurio, F., Crews, C. M., and Deshaies, R. J. (2001). Protacs: chimeric molecules that target proteins to the Skp1-Cullin-F box complex for ubiquitination and degradation. *Proc. Natl. Acad. Sci. U.S.A.* 98, 8554–8559. doi: 10.1073/pnas.141230798

Scorrano, L., De Matteis, M. A., Emr, S., Giordano, F., Hajnóczky, G., Kornmann, B., et al. (2019). Coming together to define membrane contact sites. *Nat. Commun.* 10:1287. doi: 10.1038/s41467-019-09253-3

Takahashi, D., Moriyama, J., Nakamura, T., Miki, E., Takahashi, E., Sato, A., et al. (2019). AUTACs: cargo-specific degraders using selective autophagy. *Mol. Cell* 76, 797–810.e10. doi: 10.1016/j.molcel.2019.09.009

Wheeler, A. C., Sacco, P., and Cabo, R. (2017). Unmet clinical needs and burden in Angelman syndrome: a review of the literature. *Orphanet J. Rare Dis.* 12:164. doi: 10.1186/s13023-017-0716-z

**Conflict of Interest:** The authors declare that the research was conducted in the absence of any commercial or financial relationships that could be construed as a potential conflict of interest.

frontiers in Physiology

MINI REVIEW
published: 19 February 2019
doi: 10.3389/fphys.2019.00104

# Sugar-Recognizing Ubiquitin Ligases: Action Mechanisms and Physiology

*Yukiko Yoshida[1], Tsunehiro Mizushima[2] and Keiji Tanaka[3]**

*[1] Ubiquitin Project, Tokyo Metropolitan Institute of Medical Science, Tokyo, Japan, [2] Graduate School of Life Science, Picobiology Institute, University of Hyogo, Kobe, Japan, [3] Laboratory of Protein Metabolism, Tokyo Metropolitan Institute of Medical Science, Tokyo, Japan*

F-box proteins, the substrate recognition subunits of SKP1–CUL1–F-box protein (SCF) E3 ubiquitin ligase complexes, play crucial roles in various cellular events mediated by ubiquitination. Several sugar-recognizing F-box proteins exist in both mammalian and plant cells. Although glycoproteins generally reside outside of cells, or in organelles of the secretory pathway, these lectin-type F-box proteins reside in the nucleocytoplasmic compartment. Mammalian sugar-recognizing F-box proteins commonly bind to the innermost position of N-glycans through a unique small hydrophobic pocket in their loops. Two cytosolic F-box proteins, Fbs1 and Fbs2, recognize high-mannose glycans synthesized in the ER, and $SCF^{Fbs1}$ and $SCF^{Fbs2}$ ubiquitinate excess unassembled or misfolded glycoproteins in the ERAD pathway by recognizing the innermost glycans, which serve as signals for aberrant proteins. On the other hand, endomembrane-bound Fbs3 recognizes complex glycans as well as high-mannose glycans, and $SCF^{Fbs3}$ ubiquitinates exposed glycoproteins in damaged lysosomes fated for elimination by selective autophagy. Plants express stress-inducible lectin-type F-box proteins recognizing a wider range of N- and O-glycans, suggesting that the roles of mammalian and plant lectin-type F-box proteins have diverged over the course of evolution to recognize species-specific targets with distinct functions. These sugar-recognizing F-box proteins interpret glycans in the cytosol as markers of unwanted proteins and organelles, and degrade them *via* the proteasome or autophagy.

**Keywords: E3 ubiquitin ligase, ERAD, F-box protein, glycoprotein, N-glycan, SCF complex, sugar chain**

OPEN ACCESS

***Edited by:***
*Victor M. Bolanos-Garcia, Oxford Brookes University, United Kingdom*

***Reviewed by:***
*Sumit Sahni, University of Sydney, Australia*
*Paul Kenneth Witting, University of Sydney, Australia*

****Correspondence:***
*Keiji Tanaka*
*tanaka-kj@igakuken.or.jp*

***Specialty section:***
*This article was submitted to Integrative Physiology, a section of the journal Frontiers in Physiology*

***Received:*** *23 October 2018*
***Accepted:*** *28 January 2019*
***Published:*** *19 February 2019*

***Citation:***
*Yoshida Y, Mizushima T and Tanaka K (2019) Sugar-Recognizing Ubiquitin Ligases: Action Mechanisms and Physiology. Front. Physiol. 10:104. doi: 10.3389/fphys.2019.00104*

## INTRODUCTION

Ubiquitination occurs in a temporally and spatially specific manner. E3 ubiquitin ligases control ubiquitination by recognizing specific motifs, such as post-translational modifications induced by cell-signaling events or exposed elements that are normally hidden within proteins (Ravid and Hochstrasser, 2008). Cullin-RING E3 ligases (CRLs) are the largest family of E3 enzymes in all eukaryotes (Petroski and Deshaies, 2005). The best characterized CRLs are SCF complexes. Each SCF complex consists of four subunits: a scaffold protein CUL1, a RING protein RBX1, an adaptor protein SKP1, and one of many F-box proteins, which are responsible for substrate recognition. Each F-box proteins consists of an F-box domain, which binds to SKP1, and a

divergent carboxy-terminal substrate-binding domain (Zheng et al., 2002). Mammalian F-box proteins have been grouped into three subfamilies according to their substrate-binding domains (Jin et al., 2004): the FBXW and FBXL families possess WD40 repeats and leucine-rich repeats (LRRs) in their binding domains, respectively, whereas the FBXO family does not have any characteristic structural domain(s). The varieties of SCF complexes differ considerably among eukaryotes. For example, there are 22, 72, and 698 F-box proteins in yeast (*Saccharomyces cerevisiae*), human, plant (*Arabidopsis thaliana*), respectively (Hua et al., 2011; Lee et al., 2011; Finley et al., 2012). Furthermore, CUL1, RBX1, and SKP1 are invariable components in the SCF complex in yeasts and metazoans, but the *Arabidopsis* genome encodes 19 SKP1-like proteins (ASK1-19), and some F-box proteins probably interact with several ASK proteins, yielding more diverse SCF complexes in plants (Farras et al., 2001; Gagne et al., 2002; Kuroda et al., 2012).

F-box proteins discriminate among free metabolites and various post-translational modifications in order to correctly ubiquitinate and degrade substrates in cells. For example, the growth-regulating plant hormones auxin/indole-3-acetic acid and jasmonates bind to transport inhibitor response 1 (TIR1) and coronatine-insensitive-1 (COI-1), respectively, to form part of an enlarged protein-binding interface that allows high-affinity interaction with their specific substrate hormone repressors (Tan et al., 2007; Sheard et al., 2010). As a common mechanism in all eukaryotes, many cell-cycle–related F-box proteins recognize phosphorylation in a specific motif in their corresponding substrates (Ang and Wade Harper, 2005; Randle and Laman, 2016). In addition to phosphorylation, other posttranslational modifications are also necessary for ubiquitination of some SCF complex substrates. In mammals, for example, $SCF^{FBXO22}$-KDM4A and $SCF^{FBXL17}$ target methylated p53 and acetylated PRMT1, respectively (Johmura et al., 2016; Lai et al., 2017). In addition, glycosylation is recognized by some F-box proteins in both mammals and plants. In contrast to other posttranslational modifications, the sugar chains of glycoproteins exhibit structural complexity and diversity.

Protein glycosylation occurs in the endoplasmic reticulum (ER) and Golgi, and glycoproteins reside within the lumen of secretory pathway organelles or outside the cell. Because they are separated by an endomembrane or the plasma membrane, sugar chains are normally not accessible to the ubiquitination machinery in the cytosol or nucleus. However, there are several opportunities for glycoproteins to appear in the cytosol. The first possibility is the ER-associated degradation (ERAD) pathway, in which unfolded proteins and orphan subunits are degraded by the proteasome after retrograde transport from the ER to the cytosol (Vembar and Brodsky, 2008). In this case, the N-glycan structures of glycoproteins emerging in the cytosol are high-mannose glycans that are modified by ER-resident enzymes. On the other hand, compounds including silica, monosodium urate, and protein amyloids, which are endocytosed from the extracellular milieu, can injure endosomes and lysosomes, causing glycoproteins modified with complex- or hybrid-type glycans to be leaked from these organelles to the cytosol. Furthermore, some specific-glycans on the surfaces of viruses and bacterial toxins that invaded cells *via* the retrograde transport pathway may appear in the cytosol. Therefore, sugar chains appearing in the cytosol serve as ubiquitination signal for unwanted proteins and organelles (Yoshida and Tanaka, 2018). In this review, we focus on the substrate recognition mechanisms of sugar-recognizing F-box proteins. We will discuss the differences and similarities in the substrate recognition modes of lectin-type F-box proteins between plants and mammals, from the standpoint of their physiological roles.

# MECHANISM OF N-GLYCAN RECOGNITION BY SUGAR-RECOGNIZING F-BOX PROTEINS

## N-Glycan Recognition by Mammalian Sugar-Recognizing F-Box Proteins

F-box protein recognizing sugar chain 1 (Fbs1), the first ubiquitin ligase component identified as a sugar-recognizing F-box protein, was purified from mouse brain lysate based on its affinity for an N-glycoprotein (Yoshida et al., 2002). Of the 72 human F-box proteins, only three, Fbs1/FBXO2, Fbs2/FBXO6, and Fbs3/FBXO27, have the ability to bind glycoproteins containing high-mannose glycans, which are synthesized in the ER (Yoshida et al., 2003, 2011).

These F-box proteins recognize $Man_3GlcNAc_2$ core in N-glycans, but exhibit diverse binding to various glycan structures (Glenn et al., 2008). Structural analysis reveals that the overall architecture of Fbs1 consists of the F-box domain, a linker domain, and a substrate-binding domain (**Figure 1A**). The substrate-binding domain of Fbs1 is composed of a 10-stranded β-sandwich with an α-helix; it binds $Man_3GlcNAc_2$ through a small hydrophobic pocket in the loops located at the top of the β-sandwich, which protrudes toward E2 (**Figure 1B**). $Man_3GlcNAc_2$ interacts with Fbs1 through hydrogen bonds and/or hydrophobic interactions (**Figure 1C**; Mizushima et al., 2004, 2007). The core regions of glycans in native glycoproteins are shielded by the amino acid residues surrounding the glycosylation site, but are exposed upon denaturation. Indeed, Fbs1 and Fbs2 prefer to interact with denatured glycoproteins; thus, exposure of the innermost position of N-glycans upon glycoprotein denaturation serves as a signal of misfolding (Yoshida et al., 2005, 2007; Mallinger et al., 2012). Interestingly, a cytosolic N-Glycanase 1 (NGLY1) also recognizes the same position of glycoproteins and is involved in deglycosylation of various substrates prior to their proteasome-mediated degradation *via* the ERAD pathway (Yamaguchi et al., 2007; Suzuki, 2015). Therefore, ERAD substrates emerging in the cytosol might be denatured.

Although both Fbs1 and Fbs2 preferentially bind high-mannose glycans, Fbs3 binds to glycoproteins modified with complex-type glycans, such as transferrin and LAMP2, as well as high-mannose glycans (Glenn et al., 2008; Yoshida et al., 2017). However, the structural information of Fbs3 is not yet available until now, and the mode of recognition by Fbs3 remains to be elucidated.

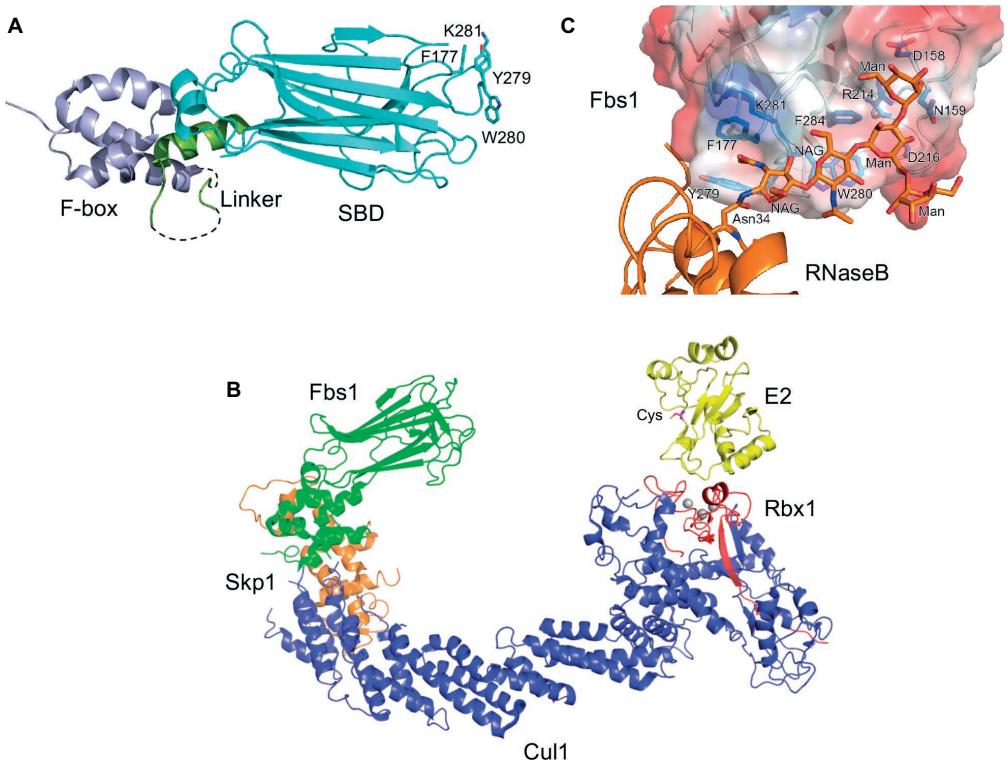


**FIGURE 1 |** Structure of Fbs1. **(A)** Overall structure of Fbs1. The F-box domain (F-box), linker, and substrate-binding domain (SBD) are shown in violet, green, and cyan, respectively. Dotted lines represent disordered regions. $GlcNAc_2$-binding residues are depicted as stick models. **(B)** Model of the $SCF^{Fbs1}$ complex bound to E2. Fbs1, Cul1, Rbx1, Skp1, and E2 are colored green, blue, red, orange, and yellow, respectively. A model of $SCF^{Fbs1}$ was constructed by superposition of the Skp1 subunits from the Skp1–Fbs1, and Skp1–Cul1–Rbx1 structures (Zheng et al., 2002) (PDB ID code 1LDK); the RING-finger domains derived from Rbx1; the c-Cbl subunit of c-Cbl–UbcH7 (Zheng et al., 2000) (PDB ID code 1FBV); and the E2 subunits of c-Cbl-UbcH7. **(C)** Surface representation of the substrate-binding site of the Fbs1 SBD bound to $Man_3GlcNAc_2$ of RNase B. The surface is colored according to the electrostatic potential of the residues (blue, positive; red, negative). Bound RNase B and $Man_3GlcNAc_2$ are orange, and the residues involved in the substrate binding are blue.

## Mammalian Fbs1-Related F-Box Proteins

Fbs1/FBXO2 exhibits high sequence similarity with other F-box proteins (Winston et al., 1999; Ilyin et al., 2002). In phylogenetic analysis, these proteins cluster into two groups: one group contains Fbs1/FBXO2, Fbs2/FBXO6, and FBXO44a, and the other contains FBXO17 and Fbs3/FBXO27 (**Figure 2A**). The genes that encode the proteins each group are arranged in tandem with very short intergenic regions, but the two groups map to different chromosomes in both human and mouse (Ilyin et al., 2002; Yoshida and Tanaka, 2010). These F-box proteins contain a highly homologous F-box domain and a substrate-binding domain (SBD) (**Figure 2B**), but the long N-terminal region and C-terminal tail are unique to Fbs1 and Fbs2, respectively. The SBD of FBXO44 has 68% identity with the corresponding region of Fbs2; the residues necessary for binding to N-glycans are conserved, and its overall structure is similar to Fbs1 and Fbs2. Nonetheless, FBXO44 has no detectable sugar-binding activity (Glenn et al., 2008; Yoshida et al., 2011). The crystal structure of FBXO44–Skp1 revealed that FBXO44 has different hydrogen bond networks than the four loops from Fbs1 and Fbs2, preventing the formation of the sugar-binding pocket (Kumanomidou et al., 2015; Nishio et al., 2016). Thus far, from a structural perspective, it has been challenging to identify factors that determine the substrate specificity of these isoforms.

## Plant Lectin-Type F-Box Proteins

These Fbs orthologues are encoded in various vertebrate genomes, but other lectin-type F-box proteins are found in plants. High levels of secretory lectins accumulate in plant seeds and vegetative storage tissues, but plants also synthesize small amounts of nucleocytoplasmic lectins in response to specific stress factors and changing environmental conditions. Among nucleocytoplasmic lectins, chimeric proteins that contain F-box domain with Jacalin-related lectins or Nictaba-like lectins were found (Lannoo and Van Damme, 2010). Nictaba, an inducible lectin found in *Nicotiana tabacum* leaves treated with jasmonates (Chen et al., 2002), recognizes $Man_3GlcNAc_2$ core as well as human Fbs family members (Lannoo et al., 2006). However, the three-dimensional conformations and sugar-recognition modes of Nictaba and mammalian Fbs1 differ considerably (Mizushima et al., 2004; Schouppe et al., 2010). *Arabidopsis* and crops such as soybean express dozens of F-box/Nictaba proteins (Delporte et al., 2015; Van Holle

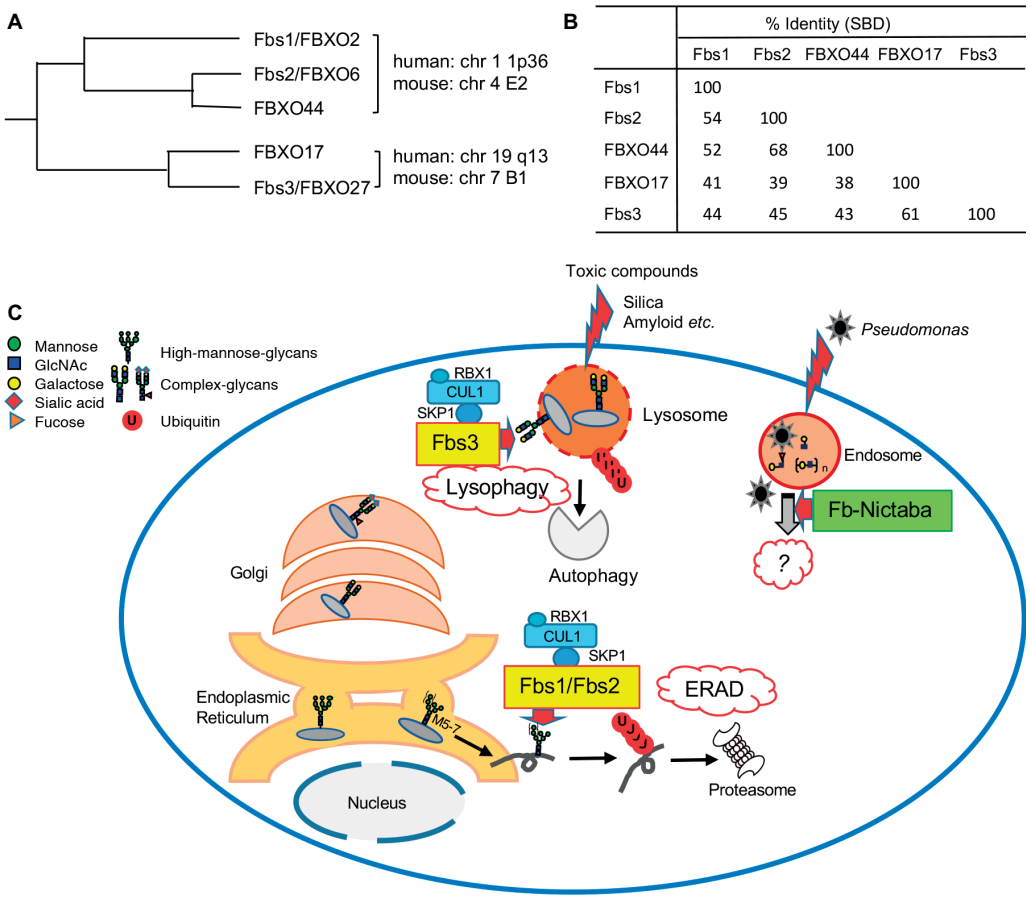


**FIGURE 2 |** Roles of sugar-recognizing F-box proteins in the cytosol. **(A)** Phylogenetic tree of Fbs1 homologs. Genomic locations of these genes on human or mouse chromosomes are also shown. **(B)** Percentage identities of substrate-binding domain (SBD) of Fbs1 homologs. **(C)** Overview of the functions of sugar-recognizing F-box proteins. Three mammalian F-box proteins (Fbs1, Fbs2, and Fbs3; yellow-colored) form SCF complexes and ubiquitinate glycoproteins in the cytosol, followed by proteasomal or autophagic degradation to maintain cellular homeostasis. They mainly recognize the innermost $Man_3GlcNAc_2$ structure in high-mannose glycans, which are attached in the ER, as a signal of misfolded glycoproteins, and act on excess unassembled subunits or misfolded glycoproteins *via* the ERAD pathway. In contrast to Fbs1 and Fbs2, Fbs3 can bind to complex-type glycans, is targeted to endomembranes via N-myristoylation, and accumulates on organelles such as lysosomes and endosomes ruptured by toxic compounds. $SCF^{Fbs3}$ ubiquitinates exposed the lysosomal glycoprotein LAMP2 to induce autophagy. Dozens of F-box/Nictaba proteins (green) are expressed in plants, but their functions have not been elucidated. These proteins recognize varieties of glycan structure in both N- and O-glycans, and their expression is induced by certain environmental stresses. The *Arabidopsis* F-box/Nictaba protein functions in defense against pathogens such as *Pseudomonas syringae*.

et al., 2017), but to date only an *Arabidopsis* F-box/Nictaba protein, At2g02360, has been characterized. The expression of At2g02360 is up-regulated after treatment with salicylic acid, heat stress, or infection with *Pseudomonas syringae*. Plants overexpressing At2g02360 exhibit milder disease symptoms after infection of pathogens, but the molecular mechanisms involved in acquisition of pathogen resistance remain to be elucidated (Stefanowicz et al., 2016). Although At2g02360 shares the highest sequence similarity (64%) to tobacco Nictaba among Arabidopsis F-box/Nictaba proteins, it binds to N- and O-glycans with Galβ1-3GlcNAc and Galβ1-4GlcNAc and poly-N-acetyllactosamine, but not to $Man_3GlcNAc_2$ core (Stefanowicz et al., 2012). It is possible that other F-box/Nictaba proteins have different sugar-binding specificities, but the roles of mammalian and plant lectin-type F-box proteins seem to have diverged substantially over the course of to recognize species-specific targets with distinct functions (**Figure 2C**).

## PHYSIOLOGICAL ROLES OF MAMMALIAN SUGAR-RECOGNIZING F-BOX PROTEINS

As described above, Fbs1 and Fbs2 specifically recognize high-mannose glycans, and in particular the innermost structure. Therefore, $SCF^{Fbs1}$ and $SCF^{Fbs2}$ can ubiquitinate excess unassembled or misfolded glycoproteins in the ERAD pathway by recognizing the innermost glycans as signals for aberrant proteins (**Figure 2B**). On the other hand, Fbs3, which can also interact with glycoproteins modified with complex-type glycans present in organelles downstream of

the Golgi or on the cell surface, contributes to maintenance of organelle homeostasis (**Figure 2C**).

$SCF^{Fbs1}$ and $SCF^{Fbs2}$ are the E3 enzymes responsible for degradation of integrin β1 that is expressed in excess over integrin α chains, or ERAD substrates such as TCRα, asialoglycoprotein receptor H2a, and CFTRΔ508 (Yoshida et al., 2002, 2003; Groisman et al., 2011; Chen et al., 2016; Ramachandran et al., 2016). The ERAD pathway is a ubiquitous protein quality control system in all eukaryotes, and ERAD substrates are generally ubiquitinated by ER membrane-embedded E3s, such as Hrd1 and gp78 (Vembar and Brodsky, 2008). However, Fbs proteins are encoded only in vertebrate genomes. In particular, Fbs1 expression is restricted to a subset of tissues, and therefore its role in in quality control may be tissue-specific.

## Roles of Fbs1 in the Brain and Inner Ear

Originally named neural F-box protein 42 kDa (NFB42) and organ of Corti protein 1 (OCP1), Fbs1 is expressed at high levels in the brain and rodent inner ear (Erhardt et al., 1998; Henzl et al., 2001). Therefore, Fbs1 may function in quality control specifically in the nervous system and inner ear, rather than in the general ERAD system.

NMDA receptors play crucial roles in neuronal development and information storage in the brain, and $SCF^{Fbs1}$ controls the abundance and localization of their specific subunits, GluN1 and GluN2A (Kato et al., 2005; Atkin et al., 2015). Furthermore, Fbs1 attenuates amyloid-β (Aβ) production through ubiquitination of β-secretase (BACE1) and amyloid precursor protein (APP), and the expression of Fbs1 decreases in the brains of Alzheimer's disease (AD) patients and Tg2576 mice, a well-characterized model of AD (Gong et al., 2010; Atkin et al., 2014). In primary neurons derived from Tg2576 mice, overexpression of Fbs1 promotes the degradation of BACE1, which is essential for Aβ generation, thereby decreasing the Aβ level (Gong et al., 2010). In addition, the total amount of amyloid precursor protein (APP) in the brain of Fbs1-KO mouse is increased but decreased on the surface of cells in hippocampal neurons, indicating that Fbs1 regulates APP protein levels and processing (Atkin et al., 2014). Interestingly, PGC-1α, a transcriptional coactivator involved in control of energy metabolism, regulates Fbs1 expression, and nicotinamide riboside upregulates BACE1 degradation through enhancing PGC-1α expression (Gong et al., 2010, 2013). Compounds such as nicotinamide that stimulate Fbs1 expression/activity may represent candidate therapeutic agents for AD.

Furthermore, Fbs1-knockout mice exhibit age-related hearing loss with cochlear degeneration and high cochlear levels of the inner-ear gap-junction protein GJB2 (Nelson et al., 2007), which is a multi-pass membrane protein that lacks glycans but nonetheless interacts with Fbs1 (Henzl et al., 2004). Fbs1 is an unusually abundant inner ear protein, and exists as a heterodimer with Skp1 but not as a component of the SCF complex, suggesting that its function in inner-ear homeostasis is distinct from that of the conventional SCF complex (Atkin et al., 2015).

Although the expression of Fbs1 is restricted to specific organs under normal condition, recent studies show that expression of Fbs1, like plant Nictaba, is up-regulated in response to some stressors. In the livers of mice with high-fat diet-induced obesity, Fbs1 expression is induced by the IKKβ/NF-κB pathway, and $SCF^{Fbs1}$ disrupts glucose homeostasis *via* degradation of the insulin receptor (Liu et al., 2017). Infection with Epstein–Barr virus (EBV) also stimulates Fbs1 expression, and induced $SCF^{Fbs1}$ ubiquitinates and degrades EBV glycoprotein B, thereby decreasing the infectivity of progeny viruses (Zhang et al., 2018). Thus, $SCF^{Fbs1}$ may function in the unusual ERAD system that is induced under certain stresses. The expression of Fbs3, like that of Fbs1, is restricted to specific organs, including the brain. Its levels are very low, but it may be induced by as-yet-undetermined stimuli.

## Roles of Fbs3

Fbs3 has a unique endomembrane localization due to N-myristoylation. This endomembrane localization, together with its glycoprotein-binding activity, is essential for effective recruitment to damaged organelles. Fbs3 accumulates within ruptured lysosomes or endosomes by treated with the lysosomal damage reagent L-leucyl-l-leucine methyl ester (LLOMe), crystalline silica, or latex beads coated with transfection reagents, whereas neither Fbs1 or Fbs2 behaves in this manner (Yoshida et al., 2017). Lysosomes are specialized organelle that contain a variety of digestive enzymes and play a crucial role in autophagy, but damaged lysosomes are themselves eliminated by a special form of autophagy known as lysophagy. Like mitophagy, a well-characterized form of selective autophagy, ubiquitination is prerequisite for lysophagy, but the ubiquitination substrates and molecular mechanisms underlying lysophagy induction have not been elucidated (Maejima et al., 2013). Following lysosomal damage, Fbs3 quickly moves to ruptured lysosomes by detecting exposed glycoproteins, and $SCF^{Fbs3}$ ubiquitinates several lysosomal glycoproteins. Among the lysosomal glycoproteins, ubiquitination of LAMP2 is especially important for recruitment of components of the autophagic machinery, such as p62 and LC3 (Yoshida et al., 2017). Although $SCF^{Fbs3}$ recognizes and ubiquitinates exposed glycoproteins that are normally sequestered in lysosomes following lysosomal damage, resulting in induction of lysophagy, other glycan-recognition systems are also involved in the autophagy-mediated response to damaged endomembranes.

Galectins are β-galactoside–binding lectins, and mostly reside in the cytosol and nucleus. Galectin-8 accumulates on damaged bacteria-containing vesicles and binds directly to NDP52, an autophagy receptor, thereby triggering a specific form of autophagy called xenophagy and restricting the growth of *Salmonella* in cells (Thurston et al., 2012; Li et al., 2013). Galectin-3 also accumulates on damaged organelles, such as phagosomes ruptured by infecting *Mycobacterium* and damaged lysosomes, and interacts with TRIM16, a RING-type ubiquitin ligase. TRIM16 further interacts with the key autophagy regulator ULK1, Beclin1, and ATG16L1, and induces autophagy following their ubiquitination (Chauhan et al., 2016). Thus, several cytosolic glycan-monitoring systems collaborate with the proteasome and autophagy to maintain cellular homeostasis.

## CONCLUSIONS AND PERSPECTIVES

Here we have summarized our current knowledge of the sugar-recognition modes and physiological roles of lectin-type F-box proteins. These proteins recognize cytosolic sugar chains, which are normally present in organelles or extracellularly, as aberrant or harmful signals that trigger ubiquitination, leading to alleviation of deleterious cellular states and maintenance of homeostasis. Mammalian sugar-recognizing F-box proteins commonly bind to the innermost position of N-glycans, and cytosolic NGLY1 removes this sugar degron. Mutations in NGLY1 cause an inherited disorder of the ERAD pathway (Enns et al., 2014), and NGLY1 knockout mice are embryonic lethal (Fujihira et al., 2017). Why would F-box proteins fail to rescue the lethality of NGLY1 deficiency, which is caused by excessive glycoprotein in the cytosol? As with Fbs3, the functions of Fbs1 and Fbs2 may be distinct from the ERAD pathway. For instance, Fbs3 accumulates in ruptured lysosomes and preferentially ubiquitinates LAMP2, which plays a crucial role for lysophagy. Thus, identification of the intrinsic substrates for Fbs1 and Fbs2 is essential for understanding their physiological relevance in maintaining cellular homeostasis. Research of these glycoprotein-related F-box proteins knockout mice in models of disease, including AD, would be also useful for assessing their physiological and pathophysiological roles.

In comparison with mammals, plants have more sugar-recognizing F-box proteins with diverse substrate specificities, but their functions have not been elucidated. The ability of these proteins to form SCF complexes remain to be determined. Among 22 yeast F-box proteins, some function in complexes that lack CUL1, suggesting that not all F-box proteins in plants must form SCF complexes. Future studies should seek to determine their sugar-binding specificities and endogenous interacting proteins, substrates, and components of the complex. The elucidation of the molecular mechanisms underlying induction of sugar-recognizing F-box proteins and promotion of SCF complex formation by various stimuli, as well as detailed analyses of their substrate recognition modes in both plants and mammals, will be crucial to understanding the functions of F-box proteins and cytosolic sugar chains.

## DATA AVAILABILITY

The datasets generated for this study are available on request to the corresponding author.

## AUTHOR CONTRIBUTIONS

YY and TM wrote the manuscript with supervision from KT. All authors critically appraised the final version of the paper.

## FUNDING

This work was supported by JSPS KAKENHI Grant Number JP16K07705 (to YY) and JP2600014 (to KT): JST CREST Grant Number JPMJCR18H3 (to YY), and the Takeda Science Foundation (KT).

## REFERENCES

Ang, X. L., and Wade Harper, J. (2005). SCF-mediated protein degradation and cell cycle control. *Oncogene* 24, 2860–2870. doi: 10.1038/sj.onc.1208614

Atkin, G., Hunt, J., Minakawa, E., Sharkey, L., Tipper, N., Tennant, W., et al. (2014). F-box only protein 2 (Fbxo2) regulates amyloid precursor protein levels and processing. *J. Biol. Chem.* 289, 7038–7048. doi: 10.1074/jbc.M113.515056

Atkin, G., Moore, S., Lu, Y., Nelson, R. F., Tipper, N., Rajpal, G., et al. (2015). Loss of F-box only protein 2 (Fbxo2) disrupts levels and localization of select NMDA receptor subunits, and promotes aberrant synaptic connectivity. *J. Neurosci.* 35, 6165–6178. doi: 10.1523/JNEUROSCI.3013-14.2015

Chauhan, S., Kumar, S., Jain, A., Ponpuak, M., Mudd, M. H., Kimura, T., et al. (2016). TRIMs and galectins globally cooperate and TRIM16 and galectin-3 co-direct autophagy in endomembrane damage homeostasis. *Dev. Cell* 39, 13–27. doi: 10.1016/j.devcel.2016.08.003

Chen, X., Duan, L. H., Luo, P. C., Hu, G., Yu, X., Liu, J., et al. (2016). FBXO6-mediated ubiquitination and degradation of Ero1L inhibits endoplasmic reticulum stress-induced apoptosis. *Cell. Physiol. Biochem.* 39, 2501–2508. doi: 10.1159/000452517

Chen, Y., Peumans, W. J., Hause, B., Bras, J., Kumar, M., Proost, P., et al. (2002). Jasmonic acid methyl ester induces the synthesis of a cytoplasmic/nuclear chito-oligosaccharide binding lectin in tobacco leaves. *FASEB J.* 16, 905–907. doi: 10.1096/fj.01-0598fje

Delporte, A., Van Holle, S., Lannoo, N., and Van Damme, E. J. (2015). The tobacco lectin, prototype of the family of Nictaba-related proteins. *Curr. Protein Pept. Sci.* 16, 5–16. doi: 10.2174/1389203716666150213154107

Enns, G. M., Shashi, V., Bainbridge, M., Gambello, M. J., Zahir, F. R., Bast, T., et al. (2014). Mutations in NGLY1 cause an inherited disorder of the endoplasmic reticulum-associated degradation pathway. *Genet. Med.* 16, 751–758. doi: 10.1038/gim.2014.22

Erhardt, J. A., Hynicka, W., Dibenedetto, A., Shen, N., Stone, N., Paulson, H., et al. (1998). A novel F box protein, NFB42, is highly enriched in neurons and induces growth arrest. *J. Biol. Chem.* 273, 35222–35227. doi: 10.1074/jbc.273.52.35222

Farras, R., Ferrando, A., Jasik, J., Kleinow, T., Okresz, L., Tiburcio, A., et al. (2001). SKP1-SnRK protein kinase interactions mediate proteasomal binding of a plant SCF ubiquitin ligase. *EMBO J.* 20, 2742–2756. doi: 10.1093/emboj/20.11.2742

Finley, D., Ulrich, H. D., Sommer, T., and Kaiser, P. (2012). The ubiquitin-proteasome system of *Saccharomyces cerevisiae*. *Genetics* 192, 319–360. doi: 10.1534/genetics.112.140467

Fujihira, H., Masahara-Negishi, Y., Tamura, M., Huang, C., Harada, Y., Wakana, S., et al. (2017). Lethality of mice bearing a knockout of the Ngly1-gene is partially rescued by the additional deletion of the Engase gene. *PLoS Genet.* 13:e1006696. doi: 10.1371/journal.pgen.1006696

Gagne, J. M., Downes, B. P., Shiu, S. H., Durski, A. M., and Vierstra, R. D. (2002). The F-box subunit of the SCF E3 complex is encoded by a diverse superfamily of genes in Arabidopsis. *Proc. Natl. Acad. Sci. USA* 99, 11519–11524. doi: 10.1073/pnas.162339999

Glenn, K. A., Nelson, R. F., Wen, H. M., Mallinger, A. J., and Paulson, H. L. (2008). Diversity in tissue expression, substrate binding, and SCF complex formation for a lectin family of ubiquitin ligases. *J. Biol. Chem.* 283, 12717–12729. doi: 10.1074/jbc.M709508200

Gong, B., Chen, F., Pan, Y., Arrieta-Cruz, I., Yoshida, Y., Haroutunian, V., et al. (2010). SCFFbx2-E3-ligase-mediated degradation of BACE1 attenuates Alzheimer's disease amyloidosis and improves synaptic function. *Aging Cell* 9, 1018–1031. doi: 10.1111/j.1474-9726.2010.00632.x

Gong, B., Pan, Y., Vempati, P., Zhao, W., Knable, L., Ho, L., et al. (2013). Nicotinamide riboside restores cognition through an upregulation of proliferator-activated receptor-gamma coactivator 1alpha regulated

beta-secretase 1 degradation and mitochondrial gene expression in Alzheimer's mouse models. *Neurobiol. Aging* 34, 1581–1588. doi: 10.1016/j.neurobiolaging.2012.12.005

Groisman, B., Shenkman, M., Ron, E., and Lederkremer, G. Z. (2011). Mannose trimming is required for delivery of a glycoprotein from EDEM1 to XTP3-B and to late endoplasmic reticulum-associated degradation steps. *J. Biol. Chem.* 286, 1292–1300. doi: 10.1074/jbc.M110.154849

Henzl, M. T., O'Neal, J., Killick, R., Thalmann, I., and Thalmann, R. (2001). OCP1, an F-box protein, co-localizes with OCP2/SKP1 in the cochlear epithelial gap junction region. *Hear. Res.* 157, 100–111. doi: 10.1016/S0378-5955(01)00285-4

Henzl, M. T., Thalmann, I., Larson, J. D., Ignatova, E. G., and Thalmann, R. (2004). The cochlear F-box protein OCP1 associates with OCP2 and connexin 26. *Hear. Res.* 191, 101–109. doi: 10.1016/j.heares.2004.01.005

Hua, Z., Zou, C., Shiu, S. H., and Vierstra, R. D. (2011). Phylogenetic comparison of F-Box (FBX) gene superfamily within the plant kingdom reveals divergent evolutionary histories indicative of genomic drift. *PLoS One* 6:e16219. doi: 10.1371/journal.pone.0016219

Ilyin, G. P., Serandour, A. L., Pigeon, C., Rialland, M., Glaise, D., and Guguen-Guillouzo, C. (2002). A new subfamily of structurally related human F-box proteins. *Gene* 296, 11–20. doi: 10.1016/S0378-1119(02)00867-3

Jin, J., Cardozo, T., Lovering, R. C., Elledge, S. J., Pagano, M., and Harper, J. W. (2004). Systematic analysis and nomenclature of mammalian F-box proteins. *Genes Dev.* 18, 2573–2580. doi: 10.1101/gad.1255304

Johmura, Y., Sun, J., Kitagawa, K., Nakanishi, K., Kuno, T., Naiki-Ito, A., et al. (2016). SCF(Fbxo22)-KDM4A targets methylated p53 for degradation and regulates senescence. *Nat. Commun.* 7:10574. doi: 10.1038/ncomms10574

Kato, A., Rouach, N., Nicoll, R. A., and Bredt, D. S. (2005). Activity-dependent NMDA receptor degradation mediated by retrotranslocation and ubiquitination. *Proc. Natl. Acad. Sci. USA* 102, 5600–5605. doi: 10.1073/pnas.0501769102

Kumanomidou, T., Nishio, K., Takagi, K., Nakagawa, T., Suzuki, A., Yamane, T., et al. (2015). The structural differences between a glycoprotein specific F-Box protein Fbs1 and its homologous protein FBG3. *PLoS One* 10:e0140366. doi: 10.1371/journal.pone.0140366

Kuroda, H., Yanagawa, Y., Takahashi, N., Horii, Y., and Matsui, M. (2012). A comprehensive analysis of interaction and localization of Arabidopsis SKP1-like (ASK) and F-box (FBX) proteins. *PLoS One* 7:e50009. doi: 10.1371/journal.pone.0050009

Lai, Y., Li, J., Li, X., and Zou, C. (2017). Lipopolysaccharide modulates p300 and Sirt1 to promote PRMT1 stability via an SCF(Fbxl17)-recognized acetyldegron. *J. Cell Sci.* 130, 3578–3587. doi: 10.1242/jcs.206904

Lannoo, N., Peumans, W. J., Pamel, E. V., Alvarez, R., Xiong, T. C., Hause, G., et al. (2006). Localization and in vitro binding studies suggest that the cytoplasmic/nuclear tobacco lectin can interact in situ with high-mannose and complex N-glycans. *FEBS Lett.* 580, 6329–6337. doi: 10.1016/j.febslet.2006.10.044

Lannoo, N., and Van Damme, E. J. (2010). Nucleocytoplasmic plant lectins. *Biochim. Biophys. Acta* 1800, 190–201. doi: 10.1016/j.bbagen.2009.07.021

Lee, J. E., Sweredoski, M. J., Graham, R. L., Kolawa, N. J., Smith, G. T., Hess, S., et al. (2011). The steady-state repertoire of human SCF ubiquitin ligase complexes does not require ongoing Nedd8 conjugation. *Mol. Cell. Proteomics* 10:M110.006460. doi: 10.1074/mcp.M110.006460

Li, S., Wandel, M. P., Li, F., Liu, Z., He, C., Wu, J., et al. (2013). Sterical hindrance promotes selectivity of the autophagy cargo receptor NDP52 for the danger receptor galectin-8 in antibacterial autophagy. *Sci. Signal.* 6:ra9. doi: 10.1126/scisignal.2003730

Liu, B., Lu, H., Li, D., Xiong, X., Gao, L., Wu, Z., et al. (2017). Aberrant expression of FBXO2 disrupts glucose homeostasis through ubiquitin-mediated degradation of insulin receptor in obese mice. *Diabetes* 66, 689–698. doi: 10.2337/db16-1104

Maejima, I., Takahashi, A., Omori, H., Kimura, T., Takabatake, Y., Saitoh, T., et al. (2013). Autophagy sequesters damaged lysosomes to control lysosomal biogenesis and kidney injury. *EMBO J.* 32, 2336–2347. doi: 10.1038/emboj.2013.171

Mallinger, A., Wen, H. M., Dankle, G. M., and Glenn, K. A. (2012). Using a ubiquitin ligase as an unfolded protein sensor. *Biochem. Biophys. Res. Commun.* 418, 44–48. doi: 10.1016/j.bbrc.2011.12.109

Mizushima, T., Hirao, T., Yoshida, Y., Lee, S. J., Chiba, T., Iwai, K., et al. (2004). Structural basis of sugar-recognizing ubiquitin ligase. *Nat. Struct. Mol. Biol.* 11, 365–370. doi: 10.1038/nsmb732

Mizushima, T., Yoshida, Y., Kumanomidou, T., Hasegawa, Y., Suzuki, A., Yamane, T., et al. (2007). Structural basis for the selection of glycosylated substrates by SCF(Fbs1) ubiquitin ligase. *Proc. Natl. Acad. Sci. USA* 104, 5777–5781.

Nelson, R. F., Glenn, K. A., Zhang, Y., Wen, H., Knutson, T., Gouvion, C. M., et al. (2007). Selective cochlear degeneration in mice lacking the F-box protein, Fbx2, a glycoprotein-specific ubiquitin ligase subunit. *J. Neurosci.* 27, 5163–5171. doi: 10.1523/JNEUROSCI.0206-07.2007

Nishio, K., Yoshida, Y., Tanaka, K., and Mizushima, T. (2016). Structural analysis of a function-associated loop mutant of the substrate-recognition domain of Fbs1 ubiquitin ligase. *Acta. Crystallogr. F Struct. Biol. Commun.* 72, 619–626. doi: 10.1107/S2053230X16011018

Petroski, M. D., and Deshaies, R. J. (2005). Function and regulation of cullin-RING ubiquitin ligases. *Nat. Rev. Mol. Cell Biol.* 6, 9–20. doi: 10.1038/nrm1547

Ramachandran, S., Osterhaus, S. R., Parekh, K. R., Jacobi, A. M., Behlke, M. A., and McCray, P. B. Jr. (2016). SYVN1, NEDD8, and FBXO2 proteins regulate DeltaF508 cystic fibrosis transmembrane conductance regulator (CFTR) ubiquitin-mediated proteasomal degradation. *J. Biol. Chem.* 291, 25489–25504. doi: 10.1074/jbc.M116.754283

Randle, S. J., and Laman, H. (2016). F-box protein interactions with the hallmark pathways in cancer. *Semin. Cancer Biol.* 36, 3–17. doi: 10.1016/j.semcancer.2015.09.013

Ravid, T., and Hochstrasser, M. (2008). Diversity of degradation signals in the ubiquitin-proteasome system. *Nat. Rev. Mol. Cell Biol.* 9, 679–690. doi: 10.1038/nrm2468

Schouppe, D., Rouge, P., Lasanajak, Y., Barre, A., Smith, D. F., Proost, P., et al. (2010). Mutational analysis of the carbohydrate binding activity of the tobacco lectin. *Glycoconj. J.* 27, 613–623. doi: 10.1007/s10719-010-9305-2

Sheard, L. B., Tan, X., Mao, H., Withers, J., Ben-Nissan, G., Hinds, T. R., et al. (2010). Jasmonate perception by inositol-phosphate-potentiated COI1-JAZ co-receptor. *Nature* 468, 400–405. doi: 10.1038/nature09430

Stefanowicz, K., Lannoo, N., Proost, P., and Van Damme, E. J. (2012). Arabidopsis F-box protein containing a Nictaba-related lectin domain interacts with N-acetyllactosamine structures. *FEBS Open Bio.* 2, 151–158. doi: 10.1016/j.fob.2012.06.002

Stefanowicz, K., Lannoo, N., Zhao, Y., Eggermont, L., Van Hove, J., Al Atalah, B., et al. (2015). Glycan-binding F-box protein from *Arabidopsis thaliana* protects plants from *Pseudomonas syringae* infection. *BMC Plant Biol.* 16:213.

Suzuki, T. The cytoplasmic peptide: N-glycanase (Ngly1)-basic science encounters a human genetic disorder. *J. Biochem.* 157, 23–34. doi: 10.1093/jb/mvu068

Tan, X., Calderon-Villalobos, L. I., Sharon, M., Zheng, C., Robinson, C. V., Estelle, M., et al. (2007). Mechanism of auxin perception by the TIR1 ubiquitin ligase. *Nature* 446, 640–645. doi: 10.1038/nature05731

Thurston, T. L., Wandel, M. P., Von Muhlinen, N., Foeglein, A., and Randow, F. (2012). Galectin 8 targets damaged vesicles for autophagy to defend cells against bacterial invasion. *Nature* 482, 414–418. doi: 10.1038/nature10744

Van Holle, S., Rouge, P., and Van Damme, E. J. M. (2017). Evolution and structural diversification of Nictaba-like lectin genes in food crops with a focus on soybean (*Glycine max*). *Ann. Bot.* 119, 901–914. doi: 10.1093/aob/mcw259

Vembar, S. S., and Brodsky, J. L. (2008). One step at a time: endoplasmic reticulum-associated degradation. *Nat. Rev. Mol. Cell Biol.* 9, 944–957. doi: 10.1038/nrm2546

Winston, J. T., Koepp, D. M., Zhu, C., Elledge, S. J., and Harper, J. W. (1999). A family of mammalian F-box proteins. *Curr. Biol.* 9, 1180–1182. doi: 10.1016/S0960-9822(00)80021-4

Yamaguchi, Y., Hirao, T., Sakata, E., Kamiya, Y., Kurimoto, E., Yoshida, Y., et al. (2007). Fbs1 protects the malfolded glycoproteins from the attack of peptide: N-glycanase. *Biochem. Biophys. Res. Commun.* 362, 712–716. doi: 10.1016/j.bbrc.2007.08.056

Yoshida, Y., Adachi, E., Fukiya, K., Iwai, K., and Tanaka, K. (2005). Glycoprotein-specific ubiquitin ligases recognize N-glycans in unfolded substrates. *EMBO Rep.* 6, 239–244. doi: 10.1038/sj.embor.7400351

Yoshida, Y., Chiba, T., Tokunaga, F., Kawasaki, H., Iwai, K., Suzuki, T., et al. (2002). E3 ubiquitin ligase that recognizes sugar chains. *Nature* 418, 438–442. doi: 10.1038/nature00890

Yoshida, Y., Murakami, A., Iwai, K., and Tanaka, K. (2007). A neural-specific F-box protein Fbs1 functions as a chaperone suppressing glycoprotein aggregation. *J. Biol. Chem.* 282, 7137–7144. doi: 10.1074/jbc.M611168200

Yoshida, Y., Murakami, A., and Tanaka, K. (2011). Skp1 stabilizes the conformation of F-box proteins. *Biochem. Biophys. Res. Commun.* 410, 24–28. doi: 10.1016/j.bbrc.2011.05.098

Yoshida, Y., and Tanaka, K. (2010). Lectin-like ERAD players in ER and cytosol. *Biochim. Biophys. Acta* 1800, 172–180. doi: 10.1016/j.bbagen.2009.07.029

Yoshida, Y., and Tanaka, K. (2018). Cytosolic N-glycans: triggers for ubiquitination directing proteasomal and autophagic degradation: molecular systems for monitoring cytosolic N-glycans as signals for unwanted proteins and organelles. *BioEssays* 40, 1700215 (1-9). doi: 10.1002/bies.201700215

Yoshida, Y., Tokunaga, F., Chiba, T., Iwai, K., Tanaka, K., and Tai, T. (2003). Fbs2 is a new member of the E3 ubiquitin ligase family that recognizes sugar chains. *J. Biol. Chem.* 278, 43877–43884. doi: 10.1074/jbc.M304157200

Yoshida, Y., Yasuda, S., Fujita, T., Hamasaki, M., Murakami, A., Kawawaki, J., et al. (2017). Ubiquitination of exposed glycoproteins by SCFFBXO27 directs damaged lysosomes for autophagy. *Proc. Natl. Acad. Sci. USA* 114, 8574–8579. doi: 10.1073/pnas.1702615114

Zhang, H. J., Tian, J., Qi, X. K., Xiang, T., He, G. P., Zhang, H., et al. (2018). Epstein-Barr virus activates F-box protein FBXO2 to limit viral infectivity by targeting glycoprotein B for degradation. *PLoS Pathog.* 14:e1007208. doi: 10.1371/journal.ppat.1007208

Zheng, N., Schulman, B. A., Song, L., Miller, J. J., Jeffrey, P. D., Wang, P., et al. (2002). Structure of the Cul1-Rbx1-Skp1-F boxSkp2 SCF ubiquitin ligase complex. *Nature* 416, 703–709. doi: 10.1038/416703a

Zheng, N., Wang, P., Jeffrey, P. D., and Pavletich, N. P. (2000). Structure of a c-Cbl-UbcH7 complex: RING domain function in ubiquitin-protein ligases. *Cell* 102, 533–539. doi: 10.1016/S0092-8674(00)00057-X

**Conflict of Interest Statement:** The authors declare that the research was conducted in the absence of any commercial or financial relationships that could be construed as a potential conflict of interest.

frontiers in Physiology

MINI REVIEW
published: 19 March 2019
doi: 10.3389/fphys.2019.00274

# Emerging Roles of the TRIM E3 Ubiquitin Ligases MID1 and MID2 in Cytokinesis

*Melania Eva Zanchetta and Germana Meroni**

*Department of Life Sciences, University of Trieste, Trieste, Italy*

Ubiquitination is a post-translational modification that consists of ubiquitin attachment to target proteins through sequential steps catalysed by activating (E1), conjugating (E2), and ligase (E3) enzymes. Protein ubiquitination is crucial for the regulation of many cellular processes not only by promoting proteasomal degradation of substrates but also re-localisation of cellular factors and modulation of protein activity. Great importance in orchestrating ubiquitination relies on E3 ligases as these proteins recognise the substrate that needs to be modified at the right time and place. Here we focus on two members of the TRIpartite Motif (TRIM) family of RING E3 ligases, MID1, and MID2. We discuss the recent findings on these developmental disease-related proteins analysing the link between their activity on essential factors and the regulation of cytokinesis highlighting the possible consequence of alteration of this process in pathological conditions.

**Keywords: ubiquitination, MID1, MID2, TRIM E3 ligase, cytokinesis, X-linked Opitz syndrome**

OPEN ACCESS

***Edited by:***
*Julien Licchesi,*
*University of Bath, United Kingdom*

***Reviewed by:***
*William Alexander McEwan,*
*University of Cambridge,*
*United Kingdom*
*Filippo Turrini,*
*Vita-Salute San Raffaele University,*
*Italy*

***Correspondence:**
*Germana Meroni*
*gmeroni@units.it*

***Specialty section:***
*This article was submitted to Integrative Physiology, a section of the journal Frontiers in Physiology*

***Received:*** *14 January 2019*
***Accepted:*** *28 February 2019*
***Published:*** *19 March 2019*

***Citation:***
*Zanchetta ME and Meroni G (2019) Emerging Roles of the TRIM E3 Ubiquitin Ligases MID1 and MID2 in Cytokinesis. Front. Physiol. 10:274. doi: 10.3389/fphys.2019.00274*

## INTRODUCTION

### Cytokinesis and Ubiquitination

Cytokinesis is the final step of cell division that consists in the physical separation into two cells after nuclear and cytoplasmic content portioning. It requires coordinated actions of the cytoskeleton, membrane systems, and cell cycle engine, which are precisely controlled in space and time. Cytokinesis starts after anaphase and consists of different steps: central spindle assembly, division plane specification, contractile ring assembly, cytokinetic furrow ingression, midbody appearance, and abscission (Echard et al., 2004; Eggert et al., 2006). Following abscission, the residual midbody is either released in the extracellular medium, degraded by selective autophagy or persists in the cytoplasm of one daughter cell (Agromayor and Martin-Serrano, 2013). Interestingly, inherited midbodies can affect cell polarity, cell communication, stemness (Bernabe-Rubio et al., 2016; Antanaviciute et al., 2018; Li et al., 2018). Cytokinesis failure leads to defective mitosis and high chromosomal instability. Thus, for proper organisms growth and development a correct cell division is essential (D'Avino et al., 2015).

The activity of cytokinesis factors must be precisely orchestrated and oscillates by regulated post-translational modifications such as ubiquitination. Covalent conjugation of ubiquitin to a substrate is operated through sequential action of activating (E1), conjugating (E2), and ligase (E3) enzymes. Importantly, the E3 ubiquitin ligases recognise the specific substrates to be ubiquitinated (Komander and Rape, 2012). Ubiquitination is long known for driving cell cycle transitions.

For example, metaphase-to-anaphase transition is triggered by the E3 ligase APC/$C^{CDC20}$ that promotes the degradation of cyclin B and securin, allowing mitotic exit (Teixeira and Reed, 2013). Ubiquitination is a signal not only for protein degradation but also for non-proteolytic fate through the building of chains with different ubiquitin linkages and topologies (Kulathu and Komander, 2012). As example, the E3 $CRL3^{KLH21}$ mono-ubiquitinates Aurora B allowing its MKLP2-mediated translocation to promote correct kinetochore–microtubule attachments during metaphase (Krupina et al., 2016). Further, a giant protein possessing E2/E3 activity, BRUCE, interacts with midbody components affecting the distribution of ubiquitin at the midbody site, in that being fundamental for abscission (Pohl and Jentsch, 2009).

Many other E3 ligases have been described to dynamically control cell cycle events through both proteolytic and non-proteolytic signals (Gilberto and Peter, 2017). The TRIpartite Motif (TRIM) family is the major sub-class of RING-E3 ubiquitin ligases counting over 70 members implicated in several physiological and pathological processes (Reymond et al., 2001; Meroni and Diez-Roux, 2005; Short and Cox, 2006; Hatakeyama, 2017). Here, we will focus on the role of two members of this family, TRIM18/Midline1/MID1 and TRIM1/Midline2/MID2 (from here onward MID1 and MID2), in cytokinesis.

## MID1 and MID2 E3 Ubiquitin Ligases

Among the TRIM family, MID1, and MID2 are very close paralogues originating from a common ancestor after the invertebrate/vertebrate separation and predating the bony vertebrates appearance (Sardiello et al., 2008). Consistently, human *MID1* and *MID2* genes have a conserved genomic structure, are both located on the X chromosome, and share a high degree of identity (70%) at nucleotide level (Quaderi et al., 1997; Buchner et al., 1999). This similarity is patent also in their domain structure. MID1 and MID2 present the N-terminal hallmark of the TRIM family, the tripartite motif, composed of the catalytic RING domain followed by tandem B-Box 1 and B-box 2 and a Coiled-coil region. The TRIM family is further subdivided into 9 classes (C-I to C-IX) according to the domains present C-terminal to the tripartite module with the SPRY-containing C-IV subfamily being the most numerous (Reymond et al., 2001; Short and Cox, 2006). MID1 and MID2 C-terminus displays a COS domain, a Fibronectin type III repeat and a PRY-SPRY domain as all C-I sub-family TRIM members (Reymond et al., 2001; Short and Cox, 2006; **Table 1**). While the Fibronectin type III repeat and PRY-SPRY domain role in MID proteins is unclear, the COS domain was shown to mediate MID1 and MID2 association with the microtubular apparatus (Buchner et al., 1999; Cainarca et al., 1999; Short and Cox, 2006). Microtubular binding of MID1 is detectable also during mitosis and on the central spindle and midbody during cytokinesis (Cainarca et al., 1999). Recently, localisation at the midbody was reported also for MID2 (Gholkar et al., 2016). Whether MID proteins co-localise at the midbody in a mutual manner is still not unravelled. The coiled-coil region of MID1, besides mediating self-interaction, is also responsible for hetero-interaction with MID2 (Short et al., 2002; Meroni and Diez-Roux, 2005). The extent and stoichiometry of MID1/MID2 interaction is at present not known but one can envisage functions elicited by either homo- or hetero-complexes resulting in partial functional redundancy between MID proteins. Indeed, redundancy between the chicken orthologues of *MID* genes, *cMid1,* and *cMid2,* has been reported during the determination of avian left/right axis (Granata et al., 2005). Intriguingly, both human genes are implicated in genetic diseases: *MID1* is mutated in patients presenting a complex neurodevelopmental disorder, the X-linked Opitz G/BBB syndrome (OS) (OMIM 300000) (Quaderi et al., 1997); and *MID2* is mutated in an X-linked intellectual disability (OMIM 300928) (Geetha et al., 2014). This further suggests MID1 and MID2 overlapping functions. Along the same line, analyses of these genes during embryonic development in human, mouse and chicken show partial overlapping expression. *MID1* is mainly found in the central nervous system (CNS), the developing branchial arches, the gastrointestinal and the urogenital systems, and the developing heart correlating with the tissues affected in OS (Dal Zotto et al., 1998; Richman et al., 2002; Pinson et al., 2004). *MID2* displays low embryonic expression in the developing CNS, thymus and heart (Buchner et al., 1999). On the contrary, in human adult tissues, *MID1* and *MID2* have a distinct expression pattern: *MID2* is mainly expressed in thyroid, smooth muscle, prostate, breast, and ovary whereas *MID1* is found in the cerebellum, lung, colon, urinary bladder, prostate, placenta, breast, and ovary and retina (source[1,2]).

Regarding their E3 ligase function, *in vitro* activity for both MID1 and MID2 has been described (Han et al., 2011; Napolitano et al., 2011). In more physiological contexts, both unique and common MID proteins partners have been identified, some of which are reported as MID E3 ligases *bona fide* substrates. These data are briefly summarised in **Table 1** and recently thoroughly reviewed in Li et al. (2016); Winter et al. (2016). These findings suggest that the two TRIM paralogues evolved maintaining common roles while developing their own specificity, likely in a context-specific manner. Their expression analyses during embryonic development revealed a preference for mitotically active compartments suggesting a role during cell cycle progression and here below we will discuss recent findings that support a role of MID1 and MID2 during the cytokinetic process.

# MID1 AND MID2 INVOLVEMENT IN CYTOKINESIS

As mentioned above, recent reports suggest an involvement of MID1 and MID2 in cytokinesis. Indeed, in HeLa cells, the depletion of either MID1 or MID2 leads to cell division defects, namely, cytokinetic arrest often followed by cell death and delay or failure to divide with regression into binucleated cells (Gholkar et al., 2016). This role is likely elicited through the interaction with several partners that we discuss here below.

[1] www.proteinatlas.org

[2] www.ncbi.nlm.nih.gov/gene

**TABLE 1 |** Summary of principal MID1 and MID2 features.

| Official symbol | MID1 | MID2 |
|---|---|---|
| Official name | midline 1 | midline 2 |
| Gene ID | 4281 | 11043 |
| Aliases | FXY, MIDIN, TRIM18, RNF59 | FXY2, TRIM1 |
| Location | Xp22.2 | Xq22 |
| CDS length | 2,004 nt | 2,148 nt |
| Protein length | 667 aa | 715 aa |
| Associated Syndromes | X-linked Opitz G/BBB syndrome (OMIM #300000) | Mental retardation, X-linked (OMIM #300928) |
| Protein domains | RING domain; B-box type 1 and 2; coiled-coil; COS domain; fibronectin type 3 domain; PRY/SPRY domain | RING domain; B-box type 1 and 2; coiled-coil; COS domain; fibronectin type 3 domain; PRY/SPRY domain |
| Protein function | E3 ubiquitin ligase | E3 ubiquitin ligase |
| Subcellular location/component (UniProt) | cytosol, microtubule, spindle (www.uniprot.org/uniprot/O15344) | cytosol, microtubule, exosome (www.uniprot.org/uniprot/Q9UJV3) |
| Amino acid modification (UniProt) | Phosphoserine 92, 96, 511 (www.uniprot.org/uniprot/O15344) | Phosporylated on serine and threonine residues (www.uniprot.org/uniprot/Q9UJV3) |
| Interactors (common interactors are indicated in bold and the relative references are listed) | **MID1**, **MID2** (Short et al., 2002); **ALPHA-4**, PPP2CB, PPP2CA, PPP2R1A (Liu et al., 2001; Watkins et al., 2012); PTPA (Du et al., 2014); **ASTRIN** (Gholkar et al., 2016); BRAF35 (Zanchetta et al., 2017); MID1IP1 (Berti et al., 2004); ANXA2, EEF1A1, NPM1, HSP90AA1, RACK1, RPS3, RPS8; (Aranda-Orgilles et al., 2008b); PAX6 (Pfirrmann et al., 2016); STK36 (Schweiger et al., 2014); TRIM16 (Bell et al., 2012); **TUBB, TUBB4B** (Gholkar et al., 2016); UBC (Trockenbacher et al., 2001); **UBE2D1**, **UBE2D2**, **UBE2D3, UBE2D4**, **UBE2E1**, **UBE2E2, UBE2E3**, **UBE2N** (Napolitano et al., 2011) | **MID2**, **MID1** (Short et al., 2002); **ALPHA-4** (Short et al., 2002); **ASTRIN**, ASPM, CEP128 (Gholkar et al., 2016); LNX1 (Lenihan et al., 2017); TRIM27, TRIM42, TRIM54 (Rolland et al., 2014); TRIM29, TRIM32 (Reymond et al., 2001); **TUBB**, **TUBB4B** (Gholkar et al., 2016); **UBE2D1**, **UBE2D2**, **UBE2D3**, **UBE2D4**; **UBE2E1**; **UBE2E2**, **UBE2E3**, **UBE2N**; (Napolitano et al., 2011) |

## Astrin

A recent work uncovered that both MID1 and MID2 bind the microtubule-associated protein Astrin (also known as SPAG5) (Gholkar et al., 2016). Astrin is important in the regulation of mitotic progression since its depletion causes centrosome instability and mitotic spindle malformation in HeLa cells. Astrin associates with the spindle throughout mitosis allowing chromosome alignment and segregation (Mack and Compton, 2001; Gruber et al., 2002). Diverse kinases, such as GSK3, Aurora A and Plk1, phosphorylate Astrin to regulate its mitotic function during spindle assembly (Cheng et al., 2008; Chiu et al., 2014; Chung et al., 2016).

The interaction between Astrin and the two TRIM proteins occurs independently from the cell cycle but has consequences only on cytokinesis. MID1 and MID2 partially co-localise with Astrin at the midbody of dividing cells. Interestingly, MID2 alone promotes Astrin ubiquitination at a unique site (K409) at mitotic exit targeting the protein to proteasomal degradation. Inappropriate accumulation of Astrin at the midbody provokes cytokinetic arrest, increased binucleation and cell death. Consistently, MID2 depletion leads to minor defects in early mitosis and major defects in cytokinesis supporting the importance of its E3 ligase activity in regulating Astrin degradation (Gholkar et al., 2016).

Unexpectedly, also MID1-deprived cells display division defects, including cytokinetic arrest, delayed or aborted abscission, inducing cell binucleation or death (Gholkar et al., 2016). At present it is not known if the observed cytokinetic phenotype is related to the lack of MID1-Astrin association and which is the mechanism involved. Further, whether MID1, MID2, and Astrin form a single protein complex is still undefined. An intriguing possibility is that distinct and dynamic homo- or hetero-MID complexes exist to target not only Astrin but also other cytokinesis-related proteins.

## Alpha4/PP2Ac

The first reported target of MID1 E3 ligase activity was the catalytic subunit of serine/threonine protein phosphatase 2A (PP2Ac) driven to ubiquitin-mediated proteasomal degradation (Trockenbacher et al., 2001). MID1 directly interacts through the B-box 1 domain with Alpha4 (α4) that is one of the atypical regulatory subunits of PP2A (Nanahoshi et al., 1998; Liu et al., 2001; Trockenbacher et al., 2001; Short et al., 2002; LeNoue-Newton et al., 2011). Later on, α4 was reported to be a MID1 substrate as well (Watkins et al., 2012; Du et al., 2013). Active PP2A is a heterotrimeric holoenzyme composed of a catalytic (C subunit), a scaffold (A subunit) and a variable regulatory subunit (B, B′, B″, or B‴ subunits) that dictate substrate selectivity and subcellular localisation of the phosphatase holoenzyme. A small pool of PP2Ac was shown to form a complex containing α4 instead of the B subunit (Baskaran and Velmurugan, 2018). At cytokinesis, PP2Ac, A and B′γ1 subunits are all localised at the midbody in HeLa cells (Wu et al., 2017). In addition, PP2A-B′ holoenzyme counteracts Aurora B kinase activity controlling the length of spindle midzone through KIF4A dephosphorylation (Bastos et al., 2014).

The mechanism of self-regulation of the MID1/α4/PP2Ac complex involves a series of ubiquitination and dephosphorylation events that have been long studied but still remain to be completely unravelled. Initially, α4 was described to protect

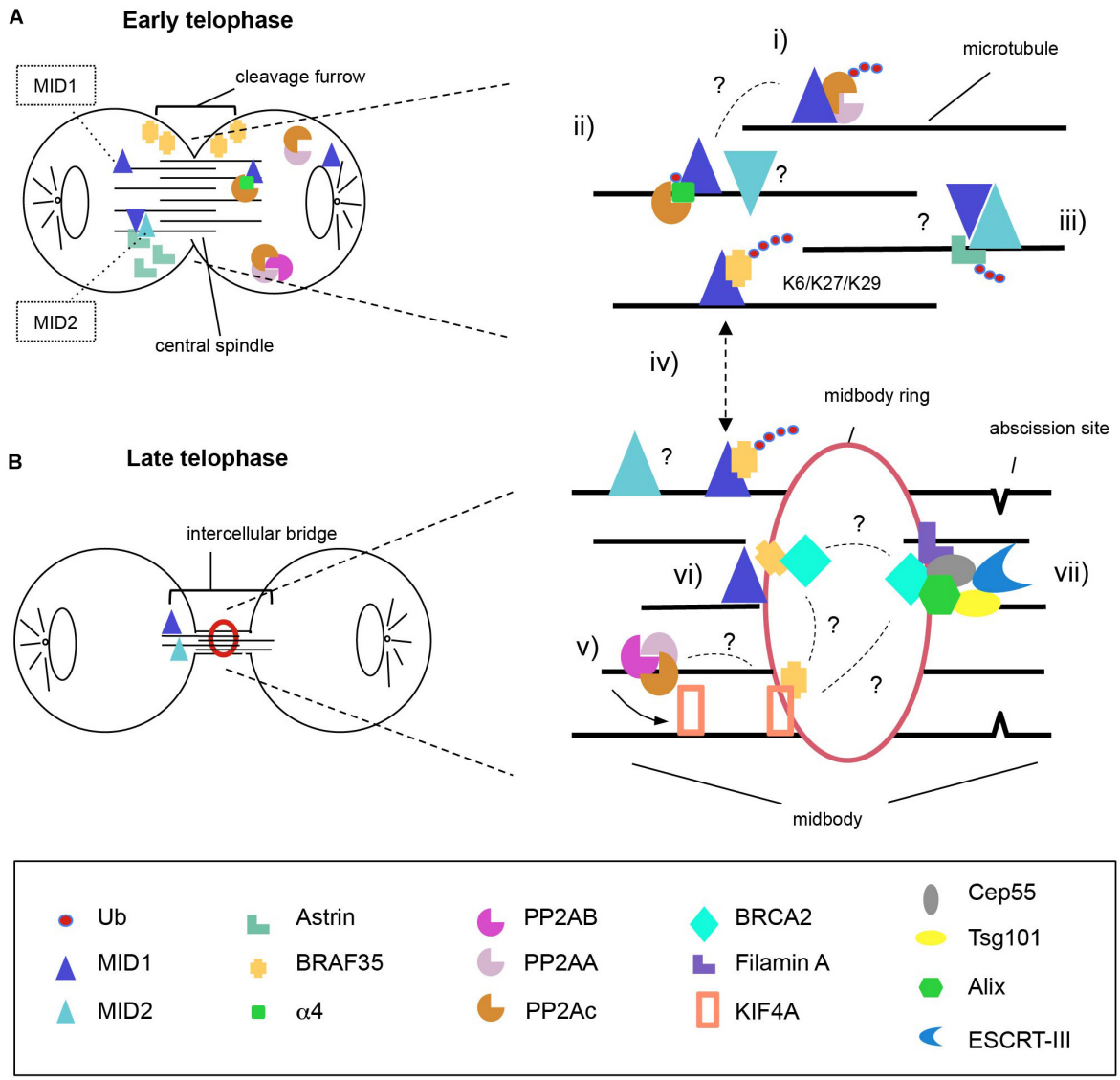


**FIGURE 1 |** Model for MID1 and MID2 complexes distribution during cytokinesis. MID1 and MID2 localise on the microtubules both at early **(A)** and late **(B)** telophase where they possibly hetero-interact. We propose action of MID proteins during both steps. At the central spindle, MID1 poly-ubiquitinates PP2Ac to regulate PP2A levels (i) and mono-ubiquitinates a4 to disrupt the association of a4-PP2Ac (ii). Available PP2Ac can be assembled into active PP2A holoenzymes that dephosphorylate KIF4A to control the length of spindle midzone (v). At early telophase, MID2 ubiquitinates Astrin inducing its proteasomal degradation and removal from the intercellular bridge in order to allow completion of cytokinesis (iii). BRAF35 abundance and localisation at the intercellular bridge is regulated through MID1-dependent ubiquitination using non-canonical ubiquitin linkages (K6, K27, and K29) (iv); there, BRAF35 associates with KIF4A and/or BRCA2 (vi); (vii) BRCA2 is recruited to the midbody through Filamin A and forms a complex with Cep55, Alix and Tsg101, allowing the recruitment of ESCRT-III to complete abscission. It is still unknown to what extent MID proteins activity on these substrates is interconnected and this is highlighted in the model with question marks (?). One intriguingly possibility is that KIF4A might represent the central player linking all the complexes regulate by MID1 and MID2.

PP2Ac from degradation. Although *in vitro* assays suggested that MID1 catalyses mono- and di-ubiquitination of PP2Ac it is likely that other E3 ligases synergistically or alternatively are required to target its proteasomal degradation (Watkins et al., 2012; Du et al., 2014). Interestingly, MID1 not only targets a sub-pool of α4 for poly-ubiquitination-mediated degradation but also mono-ubiquitinates α4, triggering calpain mediated cleavage and degradation of its C-terminus containing the MID1 binding region (Watkins et al., 2012; Du et al., 2013). Whatever the mechanism, α4 cleavage disrupts the MID1/α4/PP2Ac complex, influencing PP2Ac stability (Winter et al., 2016). Altered PP2Ac activity affects mTORC1 complex formation and signalling (Liu et al., 2011). This pathway can play a significant role in the pathogenesis of OS and it would be interesting to investigate a possible MID1-mediated mTORC1 involvement in cytokinesis.

MID proteins contain two conserved phosphorylation consensus sites (Ser92 and Ser96) for GSK3 and MAPK, respectively (Short et al., 2002). Interestingly, MID1 interaction

with α4 results in PP2Ac recruitment on microtubules and MID1 dephosphorylation at Ser96 (Aranda-Orgilles et al., 2008a). It is tempting to speculate that a similar regulatory mechanism involves MID2 as it binds α4 as well (Short et al., 2002). A fine balance of MID1 phosphorylation and dephosphorylation via MAPK and PP2A is important for regulating its affinity and its bi-directional movement along the microtubule network through kinesins and dyneins (Liu et al., 2001; Trockenbacher et al., 2001; Aranda-Orgilles et al., 2008a). Whether MID1 phosphorylation status affects E3 ligase activity or influences the interaction with α4 have not been addressed yet.

These findings leave some questions open and some issues still controversial. Indeed, α4 was shown to serve as a binding partner of PP2Ac rendering the latter catalytically inactive to avoid improper protein dephosphorylation. Then, when needed, α4 contributes to stabilise newly synthetised PP2Ac preventing its ubiquitin-mediated degradation thus permitting its assembly into functional PP2A holoenzymes (Kong et al., 2009). It is possible that binding of α4 to MID1 is needed to preserve a pool of newly available PP2Ac that can be transported along the microtubules to the spindle midzone. At this point, PP2Ac might become available for incorporation into active PP2A to dephosphorylate a pool of microtubule-associated phosphoproteins, such as KIF4A, to precisely control cytokinesis.

## BRAF35

A recently identified MID1 substrate is the BRCA2-associated factor BRAF35 (also known as HMG20B) (Zanchetta et al., 2017) that was first isolated as part of a large nuclear multi-protein complex containing BRCA2 (Marmorstein et al., 2001).

MID1 ubiquitinates BRAF35 and is necessary for its turnover mainly outside the nucleus. Strikingly, although BRAF35 protein levels are regulated by the proteasome, atypical linkages are preferred in MID1-mediated ubiquitination, involving K6, K27, and K29 poly-ubiquitin chains. Among them, only K6 poly-ubiquitination promotes BRAF35 proteasomal degradation while K27 and K29 chains have no degradative effects (Zanchetta et al., 2017). The present knowledge does not offer insights to infer the effect of these modifications on BRAF35 (Kulathu and Komander, 2012). Of note, MID1 and BRAF35 co-localise in the cytoplasmic compartment and BRAF35 accumulates in larger cytoplasmic bodies when MID1 is depleted from HeLa cells (Zanchetta et al., 2017).

Recently BRAF35 was found in a region of the midbody compatible with MID1 localisation (Cainarca et al., 1999; Lee and Venkitaraman, 2014; Gholkar et al., 2016). Consistently, BRAF35 also associates with the previously mentioned PP2A target KIF4A, a motor protein that is essential for central spindle midzone and midbody organisation (Lee and Kim, 2003). Direct interaction between the cargo domain of KIF4A and BRCA2 was also proved, suggesting the existence of a multi-protein complex in which also BRAF35 takes part (Wu et al., 2008). BRCA2 is recruited on the midbody by the actin-binding protein Filamin A and is necessary for correct localisation of other midbody proteins, such as MKLP1, MKLP2, and PRC1 (Mondal et al., 2012). On the midbody BRCA2 forms a complex with CEP55, Alix, and Tsg101 and is required for the recruitment of the ESCRT machinery, necessary for abscission (Mondal et al., 2012). Depletion of BRAF35 from HeLa cells results in a delayed transition from anaphase to the completion of cell division (Lee et al., 2011). About half of BRAF35-depleted cells start cleavage furrowing but fail to divide, becoming binucleated (Lee et al., 2011). Interestingly, the same phenotype had previously been observed in BRCA2-deficient cells (Daniels et al., 2004). It is interesting that MID1 depletion phenocopies the cytokinesis failure-derived defects that were observed in the absence of BRAF35 or BRCA2 (Gholkar et al., 2016).

The C-terminal portion of BRAF35 spanning aa 173–276 is the minimal fragment required for BRCA2 binding and is also sufficient for its midbody localisation (Lee and Venkitaraman, 2014). However, contrary to the entire C-terminal fragment (aa 173–317), expression of the 173–276 aa fragment fails to restore cytokinesis in BRAF35-depleted cells suggesting the need of an additional factor (Lee and Venkitaraman, 2014). MID1 could represent such interactor, as the binding to BRAF35 occurs in an overlapping region (aa 230–317) to that necessary to form the BRAF35/BRCA2 complex, thus contributing to proper cytokinesis (Zanchetta et al., 2017).

The findings discussed here support the role of MID proteins in cell division through activities on multiple targets likely not only promoting their proteasomal degradation. However, it is still not clear to what extent their E3 ligase activity on the substrates cited in this review and graphically summarised in **Figure 1** are interconnected. In this model, KIF4A might play a central role in the MID1- and MID2-regulated network. It is a matter of fact that both MID1 and MID2 are needed for successful cytokinesis with consequences in physiological and pathological conditions.

## CONCLUSION

Although tightly regulated, cytokinesis lacks an effective checkpoint to ensure its fidelity. Cytokinesis can fail at different steps, because cleavage furrow ingression is inhibited or incomplete, or abscission is defective. The originated cells show increased chromosomal instability resulting in the generation of multipolar spindles and chromosome segregation defects (Sagona and Stenmark, 2010). Errors in cytokinesis may thus have dramatic consequences ranging from embryonic defects to cancer. Aberrant expression of cytokinesis regulators is indeed largely associated with many cancer types (Lens and Medema, 2019).

Recent findings showed elevated MID1 expression in prostate cancer and alteration of the MID1/a4/PP2A axis in lung adenocarcinoma and MID1 expression levels positively correlate with tumour Gleason scores (Kohler et al., 2014; Zhang et al., 2018). Similarly, high level of MID2 expression was significantly correlated with breast cancer progression (Wang et al., 2016). On the contrary, down-regulation of MID1 mediated by miR-135b has been shown to promote tumour progression of mammary carcinomas (Arigoni et al., 2013). Of note, high levels of Astrin have been described in cervical, pancreatic, hepatocellular carcinoma, and non-small-cell lung cancers (Valk et al., 2010;

Yuan et al., 2014; Ansari et al., 2015; Liu et al., 2018; Yang et al., 2018). In the case of BRAF35, the A247P mutation reported in a case of lung carcinoma was shown to interfere with its midbody localisation and BRCA2 binding (Lee and Venkitaraman, 2014). This mutation induces cytokinesis failure through a dominant negative mechanism possibly affecting MID1 activity. Thus, it appears that dysregulation of MID1 plays a role in tumourigenesis, likely affecting factors that control somatic cell proliferation.

Clinically, MID1 and MID2 are implicated also in genetic developmental disorders (Quaderi et al., 1997; Geetha et al., 2014). Their involvement in cytokinesis does not come as a surprise as embryonic development is the organism phase with the highest mitotic index. During development, aberrant cytokinesis can have a strong impact not only on cell proliferation but also on morphogenetic processes. In fact, inherited midbodies can affect cell polarity and cell communication and, in epithelia, midbody positioning influences planar tissue architecture (Herszterg et al., 2014; Bernabe-Rubio et al., 2016; Antanaviciute et al., 2018).

The identification of the involvement of MID1 and MID2 in cytokinesis is intriguingly though we are still far from clarifying the precise dynamics of the occurring events. Further investigations will be necessary to understand the dynamics of the complexes containing MID proteins and Astrin, BRAF35 and PP2A and their interplay, if any. The future dissection of these mechanisms, together with parallel *in vivo* studies, will be necessary to get a comprehensive picture and for future clinical application.

## AUTHOR CONTRIBUTIONS

MZ and GM conceived the study, drafted the manuscript, and reviewed and edited the manuscript. GM acquired the funding.

## FUNDING

This work was supported by PRIN2015-MIUR (Ministry of Education, University and Research), grant number 20152CB22L.

## REFERENCES

Agromayor, M., and Martin-Serrano, J. (2013). Knowing when to cut and run: mechanisms that control cytokinetic abscission. *Trends Cell Biol.* 23, 433–441. doi: 10.1016/j.tcb.2013.04.006

Ansari, D., Andersson, R., Bauden, M. P., Andersson, B., Connolly, J. B., Welinder, C., et al. (2015). Protein deep sequencing applied to biobank samples from patients with pancreatic cancer. *J. Cancer Res. Clin. Oncol.* 141, 369–380. doi: 10.1007/s00432-014-1817-x

Antanaviciute, I., Gibieza, P., Prekeris, R., and Skeberdis, V. A. (2018). Midbody: from the regulator of cytokinesis to postmitotic signaling organelle. *Medicina* 54:E53. doi: 10.3390/medicina54040053

Aranda-Orgilles, B., Aigner, J., Kunath, M., Lurz, R., Schneider, R., and Schweiger, S. (2008a). Active transport of the ubiquitin ligase MID1 along the microtubules is regulated by protein phosphatase 2A. *PLoS One* 3:e3507. doi: 10.1371/journal.pone.0003507

Aranda-Orgilles, B., Trockenbacher, A., Winter, J., Aigner, J., Kohler, A., Jastrzebska, E., et al. (2008b). The Opitz syndrome gene product MID1 assembles a microtubule-associated ribonucleoprotein complex. *Hum. Genet.* 123, 163–176. doi: 10.1007/s00439-007-0456-6

Arigoni, M., Barutello, G., Riccardo, F., Ercole, E., Cantarella, D., Orso, F., et al. (2013). miR-135b coordinates progression of ErbB2-driven mammary carcinomas through suppression of MID1 and MTCH2. *Am. J. Pathol.* 182, 2058–2070. doi: 10.1016/j.ajpath.2013.02.046

Baskaran, R., and Velmurugan, B. K. (2018). Protein phosphatase 2A as therapeutic targets in various disease models. *Life Sci.* 210, 40–46. doi: 10.1016/j.lfs.2018.08.063

Bastos, R. N., Cundell, M. J., and Barr, F. A. (2014). KIF4A and PP2A-B56 form a spatially restricted feedback loop opposing Aurora B at the anaphase central spindle. *J. Cell Biol.* 207, 683–693. doi: 10.1083/jcb.201409129

Bell, J. L., Malyukova, A., Holien, J. K., Koach, J., Parker, M. W., Kavallaris, M., et al. (2012). TRIM16 acts as an E3 ubiquitin ligase and can heterodimerize with other TRIM family members. *PLoS One* 7:e37470. doi: 10.1371/journal.pone.0037470

Bernabe-Rubio, M., Andres, G., Casares-Arias, J., Fernandez-Barrera, J., Rangel, L., Reglero-Real, N., et al. (2016). Novel role for the midbody in primary ciliogenesis by polarized epithelial cells. *J. Cell Biol.* 214, 259–273. doi: 10.1083/jcb.201601020

Berti, C., Fontanella, B., Ferrentino, R., and Meroni, G. (2004). Mig12, a novel Opitz syndrome gene product partner, is expressed in the embryonic ventral midline and co-operates with Mid1 to bundle and stabilize microtubules. *BMC Cell Biol.* 5:9. doi: 10.1186/1471-2121-5-9

Buchner, G., Montini, E., Andolfi, G., Quaderi, N., Cainarca, S., Messali, S., et al. (1999). MID2, a homologue of the Opitz syndrome gene MID1: similarities in subcellular localization and differences in expression during development. *Hum. Mol. Genet.* 8, 1397–1407. doi: 10.1093/hmg/8.8.1397

Cainarca, S., Messali, S., Ballabio, A., and Meroni, G. (1999). Functional characterization of the Opitz syndrome gene product (midin): evidence for homodimerization and association with microtubules throughout the cell cycle. *Hum. Mol. Genet.* 8, 1387–1396. doi: 10.1093/hmg/8.8.1387

Cheng, T. S., Hsiao, Y. L., Lin, C. C., Yu, C. T., Hsu, C. M., Chang, M. S., et al. (2008). Glycogen synthase kinase 3beta interacts with and phosphorylates the spindle-associated protein astrin. *J. Biol. Chem.* 283, 2454–2464. doi: 10.1074/jbc.M706794200

Chiu, S. C., Chen, J. M., Wei, T. Y., Cheng, T. S., Wang, Y. H., Ku, C. F., et al. (2014). The mitosis-regulating and protein-protein interaction activities of astrin are controlled by aurora-A-induced phosphorylation. *Am. J. Physiol. Cell Physiol.* 307, C466–C478. doi: 10.1152/ajpcell.00164.2014

Chung, H. J., Park, J. E., Lee, N. S., Kim, H., and Jang, C. Y. (2016). Phosphorylation of astrin regulates its kinetochore function. *J. Biol. Chem.* 291, 17579–17592. doi: 10.1074/jbc.M115.712745

Dal Zotto, L., Quaderi, N. A., Elliott, R., Lingerfelter, P. A., Carrel, L., Valsecchi, V., et al. (1998). The mouse Mid1 gene: implications for the pathogenesis of Opitz syndrome and the evolution of the mammalian pseudoautosomal region. *Hum. Mol. Genet.* 7, 489–499. doi: 10.1093/hmg/7.3.489

Daniels, M. J., Wang, Y., Lee, M., and Venkitaraman, A. R. (2004). Abnormal cytokinesis in cells deficient in the breast cancer susceptibility protein BRCA2. *Science* 306, 876–879. doi: 10.1126/science.1102574

D'Avino, P. P., Giansanti, M. G., and Petronczki, M. (2015). Cytokinesis in animal cells. *Cold Spring Harb. Perspect. Biol.* 7:a015834. doi: 10.1101/cshperspect.a015834

Du, H., Huang, Y., Zaghlula, M., Walters, E., Cox, T. C., and Massiah, M. A. (2013). The MID1 E3 ligase catalyzes the polyubiquitination of Alpha4 (alpha4), a regulatory subunit of protein phosphatase 2A (PP2A): novel insights into MID1-mediated regulation of PP2A. *J. Biol. Chem.* 288, 21341–21350. doi: 10.1074/jbc.M113.481093

Du, H., Wu, K., Didoronkute, A., Levy, M. V., Todi, N., Shchelokova, A., et al. (2014). MID1 catalyzes the ubiquitination of protein phosphatase 2A and mutations within its Bbox1 domain disrupt polyubiquitination of alpha4 but not of PP2Ac. *PLoS One* 9:e107428. doi: 10.1371/journal.pone.0107428

Echard, A., Hickson, G. R., Foley, E., and O'Farrell, P. H. (2004). Terminal cytokinesis events uncovered after an RNAi screen. *Curr. Biol.* 14, 1685–1693. doi: 10.1016/j.cub.2004.08.063

Eggert, U. S., Mitchison, T. J., and Field, C. M. (2006). Animal cytokinesis: from parts list to mechanisms. *Annu. Rev. Biochem.* 75, 543–566. doi: 10.1146/annurev.biochem.74.082803.133425

Geetha, T. S., Michealraj, K. A., Kabra, M., Kaur, G., Juyal, R. C., and Thelma, B. K. (2014). Targeted deep resequencing identifies MID2 mutation for X-linked intellectual disability with varied disease severity in a large kindred from India. *Hum. Mutat.* 35, 41–44. doi: 10.1002/humu.22453

Gholkar, A. A., Senese, S., Lo, Y. C., Vides, E., Contreras, E., Hodara, E., et al. (2016). The X-linked-intellectual-disability-associated ubiquitin ligase Mid2 interacts with astrin and regulates astrin levels to promote cell division. *Cell Rep.* 14, 180–188. doi: 10.1016/j.celrep.2015.12.035

Gilberto, S., and Peter, M. (2017). Dynamic ubiquitin signaling in cell cycle regulation. *J. Cell Biol.* 216, 2259–2271. doi: 10.1083/jcb.201703170

Granata, A., Savery, D., Hazan, J., Cheung, B. M., Lumsden, A., and Quaderi, N. A. (2005). Evidence of functional redundancy between MID proteins: implications for the presentation of Opitz syndrome. *Dev. Biol.* 277, 417–424. doi: 10.1016/j.ydbio.2004.09.036

Gruber, J., Harborth, J., Schnabel, J., Weber, K., and Hatzfeld, M. (2002). The mitotic-spindle-associated protein astrin is essential for progression through mitosis. *J. Cell Sci.* 115, 4053–4059. doi: 10.1242/jcs.00088

Han, X., Du, H., and Massiah, M. A. (2011). Detection and characterization of the in vitro E3 ligase activity of the human MID1 protein. *J. Mol. Biol.* 407, 505–520. doi: 10.1016/j.jmb.2011.01.048

Hatakeyama, S. (2017). TRIM family proteins: roles in autophagy, immunity, and carcinogenesis. *Trends Biochem. Sci.* 42, 297–311. doi: 10.1016/j.tibs.2017.01.002

Herszterg, S., Pinheiro, D., and Bellaiche, Y. (2014). A multicellular view of cytokinesis in epithelial tissue. *Trends Cell Biol.* 24, 285–293. doi: 10.1016/j.tcb.2013.11.009

Kohler, A., Demir, U., Kickstein, E., Krauss, S., Aigner, J., Aranda-Orgilles, B., et al. (2014). A hormone-dependent feedback-loop controls androgen receptor levels by limiting MID1, a novel translation enhancer and promoter of oncogenic signaling. *Mol. Cancer* 13:146. doi: 10.1186/1476-4598-13-146

Komander, D., and Rape, M. (2012). The ubiquitin code. *Annu. Rev. Biochem.* 81, 203–229. doi: 10.1146/annurev-biochem-060310-170328

Kong, M., Ditsworth, D., Lindsten, T., and Thompson, C. B. (2009). Alpha4 is an essential regulator of PP2A phosphatase activity. *Mol. Cell* 36, 51–60. doi: 10.1016/j.molcel.2009.09.025

Krupina, K., Kleiss, C., Metzger, T., Fournane, S., Schmucker, S., Hofmann, K., et al. (2016). Ubiquitin receptor protein UBASH3B drives aurora B recruitment to mitotic microtubules. *Dev. Cell* 36, 63–78. doi: 10.1016/j.devcel.2015.12.017

Kulathu, Y., and Komander, D. (2012). Atypical ubiquitylation - the unexplored world of polyubiquitin beyond Lys48 and Lys63 linkages. *Nat. Rev. Mol. Cell Biol.* 13, 508–523. doi: 10.1038/nrm3394

Lee, M., Daniels, M. J., Garnett, M. J., and Venkitaraman, A. R. (2011). A mitotic function for the high-mobility group protein HMG20b regulated by its interaction with the BRC repeats of the BRCA2 tumor suppressor. *Oncogene* 30, 3360–3369. doi: 10.1038/onc.2011.55

Lee, M., and Venkitaraman, A. R. (2014). A cancer-associated mutation inactivates a region of the high-mobility group protein HMG20b essential for cytokinesis. *Cell Cycle* 13, 2554–2563. doi: 10.4161/15384101.2014.942204

Lee, Y. M., and Kim, W. (2003). Association of human kinesin superfamily protein member 4 with BRCA2-associated factor 35. *Biochem. J.* 374, 497–503. doi: 10.1042/bj20030452

Lenihan, J. A., Saha, O., and Young, P. W. (2017). Proteomic analysis reveals novel ligands and substrates for LNX1 E3 ubiquitin ligase. *PLoS One* 12:e0187352. doi: 10.1371/journal.pone.0187352

LeNoue-Newton, M., Watkins, G. R., Zou, P., Germane, K. L., McCorvey, L. R., Wadzinski, B. E., et al. (2011). The E3 ubiquitin ligase- and protein phosphatase 2A (PP2A)-binding domains of the Alpha4 protein are both required for Alpha4 to inhibit PP2A degradation. *J. Biol. Chem.* 286, 17665–17671. doi: 10.1074/jbc.M111.222414

Lens, S. M. A., and Medema, R. H. (2019). Cytokinesis defects and cancer. *Nat. Rev. Cancer* 19, 32–45. doi: 10.1038/s41568-018-0084-6

Li, B., Zhou, T., and Zou, Y. (2016). Mid1/Mid2 expression in craniofacial development and a literature review of X-linked opitz syndrome. *Mol. Genet. Genomic Med.* 4, 95–105. doi: 10.1002/mgg3.183

Li, Y., Junge, J. A., Arnesano, C., Gross, G. G., Miner, J. H., Moats, R., et al. (2018). Discs large 1 controls daughter-cell polarity after cytokinesis in vertebrate morphogenesis. *Proc. Natl. Acad. Sci. U.S.A.* 115, E10859–E10868. doi: 10.1073/pnas.1713959115

Liu, E., Knutzen, C. A., Krauss, S., Schweiger, S., and Chiang, G. G. (2011). Control of mTORC1 signaling by the Opitz syndrome protein MID1. *Proc. Natl. Acad. Sci. U.S.A.* 108, 8680–8685. doi: 10.1073/pnas.1100131108

Liu, H., Hu, J., Wei, R., Zhou, L., Pan, H., Zhu, H., et al. (2018). SPAG5 promotes hepatocellular carcinoma progression by downregulating SCARA5 through modifying beta-catenin degradation. *J. Exp. Clin. Cancer Res.* 37:229. doi: 10.1186/s13046-018-0891-3

Liu, J., Prickett, T. D., Elliott, E., Meroni, G., and Brautigan, D. L. (2001). Phosphorylation and microtubule association of the Opitz syndrome protein mid-1 is regulated by protein phosphatase 2A via binding to the regulatory subunit alpha 4. *Proc. Natl. Acad. Sci. U.S.A.* 98, 6650–6655. doi: 10.1073/pnas.111154698

Mack, G. J., and Compton, D. A. (2001). Analysis of mitotic microtubule-associated proteins using mass spectrometry identifies astrin, a spindle-associated protein. *Proc. Natl. Acad. Sci. U.S.A.* 98, 14434–14439. doi: 10.1073/pnas.261371298

Marmorstein, L. Y., Kinev, A. V., Chan, G. K., Bochar, D. A., Beniya, H., Epstein, J. A., et al. (2001). A human BRCA2 complex containing a structural DNA binding component influences cell cycle progression. *Cell* 104, 247–257. doi: 10.1016/S0092-8674(01)00209-4

Meroni, G., and Diez-Roux, G. (2005). TRIM/RBCC, a novel class of 'single protein RING finger' E3 ubiquitin ligases. *Bioessays* 27, 1147–1157. doi: 10.1002/bies.20304

Mondal, G., Rowley, M., Guidugli, L., Wu, J., Pankratz, V. S., and Couch, F. J. (2012). BRCA2 localization to the midbody by filamin A regulates cep55 signaling and completion of cytokinesis. *Dev. Cell* 23, 137–152. doi: 10.1016/j.devcel.2012.05.008

Nanahoshi, M., Nishiuma, T., Tsujishita, Y., Hara, K., Inui, S., Sakaguchi, N., et al. (1998). Regulation of protein phosphatase 2A catalytic activity by alpha4 protein and its yeast homolog Tap42. *Biochem. Biophys. Res. Commun.* 251, 520–526. doi: 10.1006/bbrc.1998.9493

Napolitano, L. M., Jaffray, E. G., Hay, R. T., and Meroni, G. (2011). Functional interactions between ubiquitin E2 enzymes and TRIM proteins. *Biochem. J.* 434, 309–319. doi: 10.1042/BJ20101487

Pfirrmann, T., Jandt, E., Ranft, S., Lokapally, A., Neuhaus, H., Perron, M., et al. (2016). Hedgehog-dependent E3-ligase Midline1 regulates ubiquitin-mediated proteasomal degradation of Pax6 during visual system development. *Proc. Natl. Acad. Sci. U.S.A.* 113, 10103–10108. doi: 10.1073/pnas.1600770113

Pinson, L., Auge, J., Audollent, S., Mattei, G., Etchevers, H., Gigarel, N., et al. (2004). Embryonic expression of the human MID1 gene and its mutations in Opitz syndrome. *J. Med. Genet.* 41, 381–386. doi: 10.1136/jmg.2003.014829

Pohl, C., and Jentsch, S. (2009). Midbody ring disposal by autophagy is a post-abscission event of cytokinesis. *Nat. Cell Biol.* 11, 65–70. doi: 10.1038/ncb1813

Quaderi, N. A., Schweiger, S., Gaudenz, K., Franco, B., Rugarli, E. I., Berger, W., et al. (1997). Opitz G/BBB syndrome, a defect of midline development, is due to mutations in a new RING finger gene on Xp22. *Nat. Genet.* 17, 285–291. doi: 10.1038/ng1197-285

Reymond, A., Meroni, G., Fantozzi, A., Merla, G., Cairo, S., Luzi, L., et al. (2001). The tripartite motif family identifies cell compartments. *EMBO J.* 20, 2140–2151. doi: 10.1093/emboj/20.9.2140

Richman, J. M., Fu, K. K., Cox, L. L., Sibbons, J. P., and Cox, T. C. (2002). Isolation and characterisation of the chick orthologue of the Opitz syndrome gene, Mid1, supports a conserved role in vertebrate development. *Int. J. Dev. Biol.* 46, 441–448.

Rolland, T., Tasan, M., Charloteaux, B., Pevzner, S. J., Zhong, Q., Sahni, N., et al. (2014). A proteome-scale map of the human interactome network. *Cell* 159, 1212–1226. doi: 10.1016/j.cell.2014.10.050

Sagona, A. P., and Stenmark, H. (2010). Cytokinesis and cancer. *FEBS Lett.* 584, 2652–2661. doi: 10.1016/j.febslet.2010.03.044

Sardiello, M., Cairo, S., Fontanella, B., Ballabio, A., and Meroni, G. (2008). Genomic analysis of the TRIM family reveals two groups of genes with distinct evolutionary properties. *BMC Evol. Biol.* 8:225. doi: 10.1186/1471-2148-8-225

Schweiger, S., Dorn, S., Fuchs, M., Kohler, A., Matthes, F., Muller, E. C., et al. (2014). The E3 ubiquitin ligase MID1 catalyzes ubiquitination and cleavage of Fu. *J. Biol. Chem.* 289, 31805–31817. doi: 10.1074/jbc.M113.541219

Short, K. M., and Cox, T. C. (2006). Sub-classification of the RBCC/TRIM superfamily reveals a novel motif necessary for microtubule binding. *J. Biol. Chem.* 281, 8970–8980. doi: 10.1074/jbc.M512755200

Short, K. M., Hopwood, B., Yi, Z., and Cox, T. C. (2002). MID1 and MID2 homo- and heterodimerise to tether the rapamycin- sensitive PP2A regulatory subunit, Alpha 4, to microtubules: implications for the clinical variability of X-linked Opitz GBBB syndrome and other developmental disorders. *BMC Cell Biol.* 3:1. doi: 10.1186/1471-2121-3-1

Teixeira, L. K., and Reed, S. I. (2013). Ubiquitin ligases and cell cycle control. *Annu. Rev. Biochem.* 82, 387–414. doi: 10.1146/annurev-biochem-060410-105307

Trockenbacher, A., Suckow, V., Foerster, J., Winter, J., Krauss, S., Ropers, H. H., et al. (2001). MID1, mutated in Opitz syndrome, encodes an ubiquitin ligase that targets phosphatase 2A for degradation. *Nat. Genet.* 29, 287–294. doi: 10.1038/ng762

Valk, K., Vooder, T., Kolde, R., Reintam, M. A., Petzold, C., Vilo, J., et al. (2010). Gene expression profiles of non-small cell lung cancer: survival prediction and new biomarkers. *Oncology* 79, 283–292. doi: 10.1159/000322116

Wang, L., Wu, J., Yuan, J., Zhu, X., Wu, H., and Li, M. (2016). Midline2 is overexpressed and a prognostic indicator in human breast cancer and promotes breast cancer cell proliferation in vitro and in vivo. *Front. Med.* 10, 41–51. doi: 10.1007/s11684-016-0429-z

Watkins, G. R., Wang, N., Mazalouskas, M. D., Gomez, R. J., Guthrie, C. R., Kraemer, B. C., et al. (2012). Monoubiquitination promotes calpain cleavage of the protein phosphatase 2A (PP2A) regulatory subunit alpha4, altering PP2A stability and microtubule-associated protein phosphorylation. *J. Biol. Chem.* 287, 24207–24215. doi: 10.1074/jbc.M112.368613

Winter, J., Basilicata, M. F., Stemmler, M. P., and Krauss, S. (2016). The MID1 protein is a central player during development and in disease. *Front. Biosci.* 21, 664–682. doi: 10.2741/4413

Wu, C. G., Chen, H., Guo, F., Yadav, V. K., McIlwain, S. J., Rowse, M., et al. (2017). PP2A-B' holoenzyme substrate recognition, regulation and role in cytokinesis. *Cell Discov.* 3:17027. doi: 10.1038/celldisc.2017.27

Wu, G., Zhou, L., Khidr, L., Guo, X. E., Kim, W., Lee, Y. M., et al. (2008). A novel role of the chromokinesin Kif4A in DNA damage response. *Cell Cycle* 7, 2013–2020. doi: 10.4161/cc.7.13.6130

Yang, Y. F., Zhang, M. F., Tian, Q. H., Fu, J., Yang, X., Zhang, C. Z., et al. (2018). SPAG5 interacts with CEP55 and exerts oncogenic activities via PI3K/AKT pathway in hepatocellular carcinoma. *Mol. Cancer* 17:117. doi: 10.1186/s12943-018-0872-3

Yuan, L. J., Li, J. D., Zhang, L., Wang, J. H., Wan, T., Zhou, Y., et al. (2014). SPAG5 upregulation predicts poor prognosis in cervical cancer patients and alters sensitivity to taxol treatment via the mTOR signaling pathway. *Cell Death Dis.* 5:e1247. doi: 10.1038/cddis.2014.222

Zanchetta, M. E., Napolitano, L. M. R., Maddalo, D., and Meroni, G. (2017). The E3 ubiquitin ligase MID1/TRIM18 promotes atypical ubiquitination of the BRCA2-associated factor 35, BRAF35. *Biochim. Biophys. Acta Mol. Cell Res.* 1864, 1844–1854. doi: 10.1016/j.bbamcr.2017.07.014

Zhang, L., Li, J., Lv, X., Guo, T., Li, W., and Zhang, J. (2018). MID1-PP2A complex functions as new insights in human lung adenocarcinoma. *J. Cancer Res. Clin. Oncol.* 144, 855–864. doi: 10.1007/s00432-018-2601-0

**Conflict of Interest Statement:** The authors declare that the research was conducted in the absence of any commercial or financial relationships that could be construed as a potential conflict of interest.

frontiers in Physiology

MINI REVIEW
published: 03 April 2019
doi: 10.3389/fphys.2019.00370

# HECT E3 Ligases: A Tale With Multiple Facets

*Janine Weber[1], Simona Polo[1,2]* and Elena Maspero[1]**

*[1] Fondazione Istituto FIRC di Oncologia Molecolare, Milan, Italy, [2] Dipartimento di Oncologia ed Emato-Oncologia, Università degli Studi di Milano, Milan, Italy*

Ubiquitination plays a pivotal role in several cellular processes and is critical for protein degradation and signaling. E3 ubiquitin ligases are the matchmakers in the ubiquitination cascade, responsible for substrate recognition. In order to achieve selectivity and specificity on their substrates, HECT E3 enzymes are tightly regulated and exert their function in a spatially and temporally controlled fashion in the cells. These characteristics made HECT E3s intriguing targets in drug discovery in the context of cancer biology.

**Keywords: ubiquitin, E3 ligase, cancer, inhibitor, HECT regulations**

OPEN ACCESS

***Edited by:***
*Julien Licchesi,*
*University of Bath, United Kingdom*

***Reviewed by:***
*Pierre G. Lutz,*
*Centre National de la Recherche Scientifique (CNRS), France*
*Olivier Staub,*
*Université de Lausanne, Switzerland*

****Correspondence:***
*Simona Polo*
*simona.polo@ifom.eu*
*Elena Maspero*
*elena.maspero@ifom.eu*

***Specialty section:***
*This article was submitted to Integrative Physiology, a section of the journal Frontiers in Physiology*

***Received:*** *18 December 2018*
***Accepted:*** *18 March 2019*
***Published:*** *03 April 2019*

***Citation:***
*Weber J, Polo S and Maspero E (2019) HECT E3 Ligases: A Tale With Multiple Facets. Front. Physiol. 10:370. doi: 10.3389/fphys.2019.00370*

## HECT E3 LIGASES

Post-translational modification of proteins by the addition of a ubiquitin (Ub) moiety can induce alteration in protein stability, function, activity, localization and interaction (Komander and Rape, 2012). This tightly regulated process (reviewed in Oh et al., 2018) requires the sequential action of a cascade of three enzymes: the Ub-activating enzyme (E1), Ub-conjugating enzymes (E2s), and Ub ligases (E3s). E3 ligases are the matchmakers of the enzymatic cascade, as they are capable of conferring a high degree of specificity and selectivity toward target substrates in cells. The human proteome codifies for more than 600 E3s (Li et al., 2008; Berndsen and Wolberger, 2014) that can be divided into three classes: the largest class is the RING (Really Interesting New Gene/U-box)-type E3s with about 600 members (reviewed in Metzger et al., 2014), followed by the HECT (Homologous to E6AP C-Terminus)-type E3s with about 28 members (reviewed in Rotin and Kumar, 2009 and Sluimer and Distel, 2018) and the RBR (RING between RING)-type E3s with about 14 members (reviewed in Dove and Klevit, 2017 and Reiter and Klevit, 2018). Whereas the RING E3 ligases function as allosteric activators of the E2 and scaffolds that bring the latter in close proximity to the substrate, the HECT and RBR E3 ligases catalyze substrate ubiquitination in a two-step reaction: in the first step, they accept the activated Ub from the E2 in a transthiolation reaction on their catalytic cysteine, and in the second step, the Ub moiety is transferred to a lysine on the target substrate.

In this review, we focus on the HECT-containing E3 ligases. Invariably at their C-terminus, all HECT E3s present the catalytic HECT domain, composed of a bulkier N-terminal lobe (N-lobe) that contains the E2 binding domain, and a C-terminal lobe (C-lobe) carrying the catalytic cysteine. The two lobes are connected by a flexible hinge region that allows the C-lobe to move around in order to facilitate the Ub transfer from the E2 to the E3 (Huang et al., 1999; Verdecia et al., 2003; Kamadurai et al., 2009).

According to the domain organization present in the N-terminal part of the proteins, the HECT E3s can be subdivided into three main families (**Table 1**; Rotin and Kumar, 2009; Scheffner and Kumar, 2014; Sluimer and Distel, 2018). The best characterized family is the NEDD4 family, consisting of nine human members: ITCH, SMURF1, SMURF2, WWP1, WWP2, NEDD4, NEDD4-2, HECW1, and HECW2. The NEDD4 members share similar domain structure and consist of a membrane/lipid-binding C2 domain, two to four WW domains for substrate

recognition and a C-terminal HECT domain (Fajner et al., 2017). The second class, the HERC family, is characterized by one or more regulators of chromatin condensation 1 (RCC)-like domains (RLD), which serve as a guanine nucleotide exchange factor (GEF) for the small GTPase in membrane trafficking processes (Sanchez-Tena et al., 2016). This family consists of six members that can be subdivided into four 'small' and two 'large' HERCs, where the latter, HERC1 and HERC2, are the largest HECT E3s with about 5000 residues. The remaining 13 HECTs do not share specific domains at the N-terminus and, for this reason, are classified as "other" HECT ligases (Scheffner and Kumar, 2014).

## REGULATION OF HECT E3 LIGASE ACTIVITY

The activity of HECT E3s is tightly regulated in terms of chain specificity (mono- or poly-ubiquitination and Ub chain linkage), interaction with the E2 and recognition of the substrate.

**TABLE 1 |** Overview of the human HECT E3 ligase subfamilies with the respective members, including their domain organization.

| Subfamily | Domains | Members |
|---|---|---|
| NEDD4 | C2, WW (4x), HECT | NEDD4, NEDD4-2, ITCH, WWP1, WWP2 |
| | C2, WW (3x), HECT | SMURF2 |
| | C2, WW (2x), HECT | SMURF1, HECW1, HECW2 |
| HERC | RLD (2x), SPRY, WD40, HECT | HERC1 |
| | RLD (3x), Cytb5, MIB, ZnF, DOC, HECT | HERC2 |
| | RLD, HECT | HERC3, HERC4, HERC5, HERC6 |
| "Other" HECT | AZUL, HECT | E6AP |
| | ARM, UBA, WWE, BH3, UBM, HECT | HUWE1 |
| | ANK, HECT | HACE1 |
| | ARM (2x), WWE, HECT | TRIP12 |
| | UBA, ZnF, PABC, HECT | UBR5 |
| | IQ, HECT | UBE3B, UBE3C |
| | ANK, SUN, MIB, HECT | HECTD1 |
| | HECT | HECTD2, HECTD4 |
| | DOC, HECT | HECTD3 |
| | PHD/RING, HECT | G2E3 |
| | Filamin, HECT | AREL1 |

*Protein domains were predicted by the InterPro server (Finn et al., 2017). HECT E3 ligases are grouped into three subfamilies, NEDD4, HERC, and "other" HECT E3 ligases based on their domain architecture N-terminal to the HECT domain. Domain abbreviations used are as follows: C2, C2 domain ($Ca^{2+}$-binding domain); WW, WW domain; HECT, homologous to E6AP C-terminus; RLD, Regulator of Chromosome Condensation 1 repeat-like domain; SPRY, B30.2/SPRY domain; WD40, W-D repeat domain; Cytb5, cytochrome b5-like heme/steroid-binding domain; DOC, APC10/DOC domain; MIB, MIB-HERC2 domain; ZnF, Zinc finger domain; AZUL, amino-terminal Zn-binding domain of UBE3A ligase; ARM, Armadillo repeat-containing domain; UBA, ubiquitin-associated domain; WWE, WWE domain; BH3, Bcl-2 homology 3 domain; UBM, ubiquitin-binding motif; ANK, Ankyrin repeat-containing domain; PABC, polyadenylate-binding protein C-terminal domain; IQ, IQ motif/EF-hand binding site; SUN, SAD1/UNC domain; PHD, PHD-type zinc finger; Filamin, filamin/ABP280 repeat-like domain.*

The ability to build linkage-specific poly-Ub chains appears to be an intrinsic feature of the HECT enzymes, as they are able to generate distinct Ub chains regardless of the paired E2 enzymes. NEDD4 family members primarily synthesize K63 chains (Kim and Huibregtse, 2009; Maspero et al., 2013; Kristariyanto et al., 2015), while E6AP is a K48-specific enzyme (Wang and Pickart, 2005; Kim and Huibregtse, 2009) and HUWE1 generates K6-, K11-, and K48- linked poly-Ub chains (Jackl et al., 2018). In most of the cases, the detailed mechanism through which they assemble specific poly-Ub chains remains unknown. In the case of NEDD4, the presence of a non-covalent Ub-binding site, called the Ub exosite, in the N-lobe appears to be required for enzyme processivity, possibly by stabilizing and orienting the distal end of growing Ub chains on the substrate (Maspero et al., 2011, 2013).

Precise control of E3 ligase activity is needed to ensure that their functions are restricted until required. Several HECT E3s are kept in a catalytically inactive state by intramolecular interactions between the N-terminal region (either the C2 or the linker region between the WW domains) and the C-terminal HECT domain (Wiesner et al., 2007; Mari et al., 2014; Riling et al., 2015; Chen et al., 2017; Zhu et al., 2017). For other E3s, such as E6AP and HUWE1, the mechanism is different but always requires intermolecular interactions. The crystal structure of the free HECT domain of E6AP suggests that it forms a trimer (Huang et al., 1999) and that the trimeric state activates the E3 ligase (Ronchi et al., 2014). In contrast, the C-terminal region of HUWE1 is maintained in an inactive conformation by homo-dimerization that occurs at the HECT domain. The engagement of the dimerization region by an activation segment located at the N-terminal of the protein seems to relieve this inhibitory mechanism (Sander et al., 2017).

A third level of regulation is represented by adaptor proteins that can modulate both the E2–E3 interaction and the interaction with the substrate. An example of the former is represented by SMAD7. SMURF1 and SMURF2 have low binding affinities for the E2-conjugating enzyme UbcH7, providing a point of control for regulating the Ub ligase activity through the action of auxiliary proteins. Indeed, SMAD7, functioning as a bridge between the E2 and E3, stabilizes an active complex and promotes, thus, the ligase activity (Ogunjimi et al., 2005). In other cases, adaptor proteins may regulate the E3 ligase by promoting its engagement with the substrate. The most famous example is represented by the adaptor protein E6 that binds to a LxxLL motif of the E6AP HECT ligase and forms, together with E6AP, a binding surface for the p53 protein. Consequently, p53 becomes K48-poly-ubiquitinated and degraded by the 26S proteasome (Huibregtse et al., 1993; Martinez-Zapien et al., 2016). NEDD4 family E3s usually recruit substrates via the WW domains that serve as direct binding sites for PPxY motifs present on the targets (Persaud et al., 2009). In this case, cooperation with auxiliary proteins confers the ability to cope with a larger number of substrates. Indeed, in the last decade, proteins such as ARTs in yeast and ARRDCs in mammals were found to modulate the ubiquitination of PY-negative substrates (Lin et al., 2008; Polo and Di Fiore, 2008; Mund and Pelham, 2009; Han et al., 2013). Other adaptor proteins which contribute to NEDD4 family members regulation are NDFIP1 and NDFIP2, transmembrane proteins that localize

to Golgi, endosomes, and multivesicular bodies (Harvey et al., 2002; Shearwin-Whyatt et al., 2006). Through their cytoplasmic PY motifs they allow the association of NEDD4 family members to their specific substrates [e.g., DMT1 (Foot et al., 2008), ENaC (Konstas et al., 2002) the water channel AQP2 (Trimpert et al., 2017)] and directly modulate the activity of these E3s (Mund and Pelham, 2009, 2010).

Notably, HECTs themselves can function as adaptors for other conjugating enzymes as in the case of HERC2 whose binding to the N-terminal domain of E6AP increases the catalytic activity of E6AP (Kuhnle et al., 2011).

Finally, the catalytic activity of the HECT enzymes is often spatially and temporally regulated by post-translational modifications. Activating modifications can contribute to the release of auto-inhibiting conformational states of the E3s. For example, the phosphorylation of ITCH on the three residues of the proline-rich region releases the auto-inhibitory state generated by the binding of the C2 and the first WW domain to the HECT domain (Gallagher et al., 2006). Likewise, FGFR and EGFR activate NEDD4 by inducing a Src-dependent phosphorylation of specific tyrosine residues in the C2 and HECT domains, opening thus the closed conformation (Persaud et al., 2014); a mechanism that seems to be in place also for NEDD4-2 (Grimsey et al., 2018). With an opposite behavior, phosphorylation of a specific residue in the HECT domain of E6AP by the kinase c-Abl disrupts the trimeric state and therefore inhibits the ligase (Chan et al., 2013).

## HECT E3 LIGASES AND THEIR UNDEFINED ROLE IN TUMORIGENESIS

Ubiquitin ligases regulate a wide range of cellular processes and are involved in many human pathologies. Abnormal expression or dysfunction of HECT E3s have been shown in many different cancers. The current knowledge often suggests a dual role for these ligases in tumorigenesis, which might depend on the tissue context and/or additional events that affect their activity. Here, we will review the recent literature on E6AP, NEDD4, and HUWE1, and highlight excellent reviews for additional reading (Bernassola et al., 2008; Rotin and Kumar, 2009; Scheffner and Kumar, 2014; Zou et al., 2015; Wang et al., 2017; Kao et al., 2018).

The classical example of an HECT associated with cancer is E6AP. Since its discovery in 1993, it was evident that E6AP drives human papilloma virus (HPV)-induced cervical carcinogenesis, exerting its activity toward the tumor suppressor p53 through its association with the viral protein E6. E6 is an adaptor protein of the HPV and it is capable of binding to the N-terminal of EA6P and the DNA-binding domain of p53 (Huibregtse et al., 1993; Scheffner et al., 1993; Beaudenon and Huibregtse, 2008), acting as an allosteric activator of E6AP (Mortensen et al., 2015), similarly to HERC2 that binds to the same region (Kuhnle et al., 2011). In addition to HPV-induced cancer, E6AP drives cancer progression in B-cell lymphoma where it degrades PML, allowing the tumor cells to bypass PML-induced senescence (Wolyniec et al., 2012). While E6AP appears to have a pro-oncogenic function, a few papers support a tumor-suppressive function for E6AP in breast and prostate cancers (Srinivasan and Nawaz, 2011; Levav-Cohen et al., 2012; Ramamoorthy et al., 2012; Mansour et al., 2016) and in non-small cell lung cancer where depletion of E6AP contributes to a decreased expression of the INK4/ARF locus (Gamell et al., 2017).

NEDD4 and NEDD4-2 E3s are instead modulators of endocytosis of several membrane proteins such as growth factor receptors [EGFR (Katz et al., 2002) and IGFR (Vecchione et al., 2003; Cao et al., 2008)] and ion channels [ENaC (Staub et al., 1996; Harvey et al., 2001), $Na_v$s (Fotia et al., 2004), and KCNQs (Ekberg et al., 2007; Jespersen et al., 2007)] therefore they are important players in the maintenance of cellular homeostasis. Mutations at the C-terminal of ENaC subunits that abrogate the interaction with NEDD4-2 are the cause of Liddle's syndrome, an autosomal dominant disorder with severe sodium retention and hypertension (Staub et al., 1996).

Overexpression of NEDD4 has been reported in several cancer types and downregulation of NEDD4 appears to reduce proliferation, migration and invasion of cancer cells (reviewed in Zou et al., 2015). The relevance of NEDD4 in the tumorigenic process was initially associated with the identification of the tumor suppressor PTEN as a NEDD4 substrate (Trotman et al., 2007; Wang et al., 2007; Kim et al., 2008; Amodio et al., 2010). Later observations linked RAS activation to NEDD4 overexpression and subsequent PTEN degradation in human colorectal cancer (Zeng et al., 2014). However, studies conducted in NEDD4 knock out (KO) mice showed that PTEN stability was not affected by the E3 ligase deficiency (Fouladkou et al., 2008), while others showed that overexpression of NEDD4 in colorectal cancers promotes cancer cell growth independently of PTEN and PI3K/AKT signaling, arguing that NEDD4-mediated regulation of PTEN is microenvironment and/or cell-type specific, and that other yet-unknown substrates are implicated in the process (Eide et al., 2013). While this latter remains an intriguing hypothesis, it is interesting to note that *in vivo* NEDD4 is reported to degrade many of its substrates, while *in vitro* its activity is clearly K63-specific (Kim and Huibregtse, 2009; Maspero et al., 2013). A possible explanation for this behavior resides in the involvement of adaptor proteins that could influence the specific type of Ub chains catalyzed by E3s [e.g., NUMB (Shao et al., 2017)] or deubiquitinases that may edit the Ub chains.

A last case study is represented by HUWE1, which is also frequently overexpressed in tumors (Chen et al., 2005; Confalonieri et al., 2009; Myant et al., 2017). Again, HUWE1 has been associated with both pro-oncogenic and tumor suppressor functions since it is responsible for K48-mediated degradation of a great variety of substrates ranging from the oncoprotein MYC (Zhao et al., 2008; Inoue et al., 2013; Myant et al., 2017) to the anti-apoptotic protein MCL1, (Zhong et al., 2005) to the tumor suppressor p53 (Chen et al., 2005) and BRCA1 (Wang et al., 2014). Particularly controversial is the role of HUWE1 in the regulation of MYC. On the one hand, HUWE1 is able to enhance tumor cell proliferation by K63-poly ubiquitination and activation of the transcription regulator MYC (Adhikary et al., 2005), on the other hand, depletion (Inoue et al., 2013) or mutation (Myant et al., 2017) of HUWE1 lead to increased MYC levels, thereby promoting skin and colon tumorigenesis.

Clearly, a precise understanding of HUWE1 function in the various cancers relies heavily on the identification of its direct substrates and the type of Ub modification occurring to them.

## TARGET SITES AND SPECIFICITY OF HECT E3 LIGASE INHIBITORS

As previously described, the regulatory mechanisms of HECT E3s are quite diverse and, therefore, provide a promising opportunity for drug discovery (Chen et al., 2018). Based on the actual knowledge, we can imagine different ways to inhibit their activity, namely: (i) by blocking the binding of the E2 enzymes or adaptor proteins; (ii) by tackling the catalytic cysteine of the enzymes; (iii) by targeting specific regulatory surfaces such as the Ub exosite; (iv) by impairing substrate recognition; and (v) by modulating the oligomeric state (**Figure 1**).

Molecules that block the HECT-E2 binding were found by Mund et al. (2014). By using a phage library, the authors isolated and modified bicyclic peptides that specifically bind to the HECT domains of SMURF2, NEDD4-1, WWP1, and HUWE1, competing with the E2 binding. Further improvement of the most promising peptide generated Heclin (HECT ligase inhibitor), a reversible inhibitor with a low micromolar affinity that, however, did not inhibit the E2 binding of the HECTs but rather caused a conformational change that renders their catalytic cysteine more susceptible to oxidation.

With the idea of identifying covalent modifiers of the catalytic cysteine of NEDD4, Kathman et al. (2015) found compounds that selectively react with a non-catalytic cysteine present in the Ub exosite of NEDD4 and NEDD4-2. Interestingly, no inhibition was observed for the NEDD4 family member WWP1 that also contains a cysteine in close proximity to the one seen in NEDD4, or for E6AP that does not contain

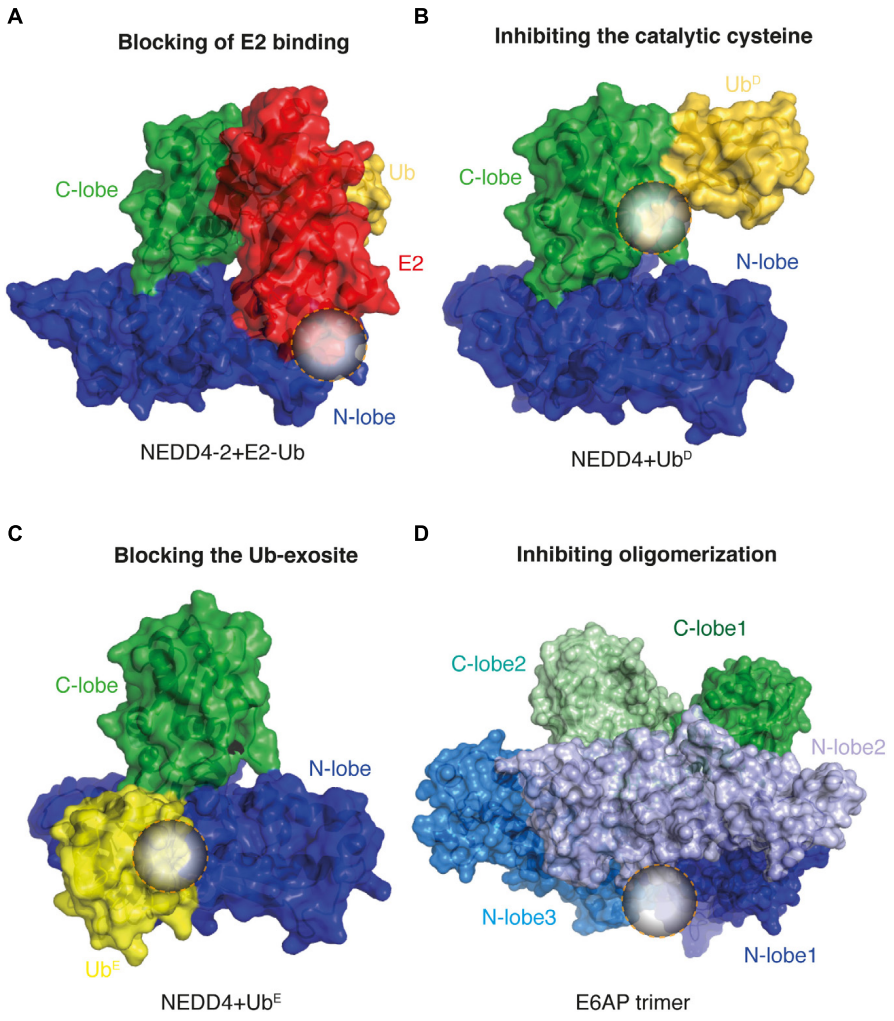


**FIGURE 1 |** Predicted inhibitory targets for HECT E3s activity. Surface representations of known crystal structures of HECT E3s. In circles are highlighted the possible binding sites for small molecules. **(A)** Blocking the E2 binding: $HECT^{NEDD4-2}$ in complex with Ub (gold)-loaded E2 (red; PDB 3JVZ). **(B)** Inhibition of the catalytic cysteine: Ub ($Ub^D$, gold)-loaded $HECT^{NEDD4}$ complex; PDB 4BBN. **(C)** Blocking the Ub exosite: $HECT^{NEDD4}$ in complex with Ub bound to the exosite ($Ub^E$, yellow; PDB 4BBN). **(D)** Inhibition of the oligomerization: $HECT^{E6AP}$ trimeric complex (1D5F). C-lobes and N-lobes are depicted in green and blue, respectively.

a cysteine in this region (Kathman et al., 2015). Another compound that may bind to the Ub exosite of the HECT domain is I3C (1H-indol-3-yl-carbinol), a phytochemical found in cruciferous vegetables that has an antiproliferative effect in cancers (Ahmad et al., 2010). I3C was found to interact with NEDD4 *in vitro* at micromolar concentrations (Adhikary et al., 2005). Through *in silico* binding simulations between I3C and the NEDD4 crystal structure, I3C was predicted to bind to the hydrophobic pocket of the N-lobe near the Ub exosite. In a follow-up study, Quirit et al. (2017) overcame the low binding affinity of I3C by screening a small library of *N*-benzyl or *N*-phenyl I3C analogs and identified 1-benzyl-indole-3-carbinol (1-benzyl-I3C) as a more potent inhibitor. However, the binding mode and the specificity of this compound has not been experimentally validated.

A recent approach suggests the use of specific Ub mutants identified by phage display (Ub variant, UbV) to modulate HECT catalysis (Zhang et al., 2016). The screen performed against 19 of the 28 human HECT enzymes lead to the identification of variants that are capable to bind the N-lobe exosite but also the N-lobe surface involved in the interaction with the E2 (Zhang et al., 2016). Binding of these variants promote inhibition or activation depending on the E3 tested and the type of modifications present in the UbV underlying the complexity of the catalytic mechanism in place. While a generalization of the process is impossible, these reagents appear to be interesting tools for further studies.

A few molecules have been found to inhibit the HECTs, impairing substrate binding. An *in silico* screening of the hydrophobic pocket of the WW domains of SMURF1 led to the identification of compounds that possess features similar to the PPXY motif. These compounds bind the ligase and block SMAD1 ubiquitination, possibly disrupting the WW domain:SMAD1 interaction (Okada et al., 2009; Kato et al., 2011; Cao et al., 2014). However, affinity, binding mode and selectivity remain to be tested.

For many small molecules and inhibitors, the binding sites, the mechanism or the specificity have not been determined. By a high-throughput screening of small molecules, Eilers and co-workers identified two compounds that selectively inhibit the enzyme activity of HUWE1, as seen by a reduced substrate ubiquitination. Both compounds were found to inhibit the ligase activity with $IC_{50}$ values in the low micromolar range, leaving NEDD4 family members or the E1 and E2 enzymes unaffected. The compounds reduced the growth of colorectal cancer cells, but not that of HUWE1-depleted or normal epithelial cells of the colon (Peter et al., 2014). However, how these compounds work on HUWE1 remains unknown (Peter et al., 2014). With a similar approach, Rossi and co-workers identified several putative ITCH inhibitors, including Clomipramine, an FDA-approved drug that is used in the clinic to treat psychiatric disorders. Clomipramine and its analogs specifically block the HECT catalytic activity of the NEDD4 family member ITCH but not that of the RING ligase Ring1B (Rossi et al., 2014). The authors clarified the mode of action of this class of drugs, showing that it specifically inhibits the transthioesterification reaction (the transfer of Ub from the E2 to the HECT domain), implying some common features at the level of the HECT members (Rossi et al., 2014).

## CONCLUDING REMARKS

Although tackling the ubiquitination system rather than the proteasome seems to be a promising avenue for therapeutic drug discovery, targeting HECT E3s to manipulate their activity is challenging for several reasons. First of all, we still lack the complete picture of their ubiquitome and their mechanism of action. Which substrates do HECT E3s ubiquitinate? What impact does ubiquitination have on their function proteolytic or non-proteolytic? How are these substrates recognized and how is their ubiquitination regulated in time and space and in different cellular conditions? What are the mechanisms the different HECT E3s apply to ubiquitinate their targets? So far, we only have a few answers for a small number of ligases and substrates due to the fact that ubiquitination is a dynamic and highly regulated process, and that the interaction with substrates is often transient with a low binding affinity. Besides the PPxY motif that is recognized by the WW domains of NEDD4 family members, no other substrate binding motif is known. An additional challenge is represented by redundancy. While E3s target multiple substrates, a specific substrate may be modulated by several E3s, depending also on the cell context. The high conservation of the HECT domain within the HECT family makes it a difficult target for which to develop specific inhibitory compounds. Finally, most of the HECTs act as both tumor suppressors and oncogenes, and more information is needed in order to find specific and effective compounds. Thus, acquiring more insights into the structural composition and the ubiquitination mechanism used by the different HECT E3s is of paramount importance in order to open new avenues for therapeutic interventions.

## AUTHOR CONTRIBUTIONS

JW, EM, and SP conceptualized and wrote this review. JW prepared the figure. All authors approved the final version of the manuscript and agreed to be accountable for the content of the work.

## FUNDING

Work in SP's laboratory was supported by the Associazione Italiana per la Ricerca sul Cancro (AIRC-IG#IG19875) and the Italian Ministry of Education, Universities and Research (PRIN 20152CB22L). EM was supported by CARIPLO (2017-0746).

## ACKNOWLEDGMENTS

We thank Wessen Maruwge for critically reading and editing the manuscript.

## REFERENCES


Adhikary, S., Marinoni, F., Hock, A., Hulleman, E., Popov, N., Beier, R., et al. (2005). The ubiquitin ligase HectH9 regulates transcriptional activation by Myc and is essential for tumor cell proliferation. *Cell* 123, 409–421. doi: 10.1016/j.cell.2005.08.016

Ahmad, A., Sakr, W. A., and Rahman, K. M. (2010). Anticancer properties of indole compounds: mechanism of apoptosis induction and role in chemotherapy. *Curr. Drug Targets* 11, 652–666. doi: 10.2174/138945010791170923

Amodio, N., Scrima, M., Palaia, L., Salman, A. N., Quintiero, A., Franco, R., et al. (2010). Oncogenic role of the E3 ubiquitin ligase NEDD4-1, a PTEN negative regulator, in non-small-cell lung carcinomas. *Am. J. Pathol.* 177, 2622–2634. doi: 10.2353/ajpath.2010.091075

Beaudenon, S., and Huibregtse, J. M. (2008). HPV E6, E6AP and cervical cancer. *BMC Biochem.* 9(Suppl. 1):S4. doi: 10.1186/1471-2091-9-S1-S4

Bernassola, F., Karin, M., Ciechanover, A., and Melino, G. (2008). The HECT family of E3 ubiquitin ligases: multiple players in cancer development. *Cancer Cell* 14, 10–21. doi: 10.1016/j.ccr.2008.06.001

Berndsen, C. E., and Wolberger, C. (2014). New insights into ubiquitin E3 ligase mechanism. *Nat. Struct. Mol. Biol.* 21, 301–307. doi: 10.1038/nsmb.2780

Cao, X. R., Lill, N. L., Boase, N., Shi, P. P., Croucher, D. R., Shan, H. B., et al. (2008). Nedd4 controls animal growth by regulating IGF-1 signaling. *Sci. Signal.* 1:ra5. doi: 10.1126/scisignal.1160940

Cao, Y., Wang, C., Zhang, X., Xing, G., Lu, K., Gu, Y., et al. (2014). Selective small molecule compounds increase BMP-2 responsiveness by inhibiting Smurf1-mediated Smad1/5 degradation. *Sci. Rep.* 4:4965. doi: 10.1038/srep04965

Chan, A. L., Grossman, T., Zuckerman, V., Campigli Di Giammartino, D., Moshel, O., Scheffner, M., et al. (2013). c-Abl phosphorylates E6AP and regulates its E3 ubiquitin ligase activity. *Biochemistry* 52, 3119–3129. doi: 10.1021/bi301710c

Chen, D., Gehringer, M., and Lorenz, S. (2018). Developing small-molecule inhibitors of HECT-type ubiquitin ligases for therapeutic applications: challenges and opportunities. *Chembiochem* 19, 2123–2135. doi: 10.1002/cbic.201800321

Chen, D. L., Kon, N., Li, M. Y., Zhang, W. Z., Qin, J., and Gu, W. (2005). ARF-BP1/mule is a critical mediator of the ARF tumor suppressor. *Cell* 121, 1071–1083. doi: 10.1016/j.cell.2005.03.037

Chen, Z., Jiang, H., Xu, W., Li, X., Dempsey, D. R., Zhang, X., et al. (2017). A tunable brake for HECT ubiquitin ligases. *Mol. Cell* 66, 345.e6–357.e6. doi: 10.1016/j.molcel.2017.03.020

Confalonieri, S., Quarto, M., Goisis, G., Nuciforo, P., Donzelli, M., Jodice, G., et al. (2009). Alterations of ubiquitin ligases in human cancer and their association with the natural history of the tumor. *Oncogene* 28, 2959–2968. doi: 10.1038/onc.2009.156

Dove, K. K., and Klevit, R. E. (2017). RING-between-RING E3 ligases: emerging themes amid the variations. *J. Mol. Biol.* 429, 3363–3375. doi: 10.1016/j.jmb.2017.08.008

Eide, P. W., Cekaite, L., Danielsen, S. A., Eilertsen, I. A., Kjenseth, A., Fykerud, T. A., et al. (2013). NEDD4 is overexpressed in colorectal cancer and promotes colonic cell growth independently of the PI3K/PTEN/AKT pathway. *Cell Signal* 25, 12–18. doi: 10.1016/j.cellsig.2012.08.012

Ekberg, J., Schuetz, F., Boase, N. A., Conroy, S. J., Manning, J., Kumar, S., et al. (2007). Regulation of the voltage-gated K(+) channels KCNQ2/3 and KCNQ3/5 by ubiquitination. *Novel role for Nedd*4-2. *J. Biol. Chem.* 282, 12135–12142. doi: 10.1074/jbc.M609385200

Fajner, V., Maspero, E., and Polo, S. (2017). Targeting HECT-type E3 ligases - insights from catalysis, regulation and inhibitors. *FEBS Lett.* 591, 2636–2647. doi: 10.1002/1873-3468.12775

Finn, R. D., Attwood, T. K., Babbitt, P. C., Bateman, A., Bork, P., Bridge, A. J., et al. (2017). InterPro in 2017-beyond protein family and domain annotations. *Nucleic Acids Res.* 45, D190–D199. doi: 10.1093/nar/gkw1107

Foot, N. J., Dalton, H. E., Shearwin-Whyatt, L. M., Dorstyn, L., Tan, S. S., Yang, B., et al. (2008). Regulation of the divalent metal ion transporter DMT1 and iron homeostasis by a ubiquitin-dependent mechanism involving Ndfips and WWP2. *Blood* 112, 4268–4275. doi: 10.1182/blood-2008-04-150953

Fotia, A. B., Ekberg, J., Adams, D. J., Cook, D. I., Poronnik, P., and Kumar, S. (2004). Regulation of neuronal voltage-gated sodium channels by the ubiquitin-protein ligases Nedd4 and Nedd4-2. *J. Biol. Chem.* 279, 28930–28935. doi: 10.1074/jbc.M402820200

Fouladkou, F., Landry, T., Kawabe, H., Neeb, A., Lu, C., Brose, N., et al. (2008). The ubiquitin ligase Nedd4-1 is dispensable for the regulation of PTEN stability and localization. *Proc. Natl. Acad. Sci. U.S.A.* 105, 8585–8590. doi: 10.1073/pnas.0803233105

Gallagher, E., Gao, M., Liu, Y. C., and Karin, M. (2006). Activation of the E3 ubiquitin ligase Itch through a phosphorylation-induced conformational change. *Proc. Natl. Acad. Sci. U.S.A.* 103, 1717–1722. doi: 10.1073/pnas.0510664103

Gamell, C., Gulati, T., Levav-Cohen, Y., Young, R. J., Do, H., Pilling, P., et al. (2017). Reduced abundance of the E3 ubiquitin ligase E6AP contributes to decreased expression of the INK4/ARF locus in non-small cell lung cancer. *Sci. Signal* 10:eaaf8223. doi: 10.1126/scisignal.aaf8223 doi: 10.1126/scisignal.aaf8223

Grimsey, N. J., Narala, R., Rada, C. C., Mehta, S., Stephens, B. S., Kufareva, I., et al. (2018). A tyrosine switch on NEDD4-2 E3 ligase transmits GPCR inflammatory signaling. *Cell Rep.* 24, 3312.e5–3323.e5. doi: 10.1016/j.celrep.2018.08.061

Han, S. O., Kommaddi, R. P., and Shenoy, S. K. (2013). Distinct roles for beta-arrestin2 and arrestin-domain-containing proteins in beta2 adrenergic receptor trafficking. *EMBO Rep.* 14, 164–171. doi: 10.1038/embor.2012.187

Harvey, K. F., Dinudom, A., Cook, D. I., and Kumar, S. (2001). The Nedd4-like protein KIAA0439 is a potential regulator of the epithelial sodium channel. *J. Biol. Chem.* 276, 8597–8601. doi: 10.1074/jbc.C000906200

Harvey, K. F., Shearwin-Whyatt, L. M., Fotia, A., Parton, R. G., and Kumar, S. (2002). N4WBP5, a potential target for ubiquitination by the Nedd4 family of proteins, is a novel Golgi-associated protein. *J. Biol. Chem.* 277, 9307–9317. doi: 10.1074/jbc.M110443200

Huang, L., Kinnucan, E., Wang, G., Beaudenon, S., Howley, P. M., Huibregtse, J. M., et al. (1999). Structure of an E6AP-UbcH7 complex: insights into ubiquitination by the E2-E3 enzyme cascade. *Science* 286, 1321–1326. doi: 10.1126/science.286.5443.1321

Huibregtse, J. M., Scheffner, M., and Howley, P. M. (1993). Localization of the E6-AP regions that direct human papillomavirus E6 binding, association with p53, and ubiquitination of associated proteins. *Mol. Cell Biol.* 13, 4918–4927. doi: 10.1128/MCB.13.8.4918

Inoue, S., Hao, Z. Y., Elia, A. J., Cescon, D., Zhou, L., Silvester, J., et al. (2013). Mule/Huwe1/Arf-BP1 suppresses Ras-driven tumorigenesis by preventing c-Myc/Miz1-mediated down-regulation of p21 and p15. *Genes Dev.* 27, 1101–1114. doi: 10.1101/gad.214577.113

Jackl, M., Stollmaier, C., Strohaker, T., Hyz, K., Maspero, E., Polo, S., et al. (2018). beta-sheet augmentation is a conserved mechanism of priming HECT E3 ligases for ubiquitin ligation. *J. Mol. Biol.* 430(18 Pt B), 3218–3233. doi: 10.1016/j.jmb.2018.06.044

Jespersen, T., Membrez, M., Nicolas, C. S., Pitard, B., Staub, O., Olesen, S. P., et al. (2007). The KCNQ1 potassium channel is down-regulated by ubiquitylating enzymes of the Nedd4/Nedd4-like family. *Cardiovasc. Res.* 74, 64–74. doi: 10.1016/j.cardiores.2007.01.008

Kamadurai, H. B., Souphron, J., Scott, D. C., Duda, D. M., Miller, D. J., Stringer, D., et al. (2009). Insights into ubiauitin transfer cascades from a structure of a UbcH5B similar to Ubiauitin-HECTNEDD4L complex. *Mol. Cell* 36, 1095–1102. doi: 10.1016/j.molcel.2009.11.010

Kao, S. H., Wu, H. T., and Wu, K. J. (2018). Ubiquitination by HUWE1 in tumorigenesis and beyond. *J. Biomed. Sci.* 25:67. doi: 10.1186/s12929-018-0470-0

Kathman, S. G., Span, I., Smith, A. T., Xu, Z., Zhan, J., Rosenzweig, A. C., et al. (2015). A small molecule that switches a ubiquitin ligase from a processive to a distributive enzymatic mechanism. *J. Am. Chem. Soc.* 137, 12442–12445. doi: 10.1021/jacs.5b06839

Kato, S., Sangadala, S., Tomita, K., Titus, L., and Boden, S. D. (2011). A synthetic compound that potentiates bone morphogenetic protein-2-induced transdifferentiation of myoblasts into the osteoblastic phenotype. *Mol. Cell. Biochem.* 349, 97–106. doi: 10.1007/s11010-010-0664-6

Katz, M., Shtiegman, K., Tal-Or, P., Yakir, L., Mosesson, Y., Harari, D., et al. (2002). Ligand-independent degradation of epidermal growth factor receptor involves

receptor ubiquitylation and Hgs, an adaptor whose ubiquitin-interacting motif targets ubiquitylation by Nedd4. *Traffic* 3, 740–751. doi: 10.1034/j.1600-0854.2002.31006.x

Kim, H. C., and Huibregtse, J. M. (2009). Polyubiquitination by HECT E3s and the determinants of chain type specificity. *Mol. Cell Biol.* 29, 3307–3318. doi: 10.1128/MCB.00240-09

Kim, S. S., Yoo, N. J., Jeong, E. G., Kim, M. S., and Lee, S. H. (2008). Expression of NEDD4-1, a PTEN regulator, in gastric and colorectal carcinomas. *APMIS* 116, 779–784. doi: 10.1111/j.1600-0463.2008.00999.x

Komander, D., and Rape, M. (2012). The ubiquitin code. *Annu. Rev. Biochem.* 81, 203–229. doi: 10.1146/annurev-biochem-060310-170328

Konstas, A. A., Shearwin-Whyatt, L. M., Fotia, A. B., Degger, B., Riccardi, D., Cook, D. I., et al. (2002). Regulation of the epithelial sodium channel by N4WBP5A, a novel Nedd4/Nedd4-2-interacting protein. *J. Biol. Chem.* 277, 29406–29416. doi: 10.1074/jbc.M203018200

Kristariyanto, Y. A., Choi, S. Y., Rehman, S. A., Ritorto, M. S., Campbell, D. G., Morrice, N. A., et al. (2015). Assembly and structure of Lys33-linked polyubiquitin reveals distinct conformations. *Biochem. J.* 467, 345–352. doi: 10.1042/BJ20141502

Kuhnle, S., Kogel, U., Glockzin, S., Marquardt, A., Ciechanover, A., Matentzoglu, K., et al. (2011). Physical and functional interaction of the HECT ubiquitin-protein ligases E6AP and HERC2. *J. Biol. Chem.* 286, 19410–19416. doi: 10.1074/jbc.M110.205211

Levav-Cohen, Y., Wolyniec, K., Alsheich-Bartok, O., Chan, A. L., Woods, S. J., Jiang, Y. H., et al. (2012). E6AP is required for replicative and oncogene-induced senescence in mouse embryo fibroblasts. *Oncogene* 31, 2199–2209. doi: 10.1038/onc.2011.402

Li, W., Bengtson, M. H., Ulbrich, A., Matsuda, A., Reddy, V. A., Orth, A., et al. (2008). Genome-wide and functional annotation of human E3 ubiquitin ligases identifies MULAN, a mitochondrial E3 that regulates the organelle's dynamics and signaling. *PLoS One* 3:e1487. doi: 10.1371/journal.pone.0001487

Lin, C. H., MacGurn, J. A., Chu, T., Stefan, C. J., and Emr, S. D. (2008). Arrestin-related ubiquitin-ligase adaptors regulate endocytosis and protein turnover at the cell surface. *Cell* 135, 714–725. doi: 10.1016/j.cell.2008.09.025

Mansour, M., Haupt, S., Chan, A. L., Godde, N., Rizzitelli, A., Loi, S., et al. (2016). The E3-ligase E6AP represses breast cancer metastasis via regulation of ECT2-Rho signaling. *Cancer Res.* 76, 4236–4248. doi: 10.1158/0008-5472.CAN-15-1553

Mari, S., Ruetalo, N., Maspero, E., Stoffregen, M. C., Pasqualato, S., Polo, S., et al. (2014). Structural and functional framework for the autoinhibition of Nedd4-family ubiquitin ligases. *Structure* 22, 1639–1649. doi: 10.1016/j.str.2014.09.006

Martinez-Zapien, D., Ruiz, F. X., Poirson, J., Mitschler, A., Ramirez, J., Forster, A., et al. (2016). Structure of the E6/E6AP/p53 complex required for HPV-mediated degradation of p53. *Nature* 529, 541–545. doi: 10.1038/nature16481

Maspero, E., Mari, S., Valentini, E., Musacchio, A., Fish, A., Pasqualato, S., et al. (2011). Structure of the HECT:ubiquitin complex and its role in ubiquitin chain elongation. *EMBO Rep.* 12, 342–349. doi: 10.1038/embor.2011.21

Maspero, E., Valentini, E., Mari, S., Cecatiello, V., Soffientini, P., Pasqualato, S., et al. (2013). Structure of a ubiquitin-loaded HECT ligase reveals the molecular basis for catalytic priming. *Nat. Struct. Mol. Biol.* 20, 696–701. doi: 10.1038/nsmb.2566

Metzger, M. B., Pruneda, J. N., Klevit, R. E., and Weissman, A. M. (2014). RING-type E3 ligases: master manipulators of E2 ubiquitin-conjugating enzymes and ubiquitination. *Biochim. Biophys. Acta* 1843, 47–60. doi: 10.1016/j.bbamcr.2013.05.026

Mortensen, F., Schneider, D., Barbic, T., Sladewska-Marquardt, A., Kuhnle, S., Marx, A., et al. (2015). Role of ubiquitin and the HPV E6 oncoprotein in E6AP-mediated ubiquitination. *Proc. Natl. Acad. Sci. U.S.A.* 112, 9872–9877. doi: 10.1073/pnas.1505923112

Mund, T., Lewis, M. J., Maslen, S., and Pelham, H. R. (2014). Peptide and small molecule inhibitors of HECT-type ubiquitin ligases. *Proc. Natl. Acad. Sci. U.S.A.* 111, 16736–16741. doi: 10.1073/pnas.1412152111

Mund, T., and Pelham, H. R. (2009). Control of the activity of WW-HECT domain E3 ubiquitin ligases by NDFIP proteins. *EMBO Rep.* 10, 501–507. doi: 10.1038/embor.2009.30

Mund, T., and Pelham, H. R. (2010). Regulation of PTEN/Akt and MAP kinase signaling pathways by the ubiquitin ligase activators Ndfip1 and Ndfip2. *Proc. Natl. Acad. Sci. U.S.A.* 107, 11429–11434. doi: 10.1073/pnas.0911714107

Myant, K. B., Cammareri, P., Hodder, M. C., Wills, J., Von Kriegsheim, A., Gyorffy, B., et al. (2017). HUWE1 is a critical colonic tumour suppressor gene that prevents MYC signalling, DNA damage accumulation and tumour initiation. *EMBO Mol. Med.* 9, 181–197. doi: 10.15252/emmm.201606684

Ogunjimi, A. A., Briant, D. J., Pece-Barbara, N., Le Roy, C., Di Guglielmo, G. M., Kavsak, P., et al. (2005). Regulation of Smurf2 ubiquitin ligase activity by anchoring the E2 to the HECT domain. *Mol. Cell* 19, 297–308. doi: 10.1016/j.molcel.2005.06.028

Oh, E., Akopian, D., and Rape, M. (2018). Principles of ubiquitin-dependent signaling. *Annu. Rev. Cell Dev. Biol.* 34, 137–162. doi: 10.1146/annurev-cellbio-100617-062802

Okada, M., Sangadala, S., Liu, Y., Yoshida, M., Reddy, B. V., Titus, L., et al. (2009). Development and optimization of a cell-based assay for the selection of synthetic compounds that potentiate bone morphogenetic protein-2 activity. *Cell Biochem. Funct.* 27, 526–534. doi: 10.1002/cbf.1615

Persaud, A., Alberts, P., Amsen, E. M., Xiong, X., Wasmuth, J., Saadon, Z., et al. (2009). Comparison of substrate specificity of the ubiquitin ligases Nedd4 and Nedd4-2 using proteome arrays. *Mol. Syst. Biol.* 5:333. doi: 10.1038/msb.2009.85

Persaud, A., Alberts, P., Mari, S., Tong, J., Murchie, R., Maspero, E., et al. (2014). Tyrosine phosphorylation of NEDD4 activates its ubiquitin ligase activity. *Sci. Signal.* 7:ra95. doi: 10.1126/scisignal.2005290

Peter, S., Bultinck, J., Myant, K., Jaenicke, L. A., Walz, S., Muller, J., et al. (2014). H Tumor cell-specific inhibition of MYC function using small molecule inhibitors of the HUWE1 ubiquitin ligase. *EMBO Mol. Med.* 6, 1525–1541. doi: 10.15252/emmm.201403927

Polo, S., and Di Fiore, P. P. (2008). Finding the right partner: science or ART? *Cell* 135, 590–592. doi: 10.1016/j.cell.2008.10.032

Quirit, J. G., Lavrenov, S. N., Poindexter, K., Xu, J., Kyauk, C., Durkin, K. A., et al. (2017). Indole-3-carbinol (I3C) analogues are potent small molecule inhibitors of NEDD4-1 ubiquitin ligase activity that disrupt proliferation of human melanoma cells. *Biochem. Pharmacol.* 127, 13–27. doi: 10.1016/j.bcp.2016.12.007

Ramamoorthy, S., Tufail, R., Hokayem, J. E., Jorda, M., Zhao, W., Reis, Z., et al. (2012). Overexpression of ligase defective E6-associated protein, E6-AP, results in mammary tumorigenesis. *Breast Cancer Res. Treat.* 132, 97–108. doi: 10.1007/s10549-011-1567-2

Reiter, K. H., and Klevit, R. E. (2018). Characterization of RING-Between-RING E3 ubiquitin transfer mechanisms. *Methods Mol. Biol.* 1844, 3–17. doi: 10.1007/978-1-4939-8706-1_1

Riling, C., Kamadurai, H., Kumar, S., O'Leary, C. E., Wu, K. P., Manion, E. E., et al. (2015). Itch WW domains inhibit its E3 ubiquitin ligase activity by blocking E2-E3 ligase trans-thiolation. *J. Biol. Chem.* 290, 23875–23887. doi: 10.1074/jbc.M115.649269

Ronchi, V. P., Klein, J. M., Edwards, D. J., and Haas, A. L. (2014). The active form of E6-associated protein (E6AP)/UBE3A ubiquitin ligase is an oligomer. *J. Biol. Chem.* 289, 1033–1048. doi: 10.1074/jbc.M113.517805

Rossi, M., Rotblat, B., Ansell, K., Amelio, I., Caraglia, M., Misso, G., et al. (2014). High throughput screening for inhibitors of the HECT ubiquitin E3 ligase ITCH identifies antidepressant drugs as regulators of autophagy. *Cell Death Dis.* 5:e1203. doi: 10.1038/cddis.2014.113

Rotin, D., and Kumar, S. (2009). Physiological functions of the HECT family of ubiquitin ligases. *Nat. Rev. Mol. Cell. Biol.* 10, 398–409. doi: 10.1038/nrm2690

Sanchez-Tena, S., Cubillos-Rojas, M., Schneider, T., and Rosa, J. L. (2016). Functional and pathological relevance of HERC family proteins: a decade later. *Cell Mol. Life Sci.* 73, 1955–1968. doi: 10.1007/s00018-016-2139-8

Sander, B., Xu, W., Eilers, M., Popov, N., and Lorenz, S. (2017). A conformational switch regulates the ubiquitin ligase HUWE1. *Elife* 6:e21036. doi: 10.7554/eLife.21036

Scheffner, M., Huibregtse, J. M., Vierstra, R. D., and Howley, P. M. (1993). The HPV-16 E6 and E6-AP complex functions as a ubiquitin-protein ligase in the ubiquitination of p53. *Cell* 75, 495–505. doi: 10.1016/0092-8674(93)90384-3

Scheffner, M., and Kumar, S. (2014). Mammalian HECT ubiquitin-protein ligases: biological and pathophysiological aspects. *Biochim. Biophys. Acta Mol. Cell Res.* 1843, 61–74. doi: 10.1016/j.bbamcr.2013.03.024

Shao, C., Li, Z., Ahmad, N., and Liu, X. (2017). Regulation of PTEN degradation and NEDD4-1 E3 ligase activity by Numb. *Cell Cycle* 16, 957–967. doi: 10.1080/15384101.2017.1310351

Shearwin-Whyatt, L., Dalton, H. E., Foot, N., and Kumar, S. (2006). Regulation of functional diversity within the Nedd4 family by accessory and adaptor proteins. *Bioessays* 28, 617–628. doi: 10.1002/bies.20422

Sluimer, J., and Distel, B. (2018). Regulating the human HECT E3 ligases. *Cell Mol. Life Sci.* 75, 3121–3141. doi: 10.1007/s00018-018-2848-2

Srinivasan, S., and Nawaz, Z. (2011). E3 ubiquitin protein ligase, E6-associated protein (E6-AP) regulates PI3K-Akt signaling and prostate cell growth. *Biochim. Biophys. Acta* 1809, 119–127. doi: 10.1016/j.bbagrm.2010.08.011

Staub, O., Dho, S., Henry, P., Correa, J., Ishikawa, T., McGlade, J., et al. (1996). WW domains of Nedd4 bind to the proline-rich PY motifs in the epithelial Na+ channel deleted in Liddle's syndrome. *EMBO J.* 15, 2371–2380. doi: 10.1002/j.1460-2075.1996.tb00593.x

Trimpert, C., Wesche, D., de Groot, T., Pimentel Rodriguez, M. M., Wong, V., van den Berg, D. T. M., et al. (2017). NDFIP allows NEDD4/NEDD4L-induced AQP2 ubiquitination and degradation. *PLoS One* 12:e0183774. doi: 10.1371/journal.pone.0183774

Trotman, L. C., Wang, X., Alimonti, A., Chen, Z., Teruya-Feldstein, J., Yang, H., et al. (2007). Ubiquitination regulates PTEN nuclear import and tumor suppression. *Cell* 128, 141–156. doi: 10.1016/j.cell.2006.11.040

Vecchione, A., Marchese, A., Henry, P., Rotin, D., and Morrione, A. (2003). The Grb10/Nedd4 complex regulates ligand-induced ubiquitination and stability of the insulin-like growth factor I receptor. *Mol. Cell Biol.* 23, 3363–3372. doi: 10.1128/MCB.23.9.3363-3372.2003

Verdecia, M. A., Joazeiro, C. A., Wells, N. J., Ferrer, J. L., Bowman, M. E., Hunter, T., et al. (2003). Conformational flexibility underlies ubiquitin ligation mediated by the WWP1 HECT domain E3 ligase. *Mol. Cell* 11, 249–259. doi: 10.1016/S1097-2765(02)00774-8

Wang, D., Ma, L., Wang, B., Liu, J., and Wei, W. (2017). E3 ubiquitin ligases in cancer and implications for therapies. *Cancer Metastasis Rev.* 36, 683–702. doi: 10.1007/s10555-017-9703-z

Wang, M., and Pickart, C. M. (2005). Different HECT domain ubiquitin ligases employ distinct mechanisms of polyubiquitin chain synthesis. *Embo J.* 24, 4324–4333. doi: 10.1038/sj.emboj.7600895

Wang, X., Lu, G., Li, L., Yi, J., Yan, K., Wang, Y., et al. (2014). HUWE1 interacts with BRCA1 and promotes its degradation in the ubiquitin-proteasome pathway. *Biochem. Biophys. Res. Commun.* 444, 290–295. doi: 10.1016/j.bbrc.2013.12.053

Wang, X., Trotman, L. C., Koppie, T., Alimonti, A., Chen, Z., Gao, Z., et al. (2007). NEDD4-1 is a proto-oncogenic ubiquitin ligase for PTEN. *Cell* 128, 129–139. doi: 10.1016/j.cell.2006.11.039

Wiesner, S., Ogunjimi, A. A., Wang, H. R., Rotin, D., Sicheri, F., Wrana, J. L., et al. (2007). Autoinhibition of the HECT-type ubiquitin ligase Smurf2 through its C2 domain. *Cell* 130, 651–662. doi: 10.1016/j.cell.2007.06.050

Wolyniec, K., Shortt, J., de Stanchina, E., Levav-Cohen, Y., Alsheich-Bartok, O., Louria-Hayon, I., et al. (2012). E6AP ubiquitin ligase regulates PML-induced senescence in Myc-driven lymphomagenesis. *Blood* 120, 822–832. doi: 10.1182/blood-2011-10-387647

Zeng, T., Wang, Q., Fu, J., Lin, Q., Bi, J., Ding, W., et al. (2014). Impeded Nedd4-1-mediated Ras degradation underlies Ras-driven tumorigenesis. *Cell Rep.* 7, 871–882. doi: 10.1016/j.celrep.2014.03.045

Zhang, W., Wu, K. P., Sartori, M. A., Kamadurai, H. B., Ordureau, A., Jiang, C., et al. (2016). System-wide modulation of HECT E3 ligases with selective ubiquitin variant probes. *Mol. Cell* 62, 121–136. doi: 10.1016/j.molcel.2016.02.005

Zhao, X., Heng, J. I., Guardavaccaro, D., Jiang, R., Pagano, M., Guillemot, F., et al. (2008). The HECT-domain ubiquitin ligase Huwe1 controls neural differentiation and proliferation by destabilizing the N-Myc oncoprotein. *Nat. Cell Biol.* 10, 643–653. doi: 10.1038/ncb1727

Zhong, Q., Gao, W., Du, F., and Wang, X. (2005). Mule/ARF-BP1, a BH3-only E3 ubiquitin ligase, catalyzes the polyubiquitination of Mcl-1 and regulates apoptosis. *Cell* 121, 1085–1095. doi: 10.1016/j.cell.2005.06.009

Zhu, K., Shan, Z., Chen, X., Cai, Y., Cui, L., Yao, W., et al. (2017). Allosteric auto-inhibition and activation of the Nedd4 family E3 ligase Itch. *EMBO Rep.* 18, 1618–1630. doi: 10.15252/embr.201744454

Zou, X., Levy-Cohen, G., and Blank, M. (2015). Molecular functions of NEDD4 E3 ubiquitin ligases in cancer. *Biochim. Biophys. Acta* 1856, 91–106. doi: 10.1016/j.bbcan.2015.06.005 doi: 10.1016/j.bbcan.2015.06.005

**Conflict of Interest Statement:** The authors declare that the research was conducted in the absence of any commercial or financial relationships that could be construed as a potential conflict of interest.

frontiers in Physiology

ORIGINAL RESEARCH
published: 09 April 2019
doi: 10.3389/fphys.2019.00390

# A Single Conserved Amino Acid Residue as a Critical Context-Specific Determinant of the Differential Ability of Mdm2 and MdmX RING Domains to Dimerize

*Pavlína Kosztyu[1], Iva Slaninová[1], Barbora Valčíková[1,2], Amandine Verlande[1,2], Petr Müller[3], Jan J. Paleček[4,5] and Stjepan Uldrijan[1,2]**

*[1]Department of Biology, Faculty of Medicine, Masaryk University, Brno, Czechia, [2]International Clinical Research Center, St. Anne's University Hospital, Brno, Czechia, [3]Regional Centre for Applied Molecular Oncology, Masaryk Memorial Cancer Institute, Brno, Czechia, [4]Central European Institute of Technology, Masaryk University, Brno, Czechia, [5]National Centre for Biomolecular Research, Faculty of Science, Masaryk University, Brno, Czechia*

OPEN ACCESS

**Edited by:**
*Victor M. Bolanos-Garcia, Oxford Brookes University, United Kingdom*

**Reviewed by:**
*Michael B. Morris, University of Sydney, Australia*
*Ana Isabel García-Guillén, University of Murcia, Spain*

***Correspondence:**
*Stjepan Uldrijan*
*uldrijan@med.muni.cz*

**Specialty section:**
*This article was submitted to Integrative Physiology, a section of the journal Frontiers in Physiology*

**Received:** *05 November 2018*
**Accepted:** *21 March 2019*
**Published:** *09 April 2019*

**Citation:**
*Kosztyu P, Slaninová I, Valčíková B, Verlande A, Müller P, Paleček JJ and Uldrijan S (2019) A Single Conserved Amino Acid Residue as a Critical Context-Specific Determinant of the Differential Ability of Mdm2 and MdmX RING Domains to Dimerize. Front. Physiol. 10:390. doi: 10.3389/fphys.2019.00390*

Mdm2 and MdmX are related proteins serving in the form of the Mdm2 homodimer or Mdm2/MdmX heterodimer as an E3 ubiquitin ligase for the tumor suppressor p53. The dimerization is required for the E3 activity and is mediated by the conserved RING domains present in both proteins, but only the RING domain of Mdm2 can form homodimers efficiently. We performed a systematic mutational analysis of human Mdm2, exchanging parts of the RING with the corresponding MdmX sequence, to identify the molecular determinants of this difference. Mdm2 can also promote MdmX degradation, and we identified several mutations blocking it. They were located mainly at the Mdm2/E2 interface and did not disrupt the MdmX-Mdm2 interaction. Surprisingly, some mutations of the Mdm2/E2 interface inhibited MdmX degradation, which is mediated by the Mdm2/MdmX heterodimer, but did not affect p53 degradation, mediated by the Mdm2 homodimer. Only one mutant, replacing a conserved cysteine 449 with asparagine (C449N), disrupted the ability of Mdm2 to dimerize with MdmX. When we introduced the cysteine residue into the corresponding site in MdmX, the RING domain became capable of forming dimers with other MdmX molecules *in vivo*, suggesting that one conserved amino acid residue in the RINGs of Mdm2 and MdmX could serve as the determinant of the differential ability of these domains to form dimers and their E3 activity. In immunoprecipitations, however, the homodimerization of MdmX could be observed only when the asparagine residue was replaced with cysteine in both RINGs. This result suggested that heterocomplexes consisting of one mutated MdmX RING with cysteine and one wild-type MdmX RING with asparagine might be less stable, despite being readily detectable in the cell-based assay. Moreover, Mdm2 C449N blocked Mdm2-MdmX heterodimerization but did not disrupt the ability of Mdm2 homodimer to promote p53 degradation, suggesting that the effect of the conserved cysteine and asparagine residues on dimerization was context-specific. Collectively, our results indicate that the effects of individual exchanges of conserved

residues between Mdm2 and MdmX RING domains might be context-specific, supporting the hypothesis that Mdm2 RING homodimers and Mdm2-MdmX heterodimers may not be entirely structurally equivalent, despite their apparent similarity.

**Keywords: Mdm2, Mdm4, MdmX, RING domain ubiquitin protein ligase, dimerization, mutagenesis, E3, p53**

## INTRODUCTION

Mdm2 and MdmX (also known as Mdm4) are closely related proteins which work together to control the levels and activity of the tumor suppressor p53 during embryonic development and in unstressed healthy cells (Jones et al., 1995; Montes de Oca Luna et al., 1995; Parant et al., 2001; Migliorini et al., 2002; Marine et al., 2006; Ringshausen et al., 2006). However, in human cancers retaining wild-type *p53* gene, Mdm2 and MdmX proteins are often expressed at high levels, overcoming the growth-suppressive functions of p53 and contributing to tumor development (Momand et al., 1998; Toledo and Wahl, 2006). Mdm2 and MdmX can directly interact with p53 and inhibit its transcription activity (Momand et al., 1992; Chen et al., 1993; Shvarts et al., 1996). Both proteins also serve as RING finger E3 ubiquitin ligases for p53, either in the form of an Mdm2 homodimer or Mdm2-MdmX heterodimer (Fang et al., 2000; Uldrijan et al., 2007). Mdm2 can also serve as E3 for MdmX and for Mdm2 itself. In the absence of MdmX, Mdm2 is unstable and less active toward p53. Dimerization with MdmX increases its stability and E3 activity toward p53. At the same time, the interaction with Mdm2 promotes the translocation of MdmX from the cytoplasm to the nucleus where the wild-type p53 protein predominantly resides (Stad et al., 2001; Gu et al., 2002; Li et al., 2002).

The N-terminal p53 binding domains and the RING domains of Mdm2 and MdmX are highly conserved in evolution (**Figure 1A**), as is the central acidic domain of Mdm2, which also actively participates in p53 ubiquitination and degradation (Argentini et al., 2001; Kawai et al., 2003; Meulmeester et al., 2003; Dolezelova et al., 2012b; Tan et al., 2016). The RING domains are in both proteins located very close to the C-terminus (**Figure 1A**) and the adjacent C-terminal tails, conserved in length and sequence, also participate in the RING domain function (Poyurovsky et al., 2007; Uldrijan et al., 2007). Although the structures of the two RING domains are very similar (Kostic et al., 2006; Linke et al., 2008), the Mdm2 homodimers and Mdm2/MdmX heterodimers do not seem to be structurally and functionally fully equivalent (Dolezelova et al., 2012a). The MdmX RING finger does not possess the ubiquitin ligase activity toward p53 on its own but can stimulate the Mdm2-mediated p53 ubiquitination and restore the E3 activity of Mdm2 mutants disrupting the function of the C-terminal tail (Linares et al., 2003; Uldrijan et al., 2007). This difference between MdmX and Mdm2 could be in part caused by intramolecular interactions mediated by other regions of the proteins. MdmX has been reported to contain autoinhibitory sequence elements that compete with the binding of MdmX to the transactivation domain of p53 (Bista et al., 2013; Chen et al., 2015). The RING domain of Mdm2 was shown to physically interact with the central acidic region of Mdm2 (Dang et al., 2002). The primary amino acid sequences of the central domains are less conserved between Mdm2 and MdmX, and MdmX cannot provide the critical function of the acidic domain in Mdm2-mediated p53 ubiquitination. A short sequence within the acidic domain of Mdm2 has been identified as necessary for p53 ubiquitination and a 30-amino acid region encompassing this sequence has been shown to promote the ubiquitin ligase activity of Mdm2 by an intramolecular interaction with the RING domain (Dolezelova et al., 2012b; Cheng et al., 2014).

A notable feature of RING-type E3s is their tendency to form homodimers and heterodimers that seems to be the prerequisite for the E3 activity for many RING finger ubiquitin ligases (Metzger et al., 2014). The RING domain of Mdm2 is capable of forming both homodimers and heterodimers with MdmX RING, while the RING domain of MdmX does not homodimerize and can form active ubiquitin ligase only in the form of MdmX-Mdm2 heterodimer (Tanimura et al., 1999; Kawai et al., 2007). MdmX stabilizes Mdm2 and stimulates Mdm2-mediated p53 ubiquitination and degradation (Sharp et al., 1999; Stad et al., 2000; Gu et al., 2002; Linares et al., 2003). Hetero-oligomerization with MdmX rescues the ubiquitin ligase activity of Mdm2 C-terminal mutants (Poyurovsky et al., 2007; Singh et al., 2007; Dolezelova et al., 2012a). Moreover, the Mdm2/MdmX heterocomplex seems to be the predominant form present in cells, required for the control of p53 activity *in vivo* (Kawai et al., 2007; Huang et al., 2011). A precise understanding of the nature of Mdm2-MdmX interactions can be critical to exploiting them as potential therapeutic targets for reactivation of p53 function in tumors. In this study, we systematically analyzed the primary structure of Mdm2 and MdmX RING domains to identify critical differences that render the MdmX RING inactive by preventing its dimerization and E3 activity.

## MATERIALS AND METHODS

### Cell Culture

Human U2OS and HEK293 cell lines were obtained from ECACC and DSMZ, respectively. Cells were cultured at 37°C / 5% $CO_2$ in Dulbecco's modified Eagle's medium (DMEM) supplemented with 10% fetal calf serum, 2 mM L-glutamine, 50 U/ml penicillin G, and 50 μg/ml streptomycin sulfate (all from Sigma-Aldrich).

### Plasmids and Mutagenesis

Mammalian expression plasmids coding for wild-type Mdm2, Mdm2 mutant Mdm2Δ9, lacking the conserved C-terminal tail required for RING dimerization, Mdm2 mutant C464A, disrupting the RING domain structure and function, Myc-tagged

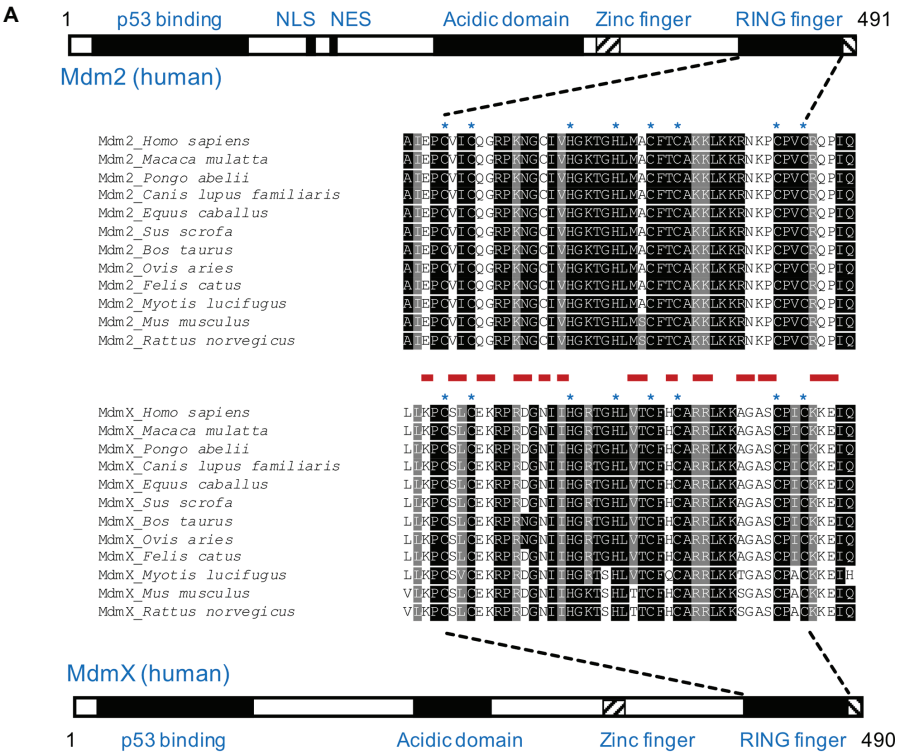


**B**

| Mdm2 RING mutagenesis (Mdm2 → MdmX exchanges) | |
|---|---|
| 436 | E → K |
| 439-440 | VI → SL |
| 442-443 | QG → EK |
| 446-447 | KN → RD |
| *449* | C → N (*A,S*) |
| *451* | *V → I* |
| 459-460 | MA → VT |
| 463 | T → H |
| *466-467* | *KK → RR* |
| 471-472 | RN → AG |
| 473-474 | KP → AS |
| 479-481 | RQP → KKE |

**C**

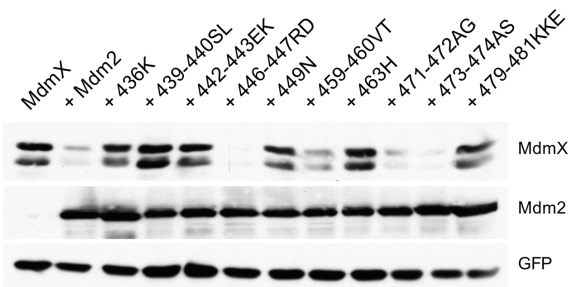


**FIGURE 1 |** Mutations mimicking MdmX RING sequence inhibit Mdm2 activity toward MdmX. **(A)** Schematic representation of human Mdm2 and MdmX proteins. RING domain sequences of selected mammalian Mdm2 and MdmX proteins were aligned using BOXSHADE 3.21 software at http://www.ch.embnet.org/software/BOX_form.html. Zinc coordinating residues are marked with an asterisk (*). Sites individually mutated in this study are marked in red. **(B)** Mdm2 mutants generated for this study. Selected amino acid residues were replaced with the corresponding MdmX RING residues. Some mutants presented in the table were created at later stages of the project (shown in *italics*). **(C)** The activity of selected mutants was tested in the MdmX degradation assay. U2OS cells were transiently transfected with combinations of plasmid vectors coding for Myc-tagged MdmX, GFP, and wild-type Mdm2 or the RING domain Mdm2 mutants. Lysates of transfected cells were analyzed by Western blotting.

MdmX, FLAG-tagged human wild-type p53 (pcDNA3-FLAG-p53), and the Mdm2/MdmX chimera (MDM2/MDMXRFD) have been described previously (Chen et al., 1993; Sharp et al., 1999; Kawai et al., 2003; Uldrijan et al., 2007). GFP-MdmX expression plasmid coding for N-terminally tagged full-length human MdmX was kindly provided by Robert Ludwig (The Beatson Institute, Glasgow, UK). Plasmid pRK5-HA-Ubiquitin-WT encoding hemagglutinin-tagged ubiquitin was a gift from Ted Dawson (Addgene plasmid # 17608). Empty vectors pcDNA3.1 and pEGFP-N1 were obtained from

Invitrogen and Clontech, respectively. All mutations within the RING domains of Mdm2 and MdmX were generated by PCR-mediated site-directed mutagenesis using Pfu DNA polymerase (Stratagene) and verified by DNA sequencing.

## p53 Degradation Assay

U2OS cells in 60-mm dishes were transfected with 0.1 μg FLAG-p53 and 1.4 μg Mdm2 mutant plasmid constructs using Effectene transfection reagent according to guidelines of the manufacturer (Qiagen). Each transfection mixture also contained 0.2 μg pEGFP-N1 (Clontech) to control for transfection efficiency, and empty plasmid pcDNA3.1 (Invitrogen) was used to bring the total amount of transfected DNA to 1.7 μg. Cells were washed with cold PBS 30 h post-transfection and lysed with 0.25 ml of SDS sample buffer. Proteins were resolved by SDS-polyacrylamide gel electrophoresis (SDS-PAGE) and analyzed by Western blotting with anti-Flag M2 (Sigma-Aldrich, F3165, 1:3,000), anti-Mdm2 Ab-1 (Merck, OP46, 1:1,000), and anti-GFP 7.1/13.1 (Roche, 11814460, 1:5,000) antibodies. In some experiments, p53 was also detected using the anti-p53 monoclonal antibody DO-1 (used at 0.2 μg/ml, kindly provided by Borivoj Vojtesek, Masaryk Memorial Cancer Institute, Brno).

## MdmX Degradation Assay

U2OS cells grown in 60-mm dishes were transfected with 1 μg Myc-MdmX and 6 μg wild-type Mdm2 or Mdm2 mutant plasmid constructs using Lipofectamine 2000 transfection reagent (Invitrogen) and DMEM was changed 4 h later. Each transfection mixture also contained 0.1 μg pEGFP-N1 as a control for transfection efficiency. The empty plasmid pcDNA3.1 was used to bring the total amount of transfected DNA to 7.1 μg in cells transfected with MdmX expression plasmid alone. Cells were cultured for 30 h, washed with cold PBS, and lysed with 0.3 ml of SDS-PAGE sample buffer. Proteins were resolved by SDS-PAGE and analyzed by Western blotting with anti-Myc 9E10 (Merck, MABE282, 1:1,000), anti-Mdm2 Ab-1 (Merck, OP46, 1:1,000), and anti-GFP 7.1/13.1 (Roche, 11814460, 1:5,000) antibodies.

## MdmX Relocalization Assay

U2OS cells grown on coverslips were transfected with Myc-tagged MdmX or GFP-tagged MdmX (0.3 μg), and wild-type Mdm2 expression plasmids or the Mdm2/MdmX chimeric construct (1.2 μg) using Effectene transfection reagent (Qiagen) and the culture medium was changed 4 h later. The empty plasmid pcDNA3.1 was used to bring the total amount of transfected DNA to 1.5 μg in cells transfected with MdmX expression plasmid alone. Twenty-four hours post-transfection, cells were treated with 15 μM MG132 (Sigma-Aldrich) in DMEM for 3 h, washed with PBS, and fixed in 4% paraformaldehyde in PBS for 10 min at room temperature. After fixation, cells were washed with PBS and permeabilized with PBS containing 0.2% Triton X-100 (Sigma-Aldrich) for 5 min. Cells were blocked with PBS containing 0.5% bovine serum albumin at room temperature for 30 min and then incubated for 2 h at room temperature with anti-Mdm2 mouse monoclonal antibody IF2 (Ab-1, Merck, OP46, 1:200) in the blocking solution or the anti-Mdm2 antibody together with anti-c-Myc rabbit polyclonal antibody (A-14, Santa Cruz Biotechnology sc-789, 1:250). Cells were washed with PBS and incubated for 1 h at room temperature with FITC- or DyLight™594-conjugated secondary antibodies (Jackson ImmunoResearch) in the blocking solution containing 1 μg/ml DAPI (Sigma-Aldrich). Cells were washed with PBS and mounted with VECTASHIELD HardSet Antifade Mounting Medium (Vector Laboratories). Images were taken with the FluoView 500 confocal laser scanning fluorescence microscopes (Olympus).

## Immunoprecipitations

HEK293 cells were transfected with 6 μg DNA per 100-mm plate using Lipofectamine 2000 reagent (Invitrogen). Cells were treated with a proteasome inhibitor (10 μM MG132 in cell culture medium) 24–36 h post-transfection, 4 h later washed with PBS, and lysed in Triton X-100 lysis buffer (1% Triton X-100, 150 mM NaCl, and 50 mM Tris pH 8.0) containing protease inhibitors (Complete Mini, Roche). Lysates were pre-cleared with 50 μl of protein G-Sepharose (Millipore). Immunoprecipitations were performed at 4°C with 1–2 μg of an antibody bound to 50 μl of protein G-Sepharose for 1 h. Mdm2 was immunoprecipitated with anti-Mdm2 antibody IF2 (Ab-1, Merck, OP46) and Myc-MdmX with anti-Myc antibody 9E10 (Merck, MABE282). Immunoprecipitated proteins were washed with lysis buffer and resuspended in SDS-PAGE sample buffer. Proteins from whole-cell extracts and immunoprecipitations were resolved by SDS-PAGE and analyzed by Western blotting with anti-Mdm2 Ab-1 (Merck, OP46, 1:1,000) and anti-Myc 9E10 (Merck, MABE282, 1:1,000) or anti-Myc A-14 (Santa Cruz Biotechnology, sc-789, 1:1,000).

## Mdm2-Mediated p53 Ubiquitylation in Cells

U2OS cells grown in 60-mm dishes were transiently transfected with FLAG-p53 (0.5 μg), hemagglutinin (HA)-ubiquitin (0.5 μg), and Mdm2 plasmid constructs (5 μg) using Lipofectamine 2000 reagent (Invitrogen) according to the manufacturer's recommendations. Empty plasmid pcDNA3.1 (Invitrogen) was used to bring the total amount of transfected DNA to 6 μg. Cells were treated 24 h post-transfection with 15 μM MG132 for 3 h, washed with PBS, and lysed in 0.3 ml 0.5% SDS. Lysates were boiled for 5 min, vortexed, cooled down to room temperature, and diluted with 1 ml of Triton X-100 lysis buffer. p53 was immunoprecipitated using 1 μg of anti-p53 monoclonal antibody DO-1 on a rotating wheel at 4°C. After 1 h of incubation, 20 μl of protein G-Sepharose beads (Sigma-Aldrich) were added for 45 min. The immunoprecipitates were washed three times with lysis buffer and analyzed by Western blotting. Ubiquitylated p53 was detected using anti-HA-Peroxidase antibody (Roche, 12013819001, 1:2,000); FLAG-p53 and MDM2 levels in the input were detected using anti-FLAG antibody M2 (Sigma-Aldrich), anti-Mdm2 Ab-1 (Merck).

## Modeling the MdmX-Mdm2-E2 Interactions

The Mdm2 contact residues mediating its binding to the MdmX and UbcH5b partners have been identified using COZOID (COntact ZOne IDentifier) tool (Furmanová et al., 2018; http://decibel.fi.muni.cz/cozoid/). The 2VJF, 2HDP, and 5MNJ structural data have been used for the Mdm2/MdmX analysis and visualization. Structures were visualized and simulated using the PyMOL tool (Molecular Graphics System, Version 1.7.2, Schrodinger, LLC; http://www.pymol.org).

# RESULTS

## The Systematic Mutational Analysis Identifies Mdm2 RING Residues Participating in MdmX Degradation

To identify conserved regions that could be responsible for the differential ability of Mdm2 and MdmX to form homodimers, we performed multiple alignments of Mdm2 and MdmX RING domain primary amino acid sequences of various mammalian species (**Figure 1A**). PCR-mediated site-directed mutagenesis was then used to introduce amino acid changes in the RING domain of full-length human Mdm2. In each of the mutants, a tiny part of the Mdm2 sequence (one, two, or three amino acids) was exchanged with the amino acid residues present in the corresponding region of human MdmX RING domain (**Figure 1B**). A cell-based MdmX degradation assay showed that many of the mutations introduced into Mdm2 RING disrupted the ability to target MdmX for degradation (**Figure 1C**). More specifically, the mutants 436K, 439–440SL, 442–443EK, 449N, 463H, and 479–481KKE had significantly impaired capacity to promote MdmX degradation, indicating that multiple differences between Mdm2 and MdmX could be responsible for the lack of E3 activity in MdmX RING and possibly also for its inability to form dimers. Therefore, in the next set of experiments, we analyzed the potential impact of the mutations on the physical interaction of the Mdm2 RING with the MdmX RING domain.

## A Single MdmX Residue Disrupts the Ability of Mdm2 RING to Bind MdmX

As already mentioned, Mdm2 not only regulates the stability of MdmX but can also induce changes in the subcellular localization of MdmX and promote its nuclear accumulation (Stad et al., 2001; Li et al., 2002). Mdm2 and MdmX proteins differ in the presence of signals for subcellular localization (**Figure 1A**). MdmX lacks the nuclear localization signal (NLS) and the nuclear export signal (NES) and is predominantly located in the cytoplasm, while Mdm2 contains both signals and shuttles continuously between the cell nucleus and cytoplasm. Despite this ability to dynamically change subcellular location, the majority of ectopically expressed Mdm2 protein can be detected in the nucleus of U2OS osteosarcoma cells. Importantly, when wild-type Mdm2 and MdmX are co-expressed at approximately 1:1 ratio, they dimerize through their respective RING domains, and the Mdm2-MdmX heterodimer localizes mainly to cell nucleus (Uldrijan et al., 2007). We performed this relocalization assay with all the Mdm2→MdmX RING domain mutants. Additional mutants 451I and 466-467RR were generated at this stage and included in the relocalization experiment to more thoroughly cover the differences between Mdm2 and MdmX RING domains.

To our surprise, the results suggested that all but one could physically interact with MdmX in living cells (**Figure 2A**). The only exception was the 449N mutant in which a single cysteine residue at position 449 of Mdm2 (C449) was exchanged with asparagine that is present at the corresponding position of MdmX RING (N448). The defect in MdmX interaction of the 449N Mdm2 mutant was confirmed in immunoprecipitations (**Figure 2B**). Wild-type Mdm2 and the 439–440SL and 442–443EK mutants that did not induce MdmX degradation but did not show a defect in the MdmX relocalization assay were used as positive controls, while the Mdm2Δ9 mutant lacking the conserved C-terminal tail required for Mdm2 RING dimerization was used as a negative control.

Both C449 and N448 are conserved in the Mdm2 and MdmX RING domains of all analyzed mammalian species (**Figure 1A**). As they are situated at the Mdm2-MdmX RING-RING interface (Linke et al., 2008; Nomura et al., 2017), these specific residues might be required for the optimal regulation of Mdm2-MdmX interactions. To test this hypothesis, we created additional Mdm2 RING mutants in which C449 was exchanged with alanine (449A) and serine (449S) residues. Analyses of the ability of the new mutants to interact with MdmX in the relocalization assays (**Figure 3A**) and immunoprecipitations (**Figure 3B**) indicated that, unlike 449N, they retained the ability to bind MdmX. However, the results of the immunoprecipitations suggested that the interaction between MdmX and the 449S mutant might be weaker than the interaction with wild-type Mdm2. These results indicated that only some residues at position 449 might be optimal for Mdm2 activity toward MdmX, potentially contributing to the conservation of cysteine 449 of Mdm2 in evolution.

## Exchange of a Single Residue Stimulates MdmX RING Domain Homodimerization

In the next set of experiments, we turned our attention to the RING domain of MdmX. We performed site-directed mutagenesis of the conserved asparagine 448 in MdmX RING into cysteine to mimic the critical C449 residue of Mdm2. However, to be able to test the effect of the mutation on MdmX homodimerization in the relocalization assay, we mutated N448 not only in the context of the full-length MdmX protein but also in a previously constructed Mdm2/MdmX chimera (Mdm2/X). This protein retains most of the Mdm2 sequence (including the NLS and NES localization signals) but the C-terminal portion of Mdm2 including the RING domain was exchanged with the MdmX sequence [**Figure 4A**, (Kawai et al., 2003)]. Like wild-type Mdm2, the Mdm2/X chimeric protein localizes mainly to the nucleus, but it is not able to relocalize wild-type MdmX into cell nucleus as two MdmX RING domains

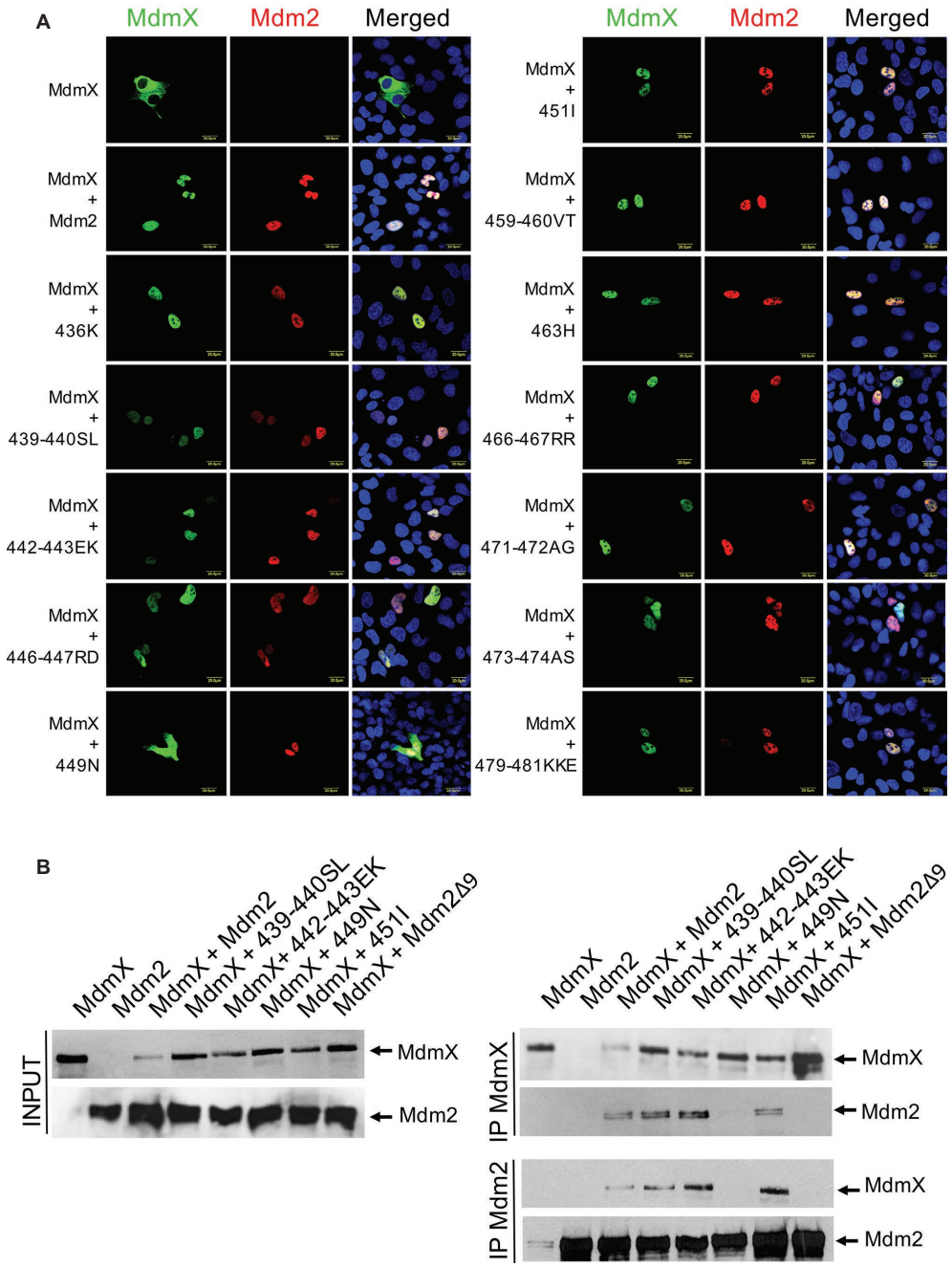


**FIGURE 2 |** Most Mdm2 mutants mimicking MdmX RING sequence retain the ability to heterodimerize with MdmX. **(A)** MdmX relocalization assay. U2OS cells were transfected with GFP-tagged MdmX expression plasmid together with plasmids coding for wild-type Mdm2 or the Mdm2 RING mutants. MdmX was detected by GFP fluorescence (green) and Mdm2 by immunofluorescence (red). DAPI was used to label cell nuclei (blue). **(B)** Immunoprecipitations. Plasmid constructs encoding selected Mdm2 mutants were transiently transfected into HEK293 cells together with Myc-tagged MdmX plasmid construct. Cells were treated 24 h post-transfection with the proteasome inhibitor MG132 for 4 h, lysed, and immunoprecipitated with anti-Mdm2 and anti-Myc antibodies. Immunoprecipitates were analyzed by Western blotting. INPUT: Mdm2 and MdmX levels in cell lysates. IP MdmX: Mdm2 and MdmX levels in samples immunoprecipitated using the anti-Myc tag antibody. IP Mdm2: MdmX and Mdm2 levels in samples immunoprecipitated with the anti-Mdm2 antibody.

do not interact. However, when we introduced cysteine instead of asparagine at the position corresponding to N448 in the MdmX RING domain of the chimera (Mdm2/X:448C), it induced nuclear localization of the wild-type MdmX protein (**Figure 4B**). Analogically, when the cysteine residue was introduced into the MdmX protein (MdmX:448C), the unmutated Mdm2/X chimera, retaining asparagine at the position corresponding to 448 of MdmX, was able to relocalize the

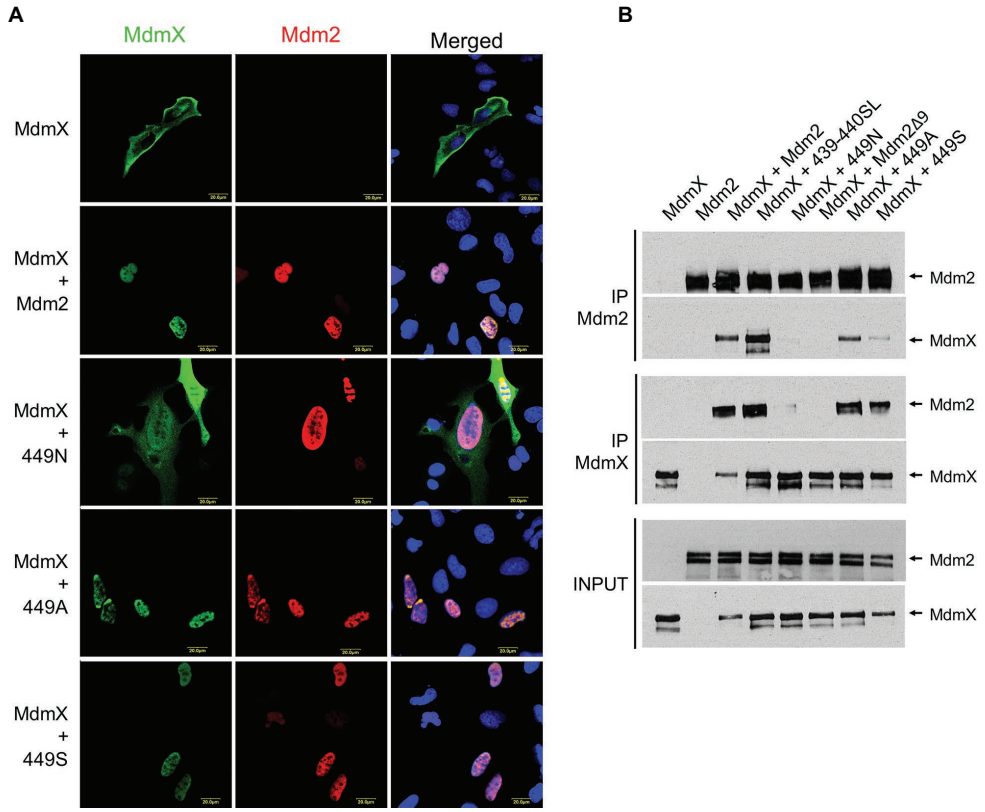


**FIGURE 3 |** C449N mutation disrupts Mdm2-MdmX heterodimerization and MdmX degradation. **(A)** MdmX relocalization assay. U2OS cells were transfected with GFP-tagged MdmX together with wild-type Mdm2 or selected Mdm2 C449 mutants. MdmX was detected by GFP fluorescence (green) and Mdm2 by immunofluorescence (red). DAPI was used to label cell nuclei (blue). **(B)** Immunoprecipitations. Selected Mdm2 mutants were transiently transfected into HEK293 cells together with Myc-tagged MdmX. Cells were treated 24 h post-transfection with the proteasome inhibitor MG132 for 4 h, lysed, and immunoprecipitated with anti-Mdm2 and anti-Myc antibodies. Immunoprecipitates were analyzed by Western blotting. INPUT: Mdm2 and MdmX levels in cell lysates. IP MdmX: Mdm2 and MdmX levels in samples immunoprecipitated using the anti-Myc tag antibody. IP Mdm2: MdmX and Mdm2 levels in samples immunoprecipitated with the anti-Mdm2 antibody.

mutated MdmX protein to the nucleus (**Figure 4C**). This result confirmed the critical importance of the cysteine residue present in Mdm2 at position 449 for the RING domain-mediated dimerization. Moreover, it indicated that the ability of two MdmX RING domains to dimerize could be induced already by introducing the critical cysteine residue into one of the interacting RING domains, in a manner similar to the heterodimerization between Mdm2 and MdmX RING domains.

Interestingly, in immunoprecipitations, the interaction of two MdmX RINGs was observed only when the cysteine residue was introduced into both of them (**Figure 5A**), suggesting that heterocomplexes containing one MdmX RING with cysteine at position 448 and one wild-type MdmX RING with arginine at the same position might be less stable. Interestingly, two out of three performed immunoprecipitation assays showed that MdmX 448C could also interact with wild-type Mdm2, but not with Mdm2 449N (**Figure 5B**). A similar difference was also seen in the cell-based relocalization assay (**Figure 5C**). This result suggested that we could not recapitulate the normal mode of Mdm2-MdmX interactions by merely swapping the critical C449/N448 residues between Mdm2 and MdmX. Therefore, it is probable that other residues in the context of the RING domains are also significantly contributing to the optimal Mdm2-MdmX dimerization.

## Differential Participation of the Conserved RING Residues in the Activity of Mdm2 Homodimers and Mdm2/MdmX Heterodimers

The structural analyses of Mdm2 homodimers and Mdm2-MdmX heterodimers indicated that Mdm2 RING binds both the E2 ubiquitin-conjugating enzyme and ubiquitin, while MdmX does not bind E2 and contacts only ubiquitin, *via* its C-terminal tail (Kostic et al., 2006; Linke et al., 2008; Nomura et al., 2017). We modeled the Mdm2/E2 interface using the recently published MdmX-Mdm2-E2 structure and found that potentially critical residues E436, V439, I440, Q442, and R479 were disrupted in the mutants that were inactive in the MdmX degradation assay (**Figures 6A,B**). Their location at the Mdm2/E2 interface could help to explain why the MdmX

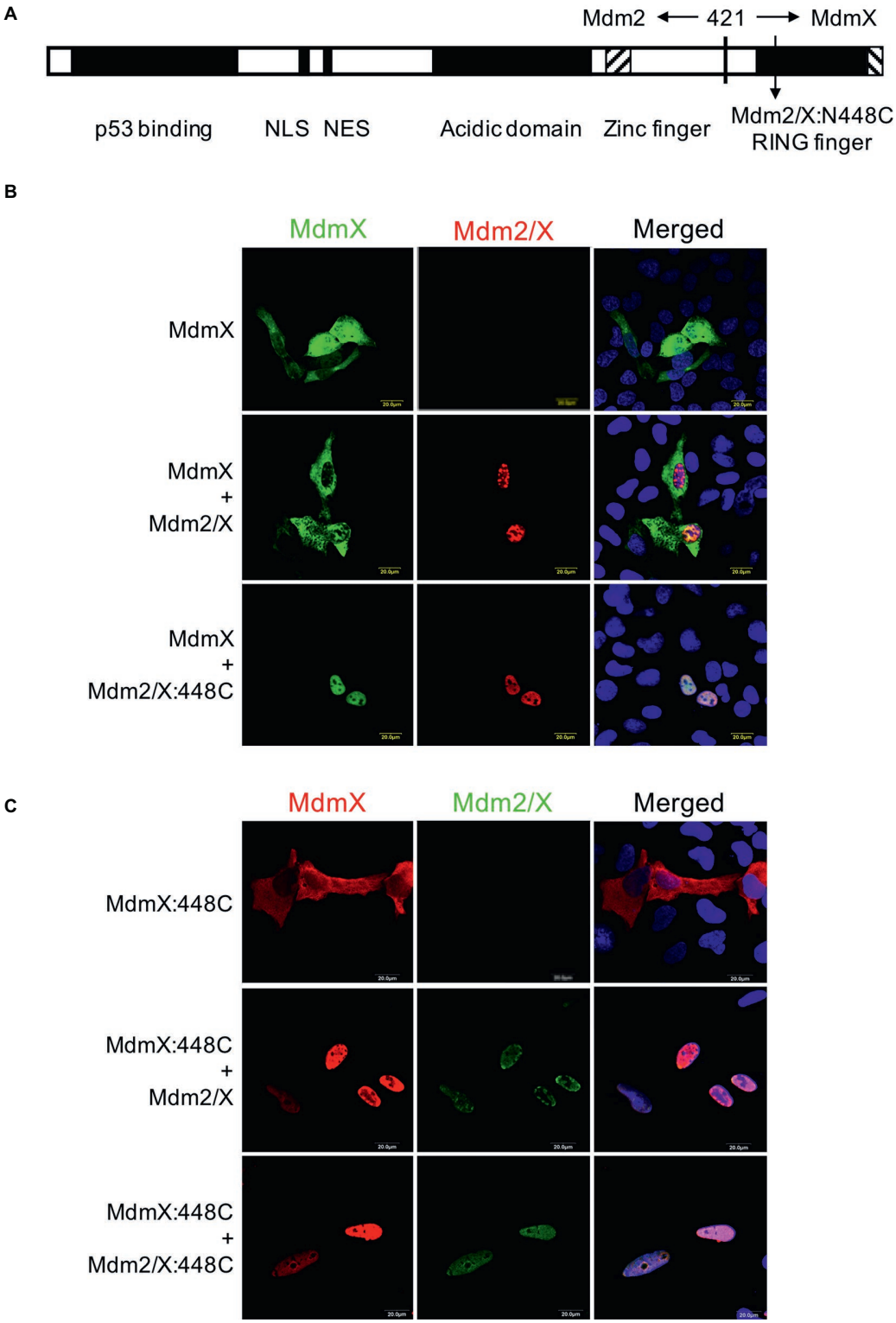


**FIGURE 4 |** Replacing N448 of MdmX RING with cysteine to mimic Mdm2 C449 promotes MdmX homodimerization *in vivo*. **(A)** Schematic representation of the Mdm2/MdmX chimeric protein (Mdm2/X). **(B)** MdmX relocalization assay. U2OS cells were transfected with GFP-tagged MdmX plasmid construct together with plasmids coding for Mdm2/X or Mdm2/X:448C in which the critical asparagine residue was replaced with cysteine. MdmX was detected by GFP fluorescence (green) and Mdm2/X by immunofluorescence (red). DAPI was used to label cell nuclei (blue). **(C)** MdmX relocalization assay. U2OS cells were transfected with plasmid construct encoding Myc-MdmX, in which the critical asparagine residue was replaced with cysteine (MdmX:448C), together with plasmids coding for Mdm2/X or Mdm2/X:448C. MdmX (red) and Mdm2/X (green) were detected by immunofluorescence. DAPI was used to label cell nuclei (blue).

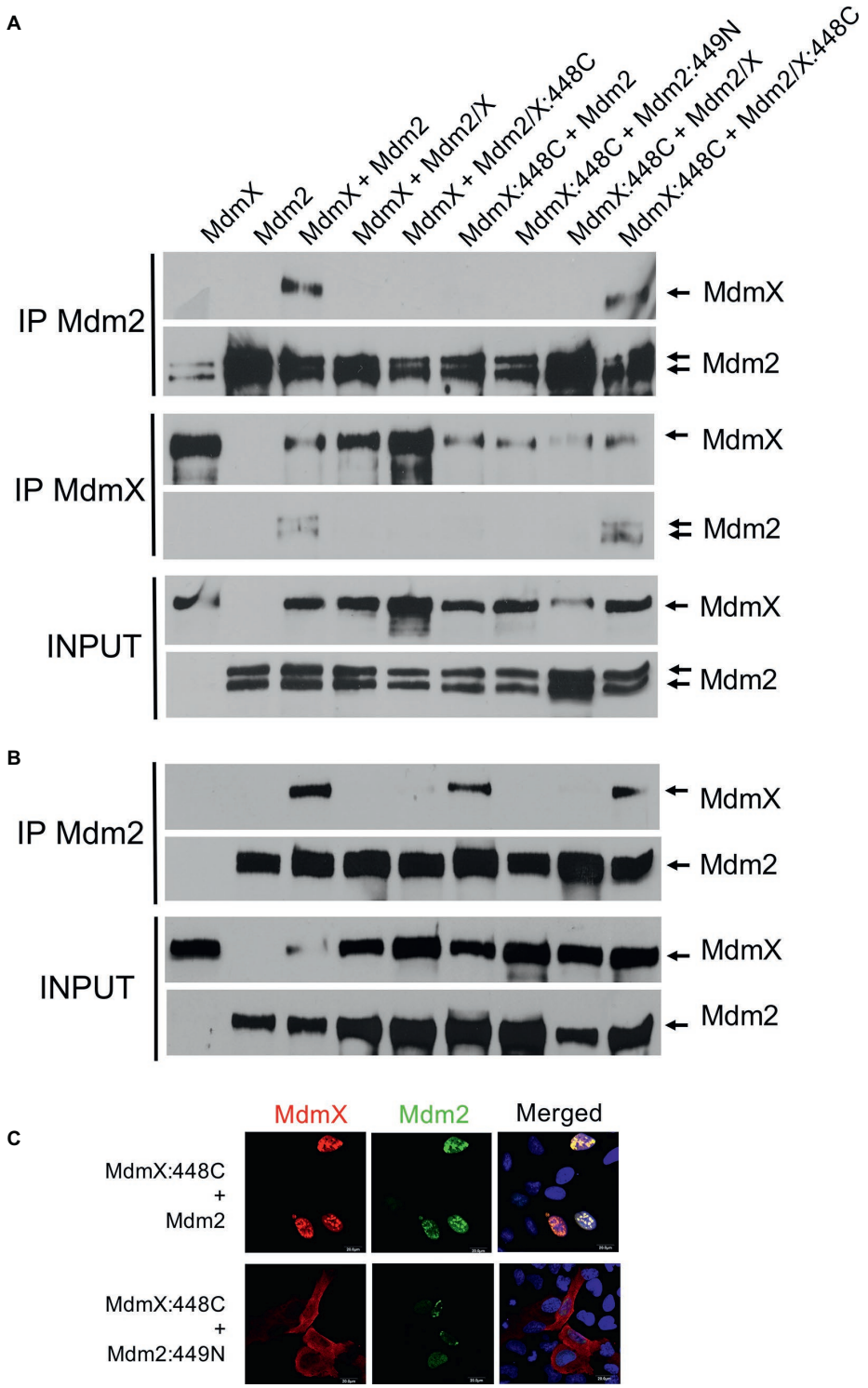


**FIGURE 5 |** MdmX N448C RING domain dimerization **(A)** Immunoprecipitations. Mdm2, Myc-MdmX, and Mdm2/X plasmid constructs were transiently transfected into HEK293 cells. Cells were treated 24 h post-transfection with proteasome inhibitor MG132 for 4 h, lysed, and immunoprecipitated with an anti-Mdm2 antibody. Immunoprecipitates were analyzed by Western blotting. INPUT: Mdm2 and MdmX levels in cell lysates. IP MdmX: Mdm2 and MdmX levels in samples immunoprecipitated using the anti-Myc tag antibody. IP Mdm2: MdmX and Mdm2 levels in samples immunoprecipitated with the anti-Mdm2 antibody. MdmX RING homodimerization was observed only when both RINGs contained a cysteine residue at position 448. **(B)** Immunoprecipitations. In addition to the MdmX 448C-MdmX 448C homodimerization, the interaction between MdmX 448C and wild-type Mdm2 was also observed in some immunoprecipitation experiments. Samples were loaded in the same order as in **(A)**. **(C)** MdmX relocalization assay. The interaction between MdmX 448C (red) and Mdm2 (green) was observed also in this assay. Experiment performed as in **Figure 4C**.

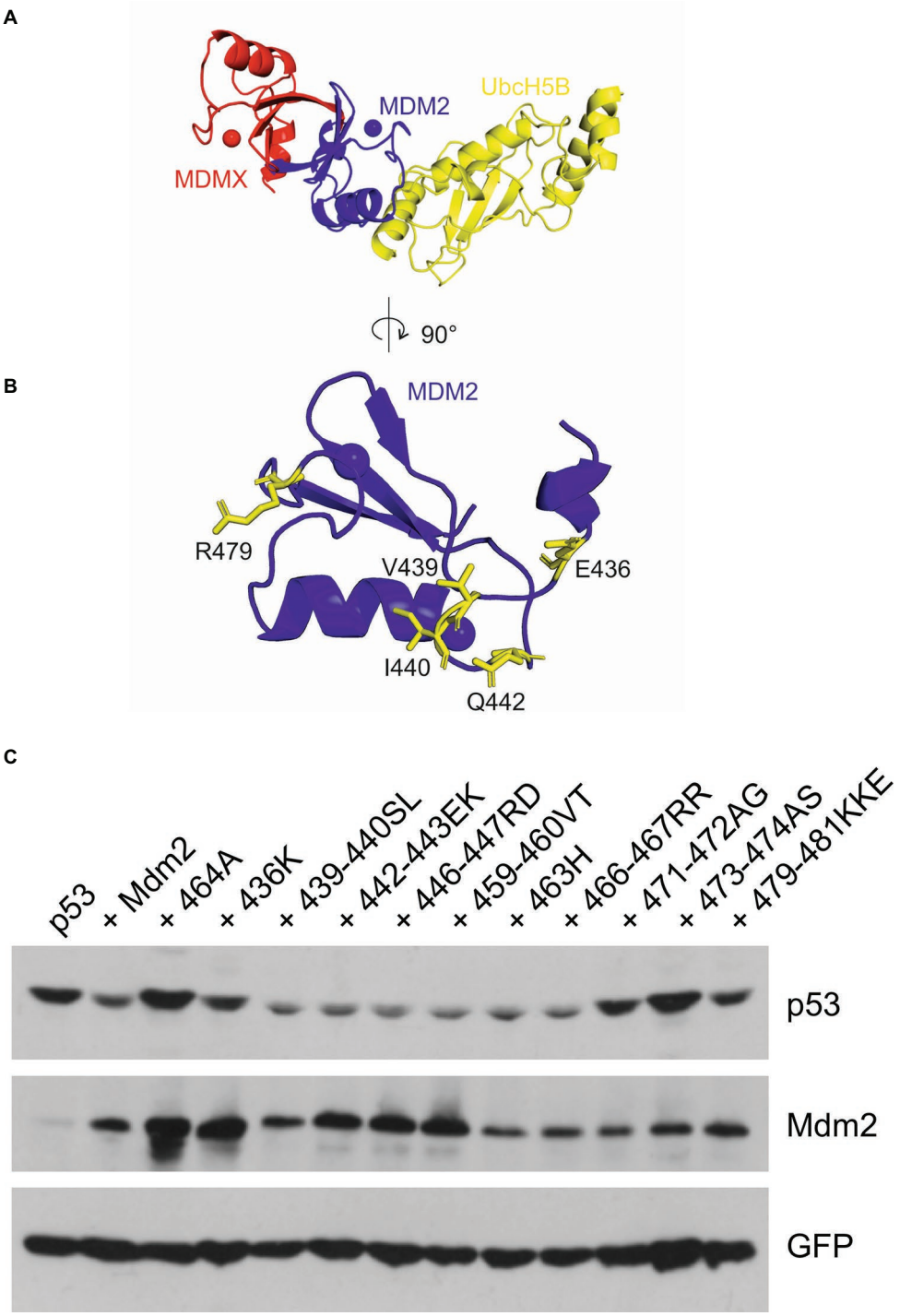


**FIGURE 6 |** Mutations of Mdm2/E2 contact residues can have a different impact on Mdm2 activity toward different targets. **(A)** Structure of the MdmX-Mdm2-UbcH5b complex (PDB: 5MNJ) (Nomura et al., 2017). Mdm2 (blue) binds MdmX (red) and UbcH5b (yellow) *via* opposite contact surfaces. **(B)** The Mdm2 contact surface view with the E436, V439, I440, Q442, and R479 contact residues mediating Mdm2-UbcH5b interaction highlighted in yellow. (**C**) p53 degradation assay. U2OS cells were transfected with plasmids coding for GFP, FLAG-tagged p53, and wild-type Mdm2 or selected Mdm2 mutants. Cells were lysed 30 h post-transfection and proteins were resolved by SDS-PAGE and analyzed by Western blotting.

residues in 436K, 439–440SL, 442–443EK, and 479–481KKE inhibited the activity of these mutants toward MdmX. We reasoned that mutations actively disrupting the Mdm2/E2 interface and E2 binding should inhibit the E3 activity of not only Mdm2-MdmX heterodimers but also Mdm2 homodimers. To our surprise, however, in a p53 degradation assay, we observed

a decreased activity toward p53 of mutants 436K and 479–481KKE, while mutants 439–440SL and 442-442EK remained fully active (**Figure 6C**). These results indicated that the contribution of individual residues at the Mdm2/E2 interface to E2 binding might differ in Mdm2 homodimers and Mdm2-MdmX heterodimers. Interestingly, we also identified two mutants that were able to degrade MdmX, 471-472AG, and 473-474AS (**Figure 1C**), but could not efficiently target p53 for degradation. This result suggested that residues 471–474 could specifically be required for the E3 activity of Mdm2 homodimer and p53 degradation (**Figure 6C**).

We also modeled the RING-RING interface and mapped the position of the critical cysteine 449 and asparagine 448 residues. Two cysteine residues could serve as contact sites at the interface of the Mdm2 RING homodimer (**Figures 7A,B**). In contrast, in a simulated MdmX RING homodimer, the two asparagine residues clashed and did not seem compatible with homodimerization (**Figure 7C**). The apparent structural similarity of the RING domains of Mdm2 and MdmX suggested that replacing C449 of Mdm2 with asparagine would disrupt not only its interaction with MdmX but also the homodimerization of the Mdm2 RING and its activity

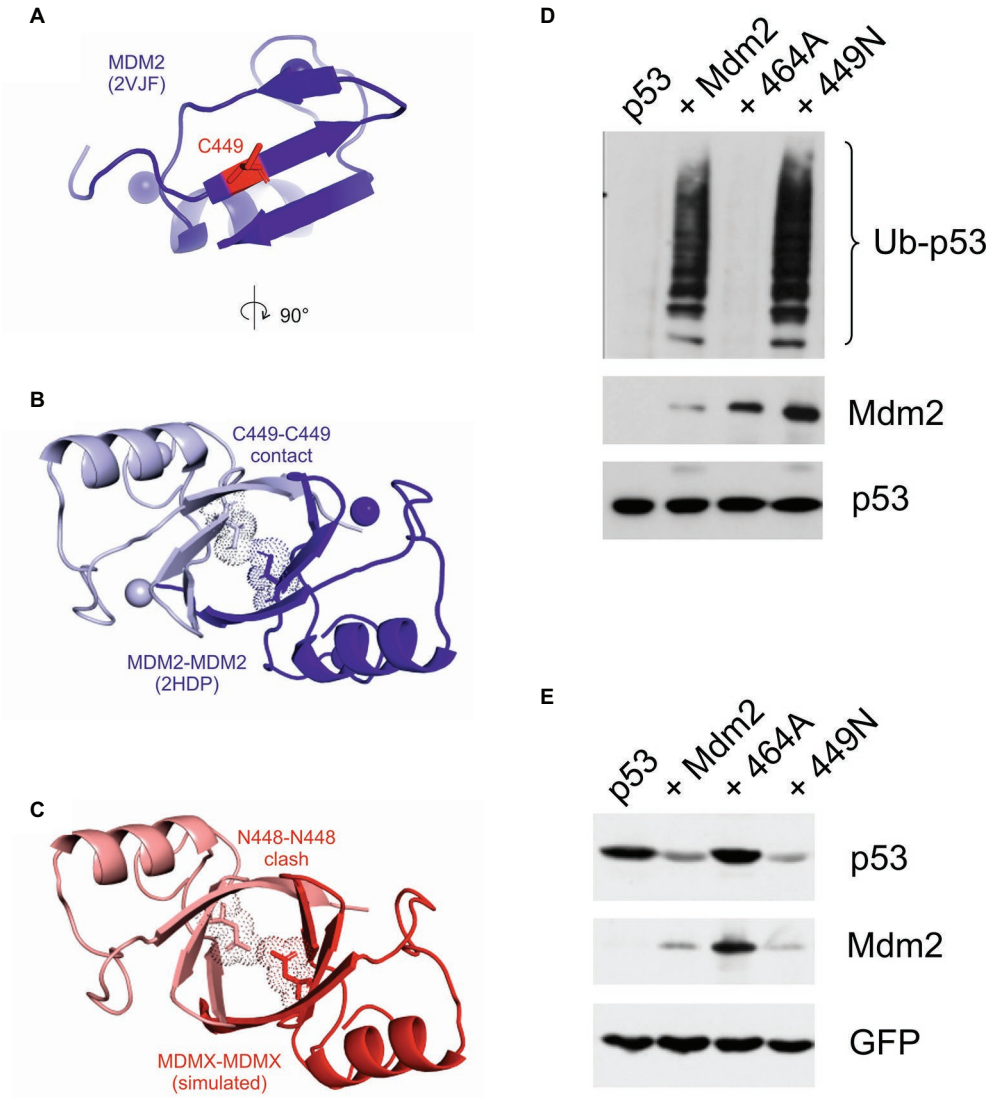


**FIGURE 7 |** Mutations of the conserved C449 residue can have a different impact on Mdm2 activity toward different targets. **(A)** The Mdm2 dimerization interface (2VJF) (blue) with highlighted central C449 residue (red stick). **(B)** The Mdm2-Mdm2 homodimer (2HDP) with highlighted central C449-C449 contact (sticks and dots). **(C)** In the simulated MdmX-MdmX homodimer (red), the central N448 residues (sticks and dots) are clashing at the dimer interface. **(D)** Cell-based p53 ubiquitylation assay. U2OS cells were transfected with plasmids encoding HA-tagged ubiquitin, FLAG-tagged p53, and wild-type Mdm2 or selected Mdm2 mutants. Cells were treated with a proteasome inhibitor 24 h post-transfection, lysed under denaturing conditions to disrupt non-covalent protein–protein interactions, lysates were diluted, and p53 was immunoprecipitated. Samples were resolved by SDS-PAGE and Western blotting was used to determine the levels of p53 and Mdm2 in cell lysates and HA-ubiquitin linked to p53 in immunoprecipitates. **(E)** p53 degradation assay. U2OS cells were transfected with GFP, FLAG-tagged p53, and wild-type Mdm2 or selected Mdm2 mutants. Cells were lysed 30 h post-transfection and proteins were resolved by SDS-PAGE and analyzed by Western blotting.

toward p53. Surprisingly, the 449N mutant was active in a p53 ubiquitylation assay (**Figure 7D**) and capable of inducing p53 degradation (**Figure 7E**), strongly suggesting that the replacement of C449 with asparagine did not disrupt Mdm2 RING homodimerization. These results indicated that the impact of the two critical residues C449 and N448 on RING dimerization could be context-specific and modified by other RING domain residues.

## DISCUSSION

The complex and dynamic relationship between Mdm2 and MdmX, which is key to the regulation of p53 stability and function, is enabled, at least in part, by the differential ability of the Mdm2 and MdmX RING domains to form dimers and serve as E3 ubiquitin ligases. Although the conserved RING domains of the two proteins exhibit a high degree of homology and structural similarity (Kostic et al., 2006; Linke et al., 2008; Tan et al., 2016), only Mdm2 RING can form homodimers and serve as E3 on its own, while the MdmX RING domain does not appear to have appreciable E3 ubiquitin ligase activity. On the other hand, the MdmX RING domain can actively contribute to Mdm2 E3 activity in the form of the Mdm2-MdmX heterodimer (Kawai et al., 2007; Poyurovsky et al., 2007; Singh et al., 2007; Uldrijan et al., 2007).

The previously published structural analyses indicated possible molecular determinants of the difference in E3 activity between the Mdm2 and MdmX RINGs. Linke et al. have predicted the putative E2-binding site on the Mdm2 RING domain by comparison with the E2/E3 complex of UbcH7 and the RING domain of c-Cbl, and mapped the residues required for functional interaction with the E2 enzyme UbcH5b by mutating the predicted residues to alanine (Linke et al., 2008). Hydrophobic contacts appeared critical since mutations of I440, L468, and P476 abolished activity. Adjacent residues were also deemed important since a mutation of R479 disrupted activity, while mutations of V439 and R471 reduced E3 activity. Many of the surface-exposed residues within Mdm2 predicted to be required for recruiting the E2 are conserved in MdmX, while some of the surrounding residues differ. To determine if these differences render MdmX inactive, Linke et al. mutated selected residues in MdmX to their Mdm2 equivalents, but none of these changes were able to turn on the E3 activity in the MdmX RING domain. The authors concluded that many small differences might contribute to the inactivity of MdmX (Linke et al., 2008).

A recent analysis of the Mdm2RING-MdmXRING-E2(UbcH5b)-ubiquitin complex suggested that despite their apparent structural similarity, the Mdm2 homodimer and Mdm2-MdmX heterodimer have differing abilities to transfer Ub due to their abilities to interact with E2~Ub complexes (~ indicates thioester bond). While Mdm2 RING could bind both UbcH5b and ubiquitin, MdmX did not bind the E2 enzyme and contacted only ubiquitin, *via* its C-terminal tail. The study also identified the conserved arginine residue at position 479 as critical for stabilizing the closed conformation of E2~Ub and the 479K mutant was shown to be defective in discharging UbcH5b~Ub (Nomura et al., 2017).

In the present study, we used PCR-mediated site-directed mutagenesis of the Mdm2 RING domain in the context of full-length Mdm2 to identify residues that could be responsible for the apparent lack of the capacity to homodimerize and low intrinsic E3 activity of the MdmX RING. We mutated parts of the Mdm2 RING into the corresponding MdmX residues and observed a significant drop in the activity toward MdmX in mutants affecting E436, VI439–440, QG442–443, C449, T463, and RQP479–481. Of these mutants, 436K, 439–440SL, 442-442EK, and 479–481KKE could be inactive because they lost at least one residue predicted to participate in the interaction with E2. Surprisingly, however, mutants 439–440SL and 442-442EK were still capable of targeting p53 for degradation, indicating that they remained active in the form of the Mdm2-Mdm2 homodimer. Such a result might suggest that a different set of residues at the Mdm2/E2 interface might be required for E2 binding in Mdm2 homodimers and Mdm2-MdmX heterodimers. Importantly, our mutant 479–481KKE was inactive both in the form of heterodimer and homodimer, confirming the critical contribution of R479 to the ubiquitin ligase activity of Mdm2 (Nomura et al., 2017).

Our study also identified the conserved cysteine 449 of Mdm2 and asparagine 448 of MdmX located at the RING-RING interface as critical determinants of the ability of Mdm proteins to form dimers *in vivo*. When cysteine was introduced into the corresponding position in the MdmX RING, the mutant MdmX protein gained the ability to form homodimers. Our data are consistent with earlier studies in which the RING domain of MdmX was mutated to contain selected Mdm2 residues. Iyappan et al. turned MdmX into an active ubiquitin ligase by mutating N448 to cysteine and replacing residues 465–480 with the corresponding Mdm2 sequence (Iyappan et al., 2010). Egorova and Sheng performed mutational analysis of isolated MdmX RING domain and tested the ubiquitin ligase activity of the mutants *in vitro*. They found that substitution of N448 for cysteine and K478 for arginine granted the MdmX RING domain the E3 activity. Based on subsequent structural analysis, the authors reasoned that C449 of Mdm2 is critical for the stability of the RING dimer structure, while R479 could play a role in recruiting and activating the ubiquitin E2 conjugating enzyme (Egorova and Sheng, 2014). The critical role of cysteine 449 and arginine 479 in the E3 activity of Mdm2 RING was also confirmed by Nomura et al., who found that substituting N448 and K478 to cysteine and arginine, respectively, was sufficient to unmask the ubiquitin ligase activity toward p53 in the Mdm2/X chimera (Nomura et al., 2017).

Interestingly, we found that only one RING with the N448C exchange was required for MdmX RING homodimerization *in vivo*, in line with the results of structural analyses indicating that cysteine and asparagine residues contact in the Mdm2-MdmX heterodimer, but two asparagine residues would clash, preventing MdmX homodimerization. However, in immunoprecipitations, we could detect MdmX homodimerization only when N448 was mutated to cysteine in both MdmX RING domains, suggesting that the context of the RING domain also plays a role. Moreover, the interaction between Mdm2 and MdmX RING domains also

seemed unstable when the two critical residues were swapped, as we could not detect the binding of Mdm2 449N to MdmX 448C in the immunoprecipitation assay, despite the predicted compatibility of the two residues. Last but not least, the Mdm2 449N mutant still served as E3 ubiquitin ligase targeting p53 for degradation, again suggesting that the asparagine and cysteine residues had a differential impact on Mdm RING domain function depending on the structural context.

It seems that the tight mutual regulation of Mdm2, MdmX, and p53 activity in cells is enabled by many individual differences between the RINGs of Mdm2 and MdmX that participate in the control of RING dimerization and E2 binding.

## AUTHOR CONTRIBUTIONS

PK, IS, and AV performed experiments and prepared the figures. BV, PM, and JP analyzed the results and prepared the figures. SU conceived the study, performed experiments, analyzed the results, and wrote the manuscript.

## FUNDING

This work was supported by the Czech Science Foundation (GA14-12166S), the Specific University Research (MUNI/A/0754/2017), the National Program of Sustainability II (MEYS CR, project No. LQ1605), and Internal Masaryk University grant (MU/0822/2015).

## ACKNOWLEDGMENTS

We thank Karen Vousden, Robert Ludwig, Donna George, Arnie Levine, Ted Dawson, and Zhi-Min Yuan for the expression plasmids and Borivoj Vojtesek for the anti-p53 antibody.

## REFERENCES

Argentini, M., Barboule, N., and Wasylyk, B. (2001). The contribution of the acidic domain of MDM2 to p53 and MDM2 stability. *Oncogene* 20, 1267–1275. doi: 10.1038/sj.onc.1204241

Bista, M., Petrovich, M., and Fersht, A. R. (2013). MDMX contains an autoinhibitory sequence element. *Proc. Natl. Acad. Sci. USA* 110, 17814–17819. doi: 10.1073/pnas.1317398110

Chen, L., Borcherds, W., Wu, S., Becker, A., Schonbrunn, E., Daughdrill, G. W., et al. (2015). Autoinhibition of MDMX by intramolecular p53 mimicry. *Proc. Natl. Acad. Sci. USA* 112, 4624–4629. doi: 10.1073/pnas.1420833112

Chen, J., Marechal, V., and Levine, A. J. (1993). Mapping of the p53 and mdm-2 interaction domains. *Mol. Cell. Biol.* 13, 4107–4114. doi: 10.1128/MCB.13.7.4107

Cheng, Q., Song, T., Chen, L., and Chen, J. (2014). Autoactivation of the MDM2 E3 ligase by intramolecular interaction. *Mol. Cell. Biol.* 34, 2800–2810. doi: 10.1128/MCB.00246-14

Dang, J., Kuo, M., Eischen, C., Stepanova, L., Sherr, C. J., and Roussel, M. F. (2002). The RING domain of Mdm2 can inhibit cell proliferation. *Cancer Res.* 62, 1222–1230.

Dolezelova, P., Cetkovska, K., Vousden, K. H., and Uldrijan, S. (2012a). Mutational analysis of Mdm2 C-terminal tail suggests an evolutionarily conserved role of its length in Mdm2 activity toward p53 and indicates structural differences between Mdm2 homodimers and Mdm2 / MdmX heterodimers. *Cell Cycle* 11, 953–962. doi: 10.4161/cc.11.5.19445

Dolezelova, P., Cetkovska, K., Vousden, K. H., and Uldrijan, S. (2012b). Mutational analysis reveals a dual role of Mdm2 acidic domain in the regulation of p53 stability. *FEBS Lett.* 586, 2225–2231. doi: 10.1016/j.febslet.2012.05.034

Egorova, O., and Sheng, Y. (2014). A site-directed mutagenesis study of the MdmX RING domain. *Biochem. Biophys. Res. Commun.* 447, 696–701. doi: 10.1016/j.bbrc.2014.04.065

Fang, S., Jensen, J. P., Ludwig, R. L., Vousden, K. H., and Weissman, A. M. (2000). Mdm2 is a RING finger-dependent ubiquitin protein ligase for itself and p53. *J. Biol. Chem.* 275, 8945–8951. doi: 10.1074/jbc.275.12.8945

Furmanová, K., Byška, J., Gröller, E. M., Viola, I., Paleček, J. J., and Kozlíková, B. (2018). COZOID: contact zone identifier for visual analysis of protein-protein interactions. *BMC Bioinform.* 19, 1–17. doi: 10.1186/s12859-018-2113-6

Gu, J., Kawai, H., Nie, L., Kitao, H., Wiederschain, D., Jochemsen, A. G., et al. (2002). Mutual dependence of MDM2 and MDMX in their functional inactivation of p53. *J. Biol. Chem.* 277, 19251–19254. doi: 10.1074/jbc.C200150200

Huang, L., Yan, Z., Liao, X., Li, Y., Yang, J., Wang, Z.-G., et al. (2011). The p53 inhibitors MDM2/MDMX complex is required for control of p53 activity in vivo. *Proc. Natl. Acad. Sci. USA* 108, 12001–12006. doi: 10.1073/pnas.1102309108

Iyappan, S., Wollscheid, H. P., Rojas-Fernandez, A., Marquardt, A., Tang, H. C., Singh, R. K., et al. (2010). Turning the RING domain protein MdmX into an active ubiquitin-protein ligase. *J. Biol. Chem.* 285, 33065–33072. doi: 10.1074/jbc.M110.115113

Jones, S. N., Roe, A. E., Donehower, L. A., and Bradley, A. (1995). Rescue of embryonic lethality in Mdm2-deficient mice by absence of p53. *Nature* 378, 206–208. doi: 10.1038/378206a0

Kawai, H., Lopez-Pajares, V., Kim, M. M., Wiederschain, D., and Yuan, Z.-M. (2007). RING domain-mediated interaction is a requirement for MDM2's E3 ligase activity. *Cancer Res.* 67, 6026–6030. doi: 10.1158/0008-5472.CAN-07-1313

Kawai, H., Wiederschain, D., and Yuan, Z. (2003). Critical contribution of the MDM2 acidic domain to p53 ubiquitination. *Mol. Cell. Biol.* 23, 4939–4947. doi: 10.1128/mcb.23.14.4939-4947.2003

Kostic, M., Matt, T., Martinez-Yamout, M. A., Dyson, H. J., and Wright, P. E. (2006). Solution structure of the Hdm2 C2H2C4 RING, a domain critical for ubiquitination of p53. *J. Mol. Biol.* 363, 433–450. doi: 10.1016/j.jmb.2006.08.027

Li, C., Chen, L., and Chen, J. (2002). DNA damage induces MDMX nuclear translocation by p53-dependent and -independent mechanisms. *Mol. Cell. Biol.* 22, 7562–7571. doi: 10.1128/mcb.22.21.7562-7571.2002

Linares, L. K., Hengstermann, A., Ciechanover, A., Müller, S., and Scheffner, M. (2003). HdmX stimulates Hdm2-mediated ubiquitination and degradation of p53. *Proc. Natl. Acad. Sci. USA* 100, 12009–12014. doi: 10.1073/pnas.2030930100

Linke, K., Mace, P. D., Smith, C. A., Vaux, D. L., Silke, J., and Day, C. L. (2008). Structure of the MDM2/MDMX RING domain heterodimer reveals dimerization is required for their ubiquitylation in trans. *Cell Death Differ.* 15, 841–848. doi: 10.1038/sj.cdd.4402309

Marine, J.-C., Francoz, S., Maetens, M., Wahl, G., Toledo, F., and Lozano, G. (2006). Keeping p53 in check: essential and synergistic functions of Mdm2 and Mdm4. *Cell Death Differ.* 13, 927–934. doi: 10.1038/sj.cdd.4401912

Metzger, M. B., Pruneda, J. N., Klevit, R. E., and Weissman, A. M. (2014). RING-type E3 ligases: master manipulators of E2 ubiquitin-conjugating enzymes and ubiquitination. *Biochim. Biophys. Acta Mol. Cell Res.* 1843, 47–60. doi: 10.1016/j.bbamcr.2013.05.026

Meulmeester, E., Frenk, R., Stad, R., de Graaf, P., Marine, J., Vousden, K. H., et al. (2003). Critical role for a central part of Mdm2 in the ubiquitylation of p53. *Mol. Cell. Biol.* 23, 4929–4938. doi: 10.1128/mcb.23.14.4929-4938.2003

Migliorini, D., Lazzerini Denchi, E., Danovi, D., Jochemsen, A., Capillo, M., Gobbi, A., et al. (2002). Mdm4 (Mdmx) regulates p53-induced growth arrest and neuronal cell death during early embryonic mouse development. *Mol. Cell. Biol.* 22, 5527–5538. doi: 10.1128/MCB.22.15.5527-5538.2002

Momand, J., Jung, D., Wilczynski, S., and Niland, J. (1998). The MDM2 gene amplification database. *Nucleic Acids Res.* 26, 3453–3459. doi: 10.1093/nar/26.15.3453

Momand, J., Zambetti, G. P., Olson, D. C., George, D., and Levine, A. J. (1992). The mdm-2 oncogene product forms a complex with the p53 protein and inhibits p53-mediated transactivation. *Cell* 69, 1237–1245. doi: 10.1016/0092-8674(92)90644-R

Montes de Oca Luna, R., Wagner, D. S., and Lozano, G. (1995). Rescue of early embryonic lethality in mdm2-deficient mice by deletion of p53. *Nature* 378, 203–206. doi: 10.1038/378203a0

Nomura, K., Klejnot, M., Kowalczyk, D., Hock, A. K., Sibbet, G. J., Vousden, K. H., et al. (2017). Structural analysis of MDM2 RING separates degradation from regulation of p53 transcription activity. *Nat. Struct. Mol. Biol.* 24, 578–587. doi: 10.1038/nsmb.3414

Parant, J., Chavez-Reyes, A., Little, N. A., Yan, W., Reinke, V., Jochemsen, A. G., et al. (2001). Rescue of embryonic lethality in Mdm4-null mice by loss of Trp53 suggests a nonoverlapping pathway with MDM2 to regulate p53. *Nat. Genet.* 29, 92–95. doi: 10.1038/ng714

Poyurovsky, M. V., Priest, C., Kentsis, A., Borden, K. L. B., Pan, Z.-Q., Pavletich, N., et al. (2007). The Mdm2 RING domain C-terminus is required for supramolecular assembly and ubiquitin ligase activity. *EMBO J.* 26, 90–101. doi: 10.1038/sj.emboj.7601465

Ringshausen, I., O'Shea, C. C., Finch, A. J., Swigart, L. B., and Evan, G. I. (2006). Mdm2 is critically and continuously required to suppress lethal p53 activity in vivo. *Cancer Cell* 10, 501–514. doi: 10.1016/j.ccr.2006.10.010

Sharp, D. A., Kratowicz, S. A., Sank, M. J., and George, D. L. (1999). Stabilization of the MDM2 oncoprotein by interaction with the structurally related MDMX protein. *J. Biol. Chem.* 274, 38189–38196. doi: 10.1074/jbc.274.53.38189

Shvarts, A., Steegenga, W. T., Riteco, N., van Laar, T., Dekker, P., Bazuine, M., et al. (1996). MDMX: a novel p53-binding protein with some functional properties of MDM2. *EMBO J.* 15, 5349–5357. doi: 10.1002/j.1460-2075.1996.tb00919.x

Singh, R. K., Iyappan, S., and Scheffner, M. (2007). Hetero-oligomerization with MdmX rescues the ubiquitin/Nedd8 ligase activity of RING finger mutants of Mdm2. *J. Biol. Chem.* 282, 10901–10907. doi: 10.1074/jbc.M610879200

Stad, R., Little, N. A., Xirodimas, D. P., Frenk, R., van der Eb, A. J., Lane, D. P., et al. (2001). Mdmx stabilizes p53 and Mdm2 via two distinct mechanisms. *EMBO Rep.* 2, 1029–1034. doi: 10.1093/embo-reports/kve227

Stad, R., Ramos, Y. F. M., Little, N., Grivell, S., Attema, J., Van der Eb, A. J., et al. (2000). Hdmx stabilizes Mdm2 and p53. *J. Biol. Chem.* 275, 28039–28044. doi: 10.1074/jbc.M003496200

Tan, B. X., Liew, H. P., Chua, J. S., Ghadessy, F. J., Tan, Y. S., Lane, D. P., et al. (2016). Anatomy of Mdm2 and Mdm4 in evolution. *J. Mol. Cell Biol.* 9, 3–15. doi: 10.1093/jmcb/mjx002

Tanimura, S., Ohtsuka, S., Mitsui, K., Shirouzu, K., Yoshimura, A., and Ohtsubo, M. (1999). MDM2 interacts with MDMX through their RING finger domains. *FEBS Lett.* 447, 5–9. doi: 10.1016/S0014-5793(99)00254-9

Toledo, F., and Wahl, G. M. (2006). Regulating the p53 pathway: in vitro hypotheses, in vivo veritas. *Nat. Rev. Cancer* 6, 909–923. doi: 10.1038/nrc2012

Uldrijan, S., Pannekoek, W.-J., and Vousden, K. H. (2007). An essential function of the extreme C-terminus of MDM2 can be provided by MDMX. *EMBO J.* 26, 102–112. doi: 10.1038/sj.emboj.7601469

**Conflict of Interest Statement:** The authors declare that the research was conducted in the absence of any commercial or financial relationships that could be construed as a potential conflict of interest.

frontiers in Physiology

ORIGINAL RESEARCH
published: 03 May 2019
doi: 10.3389/fphys.2019.00534

# Detailed Dissection of UBE3A-Mediated DDI1 Ubiquitination

*Nagore Elu[1], Nerea Osinalde[2], Javier Beaskoetxea[1], Juanma Ramirez[1], Benoit Lectez[1], Kerman Aloria[3], Jose Antonio Rodriguez[4], Jesus M. Arizmendi[1] and Ugo Mayor[1,5]**

*[1] Department of Biochemistry and Molecular Biology, Faculty of Science and Technology, University of the Basque Country (UPV/EHU), Leioa, Spain, [2] Department of Biochemistry and Molecular Biology, Faculty of Pharmacy, University of the Basque Country (UPV/EHU), Vitoria-Gasteiz, Spain, [3] Proteomics Core Facility-SGIKER, University of the Basque Country (UPV/EHU), Leioa, Spain, [4] Department of Genetics, Physical Anthropology and Animal Physiology, University of the Basque Country (UPV/EHU), Leioa, Spain, [5] Ikerbasque – Basque Foundation for Science, Bilbao, Spain*

The ubiquitin E3 ligase UBE3A has been widely reported to interact with the proteasome, but it is still unclear how this enzyme regulates by ubiquitination the different proteasomal subunits. The proteasome receptor DDI1 has been identified both in *Drosophila* photoreceptor neurons and in human neuroblastoma cells in culture as a direct substrate of UBE3A. Here, we further characterize this regulation, by identifying the UBE3A-dependent ubiquitination sites and ubiquitin chains formed on DDI1. Additionally, we found one deubiquitinating enzyme that is capable of reversing the action of UBE3A on DDI1. The complete characterization of the ubiquitination pathway of an UBE3A substrate is important due to the role of this E3 ligase in rare neurological disorders as Angelman syndrome.

**Keywords: UBE3A, ubiquitin E3 ligase, Angelman syndrome, proteasome, mass-spectrometry, GFP pull-down**

OPEN ACCESS

***Edited by:***
*Julien Licchesi,*
*University of Bath, United Kingdom*

***Reviewed by:***
*Manuel Ramírez-Sánchez,*
*Universidad de Jaén, Spain*
*Pierre G. Lutz,*
*Centre National de la Recherche Scientifique (CNRS), France*

***Correspondence:**
*Ugo Mayor*
*ugo.mayor@ehu.eus*

***Specialty section:***
*This article was submitted to Integrative Physiology, a section of the journal Frontiers in Physiology*

***Received:*** *16 December 2018*
***Accepted:*** *15 April 2019*
***Published:*** *03 May 2019*

***Citation:***
*Elu N, Osinalde N, Beaskoetxea J, Ramirez J, Lectez B, Aloria K, Rodriguez JA, Arizmendi JM and Mayor U (2019) Detailed Dissection of UBE3A-Mediated DDI1 Ubiquitination. Front. Physiol. 10:534. doi: 10.3389/fphys.2019.00534*

## INTRODUCTION

The lack of functional UBE3A E3 ubiquitin ligase in the brain is responsible for a rare neurodevelopmental disorder called Angelman syndrome (AS). With an incidence of 1:15.000 births (Margolis et al., 2015), the disease is characterized by episodes of frequent laughter, language impairment, severe developmental delay, ataxic movements, hypopigmentation, seizure disorder, sleep disturbances, muscular hypotonia, and motor delay (Buiting et al., 2016). Clinical features of AS were first described in 1965, and since then, the diagnosis criteria has been well established (Williams et al., 2006). Moreover, some studies established a link between the affected molecular mechanisms and their consecutive symptoms in patients. For example, seizure disorders have been associated to haploinsufficiency of GABA receptor genes (Moncla et al., 1999) and hypopigmentation of the skin has been explained by UBE3A regulating the melanocortin 1 receptor (Low and Chen, 2011). However, the role of UBE3A on the brain and how the lack of it can cause such a severe clinical scenario is still unknown.

Protein ubiquitination involves the coordinated action of three complementary enzymes. Upon E1-mediated activation, ubiquitin (Ub) is transferred to an E2 ubiquitin-conjugating enzyme, and subsequently to an E3 ubiquitin ligase, which is the ultimate responsible for attaching the ubiquitin moiety to the substrate (Glickman and Ciechanover, 2002). UBE3A is a HECT-type E3 ligase that catalyzes Ub transfer to the substrate through a two-step reaction that involves first, the transfer of Ub to a catalytic cysteine on the E3, and then, from the E3 to the substrate (Glickman and Ciechanover, 2002). Ub is usually attached to the side chain of lysine residues,

and thus, any lysine-containing protein could potentially be modified with ubiquitin. Such modification may occur as a single Ub attached to a single lysine (mono-ubiquitination) or to several lysines (multiple mono-ubiquitination). In addition, ubiquitin itself contains eight available amide groups: 7 lysines (K6, K11, K27, K29, K33, K48, K63) and a *N*-terminal amide group (M1) by which additional ubiquitin moieties can be attached, forming a wide range of poly-ubiquitin chains (Komander and Rape, 2012). Linkages in a poly-ubiquitin chain can be mediated by the same lysines across the chain or by different lysines, which results in the formation of homogenous and heterogeneous chain types, respectively. Additionally, if multiple lysines in each Ub are involved in the linkage formation, branched chains are formed.

Different ubiquitin chain types assign proteins a great variety of functions (Swatek and Komander, 2016). Mono-ubiquitination is involved in many essential cellular roles, including receptor internalization (Haglund et al., 2003), subcellular localization (Landré et al., 2017) and regulation of transcriptional activity (Pham and Sauer, 2000). Among poly-ubiquitin chains, K48 chains are the best characterized and are typically associated to protein degradation (Glickman and Ciechanover, 2002; Ciechanover, 2013). Indeed, *in vitro* studies have demonstrated that UBE3A ubiquitin ligase mainly forms K48 chains and hence, likely targets proteins to the proteasome (Wang and Pickart, 2005; Kim and Huibregtse, 2009). Nevertheless, poly-ubiquitin chains also exert a number of non-degradative roles. It has recently been shown that K11/K48-linked ubiquitin chains play a key role in cell cycle and quality control (Yau et al., 2017). Additionally, K63-linked poly-ubiquitination is required for the cytoplasmic localization of MBNL1 (Wang et al., 2018). K29 poly-ubiqutination is a negative regulator of Wnt/β-catenin signaling (Fei et al., 2013), whereas M1, K11 and M1/K63 mixed Ub chains modulate the NF-κb signaling pathways (Tokunaga et al., 2009; Dynek et al., 2010; Yau et al., 2017). There is also evidence for the involvement of K6-, K27- and K33-linked ubiquitination in the DNA damage response (Elia et al., 2015). Altogether, it is evident that in order to characterize the role of ubiquitination in the regulation of a given protein, it is essential to first identify the types of ubiquitin chain linkages that are formed on it.

Since ubiquitination controls the diverse endpoints of proteins, in Angelman syndrome patients, UBE3A substrates are likely to be negatively affected by the lack of functional UBE3A in neurons. In order to better understand the molecular mechanisms involved in this disease, it is pivotal not only to identify the neuronal substrates of UBE3A *in vivo*, but also to characterize their ubiquitin chains. In previous *in vivo* studies using flies, we searched for UBE3A substrates (Ramirez et al., 2018), and noted that the ubiquitination levels of many proteasomal subunits were significantly enhanced upon UBE3A overexpression. In agreement with other studies (Jacobson et al., 2014; Tomaić and Banks, 2015; Yi et al., 2017), this leads to the idea that UBE3A could regulate the activity of the proteasome. In this regard, we confirmed that the proteasomal shuttling protein Rngo/DDI1, which itself targets poly-ubiquitinated proteins to proteasomal degradation (Saeki et al., 2002; Kaplun et al., 2005; Ivantsiv et al., 2006; Voloshin et al., 2012; Ramirez et al., 2018), is a direct substrate of UBE3A (Ramirez et al., 2018). Nevertheless, it remains to be elucidated how UBE3A modulates the ubiquitination pattern of DDI1, and how this modification affects DDI1.

Overall, protein ubiquitination is not only modulated by E3 ligases, but also by deubiquitinating (DUB) enzymes that are responsible for removing the ubiquitin moiety from substrates. The human genome codes for almost a hundred DUBs that based on sequence similarity and likely mechanisms of action are divided into six groups: UCH, USP, OTU, JAMM, MJD, and the most recently discovered MINDY (Amerik and Hochstrasser, 2004; Abdul Rehman et al., 2016). It could be anticipated that there might be at least one specific DUB that counteracts the action of UBE3A. Numerous studies have shown the great potential of DUBs as suitable drug targets to treat cancer, neurodegenerative diseases and viral infection (Edelmann et al., 2011; Huang and Dixit, 2016). Therefore, identifying the DUB responsible for deubiquitinating UBE3A substrates is of pivotal relevance in the development of successful therapies to treat Angelman syndrome. More precisely, pharmacological inhibition of such DUB might help recovering the non-pathological condition of those patients, recovering to some degree the ubiquitination of those substrates shared with UBE3A.

In the present study, we have characterized the UBE3A-dependent ubiquitination of the proteasomal shuttling protein DDI1. From six ubiquitination sites detected on DDI1, we have discovered that the presence of K133 is necessary for DDI1 to be ubiquitinated by UBE3A. Additionally, investigation of the ubiquitin linkages has shown that UBE3A forms K11- and K48-linked ubiquitin chains on DDI1. We also screened a siRNA library to search for the DUB involved in the deubiquitination of UBE3A substrates, and found that USP9X has the capacity to regulate DDI1 ubiquitination levels. Overall, our data shed light into the molecular mechanisms underlying Angelman syndrome, and reveal USP9X as a potential therapeutic target that may help restoring the non-pathological ubiquitination pattern on Angelman syndrome patients, and hence, ameliorate their symptoms.

# MATERIALS AND METHODS

## Plasmids

*C*-terminally GFP-tagged DDI1 (DDI1-GFP) vector was generated using the commercial pEGFP-N1 vector (Clontech), while *N*-terminally GFP-tagged DDI1 (GFP-DDI1) was cloned into a PM-cherry-C1 vector kindly provided by Dr. Daniel Abankwa (see section "Cloning Procedures"). The plasmids used to express the *N*-terminally FLAG-tagged versions of the wild type (FLAG-UBE3A-pCMV, UBE3A$^{WT}$) and catalytically inactive (FLAG-UBE3A$^{LD}$-pCMV, UBE3A$^{LD}$) human UBE3A (Tomaić et al., 2009) were a gift from Dr. Vjekoslav Tomaic. FLAG-tagged ubiquitin (FLAG-Ub) cloned in pCDNA3.1 vector (Invitrogen) was used (Ramirez et al., 2018). A previously described untagged human Parkin plasmid (Martinez et al., 2017) was used and the empty pCDNA3.1 vector (Invitrogen) was used as control (Ramirez et al., 2018).

## Cloning Procedures

Gene for human DDI1 protein (Uniprot Q8WTU0) was synthesized by GenScript and further amplified using 5′-TATAGGTACCATGCTGATCACCGTG-3′ forward primer and 5′-TATAACCGGTATGCTCTTTTCGTCC-3′ reverse primer and inserted between the Acc65I and AgeI sites of the pEGFPN1 vector. For the generation of GFP-DDI1, human DDI1 sequence was amplified using 5′-CGCGTGTACAGTATGAATATAGCGATA-3′ forward primer and 5′-CGCAAGCTTTCAATGCTCTTTTCG-3′ reverse primer. Amplified DDI1 was then inserted between BsrGI and HindIII sites of the PM-cherry-C1 where mCherry had been previously replaced by GFP. All PCR reactions were carried out with Phusion High-Fidelity DNA polymerase (Thermo Scientific). PCR product gel extractions and plasmid purifications were performed with the E.Z.N.A. Gel Extraction Kit and E.Z.N.A. plasmid mini and midi kits (Omega Bio-tek), respectively. Correct sequence for all plasmids was confirmed by sequencing either by the Eurofins GATC Biotech Company (Köln, Germany) or the SGIKER Unit of Sequencing and Genotyping at the University of the Basque Country (Leioa, Spain).

## Cell Culture and Transfection

Human Embryonic Kidney cells (HEK293T) were cultured under standard conditions (37°C, 5% CO2) using Dulbecco's modified Eagle medium/nutrient mixture F-12 (DMEM/F-12) with GlutaMAX (Thermo Scientific) and supplemented with 10% fetal bovine serum (Thermo Scientific), 100 U/ml of penicillin (Invitrogen) and 100 mg of streptomycin (Invitrogen). For ubiquitination sites and chain-types experiments by mass spectrometry, HEK293T cells were seeded in 100 mm plates ($2 \times 10^6$ cells). After 24 h from seeding, cells were co-transfected with 12,5 μg of DDI1-GFP and 12,5 μg of $UBE3A^{WT}$ or $UBE3A^{LD}$ for 72 h using Lipofectamine 3000 transfection reagent (Invitrogen) and according to manufacturer's instructions. For the DUB silencing experiment, HEK293T cells were seeded the previous day in six-well plates ($6 \times 10^5$ cells). Each well was then transfected with 10 nM siRNA targeting specific DUBs (Ambion; life technologies). For that purpose Lipofectamine RNAiMAX transfection reagent (Thermo Fischer) was used according to manufacturer's instructions. After 24 h incubation, 1,5 μg of DDI1-GFP and 1,5 μg of FLAG-Ub were co-transfected for another 48 h using again Lipofectamine 3000 transfection reagent (Invitrogen). For all experiments, cells were washed twice in PBS after the transfection periods and stored at −20°C until required.

## GFP Pull-Down Protocol

Transfected HEK293T cells were lysed with 500 μl of lysis buffer in six-well plates and with 2 mL in 100 mm dishes (50 mM Tris–HCl pH 7.5, 150 mM NaCl, 1 mM EDTA, 0.5% Triton, 1× protease inhibitor cocktail from Roche Applied Science and 50 mM *N*-ethylmaleimide from Sigma) and centrifuged at 14 000 *g* for 10 min. Supernatants were mixed with 25 μl/well (6-well plate) and 50 μL/well (100 mm plates) of GFPTrap-A agarose beads suspension (Chromotek GmbH), which had been previously washed twice with a Dilution buffer (10 mM Tris–HCl pH 7.5, 150 mM NaCl, 0.5 mM EDTA, 1× protease inhibitor cocktail, 50 mM *N*-ethylmaleimide). After incubation for 3 h at room temperature with gentle rolling, samples were centrifuged at 2700 *g* for 2 min to separate the beads from the unbound material. GFP beads were then subjected to three washing steps; once with the dilution buffer, thrice with washing buffer (8 M urea, 1% SDS in PBS) and once with 1% SDS in PBS. GFP-tagged proteins bound to the beads were eluted by incubating at 95°C for 10 min with 25 μl elution buffer (250 mM Tris–HCl pH 7.5, 40% glycerol, 4% SDS, 0.2% bromophenol blue, 100 mM DTT).

## Western Blotting and Silver Staining

For SDS–PAGE, 4–12% Bolt Bis–Tris Plus pre-cast gels (Invitrogen) were used. Proteins were then transferred to PVDF membranes using the iBlot system (Invitrogen). Membranes were blocked using 5% powdered milk in PBS-Tween (PBS-T). Following primary and secondary antibody incubation, membranes were developed with an ECL kit (Biorad Clarity). To create dual-color westerns independent color channels were assigned to two independent westerns that were developed in the same membrane. The amount of material loaded for western blot analysis was between 10–30% of neat inputs and 30–50% of neat elution samples. The following primary antibodies were used at 1/1000 concentration: mouse monoclonal anti-GFP antibody (Roche Applied Science; catalog number 11814460001); mouse monoclonal anti-FLAG M2-HRP conjugated antibody (Sigma; catalog number A8592); mouse monoclonal anti-UBE3A (clone E6AP-300) antibody (Sigma; catalog number E8655), rabbit monoclonal anti-UCHL-5 (Abcam, ab124931), rabbit polyclonal anti-USP9X (Proteintech, 55054-1-AP), anti-USP7 (kindly provided by Dr. Emilio Lecona), rabbit polyclonal anti-USP42 (Sigma, HPA006752). The following secondary antibodies were used at 1/4000 concentration: goat anti-mouse-HRP-labeled antibody (Thermo Scientific; catalog number 62-6520) and goat anti-rabbit-HRP labeled antibody (Cell Signaling; catalog number 7074).

Prior to MS analysis, the efficiency of GFP pull-downs was evaluated by silver staining. Briefly, the 10% of each neat elution was resolved by SDS–PAGE (4–12% Bolt Bis–Tris Plus precast gels, Invitrogen), and after fixing the proteins within the gel with 40% methanol/10% acetic acid, gel bands were visualized using the SilverQuest kit following manufacturer's instructions (Invitrogen).

## In-Gel Trypsin Digestion and Peptide Extraction

Ninety percent of the neat elution from each GFP pull-down was resolved by SDS–PAGE (4–12% Bolt Bis–Tris Plus precast gels, Invitrogen) and visualized with Colloidal Blue (Invitrogen) following manufacturer's instructions. Aiming to isolate mono- and poly-ubiquitinated DDI1, each gel lane was excised into two slices above the clear band of approximately 75 KDa that corresponds to non-modified DDI1 (**Figure 1**). Subsequently, each gel lane was chopped, and proteins were subjected to in-gel digestion protocol using trypsin as described before (Osinalde et al., 2015). Briefly, gel pieces, previously

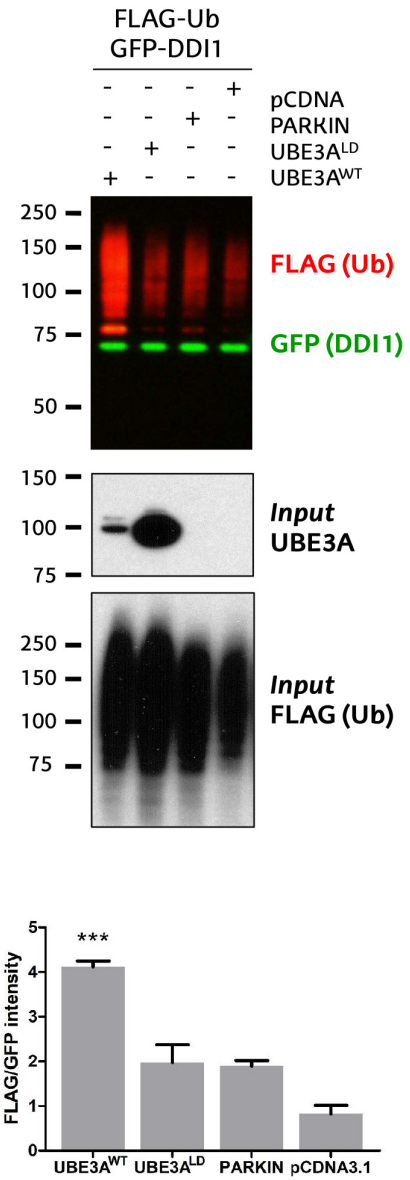


**FIGURE 1 |** Validation of DDI1 as a substrate of UBE3A in HEK293T cells. DDI1 ubiquitination was detected by western blot upon overexpression of wild-type UBE3A (UBE3A$^{WT}$), ligase dead UBE3A (UBE3A$^{LD}$), Parkin E3 ligase (PARKIN) and control vector (pCDNA3.1) in HEK293T cells. Anti-FLAG antibody (red) was used to detect the ectopically expressed ubiquitin, whereas the non-modified GFP-tagged DDI1 was detected by anti-GFP antibody (green). UBE3A overexpression was confirmed in whole cell lysates using anti-UBE3A antibody (*Input* UBE3A) while the FLAG signal in the inputs corroborated equivalent transfections in all samples [Input FLAG-(Ub)]. Quantification of western blots was performed with Image-J, by normalizing the FLAG intensities to the GFP signal. The analysis showed a statistically significant increase [one-way ANOVA, ***$p$-value $< 0.0001$, (mean ± S.E.M., $n = 3$)] of GFP-DDI1 ubiquitination upon UBE3A$^{WT}$ overexpression in comparison to overexpression of UBE3A$^{LD}$.

dehydrated with acetonitrile (ACN), were reduced with 10 mM dithiothreitol (DTT), alkylated with 55 mM chloroacetamide, and finally rehydratated in 12.5 ng/ml trypsin and incubated overnight at 37°C. The following day, resulting tryptic peptides were extracted from the gel by serial incubation with 100% ACN and 1% trifluoroacetic acid in 30% ACN. Finally, prior to MS analysis, peptide solutions were dried down in a SpeedVac centrifuge (Thermo Scientific).

## LC-MS/MS Analysis

Mass spectrometric analyses were performed on an EASY-nLC 1200 liquid chromatography system interfaced with a Q Exactive HF-X mass spectrometer (Thermo Scientific) via a nanospray flex ion source. Dried peptides were dissolved in 0.1% formic acid and loaded onto an Acclaim PepMap100 pre-column (75 μm × 2 cm, Thermo Scientific) connected to an Acclaim PepMap RSLC C18 (75 μm × 25 cm, Thermo Scientific) analytical column. Peptides were eluted from the column using the following gradient: 18 min from 2.4 to 24%, 2 min from 24 to 32% and 12 min at 80% of acetonitrile in 0.1% formic acid at a flow rate of 300 nl min$^{-1}$. The mass spectrometer was operated in positive ion mode. Full MS scans were acquired from m/z 375 to 1800 with a resolution of 120,000 at m/z 200. The 10 most intense ions were fragmented by higher energy *C*-trap dissociation with normalized collision energy of 28 and MS/MS spectra were recorded with a resolution of 15,000 at m/z 200. The maximum ion injection time were 100 ms and 120 ms, whereas AGC target values were $3 \times 10^6$ and $5 \times 10^5$ for survey and MS/MS scans, respectively. In order to avoid repeat sequencing of peptides, dynamic exclusion was applied for 12 s. Singly charged ions or ions with unassigned charge state were also excluded from MS/MS. Data were acquired using Xcalibur software (Thermo Scientific).

## Data Processing and Bioinformatics Analysis

Acquired raw data files were processed with the MaxQuant (Cox and Mann, 2008) software (version 1.5.3.17) using the internal search engine Andromeda (Cox et al., 2011) and searched against the UniProt database restricted to *Homo sapiens* entries (release 2017_03; 42165 entries) where the sequences of FLAG_UBIQUITIN and DDI1_GFP proteins were manually added. To assess ubiquitin chains types present on DDI1, only raw files corresponding to poly-ubiquitinated DDI1 were processed. By contrast, to infer the DDI1 ubiquitination sites, raw files corresponding to both mono- and poly-ubiquitinated DDI1 were processed together. Carbamidomethylation (C) was set as fixed modification whereas Met oxidation, protein *N*-terminal acetylation and Lys GlyGly (not *C*-term) were defined as variable modifications. Mass tolerance was set to 8 and 20 ppm at the MS and MS/MS level, respectively. Enzyme specificity was set to trypsin, allowing for a maximum of three missed cleavages. Match between runs option was enabled with 1.5 min match time window and 20 min alignment window to match identification across samples. The minimum peptide length was set to seven amino acids. The false discovery rate for peptides and proteins was set to 1%. For the analysis of ubiquitination sites, a minimum localization probability of 0.75 was used. Normalized spectral protein

label-free quantification (LFQ) intensities were calculated using the MaxLFQ algorithm.

# RESULTS

## UBE3A-Dependent Ubiquitination Sites on DDI1

We recently discovered that Ube3a ubiquitinates endogenous Rngo in flies, and also its human homolog DDI1 when transfected in S5-SYHY neuroblastoma cells (Ramirez et al., 2018). Using a GFP-based pulldown protocol (Ramirez et al., 2016), we now confirm that UBE3A ubiquitinates also DDI1 in HEK293T kidney cells. As compared to co-transfection with an empty vector (pCDNA3.1), or another E3 ligase such as PARKIN, a ligase dead version of UBE3A ($UBE3A^{LD}$) does not increase the ubiquitination of GFP-tagged DDI1. By contrast, wild type UBE3A ($UBE3A^{WT}$) enhances the ubiquitination of DDI1 while the level of non-modified DDI1 remains unchanged (**Figure 1** and **Supplementary Figure 1**). This effect is independent of whether DDI1 is *N*- or *C*-terminally fused to GFP (**Supplementary Figure 2**). Interestingly, UBE3A-mediated ubiquitination of DDI1 does not seem to target it for degradation, as total GFP-tagged DDI1 levels are equivalent in all samples.

According to PhosphositePlus database – the most comprehensive repository of PTM sites – (Hornbeck et al., 2015), human DDI1 can be ubiquitinated on K345 and K346. Nevertheless, DDI1 contains twelve additional lysines that may potentially be modified by ubiquitin. With the aim to identify the ubiquitination sites on DDI1 that are modified by UBE3A, we followed an approach that optimized the GFP pull-down protocol (Ramirez et al., 2016) for mass spectrometry (MS)-based detection (**Figure 2**).

First, GFP-tagged DDI1 was transfected on HEK293T cells together with wild type or, as control, ligase dead UBE3A ($UBE3A^{WT}$ and $UBE3A^{LD}$, respectively). Then, DDI1 was isolated from both experimental conditions by GFP pull-down procedure, and subsequently resolved by SDS–PAGE. Coomassie staining revealed a band just below 75 kDa corresponding to GFP-tagged DDI1, as earlier identified by western blotting (**Figure 1**). As we were interested in the ubiquitinated fraction of DDI1, we excised a slice of the gel directly above that band (**Figure 2**). Aiming to separate mono- and poly-ubiquitinated DDI1, this gel piece was further divided into two subsequent slices based on the observations by silver staining (**Supplementary Figure 3**) as well as by previous immunoblotting results (**Figure 1**): a tight band just above the non-modified DDI1 should correspond to mono-ubiquitinated DDI1-GFP and a bigger slice above this one, corresponding to the smear of poly-ubiquitinated DDI1 observed by immunobloting. Then, proteins within each gel slice were subjected to trypsin digestion, resulting peptides were extracted from the gel, and analyzed by MS; this protocol from the transfection of cells to the MS analysis was performed in triplicate for each experimental sample.

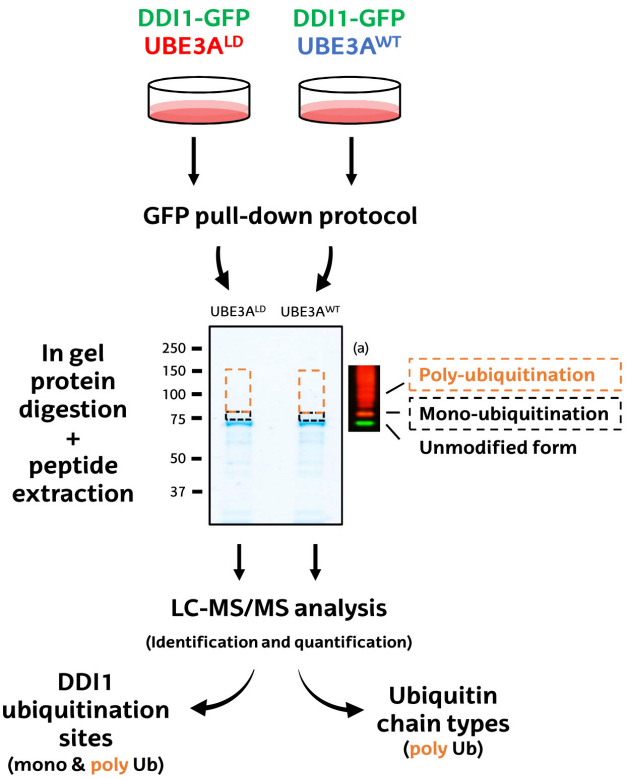


**FIGURE 2 |** Schematic diagram of the MS-based procedure used to study ubiquitination sites and ubiquitin chain types on DDI1. HEK293T cells were co-transfected with DDI1-GFP and wild type UBE3A ($UBE3A^{WT}$) or ligase dead UBE3A ($UBE3A^{LD}$). Unmodified DDI1-GFP as well as its ubiquitinated forms were isolated by GFP pull-down, and separated by SDS–PAGE. The gel slice corresponding to ubiquitinated DDI1-GFP was excised and divided into two, basing on a previous western blot (a); a lower band corresponding for mono-ubiquitinated DDI1-GFP (black), and a band above it corresponding to poly-ubiquitinated DDI1-GFP (orange). Gel slices were digested with trypsin, and resulting peptides were extracted from the gel to further identify and quantify them by LC-MS/MS. Both bands were analyzed to infer DDI1 ubiquitination sites, whereas only the poly-ubiquitination band was used to detect the nature of the ubiquitin chain types formed on DDI1.

To infer DDI1 ubiquitination sites, MS-derived raw files corresponding to the slices of both mono- and poly-ubiquitinated DDI1 were jointly analyzed using MaxQuant software. Based both on MS/MS counts and LFQ intensity values, GFP-tagged DDI1 was, as expected, the most abundant protein detected by mass spectrometry (**Figure 3A** and **Supplementary Table 1**). The second most abundant protein was ubiquitin (**Figure 3A**) despite the lack of ectopic ubiquitin expression in this experiment; given the stringent washing conditions used in the pull-down protocol, it could be postulated that those ubiquitin moieties were covalently attached to DDI1. While the levels of DDI1 were practically the same independently of UBE3A activity, Ub levels were significantly increased in the sample transfected with $UBE3A^{WT}$ (**Figure 3B**).

We detected numerous unmodified peptides that covered 76% of the DDI1-GFP sequence (**Supplementary Figure 4A**), but more interestingly we identified six diGly-modified

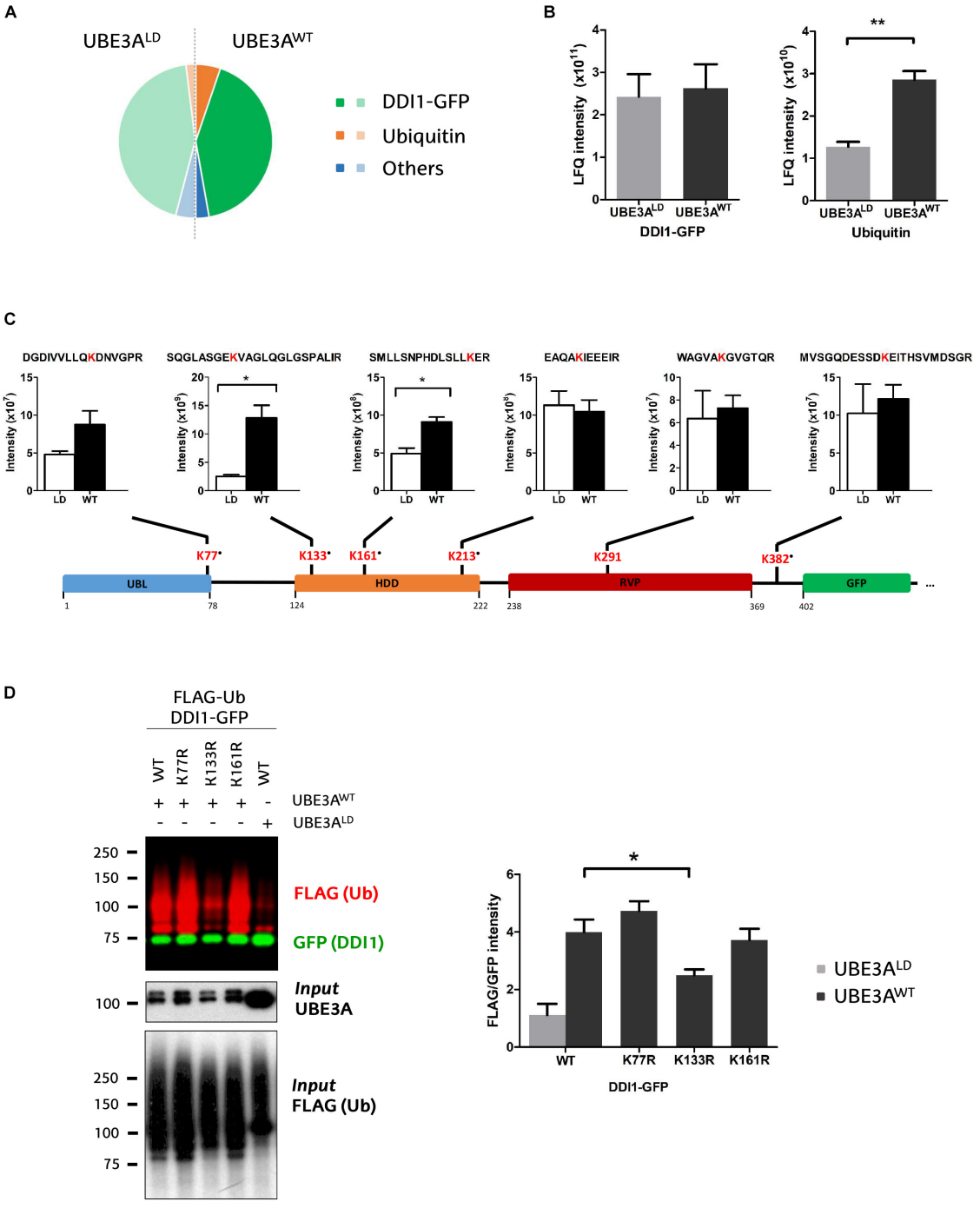


**FIGURE 3 |** Identification and quantification of DDI1 ubiquitination sites. **(A)** Relative LFQ intensity of all the proteins detected by MS demonstrate that DDI1-GFP is the most abundant protein (green) in the GFP pull-down samples, followed by ubiquitin (orange). 287 more proteins (blue) were identified with marginal intensities. **(B)** Comparison of the intensities recorded for the two most abundant proteins in UBE3A$^{WT}$ and UBE3A$^{LD}$ reveal that whereas the levels of DDI1 detected are similar in both conditions, more ubiquitin was detected in the presence of UBE3A$^{WT}$ overexpression [*t*-test, $^{**}p$-value $< 0.05$, (mean ± S.E.M., $n = 3$)]. **(C)** Schematic illustration of DDI1-GFP sequence, its domains (blue, UBL, ubiquitin-like domain; orange, HDD, helical-double domain; red, RVP, retroviral protease domain; green, GFP, GFP-tag of DDI1 protein) and the localization of the ubiquitination sites detected by mass spectrometry. Additionally, the diGly-modified peptides identified, within the ubiquitinated lysine marked in red, and the intensity values measured in each condition (WT, UBE3A$^{WT}$ and LD, UBE3A$^{LD}$) are also indicated. "•" indicates that the ubiquitination site is not reported in PhosphoSitePlus database. DiGly peptides encompassing K133 and K161 were statistically more abundant upon UBE3A$^{WT}$ overexpression [*t*-test, $^{*}p$-value $< 0.05$, (mean ± S.E.M., $n = 3$)]. **(D)** UBE3A-dependent ubiquitination of three distinct DDI1-GFP mutants (K77R, K133R, or K161R) was monitored by western blot after isolating by GFP-pulldown. In red it is illustrated the ubiquitination pattern of DDI1, and in green the unmodified version of DDI1-GFP. Quantification and statistical analysis of the ubiquitination was performed with Image-J after normalizing FLAG intensities to GFP levels. Mutation on DDI1 lysine 133 significantly [one-way ANOVA, $^{*}p$-value $< 0.05$, (mean ± S.E.M., $n = 3$)] abolishes its ubiquitination by UBE3A$^{WT}$.

peptides across the whole sequence of DDI1 (**Figure 3C** and **Supplementary Table 2**), and one on the *C*-terminally fused GFP protein (**Supplementary Figure 4B**). More precisely, we found that ubiquitin was conjugated to the following residues on DDI1: K77, which localizes in the *N*-terminal ubiquitin-like (UBL) domain; K133, K161 and K213 within the helical domain (HDD); K291, that resides in the aspartyl protease-like RVP domain; and K382, on the *C*-terminal end of the protein (**Figure 3C**). It is remarkable that besides K291 ubiquitination, whose homolog lysine had been previously reported to be ubiquitinated on experiments performed in rat brain (Na et al., 2012), the remaining five lysines detected in the present study (K77, K133, K161, K213, and K382) are novel ubiquitination sites of DDI1. Representative annotated spectra for these diGly modified peptides are shown on **Supplementary Figure 4C**.

Aiming to evaluate the effect of UBE3A on DDI1 ubiquitination, we compared the intensity of the diGly peptides between UBE3A$^{WT}$ and UBE3A$^{LD}$ overexpressing cells. The intensities of DDI1 ubiquitination sites K213-, K291-, and K382- containing diGly peptides were similar in both experimental conditions, indicating that UBE3A is not involved in modifying such resides (**Figure 3C**). On the contrary, the intensity of K133- and K161-bearing diGly peptides was induced 5- and 2- fold, respectively, in the UBE3A$^{WT}$ overexpressing condition (**Figure 3C**), while total DDI1 levels remained constant (**Figure 3B**). Similarly, ubiquitination on lysine 77 also appeared to be enhanced upon UBE3A$^{WT}$ overexpression, although this increase did not appear to be statistically significant, most probably due to the low MS/MS counts recorded (**Supplementary Table 3**). Overall, our data suggest that UBE3A may be involved in the ubiquitination of three (K77, K133, and K161) out of the six ubiquitination sites detected on DDI1.

To confirm that indeed UBE3A is responsible for ubiquitinating DDI1 on K77, K131, and K161, we generated three DDI1 point mutations, each with one of the above-mentioned lysines replaced by arginine. Following the same GFP pull-down procedure mentioned above, we isolated the DDI1-GFP mutants and monitored their ubiquitination by immunoblotting. As shown in **Figure 3D**, DDI1 ubiquitination upon UBE3A$^{WT}$ overexpression was still observed for the K77R and K161R mutants to similar level as for wild type DDI1. Having detected by MS in wild type DDI1 a moderate increase of ubiquitination at those two lysines, their removal did, however, not prevent UBE3A to still ubiquitinate DDI1, probably due to the ubiquitination being transferred to an alternative lysine. By contrast, UBE3A-dependent DDI1 ubiquitination was significantly reduced in the case of the K133R mutant (**Figure 3D** and **Supplementary Figure 4D**). It must be noted that position K133 was the one at which the highest ubiquitinated peptide intensity increase had been observed by MS upon UBE3A$^{WT}$ co-expression. In fact, the ubiquitination pattern of K133R co-expressed with UBE3A$^{WT}$ was very similar to the pattern exhibited by wild type DDI1 co-expressed with UBE3A$^{LD}$. These results indicate that UBE3A is responsible for ubiquitinating DDI1 on K133, and that the presence of this lysine 133 is necessary for UBE3A-mediated ubiquitination of DDI1.

## UBE3A-Dependent Ubiquitin Linkage Types on DDI1

Next, we studied the types of ubiquitin linkage formed on poly-ubiquitinated DDI1. For that purpose, we focused on the diGly peptides corresponding to ubiquitin within the gel slice containing poly-ubiquitinated DDI1-GFP (**Figure 2**). In line with previous results (**Figures 1**, **3B**), the ubiquitin levels in this slice were also more abundant upon overexpression of UBE3A$^{WT}$, and the ubiquitin intensity ratio between UBE3A$^{WT}$ and UBE3A$^{LD}$ samples displayed an approximately two-fold increase (**Figure 4**). MaxQuant analysis of this slice confidently detected four ubiquitination sites within ubiquitin: K11, K29, K48, and K63. The levels of K63 chains remained unaffected upon overexpression of UBE3A$^{WT}$. K29 ubiquitin linkages appeared to be increased in the presence of UBE3A$^{WT}$, in line with some earlier reports for UBE3A and other HECT E3 ligases (Chastagner et al., 2006; Xu et al., 2018), but we should note that those linkages were detected with very few counts and overlapped with a possible ubiquitination event also in K27 (**Supplementary Table 3**). More convincingly, the average from the three biological replicates analyzed displayed a clear increase of approximately two fold for both K48 and K11 chains in the UBE3A$^{WT}$ over-expressing cells with respect to the control sample (**Figure 4** and **Supplementary Table 3**). It is worth noting that the intensity fold change measured for the K48 and K11 diGly peptides were similar to the global fold-change observed for ubiquitin itself. Based on this data, and in partial agreement with earlier reports (Kim and Huibregtse, 2009), we conclude that UBE3A$^{WT}$ overexpression indeed induces both K48 and K11 ubiquitin chains on DDI1.

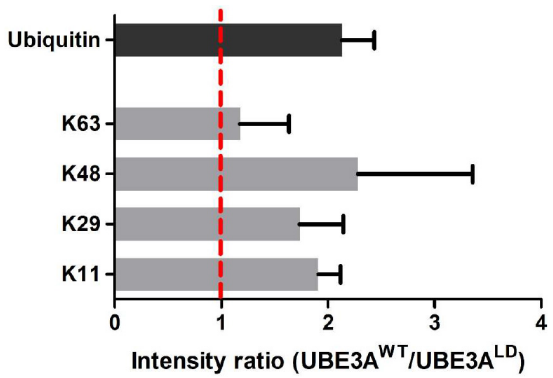


**FIGURE 4 |** Analysis of the ubiquitin linkages formed in DDI1. Four ubiquitination sites on ubiquitin were confidently identified and quantified by mass spectrometry. The intensity ratios for each ubiquitin chain type are given as the ratio of the UBE3A$^{WT}$ overexpressing condition over the intensity recorded for the UBE3A$^{LD}$ sample. The intensity ratio for ubiquitin is also indicated for reference. As K29 was not detected in neither of the UBE3A$^{LD}$ samples, its missing values were substituted by the lowest intensity value found in each replica.

## Identification of USP9X as the DUB Responsible for Deubiquitination of Human DDI1

The ubiquitination state of any given protein is determined by the balance between the conjugating action of E3 ubiquitin ligases and their counteracting deubiquitinating (DUB) enzymes. Having demonstrated that UBE3A ubiquitinates DDI1, we next aimed to discover the DUB capable of deubiquitinating it. We screened an RNAi library in order to identify the DUB whose silencing would enhance DDI1 ubiquitination. For that purpose, we used HEK293T cells expressing DDI1-GFP and FLAG-Ub, in which 41 different DUBs were silenced individually. More precisely, we silenced 36 members of the USP family, as well as 3 and 2 members, respectively, of the UCH and OTU families (**Figure 5A**). To measure DDI1 ubiquitination, GFP-tagged DDI1 was first isolated by GFP pull-down, and then ubiquitin was

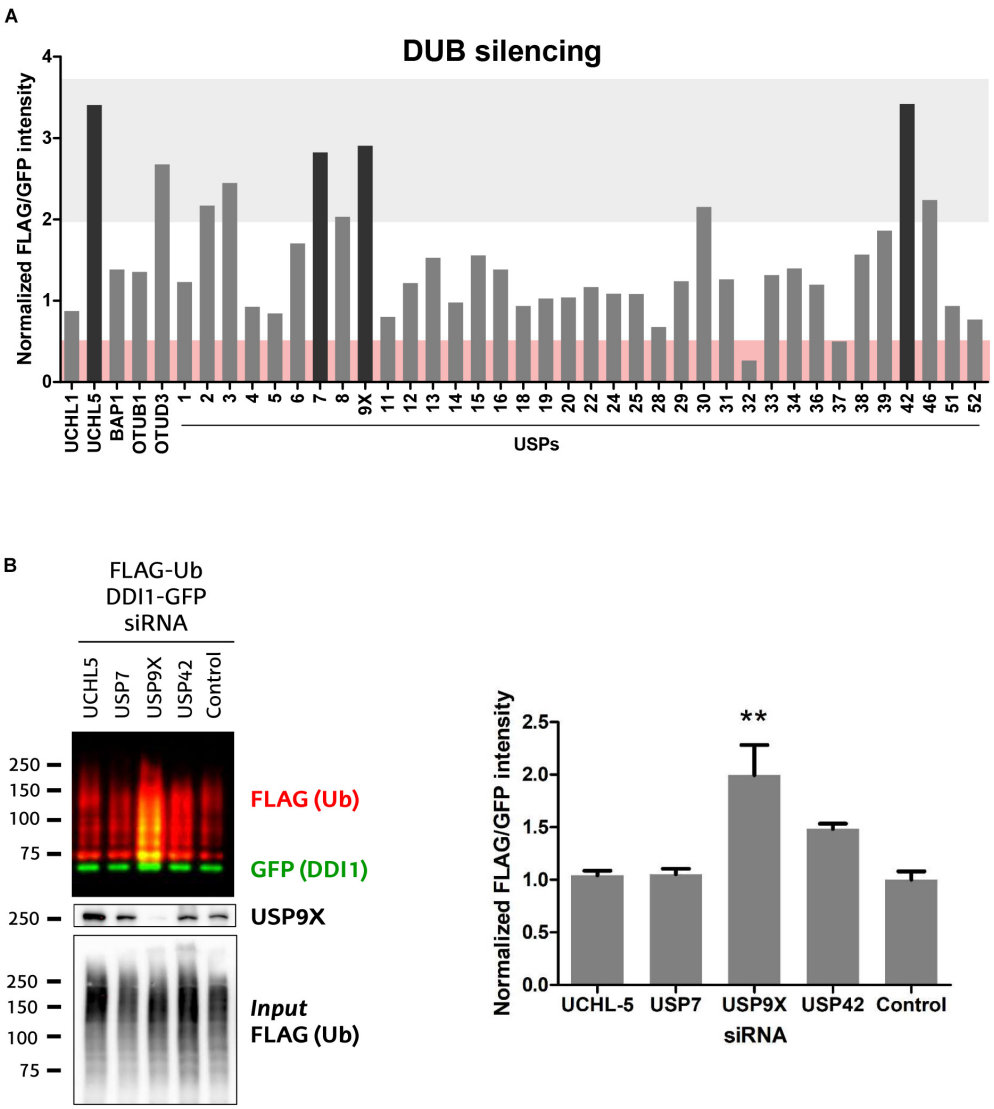


**FIGURE 5 |** Screen of 41 human DUBs indicates USP9X to be the counteracting DUB of UBE3A. **(A)** 41 different human DUBs were silenced using 10 nM siRNAi. After GFP-pulldown of DDI1-GFP, FLAG/GFP intensity ratios were determined. Those ratios were normalized to the average of three lowest values on each 6-well experimental dataset. Upon silencing of most DUBs, the ubiquitination of DDI1 did not change quantitatively (0.5 < fold-change < 2, white). However, silencing of some DUBs decreased DDI1 ubiquitination (fold-change < 0.5, red), while some others increased it (fold-change > 2, gray). Black bars highlight the DUBs that affect more severely DDI1 ubiquitination (UCHL-5, USP7, USP9X, and USP42). **(B)** siRNAs were used to silence UCHL-5, USP7, USP9X, and USP42 DUBs and scramble siRNAi was used as a control. After GFP-pulldown, DDI1 ubiquitination was detected by western blot analysis using anti-FLAG (red) and anti-GFP (green) antibodies. Equivalent amounts of ectopically overexpressed ubiquitin was detected in the cell lysates [*Input* FLAG-(Ub)], while USP9X silencing was corroborated by anti-USP9X antibody (USP9X). Quantification was performed with Image-J after normalizing FLAG/GFP intensities. USP9X inhibition significantly enhanced DDI1 ubiquitination [one-way ANOVA, $^{**}p$-value < 0.05, (mean ± S.E.M., $n = 3$)]. DDI1 ubiquitination also increased upon USP42 silencing, but not significantly, while no changes were observed for the UCHL-5 and USP7 experiments.

detected by immunoblot with an anti-FLAG antibody. Changes in DDI1 ubiquitination were measured by normalizing the FLAG-Ub signal for each sample against its own GFP signal. Additionally, aiming to compare the results obtained in the several 6-well plate based experiments, we normalized this ratio to the average of the 3 lowest ratios on each dataset of 6 silencing experiments. As shown in **Figure 5A**, silencing of most DUBs did not substantially modify the ubiquitination state of DDI1 (normalized GFP/FLAG intensity between 0.5–2). Interestingly, upon silencing of UCHL-5, OTUD3 and 8 USP family members (USP2, 3, 7, 8, 9X, 30, 42, and 46) ubiquitination of DDI1 was quantitatively enhanced (normalized GFP/FLAG intensity > 2). From those 10 candidates, we focused our attention on the four DUBs having the greatest influence on DDI1 ubiquination: UCHL-5, USP7, USP9X, and USP42.

We then silenced the above mentioned four DUBs separately, and used a scramble siRNA as a control for this validation experiment that was performed in triplicate (**Supplementary Figure 5A**). The silencing of DUBs – UCHL-5, USP7, USP9X and USP42 – was confirmed by immunoblotting (**Supplementary Figure 5B**). After DDI1-GFP and FLAG-Ub overexpression in HEK293T cells, DDI1-GFP was isolated by GFP-pulldown, and the ubiquitination of DDI1 monitored by immunoblotting. As shown in **Figure 5B**, silencing of neither USP7 nor UCHL-5 had any influence on the ubiquitination state of DDI1. Downregulation of USP42, on the other hand, showed an increase on DDI1 ubiquitination, but this increase resulted to be statistically no significant. Importantly, this second round of screening clearly demonstrated that USP9X silencing results in enhanced DDI1 ubiquitination, and hence confirms that USP9X is required for deubiquitinating DDI1 (**Figure 5B**).

DUB inhibition has been considered as a potential therapeutic strategy for those diseases on which the function of a given E3 ligase is lost, and certain essential substrates are ubiquitinated at levels below their physiological requirement. A compound termed WP1130 has been previously used to experimentally inhibit USP9X (Kapuria et al., 2010; Sun et al., 2011), even if it is known that it also targets other DUBs (Kapuria et al., 2010). Since highly selective USP9X inhibitors are not yet available, we tested whether WP1130 would –presumably through USP9X– enhance the ubiquitination of DDI1. For that purpose, HEK293T cells were incubated for 1 h with 5 μM WP1130 or with DMSO as control. We then checked the ubiquitination pattern of GFP-DDI1 by immunoblotting, using the same GFP-pulldown protocol described above. Ubiquitination of DDI1 was significantly enhanced in cells treated with USP9X inhibitor WP1130 (**Figure 6**), supporting the earlier observations that DDI1 is an USP9X-regulated substrate.

Overall, our data indicate that UBE3A and USP9X are the E3 ligase and DUB, respectively, involved in modulating the ubiquitination of DDI1.

## DISCUSSION

Poly-ubiquitinated proteins targeted for degradation might be recognized directly by proteasomal receptors or by proteasomal shuttling proteins. The first shuttling proteins – Ddi1, Rad23 and Dsk2 – were identified and characterized in *Saccharomyces cerevisiae* (Lambertson et al., 1999; Kaplun et al., 2005). Proteasomal shuttles contain an *N*-terminal ubiquitin-like (UBL) domain that interacts with the 26S proteasome (Finley, 2009), and a *C*-terminal ubiquitin-binding domain domain (UBD) that

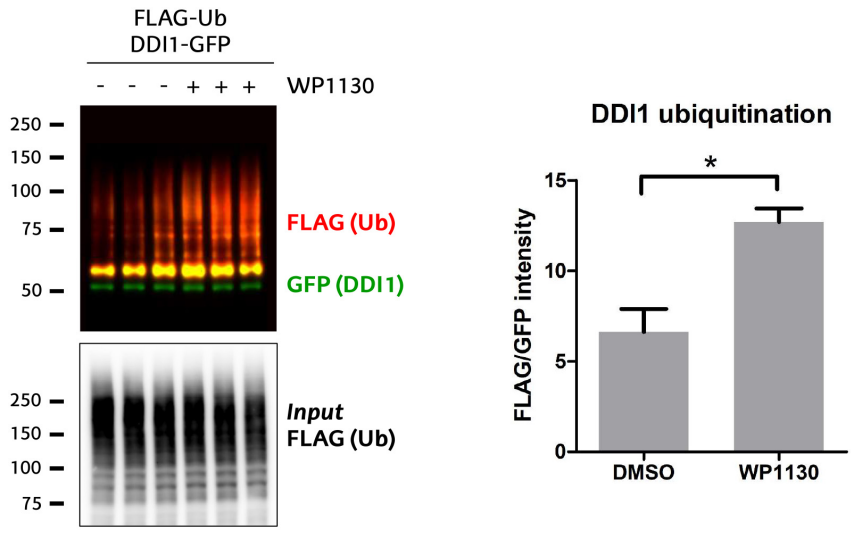


**FIGURE 6 |** USP9X inhibition by WP1130 enhances DDI1 ubiquitination. Cells expressing GFP-DDI1 and FLAG-Ub were treated with 5 μM WP1130 or DMSO for 1 h. GFP-DDI1 was pulled down and its ubiquitination monitored by western blot. Anti-GFP antibody was used to detect unmodified GFP-DDI1 levels whereas anti-FLAG antibody was used to detect ubiquitination. The signal of FLAG was normalized to the GFP signal. Equivalent amount of transfected ubiquitin was detected in the cell lysates by measuring FLAG-Ub levels [*Input* FLAG-(Ub)]. Quantification using Image-J showed a statistically significant increase in DDI1 ubiquitination after WP1130 treatment [*t*-test, **p*-value < 0.05, (mean ± S.E.M., *n* = 3)].

binds to ubiquitin or poly-ubiquitin chains (Bertolaet et al., 2001). When ubiquitinated, substrates are captured by the UBD domain, whereas the UBL domain binds to UBL receptors of the proteasome, delivering the substrates for degradation (Finley, 2009). Yeast Ddi1 and Ddi1-like shuttling proteins (e.g., Ddi2) show unique properties among canonical proteasomal shuttles. On the one hand, their UBL domain is able to bind ubiquitin (Nowicka et al., 2015), and despite having a ubiquitin-like fold, it does not interact or very weakly interacts with typical UBL receptors, including Rpn10 (Zhang et al., 2009) and Rpn1 (Rosenzweig et al., 2012). On the other hand, human DDI1 and Ddi1-like proteins from vertebrates lack the UBA domain (a type of UBD), but instead interact with ubiquitin through their UBL domain (Nowicka et al., 2015) or the ubiquitin-interacting motif (UIM) in the case of Ddi1-like proteins (Nowicka et al., 2015; Sivá et al., 2016). In line with this, a novel proteasomal shuttling mechanism has been proposed for yeast Ddi1 (Nowicka et al., 2015). Furthermore, Ddi1 and Ddi1-like proteins contain an additional domain called the retroviral protease-like (RVP) domain (Sirkis et al., 2006), making it very likely that besides their role in targeting substrates for proteasomal degradation, they may exert additional roles in the cell. Thus, further studies are necessary to fully understand the shuttling mechanism mediated by DDI1, but also to discover in which other cellular functions is involved.

Post-translation modifications (PTMs), including protein ubiquitination and phosphorylation, play a critical role in essentially all cellular processes by regulating the activity, localization or interactions of proteins. For example, it has been shown that the interaction between the proteasome and the proteasomal shuttle Rad23 is regulated by a phosphorylation occurring on the UBL domain of Rad23 (Liang et al., 2014, 23). In a recent study, we uncovered that human DDI1 is a substrate of the E3 ubiquitin ligase UBE3A, and as a consequence is ubiquitinated (Ramirez et al., 2018). Therefore, and bearing in mind the relevance of PTMs, we postulated that studying how DDI1 is ubiquitinated, or more precisely, identifying the DDI1 ubiquitination sites and chain types, may shed light into its regulation and the mechanism by which this proteasomal shuttle targets proteins to degradation. A recent large-scale proteomic study has reported that human DDI1 is ubiquitinated in K345 and K346, which reside in the RVP domain (Akimov et al., 2018). Moreover, studies in rat brain revealed that rat DDI1 K297 is also ubiquitinated (Na et al., 2012). In line with these studies, we here present the first evidence indicating that its human homolog DDI1 K291, which is also located in the RVP domain, is also ubiquitinated. As mentioned above, the function of the RVP domain, which is only present in Ddi1 and Ddi1-like proteins, is obscure. Therefore, the recent findings regarding ubiquitination events occurring on human DDI1 RVP domain might provide a baseline for future studies on deciphering the role of this unique domain.

Furthermore, our mass spectrometry-based approach revealed five novel ubiquitination sites in human DDI1: K77 on the UBL domain, K133, K161 and K213 in the HDD domain and K382 in the *C*-terminal of the protein. It is likely that ubiquitination of different residues on specific domains may affect differentially DDI1 function. Hence, future work will be necessary to elucidate the biological significance of each modification.

We are interested in elucidating the molecular mechanisms underlying Angelman syndrome, a rare neurological disease caused by the lack of functional E3 ubiquitin ligase UBE3A in the brain. For that reason, among the six DDI1 ubiquitination sites detected in the present study, our interest focused on the ones mediated by UBE3A, as it is likely that UBE3A-dependent ubiquitination events are altered in Angelman syndrome patients. Comparing the intensity of the diGly-modified peptides corresponding to DDI1 in samples overexpressing $UBE3A^{WT}$ and $UBE3A^{LD}$, we found that peptides bearing ubiquitinated K77, K133 and K161 appeared more abundant upon overexpression of $UBE3A^{WT}$. Altogether, these results pointed to the N-terminal region of DDI1, including the ubiquitin-like domain and the double helical domain (HDD), as a ubiquitination hotspot region, where UBE3A mostly acts.

Out of the three putative UBE3A-dependent DDI1 ubiquitination sites detected, K133- and K161-containing peptides reached statistical significance. However, to further corroborate previous results, DDI1 K77, K133 and K161 were individually mutated to arginines. UBE3A-dependent ubiquitination of DDI1 was only significantly reduced when residue K133 was mutated, indicating that undoubtedly UBE3A is responsible for modifying this residue. It has been postulated that the HDD domain, which contains the K133 residue, may play a role in substrate recognition (Trempe et al., 2016). Therefore, it is plausible that UBE3A-dependent ubiquitination of DDI1 K133 has an influence on such recognition.

The fate of an ubiquitinated protein does not only depend on the specific residue that is modified, but also on the type of ubiquitin linkage that is formed in such residue (Swatek and Komander, 2016). A large variety of ubiquitin linkages differentially modulate proteins and their function in multiple cellular processes. Thus, we investigated using a high stringency pull-down protocol the ubiquitin chain types specifically and covalently linked to DDI1. In parallel to the overall increase in ubiquitin signal observed upon $UBE3A^{WT}$ overexpression, a detailed MS-based analysis of the DDI1 ubiquitinated fraction revealed K48 and K11 as the chain types most prominently induced by overexpression of this E3 ligase, suggesting that the increase in ubiquitin signal most likely corresponds to the formation of those chain types.

K48-linked ubiquitin chains have been widely described to direct proteins to degradation via the proteasome (Finley, 2009; Grice and Nathan, 2016). Indeed, several studies have shown that UBE3A forms K48-type linkages, and consequently, modified proteins are predicted to be targeted for degradation (Wang and Pickart, 2005). K11 chains also improve the signal for proteasomal degradation, as evident from the fact that branched K11-linked chains formed by the anaphase-promoting complex (APC/C) increase the efficiency of proteasomal substrate recognition (Meyer and Rape, 2014). However, and in agreement with our previous work (Ramirez et al., 2018), the unchanged GFP signal on the various western blots (**Figures 1**, **3D**) clearly indicates that UBE3A-dependent ubiquitination of

DDI1 does not target this shuttling protein to degradation. One plausible explanation could be that this ubiquitination event leads to a neutralization of this proteasomal shuttle. If the role of DDI1 is to transport K48- or K11-modified proteins to the proteasome, when the client is the shuttle itself, shuttling might be interrupted, by blocking both the proteasomal interaction, as well as the recruitment of further clients. This UBE3A-mediated ubiquitination of DDI1 could thus explain our previous observations that overall proteasomal function is somehow dependent on UBE3A (Lee et al., 2014; Ramirez et al., 2018). Further analysis to decipher the function of K48 and K11 ubiquitin chains in DDI1 *in vivo* is likely to provide more light in this issue.

Most PTMs, including ubiquitination, are reversible modifications modulated by the co-ordinated action of two opposing enzymes: one adding a given chemical group to the protein, the other one removing it. In particular, protein ubiquitination is modulated by E3/DUB pairs. The regulation of the enzymes modulating protein PTMs is crucial for maintaining the appropriate balance of protein modification required for cellular homeostasis. In fact, as already mentioned, deregulation of these enzymes is implicated in a number of diseases, including cancer and rare neurological diseases (Ruprecht and Lemeer, 2014; Osinalde et al., 2018). Therefore, emerging therapeutic strategies are focused on the design of drugs that modify the biological action of these enzymes, and consequently restore appropriate cellular PTM levels. Indeed, in the past two decades, kinase inhibitors have been successfully used to treat cancer and other diseases (Bhullar et al., 2018). At present, great efforts are being made to develop similar strategies to treat diseases caused by altered protein ubiquitination. More precisely, DUBs are emerging as druggable targets for different diseases. Attempts have been done to inhibit DUBs in cancer therapy (D'Arcy et al., 2015), aiming to increase ubiquitination, and subsequent degradation, of substrates (Pinto-Fernandez and Kessler, 2016). Here we propose that modulating protein ubiquitination may represent a therapeutic approach for Angelman syndrome patients that lack UBE3A activity in the brain. More precisely, inhibition of the DUB counteracting the action of the E3 ligase UBE3A may help restoring the non-pathological ubiquitination levels of UBE3A substrates in Angelman syndrome patients.

So far, there are few studies showing that E3/DUB pairs act in a highly co-ordinated manner to regulate the ubiquitination and, hence, the activity of common substrates (Kee et al., 2005; Xie et al., 2013; Bingol et al., 2014; Sharma et al., 2014). It has been shown that Ubp2 antagonizes Rsp5 E3 ligase activity by forming a complex together with Rsp5 and Rup1 that deubquitinate Rsp5 substrates (Kee et al., 2005). Additionally, the E3/DUB pair UBR5/DUBA acts to modulate the production of IL-17 in T-cells (Rutz et al., 2015). Nevertheless, the identity of the DUB antagonizing the action of UBE3A has remained elusive, so far. Our study is pioneer in revealing USP9X as the DUB counteracting UBE3A. We demonstrate that siRNA-directed USP9X silencing, as well as treatment with WP1130 (a previously used partially specific USP9x inhibitor) significantly enhance human DDI1 ubiquitination. While it is true that the partial specificity of WP11330 could confound the obtained results, interestingly, USP9X has been earlier reported to be involved in X-linked intellectual disability (Homan et al., 2014). Furthermore USP9X is also known to have roles on axonal growth and neuronal cell migration (Homan et al., 2014) as well as in the regulation of seizures (Paemka et al., 2015). USP9X is also known to deubiquitinate α-synuclein, which is central to the pathogenesis of Parkinson disease (PD) (Rott et al., 2011). It has been suggested that drugs that modulate the activity of USP9X, together with enhancers of autophagy or proteasomal activity, may help decrease the levels of α-synuclein and provide a novel therapeutic strategy to treat α-synucleinopathies. Similarly, based on our results, we propose that attenuating the activity of USP9X may contribute to enhance the ubiquitination levels of UBE3A substrates that might be decreased in Angelman syndrome patients.

## AUTHOR CONTRIBUTIONS

NE, JAR, JMA, and UM designed the experiments. NE, JB, and KA performed the experiments. NE, NO, JR, BL, KA, and UM analyzed the experiments. NE, NO, and UM wrote the manuscript.

## FUNDING

This work was supported by March of Dimes (Research Grant 1-FY15-339); Spanish MINECO (grant SAF2016-76898-P) cofinanced with FEDER funds, and grant PRB3 (IPT17/0019 - ISCIII-SGEFI / ERDF). UM is also part of COST action Proteostasis. This work was also partially supported by Fondation Jérôme Lejeune grant 1381-MU2015A.

## SUPPLEMENTARY MATERIAL

The Supplementary Material for this article can be found online at: https://www.frontiersin.org/articles/10.3389/fphys.2019.00534/full#supplementary-material

## REFERENCES

Abdul Rehman, S. A., Kristariyanto, Y. A., Choi, S.-Y., Nkosi, P. J., Weidlich, S., Labib, K., et al. (2016). MINDY-1 is a member of an evolutionarily conserved and structurally distinct new family of deubiquitinating enzymes. *Mol. Cell* 63, 146–155. doi: 10.1016/j.molcel.2016.05.009

Akimov, V., Barrio-Hernandez, I., Hansen, S. V. F., Hallenborg, P., Pedersen, A.-K., Bekker-Jensen, D. B., et al. (2018). UbiSite approach for comprehensive mapping of lysine and N-terminal ubiquitination sites. *Nat. Struct. Mol. Biol.* 25, 631–640. doi: 10.1038/s41594-018-0084-y

Amerik, A. Y., and Hochstrasser, M. (2004). Mechanism and function of deubiquitinating enzymes. *Biochim. Biophys. Acta* 1695, 189–207. doi: 10.1016/j.bbamcr.2004.10.003

Bertolaet, B. L., Clarke, D. J., Wolff, M., Watson, M. H., Henze, M., Divita, G., et al. (2001). UBA domains of DNA damage-inducible proteins interact with ubiquitin. *Nat. Struct. Mol. Biol.* 8:417.

Bhullar, K. S., Lagarón, N. O., McGowan, E. M., Parmar, I., Jha, A., Hubbard, B. P., et al. (2018). Kinase-targeted cancer therapies: progress, challenges and future directions. *Mol. Cancer* 17:48. doi: 10.1186/s12943-018-0804-2

Bingol, B., Tea, J. S., Phu, L., Reichelt, M., Bakalarski, C. E., Song, Q., et al. (2014). The mitochondrial deubiquitinase USP30 opposes parkin-mediated mitophagy. *Nature* 510, 370–375. doi: 10.1038/nature13418

Buiting, K., Williams, C., and Horsthemke, B. (2016). Angelman syndrome — insights into a rare neurogenetic disorder. *Nat. Rev. Neurol.* 12, 584–593. doi: 10.1038/nrneurol.2016.133

Chastagner, P., Israël, A., and Brou, C. (2006). Itch/AIP4 mediates Deltex degradation through the formation of K29-linked polyubiquitin chains. *EMBO Rep.* 7, 1147–1153. doi: 10.1038/sj.embor.7400822

Ciechanover, A. (2013). Intracellular protein degradation: from a vague idea through the lysosome and the ubiquitin–proteasome system and onto human diseases and drug targeting. *Bioorg. Med. Chem.* 21, 3400–3410. doi: 10.1016/j.bmc.2013.01.056

Cox, J., and Mann, M. (2008). MaxQuant enables high peptide identification rates, individualized p.p.b.-range mass accuracies and proteome-wide protein quantification. *Nat. Biotechnol.* 26, 1367–1372. doi: 10.1038/nbt.1511

Cox, J., Neuhauser, N., Michalski, A., Scheltema, R. A., Olsen, J. V., and Mann, M. (2011). Andromeda: a peptide search engine integrated into the maxquant environment. *J. Proteome Res.* 10, 1794–1805. doi: 10.1021/pr101065j

D'Arcy, P., Wang, X., and Linder, S. (2015). Deubiquitinase inhibition as a cancer therapeutic strategy. *Pharmacol. Ther.* 147, 32–54. doi: 10.1016/j.pharmthera.2014.11.002

Dynek, J. N., Goncharov, T., Dueber, E. C., Fedorova, A. V., Izrael-Tomasevic, A., Phu, L., et al. (2010). c-IAP1 and UbcH5 promote K11-linked polyubiquitination of RIP1 in TNF signalling. *EMBO J.* 29, 4198–4209. doi: 10.1038/emboj.2010.300

Edelmann, M. J., Nicholson, B., and Kessler, B. M. (2011). Pharmacological targets in the ubiquitin system offer new ways of treating cancer, neurodegenerative disorders and infectious diseases. *Expert Rev. Mol. Med.* 13, e35. doi: 10.1017/S1462399411002031

Elia, A. E. H., Boardman, A. P., Wang, D. C., Huttlin, E. L., Everley, R. A., Dephoure, N., et al. (2015). Quantitative proteomic atlas of ubiquitination and acetylation in the DNA damage response. *Mol. Cell* 59, 867–881. doi: 10.1016/j.molcel.2015.05.006

Fei, C., Li, Z., Li, C., Chen, Y., Chen, Z., He, X., et al. (2013). Smurf1-mediated Lys29-linked nonproteolytic polyubiquitination of axin negatively regulates Wnt/ -catenin signaling. *Mol. Cell. Biol.* 33, 4095–4105. doi: 10.1128/MCB.00418-13

Finley, D. (2009). Recognition and processing of ubiquitin-protein conjugates by the proteasome. *Annu. Rev. Biochem.* 78, 477–513. doi: 10.1146/annurev.biochem.78.081507.101607

Glickman, M. H., and Ciechanover, A. (2002). The ubiquitin-proteasome proteolytic pathway: destruction for the sake of construction. *Physiol. Rev.* 82, 373–428. doi: 10.1152/physrev.00027.2001

Grice, G. L., and Nathan, J. A. (2016). The recognition of ubiquitinated proteins by the proteasome. *Cell. Mol. Life Sci.* 73, 3497–3506. doi: 10.1007/s00018-016-2255-5

Haglund, K., Sigismund, S., Polo, S., Szymkiewicz, I., Di Fiore, P. P., and Dikic, I. (2003). Multiple monoubiquitination of RTKs is sufficient for their endocytosis and degradation. *Nat. Cell Biol.* 5, 461–466. doi: 10.1038/ncb983

Homan, C. C., Kumar, R., Nguyen, L. S., Haan, E., Raymond, F. L., Abidi, F., et al. (2014). Mutations in *USP9X* are associated with X-linked intellectual disability and disrupt neuronal cell migration and growth. *Am. J. Hum. Genet.* 94, 470–478. doi: 10.1016/j.ajhg.2014.02.004

Hornbeck, P. V., Zhang, B., Murray, B., Kornhauser, J. M., Latham, V., and Skrzypek, E. (2015). PhosphoSitePlus, 2014: mutations, PTMs and recalibrations. *Nucleic Acids Res.* 43, D512–D520. doi: 10.1093/nar/gku1267

Huang, X., and Dixit, V. M. (2016). Drugging the undruggables: exploring the ubiquitin system for drug development. *Cell Res.* 26:484. doi: 10.1038/cr.2016.31

Ivantsiv, Y., Kaplun, L., Tzirkin-Goldin, R., Shabek, N., and Raveh, D. (2006). Unique role for the UbL-UbA Protein Ddi1 in turnover of SCFUfo1 complexes. *Mol. Cell. Biol.* 26, 1579–1588. doi: 10.1128/MCB.26.5.1579-1588.2006

Jacobson, A. D., MacFadden, A., Wu, Z., Peng, J., and Liu, C.-W. (2014). Autoregulation of the 26S proteasome by in situ ubiquitination. *Mol. Biol. Cell* 25, 1824–1835. doi: 10.1091/mbc.E13-10-0585

Kaplun, L., Tzirkin, R., Bakhrat, A., Shabek, N., Ivantsiv, Y., and Raveh, D. (2005). The DNA damage-inducible UbL-UbA protein Ddi1 participates in Mec1-mediated degradation of Ho endonuclease. *Mol. Cell. Biol.* 25, 5355–5362. doi: 10.1128/MCB.25.13.5355-5362.2005

Kapuria, V., Peterson, L. F., Fang, D., Bornmann, W. G., Talpaz, M., and Donato, N. J. (2010). Deubiquitinase inhibition by small-molecule WP1130 triggers aggresome formation and tumor cell Apoptosis. *Cancer Res.* 70, 9265–9276. doi: 10.1158/0008-5472.CAN-10-1530

Kee, Y., Lyon, N., and Huibregtse, J. M. (2005). The Rsp5 ubiquitin ligase is coupled to and antagonized by the Ubp2 deubiquitinating enzyme. *EMBO J.* 24, 2414–2424. doi: 10.1038/sj.emboj.7600710

Kim, H. C., and Huibregtse, J. M. (2009). Polyubiquitination by HECT E3s and the determinants of chain type specificity. *Mol. Cell. Biol.* 29, 3307–3318. doi: 10.1128/MCB.00240-09

Komander, D., and Rape, M. (2012). The ubiquitin code. *Annu. Rev. Biochem.* 81, 203–229. doi: 10.1146/annurev-biochem-060310-170328

Lambertson, D., Chen, L., and Madura, K. (1999). Pleiotropic defects caused by loss of the proteasome-interacting factors Rad23 and Rpn10 of *Saccharomyces cerevisiae*. *Genetics* 153, 69–79.

Landré, V., Revi, B., Mir, M. G., Verma, C., Hupp, T. R., Gilbert, N., et al. (2017). Regulation of transcriptional activators by DNA-binding domain ubiquitination. *Cell Death Differ.* 24, 903–916. doi: 10.1038/cdd.2017.42

Lee, S. Y., Ramirez, J., Franco, M., Lectez, B., Gonzalez, M., Barrio, R., et al. (2014). Ube3a, the E3 ubiquitin ligase causing Angelman syndrome and linked to autism, regulates protein homeostasis through the proteasomal shuttle Rpn10. *Cell. Mol. Life Sci.* 71, 2747–2758. doi: 10.1007/s00018-013-1526-7

Liang, R.-Y., Chen, L., Ko, B.-T., Shen, Y.-H., Li, Y.-T., Chen, B.-R., et al. (2014). Rad23 interaction with the proteasome is regulated by phosphorylation of its ubiquitin-like (UbL) domain. *J. Mol. Biol.* 426, 4049–4060. doi: 10.1016/j.jmb.2014.10.004

Low, D., and Chen, K.-S. (2011). UBE3A regulates MC1R expression: a link to hypopigmentation in angelman syndrome: UBE3A activates MC1R promoter. *Pigment Cell Melanoma Res.* 24, 944–952. doi: 10.1111/j.1755-148X.2011.00884.x

Margolis, S. S., Sell, G. L., Zbinden, M. A., and Bird, L. M. (2015). Angelman syndrome. *Neurotherapeutics* 12, 641–650. doi: 10.1007/s13311-015-0361-y

Martinez, A., Lectez, B., Ramirez, J., Popp, O., Sutherland, J. D., Urbé, S., et al. (2017). Quantitative proteomic analysis of Parkin substrates in Drosophila neurons. *Mol. Neurodegener.* 12:29. doi: 10.1186/s13024-017-0170-3

Meyer, H.-J., and Rape, M. (2014). Enhanced protein degradation by branched ubiquitin chains. *Cell* 157, 910–921. doi: 10.1016/j.cell.2014.03.037

Moncla, A., Malzac, P., Voelckel, M.-A., Auquier, P., Girardot, L., Mattei, M.-G., et al. (1999). Phenotype–genotype correlation in 20 deletion and 20 non-deletion Angelman syndrome patients. *Eur. J. Hum. Genet.* 7, 131–139. doi: 10.1038/sj.ejhg.5200258

Na, C.-H., Jones, D. R., Yang, Y., Wang, X., Xu, Y., and Peng, J. (2012). Synaptic protein ubiquitination in rat brain revealed by antibody-based ubiquitome analysis. *J. Proteome Res.* 11, 4722–4732. doi: 10.1021/pr300536k

Nowicka, U., Zhang, D., Walker, O., Krutauz, D., Castañeda, C. A., Chaturvedi, A., et al. (2015). DNA-damage-inducible 1 protein (Ddi1) contains an uncharacteristic ubiquitin-like domain that binds ubiquitin. *Structure* 23, 542–557. doi: 10.1016/j.str.2015.01.010

Osinalde, N., Duarri, A., Ramirez, J., Barrio, R., Perez de Nanclares, G., and Mayor, U. (2018). Impaired proteostasis in rare neurological diseases. *Semin. Cell Dev. Biol.* doi: 10.1016/j.semcdb.2018.10.007 [Epub ahead of print].

Osinalde, N., Sánchez-Quiles, V., Akimov, V., Blagoev, B., and Kratchmarova, I. (2015). SILAC-based quantification of changes in protein tyrosine phosphorylation induced by Interleukin-2 (IL-2) and IL-15 in T-lymphocytes. *Data Brief* 5, 53–58. doi: 10.1016/j.dib.2015.08.007

Paemka, L., Mahajan, V. B., Ehaideb, S. N., Skeie, J. M., Tan, M. C., Wu, S., et al. (2015). Seizures are regulated by ubiquitin-specific peptidase 9 X-linked

(USP9X), a de-ubiquitinase. *PLoS Genet*. 11:e1005022. doi: 10.1371/journal.pgen.1005022

Pham, A. D., and Sauer, F. (2000). Ubiquitin-activating/conjugating activity of TAFII250, a mediator of activation of gene expression in Drosophila. *Science* 289, 2357–2360. doi: 10.1126/science.289.5488.2357

Pinto-Fernandez, A., and Kessler, B. M. (2016). DUBbing cancer: deubiquitylating enzymes involved in epigenetics, DNA damage and the cell cycle as therapeutic targets. *Front. Genet.* 7:133. doi: 10.3389/fgene.2016.00133

Ramirez, J., Lectez, B., Osinalde, N., Sivá, M., Elu, N., Aloria, K., et al. (2018). Quantitative proteomics reveals neuronal ubiquitination of Rngo/Ddi1 and several proteasomal subunits by Ube3a, accounting for the complexity of Angelman syndrome. *Hum. Mol. Genet.* 27, 1955–1971. doi: 10.1093/hmg/ddy103

Ramirez, J., Min, M., Barrio, R., Lindon, C., and Mayor, U. (2016). "Isolation of ubiquitinated proteins to high purity from in vivo samples," in *Proteostasis: Methods and Protocols* Methods in Molecular Biology, ed. R. Matthiesen (New York, NY: Springer), 193–202. doi: 10.1007/978-1-4939-3756-1_10

Rosenzweig, R., Bronner, V., Zhang, D., Fushman, D., and Glickman, M. H. (2012). Rpn1 and Rpn2 coordinate ubiquitin processing factors at proteasome. *J. Biol. Chem.* 287, 14659–14671. doi: 10.1074/jbc.M111.316323

Rott, R., Szargel, R., Haskin, J., Bandopadhyay, R., Lees, A. J., Shani, V., et al. (2011). α-Synuclein fate is determined by USP9X-regulated monoubiquitination. *Proc. Natl. Acad. Sci. U.S.A.* 108, 18666–18671. doi: 10.1073/pnas.1105725108

Ruprecht, B., and Lemeer, S. (2014). Proteomic analysis of phosphorylation in cancer. *Expert Rev. Proteomics* 11, 259–267. doi: 10.1586/14789450.2014.901156

Rutz, S., Kayagaki, N., Phung, Q. T., Eidenschenk, C., Noubade, R., Wang, X., et al. (2015). Deubiquitinase DUBA is a post-translational brake on interleukin-17 production in T cells. *Nature* 518, 417–421. doi: 10.1038/nature13979

Saeki, Y., Saitoh, A., Toh-e, A., and Yokosawa, H. (2002). Ubiquitin-like proteins and Rpn10 play cooperative roles in ubiquitin-dependent proteolysis. *Biochem. Biophys. Res. Commun.* 293, 986–992. doi: 10.1016/s0006-291x(02)00340-6

Sharma, N., Zhu, Q., Wani, G., He, J., Wang, Q.-E., and Wani, A. A. (2014). USP3 counteracts RNF168 via deubiquitinating H2A and γH2AX at lysine 13 and 15. *Cell Cycle* 13, 106–114. doi: 10.4161/cc.26814

Sirkis, R., Gerst, J. E., and Fass, D. (2006). Ddi1, a eukaryotic protein with the retroviral protease fold. *J. Mol. Biol.* 364, 376–387. doi: 10.1016/j.jmb.2006.08.086

Sivá, M., Svoboda, M., Veverka, V., Trempe, J.-F., Hofmann, K., Kožíšek, M., et al. (2016). Human DNA-damage-inducible 2 protein is structurally and functionally distinct from its yeast ortholog. *Sci. Rep.* 6:30443. doi: 10.1038/srep30443

Sun, H., Kapuria, V., Peterson, L. F., Fang, D., Bornmann, W. G., Bartholomeusz, G., et al. (2011). Bcr-Abl ubiquitination and Usp9x inhibition block kinase signaling and promote CML cell apoptosis. *Blood* 117, 3151–3162. doi: 10.1182/blood-2010-03-276477

Swatek, K. N., and Komander, D. (2016). Ubiquitin modifications. *Cell Res.* 26, 399–422. doi: 10.1038/cr.2016.39

Tokunaga, F., Sakata, S., Saeki, Y., Satomi, Y., Kirisako, T., Kamei, K., et al. (2009). Involvement of linear polyubiquitylation of NEMO in NF-κB activation. *Nat. Cell Biol.* 11, 123–132. doi: 10.1038/ncb1821

Tomaić, V., and Banks, L. (2015). Angelman syndrome-associated ubiquitin ligase UBE3A/E6AP mutants interfere with the proteolytic activity of the proteasome. *Cell Death Dis.* 6, e1625. doi: 10.1038/cddis.2014.572

Tomaić, V., Pim, D., and Banks, L. (2009). The stability of the human papillomavirus E6 oncoprotein is E6AP dependent. *Virology* 393, 7–10. doi: 10.1016/j.virol.2009.07.029

Trempe, J.-F., Šašková, K. G., Sivá, M., Ratcliffe, C. D. H., Veverka, V., Hoegl, A., et al. (2016). Structural studies of the yeast DNA damage-inducible protein Ddi1 reveal domain architecture of this eukaryotic protein family. *Sci. Rep.* 6:33671. doi: 10.1038/srep33671

Voloshin, O., Bakhrat, A., Herrmann, S., and Raveh, D. (2012). Transfer of Ho endonuclease and Ufo1 to the proteasome by the UbL-UbA shuttle protein, Ddi1, analysed by complex formation in vitro. *PLoS One* 7:e39210. doi: 10.1371/journal.pone.0039210

Wang, M., and Pickart, C. M. (2005). Different HECT domain ubiquitin ligases employ distinct mechanisms of polyubiquitin chain synthesis. *EMBO J.* 24, 4324–4333. doi: 10.1038/sj.emboj.7600895

Wang, P.-Y., Chang, K.-T., Lin, Y.-M., Kuo, T.-Y., and Wang, G.-S. (2018). Ubiquitination of MBNL1 is required for its cytoplasmic localization and function in promoting neurite outgrowth. *Cell Rep.* 22, 2294–2306. doi: 10.1016/j.celrep.2018.02.025

Williams, C. A., Beaudet, A. L., Clayton-Smith, J., Knoll, J. H., Kyllerman, M., Laan, L. A., et al. (2006). Angelman syndrome 2005: updated consensus for diagnostic criteria. *Am. J. Med. Genet. A.* 140A, 413–418. doi: 10.1002/ajmg.a.31074

Xie, Y., Avello, M., Schirle, M., McWhinnie, E., Feng, Y., Bric-Furlong, E., et al. (2013). Deubiquitinase FAM/USP9X interacts with the E3 ubiquitin ligase SMURF1 protein and protects it from ligase activity-dependent self-degradation. *J. Biol. Chem.* 288, 2976–2985. doi: 10.1074/jbc.M112.430066

Xu, X., Li, C., Gao, X., Xia, K., Guo, H., Li, Y., et al. (2018). Excessive UBE3A dosage impairs retinoic acid signaling and synaptic plasticity in autism spectrum disorders. *Cell Res.* 28, 48–68. doi: 10.1038/cr.2017.132

Yau, R. G., Doerner, K., Castellanos, E. R., Haakonsen, D. L., Werner, A., Wang, N., et al. (2017). Assembly and function of heterotypic ubiquitin chains in cell cycle and protein quality control. *Cell* 171, 918–933.e20. doi: 10.1016/j.cell.2017.09.040

Yi, J. J., Paranjape, S. R., Walker, M. P., Choudhury, R., Wolter, J. M., Fragola, G., et al. (2017). The autism-linked UBE3A T485A mutant E3 ubiquitin ligase activates the Wnt/β-catenin pathway by inhibiting the proteasome. *J. Biol. Chem.* 292, 12503–12515. doi: 10.1074/jbc.M117.788448

Zhang, D., Chen, T., Ziv, I., Rosenzweig, R., Matiuhin, Y., Bronner, V., et al. (2009). Together, Rpn10 and Dsk2 can serve as a polyubiquitin chain-length sensor. *Mol. Cell* 36, 1018–1033. doi: 10.1016/j.molcel.2009.11.012

**Conflict of Interest Statement:** The authors declare that the research was conducted in the absence of any commercial or financial relationships that could be construed as a potential conflict of interest.

frontiers in Physiology

REVIEW
published: 09 May 2019
doi: 10.3389/fphys.2019.00517

# Mitofusins: Disease Gatekeepers and Hubs in Mitochondrial Quality Control by E3 Ligases

*Mafalda Escobar-Henriques*†* and *Mariana Joaquim*†

*Center for Molecular Medicine Cologne (CMMC), Institute for Genetics, Cologne Excellence Cluster on Cellular Stress Responses in Aging-Associated Diseases (CECAD), University of Cologne, Cologne, Germany*

Mitochondria are dynamic organelles engaged in quality control and aging processes. They constantly undergo fusion, fission, transport, and anchoring events, which empower mitochondria with a very interactive behavior. The membrane remodeling processes needed for fusion require conserved proteins named mitofusins, MFN1 and MFN2 in mammals and Fzo1 in yeast. They are the first determinants deciding on whether communication and content exchange between different mitochondrial populations should occur. Importantly, each cell possesses hundreds of mitochondria, with a different severity of mitochondrial mutations or dysfunctional proteins, which potentially spread damage to the entire network. Therefore, the degree of their merging capacity critically influences cellular fitness. In turn, the mitochondrial network rapidly and dramatically changes in response to metabolic and environmental cues. Notably, cancer or obesity conditions, and stress experienced by neurons and cardiomyocytes, for example, triggers the downregulation of mitofusins and thus fragmentation of mitochondria. This places mitofusins upfront in sensing and transmitting stress. In fact, mitofusins are almost entirely exposed to the cytoplasm, a topology suitable for a critical relay point in information exchange between mitochondria and their cellular environment. Consistent with their topology, mitofusins are either activated or repressed by cytosolic post-translational modifiers, mainly by ubiquitin. Ubiquitin is a ubiquitous small protein orchestrating multiple quality control pathways, which is covalently attached to lysine residues in its substrates, or in ubiquitin itself. Importantly, from a chain of events also mediated by E1 and E2 enzymes, E3 ligases perform the ultimate and determinant step in substrate choice. Here, we review the ubiquitin E3 ligases that modify mitofusins. Two mitochondrial E3 enzymes—March5 and MUL1—one ligase located to the ER—Gp78—and finally three cytosolic enzymes—MGRN1, HUWE1, and Parkin—were shown to ubiquitylate mitofusins, in response to a variety of cellular inputs. The respective outcomes on mitochondrial morphology, on contact sites to the endoplasmic reticulum and on destructive processes, like mitophagy or apoptosis, are presented. Ultimately, understanding the mechanisms by which E3 ligases and mitofusins sense and bi-directionally signal mitochondria-cytosolic dysfunctions could pave the way for therapeutic approaches in neurodegenerative, cardiovascular, and obesity-linked diseases.

**Keywords: E3 ligases, ubiquitin, mitofusins, MFN1/MFN2, mitochondria, quality control, mitophagy, ER**

OPEN ACCESS

***Edited by:***
*Julien Licchesi,*
*University of Bath, United Kingdom*

***Reviewed by:***
*Michael Huang,*
*University of Sydney, Australia*
*Derek Narendra,*
*National Institutes of Health (NIH), United States*

***Correspondence:**
*Mafalda Escobar-Henriques*
*mafalda.escobar@uni-koeln.de*

*†These authors have contributed equally to this work*

***Specialty section:***
*This article was submitted to Integrative Physiology, a section of the journal Frontiers in Physiology*

***Received:*** *20 February 2019*
***Accepted:*** *11 April 2019*
***Published:*** *09 May 2019*

***Citation:***
*Escobar-Henriques M and Joaquim M (2019) Mitofusins: Disease Gatekeepers and Hubs in Mitochondrial Quality Control by E3 Ligases. Front. Physiol. 10:517. doi: 10.3389/fphys.2019.00517*

## INTRODUCTION

Mitochondria were considered as static and isolated bean-shaped organelles for a long time, being labeled "power house of the cell" given the assumption that ATP production by oxidative phosphorylation (OXPHOS) was their main function (Mcbride and Neuspiel, 2006). However, as soon as researchers started to look into it by live imaging, it was quickly perceptible the existence of a high dynamism (Bereiter-Hahn and Voth, 1994; Nunnari et al., 1997), later proved to be associated with many new mitochondrial functions (Westermann, 2010). Mitochondria possess proteins that enable plastic responses, depending on the cellular conditions, by fusion, fission, and transport processes (Friedman and Nunnari, 2014). Another hallmark in the field was the awareness of the importance of mitochondrial transport and positioning within the cell and thereby interaction with other cellular compartments surrounding it. Pioneering studies unraveling physical tethering between mitochondria and the endoplasmic reticulum (ER; Kornmann et al., 2009) paved the way for subsequent discoveries on several other mitochondrial contact sites (Eisenberg-bord and Schuldiner, 2017; Cohen et al., 2018). These contacts coordinate a continuous communication of mitochondria with other organelles to support important cellular functions. Finally, the functional impact of mitochondrial interaction with soluble components present in the cytoplasm, like ubiquitin, revealed another layer of the integrative behavior of these organelles (Escobar-Henriques and Langer, 2014; Bragoszewski et al., 2017).

Ubiquitylation is a post-translational modification (PTM) that occurs through the addition of a ubiquitin moiety to substrates (Yau and Rape, 2016; Kwon and Ciechanover, 2017). Ubiquitin is required for many cellular pathways, and the discovery of its regulatory functions is constantly increasing (Rape, 2018). Consistently, ubiquitin targets at mitochondria are associated with several distinct and important cellular processes, mainly with cellular quality control functions (Escobar-Henriques and Langer, 2014).

Here we present the current knowledge on the E3 ligases modifying mitochondrial proteins, focusing on the mitochondrial fusion factors Mitofusin 1 (MFN1) and Mitofusin 2 (MFN2). Mitofusins appear to be preferred targets, constituting a cellular hub in response to metabolic needs of the cell (Chan et al., 2011; Sarraf et al., 2013; Bingol et al., 2014).

### Ubiquitylation

Ubiquitylation of proteins is one of the cellular PTMs, which allow diversifying the coding capacity of genes by covalent modifications, mostly enzyme-catalyzed, of nascent or folded proteins. Therefore, PTMs create a bigger pool of protein diversity (Walsh et al., 2005). The most common small PTMs are phosphorylation, acetylation, glycosylation, carboxylation, methylation, nitrosylation, and S-glycation, which are characterized by the addition of the respective chemical moieties to proteins (Walsh et al., 2005). Moreover, ubiquitin and ubiquitin-like modifiers constitute a set of additional PTMs: ubiquitylation, sumoylation, rubylation, lipidation, ISGylation, and FATylation (Cappadocia and Lima, 2017). Interestingly, ubiquitin itself was shown to be post-translationally modified by phosphorylation and acetylation (Herhaus and Dikic, 2015; Swatek and Komander, 2016).

Ubiquitin is a small highly conserved eukaryotic protein and ubiquitylation is the process by which ubiquitin molecules are added to a substrate (Ciechanover, 2005) (**Figure 1**). It occurs *via* an enzymatic cascade involving three elements: an E1 ubiquitin-activating enzyme, an E2 ubiquitin-conjugating enzyme, and an E3 ubiquitin ligase. First, the E1 enzyme activates ubiquitin and transfers it to the E2 enzyme, in an ATP-dependent manner. Subsequently, the ubiquitin molecule is transferred from the E2 enzyme to a specific target substrate. This requires substrate recognition by an E3 ligase, which either actively receives ubiquitin from the E2 and then covalently binds it to the substrate (HECT, RBR) or serves as a binding platform between the E2 and the substrate (RING) (Komander and Rape, 2012; Yau and Rape, 2016). E3 ligases are of extreme importance in this enzymatic cascade, since they select the specific substrates to be modified (Zheng and Shabek, 2017). Importantly, ubiquitylation is a reversible process, where deubiquitylases are able to remove the ubiquitin moiety from a substrate, resulting in free ubiquitin (Mevissen and Komander, 2017;

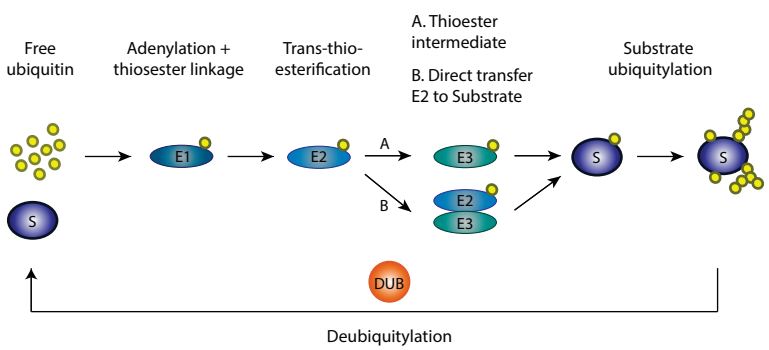


**FIGURE 1 |** Ubiquitylation cascade. Ubiquitylation of substrates requires a cascade of events involving three enzymes: an E1 ubiquitin-activating enzyme, an E2 ubiquitin-conjugating enzyme, and an E3 ubiquitin ligase. First in this cascade, the E1 enzyme activates ubiquitin and transfers it to the E2 enzyme in an ATP-dependent manner with which ubiquitin is conjugated. Afterward, the ubiquitin molecule is transferred from the E2 enzyme to the specific target substrate by the E3 ligase enzymes, which either actively receives ubiquitin from E2 and then transfers it to the substrate or serves as a binding platform between the E2 and the substrate. Finally, on the target substrate, mono, mono-multi, or polyubiquitylation can occur.

Clague et al., 2019). Ubiquitin can be present in substrates in the form of one ubiquitin moiety (mono-ubiquitylation) or several moieties (multi-monoubiquitylation). Moreover, poly-ubiquitin chains of different topologies can also form, *via* any of the seven internal lysine residues in ubiquitin (Lys6, Lys11, Lys27, Lys29, Lys33, Lys48, and Lys63; Komander and Rape, 2012; Yau and Rape, 2016). Due to their different surfaces, these ubiquitin chains attract diverse effectors, giving origin to a variety of functions (Kwon and Ciechanover, 2017). For example, Lys48-linked chains are mostly known to mark proteins for proteasomal degradation *via* the ubiquitin-proteasome system (UPS), whereas Lys63-linked chains are mainly associated with regulatory functions (Kwon and Ciechanover, 2017).

## Mitochondria and Mitofusins

Mitochondria are double membrane organelles composed by the outer mitochondrial membrane (OMM) and the inner mitochondrial membrane (IMM), which are separated by the intermembrane space (IMS; **Figure 2**; Pfanner et al., 2019). The IMM encloses the mitochondrial matrix and forms invaginations called cristae (Frey et al., 2002). The OXPHOS system locates along the cristae and provides the mitochondrial membrane potential, necessary for the production of energy in the form of ATP (Nunnari and Suomalainen, 2012). Besides oxidative phosphorylation, mitochondria perform several other important functions, such as phospholipid synthesis and assembly of iron-sulfur clusters (Braymer and Lill, 2017; Tatsuta and Langer, 2017; Cardenas et al., 2018). In addition, mitochondria are important for cellular responses, such as calcium ($Ca^{2+}$) buffering (Marchi et al., 2017; Xie et al., 2018), mitophagy (Harper et al., 2018; Pickles et al., 2018), and regulation of programmed cell death (Xie et al., 2018; Sedlackova and Korolchuk, 2019).

The functional plasticity of mitochondria is intimately linked to its morphology (Friedman and Nunnari, 2014; Tilokani et al., 2018). Fusion and fission events are majorly important for the regulation of mitochondrial morphology, whereas mitochondrial transport is of particular importance in cells with high-energy demands, such as neurons (Knott and Bossy-Wetzel, 2008; Rakovic et al., 2011). The dynamics between mitochondrial fusion and fission may result in several possible morphological outcomes, from a tubular mitochondrial network, sometimes massively interconnected, to several fragments. This plasticity is fundamental for the maintenance of proper mitochondrial function and to assist mitochondria in response to several stress situations (Liesa and Shirihai, 2013; Schrepfer and Scorrano, 2016; Chen and Chan, 2017). For example, loss of membrane potential and nutrient excess have been shown to induce mitochondrial fragmentation (Yu et al., 2006), whereas nutrient starvation was shown to shift the balance toward a tubular mitochondrial network (Tondera et al., 2009; Gomes et al., 2011; Rambold et al., 2011). These membrane remodeling events are mediated by conserved large dynamin-like GTPase proteins (Praefcke and McMahon, 2004). Drp1 is responsible for fission (Dnm1 in yeast), MFN1/MFN2 for OMM fusion (Fzo1 in yeast), and Opa1 for IMM fusion (Mgm1 in yeast; Youle and van der Bliek, 2012). They are main targets of PTMs, being either activated or repressed in order to push the morphology toward a fused or a fragmented state (**Figure 2**; Escobar-Henriques and Langer, 2014; Macvicar and Langer, 2016; Mishra and Chan, 2016).

Mitofusins are OMM proteins, with the GTPase domain locating at the N-terminal, followed by one hydrophobic heptad repeat (HR1), the transmembrane anchor(s) and finally possessing a second protein-protein interaction domain, HR2 (**Figure 3**). First, it was proposed that both N- and C-terminus face the cytosol, connected by two transmembrane domains and a short loop in the IMS (Rojo et al., 2002). This topology is in agreement with fusion-compatible structural information from both MFN1 and the bacterial homologue BDLP (Low and Löwe, 2006; Low et al., 2009; Qi et al., 2016; Cao et al., 2017). However, an alternative topology for MFN1 and MFN2 was proposed,

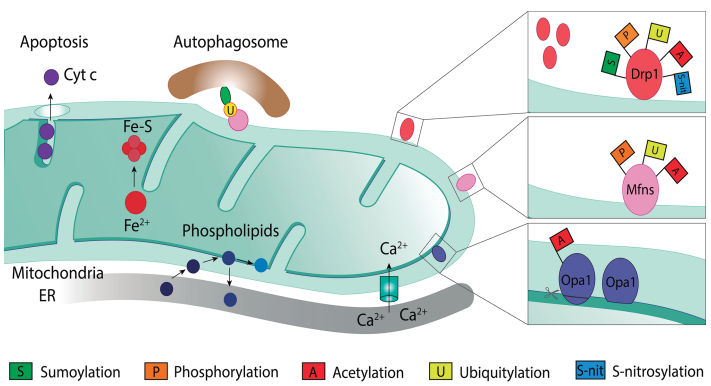


**FIGURE 2 |** Mitochondrial roles and post-translational modifications of mitochondrial dynamic proteins. Mitochondria are involved in several cellular processes other than ATP production, such as calcium ($Ca^{2+}$) buffering, phospholipid biosynthesis, iron-sulfur clusters (Fe-S) assembly from iron ($Fe^{2+}$), regulation of programmed cell death *via* cytochrome c (Cytc c) release, and mitophagy. Mitochondrial proteins known for their role in mitochondrial dynamics, such as Drp1, Mfn1/2, and Opa1, are a target for several post-translational modifications, which differently regulate their level and, hence, function. Drp1, on the OMM, can be modified by sumoylation, phosphorylation, acetylation, ubiquitylation, and S-nitrosylation. Mitofusins, also on the OMM, can be a target for phosphorylation, ubiquitylation, or acetylation. Opa1, in the IMM, can suffer processing or be modified through acetylation.

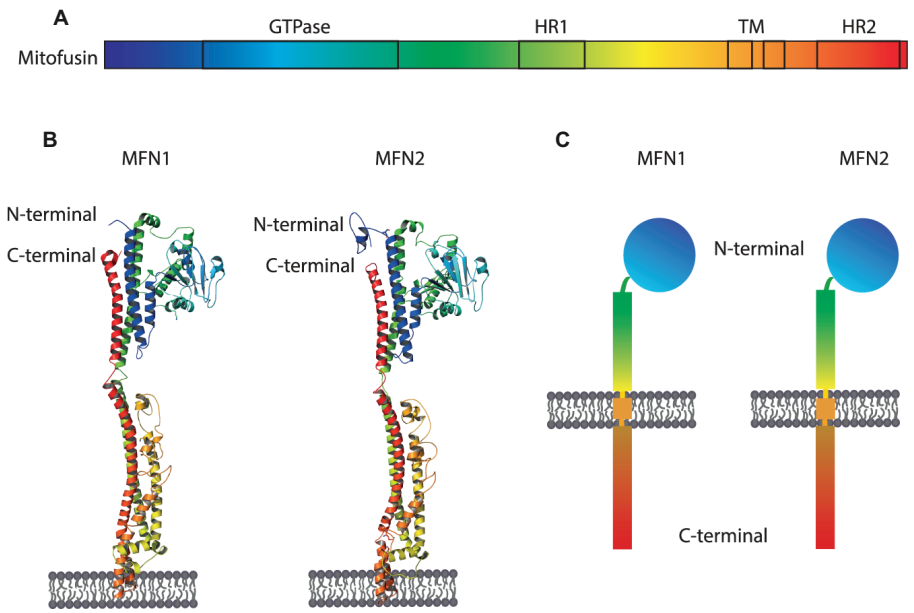


**FIGURE 3 |** Structure and topology models of mitofusins. **(A)** Linear structure of mitofusin, with the GTPase domain locating at the N-terminal, one hydrophobic heptad repeat (HR1), the transmembrane anchor(s), and a second hydrophobic heptad repeat (HR2). **(B)** Crystal structure of MFN1 and MFN2 modeled on BDLP and mini-MFN1, according to the first topology proposed, with two transmembrane domains and both the N- and C-terminus facing the cytosol (Rojo et al., 2002; Low and Löwe, 2006; Low et al., 2009; Qi et al., 2016; Cao et al., 2017). **(C)** Structural scheme of MFN1 and MFN2 according to the second topology proposed with a single spanning-membrane domain, instead of two, and the C-terminus residing in the IMS and not facing the cytosol (Mattie et al., 2018).

with a single spanning-membrane domain, instead of two, therefore placing the C-terminus in the IMS (Mattie et al., 2018). Further studies will be necessary to elucidate which topology of mitofusins reflects fusion-dependent or perhaps fusion-independent roles of mitofusins. MFN1 and MFN2 proteins are 62% identical and 77% similar to each other (Zorzano and Pich, 2006). Interestingly, despite being extremely similar, depletion of each mitofusin has different effects on mitochondrial morphology. While depletion of MFN1 leads to highly fragmented mitochondria, in the shape of small fragments, depletion of MFN2 leads to bigger mitochondrial fragments that aggregate into clusters (**Figure 4**; Chen et al., 2003). Strikingly, homozygous knockout of either MFN1 or MFN2 in mice was shown to be lethal, with death occurring in midgestation (Chen et al., 2003). Additionally, MFN2 depleted mice presented placental defects within the giant cell layer, with a reduced number of giant cells and a reduced number of nuclei on the few cells still observed. However, no placental developmental defects were observed in MFN1 mutants. This suggests that MFN1 and MFN2 may have distinct functions, perhaps independent of their roles in mitochondrial fusion (Loiseau et al., 2007; Guillet et al., 2010; Codron et al., 2016; Beręsewicz et al., 2017; El Fissi et al., 2018; Zhou et al., 2019). For example, a correlation observed between the levels of MFN2 and oxidative phosphorylation was suggested to be dependent on coenzyme Q deficiency, independently of the fusion capacity of MFN2 (Pich et al., 2005; Segalés et al., 2013; Mourier et al., 2015).

## CELLULAR PROCESSES AFFECTED BY UBIQUITYLATION OF MITOFUSINS

Ubiquitylation of both MFN1 and MFN2 has been reported and associated with diverse cellular processes. First, responses directly affecting mitochondria themselves were described, either by changing their morphology or by extending mitochondrial contacts to the ER. Second, effects on mitophagy or apoptosis are the most described effects. Nonetheless, links of mitofusin ubiquitylation with hypoxic and genotoxic stress have also been made.

### Mitochondrial Morphology

Ubiquitylation of mitofusins is promptly observed in yeast, flies, and mammals (Cohen et al., 2008; Ziviani et al., 2010; Rakovic et al., 2011). Interestingly, it plays a dual role in mitochondrial morphology either by addressing mitofusins for proteasomal turnover or by activating mitofusins and therefore promoting membrane merging. It was first suggested that the steady-state levels of Fzo1 are regulated (Fritz et al., 2003), and it was later shown that the turnover of this protein is proteasome-dependent in response to mating factor (Neutzner and Youle, 2005). Moreover, it was shown that the AAA protein and ubiquitin-selective chaperone VCP/p97/Cdc48 is required for proteasomal-dependent degradation of mitofusins (Tanaka et al., 2010; Kim et al., 2013; Zhang et al., 2017). This results in mitochondrial fragmentation, due to ongoing fission events. Moreover, it is associated with

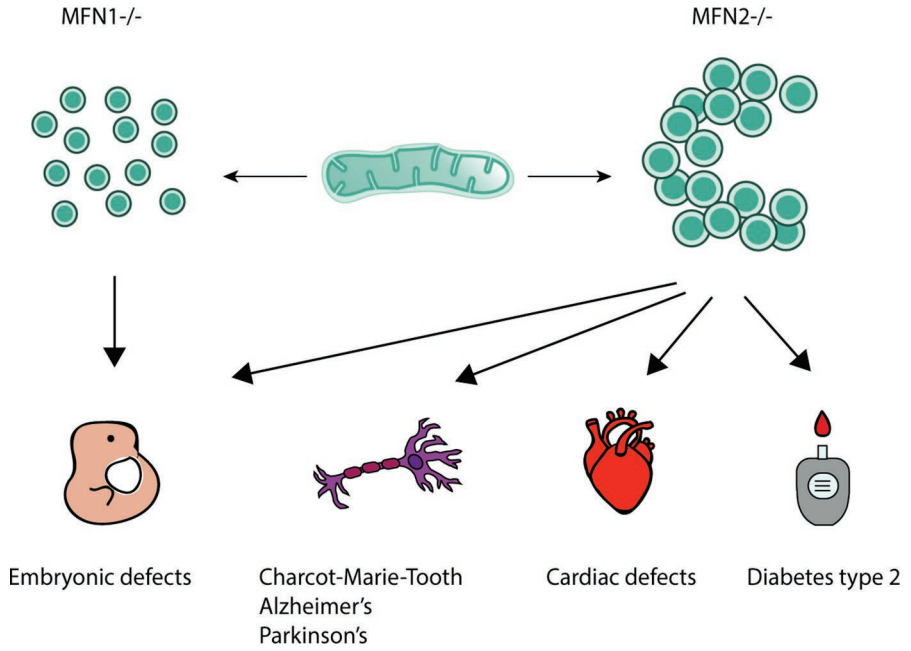


**FIGURE 4 |** Mitochondrial morphology upon knockout of Mitofusin 1 or 2 and its disease-associated roles. Although extremely similar in their sequence and structure, each mitofusin ablation leads to strikingly different mitochondrial morphologies. Mitofusin 1 knockout gives origin to a highly fragmented mitochondrial network composed of many small fragments, whereas depletion of Mitofusin 2 leads to a network where mitochondrial fragments are found enlarged and aggregated in clusters, commonly perinuclearly organized. Several diseases have been associated with knockout of Mitofusin 1 or 2. Homozygous knockout of Mitofusin 1 or 2 leads to embryonic defects such as defective giant cell layer and leads, ultimately, to lethality. While Mitofusin 1 only appears to have an effect at the embryonic level, knockout of its homologue protein, Mitofusin 2, has been shown to relate to several other defects. Animal models depleted for Mitofusin 2 display severe cardiac defects such as cardiomyocyte dysfunction, rapid progressive dilated cardiomyopathy, and final heart failure. Moreover, Mitofusin 2 mutations are the primary cause of the incurable neuropathy Charcot-Marie Tooth Type 2A for which no disease-underlying functions have been yet identified. Additionally, links with other neurodegenerative diseases such as Alzheimer's and Parkinson's diseases have been made, although the molecular mechanisms underlying it are not fully understood. Low levels of Mitofusin 2 were also shown to have a strong positive correlation with diabetes type 2 and obesity.

stress responses, mediated by several E3 ligases, as outlined later. This induces different outcomes, either regulating mitochondria-ER contact sites or affecting mitophagy and apoptosis. On the other hand, pro-fusion ubiquitylation of Fzo1 occurs constitutively and is tightly controlled by deubiquitylases and Cdc48 (Anton et al., 2013; Yue et al., 2014; Simões et al., 2018).

## ER-Mitochondria Contacts

Mitochondria are responsible for a number of cellular and subcellular processes. Consistently, mitochondria form a dynamic network with several other organelles. For example, the junctions formed with the ER are known as the mitochondria-associated ER membrane (MAM) sites and can cover up to 5% of mitochondria (Wu et al., 2018). These junctions are of extreme importance for several processes such as lipids biosynthesis, mitochondrial dynamics, and $Ca^{2+}$ transfer (**Figure 5**; Szabadkai et al., 2006; Friedman et al., 2011; Rowland and Voeltz, 2012; Kojima et al., 2016; Wu et al., 2018; Doghman-Bouguerra and Lalli, 2019).

The majority of enzymes necessary for lipid biosynthesis are found on the ER membrane. However, synthesis of phosphatidylethanolamine (PE) and phosphatidylcholine (PC), the two most abundant phospholipids, requires lipid trafficking between mitochondria and ER, due to the localization of the required enzymes (Rowland and Voeltz, 2012; Kojima et al., 2016; Tatsuta and Langer, 2017). PE is produced from phosphatidylserine (PS), which is synthetized on the ER membrane. In turn, the enzyme phosphatidylserine decarboxylase, which is responsible for the majority of PE biosynthesis, locates mostly at the IMM of mitochondria (Tatsuta and Langer, 2017; Friedman et al., 2018). Therefore, PS must be transferred to mitochondria. In turn, to produce PC, PE must be transferred back to the ER, again requiring lipid transfer events. In conclusion, the biosynthesis of both PE and PC demonstrates the importance of ER-mitochondria contact sites in lipid biosynthesis (**Figure 5**).

Interestingly, the ER was shown to be an active regulator of mitochondrial dynamics. ER tubules that contact with mitochondria were found to correlate with the presence of the mitochondrial fission factor Drp1 (Friedman et al., 2011). In agreement with the idea that ER-mitochondria contacts might regulate mitochondrial division, they correlated with the presence of constricted mitochondria, prior to Drp1 recruitment (**Figure 5**; Friedman et al., 2011). In addition, MFN2 was suggested to be present at the ER, in MAM sites, directly acting as a tether between these two organelles (De Brito and Scorrano, 2008). However, whether ER-mitochondria juxtaposition is promoted (De Brito and Scorrano, 2008; Naon et al., 2016; Basso et al., 2018; McLelland et al., 2018)

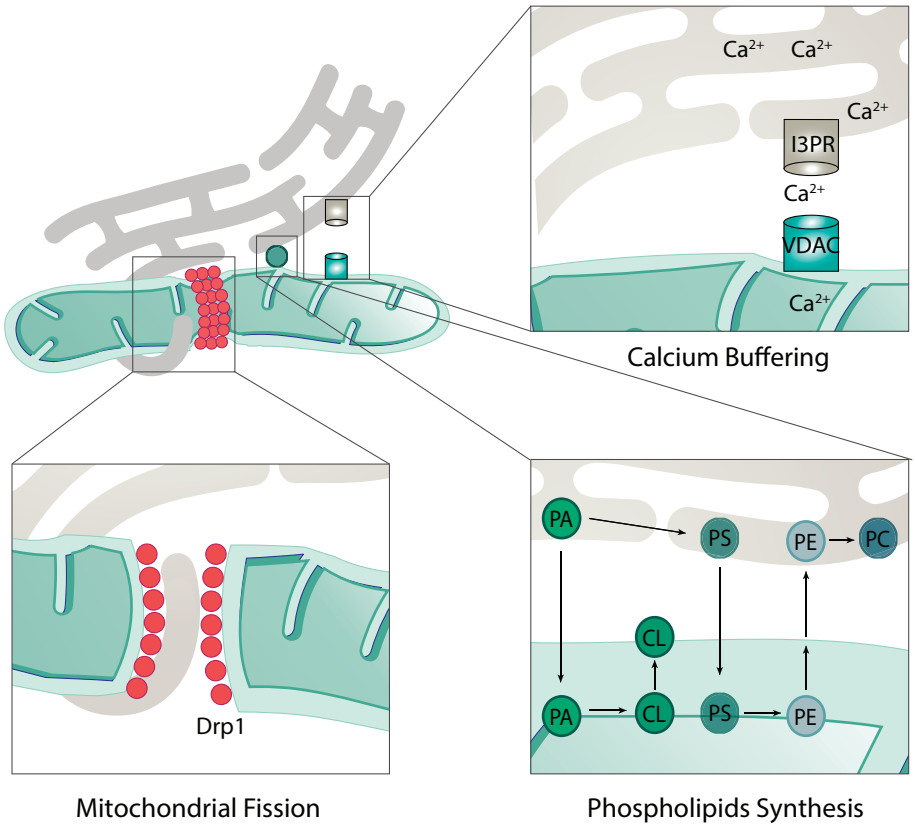


**FIGURE 5 |** Roles of mitochondria-ER contacts. The physical contacts established between mitochondria and ER are responsible for several cellular processes such as mitochondrial fission, calcium buffering, and phospholipid synthesis. During mitochondrial fission, ER tubules are found in contact with mitochondria in the future fission sites. Drp1 is recruited to these sites and, together with ER tubules, promotes constriction and fission of mitochondria. Calcium ($Ca^{2+}$) is transported from the ER to mitochondria *via* transporters in each membrane. On the ER membrane, $Ca^{2+}$ is exported *via* the inositol 1,4,5-triphosphate receptor (I3PR) to the voltage-dependent anion-selective channel (VDAC) on the mitochondrial outer membrane. For the synthesis of some phospholipids, the required enzymes are found in the mitochondria and not in the endoplasmic reticulum (ER). This implies the transfer of precursor forms of phospholipids from the ER to mitochondria where they can be modified and then re-transferred to the ER. For example, the production of the mitochondrial phospholipid cardiolipin (CL) depends on precursor lipids present at the ER. Phosphatidic acid (PA) is transferred from the ER, across the IMS to the IMM, where it is enzymatically modified to form CL, which is further transported to the OMM. An example of a bidirectional movement of lipids between the ER and mitochondria is the production of phosphatidylethanolamine (PE) and phosphatidylcholine (PC). Phosphatidylserine (PS) is first produced on the ER membrane and then translocated to the OMM. On the OMM, PS is transferred to the IMM where it is enzymatically modified to form PE. Finally, in order to produce PC, the precursor PE must be transferred back to the ER where specific enzymes modify it into PC.

or inhibited (Cosson et al., 2012; Filadi et al., 2015; Wang et al., 2015) by MFN2 is controversially discussed, depending perhaps on the cellular growth conditions. Interestingly, a role in ER-mitochondria contacts in inhibiting mitophagy was recently shown (Basso et al., 2018; McLelland et al., 2018).

One of the most well-characterized processes where ER-mitochondria contacts are indispensable is $Ca^{2+}$ buffering (Marchi et al., 2017). $Ca^{2+}$ is transferred from the ER through the inositol 1, 4,5-triphosphate receptor (I3PR) to the voltage-dependent anion-selective channel (VDAC) on the OMM (**Figure 5**; Rizzuto et al., 1998; Szabadkai et al., 2006). In turn, $Ca^{2+}$ influx to the mitochondrial matrix occurs *via* the mitochondrial calcium uniporter (MCU; Kirichok et al., 2004; Baughman et al., 2012). The transfer of $Ca^{2+}$ to mitochondria is required for several mitochondrial proteins or processes, including the TCA cycle enzymes (Bustos et al., 2017). In addition, mitochondrial division has been shown to be affected by $Ca^{2+}$ levels, in a Drp1-dependent manner (Friedman et al., 2011). In fact, some factors required for mitochondrial division and found in MAM sites are regulated by $Ca^{2+}$ binding, as for example MIRO, a protein mainly required for mitochondrial trafficking (Saotome et al., 2008). Finally, $Ca^{2+}$ transferring at the ER-mitochondria contacts was also shown to activate apoptosis (Doghman-Bouguerra and Lalli, 2019). $Ca^{2+}$ influx to mitochondria is able to open the mitochondrial permeability transition pore, leading to the release of cytochrome c and further apoptosis induction (Scorrano et al., 2003).

## Apoptosis

Apoptosis is a highly regulated programmed form of cell death that occurs in response to stress. The apoptotic cascade can be activated *via* the extrinsic or the intrinsic pathway depending on whether the stress signals are extra or intracellular, respectively (Elmore, 2007; Galluzzi and Vitale, 2018). Both pathways culminate with the activation of caspases, the final effectors of apoptosis. The extrinsic pathway is initiated with

the binding of an extracellular death ligand to a cell-surface death receptor. In turn, internal death stimuli are, for example, DNA damage, oncogene activation, the absence of certain growth factors/hormones, or viral infection. The apoptotic intrinsic pathway is mediated by mitochondria (and therefore also known as mitochondrial pathway). It occurs through the release of pro-apoptotic molecules from the IMS to the cytosol, for example, cytochrome c or SMAC/DIABLO (**Figure 6**; Xiong et al., 2014; Ugarte-Uribe and García-Sáez, 2017).

The major players in the apoptotic mitochondrial pathway are proteins belonging to the Bcl-2 family, which can be divided into pro-survival, pro-apoptotic, or apoptosis initiators (Xiong et al., 2014). Within the pro-apoptotic Bcl-2 proteins, BAX and BAK are the two main regulators (Wei et al., 2001; Ugarte-Uribe and García-Sáez, 2017). BAX is a cytosolic protein that translocates to mitochondria upon apoptotic stimuli, where it oligomerizes (Antonsson et al., 2001). Simultaneously, BAK, which locates to mitochondria, undergoes conformational changes and oligomerization upon death stimuli (Griffiths et al., 1999). Although not completely understood how, both BAX and BAK form pores on the OMM, enabling the release of pro-apoptotic molecules from the IMS to the cytosol (Wang and Youle, 2009). Once in the cytosol, cytochrome c binds to the apoptotic protease activating factor 1 (Apaf-1) (Liu et al., 1996), forming the apoptosome. This complex cleaves and activates the pro-caspase 9, followed by the activation of effector caspases (Xiong et al., 2014).

Interestingly, BAX and BAK can interact with mitofusins and Drp1, thus placing apoptosis in close relation with mitochondrial dynamics (Karbowski et al., 2002; Brooks et al., 2007). However, the impact of mitochondrial dynamics and morphology on apoptosis is still controversially discussed (Xie et al., 2018). On one hand, mitochondrial fragmentation was suggested to induce cell death, because fragmented or clustered mitochondria correlated with increased apoptosis, whereas Drp1 loss-of-function prevented apoptosis (Frank et al., 2001; Huang et al., 2007). BAX was shown to translocate to specific sites on mitochondria during the early stages of apoptosis, which subsequently become mitochondrial fission sites (Karbowski et al., 2002), Consistently, Drp1 was able to permeabilize the OMM by BAX recruitment to mitochondria (Montessuit et al., 2010). Moreover, a pro-apoptotic role of Drp1 by stabilizing ER-mitochondria contact sites was recently shown (Prudent et al., 2015; Prudent and Mcbride, 2017). On the other hand, caspase-3 activation and enhanced apoptosis could be observed in Drp1-deficient mice or derived colon cancer cells, attributing an anti-apoptotic role to mitochondrial fragmentation (Wakabayashi et al., 2009; Inoue-yamauchi and Oda, 2012). Reciprocally, a role of BAK and BAX in the regulation of mitochondrial fusion was proposed (Brooks et al., 2007; Hoppins et al., 2011). First, a role of BAK in promoting mitochondrial fragmentation during apoptosis was suggested, along with the disassociation from MFN2 and association with MFN1 (Brooks et al., 2007). Second, under non-apoptotic conditions, soluble BAK activated mitochondrial fusion *via* MFN2 (Hoppins et al., 2011). In conclusion, the reciprocal relation between mitochondrial dynamics and apoptosis is complex and context-specific.

## Mitophagy

Mitochondria are kept in vigilance by a multi-layered quality control system that protects it against all sorts of stress, ensuring maintenance of healthy mitochondria (Harper et al., 2018; Pickles et al., 2018). Upon extreme stress, such as loss of membrane potential, failure of mitochondrial

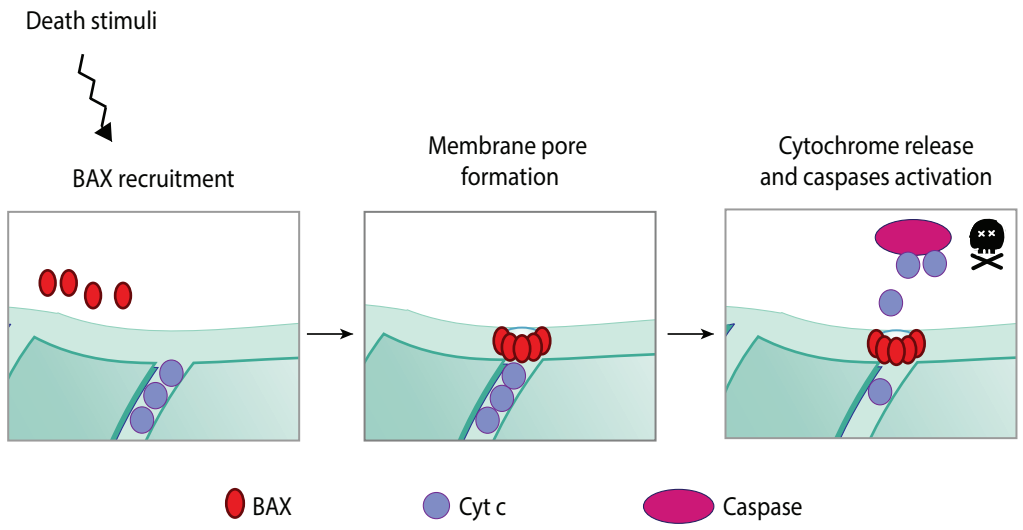


**FIGURE 6 |** Apoptotic intrinsic pathway mediated by mitochondria. The programmed and regulated cell death, apoptosis, can occur *via* two different pathways—intrinsic or extrinsic—according to the origin of the death stimuli, whether it is intrinsic or extrinsic to the cell. Upon intrinsic death stimuli, such as, for example, DNA damage or oncogene activation, the intrinsic apoptotic pathway is activated, which is mediated by mitochondria. Intrinsic stimuli induce the oligomerization of a pro-apoptotic BcL-2 protein—BAX. These oligomers are able to permeabilize the mitochondrial membrane by pore formation on the OMM. Membrane permeabilization allows the release of pro-apoptotic molecules from the IMS, importantly, cytochrome c. In a complex together with other pro-apoptotic proteins, cytochrome c activates caspases, the effectors of apoptosis.

channels, or severe mitochondrial dysfunction, the quality control mechanism activated is mitophagy. Mitophagy is a selective form of macroautophagy that eliminates damaged mitochondrial proteins, or portions of damaged mitochondrial network. It occurs *via* their engulfment by autophagosomes, which subsequently fuse with the lysosome, where degradation occurs (**Figure 7**).

Mitophagy requires the presence of specific receptors linking the autophagosome membrane to the mitochondrial portion destined for degradation, and it can be either dependent or independent on ubiquitin. Moreover, in most cases, mitophagy is also dependent on the ubiquitin-like modifier Atg8 (yeast)/LC3 (mammals), whose lipidated and active form (LC3-II) integrates in the autophagosome membrane. However, LC3-independent mitophagy has also been reported (Nishida et al., 2009; Saito et al., 2019). In *Saccharomyces cerevisiae*, mitochondria are targeted *via* the OMM protein receptor Atg32, its binding to Atg8, and, consequently, the activation of mitophagy (Kanki et al., 2009; Okamoto et al., 2009). In mammals, the homologue of Atg32, Bcl2-L-13, was reported to bind LC3-II on the autophagosome membrane and to be required for mitophagy induction (Otsu et al., 2015). Furthermore, other OMM proteins containing an LC3 interacting (LIR) motif, such as BNIP3, NIX and FUNDC1, were also described to target mitochondria for mitophagic destruction (Novak et al., 2010; Rikka et al., 2011; Liu et al., 2012; Wu et al., 2014).

The mostly described factors mediating ubiquitin-dependent regulation of mitophagy are the kinase PINK1 and the E3 ligase Parkin (**Figure 7**). Upon loss of membrane potential, PINK1 accumulates at the OMM and recruits Parkin to the mitochondria. Once at the OMM, Parkin is phosphorylated by PINK1 and thereby activated (Shiba-Fukushima et al., 2012). Activated Parkin initiates ubiquitylation of several OMM proteins, including MFN1 and MFN2, which immediately leads to loss of fusion events and to mitochondrial fragmentation, characteristic of mitophagy (Gegg et al., 2010; Poole et al., 2010; Tanaka et al., 2010; Ziviani et al., 2010). Furthermore, the poly-ubiquitin chains on surface proteins get bound to LC3-II *via* several adaptors, such as optineurin, NDP52, and p62 (Geisler et al., 2010; Narendra et al., 2010b; Lazarou et al., 2015; Khaminets et al., 2016; Mcwilliams and Muqit, 2017), thus allowing the association of mitochondria to the autophagosomes (Geisler et al., 2010).

In addition to Parkin, the E3 ligase Gp78 also activates mitophagy upon mitochondrial depolarization (Fu et al., 2013). Moreover, other ligases were reported to induce mitophagy as a response to other stress factors, for example, MARCH5, upon disruption of oxygen homeostasis (Daskalaki et al., 2018; Ferrucci et al., 2018; Shefa et al., 2019). In fact, deficiency of $O_2$ causes hypoxic stress, but excess of $O_2$ may lead to excessive reactive oxygen species, both with toxic consequences for the cells. Consequently, eukaryotes have developed complex systems to maintain their oxygen homeostasis. Not surprisingly, hypoxic stress was shown to induce mitophagy, dependent on the receptor FUNDC1 (Liu et al., 2012; Lampert et al., 2019) and its ubiquitin-dependent regulation by MARCH5 (Chen et al., 2017).

## E3 LIGASES ACTING ON MITOFUSINS

Various E3 ligases, soluble or membrane embedded and either located to the cytoplasm, the OMM, or the ER, have been shown to regulate either one or both mitofusins, as a response to various physiological or stress-induced conditions (**Figures 8, 9A,B**). The OMM E3 MARCH5 was implicated in the regulation of mitochondrial morphology, apoptosis, and ER-mitochondria contacts and in responses to toxic stress, *via* both MFN1 and MFN2. In turn, ubiquitylation of MFN2 by the OMM E3 MUL1 is linked to mitochondrial morphology, mitophagy, and neurodegeneration (Cilenti et al., 2014; Yun et al., 2014; Tang et al., 2015). The ER-located E3 Gp78 affected mitophagy and ER-mitochondria contacts, *via* ubiquitylation of both mitofusins (Fu et al., 2013;

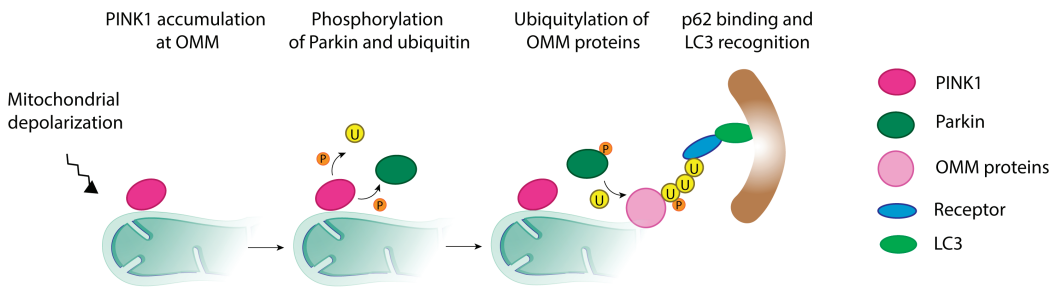


**FIGURE 7 |** Mitochondrial clearance *via* the ubiquitin-mediated pathway. Upon mitochondrial depolarization, a cascade of events is initiated, which targets damaged mitochondria, or portions of it, for degradation by the autophagy machinery. In a first step, the kinase PINK1 accumulates at the mitochondrial outer membrane and initiates phosphorylation (P) and recruitment of the E3 ligase Parkin. Activated Parkin ubiquitylates (U) several outer mitochondrial membrane proteins such as Mitofusins 1 and 2. Additional phosphorylation of ubiquitin generates a positive feedback loop increasing Parkin recruitment and further ubiquitylation. The formation of ubiquitin chains on mitochondrial surface proteins promotes its binding to lipidated LC3, an autophagosome receptor, *via* the mitochondrial receptors (R) such as optineurin, NDP52, or p62. From this point, the mitochondria, or its fragments, meant to be degraded are surrounded by the autophagosome, which finally fuses with the lysosome for final destruction.

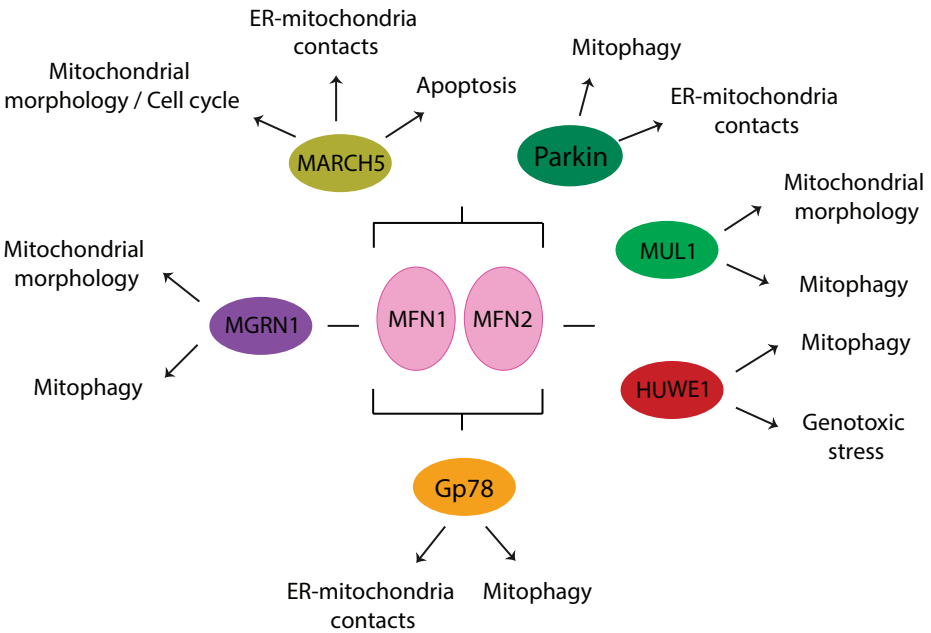


**FIGURE 8 |** E3 ligases that modify mitofusins and cellular processes associated. MARCH5, Parkin, and Gp78 regulate both mitofusins, whereas MGRN1 affects MFN1 and HUWE1 and MUL1 affect MFN2.

Wang et al., 2015). Interestingly, the cytosolic E3 MGRN1 was proposed to coordinate the balance between mitochondrial fusion and mitophagy, *via* Gp78 (Mukherjee and Chakrabarti, 2016a,b). Constitutively, MGRN1 promotes a stabilizing ubiquitylation on MFN1, concomitant with a destabilizing ubiquitylation on Gp78, thus preventing mitophagy and instead promoting fusion. By contrast, stress prevented MGRN1-dependent ubiquitylation and turnover of Gp78, consequently leading to MFN1 turnover, mitochondrial fragmentation, and induction of mitophagy. Ubiquitylation of mitofusins by another cytosolic E3, HUWE1, is linked to both genotoxic stress and mitophagy (Leboucher et al., 2012; Di Rita et al., 2018). Finally, the cytosolic E3 Parkin was shown to be recruited to mitochondria under stress, thus ubiquitylating mitofusins and promoting mitophagy, but was also suggested to regulate ER-mitochondria contact sites, both in mammals and in *Drosophila* (Narendra et al., 2008; Gegg et al., 2010; Poole et al., 2010; Tanaka et al., 2010; Ziviani et al., 2010; Glauser et al., 2011; Rakovic et al., 2011).

## MARCH5

The E3 ligase Human membrane-associated RING-CH-V (MARCH5, also named MARCHV or MITOL) is an integral OMM protein with four membrane-spanning segments and a RING-finger domain at its N-terminus (Nakamura et al., 2006; Yonashiro et al., 2006). MARCH5 is associated with the ubiquitylation and degradation of proteins regulating mitochondrial dynamics. It was shown that its overexpression increased mitochondrial tubulation and that its depletion or the presence of a RING-inactive mutant leads to mitochondrial fragmentation (Nakamura et al., 2006; Yonashiro et al., 2006). These results supporting a "pro-tubulation" role of MARCH5, meaning either promoting fusion or *via* inhibition of mitochondrial fission, the later suggested by Xu et al. (2016). However and by contrast, downregulation or RING-inactive mutants of MARCH5 were also shown to induce abnormal elongation of mitochondria (Karbowski et al., 2007; Park et al., 2010). In fact, depending on the circumstances, MARCH5 ubiquitylates or interacts with both fission and fusion components, suggesting a plastic role in the regulation of mitochondrial morphology, as a response to different stimuli.

Consistent with a plastic role of MARCH5, this ligase was reported to control a fine balance of MFN1 levels and mitochondrial fusion, in order to avoid cellular senescence (Park et al., 2014). First, MARCH5 downregulation led to intense elongation of mitochondria, a pro-survival effect (Park et al., 2010). However, persistent downregulation caused aggregation of mitochondria, progressive cellular enlargement and flattening as well as increased senescence (Park et al., 2010). Consistently, the same authors showed that upon mitochondrial stress, caused by Antimycin A (an inhibitor of complex 3 of the respiratory chain), mitochondria first elongate along with increased levels of MFN1. However, excessive MFN1 leads to mitochondrial aggregation and cellular senescence, which is counteracted by MARCH5. MARCH5 interacts with MFN1 (Park et al., 2010), preferentially binding to acetylated MFN1 on K491 (Park et al., 2014), which is conserved in yeast but not in MFN2. Then, MARCH5 assembles K-48-linked ubiquitin chains on MFN1, addressing it for proteasomal degradation (Park et al., 2014). Moreover, cellular senescence of MARCH5 depleted cells could be rescued by further knockdown of MFN1, especially under Antimycin A induced stress (Park et al., 2014). This suggests an important pro-survival role of MARCH5 upon mitochondrial stress *via* MFN1, concomitant with increased acetylation of

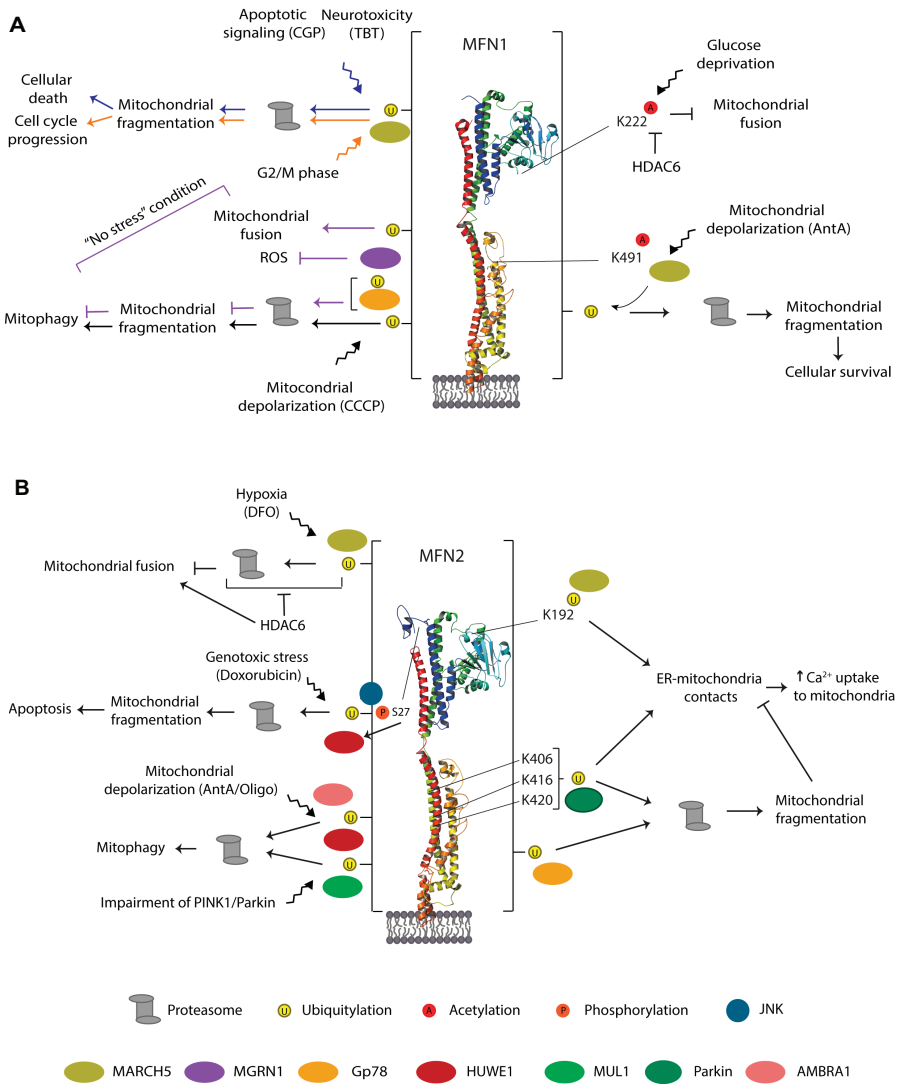


**FIGURE 9 |** Residues, E3 ligases, and processes regulating MFN1 **(A)** MFN2 **(B)**. Representation of the triggers identified to modify mammalian mitofusins by ubiquitylation, phosphorylation, and acetylation. The enzymes evolved in each case, and the cellular outcome is also depicted. The vertical bar on each side of the structure denotes that the residues modified by ubiquitylation in MFN1 or MFN2 are not known. See text for details.

MFN1, rendering it a preferential substrate for MARCH5-dependent degradation (Park et al., 2014).

A link of MARCH5 with cell death, mediated by ubiquitylation of MFN1, was observed upon the addition of CGP37157 (CGP), an inhibitor of mitochondrial calcium efflux, thus an enhancer of apoptosis (Choudhary et al., 2014). Induction of cell death in prostate cancer cells with CGP led to ubiquitylation and degradation of MFN1. MFN1 turnover was dependent on MARCH5, suggesting that it could directly modify MFN1. Moreover, MFN1 depletion in prostate cancer cells increased the cell death response to CGP. Therefore, a pro-apoptotic role of MARCH5 and the potential therapeutic benefits of MFN1 inhibition are suggested (Choudhary et al., 2014). Consistently, in induced pluripotent stem cells (iPSCs), a decrease in cell viability and ATP content, as well as mitochondrial fragmentation, was observed with tributyltin (TBT; Yamada et al., 2016), an endocrine disruptor that causes neurotoxicity and immunotoxicity (Kotake, 2012). TBT led to a decrease in MFN1 levels, which depended on MARCH5, presumably *via* direct ubiquitylation of MFN1 (Yamada et al., 2016).

The apparent contradictory observations of a pro- and anti-survival role of MARCH5 upon Antimycin A or CGP/TBT treatment, respectively, could be explained by the extension of MFN1 overexpression achieved by each stress. Consistently, the levels of acetylated MFN1 probably regulate a fine-tuned balance of fusion activity as well. Indeed, the ubiquitin binding deacetylase HDAC6, mostly cytosolic, was shown to interact with MFN1, mainly under glucose deprivation (Lee et al., 2014). Interestingly, HDAC6 also bound to MFN2, but its acetylation or interaction with HDAC6 was not altered under glucose deprivation (Lee et al., 2014). Importantly, acetylation of MFN1 at K222 was shown to inhibit its fusogenic activity. Moreover, HDAC6-dependent deacetylation of MFN1 ameliorated

ROS production during glucose starvation, supporting a role of MFN1-mediated fusion to cope with metabolic stress (Lee et al., 2014). Therefore, HDAC6 promotes MFN1-dependent hyperfusion, observed both upon glucose starvation in cells and upon fasting in mice (Lee et al., 2014). In conclusion, various stress conditions lead to MARCH5-dependent ubiquitylation and degradation of MFN1.

In addition to MFN1, MARCH5 and HDAC6 regulate stress-induced MFN2 turnover (Kim et al., 2015). MARCH5 interacts with MFN2 (Nakamura et al., 2006), which occurs between the C-terminal domain of MARCH5 and the HR1 domain of MFN2 (Sugiura et al., 2013). Moreover, MARCH5 was shown to be responsible for ubiquitylation and degradation of MFN2 under hypoxic stress, provoked by adding deferoxamine (DFO), in cells lacking HDAC6 (Kim et al., 2015). However, HDAC6 bound strongly to MFN2 in the presence of DFO, thus inhibiting MFN2 turnover and preventing mitochondrial fragmentation (Kim et al., 2015). Therefore, HDAC6 can protect mitochondria and activate adaptive mitochondrial fusion under hypoxic stress (*via* deacetylation of MFN2) and under starvation (*via* deacetylation of MFN1). In both cases, deacetylation of mitofusins induced their fusogenic capacity by preventing ubiquitylation and degradation by MARCH5.

The regulation of MFN1 and MFN2 by MARCH5 was also observed in the absence of external stress, being instead either linked to cell cycle, *via* MFN1, or linked to ER-mitochondria exchanges, *via* MFN2. Cell cycle transitions are accompanied by alterations in mitochondrial morphology, which are actively regulated by both fusion and fission proteins (Mitra, 2013; Horbay and Bilyy, 2016). During the G2/M phase, mitochondria fragment; then, after cellular division, they fuse again (Mitra, 2013). Consistent with the fragmentation, it was shown that MARCH5 ubiquitylates MFN1 at G2/M, addressing it for proteasomal degradation (Park and Cho, 2012). By contrast, a non-proteolytic role of MARCH5 acting on MFN2 was demonstrated, through the addition of K63-linked polyubiquitin chains at K192, located on the GTPase domain and not conserved in MFN1 (Sugiura et al., 2013). Despite the suggestion that MFN2 also locates to the ER, MARCH5 only ubiquitylated MFN2 present at the mitochondria, not ER-associated MFN2. This created a non-proteolytic tag, instead promoting the formation of MFN2 higher oligomers, important to maintain ER-mitochondria contacts (Sugiura et al., 2013). Consistently, MARCH5 knockdown caused MFN2 decrease at MAM sites as well as reduced co-localization of mitochondria and ER, which was rescued upon re-expression of MARCH5. Moreover, a decrease in mitochondrial $Ca^{2+}$ uptake could be observed, suggesting a functional role of MFN2-mediated contact sites, dependent on MARCH5 ubiquitylation of MFN2 (Sugiura et al., 2013).

## HUWE1

HUWE1 is a multifunctional E3 ligase belonging to the HECT-domain E3 ligase family, therefore forming a ubiquitin-thioester intermediate with ubiquitin, before transferring it to the substrate (Bernassola et al., 2008). HUWE1 is composed by an ubiquitin-associated domain, a WWE domain (involved in proteolysis), a BH3 domain (common to the family), and two N-terminal domains. Finally, the HECT domain is found in its C-terminus (Kao et al., 2018). HUWE1 mediates not only K48- and K63-linked poly-ubiquitylation (Adhikary et al., 2005; Zhao et al., 2008) but also mono-ubiquitylation (Parsons et al., 2009) and K11-/K6-linked ubiquitylation (Michel et al., 2017), therefore being suggested to assemble a powerful ubiquitin combination for proteasomal turnover (Meyer and Rape, 2014). This E3 ligase is majorly known for regulation of proliferation, differentiation, and apoptosis, being therefore associated with cancer and metastasis (Kao et al., 2018).

MFN2 was recently shown to be modified in a HUWE1-dependent manner with K6-linked polyubiquitin chains (Michel et al., 2017). Moreover, it was demonstrated that HUWE1 ubiquitylates MFN2 in response to genotoxic stress (Leboucher et al., 2012) and upon induction of mitophagy (Di Rita et al., 2018), thereby addressing MFN2 for proteasomal degradation. First, in sarcoma cells, HUWE1 ubiquitylated MFN2 upon activation of the c-Jun N-terminal kinase (JNK) pathway, by the addition of Doxorubicin, a genotoxic stressor well known for inducing apoptosis (Leboucher et al., 2012). Doxorubicin led to mitochondrial fragmentation and to MFN2 ubiquitylation and phosphorylation at serine 27, signaling proteasomal-dependent loss of MFN2. The authors identified the JNK as the stress-activated kinase phosphorylating MFN2. In addition, MFN2 bound to the BH3 domain of HUWE1, suggesting a role in apoptosis. Consistently, knockdown of HUWE1 prevented apoptosis, which was restored upon further knockdown of MFN2. In summary, this study proposes that phosphorylation of MFN2 by JNK leads to recruitment of the E3 ligase HUWE1 to phosphorylated MFN2 and subsequent acceleration of its degradation by the proteasome. Consequently, degradation of MFN2 leads to enhanced mitochondrial fragmentation and apoptosis (Leboucher et al., 2012).

Second, a role of HUWE1 in mitophagy induction was recently identified. This was observed upon the addition of Oligomycin (an inhibitor of complex 5 of OXPHOS) and Antimycin A, by a pathway mediated by AMBRA1 (Di Rita et al., 2018). AMBRA1 is an inducer of autophagy and a regulator of mitophagy, involved in both PINK1/Parkin-dependent and independent pathways, through binding to LC3 (Strappazzon et al., 2015). HUWE1 interacted with AMBRA1, especially under mitophagy conditions, and translocated to mitochondria. Moreover, both HUWE1-dependent ubiquitylation and proteasomal-dependent degradation of MFN2 were observed. Importantly, HUWE1 depletion impaired AMBRA1-mediated mitophagy (Di Rita et al., 2018).

## Gp78

Glycoprotein 78 (Gp78) is an ER membrane-anchored E3 ubiquitin ligase (Nabi and Raz, 1987). Gp78 is inhibited by the ubiquitous cytokine autocrine motility factor (AMF) and was first identified as the autocrine motility factor receptor (AMFR), for its role in a signaling cascade regulating cancer cell motility and metastasis (Nabi et al., 1990; Silletti et al., 1991). Gp78 regulates protein quality control *via* the ER-associated degradation machinery (ERAD; Fang et al., 2001). ERAD is responsible for the degradation of misfolded or functionally denatured proteins from the ER, occurring *via* proteasomal degradation after their

retro-translocation to the cytosol (Mehrtash and Hochstrasser, 2018). This E3 ligase possesses a G2BR domain, for E2-binding, has five N-terminal transmembrane domains, and, in its C-terminus, has the RING-Finger and VIM domain facing the cytosol (Joshi et al., 2017). The E3 ligase activity of Gp78 is associated with cell signaling and motility, metabolism, neurodegeneration, and cancer/metastasis (Liottaab et al., 1986; Watanabes et al., 1991; Nabi et al., 1992; Luo et al., 2002).

Regarding mitofusins, a role of Gp78 was observed for mitophagy (Fu et al., 2013) and ER-mitochondria contact sites (Wang et al., 2015). First, overexpression of Gp78 was shown to induce mitochondrial fragmentation, dependent on its E3 ligase activity (Fu et al., 2013). Moreover, mitochondrial loss was observed, further aggravated upon mitochondrial uncoupling with CCCP, but rescued by Gp78 downregulation, pointing to its role in mediating mitophagy. Consistently, Gp78 expression was shown to partially recruit LC3 to the ER, co-localizing with Gp78 itself (Fu et al., 2013). Moreover, recruitment of LC3 to Gp78-positive ER domains was dramatically increased upon CCCP treatment, supporting a direct role of Gp78 for clearance of damaged mitochondria. Concomitantly, decreased levels of MFN1 and MFN2 were observed, especially in the presence of CCCP, an effect prevented by proteasomal inhibition (Fu et al., 2013). Moreover, Gp78 interacted with both mitofusins (Fu et al., 2013) and its inhibitor, AMF, prevented Gp78-induced degradation of both MFN1 and MFN2 (Shankar et al., 2013). However, knockdown of MFN1, but not of MFN2, inhibited induction of mitophagy, suggesting that albeit degraded, MFN1 is required for mitophagy. In summary, the role of Gp78 in mitophagy appears to be specifically dependent on MFN1.

In addition to mitophagy, Gp78 promoted contact sites between the ER and mitochondria, which were functional in calcium transfer (Wang et al., 2015). However, despite Gp78 being mostly localized to smooth-ER (Benlimame et al., 1998), it specifically affected contacts of mitochondria to rough ER, in fibrosarcoma cancer cells (Wang et al., 2015). Moreover, in this case, the selective regulation of rough ER by Gp78 depended specifically on the presence of MFN2. Given that MFN2 levels increased upon downregulation of Gp78, the role of the ligase in promoting rough ER-mitochondria contacts might occur *via* ubiquitylation and subsequent degradation of MFN2 (Wang et al., 2015). By contrast, although the levels of MFN1 also increased in the absence of Gp78, MFN1 knockdown did not affect rough ER-mitochondria contacts. Instead, MFN1 knockdown inhibited the contacts between mitochondria and smooth ER, which were not affected by Gp78 knockdown or by the addition of its inhibitor AMF. In summary, both MFN1 and MFN2 behaved as inhibitors of ER-mitochondria contact formation, albeit through different mechanisms and at different ER sites (Wang et al., 2015).

## MGRN1

The E3 ligase Mahogunin Ring Finger-1 (MGRN1) was first discovered to be the gene mutated in a color-coat mutant mice, *mahoganoid* (Phan et al., 2002; He et al., 2003; Upadhyay et al., 2016). MGRN1 is a soluble E3 ligase, however, locating to the cytoplasm, plasma membrane, endosomes, and nucleus (Bagher et al., 2006).

Interestingly, a relation between MGRN1 and both Gp78 and MFN1 was suggested, affecting both mitophagy and mitochondrial fusion. First, the levels of Gp78 itself were negatively regulated by MGRN1, an effect observed in the absence of external stress (Mukherjee and Chakrabarti, 2016a,b). Depletion of MGRN1, or deletion of the RING-finger domain, caused perinuclear clustering of mitochondria and increased oxidatively modified proteins, indicative of ROS (Mukherjee and Chakrabarti, 2016a,b). Moreover, MGRN1-dependent ubiquitylation of Gp78 addressed it for proteasomal degradation. Thus, by repressing Gp78, MGRN1 indirectly prevented mitophagy, MFN1 turnover, and perinuclear clustering. However, depolarization conditions compromised ubiquitylation of Gp78 by MGRN1, thus rescuing the levels of Gp78 and favoring mitophagy of damaged mitochondria (Mukherjee and Chakrabarti, 2016b). Indeed, cells expressing the Ring-Finger mutant MGRN1 reveal higher propensity for mitophagy: they displayed higher levels of LC3-positive mitochondria and presented increased co-localization of mitochondria with p62-positive autophagic vesicles.

Second, MGRN1 also preserved MFN1 stability by directly interacting with it. Moreover, expression of a RING-finger mutant impaired higher oligomerization of MFN1 and mitochondrial fusion (Mukherjee and Chakrabarti, 2016a). Thus, MGRN1 was suggested to actively promote mitochondrial fusion *via* non-degradative ubiquitylation of MFN1, consistent with previous observations (Yue et al., 2014). This is reminiscent of the E3 ligase $SCF^{Mdm30}$ that modifies the yeast mitofusin Fzo1 (Fritz et al., 2003; Escobar-henriques et al., 2006; Cohen et al., 2008, 2011; Anton et al., 2011) with a stabilizing ubiquitylation (Anton et al., 2013; Simões et al., 2018). Indeed, a dual and interdependent balance between constitutive/non-degradative ubiquitylation of MFN1 *vs.* stress-induced/degradative ubiquitylation resembles the regulation of Fzo1 in yeast (Anton et al., 2013; Simões et al., 2018).

## Parkin

Parkin, an E3 ligase associated with Parkinson's disease (Kitada et al., 1998), belongs to the RING-between-RING family of E3 ligases (Smit and Sixma, 2014; Walden and Rittinger, 2018): it has an N-terminal Ub-like (UBL) domain, a zinc-binding domain (RING0, unique to Parkin), a RING domain (RING1, a canonical domain), and two linear zinc-binding folds (IBR and RING2; Panicker et al., 2017). Importantly, Parkin recruitment to the mitochondria requires PINK1 (Geisler et al., 2010; Matsuda et al., 2010; Vives-Bauza et al., 2010; Narendra et al., 2010a), namely its kinase activity and localization at the mitochondrial surface (Okatsu et al., 2012; Shiba-Fukushima et al., 2012). Moreover, crystal structures revealed that Parkin assumes an auto-inhibited conformation that is activated by undergoing major structural rearrangements, which require PINK1-dependent phosphorylation at serine 65 of its UBL domain. In addition, it requires binding of ubiquitin itself, also phosphorylated by PINK1 at serine 65 (Riley et al., 2013; Spratt et al., 2013; Wauer and Komander, 2013; Caulfield et al., 2014; Kane et al., 2014; Kazlauskaite et al., 2014; Koyano et al., 2014; Swatek and Komander, 2016; Wauer et al., 2016; Kumar et al., 2017; Mcwilliams et al., 2018; Gladkova et al., 2019). Parkin is able

to ubiquitylate itself as well as a large variety of both cytosolic and OMM proteins. Mono-ubiquitylation and K63-, K48-, K11-, and K6-linked poly-ubiquitylation have been reported for this E3 ligase (Cunningham et al., 2015; Seirafi et al., 2015; Moutonliger et al., 2017). Despite its diverse functions (Scarffe et al., 2014), the extensive body of literature regarding Parkin and its E3 ligase activity is mainly gathered from its role on mitochondrial clearance (Harper et al., 2018; Pickles et al., 2018), whereby mitofusins are ubiquitylated. Nevertheless, Parkin has also been shown to act on mitofusins for the regulation of ER-mitochondria contact sites (Basso et al., 2018; McLelland et al., 2018).

Among the E3 ligases acting on mitofusins, Parkin is definitely the most well studied. Parkin was initially shown to translocate from the cytoplasm to depolarized mitochondria in mammalian cells (Narendra et al., 2008). This study led to the development of the hypothesis that Parkin not only is responsible for the ubiquitylation of proteins, leading to their subsequent degradation by the UPS, but also acts on the selective elimination of impaired mitochondria. Strikingly, this dramatically raised the interest of many researchers. Shortly after, several mitochondrial ubiquitylation targets of Parkin were identified (Chan et al., 2011). These included dMfn (MARF) in *Drosophila* (Poole et al., 2010; Ziviani et al., 2010) and MFN1 and MFN2 in murine and mammalian cells (Gegg et al., 2010; Tanaka et al., 2010; Glauser et al., 2011; Rakovic et al., 2011), as well as other OMM proteins like VDAC1, Fis1, or Tom20 (Chan et al., 2011). The ubiquitylation of several mitochondrial proteins by Parkin precedes mitophagy and is accomplished by the proteasome, independently of autophagy (Chan et al., 2011; Sarraf et al., 2013). Furthermore, this was shown to be essential for mitophagy, since inhibition of the 26S proteasome fully abrogated Parkin-mediated mitophagy (Tanaka et al., 2010; Chan et al., 2011). In conclusion, upon mitochondrial depolarization, Parkin mediates ubiquitylation of both mitofusins, thus addressing them for proteasomal turnover. However, whether mitofusins are actively required for Parkin-mediated mitophagy is still controversial (Narendra et al., 2008; Chan et al., 2011; Chen and Dorn, 2013), as discussed later.

Interestingly, a direct role of MFN2 in preventing mitophagy dependent on PINK1/Parkin, by keeping mitochondria tethered to the ER, was recently demonstrated (Basso et al., 2018; McLelland et al., 2018). First, depolarization impaired the connection between mitochondria and the ER, a process that depended on proteasomal turnover and was further exacerbated by overexpression of Parkin (McLelland et al., 2018). In fact, turnover of both mitofusins is a very early event after the addition of CCCP (Chan et al., 2011; Sarraf et al., 2013; McLelland et al., 2018). MFN2 was phospho-ubiquitylated, as expected, and its subsequent degradation contributed to the recruitment of Parkin to mitochondria, thus activating the general ubiquitylation of other outer membrane proteins and accelerating mitophagy (McLelland et al., 2018). Consistently, the Parkin-resistant MFN2 HR1 mutants K406R, K416R and K420R failed to induce mitophagy, a specific effect since their capacity to promote mitochondrial fusion was not affected.

Second, in contrast, Parkin-mediated ubiquitylation of mitofusins, also at K416, promoted ER-mitochondria contact sites (Basso et al., 2018). Indeed, downregulation of Parkin in *Drosophila* or mouse embryonic fibroblast (MEF) cells led to decreased ubiquitylation of mitofusins, concomitant with a significant decrease in ER-mitochondria contacts. Moreover, the ubiquitin dead mutant of dMFN, corresponding to K416R in mammals, was also deficient in establishing ER-mitochondria contacts and in mitochondrial $Ca^{2+}$ uptake (Basso et al., 2018). These results suggest that ubiquitylation of dMfn at "lysine 416" regulates physical and functional ER-mitochondria contacts in *Drosophila*. Finally, expressing an ER-mitochondria synthetic linker rescued locomotor deficits associated with Parkinson's disease. In conclusion, although somehow contradictory, both studies suggest an active role of MFN2 in preventing mitophagy by tethering mitochondria to the ER. It is possible that in the absence of external stress mild MFN2 ubiquitylation by Parkin keeps the two organelles together. Then, upon depolarization, excessive ubiquitylation occurs instead targeting MFN2 for proteasomal turnover, again reminiscent of findings in yeast (Anton et al., 2013; Simões et al., 2018).

## MUL1/MULAN/MAPL/GIDE

Like MARCH5, the E3 ligase MUL1 is an integral outer membrane protein regulating mitochondrial dynamics. MUL1/MULAN was first identified as an NF-κB activator with E3 ligase activity (Matsuda et al., 2003). Later, this E3 ligase was identified as a mitochondrial protein, being also known as mitochondria-anchored protein ligase (MAPL) or growth inhibition and death E3 (GIDE) ligase (Li et al., 2008; Neuspiel et al., 2008; Zhang et al., 2008). MUL1 has two transmembrane domains, with its RING-finger domain facing the cytosol, whose overexpression induces fragmentation and perinuclear clustering of mitochondria (Li et al., 2008; Neuspiel et al., 2008). A clear role of MUL1/MAPL as a SUMO E3 ligase was demonstrated (Braschi et al., 2009). For example, MUL1/MAPL acts in the formation of mitochondria-derived vesicles addressed to peroxisomes (Neuspiel et al., 2008; Sugiura et al., 2014), in inflammation (Barry et al., 2018), and in innate immunity (Doiron et al., 2017). In addition, other SUMO-dependent roles were shown, in the regulation of mitochondrial fission (Braschi et al., 2009) and activation of apoptosis, by stabilizing ER-mitochondria contact sites *via* Drp1 SUMOylation (Prudent et al., 2015). Consistently, Zhang et al. (2008) reported MUL1/GIDE as a pro-apoptotic enzyme. However, in what regards the regulation of mitofusins by MUL1, so far only ubiquitin ligase activity was shown (Yun et al., 2014; Tang et al., 2015).

MUL1 was suggested to compensate for PINK1 and Parkin deficiencies, for example, by ubiquitylating mitofusin in *Drosophila*, dMfn/MARF (Yun et al., 2014), and MFN2 in mammals (Tang et al., 2015), thus contributing to mitochondrial integrity by promoting mitophagy. In the fly, overexpression of dMfn aggravated the lethality and neurodegeneration phenotypes seen upon PINK1/Parkin deficiency (Yun et al., 2014). Moreover, these deficiencies could be compensated by MUL1-dependent ubiquitylation and proteasomal degradation of dMfn. Consistently, loss of MUL1 resulted in an increase in dMfn levels. Importantly, increased levels of dMfn, observed in dopaminergic neurons and muscle of PINK1/Parkin mutant

flies, could be rescued upon MUL1 overexpression. Moreover, HeLa cells exposed to cycloheximide presented decreased MFN1 and MFN2 levels, which could be stabilized upon MUL1 silencing (Yun et al., 2014). Consistently, in the mouse model for neurodegeneration, mnd2, where MUL1 accumulated, the levels of MFN2 decreased and mitophagy was enhanced (Cilenti et al., 2014). Moreover, a role of MUL1 in the degradation of MFN2 was suggested in the context of dopaminergic (DA) neuronal loss (Tang et al., 2015), closely related to Parkinson's and Alzheimer's diseases. Indeed, Parkinson's-linked mutations of VPS35, a retromer component for endosomal trafficking, correlated with increased ubiquitylation and decreased levels of MFN2, dependent on the proteasome (Tang et al., 2015). In addition, these neurons presented mitochondrial fragmentation, along with impaired OXPHOS, pointing to mitochondrial dysfunction. Finally, MUL1 inhibition re-increased MFN2, suggesting that MUL1 directly ubiquitylates MFN2, signaling its degradation by the proteasome (Tang et al., 2015). Together, these results indicate that MUL1 compensates for Parkinson's phenotypes, caused by the loss of PINK1/Parkin or VSP35, by decreasing MFN2.

## MITOFUSINS: PRO- OR ANTI-MITOPHAGIC PROTEINS?

During mitophagy induction, mitofusins are clearly among the first substrates to be ubiquitylated by Parkin (Chan et al., 2011; Sarraf et al., 2013; McLelland et al., 2018). However, it was first reported that the absence of both mitofusins did not affect mitophagy (Narendra et al., 2008; Chan et al., 2011). Nevertheless, mutations or modifications of MFN1 and MFN2, either by ubiquitylation, acetylation, or phosphorylation, have also been proposed to directly affect mitophagy (**Figure 10**). As detailed below, whether mitophagy is enhanced or instead repressed by mitofusins and their ubiquitylation is still controversially discussed.

### Pro-mitophagic Role

An active and essential role of MFN2 for mitophagy was proposed under diverse mitophagy induction conditions and different cell lines, tissues, and animal models. First, MFN2-phosphorylation by PINK1 was required for recruiting Parkin to damaged mitochondria (Chen and Dorn, 2013). This study could show that Parkin binds to MFN2 in a PINK1-dependent manner after which PINK1 phosphorylates MFN2. Phosphorylated MFN2 further promotes ubiquitylation of other OMM proteins by Parkin, targeting mitochondria for degradation. This model was supported by the observation that MFN2 depletion from murine cardiomyocytes prevented Parkin translocation to mitochondria upon membrane depolarization and, consequently, decreased mitophagy levels (Chen and Dorn, 2013). Consistently, depletion of MFN1 and MFN2 caused accumulation of defective mitochondria, but no increase in mitophagy levels was observed (Song et al., 2015). These results suggest that ablation of both mitofusins interferes with a step in the mitophagic process, stopping defective mitochondria from being degraded and leading to their accumulation, pointing, thereby, to the fact that both MFN1 and MFN2 are required for mitochondrial clearance in the murine cardiac system. However, it is important to note that other studies have reported that mitophagy still occurs in the absence of MFN1 or MFN2, pointing to the existence of other proteins that serve as Parkin receptors upon mitophagy induction (Narendra et al., 2008; Chan et al., 2011).

Further supporting a pro-mitophagic role, MFN1-knockdown inhibited mitophagy that was caused by overexpression of Gp78. (Fu et al., 2013). Induction of mitophagy by Gp78 and MFN1 was Parkin-independent (Fu et al., 2013). Moreover, MFN2 was also not required. However, MFN2 was reported as a central player in autophagosome-lysosome formation in human cardiomyocytes (Zhao et al., 2012). Deletion of MFN2 in cardiomyocytes led to the extensive accumulation of autophagosomes, in response to ischemia-reperfusion stress, a condition that induces mitophagy (Zhao et al., 2012). Nevertheless, both autophagosome and lysosome formation remained unaltered

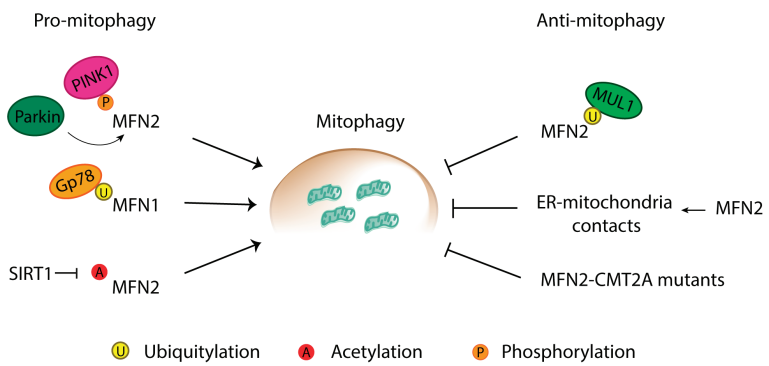


**FIGURE 10 |** Pro- and anti-mitophagic roles of mitofusins. Mitofusins are reported to induce and inhibit mitophagy through a variety of processes. Pro-mitophagic roles of mitofusins can be promoted by (1) phosphorylation of MFN2 by PINK1, and subsequent recruitment of Parkin to mitochondria, (2) Gp78-mediated ubiquitylation of MFN1, and (3) SIRT1-mediated deacetylation of MFN2. Anti-mitophagic roles have been described for Mitofusin 2 *via* (1) MULAN-mediated ubiquitylation, (2) increase of ER-mitochondria contacts directly mediated by MFN2, and (3) mutations in MFN2 associated with Charcot-Marie-Tooth Type 2A (CMT2A) neuropathy.

(Zhao et al., 2012). Instead, autophagosome accumulation was due to marked retardation of the fusion step between autophagosomes and lysosomes, in the absence of MFN2, a phenotype rescued by re-expression of MFN2 (Zhao et al., 2012).

Additional evidences for a pro-mitophagic role of MFN2 were provided in murine skeletal muscle, in the context of aging (Sebastián et al., 2016). Aging in mice was accompanied by a decrease in MFN2 levels and, consistently, MFN2 depletion generated aging signatures (Sebastián et al., 2016). In parallel, MFN2 ablation impaired autophagy and led to excessive mitochondrial dysfunction (Sebastián et al., 2016). In conclusion, during aging MFN2 levels decreased, consequently impairing mitophagy. Also in the context of aging, MFN2 was reported to induce mitophagy in aged human liver cells upon ischemia/reperfusion (I/R) injury (Chun et al., 2018). This study reported a pro-mitophagic role of MFN2, not promoted by the canonical Parkin-dependent ubiquitylation of MFN2, but by another type of PTM: deacetylation *via* sirtuin 1 (SIRT1). Overexpression of either MFN2 or SIRT1 alone failed to rescue I/R injury, mitochondrial dysfunction, and cell death. However, their co-expression promoted autophagy in aged hepatocytes (Chun et al., 2018). Furthermore, the authors showed that deacetylation of MFN2 by SIRT1 occurs at K655 and K662 residues, located in the C-terminus, and directly linked these modification to an increase in autophagy (Chun et al., 2018).

Finally, supporting pro-mitophagic evidences were shown in primary cultured neurons, where I/R injury phenotypes were ameliorated by MFN2 expression and aggravated by its downregulation (Peng et al., 2018). In fact, MFN2 expression led to increased autophagosome formation and fusion with lysosomes (Peng et al., 2018), suggesting once again an important role of MFN2 factor for mitochondrial clearance.

### Anti-mitophagic Role

In the context of the neuropathy Charcot-Marie-Tooth Type 2A (CMT2A), which is caused by dominant-negative mutations in MFN2, it was suggested that MFN2 behaves as an inhibitor of mitophagy (Rizzo et al., 2016). Indeed, motor neurons derived from iPSCS generated from CMT2A fibroblasts had an increased autophagic flux (Rizzo et al., 2016). This suggests an anti-mitophagic role of mutant MFN2 in CMT2A patients. Consistently, in the $CD4^+$ T immune system cells, and in the presence of several stimuli such as rapamycin, ionomycin, or starvation, overexpression of MFN2 led to an impairment in autophagy (Ying et al., 2017).

Moreover, an inhibitory effect of MFN2 toward mitophagy was also suggested in the context of its function as an ER-mitochondria tether. ER-mitochondria contacts are destroyed during mitochondrial clearance process, and, consistently, a reduction in these contacts leads to an increase in mitochondrial degradation (McLelland et al., 2018). Importantly, MFN2 directly promoted contacts between mitochondria and ER, therefore preventing mitophagy (McLelland et al., 2018). Moreover, degradation of MFN2 was necessary for mitophagy to occur. In fact, ubiquitylated MFN2 was suggested to be the active form of MFN2 in promoting ER-mitochondria tethering (Basso et al., 2018). Finally, another anti-mitophagic role of MFN2 was proposed, upon compromised PINK1/Parkin, which depended on ubiquitylation of MFN2 by MUL1, followed by proteasomal degradation (Yun et al., 2014).

## DISEASE-ASSOCIATED ROLES OF MFN2

A broad spectrum of disorders has been linked to mutations or altered levels in MFN2, underlining its physiological relevance (**Figure 4**). MFN2 correlation with disease also supports the idea that MFN2, more than MFN1, is involved in several other disease-relevant roles besides mitochondrial fusion.

First, MFN2 mutations cause a rare neurodegenerative disease. In addition, a link of MFN2 to the most common neuropathies has also been suggested. Importantly, so far no cure is possible for these diseases, being only symptomatic treatments available. Second, a role of MFN2 in mitophagy or ER-contact sites preventing heart failure was proposed. Finally, MFN2 is also linked to diabetes, an aspect of crucial importance in our present society.

### Neurodegeneration

The major causal link between MFN2 dysfunction and disease lies with the CMT2A neuropathy (Züchner et al., 2004; Verhoeven et al., 2006). CMT2A is a subtype of an incurable neuropathy, Charcot-Marie-Tooth (CMT), characterized by progressive distal weakness, muscular atrophy, and sensory abnormalities, affecting 1 in 2,500 people (Tazir et al., 2013, 2014; El-abassi et al., 2014; Stuppia et al., 2015; Stojkovic, 2016; Barbullushi et al., 2019). CMT is one of the most common inherited neurological diseases, usually inherited as an autosomal dominant trait but sometimes as autosomal recessive and X-linked trait. CMT2A subtype presents an earlier onset, with motor symptoms mainly affecting the lower limbs. More than hundred MFN2 mutations are described as causative of CMT2A, comprising one-fifth of all CMT2A cases (Stojkovic, 2016; Dohrn et al., 2017). Strikingly, MFN2 mutations account for approximately 90% of the most severe cases of CMT (Feely et al., 2011).

To date, the disease-underlying functions of MFN2 have not been identified. Recent studies with CMT2A-associated mutations highlighted the importance of carefully addressing membrane potential, apoptosis, ER-mitochondria contacts, and mitophagy in CMT2A, further suggesting fusion-independent roles of Mitofusin 2 (Saporta et al., 2015; Rizzo et al., 2016; Bernard-Marissal et al., 2018; Larrea et al., 2019). Two very recent studies support a pathogenic role of reduced ER-mitochondria contacts caused by MFN2 mutants associated with CMT2A. First, the presence of the most common CMT2A disease mutant $MFN2^{R94Q}$ in patient-derived fibroblasts, primary neurons, and *in vivo* motor neurons of CMT2A mouse model, impaired ER-mitochondria contacts (Bernard-Marissal et al., 2018). Importantly, ER stress, $Ca^{2+}$ defective uptake, and alteration in the axonal transport of mitochondria, could also be observed. Second, the extent of ER-mitochondria contacts also diminished with three different CMT2A variants: $MFN2^{R364W}$, $MFN2^{M376V}$, and $MFN2^{W740S}$ (Larrea et al., 2019). Moreover, phospholipid synthesis and trafficking were affected in cells

expressing these pathogenic mutants, further supporting the functional relevance of ER-mitochondria contact sites for MFN2-related neurodegeneration.

In addition to CMT, links have been made between MFN2 dysregulation and both Parkinson's and Alzheimer's diseases (Han et al., 2011). Indeed, the frontal cortex of Alzheimer's disease patients displays a reduction in MFN2 levels, as well as the hippocampal neurons of post-mortem patients (Wang et al., 2009; Manczak et al., 2011), which is recapitulated in Alzheimer's disease models. In fact, production of amyloid β-peptide (aβ), the main component of amyloid plaques causative of Alzheimer's disease, was found to be decreased upon knockdown of MFN2 (Leal et al., 2016). Furthermore, silencing of MFN2 led to an increase in ER-mitochondria contacts, characteristic of Alzheimer's (Hedskog et al., 2013). However, contradictory results suggest that overexpression of MFN2 leads instead to reduction of aβ-mediated neuronal cell death (Park et al., 2015). In addition to ER-mitochondria contacts, a protective role of mitophagy has also been suggested (Kerr et al., 2017; Fang et al., 2019). Indeed, neurons affected in Alzheimer's disease presented compromised mitophagy and accumulated defective mitochondria, consistent with the mitochondrial dysfunction characteristic of Alzheimer's disease. Importantly, mitophagy induction diminished aβ as well as tau hyperphosphorylation, two hallmarks of Alzheimer's disease (Fang et al., 2019). Supporting this idea, mitophagy induction prevented cognitive impairment in an Alzheimer's disease mouse model and reversed memory impairment in both transgenic tau nematodes and mice (Fang et al., 2019). Regarding Parkinson's disease, the link originates from MFN2 being a target of Parkin. First, loss of function mutations in the genes encoding for Parkin or PINK1 is found at the origin of early-onset PD (Kitada et al., 1998; Valente et al., 2004; Corti et al., 2011). In fact, Parkin mutations are primarily associated with autosomal recessive Parkinson's disease and are the most known cause for this neuropathy. PD is characterized by progressive loss of dopaminergic neurons within substantia nigra, which attributes to Parkin an extremely important neuroprotective role. Second, the E3 ligase Parkin ubiquitylates MFN2 (Tanaka et al., 2010), and other OM proteins (Sarraf et al., 2013), being mitofusins rapidly degraded, among other Parkin targets (Chan et al., 2011; Sarraf et al., 2013). However, causative evidence for a role of MFN2-dependent mitophagy *via* PINK1/Parkin in Parkinson's disease is still missing.

## Cardiac Dysfunction

A link between cardiac dysfunction and mitofusin impairment has been established over the years (Hall et al., 2014). First, ablation of mitofusins in cardiomyocytes, *Drosophila*, and mice caused cardiomyocyte dysfunction, rapid progressive dilated cardiomyopathy, and finally heart failure (Chen et al., 2011; Dorn et al., 2011; Papanicolaou et al., 2012; Song et al., 2017). Furthermore, heart phenotypes present in the fly were rescued upon expression of human mitofusins, supporting evolutionary conserved roles of mitofusins in the heart (Dorn et al., 2011). Interestingly, MFN2 was found to have an essential role in mice heart, in the metabolic shift from carbohydrates to fatty acids as the substrate preference, which occurs during perinatal period (Gong et al., 2015). An MFN2 mutant that cannot be phosphorylated by PINK1 and, therefore, inhibits Parkin-mediated mitophagy, prevented this mitochondrial metabolic maturation, and the respective hearts maintained the fetal metabolic signature (Gong et al., 2015). The authors suggested that mitochondria in fetal cardiomyocyte undergo MFN2-dependent mitophagy in order to allow their replacement by mature mitochondria. This places MFN2 as a central player in this essential metabolic shift. In fact, an active role of MFN2 for mitophagy of cardiac mitochondria had previously been suggested (Chen et al., 2011). Consistently, depletion of MFN1 and MFN2 in cardiomyocytes caused accumulation of defective mitochondria (Song et al., 2015, 2017). Moreover, no increase in mitophagy levels was observed, suggesting that ablation of both mitofusins interferes with a step in the mitophagic process required for the degradation of defective mitochondria (Song et al., 2015, 2017). In fact, despite the existence of fusion events in cardiac mitochondria (Weaver et al., 2014), they are discrete organelles rather than the continuous networks observed in other cell types, perhaps explaining the particular importance of mitophagy (Dorn, 2018).

## Type 2 Diabetes

A critical role of MFN2 for integrative physiology of whole body energy and glucose metabolism has been proposed, in neurons expressing orexigenic neuropeptide agouti-related protein (Agrp) and neurons expressing anorexigenic pro-opiomelanocortin (POMC; Ozcan, 2013; Dietrich et al., 2014; Schneeberger et al., 2014; Timper and Brüning, 2017). Moreover, MFN2 has been linked with diabetes and obesity, which are, *per se*, intimately related (Zorzano et al., 2009). MFN2 is found decreased in skeletal muscle from both obese and type 2 diabetic patients (Bach et al., 2005), in line with increased mitochondrial fission and reduced mitochondrial size, which are characteristic hallmarks of diabetes type 2 (Kelley et al., 2002; Toledo et al., 2006). Interestingly, body weight loss in obese subjects increased the expression of MFN2 in skeletal muscle and rescued mitochondrial size and number (Bach et al., 2005; Toledo et al., 2006). However, in adipose tissues of mice subjected to high-fat diet, the levels of MFN2 were increased, suggesting tissue-specific responses (Boutant et al., 2017). Moreover, ablation of MFN2 in adipocytes was beneficial, as it conferred better tolerance to glucose and protected against high-fat induced insulin resistance (Boutant et al., 2017; Mahdaviani et al., 2017). Interestingly, a concomitant decrease in mitochondria-lipid droplet interaction was observed, which decreased the lipolytic response of adipose tissues (Boutant et al., 2017). Lipid droplets are organelles present in adipose tissues responsible for the storage of lipid molecules. Upon specific metabolic conditions, these organelles release the lipid molecules, which can be further used for ATP production (Londos et al., 1999). Interestingly, the excessive storage of lipids in these organelles was shown to underlie metabolic disorders such as diabetes and obesity. These results suggest an interesting role of MFN2 in mitochondria-lipid droplets interaction, which had been previously described (Pidoux et al., 2011; Rambold et al., 2015). Consistently, lack of MFN2 in mice and *Drosophila*

impairs lipid droplet formation and morphology (Sandoval et al., 2014; Mcfie et al., 2016). Interestingly, enzymes necessary for specific lipids biosynthesis commonly stored in lipid droplets are found enriched at MAM sites, where human MFN2 was also found to be enriched (De Brito and Scorrano, 2008). The nature of this relation is still poorly understood but might depend on a role of MFN2 in ER-mitochondria contacts, shown to be altered in different models of obesity and insulin resistance (Sebastián et al., 2012; Schneeberger et al., 2014; Filadi et al., 2017).

## CONCLUDING REMARKS

The importance of mitochondrial morphology for cellular fitness is increasingly clear. Moreover, the role of mitofusins as a response hub to different metabolic or stress states, by their selective recognition and modification has also been demonstrated. Ubiquitylation by E3 ligases and also phosphorylation or acetylation modulate a myriad of activating or repressing states in mitofusins. Further studies are required to elucidate controversial results and decipher the pathophysiological impact of mitofusin modifications in not only neurodegeneration and cardiac diseases but also energy expenditure-related diseases, such as obesity and diabetes.

## AUTHOR CONTRIBUTIONS

Both authors wrote the manuscript. MJ drew the figures. ME-H coordinated the study.

## FUNDING

This work was supported by a Otto-Bayer fellowship from the Bayer foundation to MJ and by grants of the Deutsche Forschungsgemeinschaft (DFG; ES338/3-1, CRC 1218 TP A03; to ME-H), the Fritz-Thyssen foundation (10.15.1.018MN, to ME-H), the Center for Molecular Medicine Cologne (CMMC; CAP14, to ME-H), funded under the Institutional Strategy of the University of Cologne within the German Excellence Initiative (ZUK 81/1, to ME-H), and benefited from funds of the Faculty of Mathematics and Natural Sciences, attributed to ME-H.

## ACKNOWLEDGMENTS

We are grateful to V. Anton for the structure modeling presented in **Figures 3, 9** and to T. Simões and S. Altin for critical reading of the manuscript.

## REFERENCES

Adhikary, S., Marinoni, F., Hock, A., Hulleman, E., Popov, N., Beier, R., et al. (2005). The ubiquitin ligase HectH9 regulates transcriptional activation by Myc and is essential for tumor cell proliferation. *Cell* 123, 409–421. doi: 10.1016/j.cell.2005.08.016

Anton, F., Dittmar, G., Langer, T., and Escobar-Henriques, M. (2013). Two deubiquitylases act on mitofusin and regulate mitochondrial fusion along independent pathways. *Mol. Cell* 49, 487–498. doi: 10.1016/j.molcel.2012.12.003

Anton, F., Fres, J. M., Schauss, A., Pinson, B., Praefcke, G. J. K., Langer, T., et al. (2011). Ugo1 and Mdm30 act sequentially during Fzo1- mediated mitochondrial outer membrane fusion. *J. Cell Sci.* 124, 1126–1135. doi: 10.1242/jcs.073080

Antonsson, B., Montessuit, S., Sanchez, B., Martinou, J., and Oligomerization, B. (2001). Bax is present as a high molecular weight oligomer/complex in the mitochondrial membrane of apoptotic cells. *J. Biol. Chem.* 276, 11615–11623. doi: 10.1074/jbc.M010810200

Bach, D., Naon, D., Pich, S., Soriano, F. X., Vega, N., Rieusset, J., et al. (2005). Expression of Mfn2, the Charcot-Marie-Tooth neuropathy type 2A gene, in human skeletal muscle. *Diabetes* 54, 2685–2693. doi: 10.2337/diabetes.54.9.2685

Bagher, P., Jiao, J., Owen Smith, C., Cota, C. D., and Gunn, T. M. (2006). Characterization of Mahogunin Ring Finger-1 expression in mice. *Pigment Cell Res.* 19, 635–643. doi: 10.1111/j.1600-0749.2006.00340.x

Barbullushi, K., Abati, E., Rizzo, F., Bresolin, N., Comi, G. P., and Corti, S. (2019). Disease Modeling and Therapeutic Strategies in CMT2A: State of the Art. *Mol. Neurobiol.* doi: 10.1007/s12035-019-1533-2

Barry, R., John, S. W., Liccardi, G., Tenev, T., Jaco, I., Chen, C., et al. (2018). SUMO-mediated regulation of MLRP3 modulates inflammasome activity. *Nat. Commun.* 9, 1–14. doi: 10.1038/s41467-018-05321-2

Basso, V., Marchesan, E., Peggion, C., Chakraborty, J., von Stockum, S., Giacomello, M., et al. (2018). Regulation of endoplasmic reticulum-mitochondria contacts by Parkin via Mfn2. *Pharmacol. Res.* 138, 43–56. doi: 10.1016/j.phrs.2018.09.006

Baughman, J. M., Perocchi, F., Girgis, H. S., Plovanich, M., Belcher-Timme, C. A., Sancak, Y., et al. (2012). Integrative genomics identifies MCU as an essential component of the mitochondrial calcium uniporter. *Nature* 476, 341–345. doi: 10.1038/nature10234

Benlimame, N., Le, P. U., and Nabi, I. R. (1998). Localization of autocrine motility factor receptor to caveolae and clathrin-independent internalization of its ligand to smooth endoplasmic reticulum. *Mol. Biol. Cell* 9, 1773–1786.

Bereiter-Hahn, J., and Voth, M. (1994). Dynamics of mitochondria in living cells: shape changes, dislocations, fusion, and fission of mitochondria. *Microsc. Res. Tech.* 27, 198–219. doi: 10.1002/jemt.1070270303

Beręsewicz, M., Boratyńska-Jasińska, A., Charzewski, Ł., Kawalec, M., Kabzińska, D., Kocha, A., et al. (2017). The effect of a novel c. 820C > T (Arg274Trp) mutation in the mitofusin 2 gene on fibroblast metabolism and clinical manifestation in a patient. *PLoS One* 12, 1–25. doi: 10.1371/journal.pone.0169999

Bernard-Marissal, N., van Hameren, G., Juneja, M., Pellegrino, C., Louhivuori, L., Bartesaghi, L., et al. (2018). Altered interplay between endoplasmic reticulum and mitochondria in Charcot-Marie-Tooth type 2A neuropathy. *Proc. Natl. Acad. Sci. USA* 116, 2328–2337. doi: 10.1073/pnas.1810932116

Bernassola, F., Karin, M., Ciechanover, A., and Melino, G. (2008). The HECT family of E3 ubiquitin ligases: multiple players in cancer development. *Cancer Cell* 14, 10–21. doi: 10.1016/j.ccr.2008.06.001

Bingol, B., Tea, J. S., Phu, L., Reichelt, M., Bakalarski, C. E., Song, Q., et al. (2014). The mitochondrial deubiquitinase USP30 opposes parkin-mediated mitophagy. *Nature* 510, 370–375. doi: 10.1038/nature13418

Boutant, M., Kulkarni, S. S., Joffraud, M., Ratajczak, J., Valera-alberni, M., Combe, R., et al. (2017). Mfn 2 is critical for brown adipose tissue thermogenic function. *EMBO J.* 36, 1543–1558. doi: 10.15252/embj.201694914

Bragoszewski, P., Turek, M., and Chacinska, A. (2017). Control of mitochondrial biogenesis and function by the ubiquitin – proteasome system. *Open Biol.* 7. doi: 10.1098/rsob.170007

Braschi, E., Zunino, R., and McBride, H. M. (2009). MAPL is a new mitochondrial SUMO E3 ligase that regulates mitochondrial fission. *EMBO Rep.* 10, 748–754. doi: 10.1038/embor.2009.86

Braymer, J. J., and Lill, R. (2017). Iron – sulfur cluster biogenesis and trafficking in mitochondria. *J. Biol. Chem.* 292, 12754–12763. doi: 10.1074/jbc.R117.787101

Brooks, C., Wei, Q., Feng, L., Dong, G., Tao, Y., Mei, L., et al. (2007). Bak regulates mitochondrial morphology and pathology during apoptosis by interacting with mitofusins. *Proc. Natl. Acad. Sci. USA* 104, 11649–11654. doi: 10.1088/1757-899X/270/1/012007

Bustos, G., Lovy, A., and Cárdenas, C. (2017). Endoplasmic reticulum – mitochondria calcium communication and the regulation of mitochondrial

metabolism in cancer: a novel potential target. *Front. Oncol.* 7, 1–8. doi: 10.3389/fonc.2017.00199

Cao, Y., Meng, S., Chen, Y., Feng, J., Gu, D., Yu, B., et al. (2017). Mfn1 structures reveal nucleotide-triggered dimerization critical for mitochondrial fusion. *Nature* 542, 372–376. doi: 10.1038/nature21077

Cappadocia, L., and Lima, C. D. (2017). Ubiquitin-like protein conjugation: structures, chemistry, and mechanism. *Chem. Rev.* 118, 889–918. doi: 10.1021/acs.chemrev.6b00737

Cardenas, M., Afroditi, R., and Kostas, C. (2018). Iron – sulfur clusters: from metals through mitochondria biogenesis to disease. *J. Biol. Inorg. Chem.* 23, 509–520. doi: 10.1007/s00775-018-1548-6

Caulfield, T. R., Fiesel, F. C., Moussaud-Lamodière, E. L., Dourado, D. F. A. R., Flores, S. C., and Springer, W. (2014). Phosphorylation by PINK1 releases the UBL domain and initializes the conformational opening of the E3 ubiquitin ligase Parkin. *PLoS Comput. Biol.* 10:e1003935. doi: 10.1371/journal.pcbi.1003935

Chan, N. C., Salazar, A. M., Pham, A. H., Sweredoski, M. J., Kolawa, N. J., Graham, R. L. J., et al. (2011). Broad activation of the ubiquitin-proteasome system by Parkin is critical for mitophagy. *Hum. Mol. Genet.* 20, 1726–1737. doi: 10.1093/hmg/ddr048

Chen, H., and Chan, D. C. (2017). Mitochondrial dynamics in rgulating the ubique phenotypes of cancer ans stem cells. *Cell Metab.* 26, 39–48. doi: 10.1016/j.cmet.2017.05.016

Chen, H., Detmer, S. A., Ewald, A. J., Griffin, E. E., Fraser, S. E., and Chan, D. C. (2003). Mitofusins Mfn1 and Mfn2 coordinately regulate mitochondrial fusion and are essential for embryonic development. *J. Cell Biol.* 160, 189–200. doi: 10.1083/jcb.200211046

Chen, Y., and Dorn, G. W. II (2013). PINK1-phosphorylated mitofusin 2 is a Parkin receptor for culling damaged mitochondria. *Science* 340, 471–475. doi: 10.1126/science.1231031

Chen, Z., Liu, L., Cheng, Q., Li, Y., Wu, H., Zhang, W., et al. (2017). Mitochondrial E 3 ligase MARCH 5 regulates FUNDC 1 to fine-tune hypoxic mitophagy. *EMBO Rep.* 18, 495–509. doi: 10.15252/embr.201643309

Chen, Y., Liu, Y., and Dorn, G. W. II (2011). Mitochondrial fusion is essential for organelle function and cardiac homeostasis. *Circ. Res.* 109, 1327–1331. doi: 10.1161/CIRCRESAHA.111.258723

Choudhary, V., Kaddour-Djebbar, I., Alaisami, R., Kumar, M. V., and Bollag, W. B. (2014). Mitofusin 1 degradation is induced by a disruptor of mitochondrial calcium homeostasis, CGP37157: a role in apoptosis in prostate cancer cells. *Int. J. Oncol.* 44, 1767–1773. doi: 10.3892/ijo.2014.2343

Chun, S. K., Lee, S., Flores-Toro, J., Rebecca, Y. U., Yang, M. J., Go, K. L., et al. (2018). Loss of sirtuin 1 and mitofusin 2 contributes to enhanced ischemia/reperfusion injury in aged livers. *Aging Cell* 17, 1–16. doi: 10.1111/acel.12761

Ciechanover, A. (2005). Proteolysis from the lysosome to ubiquitin and the proteasome. *Nat. Rev. Mol. Cell Biol.* 6, 79–86. doi: 10.1038/nrm1552

Cilenti, L., Ambivero, C. T., Ward, N., Alnemri, E. S., Germain, D., and Zervos, A. S. (2014). Inactivation of Omi/HtrA2 protease leads to the deregulation of mitochondrial Mulan E3 ubiquitin ligase and increased mitophagy. *Biochim. Biophys. Acta Mol. Cell Res.* 1843, 1295–1307. doi: 10.1016/j.bbamcr.2014.03.027

Clague, M. J., Urbé, S., and Komander, D. (2019). Breaking the chains: deubiquitylating enzyme specificity begets function. *Nat. Rev. Mol. Cell Biol.* doi: 10.1038/s41580-019-0099-1

Codron, P., Chevrollier, A., Kane, M. S., Echaniz-laguna, A., Latour, P., Reynier, P., et al. (2016). Increased mitochondrial fusion in a autosomal recessive CMT2A family with mitochondrial GTPase mitofusin 2 mutations. *J. Periphral Nerv. Syst*. 21, 365–369. doi: 10.1111/jns.12192

Cohen, M. M., Amiott, E. A., Day, A. R., Leboucher, G. P., Pryce, E. N., Glickman, M. H., et al. (2011). Sequential requirements for the GTPase domain of the mitofusin Fzo1 and the ubiquitin ligase SCF Mdm30 in mitochondrial outer membrane fusion. *J. Cell Sci.* 124, 1403–1410. doi: 10.1242/jcs.079293

Cohen, M. M. J., Leboucher, G. P., Livnat-Levanon, N., Glickman, M. H., and Weissman, A. M. (2008). Ubiquitin-proteasome-dependent degradation of a mitofusin, a critical regulator of mitochondrial fusion. *Mol. Biol. Cell* 19, 2457–2464. doi: 10.1091/mbc.E08–02–0227

Cohen, S., Valm, A. M., and Lippincott-schwartz, J. (2018). Interacting organelles. *Curr. Opin. Cell Biol.* 53, 84–91. doi: 10.1016/j.ceb.2018.06.003

Corti, O., Lesage, S., and Brice, A. (2011). What genetics tells us about the causes and mechanisms of Parkinson's disease. *Physiol. Rev.* 91, 1161–1218. doi: 10.1152/physrev.00022.2010

Cosson, P., Marchetti, A., Ravazzola, M., and Orci, L. (2012). Mitofusin-2 independent juxtaposition of endoplasmic reticulum and mitochondria: an ultrastructural study. *PLoS One* 7, 1–5. doi: 10.1371/journal.pone.0046293

Cunningham, C. N., Baughman, J. M., Phu, L., Tea, J. S., Yu, C., Coons, M., et al. (2015). USP30 and parkin homeostatically regulate atypical ubiquitin chains on mitochondria. *Nat. Cell Biol.* 17, 160–171. doi: 10.1038/ncb3097

Daskalaki, I., Gkikas, I., and Tavernarakis, N. (2018). Hypoxia and selective autophagy in cancer development and therapy. *Front. Cell Dev. Biol.* 6, 1–22. doi: 10.3389/fcell.2018.00104

De Brito, O. M., and Scorrano, L. (2008). Mitofusin 2 tethers endoplasmic reticulum to mitochondria. *Nature* 456, 605–610. doi: 10.1038/nature07534

Di Rita, A., Peschiaroli, A., D'Acunzo, P., Srobbe, D., Hu, Z., Gruber, J., et al. (2018). HUWE1 E3 ligase promotes PINK1/PARKIN-independent mitophagy by regulating AMBRA1 activation via IKKα. *Nat. Commun.* 9, 1–18. doi: 10.1038/s41467-018-05722-3

Dietrich, M. O., Liu, Z.-W., and Horvath, T. L. (2014). Mitochondrial dynamics controlled by mitofusins regulate Agrp neuronal activity and diet-induced obesity. *Cell* 155, 188–199. doi: 10.1016/j.cell.2013.09.004.Mitochondrial

Doghman-Bouguerra, M., and Lalli, E. (2019). ER-mitochondria interactions: both strength and weakness within cancer cells. *BBA - Mol. Cell Res.* 1866, 650–662. doi: 10.1016/j.bbamcr.2019.01.009

Dohrn, M. F., Glöckle, N., MUlahasanovis, L., Heller, C., Mohr, J., Bauer, C., et al. (2017). Frequent genes in rare diseases: panel-based next generation sequencing to disclose causal mutation in hereditary neuropathies. *J. Neurochem.* 143, 507–522. doi: 10.1111/jnc.14217

Doiron, K., Goyon, V., Coyaud, E., Rajapakse, S., Raught, B., and Mcbride, H. M. (2017). The dynamic interacting landscape of MAPL reveals essential functions for SUMOylation in innate immunity. *Sci. Rep.* 7, 1–11. doi: 10.1038/s41598-017-00151-6

Dorn, G. W. II (2018). Cardiac-specific research platforms engender novel insights into mitochondrial dynamism. *Curr. Opin. Physiol.* 3, 110–115. doi: 10.1016/j.cophys.2018.03.006

Dorn, G. W. II, Clark, C. F., Eschenbacher, W. H., Kang, M., Engelhard, J. T., Warner, S. J., et al. (2011). MARF and Opa1 control mitochondrial and cardiac function in Drosophila. *Circ. Res.* 108, 12–17. doi: 10.1161/CIRCRESAHA.110.236745

Eisenberg-bord, M., and Schuldiner, M. (2017). Mitochatting – if only we could be a fly on the cell wall. *BBA - Mol. Cell Res.* 1864, 1469–1480. doi: 10.1016/j.bbamcr.2017.04.012

El-abassi, R., England, J. D., and Carter, G. T. (2014). Charcot-Marie-Tooth disease: an overview of genotypes, phenotypes, and clinical management strategies. *Am. Acad. Phys. Med. Rehabil.* 6, 342–355. doi: 10.1016/j.pmrj.2013.08.611

Elmore, S. (2007). Apoptosis: a review of programmed cell death. *Toxicol. Pathol.* 35, 495–516. doi: 10.1080/01926230701320337

Escobar-Henriques, M., and Langer, T. (2014). Dynamic survey of mitochondria by ubiquitin. *EMBO Rep.* 15, 231–243. doi: 10.1002/embr.201338225

Escobar-henriques, M., Westermann, B., and Langer, T. (2006). Regulation of mitochondrial fusion by the F-box protein Mdm30 involves proteasome-independent turnover of Fzo1. *J. Cell Biol.* 173, 645–650. doi: 10.1083/jcb.200512079

Fang, S., Ferrone, M., Yang, C., Jensen, J. P., Tiwari, S., and Weissman, A. M. (2001). The tumor autocrine motility factor receptor, gp78, is a ubiquitin protein ligase implicated in degradation from the endoplasmic reticulum. *Proc. Natl. Acad. Sci. USA* 98, 14422–14427. doi: 10.1073/pnas.251401598

Fang, E. F., Hou, Y., Palikaras, K., Adriaanse, B. A., Kerr, J. S., Yang, B., et al. (2019). Mitophagy inhibits amyloid-beta and tau pathology and reverses cognitive deficits in models of Alzheimer's disease. *Nat. Neurosci.* 22, 401–412. doi: 10.1038/s41593-018-0332-9

Feely, S. M. E., Siskind, C. E., Sottile, S., Davis, M., Gibbons, V. S., Reilly, M. M., et al. (2011). MFN2 mutations cause severe phenotypes in most patients with CMT2A. *Neurology* 76, 1690–1696. doi: 10.1212/WNL.0b013e31821a441e

Ferrucci, M., Biagioni, F., Ryskalin, L., Limanaqi, F., Gambardella, S., Frati, A., et al. (2018). Ambiguous effects of autophagy activation following hypoperfusion/ischemia. *Int. J. Mol. Sci.* 19, 1–24. doi: 10.3390/ijms19092756

Filadi, R., Greotti, E., Turacchio, G., Luini, A., Pozzan, T., and Pizzo, P. (2015). Mitofusin 2 ablation increases endoplasmic reticulum – mitochondria coupling. *Proc. Natl. Acad. Sci. USA* 112, E2174–E2181. doi: 10.1073/pnas.1504880112

Filadi, R., Theurey, P., and Pizzo, P. (2017). The endoplasmic reticulum-mitochondria coupling in health and disease: molecules, functions and significance. *Cell Calcium* 62, 1–15. doi: 10.1016/j.ceca.2017.01.003

El Fissi, N., Rojo, M., Aouane, A., Karatas, E., Poliacikova, G., David, C., et al. (2018). Mitofusin gain and loss of function drive pathogenesis in Drosophila models of CMT 2 A neuropathy. *EMBO Rep.* 19, 1–16. doi: 10.15252/embr.201745241

Frank, S., Gaume, B., Bergmann-Leitner, E. S., Leitner, W. W., Robert, E. G., Catez, F., et al. (2001). The role of dynamin-related protein 1, a mediator of mitochondrial fission, in apoptosis. *Dev. Cell* 1, 515–525. doi: 10.1016/S1534-5807(01)00055-7

Frey, T. G., Renken, C. W., and Perkins, G. A. (2002). Insight into mitochondrial structure and function from electron tomography. *Biochim. Biophys. Acta Bioenerg.* 1555, 196–203. doi: 10.1016/S0005-2728(02)00278-5

Friedman, J. R., Kannan, M., Toulmay, A., Jan, C. H., Weissman, J. S., Prinz, W. A., et al. (2018). Lipid homeostasis is maintained by dual targeting of the mitochondrial PE biosynthesis enzyme to the ER. *Dev. Cell* 44, 261–270. doi: 10.1016/j.devcel.2017.11.023

Friedman, J. R., Lackner, L. L., West, M., DiBenedetto, J. R., Nunnari, J., and Voeltz, G. K. (2011). ER tubules mark sites of mitochondrial division. *Science* 334, 358–362. doi: 10.1126/science.1207385

Friedman, J. R., and Nunnari, J. (2014). Mitochondrial form and function. *Nature* 505, 335–343. doi: 10.1038/nature12985

Fritz, S., Weinbach, N., and Westermann, B. (2003). Mdm30 is an F-box protein required for maintenance of fusion-competent mitochondria in yeast. *Mol. Biol. Cell* 14, 2303–2313. doi: 10.1091/mbc.E02

Fu, M., St-Pierre, P., Shankar, J., Wang, P. T. C., Joshi, B., and Nabi, I. R. (2013). Regulation of mitophagy by the Gp78 E3 ubiquitin ligase. *Mol. Biol. Cell* 24, 1153–1162. doi: 10.1091/mbc.E12-08-0607

Galluzzi, L., and Vitale, I. (2018). Molecular mechanisms of cell death: recommendations of the Nomenclature Committee on Cell Death 2018. *Cell Death Differ.* 25, 486–541. doi: 10.1038/s41418-017-0012-4

Gegg, M. E., Cooper, J. M., Chau, K. Y., Rojo, M., Schapira, A. H. V., and Taanman, J. W. (2010). Mitofusin 1 and mitofusin 2 are ubiquitinated in a PINK1/parkin-dependent manner upon induction of mitophagy. *Hum. Mol. Genet.* 19, 4861–4870. doi: 10.1093/hmg/ddq419

Geisler, S., Holmström, K. M., Skujat, D., Fiesel, F. C., Rothfuss, O. C., Kahle, P. J., et al. (2010). PINK1/Parkin-mediated mitophagy is dependent on VDAC1 and p62/SQSTM1. *Nat. Cell Biol.* 12, 119–131. doi: 10.1038/ncb2012

Gladkova, C., Maslen, S., Skehel, J. M., and Komander, D. (2019). Mechanism of Parkin activation by PINK1. *Nature* 559, 410–414. doi: 10.1038/s41586-018-0224-x.Mechanism

Glauser, L., Sonnay, S., Stafa, K., and Moore, D. J. (2011). Parkin promotes the ubiquitination and degradation of the mitochondrial fusion factor mitofusin 1. *J. Neurochem.* 118, 636–645. doi: 10.1111/j.1471-4159.2011.07318.x

Gomes, L. C., Di Benedetto, G., and Scorrano, L. (2011). During autophagy mitochondria elongate, are spared from degradation and sustain cell viability. *Nat. Cell Biol.* 13, 589–598. doi: 10.1038/ncb2220.During

Gong, G., Song, M., Csordas, G., Kelly, D. P., Matkovich, S. J., and Ii, G. W. D. (2015). Parkin-mediated mitophagy directsperinatal cardiac metabolic maturation. *Science* 350, 1–20. doi: 10.1126/science.aad2459

Griffiths, G. J., Dubrez, L., Morgan, C. P., Jones, N. A., Whitehouse, J., Corfe, B. M., et al. (1999). Cell damage-induced conformational changes of the pro-apoptotic protein bak in vivo precede the onset of apoptosis. *J. Cell Biol.* 144, 903–914. doi: 10.1083/jcb.144.5.903

Guillet, V., Gueguen, N., Verny, C., Ferre, M., Homedan, C., Loiseau, D., et al. (2010). Adenine nucleotide translocase is involved in a mitochondrial coupling defect in MFN2 -related Charcot–Marie–Tooth type 2A disease. *Neurogenetics* 11, 127–133. doi: 10.1007/s10048-009-0207-z

Hall, A. R., Burke, N., Dongworth, R. K., and Hausenloy, D. J. (2014). Mitochondrial fusion and fission proteins: novel therapeutic targets for combating cardiovascular. *Br. J. Pharmacol.* 171, 1890–1906. doi: 10.1111/bph.12516

Han, X.-J., Tomizawa, K., Fujimura, A., Ohmori, I., Nishiki, T., Matsushita, M., et al. (2011). Regulation of mitochondrial dynamics and neurodegenerative diseases. *Acta Med. Okayama* 65, 1–10. doi: 10.18926/AMO/43824

Harper, J. W., Ordureau, A., and Heo, J. M. (2018). Building and decoding ubiquitin chains for mitophagy. *Nat. Rev. Mol. Cell Biol.* 19, 93–108. doi: 10.1038/nrm.2017.129

He, L., Lu, X. Y., Jolly, A. F., Eldridge, A. G., Watson, S. J., Jackson, P. K., et al. (2003). Spongiform degeneration in mahoganoid mutant mice. *Science* 299, 710–712. doi: 10.1126/science.1079694

Hedskog, L., Moreira, C., Filadi, R., Rönnbäck, A., Hertwig, L., and Wiehager, B. (2013). Modulation of the endoplasmic reticulum–mitochondria interface in Alzheimer's disease and related models. *Proc. Natl. Acad. Sci. USA* 110, 7916–7921. doi: 10.1073/pnas.1300677110

Herhaus, L., and Dikic, I. (2015). Expanding the ubiquitin code through post-translational modification. *EMBO Rep.* 16, 1071–1083. doi: 10.15252/embr.201540891

Hoppins, S., Edlich, F., Cleland, M., Banerjee, S., Michael, J., Youle, R., et al. (2011). The soluble form of Bax regulates mitochondrial fusion via MFN2 homotypic complexes. *Mol. Cell* 41, 150–160. doi: 10.1016/j.molcel.2010.11.030

Horbay, R., and Bilyy, R. (2016). Mitochondrial dynamics during cell cycling. *Apoptosis* 21, 1327–1335. doi: 10.1007/s10495-016-1295-5

Huang, P., Yu, T., and Yoon, Y. (2007). Mitochondrial clustering induced by overexpression of the mitochondrial fusion protein Mfn2 causes mitochondrial dysfunction and cell death. *Eur. J. Cell Biol.* 86, 289–302. doi: 10.1016/j.ejcb.2007.04.002

Inoue-yamauchi, A., and Oda, H. (2012). Depletion of mitochondrial fission factor DRP1 causes increased apoptosis in human colon cancer cells. *Biochem. Biophys. Res. Commun.* 421, 81–85. doi: 10.1016/j.bbrc.2012.03.118

Joshi, V., Upadhyay, A., Kumar, A., and Mishra, A. (2017). Gp78 E3 ubiquitin ligase: essential functions and contributions in proteostasis. *Front. Cell. Neurosci.* 11, 1–18. doi: 10.3389/fncel.2017.00259

Kane, L. A., Lazarou, M., Fogel, A. I., Li, Y., Yamano, K., Sarraf, S. A., et al. (2014). PINK1 phosphorylates ubiquitin to activate Parkin E3 ubiquitin ligase activity. *J. Cell Biol.* 205, 143–153. doi: 10.1083/jcb.201402104

Kanki, T., Wang, K., Cao, Y., Baba, M., and Klionsky, D. J. (2009). Article Atg32 is a mitochondrial protein that confers selectivity during mitophagy. *Dev. Cell* 17, 98–109. doi: 10.1016/j.devcel.2009.06.014

Kao, S. H., Wu, H. T., and Wu, K. J. (2018). Ubiquitination by HUWE1 in tumorigenesis and beyond. *J. Biomed. Sci.* 25, 1–15. doi: 10.1186/s12929-018-0470-0

Karbowski, M., Lee, Y. J., Gaume, B., Jeong, S. Y., Frank, S., Nechushtan, A., et al. (2002). Spatial and temporal association of Bax with mitochondrial fission sites, Drp1, and Mfn2 during apoptosis. *J. Cell Biol.* 159, 931–938. doi: 10.1083/jcb.200209124

Karbowski, M., Neutzner, A., and Youle, R. J. (2007). The mitochondrial E3 ubiquitin ligase MARCH5 is required for Drp1 dependent mitochondrial division. *J. Cell Biol.* 178, 71–84. doi: 10.1083/jcb.200611064

Kazlauskaite, A., Kondapalli, C., Gourlay, R., Camoberll, D. G., Ritorto, M. S., Hofmann, K., et al. (2014). Parkin is activated by PINK1-dependent phosphorylation of ubiquitin at Ser 65. *Biochem. J.* 460, 127–139. doi: 10.1042/BJ20140334

Kelley, D. E., He, J., Menshikova, E. V., and Ritov, V. B. (2002). Dysfunction of mitochondria in human skeletal muscle in type 2 diabetes. *Diabetes* 51, 2944–2950. doi: 10.2337/diabetes.51.10.2944

Kerr, J. S., Adriaanse, B. A., Greig, N. H., Mattson, M. P., Cader, M. Z., Bohr, V. A., et al. (2017). Mitophagy and Alzheimer's disease: cellular and molecular mechanisms. *Trends Neurosci.* 40, 151–166. doi: 10.1016/j.tins.2017.01.002

Khaminets, A., Behl, C., and Dikic, I. (2016). Ubiquitin-dependent and independent signals in selective autophagy. *Trends Cell Biol.* 26, 6–16. doi: 10.1016/j.tcb.2015.08.010

Kim, H. J., Nagano, Y., Choi, S. J., Park, S. Y., Kim, H., Yao, T. P., et al. (2015). HDAC6 maintains mitochondrial connectivity under hypoxic stress by suppressing MARCH5/MITOL dependent MFN2 degradation. *Biochem. Biophys. Res. Commun.* 464, 1235–1240. doi: 10.1016/j.bbrc.2015.07.111

Kim, N. C., Tresse, E., Kolaitis, R. M., Molliex, A., Ruth, E., Alami, N. H., et al. (2013). VCP is essential for mitochondrial quality control by PINK1/Parkin and this function is impaired by VCP mutations. *Neuron* 78, 65–80. doi: 10.1016/j.neuron.2013.02.029

Kirichok, Y., Krapivinsky, G., and Clapham, D. E. (2004). The mitochondrial calcium uniporter is a highly selective ion channel. *Nature* 427, 360–364. doi: 10.1038/nature02246

Kitada, T., Asakawa, S., Hattori, N., Matsumine, H., Yakamura, Y., Minoshima, S., et al. (1998). Mutations in the parkin gene cause autosomal recessive jubenile parkinsonism. *Nature* 392, 605–608. doi: 10.1038/33416

Knott, A. B., and Bossy-Wetzel, E. (2008). Impairing the mitochondrial fission and fusion balance: a new mechanisms of neurodegeneration. *Ann. N. Y. Acad. Sci.* 1147, 283–292. doi: 10.1196/annals.1427.030

Kojima, R., Endo, T., and Tamura, Y. (2016). A phospholipid transfer function of ER-mitochondria encounter structure revealed in vitro. *Sci. Rep.* 6, 1–9. doi: 10.1038/srep30777

Komander, D., and Rape, M. (2012). The ubiquitin code. *Annu. Rev. Biochem.* 81, 203–229. doi: 10.1146/annurev-biochem-060310-170328

Kornmann, B., Currie, E., Collins, S. R., Schuldiner, M., Nunnari, J., Weissman, J. S., et al. (2009). An ER-mitochondria tethering complex revealed by a synthetic biology screen. *Science* 325, 477–481. doi: 10.1126/science.1175088

Kotake, Y. (2012). Molecular mechanisms of environmental organotin toxicity in mammals. *Biol. Pharm. Bull.* 35, 1876–1880. doi: 10.1248/bpb.b212017

Koyano, F., Okatsu, K., Kosako, H., Tamura, Y., Go, E., Kimura, M., et al. (2014). Ubiquitin is phosphorylated by PINK1 to activate parkin. *Nature* 510, 162–166. doi: 10.1038/nature13392

Kumar, A., Chaugule, V. K., Condos, T. E. C., Barber, K. R., Johnson, C., Toth, R., et al. (2017). Parkin-phosphoubiquitin complex reveals a cryptic ubiquitin binding site required for RBR ligase activity. *Nat. Struct. Mol. Biol.* 24, 475–483. doi: 10.1038/nsmb.3400

Kwon, Y. T., and Ciechanover, A. (2017). The ubiquitin code in the ubiquitin-proteasome system and autophagy. *Trends Biochem. Sci.* 42, 873–886. doi: 10.1016/j.tibs.2017.09.002

Lampert, M. A., Orogo, A. M., Najor, R. H., Hammerling, B. C., Leon, L. J., Wang, B. J., et al. (2019). BNIP3L/NIX and FUNDC1-mediated mitophagy is required for mitochondrial network remodeling during cardiac progenitor cell differentiation. *Autophagy* 1–17. doi: 10.1080/15548627.2019.1580095

Larrea, D., Pera, M., Gonelli, A., Cabrera, R. Q., Akman, H. O., Guardia-Laguarta, C., et al. (2019). MFN2 mutations in Charcot-Marie-Tooth disease alter mitochondria-associated ER membrane function but do not impair bioenergetics. *Hum. Mol. Genet.* 1–19. doi: 10.1093/hmg/ddz008

Lazarou, M., Sliter, D. A., Kane, L. A., Sarraf, S. A., Burman, J. L., Sideris, D. P., et al. (2015). The ubiquitin kinase PINK1 recruits autophagy receptors to induce mitophagy. *Nature* 524, 309–314. doi: 10.1038/nature14893

Leal, N. S., Schreiner, B., Pinho, C. M., Filadi, R., Pizzo, P., Ankarcrona, M., et al. (2016). Mitofusin-2 knockdown increases ER – mitochondria contact and decreases amyloid b -peptide production. *J. Cell. Mol. Med.* 20, 1686–1695. doi: 10.1111/jcmm.12863

Leboucher, G. P., Yien, T. C., Yang, M., Shaw, K. C., Zhou, M., Veenstra, T. D., et al. (2012). Stress-induced phosphorylation and preoteasomal degradation of mitofusin 2 facilitates mitochondrial fragmentation and apoptosis. *Mol. Cell* 47, 546–557. doi: 10.1016/j.molcel.2012.05.041

Lee, J., Kapur, M., Li, M., Choi, M., Choi, S., Kim, H., et al. (2014). MFN1 deacetylation activates adaptive mitochondrial fusion and protects metabolically challenged mitochondria. *J. Cell Sci.* 127, 4954–4963. doi: 10.1242/jcs.157321

Li, W., Bengtson, M. H., Ulbrich, A., Matsuda, A., Reddy, V. A., Orth, A., et al. (2008). Genome-wide and functional annotation of human E3 ubiquitin ligases identifies MULAN, a mitochondrial E3 that regulates the organelle's dynamics and signaling. *PLoS One* 3, 1–13. doi: 10.1371/journal.-pone.0001487

Liesa, M., and Shirihai, O. S. (2013). Mitochondrial dyamics in the regulatin of nutrient utilization and energy expenditure. *Cell Metab.* 17, 491–506. doi: 10.1016/j.cmet.2013.03.002

Liottaab, L. A., Mandlerc, R., Muranoc, G., Katze, D. A., Gordonf, R. K., Chiangf, P. K., et al. (1986). Tumor cell autocrine motility factor. *Proc. Natl. Acad. Sci. USA* 83, 3302–3306.

Liu, L., Feng, D., Chen, G., Chen, M., Zheng, Q., Song, P., et al. (2012). Mitochondrial outer-membrane protein FUNDC1 mediates hypoxia-induced mitophagy in mammalian cells. *Nat. Cell Biol.* 14, 177–185. doi: 10.1038/ncb2422

Liu, X., Kim, C. N., Yang, J., Jemmerson, R., and Wang, X. (1996). Induction of apoptotic program in cell-free extracts: requirement for dATP and cytochrome c. *Cell* 86, 147–157. doi: 10.1016/S0092-8674(00)80085-9

Loiseau, D., Chevrollier, A., Verny, C., Guillet, V., Amati-bonneau, P., and Malthie, Y. (2007). Mitochondrial coupling defect in Charcot–Marie–Tooth type 2A disease. *Ann. Neurol.* 61, 315–323. doi: 10.1002/ana.21086

Londos, C., Brasaemle, D. L., Schultz, C. J., Adler-wailes, D. C., Levin, D. M., Kimmel, A. R., et al. (1999). On the control of lipolysis in adipocytes. *Ann. N. Y. Acad. Sci.* 892, 155–168. doi: 10.1111/j.1749-6632.1999.tb07794.x

Low, H. H., and Löwe, J. (2006). A bacterial dynamin-like proteins. *Nature* 444, 766–769. doi: 10.1038/nature05312

Low, H. H., Sachse, C., Amos, L. A., and Löwe, J. (2009). Structure of a bacterial dynamin-like protein lipid tube provides a mechanism for assembly and membrane curving. *Cell* 139, 1342–1352. doi: 10.1016/j.cell.2009.11.003

Luo, Y., Long, J. M., Lu, C., Chan, S. L., Spangler, E. L., Mascarucci, P., et al. (2002). A link between maze learning and hippocampal expression of neuroleukin and its receptor gp78. *J. Neurochem.* 80, 354–361. doi: 10.1046/j.0022-3042.2001.00707.x

Macvicar, T., and Langer, T. (2016). OPA1 processing in cell death and disease – the long and short of it. *J. Cell Sci.* 128, 2297–2306. doi: 10.1242/jcs.159186

Mahdaviani, K., Benador, I. Y., Su, S., Gharakhanian, R. A., Stiles, L., Trudeau, K. M., et al. (2017). Mfn 2 deletion in brown adipose tissue protects from insulin resistance and impairs thermogenesis. *EMBO Rep.* 18, 1123–1138. doi: 10.15252/embr.201643827

Manczak, M., Calkins, M. J., and Reddy, P. H. (2011). Impaired mitochondrial dynamics and abnormal interaction of amyloid beta with mitochondrial protein Drp1 in neurons from patients with Alzheimer's disease: implications for neuronal damage. *Hum. Mol. Genet.* 20, 2495–2509. doi: 10.1093/hmg/ddr139

Marchi, S., Bittremieux, M., Missiroli, S., Morganti, C., Patergnani, S., Sbano, L., et al. (2017). Endoplasmic reticulum-mitochondria communication through Ca 2+ signaling: the importance of mitochondria- associated membranes (MAMs). *Adv. Exp. Med. Biol.* 997, 49–67. doi: 10.1007/978-981-10-4567-7

Matsuda, N., Sato, S., Shiba, K., Okatsu, K., Saisho, K., Gautier, C. A., et al. (2010). PINK1 stabilized by mitochondrial depolarization recruits Parkin to damaged mitochondria and activates latent Parkin for mitophagy. *J. Cell Biol.* 189, 211–221. doi: 10.1083/jcb.200910140

Matsuda, A., Suzuki, Y., Honda, G., Muramatsu, S., Matsuzaki, O., Nagano, Y., et al. (2003). Large-scale identification and characterization of human genes that activate NF-κB and MAPK signaling pathways. *Oncogene* 22, 3307–3318. doi: 10.1038/sj.onc.1206406

Mattie, S., Riemer, J., Wideman, J. G., and McBride, H. M. (2018). A new mitofusin topology places the redox-regulated C terminus in the mitochondrial intermembrane space. *J. Cell Biol.* 217, 507–515. doi: 10.1083/jcb.201611194

Mcbride, H. M., and Neuspiel, M. (2006). Mitochondria: more than just a powerhouse. *Curr. Biol.* 16, 551–560. doi: 10.1016/j.cub.2006.06.054

Mcfie, P. J., Ambilwade, P., Vu, H., and Stone, S. J. (2016). Biochemical and biophysical research communications endoplasmic reticulum-mitochondrial interaction mediated by mitofusin-1 or mitofusin-2 is not required for lipid droplet formation or adipocyte differentiation. *Biochem. Biophys. Res. Commun.* 478, 392–397. doi: 10.1016/j.bbrc.2016.07.040

McLelland, G. L., Goiran, T., Yi, W., Dorval, G., Chen, C. X., Lauinger, N. D., et al. (2018). Mfn2 ubiquitination by PINK1/parkin gates the p97-dependent release of ER from mitochondria to drive mitophagy. *elife* 7, 1–35. doi: 10.7554/eLife.32866

Mcwilliams, T. G., Barini, E., Pohjolan-pirhonen, R., Brooks, P., Burel, S., Balk, K., et al. (2018). Phosphorylation of Parkin at serine 65 is essential for its activation in vivo. *Open Biol.* 1, 1–18. doi: 10.1098/rsob.180108

Mcwilliams, T. G., and Muqit, M. M. K. (2017). Science direct PINK1 and Parkin: emerging themes in mitochondrial homeostasis. *Curr. Opin. Cell Biol.* 45, 83–91. doi: 10.1016/j.ceb.2017.03.013

Mehrtash, A. B., and Hochstrasser, M. (2018). Ubiquitin-dependent protein degradation at the endoplasmic reticulum and nuclear envelope. *Semin. Cell Dev. Biol.* 1. doi: 10.1016/j.semcdb.2018.09.013

Mevissen, T. E. T., and Komander, D. (2017). Mechanisms of deubiquitinase specificity and regulation. *Annu. Rev. Biochem.* 86, 34.1–34.33. doi: 10.1146/annurev-biochem-061516-044916

Meyer, H.-J., and Rape, M. (2014). Enhanced protein degradation by branched ubiquitin chains. *Cell* 157, 910–921. doi: 10.1016/j.cell.2014.03.037

Michel, M. A., Swatek, K. N., Hospenthal, M. K., and Komander, D. (2017). Ubiquitin linkage-specific affimers reveal insights into K6-linked ubiquitin signaling. *Mol. Cell* 68, 1–14. doi: 10.1016/j.molcel.2017.08.020

Mishra, P., and Chan, D. C. (2016). Metabolic regulation of mitochondrial dynamics. *J. Cell Biol.* 212, 379–387. doi: 10.1083/jcb.201511036

Mitra, K. (2013). Prospects & overviews mitochondrial fission-fusion as an emerging key regulator of cell proliferation and differentiation. *BioEssays* 35, 955–964. doi: 10.1002/bies.201300011

Montessuit, S., Somasekharan, S. P., Terrones, O., Lucken-Ardjomande, S., Herzig, S., Scwarzenbacher, R., et al. (2010). Membrane remodeling induced by the dynamin related protein Drp1 stimulates bax oligomerization. *Cell* 142, 889–901. doi: 10.1016/j.cell.2010.08.017

Mourier, A., Motori, E., Brandt, T., Lagouge, M., Atanassov, I., Galinier, A., et al. (2015). Mitofusin 2 is required to maintain mitochondrial coenzyme Q levels. *J. Cell Biol.* 208, 429–442. doi: 10.1083/jcb.201411100

Mouton-liger, F., Jacoupy, M., and Corvol, J. (2017). PINK1/Parkin-dependent mitochondrial surveillance: from pleiotropy to Parkinson's disease. *Front. Mol. Neurosci.* 10, 1–15. doi: 10.3389/fnmol.2017.00120

Mukherjee, R., and Chakrabarti, O. (2016a). Regulation of mitofusin1 by Mahogunin Ring Finger-1 and the proteasome modulates mitochondrial fusion. *Biochim. Biophys. Acta Mol. Cell Res.* 1863, 3065–3083. doi: 10.1016/j.bbamcr.2016.09.022

Mukherjee, R., and Chakrabarti, O. (2016b). Ubiquitin-mediated regulation of the E3 ligase GP78 by MGRN1 in trans affects mitochondrial homeostasis. *J. Cell Sci.* 129, 757–773. doi: 10.1242/jcs.176537

Nabi, I. R., and Raz, A. (1987). Cell shape modulation alters glycosylation of a metastatic melanoma cell-surface antigen. *Int. J. Cancer* 40, 396–402. doi: 10.1002/ijc.2910400319

Nabi, I. R., Watanabe, H., and Raz, A. (1990). Identification of B16-F1 melanoma autocrine motility-like factor receptor. *Cancer Res.* 50, 409–414.

Nabi, I. R., Watanabe, H., and Raz, A. (1992). Autocrine motility factor and its receptor: role in cell locomotion and metastasis. *Cancer Metastasis Rev.* 11, 5–20. doi: 10.1007/BF00047599

Nakamura, N., Kimura, Y., Tokuda, M., Honda, S., and Hirose, S. (2006). MARCH-V is a novel mitofusin 2- and Drp1-binding protein able to change mitochondrial morphology. *EMBO Rep.* 7, 1019–1022. doi: 10.1038/sj.embor.7400790

Naon, D., Zaninello, M., Giacomello, M., Varanita, T., and Grespi, F. (2016). Critical reappraisal confirms that Mitofusin 2 is an endoplasmic reticulum – mitochondria tether. *Proc. Natl. Acad. Sci. USA* 113, 11249–11254. doi: 10.1073/pnas.1606786113

Narendra, D. P., Jin, S. M., Tanaka, A., Suen, D.-F., Gautier, C. A., Shen, J., et al. (2010a). PINK1 is selectively stabilized on impaired mitochondria to activate Parkin. *PLoS Biol.* 8, 1–21. doi: 10.1371/journal.pbio.1000298

Narendra, D. P., Kane, L. A., Hauser, D. N., Fearnley, I. M., and Youle, R. J. (2010b). p62/SQSTM1 is required for Parkin-induced mitochondrial clustering but not mitophagy; VDAC1 is dispensable for both. *Autophagy* 6, 1090–1106. doi: 10.4161/auto.6.8.13426

Narendra, D., Tanaka, A., Suen, D. F., and Youle, R. J. (2008). Parkin is recruited selectively to impaired mitochondria and promotes their autophagy. *J. Cell Biol.* 183, 795–803. doi: 10.1083/jcb.200809125

Neuspiel, M., Schauss, A. C., Braschi, E., Zunino, R., Rippstein, P., Rachubinski, R. A., et al. (2008). Cargo-selected transport from the mitochondria to peroxisomes is mediated by vesicular carriers. *Curr. Biol.* 18, 102–108. doi: 10.1016/j.cub.2007.12.038

Neutzner, A., and Youle, R. J. (2005). Instability of the mitofusin Fzo1 regulates mitochondrial morphology during the mating response of the yeast *Saccharomyces cerevisiae*. *J. Biol. Chem.* 280, 18598–18603. doi: 10.1074/jbc.M500807200

Nishida, Y., Arakawa, S., Fujitani, K., Yamaguchi, H., Mizuta, T., Kanaseki, T., et al. (2009). Discovery of Atg5/Atg7-independent alternative macroautophagy. *Nature* 461, 654–658. doi: 10.1038/nature08455

Novak, I., Kirkin, V., Mcewan, D. G., Zhang, J., Wild, P., Rozenknop, A., et al. (2010). Nix is a selective autophagy receptor for mitochondrial clearance. *EMBO Rep.* 11, 45–51. doi: 10.1038/embor.2009.256

Nunnari, J., Marshall, W. F., Straight, A., Murray, A., Sedat, J. W., and Walter, P. (1997). Mitochondrial transmission during mating in *Saccharomyces cerevisiae* is determined by mitochondrial fusion and fission and the intramitochondrial segregation of mitochondrial DNA. *Mol. Biol. Cell* 8, 1233–1242.

Nunnari, J., and Suomalainen, A. (2012). Mitochondria: in sickness and in health. *Cell* 148, 1145–1159. doi: 10.1016/j.cell.2012.02.035

Okamoto, K., Kondo-Okamoto, N., and Ohsumi, Y. (2009). Mitochondria-anchored receptor Atg32 mediates degradation of mitochondria via selective autophagy. *Dev. Cell* 17, 87–97. doi: 10.1016/j.devcel.2009.06.013

Okatsu, K., Oka, T., Iguchi, M., Imamura, K., Kosako, H., Tani, N., et al. (2012). PINK1 autophosphorylation upon membrane potential dissipation is essential for Parkin recruitment to damaged mitochondria. *Nat. Commun.* 3, 1010–1016. doi: 10.1038/ncomms2016

Otsu, K., Murakawa, T., and Yamaguchi, O. (2015). BCL2L13 is a mammalian homolog of the yeast mitophagy receptor Atg32. *Autophagy* 11, 1932–1933. doi: 10.1080/15548627.2015.1084459

Ozcan, U. (2013). Mitofusins: mighty regulators of metabolism. *Cell* 155, 17–18. doi: 10.1016/j.cell.2013.09.013

Panicker, N., Dawson, V. L., and Dawson, T. M. (2017). Activation mechanisms of the E3 ubiquitin ligase parkin. *Biochem. J.* 474, 3075–3086. doi: 10.1042/BCJ20170476

Papanicolaou, K. N., Kikuchi, R., Ngoh, G. A., Coughlan, K. A., Dominguez, I., Stanley, W. C., et al. (2012). Mitofusin 1 and 2 are essentialfor posnatal metabolic remodeling in heart. *Circ. Res.* 111, 1012–1026. doi: 10.1161/CIRCRESAHA.112.274142

Park, Y. Y., and Cho, H. (2012). Mitofusin 1 is degraded at G2/M phase through ubiquitylation by MARCH5. *Cell Div.* 7, 1–6. doi: 10.1186/1747-1028-7-25

Park, J., Choi, H., Min, J.-S., Kim, B., Lee, S.-R., Yun, J. W., et al. (2015). Loss of mitofusin 2 links beta-amyloid-mediated mitochondrial fragmentation and Cdk5-induced oxidative stress in neuron cells. *J. Neurochem.* 132, 687–702. doi: 10.1111/jnc.12984

Park, Y.-Y., Lee, S., Karbowski, M., Neutzner, A., Youle, R. J., and Cho, H. (2010). Loss of MARCH5 mitochondrial E3 ubiquitin ligase induces cellular senescence through dynamin-related protein 1 and mitofusin 1. *J. Cell Sci.* 123, 619–626. doi: 10.1242/jcs.061481

Park, Y. Y., Nguyen, O. T. K., Kang, H., and Cho, H. (2014). MARCH5-mediated quality control on acetylated Mfn1 facilitates mitochondrial homeostasis and cell survival. *Cell Death Dis.* 5, 1–12. doi: 10.1038/cddis.2014.142

Parsons, J. L., Tait, P. S., Finch, D., Dianova, I. I., Edelmann, M. J., Svetlana, V., et al. (2009). Ubiquitin ligase ARF-BP1/mule modulates base excision repair. *EMBO J.* 28, 3207–3215. doi: 10.1038/emboj.2009.243

Peng, C., Rao, W., Zhang, L., Gao, F., Hui, H., Wang, K., et al. (2018). Mitofusin 2 exerts a protective role in ischemia reperfusion injury through increasing autophagy. *Cell. Physiol. Biochem.* 46, 2311–2324. doi: 10.1159/000489621

Pfanner, N., Warscheid, B., and Wiedemann, N. (2019). Mitochondrial proteins: from biogenesis to functional networks. *Nat. Rev. Mol. Cell Biol.* 20, 267–284. doi: 10.1038/s41580-018-0092-0

Phan, L. K., Lin, F., LeDuc, C. A., Chung, W. K., and Leibel, R. L. (2002). The mouse mahoganoid coat color mutation disrupts a novel C3HC4 RING domain protein. *J. Clin. Invest.* 110, 1449–1459. doi: 10.1172/JCI0216131

Pich, S., Bach, D., Briones, P., Liesa, M., Camps, M., Testar, X., et al. (2005). The Charcot-Marie-Tooth type 2A gene product, Mfn2, up-regulates fuel oxidation through expression of OXPHOS system. *Hum. Mol. Genet.* 14, 1405–1415. doi: 10.1093/hmg/ddi149

Pickles, S., Vigié, P., and Youle, R. J. (2018). Mitophagy and quality control mechanisms in mitochondrial maintenance. *Curr. Biol.* 28, R142–R143. doi: 10.1016/j.cub.2018.01.004

Pidoux, G., Witczak, O., Jarnæss, E., Myrvold, L., Urlaub, H., Stokka, A. J., et al. (2011). Optic atrophy 1 is an A-kinase anchoring protein on lipid droplets that mediates adrenergic control of lipolysis. *EMBO J.* 30, 4371–4386. doi: 10.1038/emboj.2011.365

Poole, A. C., Thomas, R. E., Yu, S., Vincow, E. S., and Pallanck, L. (2010). The mitochondrial fusion-promoting factor mitofusin is a substrate of the PINK1/parkin pathway. *PLoS One* 5, 1–8. doi: 10.1371/journal.pone.0010054

Praefcke, G. J. K., and McMahon, H. T. (2004). The dynamin superfamily: universal membrane tubulation and fission molecules? *Nat. Rev. Mol. Cell Biol.* 5, 133–147. doi: 10.1038/nrm1313

Prudent, J., and Mcbride, H. M. (2017). The mitochondria–endoplasmic reticulum contact sites: a signalling platform for cell death. *Curr. Opin. Cell Biol.* 45, 57–63. doi: 10.1016/j.ceb.2017.03.007

Prudent, J., Zunino, R., Mattie, S., Gordon, C., Mcbride, H. M., Prudent, J., et al. (2015). MAPL SUMOylation of Drp1 stabilizes an ER/mitochondrial platform required for cell death article MAPL SUMOylation of Drp1 stabilizes an ER/mitochondrial platform required for cell death. *Mol. Cell* 59, 941–955. doi: 10.1016/j.molcel.2015.08.001

Qi, Y., Yan, L., Yu, C., Guo, X., Zhou, X., Hu, X., et al. (2016). Structures of human mitofusin 1 provide insight into mitochondrial tethering. *J. Cell Biol.* 215, 621–629. doi: 10.1083/jcb.201609019

Rakovic, A., Grünewald, A., Kottwitz, J., Brüggemann, N., Pramstaller, P. P., Lohmann, K., et al. (2011). Mutations in PINK1 and Parkin impair ubiquitination of mitofusins in human fibroblasts. *PLoS One* 6, 1–13. doi: 10.1371/journal.pone.0016746

Rambold, A. S., Cohen, S., and Lippincott-schwartz, J. (2015). Fatty acid trafficking in starved cells: regulation by lipid droplet lipolysis, autophagy and mitochondrial fusion dynamics. *Dev. Cell* 32, 678–692. doi: 10.1016/j.devcel.2015.01.029

Rambold, A. S., Kostelecky, B., Elia, N., and Lippincott-Schwartz, J. (2011). Tubular network formation protects mitochondria from autophagosomal degradation during nutrient starvation. *PNAS* 108, 10190–10195. doi: 10.1073/pnas.1107402108

Rape, M. (2018). Ubiquitylation at the crossroads of development and disease. *Nat. Rev. Mol. Cell Biol.* 19, 59–70. doi: 10.1038/nrm.2017.83

Rikka, S., Quinsay, M., Thomas, R., Kubil, D., Zhang, X., AN, M., et al. (2011). Bnip3 impairs mitochondrial bioenergetics and stimulates mitochondrial turnover. *Cell Death Differ.* 18, 721–731. doi: 10.1038/cdd.2010.146

Riley, B. E., Lougheed, J. C., Callaway, K., Velasquez, M., Brecht, E., Nguyen, L., et al. (2013). Structure and function of Parkin E3 ubiquitin ligase reveals aspects of RING and HECT ligases. *Nat. Commun.* 4, 1–9. doi: 10.1038/ncomms2982

Rizzo, F., Ronchi, D., Salani, S., Nizzardo, M., Fortunato, F., Bordoni, A., et al. (2016). Selective mitochondrial depletion, apoptosis resistance, and increased mitophagy in human Charcot-Marie-Tooth 2A motor neurons. *Hum. Mol. Genet.* 25, 4266–4281. doi: 10.1093/hmg/ddw258

Rizzuto, R., Pinton, P., Carrington, W., Fay, F. S., Fogarty, K. E., Lifshitz, L. M., et al. (1998). Close contacts with the endoplasmic reticulum as determinants of close contacts with the endoplasmic reticulum as determinants of mitochondrial Ca 2 responses. *Science* 280, 1763–1766. doi: 10.1126/science.280.5370.1763

Rojo, M., Legros, F., Chateau, D., and Lombès, A. (2002). Membrane topology and mitochondrial targeting of mitofusins, ubiquitous mammalian homologs of the transmembrane GTPase Fzo. *J. Cell Sci.* 115, 1663–1674.

Rowland, A. A., and Voeltz, G. K. (2012). Endoplasmic reticulum-mitochondria contacts: function of the junction. *Nat. Rev. Mol. Cell Biol.* 13, 607–615. doi: 10.1038/nrm3440

Saito, T., Kundu, M., Sadoshima, J., Saito, T., Nah, J., Oka, S., et al. (2019). An alternative mitophagy pathway mediated by Rab9 protects the heart against ischemia graphical abstract find the latest version: an alternative mitophagy pathway mediated by Rab9 protects the heart against ischemia. *J. Clin. Invest.* 129, 802–819. doi: 10.1172/JCI122035

Sandoval, H., Yao, C., Chen, K., Jaiswal, M., Donti, T., Lin, Y. Q., et al. (2014). Mitochondrial fusion but not fission regulates larval growth and synaptic development through steroid hormone production. *elife* 3, 1–23. doi: 10.7554/eLife.03558

Saotome, M., Safiulina, D., Szabadkai, G., Das, S., Fransson, A., Aspenstrom, P., et al. (2008). Bidirectional $Ca^{2+}$-dependent control of mitochondrial dynamics by the Miro GTPase. *Proc. Natl. Acad. Sci. USA* 105, 20728–20733. doi: 10.1073/pnas.0808953105

Saporta, M. A., Dang, V., Volfson, D., Zou, B., Xie, X. S., Adebola, A., et al. (2015). Axonal Charcot-Marie-Tooth disease patient-derived motor neurons demonstrate disease-specific phenotypes including abnormal electrophysiological properties. *Exp. Neurol.* 263, 190–199. doi: 10.1016/j.expneurol.2014.10.005

Sarraf, S. A., Raman, M., Guarani-pereira, V., Sowa, M. E., Edward, L., Gygi, S. P., et al. (2013). Landscape of the PARKIN-dependent ubiquitylome in response to mitochondrial depolarization. *Nature* 496, 372–376. doi: 10.1038/nature12043

Scarffe, L. A., Stevens, D. A., Dawson, V. L., and Dawson, T. M. (2014). Parkin and PINK1: much more than mitophagy. *Trends Neurosci.* 37, 315–324. doi: 10.1016/j.tins.2014.03.004

Schneeberger, M., Dietrich, M. O., Sebástian, D., Imberón, M., Castaño, C., Garcia, A., et al. (2014). Mitofusin 2 in POMC neurons connects ER stress with leptin resistance and energy imbalance. *Cell* 155, 1–23. doi: 10.1016/j.cell.2013.09.003

Schrepfer, E., and Scorrano, L. (2016). Review mitofusins, from mitochondria to metabolism. *Mol. Cell* 61, 683–694. doi: 10.1016/j.molcel.2016.02.022

Scorrano, L., Scorrano, L., Oakes, S. A., Opferman, J. T., Cheng, E. H., Sorcinelli, M. D., et al. (2003). BAX and BAK regulation of endoplasmic reticulum Ca 2+: a control point for apoptosis. *Science* 300, 135–139. doi: 10.1126/science.1081208

Sebastián, D., Hernández-alvarez, M. I., Segalés, J., and Sorianello, E. (2012). Mitofusin 2 (Mfn2) links mitochondrial and endoplasmic reticulum function with insulin signaling and is essential for normal glucose homeostasis. *Proc. Natl. Acad. Sci. USA* 109, 5523–5528. doi: 10.1073/pnas.1108220109

Sebastián, D., Sorianello, E., Segalés, J., Irazoki, A., Ruiz-Bonilla, V., Sala, D., et al. (2016). Mfn2 deficiency links age-related sarcopenia and impaired autophagy to activation of an adaptive mitophagy pathway. *EMBO J.* 35, 1677–1693. doi: 10.15252/embj.201593084

Sedlackova, L., and Korolchuk, V. I. (2019). Mitochondrial quality control as a key determinant of cell survival. *BBA - Mol. Cell Res.* 1866, 575–587. doi: 10.1016/j.bbamcr.2018.12.012

Segalés, J., Paz, J. C., Hernández-alvarez, M. I., Sala, D., Muñoz, J. P., Noguera, E., et al. (2013). A form of mitofusin 2 (Mfn2) lacking the transmembrane domains and the COOH-terminal end stimulates metabolism in muscle and liver cells. *Am. J. Physiol. Metab.* 2, 1208–1221. doi: 10.1152/ajpendo.00546.2012

Seirafi, M., Koslov, G., and Gehring, K. (2015). Parkin structure and function. *FEBS J.* 282, 2017–2088. doi: 10.1111/febs.13249

Shankar, J., Kojic, L. D., St-pierre, P., Wang, P. T. C., Fu, M., Joshi, B., et al. (2013). Raft endocytosis of AMF regulates mitochondrial dynamics through Rac1 signaling and the Gp78 ubiquitin ligase. *J. Cell Sci.* 126, 3295–3304. doi: 10.1242/jcs.120162

Shefa, U., Jeong, N. Y., Song, I. O., Chung, H., Kim, D., Jung, J., et al. (2019). Mitophagy links oxidative stress conditions and neurodegenerative diseases. *Neural Regen. Res.* 14, 749–756. doi: 10.4103/1673-5374.249218

Shiba-Fukushima, K., Imai, Y., Yoshida, S., Ishihama, Y., Kanao, T., Sato, S., et al. (2012). PINK1-mediated phosphorylation of the parkin ubiquitin-like domain primes mitochondrial translocation of parkin and regulates mitophagy. *Sci. Rep.* 2, 1–8. doi: 10.1038/srep01002

Silletti, S., Watanabe, H., Hogan, V., Nabi, I. R., and Raz, A. (1991). Purification of B16-F1 melanoma autocrine motility factor and its receptor. *Cancer Res.* 51, 3507–3511.

Simões, T., Schuster, R., Den Brave, F., Escobar-henriques, M., and Diseases, A. (2018). Cdc48 regulates a deubiquitylase cascade critical for mitochondrial fusion. *elife* 7, 1–29. doi: 10.7554/eLife.30015

Smit, J. J., and Sixma, T. K. (2014). RBR E 3 -ligases at work. *EMBO Rep.* 15, 142–154. doi: 10.1002/embr.201338166

Song, M., Franco, A., Fleischer, J. A., Zhang, L., and Dorn, G. W. II (2017). Abrogating mitochondial dynamics in mouse hearts accelerates mitochondrial senescence. *Cell Metab.* 26, 872–883. doi: 10.1016/j.cmet.2017.09.023

Song, M., Mihara, K., Chen, Y., Scorrano, L., and Dorn, G. W. II (2015). Mitochondrial fission and fusion factors recuprocally orchestrate mitophagic culling in mouse hearts and cultures fibroblasts. *Cell Metab.* 21, 273–285. doi: 10.1016/j.cmet.2014.12.011

Spratt, D. E., Martinez-torres, R. J., Noh, Y. J., Mercier, P., Manczyk, N., Barber, K. R., et al. (2013). A molecular explanation for the recessive nature of parkin-linked Parkinson's disease. *Nat. Commun.* 4, 1–12. doi: 10.1038/ncomms2983

Stojkovic, T. (2016). Hereditary neuropathies: an update. *Rev. Neurol.* 172, 775–778. doi: 10.1016/j.neurol.2016.06.007

Strappazzon, F., Nazio, F., Corrado, M., Cianfanelli, V., Romagnoli, A., Fimia, G. M., et al. (2015). AMBRA1 is able to induce mitophagy via LC3 binding, regardless of PARKIN and p62/SQSTM1. *Cell Death Differ.* 22, 419–432. doi: 10.1038/cdd.2014.139

Stuppia, G., Rizzo, F., Riboldi, G., Del Bo, R., Nizzardo, M., Simone, C., et al. (2015). MFN2-related neuropathies: clinical features, molecular pathogenesis and therapeutic perspectives. *J. Neurol. Sci.* 356, 7–18. doi: 10.1016/j.jns.2015.05.033

Sugiura, A., Mclelland, G., Fon, E. A., and Mcbride, H. M. (2014). A new pathway for mitochondrial quality control: mitochondrial-derived vesicles. *EMBO Rep.* 33, 2142–2156. doi: 10.15252/embj.201488104

Sugiura, A., Nagashima, S., Tokuyama, T., Amo, T., Matsuki, Y., Ishido, S., et al. (2013). MITOL regulates endoplasmic contacts via mitofusin2. *Mol. Cell* 51, 20–34. doi: 10.1016/j.molcel.2013.04.023

Swatek, K. N., and Komander, D. (2016). Ubiquitin modifications. *Nat. Publ. Gr.* 26, 399–422. doi: 10.1038/cr.2016.39

Szabadkai, G., Bianchi, K., Várnai, P., De Stefani, D., Wieckowski, M. R., Cavagna, D., et al. (2006). Chaperone-mediated coupling of endoplasmic reticulum and mitochondrial Ca2+ channels. *J. Cell Biol.* 175, 901–911. doi: 10.1083/jcb.200608073

Tanaka, A., Cleland, M. M., Xu, S., Narendra, D. P., Suen, D. F., Karbowski, M., et al. (2010). Proteasome and p97 mediate mitophagy and degradation of mitofusins induced by parkin. *J. Cell Biol.* 191, 1367–1380. doi: 10.1083/jcb.201007013

Tang, F., Liu, W., Hu, J., Erion, J. R., Ye, J., Mei, L., et al. (2015). VPS35 deficiency or mutation causes dopaminergic neuronal loss by impairing mitochondrial fusion and function. *Cell Rep.* 12, 1631–1643. doi: 10.1016/j.celrep.2015.08.001

Tatsuta, T., and Langer, T. (2017). Intramitochondrial phospholipid trafficking. *Biochim. Biophys. Acta* 1862, 81–89. doi: 10.1016/j.bbalip.2016.08.006

Tazir, M., Bellatache, M., Nouioua, S., and Vallat, J. (2013). Autosomal recessive Charcot-Marie-Tooth disease: from genes to phenotypes. *J. Peripher. Nerv. Syst.* 129, 113–129. doi: 10.1111/jns5.12026

Tazir, M., Hamadouche, T., Nouioua, S., Mathis, S., and Vallat, J. (2014). Hereditary motor and sensory neuropathies or Charcot–Marie–Tooth diseases: an update. *J. Neurol. Sci.* 347, 14–22. doi: 10.1016/j.jns.2014.10.013

Tilokani, L., Nagashima, S., Paupe, V., and Prudent, J. (2018). Mitochondrial dynamics: overview of molecular mechanisms. *Essays Biochem.* 62, 341–360. doi: 10.1042/EBC20170104

Timper, K., and Brüning, J. C. (2017). Hypothalamic circuits regulating appetite and energy homeostasis: pathways to obesity. *Dis. Model. Mech.* 10, 679–689. doi: 10.1242/dmm.026609

Toledo, F. G. S., Watkins, S., and Kelley, D. E. (2006). Changes induced by physical activity and weight loss in the morphology of intermyofibrillar mitochondria in obese men and women. *J. Clin. Endocrinol. Metab.* 91, 3224–3227. doi: 10.1210/jc.2006-0002

Tondera, D., Jourdain, A., Karbowski, M., Mattenberger, Y., Da Cruz, S., Clerc, P., et al. (2009). SLP-2 is required for stress-induced mitochondrial hyperfusion. *EMBO J.* 28, 1589–1600. doi: 10.1038/emboj.2009.89

Ugarte-Uribe, B., and García-Sáez, A. J. (2017). Apoptotic foci at mitochondria: in and around Bax pores. *Philos. Trans. R. Soc. B Biol. Sci.* 372, 1–9. doi: 10.1098/rstb.2016.0217

Upadhyay, A., Amanullah, A., Chhangani, D., Mishra, R., Prasad, A., and Mishra, A. (2016). Mahogunin Ring Finger-1 (MGRN1), a multifaceted ubiquitin ligase: recent unraveling of neurobiological mechanisms. *Mol. Neurobiol.* 53, 4484–4496. doi: 10.1007/s12035-015-9379-8

Valente, E. M., Abou-sleiman, P. M., Caputo, V., Muqit, M. M. K., Harvey, K., Gispert, S., et al. (2004). Hereditary early-onset Parkinson's disease caused by mutations in PINK1. *Science* 304, 1158–1161. doi: 10.1126/science.1096284

Verhoeven, K., Claeys, Ă. K. G., Zu, Ă. S., Seeman, P., Mazanec, R., Saifi, G. M., et al. (2006). MFN2 mutation distribution and genotype/phenotype correlation in Charcot–Marie–Tooth type 2. *Brain* 129, 2093–2102. doi: 10.1093/brain/awl126

Vives-Bauza, C., Zhou, C., Huang, Y., Cui, M., de Vries, R. L. A., Kim, J., et al. (2010). PINK1-dependent recruitment of Parkin to mitochondria in mitophagy. *Proc. Natl. Acad. Sci. USA* 107, 378–383. doi: 10.1073/pnas.0911187107

Wakabayashi, J., Zhang, Z., Wakabayashi, N., Tamura, Y., Fukaya, M., Kensler, T. W., et al. (2009). The dynamin-related GTPase Drp1 is required for embryonic and brain development in mice. *J. Cell Biol.* 186, 805–816. doi: 10.1083/jcb.200903065

Walden, H., and Rittinger, K. (2018). RBR ligase-mediated ubiquitin transfer: a tale with many twists and turns. *Nat. Struct. Mol. Biol.* 25, 440–445. doi: 10.1038/s41594-018-0063-3

Walsh, C. T., Garneau-Tsodikova, S., and Gatto, G. J. (2005). Protein posttranslational modifications: the chemistry of proteome diversifications. *Angew. Chem. Int. Ed.* 44, 7342–7372. doi: 10.1002/anie.200501023

Wang, P. T. C., Garcin, P. O., Fu, M., Masoudi, M., St-Pierre, P., Pante, N., et al. (2015). Distinct mechanisms controlling rough and smooth endoplasmic reticulum contacts with mitochondria. *J. Cell Sci.* 128, 2759–2765. doi: 10.1242/jcs.171132

Wang, X., Su, B., Lee, H., Li, X., Perry, G., and Smith, M. A. (2009). Impaired balance of mitochondria fission and fusion in Alzheimer disease. *J. Neurosci.* 29, 9090–9103. doi: 10.1523/JNEUROSCI.1357-09.2009

Wang, C., and Youle, R. J. (2009). The role of mitochondria in apoptosis. *Annu. Rev. Genet.* 43, 95–118. doi: 10.1146/annurev-genet-102108-134850

Watanabes, H., Carmip, P., Hogan, V., Raz, T., Silletti, S., and Nabin, I. R. (1991). Purification of human tumor cell autocrine motility factor and molecular cloning of its receptor. *J. Biol. Chem.* 266, 13442–13448.

Wauer, T., and Komander, D. (2013). Structure of the human Parkin ligase domain in an autoinhibited state. *EMBO J.* 32, 2099–2112. doi: 10.1038/emboj.2013.125

Wauer, T., Simicek, M., Schubert, A., and Komander, D. (2016). Mechanism of phospho-ubiquitin induced PARKIN activation. *Nature* 524, 370–374. doi: 10.1038/nature14879

Weaver, D., Liu, X., Biology, C., and Jefferson, T. (2014). The distribution and apoptotic function of outer membrane proteins depend on mitochondrial fusion. *Mol. Cell* 54, 870–878. doi: 10.1016/j.molcel.2014.03.048

Wei, M. C., Zong, W., Cheng, E. H., Lindsten, T., Ross, A. J., Roth, K. A., et al. (2001). Proapoptotic BAX and BAK: a requesite gateway to mitochondrial dysfuntion and death. *Science* 292, 727–730. doi: 10.1126/science.1059108

Westermann, B. (2010). Mitochondrial fusion and fission in cell life and death. *Nat. Publ. Gr.* 11, 872–884. doi: 10.1038/nrm3013

Wu, H., Carvalho, P., and Voeltz, G. K. (2018). Here, there, and everywhere: the importance of ER membrane contact sites. *Science* 361, 1–9. doi: 10.1126/science.aan5835

Wu, W., Tian, W., Hu, Z., Chen, G., Huang, L., Li, W., et al. (2014). ULK 1 translocates to mitochondria and phosphorylates FUNDC1 to regulate mitophagy. *EMBO Rep.* 15, 566–575. doi: 10.1002/embr.201438501

Xie, L., Shi, F., Tan, Z., Li, Y., Bode, A. M., and Cao, Y. (2018). Mitochondrial network structure homeostasis and cell death. *Cancer Sci.* 109, 3686–3694. doi: 10.1111/cas.13830

Xiong, S., Mu, T., Wang, G., and Jiang, X. (2014). Mitochondria-mediated apoptosis in mammals. *Protein Cell* 5, 737–749. doi: 10.1007/s13238-014-0089-1

Xu, S., Cherok, E., Das, S., Li, S., Roelofs, B. A., Ge, S. X., et al. (2016). Mitochondrial E3 ubiquitin ligase MARCH5 controls mitochondrial fission and cell sensitivity to stress-induced apoptosis through regulation of MiD49 protein. *Mol. Biol. Cell* 27, 349–359. doi: 10.1091/mbc.E15-09-0678

Yamada, S., Asanagi, M., Hirata, N., Itagaki, H., Sekino, Y., and Kanda, Y. (2016). Tributyltin induces mitochondrial fission through Mfn1 degradation in human induced pluripotent stem cells. *Toxicol. In Vitro* 34, 257–263. doi: 10.1016/j.tiv.2016.04.013

Yau, R., and Rape, M. (2016). The increasing complexity of the ubiquitin code. *Nat. Publ. Gr.* 18, 579–586. doi: 10.1038/ncb3358

Ying, L., Zhao, G. J., Wu, Y., Ke, H. L., Hong, G. L., Zhang, H., et al. (2017). Mitofusin 2 promotes apoptosis of CD4+T cells by inhibiting autophagy in sepsis. *Mediat. Inflamm.* 2017, 1–15. doi: 10.1155/2017/4926205

Yonashiro, R., Ishido, S., Kyo, S., Fukuda, T., Goto, E., Matsuki, Y., et al. (2006). A novel mitochondrial ubiquitin ligase plays a critical role in mitochondrial dynamics. *EMBO J.* 25, 3618–3626. doi: 10.1038/sj.emboj.7601249

Youle, R. J., and van der Bliek, A. M. (2012). Mitochondrial fission, fusion and stress. *Science* 337, 1062–1065. doi: 10.1126/science.1219855

Yu, T., Robotham, J. L., and Yoon, Y. (2006). Increased production of reactive oxygen species in hyperglycemic conditions requires dynamic change of mitochondrial morphology. *PNAS* 103, 2653–2658. doi: 10.1073/pnas.0511154103

Yue, W., Chen, Z., Liu, H., Yan, C., Chen, M., Feng, D., et al. (2014). A small natural molecule promotes mitochondrial fusion through inhibition of the deubiquitinase USP30. *Cell Res.* 24, 482–496. doi: 10.1038/cr.2014.20

Yun, J., Puri, R., Yang, H., Lizzio, M. A., Wu, C., Sheng, Z. H., et al. (2014). MUL1 acts in parallel to the PINK1/parkin pathway in regulating mitofusin and compensates for loss of PINK1/parkin. *elife* 3, 1–26. doi: 10.7554/eLife.01958.001

Zhang, B., Huang, J., Li, H.-L., Liu, T., Wang, Y.-Y., Waterman, P., et al. (2008). GIDE is a mitochondrial E3 ubiquitin ligase that induces apoptosis and slows growth. *Cell Res.* 18, 900–910. doi: 10.1038/cr.2008.75

Zhang, T., Mishra, P., Hay, B. A., Chan, D., and Guo, M. (2017). Valosin-containing protein (VCP/p97) inhibitors relieve mitofusin-dependent mitochondrial defects due to VCP disease mutants. *elife* 6, 1–28. doi: 10.7554/eLife.17834

Zhao, X., Heng, J. I., Guardavaccaro, D., Jiang, R., Guillemot, F., Iavarone, A., et al. (2008). The HECT-domain ubiquitin ligase Huwe1 controls neural differentiation and proliferation by destabilizing the N-Myc oncoprotein. *Nat. Cell Biol.* 10, 643–653. doi: 10.1038/ncb1727

Zhao, T., Huang, X., Han, L., Wang, X., Cheng, H., Zhao, Y., et al. (2012). Central role of mitofusin 2 in autophagosome-lysosome fusion in cardiomyocytes. *J. Biol. Chem.* 287, 23615–23625. doi: 10.1074/jbc.M112.379164

Zheng, N., and Shabek, N. (2017). Ubiquitin ligases: structure, function, and regulation. *Annu. Rev.* 86, 129–157. doi: 10.1146/annurev-biochem-060815-014922

Zhou, Y., Carmona, S., Muhammad, A. K. M. G., Bell, S., Landeros, J., Vazquez, M., et al. (2019). Restoring mitofusin balance prevents axonal degeneration in a Charcot-Marie-Tooth type 2A model. *J. Clin. Invest.* 129, 1756–1771. doi: 10.1172/JCI124194

Ziviani, E., Tao, R. N., and Whitworth, A. J. (2010). Drosophila parkin requires PINK1 for mitochondrial translocation and ubiquitinates mitofusin. *Proc. Natl. Acad. Sci. USA* 107, 5018–5023. doi: 10.1073/pnas.0913485107

Zorzano, A., Liesa, M., Palacín, M., Zorzano, A., Liesa, M., and Palacín, M. (2009). Mitochondrial dynamics as a bridge between mitochondrial dysfunction and insulin resistance mitochondrial dynamics as a bridge between mitochondrial dysfunction and insulin resistance. *Arch. os Physiol. Biochem.* 115, 1–12. doi: 10.1080/13813450802676335

Zorzano, A., and Pich, S. (2006). What is the biological significance of the two mitofusin proteins present in the outer mitochondrial membrane of mammalian cells? *IUBMB Life* 58, 441–443. doi: 10.1080/15216540600644838

Züchner, S., Mersiyanova, I. V., Muglia, M., Bissar-tadmouri, N., Rochelle, J., Dadali, E. L., et al. (2004). Mutations in the mitochondrial GTPase mitofusin 2 cause Charcot-Marie-Tooth neuropathy type 2A. *Nat. Publ. Gr.* 36, 449–452. doi: 10.1038/ng1341

**Conflict of Interest Statement:** The authors declare that the research was conducted in the absence of any commercial or financial relationships that could be construed as a potential conflict of interest.

frontiers in Physiology

REVIEW
published: 05 July 2019
doi: 10.3389/fphys.2019.00835

# Enzymatic Logic of Ubiquitin Chain Assembly

*Kirandeep K. Deol[1], Sonja Lorenz[2]* and Eric R. Strieter[1,3]**

*[1] Department of Chemistry, University of Massachusetts, Amherst, MA, United States, [2] Rudolf Virchow Center for Experimental Biomedicine, University of Würzburg, Würzburg, Germany, [3] Department of Biochemistry and Molecular Biology, University of Massachusetts, Amherst, MA, United States*

Protein ubiquitination impacts virtually every biochemical pathway in eukaryotic cells. The fate of a ubiquitinated protein is largely dictated by the type of ubiquitin modification with which it is decorated, including a large variety of polymeric chains. As a result, there have been intense efforts over the last two decades to dissect the molecular details underlying the synthesis of ubiquitin chains by ubiquitin-conjugating (E2) enzymes and ubiquitin ligases (E3s). In this review, we highlight these advances. We discuss the evidence in support of the alternative models of transferring one ubiquitin at a time to a growing substrate-linked chain (sequential addition model) versus transferring a pre-assembled ubiquitin chain (en bloc model) to a substrate. Against this backdrop, we outline emerging principles of chain assembly: multisite interactions, distinct mechanisms of chain initiation and elongation, optimal positioning of ubiquitin molecules that are ultimately conjugated to each other, and substrate-assisted catalysis. Understanding the enzymatic logic of ubiquitin chain assembly has important biomedical implications, as the misregulation of many E2s and E3s and associated perturbations in ubiquitin chain formation contribute to human disease. The resurgent interest in bifunctional small molecules targeting pathogenic proteins to specific E3s for polyubiquitination and subsequent degradation provides an additional incentive to define the mechanisms responsible for efficient and specific chain synthesis and harness them for therapeutic benefit.

**Keywords: ubiquitin, E2 conjugating enzyme, E3 ligating enzyme, sequential addition, en bloc transfer**

OPEN ACCESS

***Edited by:***
*Brian James Morris, University of Sydney, Australia*

***Reviewed by:***
*Wuqiang Zhu, The University of Alabama at Birmingham, United States*
*Yaoliang Tang, Augusta University, United States*

****Correspondence:***
*Sonja Lorenz*
*sonja.lorenz@virchow.uni-wuerzburg.de*
*Eric R. Strieter*
*estrieter@umass.edu*

***Specialty section:***
*This article was submitted to Integrative Physiology, a section of the journal Frontiers in Physiology*

***Received:*** *27 March 2019*
***Accepted:*** *17 June 2019*
***Published:*** *05 July 2019*

***Citation:***
*Deol KK, Lorenz S and Strieter ER (2019) Enzymatic Logic of Ubiquitin Chain Assembly. Front. Physiol. 10:835. doi: 10.3389/fphys.2019.00835*

## INTRODUCTION

The small protein ubiquitin is involved in nearly every cellular pathway through its covalent attachment to target proteins (Hershko and Ciechanover, 1998; Oh et al., 2018). Ubiquitination is notorious for triggering protein degradation through the 26S proteasome (Finley, 2009; Collins and Goldberg, 2017; Yu and Matouschek, 2017). However, it can also alter protein structure and function, induce changes in protein localization, and mediate the assembly or disassembly of multi-protein complexes. What determines the fate of a ubiquitinated protein is the nature of the modification (Komander and Rape, 2012; Swatek and Komander, 2016; Yau and Rape, 2016). Ubiquitin molecules can be covalently attached to a target protein at one or several sites to afford a (multi-) monoubiquitinated product and/or in the form of polyubiquitin chains. Owing to the eight amino groups of ubiquitin (M1, K6, K11, K27, K29, K33, K48, and K63) along with the capacity to form branched structures, the number of possible chain types is staggering; each one has the

potential to govern the dynamics of a biochemical pathway in a distinct manner (**Figure 1**). Due to the diverse functional consequences, there has been intense interest in deciphering how ubiquitin chains are assembled.

Over a decade ago, a thought-provoking review was published describing the state of affairs regarding ubiquitin chain assembly (Hochstrasser, 2006). At the time, several models had been proposed, but the precise mechanisms by which ubiquitin chains are generated on a substrate by the sequential activities of E1 (ubiquitin-activating), E2 (ubiquitin-conjugating), and E3 enzymes (ubiquitin ligases) remained unclear. Since then, the picture has become much less opaque: detailed kinetic studies on several E2-E3 systems have supported a sequential addition mechanism, in which ubiquitin molecules are added one at a time, initially to the substrate and then to the distal end of the growing chain (Pierce et al., 2009; Lu et al., 2015b; French et al., 2017). In certain cases, chain initiation and elongation are performed by two distinct E2 enzymes working in collaboration with a single E3 (Rodrigo-Brenni and Morgan, 2007; Garnett et al., 2009; Williamson et al., 2009; Wu K. et al., 2010; Wu T. et al., 2010). In other instances, both steps are carried out by distinct pairs of E2s and E3s (Scott et al., 2016; Dove et al., 2017a). With some systems there is also evidence for an "en bloc" transfer of pre-assembled ubiquitin chains to substrates (Wang and Pickart, 2005; Li et al., 2007; Ravid and Hochstrasser, 2007; Masuda et al., 2012; Ronchi et al., 2013, 2017; Streich et al., 2013; Edwards et al., 2014; Todaro et al., 2017).

In this review, we focus on the mechanistic intricacies of ubiquitin chain formation. We start by providing a census of the ubiquitination/deubiquitination machinery to underscore the diversity of enzymes involved. We then revisit mechanisms of chain assembly that have been put forward over the years, providing detailed accounts in support of each one. Finally, we outline the key factors underlying the efficiency, processivity, and specificity with which E2s and E3s catalyze chain assembly.

## CELLULAR MACHINERY

A massive collection of proteins encoded by ∼5% of the human genome is responsible for sculpting the cellular ubiquitination landscape (Clague et al., 2015; **Figure 2**). The apex of the system is the E1 family of enzymes (Schulman and Wade Harper, 2009). In humans, there are two E1s selective for ubiquitin: UBA1 and UBA6. UBA1 is one of the most abundant protein in HeLa cells (Kulak et al., 2014). UBA6—which is an order of magnitude lower in abundance than UBA1—is unique in that it loads ubiquitin or the ubiquitin-like modifier FAT10 specifically onto the E2 UBE2Z (USE1), whereas UBA1 transfers ubiquitin to a wide array of E2s (Chiu et al., 2007; Jin et al., 2007; Pelzer et al., 2007; Aichem et al., 2010). The human genome encodes ∼40 E2s dedicated to ubiquitin conjugation (Michelle et al., 2009; Yates et al., 2017). Several of them are limited to monoubiquitination; others act as "chain extenders" by modifying ubiquitin itself. A subset of E2s synthesize a single linkage type between ubiquitin molecules, while others are promiscuous (Ye and Rape, 2009; Wenzel et al., 2015; Stewart et al., 2016).

By selecting substrates and modifying them with ubiquitin chains, E3s play a pivotal role in ubiquitin signaling. Considering most proteins in the cell are subject to ubiquitination, the substrate repertoire of E3s is immense. To meet this demand, the human genome encodes over 600 E3s (Li et al., 2008), which fall into three mechanistic classes: the RING (really interesting new gene)/U-box, HECT (homologous to E6AP C-terminus), and RBR (RING-between-RING) ligases (Buetow and Huang, 2016). The RING/U-box ligases are the largest of these classes and catalyze the direct transfer of ubiquitin from a thioester-linked E2-ubiquitin conjugate (E2∼ubiquitin) to a substrate (Deshaies and Joazeiro, 2009; Metzger et al., 2014). The 28 human HECT (Huibregtse et al., 1995; Lorenz, 2018; Weber et al., 2019) and 14 RBR (Marín et al., 2004; Smit and Sixma, 2014; Dove and Klevit, 2017; Walden and Rittinger, 2018) ligases proceed through a two-step mechanism, in which ubiquitin is first transferred from an E2 to the active site cysteine of the E3 to afford an E3∼ubiquitin thioester-linked intermediate and then delivered to a substrate (Huang et al., 1999; Wenzel et al., 2011).

The ∼100 human deubiquitinases (DUBs) antagonize the activity of E3s by severing the isopeptide linkage between ubiquitin and a substrate or disassembling ubiquitin chains (Clague et al., 2013, 2019; Mevissen and Komander, 2017). DUBs are sub-categorized into seven families: the ubiquitin C-terminal hydrolases (UCHs), ubiquitin specific proteases (USPs), Machado-Josephins (MJDs), ovarian tumor proteases (OTUs), JAB1/MPN domain-associated metalloisopeptidases (JAMM/MPN$^+$), the novel MIU-containing DUB family MINDY (Abdul Rehman et al., 2016), and the zinc finger with UFM1-specific peptidase domain-containing ZUFSP family (Haahr et al., 2018; Hermanns et al., 2018; Hewings et al., 2018; Kwasna et al., 2018). All but the JAMM/MPN$^+$ metalloproteases catalyze bond cleavage using an active-site cysteine residue reminiscent of canonical cysteine proteases such as papain. Proteins containing ubiquitin-binding domains (UBDs) typically act as effectors transmitting the recognition of different ubiquitin modifications into a biological response (Husnjak and Dikic, 2012).

## WHAT ARE THE DIFFERENT MECHANISMS OF CHAIN ASSEMBLY?

Several models for chain assembly have been entertained over the years (Hochstrasser, 2006). While these models involve different oligomerization states of E2s and E3s, they all follow either of two basic mechanisms—sequential addition and en bloc transfer—which differ in the directionality of chain growth and location of the growing chain. Sequential addition—presumably the predominant mechanism—requires the transfer of individual ubiquitin molecules to a substrate. By contrast, the en bloc mechanism involves transferring chains that have been pre-formed on the active-site cysteine of an E2 or HECT/RBR E3 to a substrate.

### Sequential Addition

According to the sequential addition model, each ubiquitinated substrate species acts as a substrate for the formation of

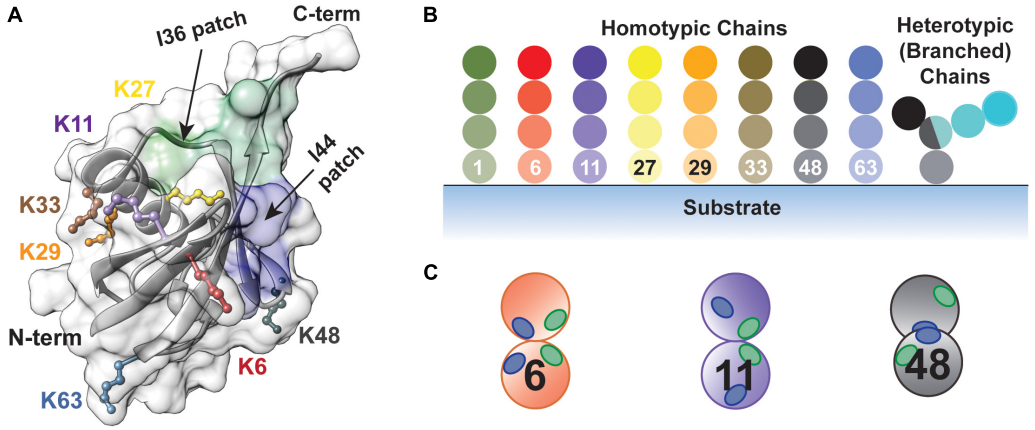


**FIGURE 1 |** The diversity of ubiquitin chains enables highly nuanced mechanisms of regulation. **(A)** Structure of ubiquitin (PDB: 1UBQ) showing the seven lysine side chains (K6, K11, K27, K29, K33, K48, and K63) and the N-terminus along with the I36 and I44-centered hydrophobic patches, highlighted in green (L8, I36, L70, and L73) and blue (L8, I44, H68, and V70), respectively. **(B)** Types of ubiquitin chains that can be produced. Homotypic chains are assembled using the same amino group of ubiquitin for each linkage, whereas heterotypic chains contain a mixture of linkages. Branched chains are a form of heterotypic chain, in which at least one ubiquitin molecule is modified by two or more ubiquitin molecules. **(C)** The relative orientation of the I36 and I44-centered hydrophobic patches controls how different chain types are recognized by effector proteins and DUBs.

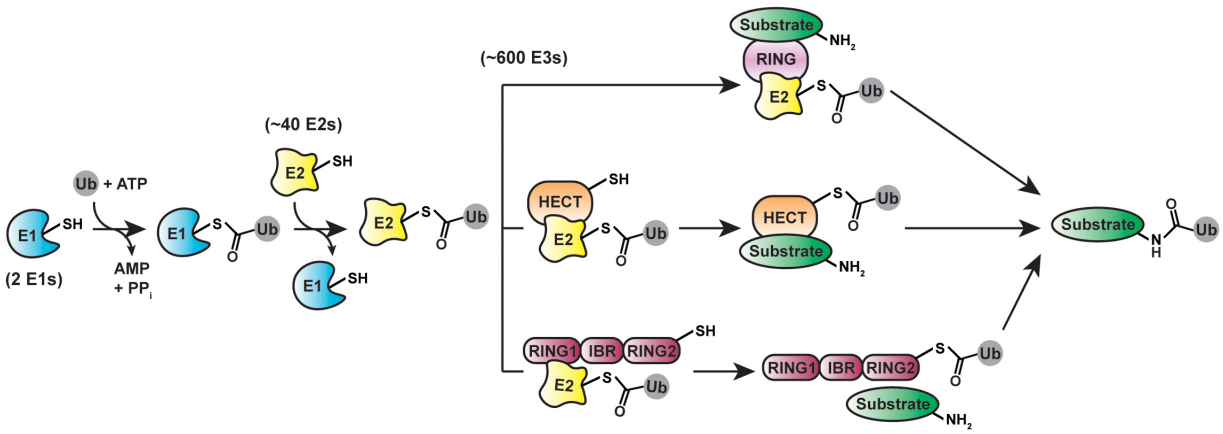


**FIGURE 2 |** Cellular machinery involved in ubiquitination. protein ubiquitination is driven by E1 (ubiquitin-activating), E2 (ubiquitin-conjugating), and E3 (ubiquitin-ligating) enzymes. Three distinct classes of ubiquitin ligases—RING/U-box (top), HECT (middle), and RBR (bottom)—utilize different structural mechanisms for mediating the final transfer of ubiquitin onto substrates.

successively longer substrate-linked chain (**Figure 3A**). Thus, new ubiquitinated species appear in a sequential manner with a lag phase proportional to chain length. The challenge in providing evidence for this mechanism lies in the necessity to detect individual reaction products/intermediates on fast timescales of milliseconds to seconds.

This was first accomplished using the yeast Skp-cullin-F-box protein complex $SCF^{Cdc4}$ (human homolog of Cdc4 is FBXW7) as a model system (Pierce et al., 2009). $SCF^{Cdc4}$ is the founding member (Feldman et al., 1997; Skowyra et al., 1997) of the largest family of E3s—the cullin-RING ligases (CRLs) (Petroski and Deshaies, 2005a)—which account for ~20% of all proteasome-dependent degradation (Soucy et al., 2009). It cooperates with the K48 linkage-specific E2 Cdc34 (human enzyme is referred to as UBE2R1) (Petroski and Deshaies, 2005b; Gazdoiu et al., 2007; Ziemba et al., 2013; Choi et al., 2014; Chong et al., 2014; Hill et al., 2016). Together, $SCF^{Cdc4}$ and Cdc34 catalyze substrate polyubiquitination within seconds. Using single-encounter assays, it was shown that most encounters of Cdc34-$SCF^{Cdc4}$ with a substrate are futile (Pierce et al., 2009); however, the vast majority of modified substrate molecules carry chains with ≥4 ubiquitin moieties (Saha and Deshaies, 2008). To determine whether substrate ubiquitination by Cdc34-$SCF^{Cdc4}$ occurs en bloc or sequentially, the distribution of ubiquitin chains conjugated to Cdc34 was measured by intact mass spectrometry (Pierce et al., 2009); the logic being that the product distribution should reflect the population of Cdc34~ubiquitin conjugates if pre-formed chains were transferred from the E2 to the substrate en bloc. However, Cdc34 conjugates bearing more than one ubiquitin could not be detected in

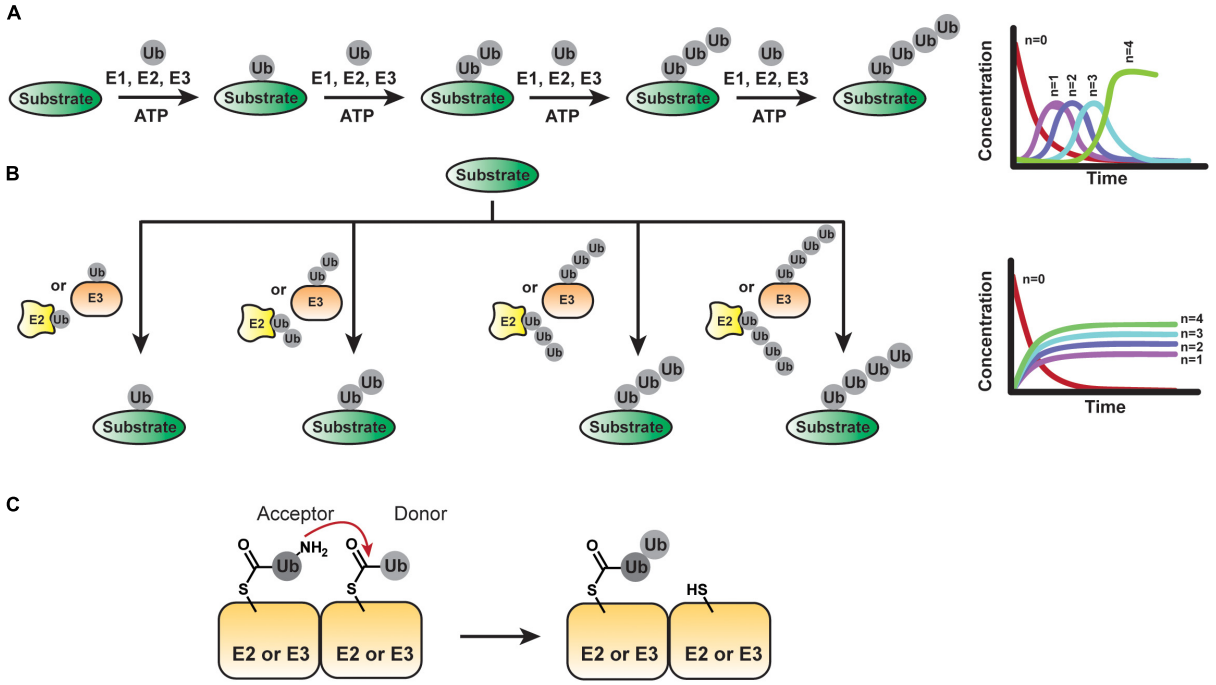


**FIGURE 3 |** Mechanisms of Ubiquitin Chain Assembly. **(A)** The sequential addition model implies the transfer of ubiquitin molecules one at a time. The fractional conversion profile of product formation will show a lag phase proportional to chain length for each new ubiquitinated species formed. **(B)** In the en bloc model, pre-assembled ubiquitin chains anchored to the active site of an E2 or E3 are transferred to a substrate. If the pre-assembly of chains is much faster than the transfer of chains to the substrate, a lag phase proportional to chain length should not be observed in the fractional conversion profile. **(C)** Basic step of an en bloc transfer mechanism: The ubiquitin conjugated to the active site of an E2 or HECT/RBR E3 provides an acceptor lysine residue to attack the C-terminus of another thioester-linked ubiquitin tethered to another E2 or E3.

this set-up, thus offering indirect support for a sequential addition mechanism.

The most compelling evidence for the sequential addition mechanism comes from millisecond kinetic measurements (Pierce et al., 2009). Such time resolution is sufficient to detect whether chains are formed sequentially or contemporaneously. In the case of Cdc34-SCF$^{Cdc4}$ and UBE2R1-SCF$^{\beta-TrCP}$, each new ubiquitinated species was found to occur sequentially with non-concurrent lag phases; in other words, each reaction intermediate acts as a substrate during each round of chain elongation. Kinetic analyses revealed that transferring the first ubiquitin (a step represented by $k_{Ub1}$) is the slowest step during ubiquitin chain assembly, which is why most enzyme-substrate encounters are unproductive. Once the first ubiquitin is in place, the rates of sequential ubiquitin additions ($k_{Ub-n}$) are markedly faster than substrate dissociation ($k_{off}$), allowing for multiple transfer events to occur before the enzyme-substrate complex dissociates. As a result, polyubiquitination is processive. Just as the probability of acquiring a chain depends on the ratio of $k_{Ub1}$ to $k_{off}$, the length of a chain is determined by the rates of the additional ubiquitin transfer ($k_{Ub-n}$) and $k_{off}$. Reductions in $k_{Ub-n}$ manifest with increasing chain length, as the distal end of the growing chain samples more conformational space.

With certain E3s, e.g., the 1.3 MDa CRL APC/C, the conformational space occupied by the growing chain can be restricted by subunits harboring ubiquitin-binding domains (Brown et al., 2014; Kelly et al., 2014), resulting in a decrease in $k_{off}$ and an increase in $k_{Ub-n}$. As described in more detail below, single-molecule measurements combined with detailed structural and biochemical studies have shown that the APC/C assembles ubiquitin chains through a feed-forward mechanism termed processive affinity amplification (PAA) (Lu et al., 2015b). The basic premise is that substrates carrying more ubiquitin molecules/longer ubiquitin chains are preferentially ubiquitinated compared to substrates carrying fewer ubiquitin molecules/shorter chains. In essence, each ubiquitin molecule added to the substrate enhances the affinity of the modified substrate for the APC/C, thus rendering chain formation processive.

A consequence of the sequential addition mechanism is that the processivity of ubiquitin linkage formation can dictate chain length and, thus, the fate of the substrate protein. In the case of the Cdc34/UBE2R1-SCF complexes, the rate-limiting transfer of the first ubiquitin affords two distinct populations of substrate–unmodified and extensively polyubiquitinated (Pierce et al., 2009). How fast a substrate is decorated with the first ubiquitin will thus largely determine how fast it is degraded by the proteasome, assuming ubiquitination is rate-limiting during degradation.

The situation is different with the HECT ligase WWP1. Time course data shows that WWP1 catalyzes K63-linked ubiquitin chains on its substrates in a sequential manner

with a lag phase proportional to chain length (French et al., 2017). Once the chain reaches ∼4 subunits in length, WWP1 switches to building chains linked through K11 and K48, presumably due to topological constraints on the distal ubiquitin within the substrate-tethered K63 chain. Thus, even if the multidirectional phase is slow, the substrate can be modified with short K63 chains to possibly direct proteasome-independent events. In contrast, branched chains, as formed during the second phase of the reaction promote proteasomal degradation of the modified substrate (Meyer and Rape, 2014; Grice et al., 2015; Liu et al., 2017; Yau et al., 2017; Ohtake et al., 2018).

Sequential addition also lends itself to fine-tuning of the polyubiquitinated protein by DUBs (Zhang et al., 2013): consider two substrates with slightly different affinities for an E3. Both acquire ubiquitin moieties at roughly the same rate, but one is released faster than the other. Every time dissociation occurs, the growing ubiquitin chain may be exposed to a DUB, thus running the risk of disassembly. Indeed, incorporating DUB activity into a kinetic model for sequential addition reveals that a two-fold increase in $k_{off}$ results in over an eight-fold decrease in chain formation. In other words, modest differences in E3-substrate affinity afford significant differences in the extent to which substrates are modified with ubiquitin in a single encounter with the E3. In turn, this affects the efficiency of their proteasome-mediated degradation or alternative downstream responses.

## En Bloc Transfer

In addition to transferring individual ubiquitin molecules to a growing substrate-linked chain, there is evidence that certain systems can pre-form chains on the active site cysteine of an E2 or E3 before transfer to a substrate (**Figure 3B**). From the perspective of maximizing the efficiency with which a substrate is polyubiquitinated, such en bloc transfer is ideal: unlike the sequential addition mechanism, an E3-substrate complex does not have to be long-lived for the substrate to receive a chain of sufficient length for downstream signaling events. Instead, the population of E2- or E3-tethered chains dictates how a substrate is modified. On the flip side, en bloc transfer requires the mechanisms of chain pre-formation on the respective enzyme to be much faster than substrate transfer.

En bloc transfer was first proposed based on biochemical studies with the K48-specific HECT E3 UBE3A (E6AP) (Wang et al., 2006). As with all HECT E3s, ubiquitin is transferred from an E2 (UBE2L3) to the active-site cysteine of UBE3A to form a thioester-linked conjugate. En bloc assembly of chains by UBE3A then implies that the ubiquitin conjugated to the active site of UBE3A provides the acceptor lysine residue (K48) to attack the C-terminus of another thioester-linked ubiquitin tethered to either a UBE3A subunit (in the context of an UBE3A oligomer) or an associated E2 (**Figure 3C**). Consistent with this notion, mixing UBE3A∼ubiquitin with a ubiquitin molecule that cannot be activated as a thioester precludes the formation of di-ubiquitin. However, di-ubiquitin can be generated upon reacting UBE3A∼ubiquitin with an E2∼K0-ubiquitin conjugate (ubiquitin variant lacking lysine residues). When a substrate is added to the picture, e.g., the ubiquitin-binding protein HHR23A, the K48-linked di-ubiquitin is transferred to HHR23A, suggesting en bloc transfer is chemically feasible. However, UBE3A-bound di-(or poly)ubiquitin has not been detected directly. Recently, steady-state kinetic analyses have led to a model in which E2∼ubiquitin conjugates bind two functionally distinct sites on trimers of the catalytic domain of UBE3A (Ronchi et al., 2013, 2014, 2017) and NEDD4 subfamily members (Todaro et al., 2017, 2018), respectively, to build active site-anchored ubiquitin chains for en bloc transfer. Yet, as mentioned above, the NEDD4-type WWP1 builds chains sequentially (French et al., 2017).

Time course analyses suggested that en bloc transfer also applies to certain E2/RING E3 systems. The human E2 UBE2G2 (Fang et al., 2001; Chen et al., 2006) and its yeast ortholog Ubc7 (Biederer et al., 1996; Hiller et al., 1996; Bays et al., 2001; Deak and Wolf, 2001) are associated with the ER membrane and responsible for K48-linked ubiquitin chain formation on misfolded polypeptides exported from the ER lumen during ERAD. In the presence of the ER-resident E3 GP78, UBE2G2 was found to catalyze the assembly of ubiquitin chains on its active-site cysteine (Li et al., 2007). The propensity for GP78 to oligomerize drives this preassembly process, as the formation of UBE2G2-GP78 hetero-oligomers brings the active sites of multiple UBE2G2 molecules into close proximity (Li et al., 2009; Liu et al., 2014). With UBE2G2∼ubiquitin conjugates juxtaposed, K48 of one ubiquitin is thought to attack the C-terminus of the neighboring thioester-linked one.

Besides UBE2G2, UBE2K, and Ubc7, have also been found conjugated to ubiquitin chains through a thioester linkage (Haldeman et al., 1997; Ravid and Hochstrasser, 2007; Bazirgan and Hampton, 2008). The rate at which chains are formed on the active-site cysteine of UBE2G2 is slightly faster than the rate of transfer to a substrate lysine residue, suggesting en bloc transfer is kinetically feasible during the polyubiquitination of a substrate (Li et al., 2007). That said, fast kinetic measurements of product distributions would be helpful to validate this mechanism and confirm that substrate-anchored ubiquitin chains indeed reflect the distribution of chains attached to the active site of UBE2G2.

# WHAT ARE THE KEY MOLECULAR FEATURES REQUIRED FOR CHAIN ASSEMBLY?

Ubiquitin chain formation requires a molecular juggling act (Lorenz et al., 2013). In the context of the sequential addition model, an E3 has to engage a substrate and a thioester-linked E2-donor ubiquitin complex, transfer ubiquitin to a primary amino group of the substrate, and then switch to one of eight primary amino groups of an acceptor ubiquitin to promote chain elongation. All of these events must occur while the substrate remains bound to

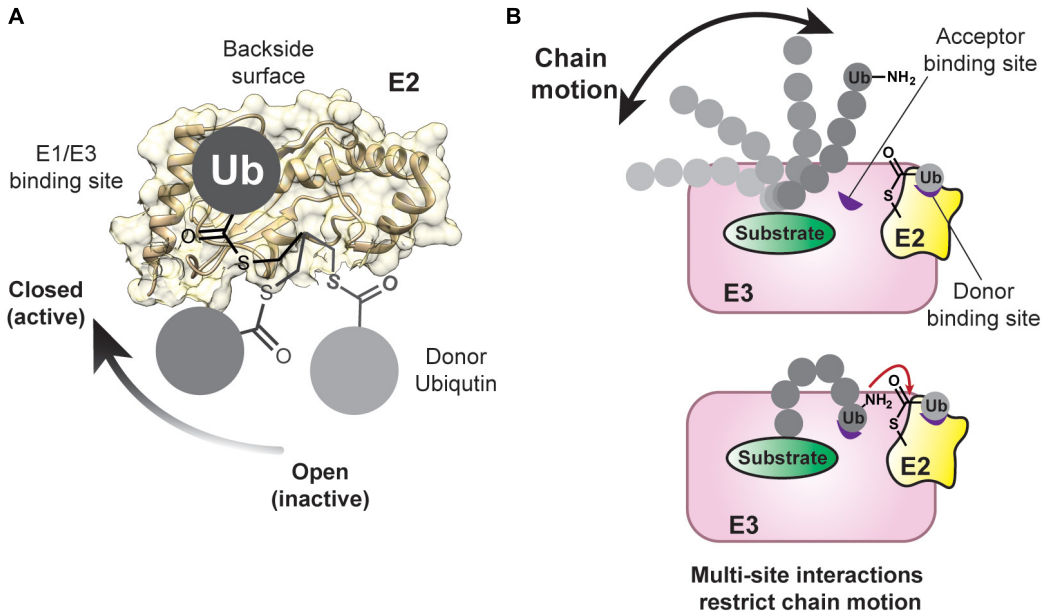


**FIGURE 4 |** Conformational Flexibility of the Donor and Acceptor Ubiquitin Are Restrained During Chain Assembly. **(A)** The donor ubiquitin covalently tethered to the active-site cysteine of an E2 can adopt multiple conformations, referred to as "open" and "closed." The closed conformation is important during catalysis with RING E3 enzymes. The E1/E3 binding site and the backside of an E2 are also highlighted on the structure of UBE2D2 (PDB: 5ULF). **(B)** As a chain increases in length, it can occupy more conformational space (top). Low-affinity ubiquitin-binding domains (shown in purple) can assist in limiting the conformational space of the chain and positioning the acceptor ubiquitin for the nucleophilic attack on the E2∼donor ubiquitin conjugate.

the E3 to minimize the number of encounters required to build a chain.

## Multisite E2-E3 Interactions During Chain Formation

Structural studies have shown that E3s interact with the same surface of E2s that is recognized by E1 enzymes (**Figure 4A**; Eletr et al., 2005; Huang et al., 2005; Kamadurai et al., 2009; Lechtenberg et al., 2016; Dove et al., 2017b; Yuan et al., 2017; Condos et al., 2018; Sauvé et al., 2018). Such mutually exclusive binding places a major constraint on the mechanism of polyubiquitination because the spent E2 must dissociate from the E3 after ubiquitin transfer to allow for ubiquitin reloading. Assuming the association between E3 and an E2∼ubiquitin conjugate is governed by short-range interactions (e.g., van der Waals), and thus diffusion-controlled, the on-rate would be $\leq 10^6$ $M^{-1}s^{-1}$ (Alsallaq and Zhou, 2008; Schreiber et al., 2009). With an intracellular concentration of E2∼ubiquitin conjugate estimated to be around 1 μM (Kleiger et al., 2009a), the complex would form at a rate of 1 $s^{-1}$. If the affinity is ∼10 μM, the off-rate would be 10 $s^{-1}$. For six rounds of conjugation, the assembly and disassembly of an E2-E3 complex would thus consume ∼6 s of the entire process. At first glance, these numbers seem reasonable, considering kinetic studies have shown that a substrate can acquire up to six ubiquitin molecules in ∼10 s, as catalyzed by the Cdc34-SCF complex (Saha and Deshaies, 2008). However, Cdc34∼ubiquitin binds tightly to SCF with a $K_d$ in the low nanomolar range (Saha and Deshaies, 2008). The overall rate of cyclical binding and release would thus not be conducive to the processive assembly of a ubiquitin chain.

A balance between affinity and processivity is achieved through bipartite interactions. Cdc34 not only engages SCF through the Rbx1 RING subunit, but also possesses an acidic C-terminal tail that interacts with a conserved basic cleft on the cullin subunit (Kleiger et al., 2009b). These electrostatic interactions govern the initial, rapid recognition, while interactions between Rbx1 and Cdc34 position and activate the ubiquitin-loaded E2 for transferring ubiquitin to the substrate. With electrostatic forces driving the interaction between Cdc34 and SCF, the on-rate is two orders of magnitude faster than the diffusion-controlled limit. The off-rate thus does not have to be slow in order to achieve nanomolar affinity. Since the off-rate is $>30$ $s^{-1}$, binding and release can occur before substrate dissociation. That electrostatic forces govern the interactions between Cdc34 and the SCF has an additional advantage: due to their weaker dependence on distance ($1/r$) compared to van-der-Waals interactions ($1/r^6$) allows the spent E2 to remain in close proximity to the E3 while it is recharged with ubiquitin by an E1. The importance of electrostatic forces in Cdc34-CRL interactions is underscored by the fact that the basic cleft is conserved across the cullin family.

Other multi-component E2-CRL assemblies have also evolved multisite binding mechanisms for processive polyubiquitination. For example, the human APC/C cooperates with two E2s, UBE2C and UBE2S, to catalyze polyubiquitination of key cell cycle regulators, thereby regulating cellular progression through mitosis—a process that has recently been reconstructed,

primarily due to the power of cryo-electron microscopy (Alfieri et al., 2017; Watson et al., 2019). UBE2C initiates chain synthesis, while UBE2S catalyzes chain elongation in a K11-linkage specific manner (Jin et al., 2008; Garnett et al., 2009; Williamson et al., 2009; Wu T. et al., 2010; Wickliffe et al., 2011). The rate ot substrate degradation is determined by the efficiency of chain initiation as well as the nature and extent of polyubiquitination (Rape et al., 2006; Williamson et al., 2011; Lu et al., 2015a). Processivity in ubiquitination, as achieved through the PAA mechanism discussed above (Lu et al., 2015b), ensures efficient substrate degradation and involves distinct multisite interactions of the APC/C with UBE2C and UBE2S.

During the priming reaction, the APC/C engages UBE2C in a canonical mode through its RING domain (APC11) and via the winged-helix B (WHB) domain of APC2 (Brown et al., 2014, 2015, 2016). The WHB domain binds the "backside" of UBE2C, which is located on the opposite side of the donor ubiquitin binding site and provides an important allosteric site in a number of E2s (Miura et al., 2002; Brzovic et al., 2006; Bocik et al., 2011; Hibbert et al., 2011; Page et al., 2012; Ranaweera and Yang, 2013). Investigations into another RING E3, RNF38, and the E2 UBE2D2 (Buetow et al., 2015) have shown that backside binding of ubiquitin to UBE2D2 limits the flexibility of the RING domain binding site and stabilizes the catalytically active closed conformation of UBE2D2∼ubiquitin (**Figure 4A**; Saha et al., 2011; Wickliffe et al., 2011; Dou et al., 2012, 2013; Plechanovová et al., 2012; Pruneda et al., 2012; Soss et al., 2013; Branigan et al., 2015; Dove et al., 2017b). The net result is a dramatic increase in catalytic efficiency. Based on these data, the WHB domain of APC2 might not only limit the search radius of the dynamic UBE2C-APC11 assembly to specific lysines of a substrate (Brown et al., 2015), but also potentiate ubiquitin transfer.

In other systems, backside interactions enable rapid cycling between E2 binding and release. For example, the G2BR domain of GP78 was found to bind to the backside of UBE2G2 with low nanomolar affinity (Das et al., 2009; Li et al., 2009). This interaction induces conformational changes in UBE2G2 that result in an increase in the affinity for the RING domain of GP78 by ∼50-fold. Assuming the binding energies are additive (Jencks, 1981), an overall $K_d$ in the picomolar range would be expected. Such tight binding could adversely affect E2 exchange from the E3 and ultimately processivity; however, the measured $K_d$ turns out to be $\sim 10^3$ times higher than calculated. As revealed through biophysical studies, UBE2G2 is released from GP78 by an allosteric feedback mechanism in which binding of the RING domain to UBE2G2 reduces the number of electrostatic interactions between UBE2G2 and G2BR (Das et al., 2013). The kinetics in this system are such that the off-rate of UBE2G2 from G2BR is much faster than the rate of ubiquitin transfer. Since the E1 cannot charge the G2BR-bound form of UBE2G2 as efficiently as free UBE2G2, complete release of the E2 is likely important for consecutive cycles of ubiquitination.

Chain elongation on APC/C substrates involves a unique set of bipartite interactions between the APC/C and UBE2S. UBE2S is primarily recruited to APC/C through its 66-residue C-terminal peptide (CTP) extension (Meyer and Rape, 2014; Brown et al., 2016), which nestles into a complementary acidic and hydrophobic groove at the interface between the APC2 and APC4 subunits. The catalytic UBC domain of UBE2S is held in place by the cullin APC2, not the APC11 RING domain, to promote chain elongation (Brown et al., 2016). The APC11 RING domain instead serves a non-canonical role during this process by tracking the distal acceptor ubiquitin molecule of the growing ubiquitin chain (Kelly et al., 2014; Brown et al., 2016).

## Distinct Enzymes for Priming and Extension

The distinct reactions of monoubiquitination/priming and polyubiquitination/elongation that are catalyzed by E3s present significant challenges. During the priming phase, ubiquitin is directly attached to a substrate protein. For this process to be site-specific, spatial restrictions (Kamadurai et al., 2013) or active participation from the substrate (Jin et al., 2008; Mattiroli et al., 2012, 2014) are required. In most cases monoubiquitination occurs at multiple lysines with little dependence on sequence context (Petroski and Deshaies, 2003; Tang et al., 2007; Fischer et al., 2011). By contrast, chain elongation often occurs with specificity for the amino group of ubiquitin that is modified (Wenzel and Klevit, 2012). To achieve specificity during sequential addition, an E3 needs to repeatedly position the distal acceptor ubiquitin molecule in a growing chain with high precision.

E3s have evolved different mechanisms to meet this demand. The APC/C, for example, uses two different E2s for priming and extension (Rodrigo-Brenni and Morgan, 2007). The recognition of a substrate's degron motif (a KEN- or D-box) by the APC/C co-factors CDH1 or CDC20, respectively, along with the APC10 subunit (Fang et al., 1998; Pfleger and Kirschner, 2000) places the substrate in close proximity to the UBE2C∼ubiquitin conjugate (Brown et al., 2016). Confined to the same space within the central cavity of APC/C, UBE2C can readily modify the substrate with individual ubiquitin molecules and/or short K11, K48, and K63 chains (Kirkpatrick et al., 2006). Thereafter, the APC/C subsequently juxtaposes UBE2S with the acceptor ubiquitin (Brown et al., 2016), thus providing an optimal geometry for processive and specific chain elongation using K11 of ubiquitin (Wickliffe et al., 2011). What is particularly interesting about the different catalytic architectures of the APC/C is the potential for differential regulation by macromolecular factors and posttranslational modifications, e.g., phosphorylation (Reimann et al., 2001; Craney et al., 2016; Qiao et al., 2016).

Similar to the APC/C, SCF ligases are known to collaborate with several E2s. In this case, UBE2D2/D3 transfers the first ubiquitin, while UBE2R1 catalyzes K48-linked chain elongation (Wu K. et al., 2010). In a surprising turn of events, SCFs were also found to team up with another E3 ligase to carry out the distinct steps of priming and extension (Scott et al., 2016; Dove et al., 2017a). Using genome and proteome-wide screens, the RBR E3 HHARI and its *Caenorhabditis elegans* ortholog ARI-1 were shown to associate with the NEDD8-modified/activated forms of CRLs. Like many RBRs, HHARI/ARI-1 exists in an autoinhibited state in which its Ariadne domain interacts with the RING2 domain (Duda et al., 2013), thereby blocking the

catalytic cysteine and preventing transfer of ubiquitin from the cognate E2 UBE2L3/UBC-18. Autoinhibition is relieved upon binding of NEDD8-modified CRLs. Once charged with ubiquitin, HHARI catalyzes the monoubiquitination of CRL substrates. With the substrate primed, UBE2R1 then works with the CRL to form a K48-linked chain. While this cooperative mode of action of HHARI and NEDD8-modified CRLs is conceptually unique, there are other examples of ubiquitin ligases that regulate each other through macromolecular interfaces (Kühnle et al., 2011).

When two E3s act independently but sequentially to prime and extend, the ubiquitin-dependent outcome can change dramatically. In response to replication fork collapse, for example, the DNA polymerase processivity factor PCNA (proliferating cell nuclear antigen) is monoubiquitinated by Rad6 (an E2) and Rad18 (an E3) to promote an error-prone damage tolerance process known as translesion DNA synthesis (Hoege et al., 2002; Stelter and Ulrich, 2003). Switching to an error-free, lesion bypass process requires collaboration between the E3 Rad5 and E2 Ubc13/Mms2 to build K63-linked chains, with the monoubiquitinated product of Rad6-Rad16 serving as the substrate for Ubc13/Mms2-Rad5 (Hoege et al., 2002; Parker and Ulrich, 2009). The HECT E3s HUWE1 and UBR5 also use ubiquitinated substrates to seed chain extension. HUWE1 has been shown to recognize substrates primed with K63-linked chains by another E3, e.g., TRAF6, and extend a K48-linked chain from a branch point (Ohtake et al., 2016), transforming the ubiquitin-dependent signal from non-degradative to degradative. Likewise, UBR5 installs K48 branch points on preexisting chains built by other E3s, e.g., ITCH and UBR4, and continues to extend the chains with K48 linkages for the purpose of creating a more potent proteasome-targeting signal (Yau et al., 2017; Ohtake et al., 2018). Whether HUWE1 and UBR5 prefer an internal ubiquitin subunit within a chain, similar to the yeast branching enzyme Ufd2 (Liu et al., 2017), or any subunit can serve as the starting point for chain extension remains unclear.

## Orienting the Acceptor Ubiquitin

While the orientation of the donor ubiquitin toward the E2 or E3 is an important part of preparing the active site for the nucleophilic attack of the acceptor, both chemically and sterically (**Figure 4A**; Saha et al., 2011; Wickliffe et al., 2011; Dou et al., 2012, 2013; Plechanovová et al., 2012; Pruneda et al., 2012; Soss et al., 2013; Branigan et al., 2015; Lorenz et al., 2016; Dove et al., 2017b), the acceptor ubiquitin must also be positioned properly to maximize the efficiency and processivity of chain formation (**Figure 4B**; Wright et al., 2016). One can think about this problem from an entropic perspective: as the length increases, a chain can occupy more conformational space. To avoid a large entropic penalty, E2s and E3s must limit the conformational freedom of a growing chain by placing the acceptor ubiquitin in close proximity to the donor. Importantly, how an acceptor ubiquitin is oriented toward the donor also determines the specificity of linkage formation.

The first clue for how an acceptor ubiquitin is positioned for the formation of a specific linkage came from structural studies of the K63-specific yeast E2 Ubc13 (human enzyme; UBE2N) and its co-factor, the ubiquitin E2 variant (UEV) Mms2 (UBE2V2). A crystal structure of the Mms2-Ubc13-donor ubiquitin conjugate showed the donor ubiquitin of one complex binding to the Mms2 molecule of a neighboring Mms2-Ubc13 complex (Eddins et al., 2006). The resulting contacts between Mms2 and ubiquitin position K63 near the active site of the adjacent Ubc13, mimicking an acceptor ubiquitin. This structure thus illustrated how an accessory protein can assist in limiting the orientation of the acceptor ubiquitin toward the catalytic center of an E2 and allow for specificity in acceptor lysine selection. More recently, the crystal structures of a UBE2V2/UBE2N-donor ubiquitin complex bound to the dimeric RING domain of RNF4 revealed that the RING domain tethers the donor ubiquitin in an activated closed conformation toward the E2, thus stimulating catalysis (Branigan et al., 2015); this mechanism has emerged as a canonical principle of RING-mediated catalysis in several E2/E2 systems (Dou et al., 2012; Plechanovová et al., 2012; Pruneda et al., 2012).

By contrast, the APC/C relies on a non-canonical interaction between its RING domain (APC11) and the acceptor ubiquitin: a hydrophobic patch of APC11 engages ubiquitin through residues surrounding K48 along with the C-terminus, thus blocking K48 from serving as an acceptor lysine (Brown et al., 2016), and allowing K11 to be presented to the activated C-terminus of the UBE2S-linked donor. Kinetic studies suggest this mechanism accounts for a 40-fold decrease in $K_m$ and an overall 175-fold increase in catalytic efficiency (Brown et al., 2016).

Interestingly, UBE2S can achieve K11 linkage specificity in the absence of the APC/C (Bremm et al., 2010; Matsumoto et al., 2010; Wickliffe et al., 2011). The key to this inherent specificity lies in the activation of the acceptor lysine, K11, by an adjacent acidic side chain, E34, of ubiquitin, which promotes the nucleophilic attack of K11 through facilitating its deprotonation (Wickliffe et al., 2011). This mechanism, known as substrate-assisted catalysis, triggers isopeptide bond formation specifically when K11 is presented to the UBE2S active site, while other acceptor orientations are catalytically disfavored. Notably, ubiquitin was also found to contribute to catalysis in HECT E3s (Ries et al., 2019) and DUBs (Keusekotten et al., 2013; Mevissen et al., 2016), suggesting substrate-assisted catalysis is a conserved theme in different classes of ubiquitinating and deubiquitinating enzymes.

Principles of acceptor ubiquitin recognition have also started to emerge outside of the RING E3 family. For instance, structural studies of the RBR-type linear ubiquitin chain assembly complex (LUBAC) has revealed dedicated interaction sites for the acceptor ubiquitin. LUBAC generates M1-linked chains to regulate innate immunity and inflammation through the NF-κB pathway (Kirisako et al., 2006; Ikeda et al., 2011; Tokunaga et al., 2011) and is composed of two RBR E3 subunits: HOIP and HOIL-1L; however, only one of the RBRs (HOIP), contains the catalytic activity necessary for generating M1-linked chains (Smit et al., 2012; Stieglitz et al., 2013). The structure of a minimal HOIP–ubiquitin transfer complex shows the α-amino group of the acceptor residue, M1, poised for the nucleophilic attack on the donor ubiquitin (Lechtenberg et al., 2016). In this complex, the RING2-domain together with the "linear ubiquitin chain determining region" (LDD) of HOIP create a platform

that ensures the α-amino group of the acceptor is positioned in proximity to the active site. Deprotonation of this amino group, as required for its nucleophilic function, is promoted by a particular histidine residue of HOIP.

In HECT E3s, the structural basis of acceptor ubiquitin recognition has remained elusive. However, a particular region, known as the "exosite," in the N-lobe of the catalytic HECT domain, was shown to engage a regulatory ubiquitin molecule, thus promoting chain elongation but not initiation (Ogunjimi et al., 2010; Kim et al., 2011; Maspero et al., 2011, 2013; Zhang et al., 2016; French et al., 2017; Ries et al., 2019). It has thus been hypothesized that the exosite contributes indirectly to stabilizing the acceptor ubiquitin in proximity to the active site by interacting with flanking ubiquitin moieties within the growing chain (Fajner et al., 2017).

Finally, Cue1, a receptor and activator of the yeast E2 Ubc7 that is crucial for ERAD (Biederer et al., 1997), provides an example of how an accessory protein can impact the acceptor ubiquitin to promote ubiquitin linkage formation. Cue1 harbors an N-terminal ubiquitin-binding CUE domain and a C-terminal Ubc7 binding region (U7BR), which likely activates Ubc7 in a manner analogous to the G2BR domain of GP78 (Bazirgan and Hampton, 2008; Kostova et al., 2009; Metzger et al., 2013). NMR studies and *in vitro* ubiquitination reactions revealed that the CUE domain accelerates chain formation by binding to the penultimate ubiquitin molecule in a growing chain, thereby assisting U7BR in orienting the distal acceptor moiety toward the active site of Ubc*7* formation (Bagola et al., 2013; von Delbrück et al., 2016). Although the overall impact of Cue1 on the kinetics of chain formation is modest *in vitro*, the mechanistic implications are rather intriguing. Kinetic measurements show that the off-rate of the CUE domain-ubiquitin complex is fast compared to the rate of isopeptide bond formation. Thus, the CUE domain can "hop" along a chain without affecting the overall rate of chain formation until it finds the ubiquitin moiety adjacent to the acceptor. E3s capable of elongating existing ubiquitin chains by installing branch points could use similar enzymatic logic (Koegl et al., 1999; Metzger and Weissman, 2010; Ohtake et al., 2016, Ohtake et al., 2018; Liu et al., 2017; Yau et al., 2017).

## OUTLOOK

The progress made over the last decade in understanding how ubiquitin chains are assembled is astonishing. Most notably, detailed kinetic analyses have illustrated the complexities of the sequential addition mechanism in the context of CRLs. Moreover, synergistic advances in structural biology, genomic engineering, quantitative mass spectrometry, and chemical biology have helped elucidate central operating principles underlying the activities of E2s and E3s, including multi-site interactions, the cooperative interplay of distinct enzymes for chain initiation and elongation, the precise positioning of the donor and acceptor ubiquitin, and substrate-assisted catalysis. While these principles have been found to recur in various model systems studied, it is important to realize that each class of E3s appears to implement these principles by distinct structural mechanisms, thus contributing to the enormous versatility and specificity of ubiquitin signaling.

Despite considerable advances in understanding the mechanistic principles of ubiquitin chain formation, reconstituting and structurally visualizing the trajectory of the functional enzyme-substrate assemblies has been challenging. This is due, for the most part, to the weak and dynamic nature of the underlying macromolecular interactions, which typically fall into the hig micromolar to millimolar affinity range *in vitro*. To overcome this challenge, crosslinking approaches have emerged as indispensable tools, opening exciting avenues to capture specific complexes for structural analyses (Witting et al., 2017).

The immense potential of ubiquitin ligases as therapeutic targets has been illustrated by the clinical efficacy of thalidomide and its derivatives in the treatment of hematological malignancies (Lindner and Krönke, 2016). However, progress toward rationally manipulating E3s has been impeded largely by our insufficient understanding of their conformational dynamics, macromolecular interactions, and functional integration into cellular pathways (Huang and Dixit, 2016; Chen et al., 2018). Over the next few years, it will be exciting to see how the mechanisms of critical, yet uncharacterized E3s unfold, especially those in the relatively poorly characterized RBR and HECT families, and how these mechanisms are altered in human diseases. For instance, the HECT ligase HUWE1 has both pro-oncogenic and tumor suppressor functions, depending on the cellular context (Zhao et al., 2008; Inoue et al., 2013; Peter et al., 2014; King et al., 2016; Myant et al., 2017). Which macromolecular complexes mediate these functions by mediating substrate selection, activity, and linkage specificity of this crucial ligase remains to be determined. It will also be important to identify the consequences of patient-derived mutations in disease-associated ligase genes in order to develop efficient strategies targeting these enzymes therapeutically. Finally, a better understanding of the mechanisms of ubiquitin chain formation will facilitate the development of bifunctional small molecules, known as PROTACs (Sakamoto et al., 2002), that re-program a particular ligase to mark a pathogenic target protein for degradation – a powerful concept that has recently entered clinical trials (Mullard, 2019).

## AUTHOR CONTRIBUTIONS

All authors listed have made a substantial, direct and intellectual contribution to the work, and approved it for publication.

## ACKNOWLEDGMENTS

We apologize to all colleagues whose work we did not include. Work in our labs is funded by grants from the National Institutes of Health (R01GM110543; ES), the Emmy Noether Program of the German Research Foundation (LO 2003/1-1; SL), and the EMBO Young Investigator Program (SL). KD holds an NSF graduate research fellowship (GRFP1451512). We thank Anna Liess for assistance in the figures.

## REFERENCES


Abdul Rehman, S. A., Kristariyanto, Y. A., Choi, S. Y., Nkosi, P. J., Weidlich, S., Labib, K., et al. (2016). MINDY-1 is a member of an evolutionarily conserved and structurally distinct new family of deubiquitinating enzymes. *Mol. Cell* 63, 146–155. doi: 10.1016/j.molcel.2016.05.009

Aichem, A., Pelzer, C., Lukasiak, S., Kalveram, B., Sheppard, P. W., Rani, N., et al. (2010). USE1 is a bispecific conjugating enzyme for ubiquitin and FAT10, which FAT10ylates itself in cis. *Nat. Commun.* 1:13. doi: 10.1038/ncomms1012

Alfieri, C., Zhang, S., and Barford, D. (2017). Visualizing the complex functions and mechanisms of the anaphase promoting complex/cyclosome (APC/C). *Open Biol.* 7:170204. doi: 10.1098/rsob.170204

Alsallaq, R., and Zhou, H. X. (2008). Electrostatic rate enhancement and transient complex of protein-protein association. *Proteins* 71, 320–335. doi: 10.1002/prot.21679

Bagola, K., vonDelbrück, M., Dittmar, G., Scheffner, M., Ziv, I., Glickman, M. H., et al. (2013). Ubiquitin binding by a CUE domain regulates ubiquitin chain formation by ERAD E3 ligases. *Mol. Cell* 50, 528–539. doi: 10.1016/j.molcel.2013.04.005

Bays, N. W., Gardner, R. G., Seelig, L. P., Joazeiro, C. A., and Hampton, R. Y. (2001). Hrd1p/Der3p is a membrane-anchored ubiquitin ligase required for ER-associated degradation. *Nat. Cell Biol.* 3, 24–29. doi: 10.1038/35050524

Bazirgan, O. A., and Hampton, R. Y. (2008). Cue1p is an activator of Ubc7p E2 activity in vitro and in vivo. *J. Biol. Chem.* 283, 12797–12810. doi: 10.1074/jbc.M801122200

Biederer, T., Volkwein, C., and Sommer, T. (1996). Degradation of subunits of the Sec61p complex, an integral component of the ER membrane, by the ubiquitin-proteasome pathway. *EMBO J.* 15, 2069–2076. doi: 10.1002/j.1460-2075.1996.tb00560.x

Biederer, T., Volkwein, C., and Sommer, T. (1997). Role of Cue1p in ubiquitination and degradation at the ER surface. *Science* 278, 1806–1809. doi: 10.1126/science.278.5344.1806

Bocik, W. E., Sircar, A., Gray, J. J., and Tolman, J. R. (2011). Mechanism of polyubiquitin chain recognition by the human ubiquitin conjugating enzyme Ube2g2. *J. Biol. Chem.* 286, 3981–3991. doi: 10.1074/jbc.M110.189050

Branigan, E., Plechanovová, A., Jaffray, E. G., Naismith, J. H., and Hay, R. T. (2015). Structural basis for the RING-catalyzed synthesis of K63-linked ubiquitin chains. *Nat. Struct. Mol. Biol.* 22, 597–602. doi: 10.1038/nsmb.3052

Bremm, A., Freund, S. M. V., and Komander, D. (2010). Lys11-linked ubiquitin chains adopt compact conformations and are preferentially hydrolyzed by the deubiquitinase Cezanne. *Nat. Struct. Mol. Biol.* 17, 939–947. doi: 10.1038/nsmb.1873

Brown, N. G., VanderLinden, R., Watson, E. R., Qiao, R., Grace, C. R. R., Yamaguchi, M., et al. (2015). RING E3 mechanism for ubiquitin ligation to a disordered substrate visualized for human anaphase-promoting complex. *Proc. Natl. Acad. Sci. U.S.A.* 112, 5272–5279. doi: 10.1073/pnas.1504161112

Brown, N. G., VanderLinden, R., Watson, E. R., Weissmann, F., Ordureau, A., Wu, K. P., et al. (2016). Dual RING E3 architectures regulate multiubiquitination and ubiquitin chain elongation by APC/C. *Cell* 165, 1440–1453. doi: 10.1016/j.cell.2016.05.037

Brown, N. G., Watson, E. R., Weissmann, F., Jarvis, M. A., VanderLinden, R., Grace, C. R. R., et al. (2014). Mechanism of polyubiquitination by human anaphase-promoting complex: ring repurposing for ubiquitin chain assembly. *Mol. Cell* 56, 246–260. doi: 10.1016/j.molcel.2014.09.009

Brzovic, P. S., Lissounov, A., Christensen, D. E., Hoyt, D. W., and Klevit, R. E. (2006). A UbcH5/ubiquitin noncovalent complex is required for processive BRCA1-directed ubiquitination. *Mol. Cell* 21, 873–880. doi: 10.1016/j.molcel.2006.02.008

Buetow, L., Gabrielsen, M., Anthony, N. G., Dou, H., Patel, A., Aitkenhead, H., et al. (2015). Activation of a primed RING E3-E2-ubiquitin complex by non-covalent ubiquitin. *Mol. Cell* 58, 297–310. doi: 10.1016/j.molcel.2015.02.017

Buetow, L., and Huang, D. T. (2016). Structural insights into the catalysis and regulation of E3 ubiquitin ligases. *Nat. Rev. Mol. Cell Biol.* 17, 626–642. doi: 10.1038/nrm.2016.91

Chen, B., Mariano, J., Tsai, Y. C., Chan, A. H., Cohen, M., and Weissman, A. M. (2006). The activity of a human endoplasmic reticulum-associated degradation E3, gp78, requires its Cue domain, RING finger, and an E2-binding site. *Proc. Natl. Acad. Sci. U.S.A.* 103, 341–346. doi: 10.1073/pnas.0506618103

Chen, D., Gehringer, M., and Lorenz, S. (2018). Developing small-molecule inhibitors of HECT-type ubiquitin ligases for therapeutic applications: challenges and opportunities. *ChemBioChem* 19, 2123–2135. doi: 10.1002/cbic.201800321

Chiu, Y. H., Sun, Q., and Chen, Z. J. (2007). E1-L2 activates both ubiquitin and FAT10. *Mol. Cell* 27, 1014–1023. doi: 10.1016/j.molcel.2007.08.020

Choi, Y.-S., Lee, Y.-J., Lee, S.-Y., Shi, L., Ha, J.-H., Cheong, H.-K., et al. (2014). Differential ubiquitin binding by the acidic loops of Ube2g1 and Ube2r1 enzymes distinguishes their Lys-48-ubiquitylation activities. *J. Biol. Chem.* 290, 2251–2263. doi: 10.1074/jbc.M114.624809

Chong, R. A., Wu, K., Spratt, D. E., Yang, Y., Lee, C., Nayak, J., et al. (2014). Pivotal role for the ubiquitin Y59-E51 loop in lysine 48 polyubiquitination. *Proc. Natl. Acad. Sci. U.S.A.* 111, 8434–8439. doi: 10.1073/pnas.1407849111

Clague, M. J., Barsukov, I., Coulson, J. M., Liu, H., Rigden, D. J., and Urbe, S. (2013). Deubiquitylases from genes to organism. *Physiol. Rev.* 93, 1289–1315. doi: 10.1152/physrev.00002.2013

Clague, M. J., Heride, C., and Urbé, S. (2015). The demographics of the ubiquitin system. *Trends Cell Biol.* 25, 417–426. doi: 10.1016/j.tcb.2015.03.002

Clague, M. J., Urbé, S., and Komander, D. (2019). Breaking the chains: deubiquitylating enzyme specificity begets function. *Nat. Rev. Mol. Cell Biol.* 20, 338–352. doi: 10.1038/s41580-019-0099-1

Collins, G. A., and Goldberg, A. L. (2017). The logic of the 26S proteasome. *Cell* 169, 792–806. doi: 10.1016/j.cell.2017.04.023

Condos, T. E., Dunkerley, K. M., Freeman, E. A., Barber, K. R., Aguirre, J. D., Chaugule, V. K., et al. (2018). Synergistic recruitment of UbcH7∼Ub and phosphorylated Ubl domain triggers parkin activation. *EMBO J.* 37:e100014. doi: 10.15252/embj.2018100014

Craney, A., Kelly, A., Jia, L., Fedrigo, I., Yu, H., and Rape, M. (2016). Control of APC/C-dependent ubiquitin chain elongation by reversible phosphorylation. *Proc. Natl. Acad. Sci. U.S.A.* 113, 1540–1545. doi: 10.1073/pnas.1522423113

Das, R., Liang, Y. H., Mariano, J., Li, J., Huang, T., King, A., et al. (2013). Allosteric regulation of E2:E3 interactions promote a processive ubiquitination machine. *EMBO J.* 32, 2504–2516. doi: 10.1038/emboj.2013.174

Das, R., Mariano, J., Tsai, Y. C., Kalathur, R. C., Kostova, Z., Li, J., et al. (2009). Allosteric activation of E2-RING finger-mediated ubiquitylation by a structurally defined specific E2-binding region of gp78. *Mol. Cell* 34, 674–685. doi: 10.1016/j.molcel.2009.05.010

Deak, P. M., and Wolf, D. H. (2001). Membrane topology and function of Der3/Hrd1p as a ubiquitin-protein ligase (E3) involved in endoplasmic reticulum degradation. *J. Biol. Chem.* 276, 10663–10669. doi: 10.1074/jbc.m008608200

Deshaies, R. J., and Joazeiro, C. A. P. (2009). RING domain E3 ubiquitin ligases. *Annu. Rev. Biochem.* 78, 399–434. doi: 10.1146/annurev.biochem.78.101807.093809

Dou, H., Buetow, L., Sibbet, G. J., Cameron, K., and Huang, D. T. (2012). BIRC7-E2 ubiquitin conjugate structure reveals the mechanism of ubiquitin transfer by a RING dimer. *Nat. Struct. Mol. Biol.* 19, 876–883. doi: 10.1038/nsmb.2379

Dou, H., Buetow, L., Sibbet, G. J., Cameron, K., and Huang, D. T. (2013). Essentiality of a non-RING element in priming donor ubiquitin for catalysis by a monomeric E3. *Nat. Struct. Mol. Biol.* 20, 982–986. doi: 10.1038/nsmb.2621

Dove, K. K., Kemp, H. A., Di Bona, K. R., Reiter, K. H., Milburn, L. J., Camacho, D., et al. (2017a). Two functionally distinct E2/E3 pairs coordinate sequential ubiquitination of a common substrate in *Caenorhabditis elegans* development. *Proc. Natl. Acad. Sci. U.S.A.* 114, E6576–E6584. doi: 10.1073/pnas.1705060114

Dove, K. K., Olszewski, J. L., Martino, L., Duda, D. M., Wu, X. S., Miller, D. J., et al. (2017b). Structural studies of HHARI/UbcH7∼Ub reveal unique E2∼Ub conformational restriction by RBR RING1. *Structure* 25, 890–900. doi: 10.1016/j.str.2017.04.013

Dove, K. K., and Klevit, R. E. (2017). RING-between-ring E3 ligases: emerging themes amid the variations. *J. Mol. Biol.* 429, 3363–3375. doi: 10.1016/j.jmb.2017.08.008

Duda, D. M., Olszewski, J. L., Schuermann, J. P., Kurinov, I., Miller, D. J., Nourse, A., et al. (2013). Structure of HHARI, a RING-IBR-RING ubiquitin ligase: autoinhibition of an ariadne-family E3 and insights into ligation mechanism. *Structure* 21, 1030–1041. doi: 10.1016/j.str.2013.04.019

Eddins, M. J., Carlile, C. M., Gomez, K. M., Pickart, C. M., and Wolberger, C. (2006). Mms2-Ubc13 covalently bound to ubiquitin reveals the structural basis

of linkage-specific polyubiquitin chain formation. *Nat. Struct. Mol. Biol.* 13, 915–920. doi: 10.1038/nsmb1148

Edwards, D. J., Streich, F. C., Ronchi, V. P., Todaro, D. R., and Haas, A. L. (2014). Convergent evolution in the assembly of polyubiquitin degradation signals by the *Shigella* flexneri IpaH9.8 ligase. *J. Biol. Chem.* 289, 34114–34128. doi: 10.1074/jbc.M114.609164

Eletr, Z. M., Huang, D. T., Duda, D. M., Schulman, B. A., and Kuhlman, B. (2005). E2 conjugating enzymes must disengage from their E1 enzymes before E3-dependent ubiquitin and ubiquitin-like transfer. *Nat. Struct. Mol. Biol.* 12, 933–934. doi: 10.1038/nsmb984

Fajner, V., Maspero, E., and Polo, S. (2017). Targeting HECT-type E3 ligases – insights from catalysis, regulation and inhibitors. *FEBS Lett.* 591, 2636–2647. doi: 10.1002/1873-3468.12775

Fang, G., Hongtao, Y., and Kirschner, M. W. (1998). Direct binding of CDC20 protein family members activates the anaphase-promoting complex in mitosis and G1. *Mol. Cell* 2, 163–171. doi: 10.1016/s1097-2765(00)80126-4

Fang, S., Ferrone, M., Yang, C., Jensen, J. P., Tiwari, S., and Weissman, A. M. (2001). The tumor autocrine motility factor receptor, gp78, is a ubiquitin protein ligase implicated in degradation from the endoplasmic reticulum. *Proc. Natl. Acad. Sci. U.S.A.* 98, 14422–14427. doi: 10.1073/pnas.251401598

Feldman, R. M. R., Correll, C. C., Kaplan, K. B., and Deshaies, R. J. (1997). A complex of Cdc4p, Skp1p, and Cdc53p/cullin catalyzes ubiquitination of the phosphorylated CDK inhibitor Sic1p. *Cell* 91, 221–230. doi: 10.1016/s0092-8674(00)80404-3

Finley, D. (2009). Recognition and processing of ubiquitin-protein conjugates by the proteasome. *Annu. Rev. Biochem.* 78, 477–513. doi: 10.1146/annurev.biochem.78.081507.101607

Fischer, E. S., Scrima, A., Böhm, K., Matsumoto, S., Lingaraju, G. M., Faty, M., et al. (2011). The molecular basis of CRL4 DDB2/CSA ubiquitin ligase architecture, targeting, and activation. *Cell* 147, 1024–1039. doi: 10.1016/j.cell.2011.10.035

French, M. E., Klosowiak, J. L., Aslanian, A., Reed, S. I., Yates, J. R., and Hunter, T. (2017). Mechanism of ubiquitin chain synthesis employed by a HECT domain ubiquitin ligase. *J. Biol. Chem.* 292, 10398–10413. doi: 10.1074/jbc.M117.789479

Garnett, M. J., Mansfeld, J., Godwin, C., Matsusaka, T., Wu, J., Russell, P., et al. (2009). UBE2S elongates ubiquitin chains on APC/C substrates to promote mitotic exit. *Nat. Cell Biol.* 11, 1363–1369. doi: 10.1038/ncb1983

Gazdoiu, S., Yamoah, K., Wu, K., and Pan, Z.-Q. (2007). Human Cdc34 employs distinct sites to coordinate attachment of ubiquitin to a substrate and assembly of polyubiquitin chains. *Mol. Cell. Biol.* 27, 7041–7052. doi: 10.1128/mcb.00812-07

Grice, G. L., Lobb, I. T., Weekes, M. P., Gygi, S. P., Antrobus, R., and Nathan, J. A. (2015). The proteasome distinguishes between heterotypic and homotypic lysine-11-Linked polyubiquitin chains. *Cell Rep.* 12, 545–553. doi: 10.1016/j.celrep.2015.06.061

Haahr, P., Borgermann, N., Guo, X., Typas, D., Achuthankutty, D., Hoffmann, S., et al. (2018). ZUFSP deubiquitylates K63-linked polyubiquitin chains to promote genome stability. *Mol. Cell* 70, 165–174. doi: 10.1016/j.molcel.2018.02.024

Haldeman, M. T., Xia, G., Kasperek, E. M., and Pickart, C. M. (1997). Structure and function of ubiquitin conjugating enzyme E2-25K: The tail is a core-dependent activity element. *Biochemistry* 36, 10526–10537. doi: 10.1021/bi970750u

Hermanns, T., Pichlo, C., Woiwode, I., Klopffleisch, K., Witting, K. F., Ovaa, H., et al. (2018). A family of unconventional deubiquitinases with modular chain specificity determinants. *Nat. Commun.* 9:799. doi: 10.1038/s41467-018-03148-5

Hershko, A., and Ciechanover, A. (1998). The ubiquitin system. *Annu. Rev. Biochem.* 67, 425–479.

Hewings, D. S., Heideker, J., Ma, T. P., AhYoung, A. P., El Oualid, F., Amore, A., et al. (2018). Reactive-site-centric chemoproteomics identifies a distinct class of deubiquitinase enzymes. *Nat. Commun.* 9:1162. doi: 10.1038/s41467-018-03511-6

Hibbert, R. G., Huang, A., Boelens, R., and Sixma, T. K. (2011). E3 ligase Rad18 promotes monoubiquitination rather than ubiquitin chain formation by E2 enzyme Rad6. *Proc. Natl. Acad. Sci. U.S.A.* 108, 5590–5595. doi: 10.1073/pnas.1017516108

Hill, S., Harrison, J. S., Lewis, S. M., Kuhlman, B., and Kleiger, G. (2016). Mechanism of lysine 48 selectivity during polyubiquitin chain formation by the Ube2R1/2 ubiquitin-conjugating enzyme. *Mol. Cell. Biol.* 36, 1720–1732. doi: 10.1128/MCB.00097-16

Hiller, M. M., Finger, A., Schweiger, M., and Wolf, D. H. (1996). ER degradation of a misfolded luminal protein by the cytosolic ubiquitin-proteasome pathway. *Science* 273, 1725–1728. doi: 10.1126/science.273.5282.1725

Hochstrasser, M. (2006). Lingering mysteries of ubiquitin-chain assembly. *Cell* 124, 27–34. doi: 10.1016/j.cell.2005.12.025

Hoege, C., Pfander, B., Moldovan, G. L., Pyrowolakis, G., and Jentsch, S. (2002). RAD6-dependent DNA repair is linked to modification of PCNA by ubiquitin and SUMO. *Nature* 419, 135–141. doi: 10.1038/nature00991

Huang, D. T., Paydar, A., Zhuang, M., Waddell, M. B., Holton, J. M., and Schulman, B. A. (2005). Structural basis for recruitment of Ubc12 by an E2 binding domain in NEDD8's E1. *Mol. Cell* 17, 341–350. doi: 10.1016/j.molcel.2004.12.020

Huang, L., Kinnucan, E., Wang, G., Beaudenon, S., Howley, P. M., Huibregtse, J. M., et al. (1999). Structure of an E6AP-UbcH7 complex: insights into ubiquitination by the E2-E3 enzyme cascade. *Science* 286, 1321–1326. doi: 10.1126/science.286.5443.1321

Huang, X., and Dixit, V. M. (2016). Drugging the undruggables: exploring the ubiquitin system for drug development. *Cell Res.* 26, 484–498. doi: 10.1038/cr.2016.31

Huibregtse, J. M., Scheffner, M., Beaudenon, S., and Howley, P. M. (1995). A family of proteins structurally and functionally related to the E6-AP ubiquitin-protein ligase. *Proc. Natl. Acad. Sci. U.S.A.* 92, 2563–2567. doi: 10.1073/pnas.92.7.2563

Husnjak, K., and Dikic, I. (2012). Ubiquitin-binding proteins: decoders of ubiquitin-mediated cellular functions. *Annu. Rev. Biochem.* 81, 291–322. doi: 10.1146/annurev-biochem-051810-094654

Ikeda, F., Deribe, Y. L., Skånland, S. S., Stieglitz, B., Grabbe, C., Franz-Wachtel, M., et al. (2011). SHARPIN forms a linear ubiquitin ligase complex regulating NF-κB activity and apoptosis. *Nature* 471, 637–641. doi: 10.1038/nature09814

Inoue, S., Hao, Z., Elia, A. J., Cescon, D., Zhou, L., Silvester, J., et al. (2013). Mule/Huwe1/Arf-BP1 suppresses Ras-driven tumorigenesis by preventing c-Myc/Miz1-mediated down-regulation of p21 and p15. *Genes Dev.* 27, 1101–1114. doi: 10.1101/gad.214577.113

Jencks, W. P. (1981). On the attribution and additivity of binding energies. *Proc. Natl. Acad. Sci. U.S.A.* 78, 4046–4050. doi: 10.1073/pnas.78.7.4046

Jin, J., Li, X., Gygi, S. P., and Harper, J. W. (2007). Dual E1 activation systems for ubiquitin differentially regulate E2 enzyme charging. *Nature* 447, 1135–1138. doi: 10.1038/nature05902

Jin, L., Williamson, A., Banerjee, S., Philipp, I., and Rape, M. (2008). Mechanism of ubiquitin-chain formation by the human anaphase-promoting complex. *Cell* 133, 653–665. doi: 10.1016/j.cell.2008.04.012

Kamadurai, H. B., Qiu, Y., Deng, A., Harrison, J. S., MacDonald, C., Actis, M., et al. (2013). Mechanism of ubiquitin ligation and lysine prioritization by a HECT E3. *eLife* 2:e00828. doi: 10.7554/eLife.00828

Kamadurai, H. B., Souphron, J., Scott, D. C., Duda, D. M., Miller, D. J., Stringer, D., et al. (2009). Insights into ubiquitin transfer cascades from a structure of a UbcH5B∼ ubiquitin-HECTNEDD4L complex. *Mol. Cell* 36, 1095–1102. doi: 10.1016/j.molcel.2009.11.010

Kelly, A., Wickliffe, K. E., Song, L., Fedrigo, I., and Rape, M. (2014). Ubiquitin chain elongation requires E3-dependent tracking of the emerging conjugate. *Mol. Cell.* 56, 232–245. doi: 10.1016/j.molcel.2014.09.010

Keusekotten, K., Elliott, P. R., Glockner, L., Fiil, B. K., Damgaard, R. B., Kulathu, Y., et al. (2013). OTULIN antagonizes LUBAC signaling by specifically hydrolyzing Met1-linked polyubiquitin. *Cell* 153, 1312–1326. doi: 10.1016/j.cell.2013.05.014

Kim, H. C., Steffen, A. M., Oldham, M. L., Chen, J., and Huibregtse, J. M. (2011). Structure and function of a HECT domain ubiquitin-binding site. *EMBO Rep.* 12, 334–341. doi: 10.1038/embor.2011.23

King, B., Boccalatte, F., Moran-Crusio, K., Wolf, E., Wang, J., Kayembe, C., et al. (2016). The ubiquitin ligase Huwe1 regulates the maintenance and lymphoid commitment of hematopoietic stem cells. *Nat. Immunol.* 17, 1312–1321. doi: 10.1038/ni.3559

Kirisako, T., Kamei, K., Murata, S., Kato, M., Fukumoto, H., Kanie, M., et al. (2006). A ubiquitin ligase complex assembles linear polyubiquitin chains. *EMBO J.* 25, 4877–4887. doi: 10.1038/sj.emboj.7601360

Kirkpatrick, D. S., Hathaway, N. A., Hanna, J., Elsasser, S., Rush, J., Finley, D., et al. (2006). Quantitative analysis of in vitro ubiquitinated cyclin B1 reveals complex chain topology. *Nat. Cell Biol.* 8, 700–710. doi: 10.1038/ncb1436

Kleiger, G., Hao, B., Mohl, D. A., and Deshales, R. J. (2009a). The acidic tail of the Cdc34 ubiquitin-conjugating enzyme functions in both binding to and catalysis with ubiquitin ligase SCFCdc4. *J. Biol. Chem.* 284, 36012–36023. doi: 10.1074/jbc.M109.058529

Kleiger, G., Saha, A., Lewis, S., Kuhlman, B., and Deshaies, R. J. (2009b). Rapid E2-E3 assembly and disassembly enable processive ubiquitylation of cullin-RING ubiquitin ligase substrates. *Cell* 139, 957–968. doi: 10.1016/j.cell.2009.10.030

Koegl, M., Hoppe, T., Schlenker, S., Ulrich, H. D., Mayer, T. U., and Jentsch, S. (1999). A novel ubiquitination factor, E4, is involved in multiubiquitin chain assembly. *Cell* 96, 635–644. doi: 10.1016/s0092-8674(00)80574-7

Komander, D., and Rape, M. (2012). The ubiquitin code. *Annu. Rev. Biochem.* 81, 203–229. doi: 10.1146/annurev-biochem-060310-170328

Kostova, Z., Mariano, J., Scholz, S., Koenig, C., and Weissman, A. M. (2009). A Ubc7p-binding domain in Cue1p activates ER-associated protein degradation. *J. Cell Sci.* 122, 1374–1381. doi: 10.1242/jcs.044255

Kühnle, S., Kogel, U., Glockzin, S., Marquardt, A., Ciechanover, A., Matentzoglu, K., et al. (2011). Physical and functional interaction of the HECT ubiquitin-protein ligases E6AP and HERC2. *J. Biol. Chem.* 286, 19410–19416. doi: 10.1074/jbc.M110.205211

Kulak, N. A., Pichler, G., Paron, I., Nagaraj, N., and Mann, M. (2014). Minimal, encapsulated proteomic-sample processing applied to copy-number estimation in eukaryotic cells. *Nat. Methods* 11, 319–324. doi: 10.1038/nmeth.2834

Kwasna, D., Rehman, S. A. A., Natarajan, J., Matthews, S., Madden, R., De Cesare, V., et al. (2018). Discovery and characterization of ZUFSP, a novel DUB class important for genome stability. *Mol. Cell* 70, 150–164. doi: 10.1016/j.molcel.2018.02.023

Lechtenberg, B. C., Rajput, A., Sanishvili, R., Dobaczewska, M. K., Ware, C. F., Mace, P. D., et al. (2016). Structure of a HOIP/E2∼ ubiquitin complex reveals RBR E3 ligase mechanism and regulation. *Nature* 529, 546–550. doi: 10.1038/nature16511

Li, W., Bengtson, M. H., Ulbrich, A., Matsuda, A., Reddy, V. A., Orth, A., et al. (2008). Genome-wide and functional annotation of human E3 ubiquitin ligases identifies MULAN, a mitochondrial E3 that regulates the organelle's dynamics and signaling. *PLoS One* 3:e1487. doi: 10.1371/journal.pone.0001487

Li, W., Tu, D., Brunger, A. T., and Ye, Y. (2007). A ubiquitin ligase transfers preformed polyubiquitin chains from a conjugating enzyme to a substrate. *Nature* 446, 333–337. doi: 10.1038/nature05542

Li, W., Tu, D., Li, L., Wollert, T., Ghirlando, R., Brunger, A. T., et al. (2009). Mechanistic insights into active site-associated polyubiquitination by the ubiquitin-conjugating enzyme Ube2g2. *Proc. Natl. Acad. Sci. U.S.A.* 106, 3722–3727. doi: 10.1073/pnas.0808564106

Lindner, S., and Krönke, J. (2016). The molecular mechanism of thalidomide analogs in hematologic malignancies. *J. Mol. Med.* 94, 1327–1334. doi: 10.1007/s00109-016-1450-z

Liu, C., Liu, W., Ye, Y., and Li, W. (2017). Ufd2p synthesizes branched ubiquitin chains to promote the degradation of substrates modified with atypical chains. *Nat. Commun.* 8, 1–15. doi: 10.1038/ncomms14274

Liu, W., Shang, Y., Zeng, Y., Liu, C., Li, Y., Zhai, L., et al. (2014). Dimeric Ube2g2 simultaneously engages donor and acceptor ubiquitins to form Lys48-linked ubiquitin chains. *EMBO J.* 33, 46–61. doi: 10.1002/embj.201385315

Lorenz, S. (2018). Structural mechanisms of HECT-type ubiquitin ligases. *Biol. Chem.* 399, 127–145. doi: 10.1515/hsz-2017-0184

Lorenz, S., Bhattacharyya, M., Feiler, C., Rape, M., and Kuriyan, J. (2016). Crystal structure of a Ube2S-Ubiquitin conjugate. *PLoS One* 11:e0147550. doi: 10.1371/journal.pone.0147550

Lorenz, S., Cantor, A. J., Rape, M., and Kuriyan, J. (2013). Macromolecular juggling by ubiquitylation enzymes. *BMC Biol.* 11:65. doi: 10.1186/1741-7007-11-65

Lu, Y., Lee, B. H., King, R. W., Finley, D., and Kirschner, M. W. (2015a). Substrate degradation by the proteasome: a single-molecule kinetic analysis. *Science* 348, 183–184. doi: 10.1126/science.1250834

Lu, Y., Wang, W., and Kirschner, M. W. (2015b). Specificity of the anaphase-promoting complex: a single-molecule study. *Science* 348:1248737. doi: 10.1126/science.1248737

Marín, I., Lucas, J. I., Gradilla, A.-C., and Ferrús, A. (2004). Parkin and relatives: the RBR family of ubiquitin ligases. *Physiol. Genomics* 17, 253–263. doi: 10.1152/physiolgenomics.00226.2003

Maspero, E., Mari, S., Valentini, E., Musacchio, A., Fish, A., Pasqualato, S., et al. (2011). Structure of the HECT:ubiquitin complex and its role in ubiquitin chain elongation. *EMBO Rep.* 12, 342–349. doi: 10.1038/embor.2011.21

Maspero, E., Valentini, E., Mari, S., Cecatiello, V., Soffientini, P., Pasqualato, S., et al. (2013). Structure of a ubiquitin-loaded HECT ligase reveals the molecular basis for catalytic priming. *Nat. Struct. Mol. Biol.* 20, 696–701. doi: 10.1038/nsmb.2566

Masuda, Y., Suzuki, M., Kawai, H., Hishiki, A., Hashimoto, H., Masutani, C., et al. (2012). En bloc transfer of polyubiquitin chains to PCNA in vitro is mediated by two different human E2-E3 pairs. *Nucleic Acids Res.* 40, 10394–10407. doi: 10.1093/nar/gks763

Matsumoto, M. L., Wickliffe, K. E., Dong, K. C., Yu, C., Bosanac, I., Bustos, D., et al. (2010). K11-linked polyubiquitination in cell cycle control revealed by a K11 linkage-specific antibody. *Mol. Cell* 39, 477–484. doi: 10.1016/j.molcel.2010.07.001

Mattiroli, F., Uckelmann, M., Sahtoe, D. D., van Dijk, W. J., and Sixma, T. K. (2014). The nucleosome acidic patch plays a critical role in RNF168-dependent ubiquitination of histone H2A. *Nat. Commun.* 5:3291. doi: 10.1038/ncomms4291

Mattiroli, F., Vissers, J. H. A., Van Dijk, W. J., Ikpa, P., Citterio, E., Vermeulen, W., et al. (2012). RNF168 ubiquitinates K13-15 on H2A/H2AX to drive DNA damage signaling. *Cell* 150, 1182–1195. doi: 10.1016/j.cell.2012.08.005

Metzger, M. B., Liang, Y. H., Das, R., Mariano, J., Li, S., Li, J., et al. (2013). A structurally unique E2-binding domain activates ubiquitination by the ERAD E2, Ubc7p, through multiple mechanisms. *Mol. Cell* 50, 516–527. doi: 10.1016/j.molcel.2013.04.004

Metzger, M. B., Pruneda, J. N., Klevit, R. E., and Weissman, A. M. (2014). RING-type E3 ligases: Master manipulators of E2 ubiquitin-conjugating enzymes and ubiquitination. *Biochim. Biophys. Acta-Mol. Cell Res.* 1843, 47–60. doi: 10.1016/j.bbamcr.2013.05.026

Metzger, M. B., and Weissman, A. M. (2010). Working on a chain: E3s ganging up for ubiquitylation. *Nat. Cell Biol.* 12, 1124–1126. doi: 10.1038/ncb1210-1124

Mevissen, T. E. T., and Komander, D. (2017). Mechanisms of deubiquitinase specificity and regulation. *Annu. Rev. Biochem.* 86, 159–192. doi: 10.1146/annurev-biochem-061516-044916

Mevissen, T. E. T., Kulathu, Y., Mulder, M. P. C., Geurink, P. P., Maslen, S. L., Gersch, M., et al. (2016). Molecular basis of Lys11-polyubiquitin specificity in the deubiquitinase Cezanne. *Nature* 538, 402–405. doi: 10.1038/nature19836

Meyer, H. J., and Rape, M. (2014). Enhanced protein degradation by branched ubiquitin chains. *Cell* 157, 910–921. doi: 10.1016/j.cell.2014.03.037

Michelle, C., Vourc'H, P., Mignon, L., and Andres, C. R. (2009). What was the set of ubiquitin and ubiquitin-like conjugating enzymes in the eukaryote common ancestor? *J. Mol. Evol.* 68, 616–628. doi: 10.1007/s00239-009-9225-6

Miura, T., Klaus, W., Gsell, B., Miyamoto, C., and Senn, H. (2002). Characterization of the binding interface between ubiquitin and class I human ubiquitin-conjugating enzyme 2b by multidimensional heteronuclear NMR spectroscopy in solution. *J. Mol. Biol.* 290, 213–228. doi: 10.1006/jmbi.1999.2859

Mullard, A. (2019). First targeted protein degrader hits the clinic. *Nat. Rev. Drug Discov.* doi: 10.1038/d41573-019-00043-6 [Epub ahead of print].

Myant, K. B., Cammareri, P., Hodder, M. C., Wills, J., Von Kriegsheim, A., Györffy, B., et al. (2017). HUWE1 is a critical colonic tumour suppressor gene that prevents MYC signalling, DNA damage accumulation and tumour initiation. *EMBO Mol. Med.* 9, 181–197. doi: 10.15252/emmm.201606684

Ogunjimi, A. A., Wiesner, S., Briant, D. J., Varelas, X., Sicheri, F., Forman-Kay, J., et al. (2010). The ubiquitin binding region of the smurf HECT domain facilitates polyubiquitylation and binding of ubiquitylated substrates. *J. Biol. Chem.* 285, 6308–6315. doi: 10.1074/jbc.M109.044537

Oh, E., Akopian, D., and Rape, M. (2018). Principles of ubiquitin-dependent signaling. *Annu. Rev. Cell Dev. Biol.* 34, 18–19.

Ohtake, F., Saeki, Y., Ishido, S., Kanno, J., and Tanaka, K. (2016). The K48-K63 branched ubiquitin chain regulates NF-κB signaling. *Mol. Cell* 64, 251–266. doi: 10.1016/j.molcel.2016.09.014

Ohtake, F., Tsuchiya, H., Saeki, Y., and Tanaka, K. (2018). K63 ubiquitylation triggers proteasomal degradation by seeding branched ubiquitin chains. *Proc. Natl. Acad. Sci. U.S.A.* 115, E1401–E1408. doi: 10.1073/pnas.1716673115

Page, R. C., Pruneda, J. N., Amick, J., Klevit, R. E., and Misra, S. (2012). Structural insights into the conformation and oligomerization of E2∼ Ubiquitin conjugates. *Biochemistry* 51, 4175–4187. doi: 10.1021/bi300058m

Parker, J. L., and Ulrich, H. D. (2009). Mechanistic analysis of PCNA poly-ubiquitylation by the ubiquitin protein ligases Rad18 and Rad5. *EMBO J.* 28, 3657–3666. doi: 10.1038/emboj.2009.303

Pelzer, C., Kassner, I., Matentzoglu, K., Singh, R. K., Wollscheid, H. P., Scheffner, M., et al. (2007). UBE1L2, a novel E1 enzyme specific for ubiquitin. *J. Biol. Chem.* 282, 23010–23014. doi: 10.1074/jbc.c700111200

Peter, S., Bultinck, J., Myant, K., Jaenicke, L. A., Walz, S., Müller, J., et al. (2014). Tumor cell-specific inhibition of MYC function using small molecule inhibitors of the HUWE1 ubiquitin ligase. *EMBO Mol. Med.* 6, 1525–1541. doi: 10.15252/emmm.201403927

Petroski, M. D., and Deshaies, R. J. (2003). Context of multiubiquitin chain attachment influences the rate of sic1 degradation. *Mol. Cell* 11, 1435–1444. doi: 10.1016/s1097-2765(03)00221-1

Petroski, M. D., and Deshaies, R. J. (2005a). Function and regulation of cullin-RING ubiquitin ligases. *Nat. Rev. Mol. Cell Biol.* 6, 9–20. doi: 10.1038/nrm1547

Petroski, M. D., and Deshaies, R. J. (2005b). Mechanism of lysine 48-linked ubiquitin-chain synthesis by the cullin-RING ubiquitin-ligase complex SCF-Cdc34. *Cell* 123, 1107–1120. doi: 10.1016/j.cell.2005.09.033

Pfleger, C. M., and Kirschner, M. W. (2000). The KEN box: an APC recognition signal distinct from the D box targeted by Cdh1. *Genes Dev.* 14, 655–665.

Pierce, N. W., Kleiger, G., Shan, S. O., and Deshaies, R. J. (2009). Detection of sequential polyubiquitylation on a millisecond timescale. *Nature* 462, 615–619. doi: 10.1038/nature08595

Plechanovová, A., Jaffray, E. G., Tatham, M. H., Naismith, J. H., and Hay, R. T. (2012). Structure of a RING E3 ligase and ubiquitin-loaded E2 primed for catalysis. *Nature* 489, 115–120. doi: 10.1038/nature11376

Pruneda, J. N., Littlefield, P. J., Soss, S. E., Nordquist, K. A., Chazin, W. J., Brzovic, P. S., et al. (2012). Structure of an E3:E2∼ Ub complex reveals an allosteric mechanism shared among RING/U-box ligases. *Mol. Cell* 47, 933–942. doi: 10.1016/j.molcel.2012.07.001

Qiao, R., Weissmann, F., Yamaguchi, M., Brown, N. G., VanderLinden, R., Imre, R., et al. (2016). Mechanism of APC/C CDC20 Activation by Mitotic Phosphorylation. *Proc. Natl. Acad. Sci. U.S.A.* 113, E2570–E2578. doi: 10.1073/pnas.1604929113

Ranaweera, R. S., and Yang, X. (2013). Auto-ubiquitination of Mdm2 enhances its substrate ubiquitin ligase activity. *J. Biol. Chem.* 288, 18939–18946. doi: 10.1074/jbc.M113.454470

Rape, M., Reddy, S. K., and Kirschner, M. W. (2006). The processivity of multiubiquitination by the APC determines the order of substrate degradation. *Cell* 124, 89–103. doi: 10.1016/j.cell.2005.10.032

Ravid, T., and Hochstrasser, M. (2007). Autoregulation of an E2 enzyme by ubiquitin-chain assembly on its catalytic residue. *Nat. Cell Biol.* 9, 422–427. doi: 10.1038/ncb1558

Reimann, J. D. R., Freed, E., Hsu, J. Y., Kramer, E. R., Peters, J. M., and Jackson, P. K. (2001). Emi1 is a mitotic regulator that interacts with Cdc20 and inhibits the anaphase promoting complex. *Cell* 105, 645–655. doi: 10.1016/s0092-8674(01)00361-0

Ries, L. K., Sander, B., Deol, K. K., Letzelter, M.-A., Strieter, E. R., and Lorenz, S. (2019). Analysis of ubiquitin recognition by the HECT ligase E6AP provides insight into its linkage specificity. *J. Biol. Chem.* 294, 6113–6129. doi: 10.1074/jbc.RA118.007014

Rodrigo-Brenni, M. C., and Morgan, D. O. (2007). Sequential E2s drive polyubiquitin chain assembly on APC targets. *Cell* 130, 127–139. doi: 10.1016/j.cell.2007.05.027

Ronchi, V. P., Kim, E. D., Summa, C. M., Klein, J. M., and Haas, A. L. (2017). In silico modeling of the cryptic E2∼ubiquitin-binding site of E6-associated protein (E6AP)/UBE3A reveals the mechanism of polyubiquitin chain assembly. *J. Biol. Chem.* 292, 18006–18023. doi: 10.1074/jbc.M117.813477

Ronchi, V. P., Klein, J. M., Edwards, D. J., and Haas, A. L. (2014). The active form of E6-associated protein (E6AP)/UBE3A ubiquitin ligase is an oligomer. *J. Biol. Chem.* 289, 1033–1048. doi: 10.1074/jbc.M113.517805

Ronchi, V. P., Klein, J. M., and Haas, A. L. (2013). E6AP/UBE3A ubiquitin ligase harbors two E2∼ ubiquitin binding sites. *J. Biol. Chem.* 288, 10349–10360. doi: 10.1074/jbc.m113.458059

Saha, A., and Deshaies, R. J. (2008). Multimodal activation of the ubiquitin ligase SCF by Nedd8 conjugation. *Mol. Cell* 32, 21–31. doi: 10.1016/j.molcel.2008.08.021

Saha, A., Lewis, S., Kleiger, G., Kuhlman, B., and Deshaies, R. J. (2011). Essential role for ubiquitin-ubiquitin-conjugating enzyme interaction in ubiquitin discharge from Cdc34 to substrate. *Mol. Cell* 42, 75–83. doi: 10.1016/j.molcel.2011.03.016

Sakamoto, K. M., Kim, K. B., Kumagai, A., Mercurio, F., Crews, C. M., and Deshaies, R. J. (2002). Protacs: Chimeric molecules that target proteins to the Skp1-Cullin-F box complex for ubiquitination and degradation. *Proc. Natl. Acad. Sci. U.S.A.* 98, 8554–8559. doi: 10.1073/pnas.141230798

Sauvé, V., Sung, G., Soya, N., Kozlov, G., Blaimschein, N., Miotto, L. S., et al. (2018). Mechanism of parkin activation by phosphorylation. *Nat. Struct. Mol. Biol.* 25, 623–630. doi: 10.1038/s41594-018-0088-7

Schreiber, G., Haran, G., and Zhou, H.-X. (2009). Fundamental aspects of protein-protein association kinetics. *Chem. Rev.* 109, 839–860. doi: 10.1021/cr800373w

Schulman, B. A., and Wade Harper, J. (2009). Ubiquitin-like protein activation by E1 enzymes: The apex for downstream signalling pathways. *Nat. Rev. Mol. Cell Biol.* 10, 319–331. doi: 10.1038/nrm2673

Scott, D. C., Rhee, D. Y., Duda, D. M., Kelsall, I. R., Olszewski, J. L., Paulo, J. A., et al. (2016). Two distinct types of E3 ligases work in unison to regulate substrate ubiquitylation. *Cell* 166, 1198–1214. doi: 10.1016/j.cell.2016.07.027

Skowyra, D., Craig, K. L., Tyers, M., Elledge, S. J., and Harper, J. W. (1997). F-box proteins are receptors that recruit phosphorylated substrates to the SCF ubiquitin-ligase complex. *Cell* 91, 209–219. doi: 10.1016/s0092-8674(00)80403-1

Smit, J. J., Monteferrario, D., Noordermeer, S. M., Van Dijk, W. J., Van Der Reijden, B. A., and Sixma, T. K. (2012). The E3 ligase HOIP specifies linear ubiquitin chain assembly through its RING-IBR-RING domain and the unique LDD extension. *EMBO J.* 31, 3833–3844. doi: 10.1038/emboj.2012.217

Smit, J. J., and Sixma, T. K. (2014). RBR E3-ligases at work. *EMBO Rep.* 15, 142–154. doi: 10.1002/embr.201338166

Soss, S. E., Klevit, R. E., and Chazin, W. J. (2013). Activation of UbcH5c∼ Ub is the result of a shift in interdomain motions of the conjugate bound to U-box E3 ligase E4B. *Biochemistry* 52, 2991–2999. doi: 10.1021/bi3015949

Soucy, T. A., Smith, P. G., Milhollen, M. A., Berger, A. J., Gavin, J. M., Adhikari, S., et al. (2009). An inhibitor of NEDD8-activating enzyme as a new approach to treat cancer. *Nature* 458, 732–736. doi: 10.1038/nature07884

Stelter, P., and Ulrich, H. D. (2003). Control of spontaneous and damage-induced mutagenesis by SUMO and ubiquitin conjugation. *Nature* 425, 188–191. doi: 10.1038/nature01965

Stewart, M. D., Ritterhoff, T., Klevit, R. E., and Brzovic, P. S. (2016). E2 enzymes: more than just middle men. *Cell Res.* 26, 423–440. doi: 10.1038/cr.2016.35

Stieglitz, B., Rana, R. R., Koliopoulos, M. G., Morris-Davies, A. C., Schaeffer, V., Christodoulou, E., et al. (2013). Structural basis for ligase-specific conjugation of linear ubiquitin chains by HOIP. *Nature* 503, 422–426. doi: 10.1038/nature12638

Streich, F. C., Ronchi, V. P., Connick, J. P., and Haas, A. L. (2013). Tripartite motif ligases catalyze polyubiquitin chain formation through a cooperative allosteric mechanism. *J. Biol. Chem.* 288, 8209–8221. doi: 10.1074/jbc.M113.451567

Swatek, K. N., and Komander, D. (2016). Ubiquitin modifications. *Cell Res.* 26, 399–422. doi: 10.1038/cr.2016.39

Tang, X., Orlicky, S., Lin, Z., Willems, A., Neculai, D., Ceccarelli, D., et al. (2007). Suprafacial orientation of the SCFCdc4 dimer accommodates multiple geometries for substrate ubiquitination. *Cell* 129, 1165–1176. doi: 10.1016/j.cell.2007.04.042

Todaro, D. R., Augustus-Wallace, A. C., Klein, J. M., and Haas, A. L. (2017). The mechanism of neural precursor cell expressed developmentally down-regulated 4-2 (Nedd4-2)/NEDD4L-catalyzed polyubiquitin chain assembly. *J. Biol. Chem.* 292, 19521–19536. doi: 10.1074/jbc.M117.817882

Todaro, D. R., Augustus-Wallace, A. C., Klein, J. M., and Haas, A. L. (2018). Oligomerization of the hect ubiquitin ligase Nedd4-2/NEDD4L is essential for polyubiquitin chain assembly. *J. Biol. Chem.* 293, 18192–18206. doi: 10.1074/jbc.RA118.003716

Tokunaga, F., Nakagawa, T., Nakahara, M., Saeki, Y., Taniguchi, M., Sakata, S., et al. (2011). SHARPIN is a component of the NF-κB-activating linear ubiquitin chain assembly complex. *Nature* 471, 633–636. doi: 10.1038/nature09815

von Delbrück, M., Kniss, A., Rogov, V. V., Pluska, L., Bagola, K., Löhr, F., et al. (2016). The CUE domain of Cue1 aligns growing ubiquitin chains with Ubc7 for rapid elongation. *Mol. Cell* 62, 918–928. doi: 10.1016/j.molcel.2016.04.031

Walden, H., and Rittinger, K. (2018). RBR ligase-mediated ubiquitin transfer: a tale with many twists and turns. *Nat. Struct. Mol. Biol.* 25, 440–445. doi: 10.1038/s41594-018-0063-3

Wang, M., Cheng, D., Peng, J., and Pickart, C. M. (2006). Molecular determinants of polyubiquitin linkage selection by an HECT ubiquitin ligase. *EMBO J.* 25, 1710–1719. doi: 10.1038/sj.emboj.7601061

Wang, M., and Pickart, C. M. (2005). Different HECT domain ubiquitin ligases employ distinct mechanisms of polyubiquitin chain synthesis. *EMBO J.* 24, 4324–4333. doi: 10.1038/sj.emboj.7600895

Watson, E. R., Brown, N. G., Peters, J. M., Stark, H., and Schulman, B. A. (2019). Posing the APC/C E3 ubiquitin ligase to orchestrate cell division. *Trends Cell Biol.* 29, 117–134. doi: 10.1016/j.tcb.2018.09.007

Weber, J., Polo, S., and Maspero, E. (2019). HECT E3 ligases: a tale with multiple facets. *Front. Physiol.* 10:370. doi: 10.3389/fphys.2019.00370

Wenzel, D. M., and Klevit, R. E. (2012). Following ariadne's thread: a new perspective on RBR ubiquitin ligases. *BMC Biol.* 10:24. doi: 10.1186/1741-7007-10-24

Wenzel, D. M., Lissounov, A., Brzovic, P. S., and Klevit, R. E. (2011). UBCH7 reactivity profile reveals parkin and HHARI to be RING/HECT hybrids. *Nature* 474, 105–108. doi: 10.1038/nature09966

Wenzel, D. M., Stoll, K. E., and Klevit, R. E. (2015). E2s: structurally economical and functionally replete. *Biochem. J.* 433, 31–42. doi: 10.1042/BJ20100985

Wickliffe, K. E., Lorenz, S., Wemmer, D. E., Kuriyan, J., and Rape, M. (2011). The mechanism of linkage-specific ubiquitin chain elongation by a single-subunit E2. *Cell* 144, 769–781. doi: 10.1016/j.cell.2011.01.035

Williamson, A., Banerjee, S., Zhu, X., Philipp, I., Iavarone, A. T., and Rape, M. (2011). Regulation of ubiquitin chain initiation to control the timing of substrate degradation. *Mol. Cell* 42, 744–757. doi: 10.1016/j.molcel.2011.04.022

Williamson, A., Wickliffe, K. E., Mellone, B. G., Song, L., Karpen, G. H., and Rape, M. (2009). Identification of a physiological E2 module for the human anaphase-promoting complex. *Proc. Natl. Acad. Sci. U.S.A.* 106, 18213–18218. doi: 10.1073/pnas.0907887106

Witting, K. F., Mulder, M. P. C., and Ovaa, H. (2017). Advancing our understanding of ubiquitination using the Ub-toolkit. *J. Mol. Biol.* 429, 3388–3394. doi: 10.1016/j.jmb.2017.04.002

Wright, J. D., Mace, P. D., and Day, C. L. (2016). Noncovalent ubiquitin interactions regulate the catalytic activity of ubiquitin writers. *Trends Biochem. Sci.* 41, 924–937. doi: 10.1016/j.tibs.2016.08.003

Wu, K., Kovacev, J., and Pan, Z. Q. (2010). Priming and extending: a UbcH5/Cdc34 E2 handoff mechanism for polyubiquitination on a SCF substrate. *Mol. Cell* 37, 784–796. doi: 10.1016/j.molcel.2010.02.025

Wu, T., Merbl, Y., Huo, Y., Gallop, J. L., Tzur, A., and Kirschner, M. W. (2010). UBE2S drives elongation of K11-linked ubiquitin chains by the anaphase-promoting complex. *Proc. Natl. Acad. Sci. U.S.A.* 107, 1355–1360. doi: 10.1073/pnas.0912802107

Yates, B., Braschi, B., Gray, K. A., Seal, R. L., Tweedie, S., and Bruford, E. A. (2017). Genenames.org: the HGNC and VGNC resources in 2017. *Nucleic Acids Res.* 45, D619–D625. doi: 10.1093/nar/gkw1033

Yau, R., and Rape, M. (2016). The increasing complexity of the ubiquitin code. *Nat. Cell Biol.* 18, 579–586. doi: 10.1038/ncb3358

Yau, R. G., Doerner, K., Castellanos, E. R., Haakonsen, D. L., Werner, A., Wang, N., et al. (2017). Assembly and function of heterotypic ubiquitin chains in cell-cycle and protein quality control. *Cell* 171, 918.e–933.e. doi: 10.1016/j.cell.2017.09.040

Ye, Y., and Rape, M. (2009). Building ubiquitin chains: E2 enzymes at work. *Nat. Rev. Mol. Cell Biol.* 10, 755–764. doi: 10.1038/nrm2780

Yu, H., and Matouschek, A. (2017). Recognition of client proteins by the proteasome. *Annu. Rev. Biophys.* 46, 149–173. doi: 10.1146/annurev-biophys-070816-033719

Yuan, L., Lv, Z., Atkison, J. H., and Olsen, S. K. (2017). Structural insights into the mechanism and E2 specificity of the RBR E3 ubiquitin ligase HHARI. *Nat. Commun.* 8:211. doi: 10.1038/s41467-017-00272-6

Zhang, W., Wu, K. P., Sartori, M. A., Kamadurai, H. B., Ordureau, A., Jiang, C., et al. (2016). System-wide modulation of HECT E3 ligases with selective ubiquitin variant probes. *Mol. Cell* 62, 121–136. doi: 10.1016/j.molcel.2016.02.005

Zhang, Z. R., Bonifacino, J. S., and Hegde, R. S. (2013). Deubiquitinases sharpen substrate discrimination during membrane protein degradation from the ER. *Cell* 154, 609–622. doi: 10.1016/j.cell.2013.06.038

Zhao, X., Heng, J. I. T., Guardavaccaro, D., Jiang, R., Pagano, M., Guillemot, F., et al. (2008). The HECT-domain ubiquitin ligase Huwe1 controls neural differentiation and proliferation by destabilizing the N-Myc oncoprotein. *Nat. Cell Biol.* 10, 643–653. doi: 10.1038/ncb1727

Ziemba, A., Sandoval, D., Webb, K., Bennett, E. J., Hill, S., and Kleiger, G. (2013). Multimodal mechanism of action for the Cdc34 acidic loop. *J. Biol. Chem.* 288, 34882–34896. doi: 10.1074/jbc.M113.509190

**Conflict of Interest Statement:** The authors declare that the research was conducted in the absence of any commercial or financial relationships that could be construed as a potential conflict of interest.

frontiers in Physiology

MINI REVIEW
published: 07 August 2019
doi: 10.3389/fphys.2019.01014

# HERCing: Structural and Functional Relevance of the Large HERC Ubiquitin Ligases

*Jesús García-Cano, Arturo Martinez-Martinez, Joan Sala-Gaston, Leonardo Pedrazza and Jose Luis Rosa**

*Ubiquitylation and Cell Signalling Lab, IDIBELL, Departament de Ciències Fisiològiques, Universitat de Barcelona, Barcelona, Spain*

Homologous to the E6AP carboxyl terminus (HECT) and regulator of chromosome condensation 1 (RCC1)-like domain-containing proteins (HERCs) belong to the superfamily of ubiquitin ligases. HERC proteins are divided into two subfamilies, Large and Small HERCs. Despite their similarities in terms of both structure and domains, these subfamilies are evolutionarily very distant and result from a convergence phenomenon rather than from a common origin. Large HERC genes, *HERC1* and *HERC2*, are present in most metazoan taxa. They encode very large proteins (approximately 5,000 amino acid residues in a single polypeptide chain) that contain more than one RCC1-like domain as a structural characteristic. Accumulating evidences show that these unusually large proteins play key roles in a wide range of cellular functions which include neurodevelopment, DNA damage repair, and cell proliferation. To better understand the origin, evolution, and function of the Large HERC family, this minireview provides with an integrated overview of their structure and function and details their physiological implications. This study also highlights and discusses how dysregulation of these proteins is associated with severe human diseases such as neurological disorders and cancer.

**Keywords: ubiquitin, ligase, HERC, structure, function, cancer, neurobiology, evolution**

OPEN ACCESS

***Edited by:***
*Julien Licchesi,*
*University of Bath, United Kingdom*

***Reviewed by:***
*Michael B. Morris,*
*University of Sydney, Australia*
*Ignacio Marín,*
*Superior Council of Scientific Investigations (CSIC), Spain*

***Correspondence:**
*Jose Luis Rosa*
*joseluisrosa@ub.edu*

***Specialty section:***
*This article was submitted to Integrative Physiology, a section of the journal Frontiers in Physiology*

***Received:*** *26 November 2018*
***Accepted:*** *23 July 2019*
***Published:*** *07 August 2019*

***Citation:***
*García-Cano J, Martinez-Martinez A, Sala-Gaston J, Pedrazza L and Rosa JL (2019) HERCing: Structural and Functional Relevance of the Large HERC Ubiquitin Ligases. Front. Physiol. 10:1014. doi: 10.3389/fphys.2019.01014*

## INTRODUCTION

Proteins containing a HECT domain are ubiquitin ligases (E3). These enzymes participate in the ubiquitylation process accepting ubiquitin from a ubiquitin-conjugating enzymes (E2) and catalysing its transfer to the protein to be ubiquitylated (Buetow and Huang, 2016). In animals, HECT E3 ligases can be divided into 16 groups including the Large HERC family (Marín, 2010), which is the subject of the present minireview. This family is comprised by HERC1 and HERC2, two gigantic proteins of close to 5,000 amino acid residues in a single polypeptide chain. They are the largest HECT-containing proteins[1].

[1]https://www.uniprot.org/uniprot/?query=reviewed%3Ayes+AND+organism%3A%22Homo+sapiens+%28Human%29+%5B9606%5D%22&sort=mass; (Bateman et al., 2017).

## LARGE HERCs EVOLUTIONARY INSIGHTS

Although traditionally classified together with the Small HERC proteins, Large and Small HERCs form two distant protein families (Marín, 2010). Large HERCs contain more than one RCC1-like domains (RLDs), differing from Small HERCs, which carry only one. Structural differences were observed between the RLDs in Large and Small HERCs (Hadjebi et al., 2008). The explanation for the differences among these two protein groups is that they result from convergent evolution of ancestors belonging to distant families (Marín, 2010).

While HERC2 appears in some choanoflagellates such as *Monosiga brevicollis* and *Salpingoeca rosetta*, the emergence of HERC1 occurred in Metazoa. Both proteins are already present in the placozoan *Trichoplax adhaerens* and in most metazoan phyla, with the absence of HERC1 in certain insect clades (Marín, 2010). Phylogenetic analysis of Large HERCs amino acid sequences segregates them in two clusters: one for HERC1 and one for HERC2; displaying higher similarity between orthologues (**Figure 1**). The phylogenetic relationships of the sequences within each cluster correlate with those in the evolution of the species. It is noteworthy that HERC2 from *S. rosetta* presents a SPRY domain, which is characteristic of HERC1 (**Figure 2A**; Garcia-Gonzalo et al., 2005). However, it cannot be considered homologous to that of *T. adhaerens* HERC1 [19.6% identity, $e = 0.17$; as shown by BLAST-p comparison (Altschul et al., 1997, 2005)]. Thus, this presence is likely due to convergence, a relatively frequent event in HECT proteins along evolution (Marín, 2010).

## STRUCTURAL FEATURES OF LARGE HERCs

### The RCC1-Like Domains, Structure, and Function

The presence of RLDs is a structural feature of Large HERCs (**Figure 2A**). RCC1 is necessary for maintaining chromosomes decondensed during DNA replication. It is also a guanine exchange factor (GEF) for the GTPase Ran, a nuclear import protein (Nishimoto et al., 1978; Bischoff and Ponstingl, 1991). RCC1 tertiary structure is composed of seven $\beta$ blades resembling the shape of a propeller (**Figure 2B**; first panel). Structure prediction models have been used since three-dimensional structure determination of Large HERCs has not been possible to date (Waterhouse et al., 2018). Large HERC RLDs structure is very similar to that of RCC1 (**Figure 2B**; framed panels).

HERC1 is implicated in intracellular vesicle trafficking by interacting through its RLD2 with ARF1 and Clathrin (Rosa et al., 1996; Rosa and Barbacid, 1997). HERC1 RLD1 may also function as a GDP releasing factor (GRF) for ARF proteins in the presence of phosphatidylinositol-4,5-bisphosphate (Garcia-Gonzalo et al., 2004, 2005). As a small GTPase regulator, HERC1 interacts, among others, with IQGAP1, which is a key interactor centre for such proteins (Jacquemet and Humphries, 2013). No GEF or GRF activities have been reported in HERC2. Of note, HERC2 forms a complex with and stimulates the E6AP ubiquitin ligase activity through its RLD2 (Kuhnle et al., 2011).

### HECT Domain Structure and Function: Ubiquitin Ligase Activity

Large HERCs display a HECT domain at their carboxyl end. *In silico* predicted models show structural similarity with the HECT domain of E6AP (**Figure 2C**). They form a bilobed structure consisting of a helix-turn-helix motif packed with two and four antiparallel $\beta$ sheets at the N and C ends, respectively. The lobes are joined to the hinge formed by a core of α helices. This bilobed structure facilitates transmission of the ubiquitin residue to its target protein. Thus, the N-terminal-facing lobe is able to bind the E2 enzyme from which the ubiquityl residue is transferred to the catalytic cysteine within the C-terminal-facing lobe of the domain (**Figure 2C**; circled). Following that, the ubiquitin is transferred to a lysyl residue or to the amino terminus in the target protein (Metzger et al., 2012; Streich and Lima, 2014).

Large HERCs play a role in protein stability. HERC1 regulates C-RAF stability through ubiquitylation leading to proteasomal degradation (Schneider et al., 2018) and is also implicated in the stability of TSC2/tuberin (Chong-Kopera et al., 2006). HERC2 ubiquitylates for proteasomal degradation proteins involved in DNA repair such as XPA and BRCA1, Ubiquitin Specific Proteases (USP) such as USP33 and USP20, and proteins involved in iron metabolism such as FBXl5 and NCOA4 (reviewed in Sánchez-Tena et al., 2016). HERC2 also promotes degradation of the LKB1 kinase when acetylated (Bai et al., 2016).

## PHYSIOLOGICAL IMPLICATIONS

### Cancer and DNA Damage Repair

HERC2 is implicated in different types of cancer. In osteosarcoma, the increase of HERC2-binding protein SOX18 enhances cell proliferation correlating with a decrease in *HERCs* mRNA levels, especially those of *HERC2* (Zhu et al., 2018). Certain *HERC2* genetic variants are risk factors in cutaneous and uveal melanomas (Ibarrola-Villava et al., 2010; Amos et al., 2011; Kosiniak-Kamysz et al., 2014). Frameshift mutations in *HERC2* have been described in gastric and colorectal carcinomas with microsatellite instability (Yoo et al., 2011).

HERC2 is also implicated in DNA damage repair (DDR). HERC2 induces BRCA1 degradation in breast cancer. This is inhibited either by binding of TUSC4 to HERC2 (Peng et al., 2015) or by BARD1 binding BRCA1 itself (Wu et al., 2010). Moreover, HERC2 targets XPA for degradation. ATR phosphorylates XPA thus preventing this ubiquitylation while WIP dephosphorylates XPA in a circadian manner (Kang et al., 2010, 2011; Lee et al., 2014). Besides, ATR phosphorylates and also stabilizes USP20 by unbinding it from HERC2. In turn, USP20 stabilizes Claspin, which increases the activity of the ATR-Chk1 axis (Yuan et al., 2014; Zhu et al., 2014).

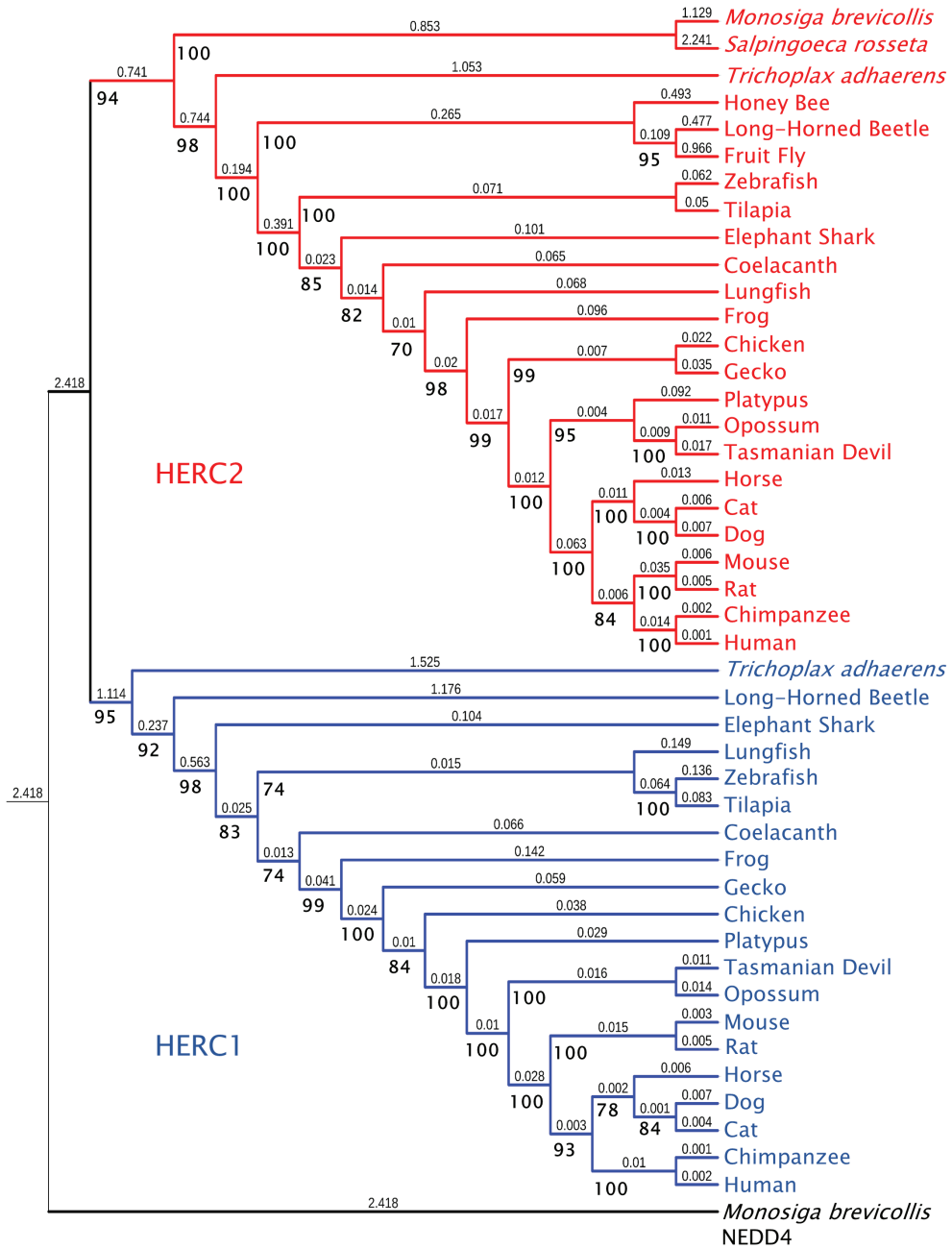


**FIGURE 1 |** Molecular phylogeny of Large HERC proteins. The tree shows the clustering of HERC1 (blue) and HERC2 (red) amino acid sequences from significative choanoflagellate and metazoan species. Ultrafast bootstrap support (1,000 replicates) is shown next to the branches in bold. Smaller numbers indicate branch lengths. NEDD4 protein from *Monosiga brevicollis* was used as a outgroup.

On the other hand, HERC2 binds Claspin among other proteins upon MCM2 phosphorylation, and facilitates replication origin firing (Izawa et al., 2011). In a different way, HERC2 promotes resistance to cisplatin and UV-induced DNA damage by stabilizing the Ubc13-RNF8 tandem and RNF168 and enhancing the recruitment of repair factors such as 53BP1, RAP80, and BRCA1 to the damaged sites (Bekker-Jensen et al., 2010; Danielsen et al., 2012; Bonanno et al., 2016; Mohiuddin et al., 2016). Ubc13-RNF8 binding is facilitated by HERC2 by interacting with the RNF8 FHA domain upon phosphorylation of threonine 4827 of HERC2 triggered by ionizing radiation (IR) (Bekker-Jensen et al., 2010) and by acting as a docking platform upon DNA damage, when HERC2 is SUMOylated by PIAS4 (Bekker-Jensen and Mailand, 2010; Danielsen et al., 2012). Both RNF8 and RNF168 are required for ubiquitin foci formation upon IR (Oestergaard et al., 2012), which are necessary for DDR maintenance. In addition to that, HERC2 stabilizes USP16 which, in turn, deubiquitylates

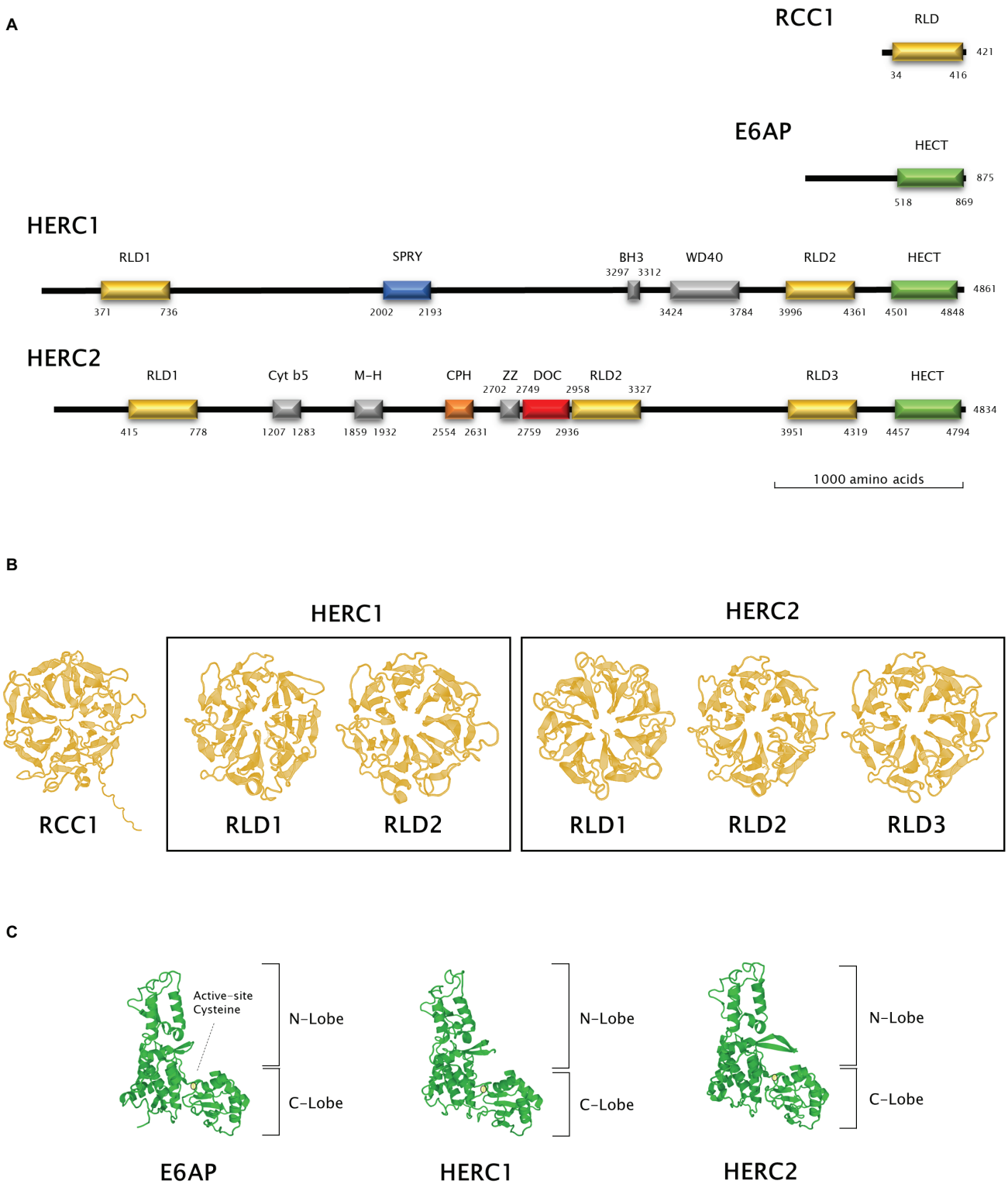


**FIGURE 2 |** Structural features of Large HERC proteins. **(A)** Primary structure of human RCC-1, E6AP, HERC1, and HERC2 proteins. Scheme shows the approximate relative position of each significative protein domain as indicated by ScanProSite domain predictions with the amino acid sequences. **(B,C)** Three-dimensional structures of homologous RCC1-like and HECT domains in HERC1 and HERC2. Three-dimensional structures of RCC1 and E6AP HECT domains were modelled using the Swiss-Model online software and used as a template for HERC1 and HERC2 RCC1-like **(B)** and HECT **(C)** domains modelling. Active-site cysteine location in the HECT domains is indicated by a pale yellow circle.

histone 2A so as to terminate the DDR (Zhang et al., 2014). Moreover, during S phase, HERC2 is necessary for RPA ubiquitylation which plays a role in clearing G-quadruplex DNA structures by binding the RecQ DNA helicases BLM and WRN (Wu et al., 2018). Finally, HERC2 along with NEURL4 controls cell proliferation by regulating the transcriptional activity of the tumour suppressor protein p53 through regulation of its oligomerization (Cubillos-Rojas et al., 2014, 2017). All these data suggest that HERC2 functions to control the cell response to genotoxic insults and helps maintain genome stability.

HERC1 is also involved in DDR and cancer. *HERC1* deletions affect MSH2 protein levels (Diouf et al., 2011). Besides, it also promotes degradation of BAK in the presence of the E6 protein from the HPV5β virus and prevents cell death in response to UV (Holloway et al., 2015). Furthermore, *HERC1* is recurrently mutated in metastatic triple negative (Craig et al., 2013) and in invasive lobular cancer in the breast (Ping et al., 2016). In addition to that, an atypical *HERC1-PML* transcript fusion mRNA (Walz et al., 2010) and HERC1 mutations are also found in leukaemia (Diouf et al., 2011; Neumann et al., 2015; Johansson et al., 2018). HERC1 binds to the M2 isoform of pyruvate kinase, which is typically found in proliferating tissues and cancer cells although the physiological role for this association has not been elucidated to date (Garcia-Gonzalo et al., 2003; Mazurek, 2008). Moreover, as stated above, HERC1 regulates cell proliferation through C-RAF stability. In particular, accumulation of C-RAF upon *HERC1* knockdown results in increased cell proliferation (Schneider et al., 2018). Finally, one singular clinical case of pulmonary sclerosing pneumocytoma revealed several somatic mutations on *HERC1* along with other genes such as *TSC1* and *AKT1* (Fan et al., 2018).

## Development and Neurobiology

In mice, recessive mutations of the *Herc2* gene are associated with defects in growth, motor coordination and fertility (Lehman et al., 1998; Walkowicz et al., 1999). While *Herc2* knockout animals are not viable, heterozygous mice have motor impairment (Cubillos-Rojas et al., 2016). In humans, the *HERC2* gene locates to chromosome 15 among genes responsible for such disorders as Angelman and Prader-Willi syndromes and Autism spectrum disorders (Ji et al., 1999; Dimitropoulos and Schultz, 2007; Roberts et al., 2014). Recessive mutations in the *HERC2* locus are related to symptoms ranging from cognitive delay, ataxia, speech disorders, microcephalia, seizures, facial dysmorphism, hypopigmentation, and other secondary signs such as infections and behavioural alterations (Puffenberger et al., 2012; Harlalka et al., 2013; Neubert et al., 2013; Han et al., 2016; Morice-Picard et al., 2016).

Little is known about the precise molecular mechanism by which HERC2 affects neuronal development and function. HERC2-NEURL4 complex binds RNF8 in neurons regulating synapse formation *in vivo*. Knockdown of HERC2 resembles the effects in RNF8 depletion and inhibition of RNF8-Ubc13 signalling – an increase in parallel fibres, synaptic boutons, and synapse formation with Purkinje cells (Valnegri et al., 2017). HERC2 could also be linked to other neurological diseases. Parkinson's disease-associated kinase LRRK2 is known to bind to the HERC2-NEURL4 complex thus regulating endosomal vesicular trafficking and promoting the internalization of the Delta-like 1/Delta Notch ligand, affecting its signalling (Imai et al., 2015).

HERC1 has also major implications in neurodevelopment. Herc1 Gly483Glu mutant mice, termed *tambaleante*, present with delayed growth, short body, high juvenile mortality, and severe ataxia, the latter due to Purkinje cell loss beyond the age of 2 months, correlating with autophagy and decreased mTOR signalling (Mashimo et al., 2009). *Tambaleante* mice have impaired neurotransmitter release in neuromuscular junctions (Bachiller et al., 2015), defective ubiquitin-proteasome-driven protein aggregate clearance, and increased autophagic flux in neocortical pyramidal, CA3 hippocampal pyramidal and spinal cord motor neurons (Ruiz et al., 2016) and poor myelinisation and delayed action potential transmission (Bachiller et al., 2018). Furthermore, they have impaired associative learning (Perez-Villegas et al., 2018). In humans, patients with recessive mutations of *HERC1* present with intellectual disability, macrocephalia, facial dysmorphism, feeding difficulties, kyphoscoliosis, thicker corpus callosum, seizures, and other clinical signs resembling autism (Ortega-Recalde et al., 2015; Aggarwal et al., 2016; Hashimoto et al., 2016; Nguyen et al., 2016; Kannan et al., 2017; Utine et al., 2017).

## Other Processes

The human *HERC2* gene locus is upstream of that of the *OCA2* gene (mutated in oculocutaneous albinism) and certain *HERC2* SNPs can interfere *OCA2*'s expression thus affecting eye, skin, and hair pigmentation (Eiberg et al., 2008; Kayser et al., 2008; Sturm et al., 2008; Branicki et al., 2009; Nan et al., 2009). Certain phenotypes are favoured by evolution with a traceable population gradient from Europe to Asia (Ulivi et al., 2013; Wilde et al., 2014). Moreover, polymorphisms in the *HERC2* locus relate to rosacea (Aponte et al., 2018), macular degeneration (Klein et al., 2014), vitiligo (Jin et al., 2012), and skin photosensitivity (Hernando et al., 2018). As for *HERC1*, some of its catalogued polymorphisms are more likely to occur in the East Asian population than in the rest of the world (Xue et al., 2009; Yuasa et al., 2009).

HERC2 is also related to inflammation and autoimmune diseases such as Crohn's disease, ulcerative colitis, type 1 diabetes mellitus, or sarcoidosis (Franke et al., 2008; Weersma et al., 2009; Wang et al., 2010; Fischer et al., 2011; Garcia-Heredia and Carnero, 2017). With regard to HERC1, a downregulation of its expression has been observed in an LPS-induced inflammation model following coenzyme $Q_{10}$ treatment. (Schmelzer and Doring, 2010).

In addition to this, HERC2 is involved in iron metabolism and ferritinophagy by regulating stability of FBXL5, IRP2, and NCOA4 proteins (Moroishi et al., 2011, 2014; Galligan et al., 2015; Mancias et al., 2015; Ryu et al., 2018) and in toxicology to the response to diisocyanate, toluene, or alcohol

intake (Sulovari et al., 2015; Yucesoy et al., 2015; Lim et al., 2017). In regard to toxicology, HERC1 may also play a role in the response of the nervous system to heroin (Drakenberg et al., 2006).

## FINAL REMARKS

Large-HERC family members are staggeringly complex proteins that can intervene in a wide range of physiological processes, such as proliferation, DNA repair, neurodevelopment, inflammation, or ferritinophagy among others. HERC1 and HERC2 sequences are quite conserved through animal evolution, evolving linearly together with the increase of complexity in nervous, endocrine, and immune systems of organisms. Mutations or reduced expression of Large HERCs are associated with neurological disorders, DNA repair defects, and cancer pointing out the importance that Large HERC proteins have in the abovementioned physiological processes.

## FIGURE SOURCES

Amino acid sequences were aligned using the Mafft FFT-NS-i algorithm (Katoh, 2002). The phylogenetic tree in **Figure 1** was inferred using the maximum likelihood method with IQ-Tree 1.6.9 software (Nguyen et al., 2015). The model used for the analysis was JTT + F + G4, determined using ModelFinder (Kalyaanamoorthy et al., 2017). The IQ-Tree search parameters were set to perturbation strength = 0.8 and 500 unsuccessful iterations to stop (numstop = 500). Ultrafast Bootstrap support (Hoang et al., 2018) was calculated from 1,000 replicates. The final tree obtained with IQ-Tree was visualized using Interactive Tree of Life v4 (Letunic and Bork, 2019). NEDD4 protein from *M. brevicollis* was used as an outgroup. The accession numbers of the sequences used are: for NEDD4: *M. brevicollis* (XP_001750085.1), for HERC1: *T. adhaerens* (XP_002116356.1), *Anoplophora glabripennis* (Asian long-horned beetle) (XP_018567016.1), *Callorhinchus milii* (Elephant shark) (XP_007906088.1), *Latimeria chalumnae* (Coelacanth) (XP_005987767.1), *Danio rerio* (Zebrafish) (XP_021333511.1), *Oreochromis niloticus* (Tilapia) (XP_013121789.1), *Xenopus tropicalis* (Frog) (XP_004916026.1), *Gekko japonicus* (Gecko) (XP_015275623.1), *Gallus gallus* (Chicken) (XP_004943789.1), *Ornithorhynchus anatinus* (Platypus) (XP_028921613), *Monodelphis domestica* (Opossum) (XP_016284147.1), *Sarcophilus harrisii* (Tasmanian devil) (XP_023353554.1), *Equus caballus* (Horse) (XP_023471806.1), *Rattus norvegicus* (Rat) (XP_017451567.1), *Mus musculus* (Mouse) (NP_663592.3), *Homo sapiens* (Human) (NP_003913.3), *Pan troglodytes* (Chimpanzee) (XP_001174017.1), *Canis lupus familiaris* (Dog) (XP_544717.3), *Felis catus* (Cat) (XP_023110993.1), and *Lepidosiren paradoxa* (Lungfish) (Translated from GEHZ01042047.1, NCBI TSA database). For HERC2: *M. brevicollis* (XP_001743304.1), *S. rosetta* (XP_004996155.1), *T. adhaerens* (XP_002112421), Asian long-horned beetle (XP_018562376.1), *Drosophila melanogaster* (Fruit fly) (NP_608388.2), *Apis mellifera* (Honey bee) (XP_01677273), Coelacanth (XP_014343905.1), Zebrafish (XP_021332870.1), Tilapia (XP_013130527.1), Frog (XP_012813156.1), Gecko (XP_015266462.1), Chicken (XP_015133197.1), Platypus (XP_016083014.1), Opossum (XP_007501467.1), Tasmanian devil (XP_023356163.1), Horse (XP_023507879.1), Mouse (NP_001347009.1), Rat (XP_006229362.1), Human (NP_004658.3), Chimpanzee (XP_024204823.1), Dog (XP_022272508.1), Cat (XP_023110801.1), Elephant shark (XP_007889299.1), and Lungfish (Translated from GEHZ01036559.1, NCBI TSA).

Human RCC1 (NCBI accession number P18754) and HECT domain from E6AP (NCBI accession number Q05086.4, amino acids from 518 to 869) three-dimensional structures were modelled using Swiss-Model online software (Waterhouse et al., 2018). RLDs and HECT domains from HERC1 and HERC2 were modelled using a User Template mode. The query sequences were the following: Q15751 for HERC1 (amino acids 371–736 and 3996–4361 for RLD1 and RLD2, respectively, and 4501–4848 for the HECT domain) and O95714 for HERC2 (amino acids 415–778, 2958–3327 and 3951–4319 for RLD1, RLD2, and RLD3, respectively, and 4457–4794 for the HECT domain). PDB files from RCC1 and E6AP HECT domain models obtained as described above were used as templates in these queries. The amino acid position of each domain identified was verified using ScanProSite domain predictions (Sigrist et al., 2012).

## AUTHOR CONTRIBUTIONS

JG-C and JR conceived and designed the manuscript. JG-C, AM-M, and JR analysed the data and performed figures and tables. JG-C, AM-M, JS-G, LP, and JR wrote the manuscript.

## FUNDING

This work was supported by the Spanish Ministerio de Economía, Industria y Competitividad (MINECO-AEI/FEDER, UE; BFU2016-80295-R; and SAF2017-90900-REDT). JG-C received a contract from the Universitat de Barcelona postdoctoral programme in collaboration with the "La Caixa" bank foundation. AM-M was awarded an "FI" PhD Fellowship by the Agència de Gestió dels Ajuts Universitaris i de Recerca (AGAUR) of the Generalitat de Catalunya regional government. JS-G was supported by an FPU PhD (FPU17/02413) grant from the Spanish Ministry of Science, Innovation and Universities and LP received a postdoctoral contract from the Conselho Nacional de Desenvolvimento Científico e Tecnológico (CNPq, 203,528/2017-4), from the Ministry of Science, Technology and Innovation Education of Brazil.

## ACKNOWLEDGMENTS

We thank Joan Martí-Carreras for technical assistance and commentaries.

## REFERENCES


Aggarwal, S., Bhowmik, A. D., Ramprasad, V. L., Murugan, S., and Dalal, A. (2016). A splice site mutation in HERC1 leads to syndromic intellectual disability with macrocephaly and facial dysmorphism: further delineation of the phenotypic spectrum. *Am. J. Med. Genet. A* 170, 1868–1873. doi: 10.1002/ajmg.a.37654

Altschul, S. F., Madden, T. L., Schäffer, A. A., Zhang, J., Zhang, Z., Miller, W., et al. (1997). Gapped BLAST and PSI-BLAST: a new generation of protein database search programs. *Nucleic Acids Res.* 25, 3389–3402. doi: 10.1093/nar/25.17.3389

Altschul, S. F., Wootton, J. C., Gertz, E. M., Agarwala, R., Morgulis, A., Schaffer, A. A., et al. (2005). Protein database searches using compositionally adjusted substitution matrices. *FEBS J.* 272, 5101–5109. doi: 10.1111/j.1742-4658.2005.04945.x

Amos, C. I., Wang, L.-E., Lee, J. E., Gershenwald, J. E., Chen, W. V., Fang, S., et al. (2011). Genome-wide association study identifies novel loci predisposing to cutaneous melanoma. *Hum. Mol. Genet.* 20, 5012–5023. doi: 10.1093/hmg/ddr415

Aponte, J. L., Chiano, M. N., Yerges-Armstrong, L. M., Hinds, D. A., Tian, C., Gupta, A., et al. (2018). Assessment of rosacea symptom severity by genome-wide association study and expression analysis highlights immuno-inflammatory and skin pigmentation genes. *Hum. Mol. Genet.* 15, 2762–2772. doi: 10.1093/hmg/ddy184

Bachiller, S., Roca-Ceballos, M. A., Garcia-Dominguez, I., Perez-Villegas, E. M., Martos-Carmona, D., Perez-Castro, M. A., et al. (2018). HERC1 ubiquitin ligase is required for normal axonal myelination in the peripheral nervous system. *Mol. Neurobiol.* 55, 8856–8868. doi: 10.1007/s12035-018-1021-0

Bachiller, S., Rybkina, T., Porras-Garcia, E., Perez-Villegas, E., Tabares, L., Armengol, J. A., et al. (2015). The HERC1 E3 ubiquitin ligase is essential for normal development and for neurotransmission at the mouse neuromuscular junction. *Cell. Mol. Life Sci.* 72, 2961–2971. doi: 10.1007/s00018-015-1878-2

Bai, B., Man, A. W. C., Yang, K., Guo, Y., Xu, C., Tse, H.-F., et al. (2016). Endothelial SIRT1 prevents adverse arterial remodeling by facilitating HERC2-mediated degradation of acetylated LKB1. *Oncotarget* 7, 39065–39081. doi: 10.18632/oncotarget.9687

Bateman, A., Martin, M. J., O'Donovan, C., Magrane, M., Alpi, E., Antunes, R., et al. (2017). UniProt: the universal protein knowledgebase. *Nucleic Acids Res.* 45, D158–D169. doi: 10.1093/nar/gkw1099

Bekker-Jensen, S., and Mailand, N. (2010). Assembly and function of DNA double-strand break repair foci in mammalian cells. *DNA Repair* 9, 1219–1228. doi: 10.1016/j.dnarep.2010.09.010

Bekker-Jensen, S., Rendtlew Danielsen, J., Fugger, K., Gromova, I., Nerstedt, A., Lukas, C., et al. (2010). HERC2 coordinates ubiquitin-dependent assembly of DNA repair factors on damaged chromosomes. *Nat. Cell Biol.* 12, 12–80. doi: 10.1038/ncb2008

Bischoff, F. R., and Ponstingl, H. (1991). Catalysis of guanine nucleotide exchange on Ran by the mitotic regulator RCC1. *Nature* 354, 80–82. doi: 10.1038/354080a0

Bonanno, L., Costa, C., Majem, M., Sanchez, J.-J., Rodriguez, I., Gimenez-Capitan, A., et al. (2016). Combinatory effect of BRCA1 and HERC2 expression on outcome in advanced non-small-cell lung cancer. *BMC Cancer* 16:312. doi: 10.1186/s12885-016-2339-5

Branicki, W., Brudnik, U., and Wojas-Pelc, A. (2009). Interactions between HERC2, OCA2 and MC1R may influence human pigmentation phenotype. *Ann. Hum. Genet.* 73, 160–170. doi: 10.1111/j.1469-1809.2009.00504.x

Buetow, L., and Huang, D. T. (2016). Structural insights into the catalysis and regulation of E3 ubiquitin ligases. *Nat. Rev. Mol. Cell Biol.* 17, 626–642. doi: 10.1038/nrm.2016.91

Chong-Kopera, H., Inoki, K., Li, Y., Zhu, T., Garcia-Gonzalo, F. R., Rosa, J. L., et al. (2006). TSC1 stabilizes TSC2 by inhibiting the interaction between TSC2 and the HERC1 ubiquitin ligase. *J. Biol. Chem.* 281, 8313–8316. doi: 10.1074/jbc.C500451200

Craig, D. W., O'Shaughnessy, J. A., Kiefer, J. A., Aldrich, J., Sinari, S., Moses, T. M., et al. (2013). Genome and transcriptome sequencing in prospective metastatic triple-negative breast cancer uncovers therapeutic vulnerabilities. *Mol. Cancer Ther.* 12, 104–116. doi: 10.1158/1535-7163.MCT-12-0781

Cubillos-Rojas, M., Amair-Pinedo, F., Peiró-Jordán, R., Bartrons, R., Ventura, F., and Rosa, J. L. (2014). The E3 ubiquitin protein ligase HERC2 modulates the activity of tumor protein p53 by regulating its oligomerization. *J. Biol. Chem.* 289, 14782–14795. doi: 10.1074/jbc.M113.527978

Cubillos-Rojas, M., Schneider, T., Bartrons, R., Ventura, F., Rosa, J. L., Cubillos-Rojas, M., et al. (2017). NEURL4 regulates the transcriptional activity of tumor suppressor protein p53 by modulating its oligomerization. *Oncotarget* 8, 61824–61836. doi: 10.18632/oncotarget.18699

Cubillos-Rojas, M., Schneider, T., Hadjebi, O., Pedrazza, L., de Oliveira, J. R., Langa, F., et al. (2016). The HERC2 ubiquitin ligase is essential for embryonic development and regulates motor coordination. *Oncotarget* 7, 56083–56106. doi: 10.18632/oncotarget.11270

Danielsen, J. R., Povlsen, L. K., Villumsen, B. H., Streicher, W., Nilsson, J., Wikstrom, M., et al. (2012). DNA damage-inducible SUMOylation of HERC2 promotes RNF8 binding via a novel SUMO-binding Zinc finger. *J. Cell Biol.* 197, 179–187. doi: 10.1083/jcb.201106152

Dimitropoulos, A., and Schultz, R. T. (2007). Autistic-like symptomatology in Prader-Willi syndrome: a review of recent findings. *Curr. Psychiatry Rep.* 9, 159–164. doi: 10.1007/s11920-007-0086-7

Diouf, B., Cheng, Q., Krynetskaia, N. F., Yang, W., Cheok, M., Pei, D., et al. (2011). Somatic deletions of genes regulating MSH2 protein stability cause DNA mismatch repair deficiency and drug resistance in human leukemia cells. *Nat. Med.* 17, 1298–1303. doi: 10.1038/nm.2430

Drakenberg, K., Nikoshkov, A., Horvath, M. C., Fagergren, P., Gharibyan, A., Saarelainen, K., et al. (2006). Opioid receptor A118G polymorphism in association with striatal opioid neuropeptide gene expression in heroin abusers. *Proc. Natl. Acad. Sci. USA* 103, 7883–7888. doi: 10.1073/pnas.0600871103

Eiberg, H., Troelsen, J., Nielsen, M., Mikkelsen, A., Mengel-From, J., Kjaer, K. W., et al. (2008). Blue eye color in humans may be caused by a perfectly associated founder mutation in a regulatory element located within the HERC2 gene inhibiting OCA2 expression. *Hum. Genet.* 123, 177–187. doi: 10.1007/s00439-007-0460-x

Fan, X., Lin, L., Wang, J., Wang, Y., Feng, A., Nie, L., et al. (2018). Genome profile in a extremely rare case of pulmonary sclerosing pneumocytoma presenting with diffusely-scattered nodules in the right lung. *Cancer Biol. Ther.* 19, 13–19. doi: 10.1080/15384047.2017.1360443

Fischer, A., Nothnagel, M., Franke, A., Jacobs, G., Saadati, H. R., Gaede, K. I., et al. (2011). Association of inflammatory bowel disease risk loci with sarcoidosis, and its acute and chronic subphenotypes. *Eur. Respir. J.* 37, 610–616. doi: 10.1183/09031936.00049410

Franke, A., Balschun, T., Karlsen, T. H., Hedderich, J., May, S., Lu, T., et al. (2008). Replication of signals from recent studies of Crohn's disease identifies previously unknown disease loci for ulcerative colitis. *Nat. Genet.* 40, 713–715. doi: 10.1038/ng.148

Galligan, J. T., Martinez-Noel, G., Arndt, V., Hayes, S., Chittenden, T. W., Harper, J. W., et al. (2015). Proteomic analysis and identification of cellular interactors of the giant ubiquitin ligase HERC2. *J. Proteome Res.* 14, 953–966. doi: 10.1021/pr501005v

Garcia-Gonzalo, F. R., Bartrons, R., Ventura, F., and Rosa, J. L. (2005). Requirement of phosphatidylinositol-4,5-bisphosphate for HERC1-mediated guanine nucleotide release from ARF proteins. *FEBS Lett.* 579, 343–348. doi: 10.1016/j.febslet.2004.11.095

Garcia-Gonzalo, F. R., Cruz, C., Munoz, P., Mazurek, S., Eigenbrodt, E., Ventura, F., et al. (2003). Interaction between HERC1 and M2-type pyruvate kinase. *FEBS Lett.* 539, 78–84. doi: 10.1016/S0014-5793(03)00205-9

Garcia-Gonzalo, F. R., Munoz, P., Gonzalez, E., Casaroli-Marano, R. P., Vilaro, S., Bartrons, R., et al. (2004). The giant protein HERC1 is recruited to aluminum fluoride-induced actin-rich surface protrusions in HeLa cells. *FEBS Lett.* 559, 77–83. doi: 10.1016/S0014-5793(04)00030-4

Garcia-Heredia, J. M., and Carnero, A. (2017). The cargo protein MAP17 (PDZK1IP1) regulates the immune microenvironment. *Oncotarget* 8, 98580–98597. doi: 10.18632/oncotarget.21651

Hadjebi, O., Casas-Terradellas, E., Garcia-Gonzalo, F. R., and Rosa, J. L. (2008). The RCC1 superfamily: from genes, to function, to disease. *Biochim. Biophys. Acta, Mol. Cell Res.* 1783, 1467–1479. doi: 10.1016/j.bbamcr.2008.03.015

Han, J. Y., Park, J., Jang, W., Chae, H., Kim, M., and Kim, Y. (2016). A twin sibling with Prader-Willi syndrome caused by type 2 microdeletion following assisted reproductive technology: a case report. *Biomed. reports* 5, 18–22. doi: 10.3892/br.2016.675

Harlalka, G. V., Baple, E. L., Cross, H., Kuhnle, S., Cubillos-Rojas, M., Matentzoglu, K., et al. (2013). Mutation of HERC2 causes developmental delay with Angelman-like features. *J. Med. Genet.* 50, 65–73. doi: 10.1136/jmedgenet-2012-101367

Hashimoto, R., Nakazawa, T., Tsurusaki, Y., Yasuda, Y., Nagayasu, K., Matsumura, K., et al. (2016). Whole-exome sequencing and neurite outgrowth analysis in autism spectrum disorder. *J. Hum. Genet.* 61, 199–206. doi: 10.1038/jhg.2015.141

Hernando, B., Sanz-Page, E., Pitarch, G., Mahiques, L., Valcuende-Cavero, F., and Martinez-Cadenas, C. (2018). Genetic variants associated with skin photosensitivity in a southern European population from Spain. *Photodermatol. Photoimmunol. Photomed.* 34, 415–422. doi: 10.1111/phpp.12412

Hoang, D. T., Chernomor, O., von Haeseler, A., Minh, B. Q., and Vinh, L. S. (2018). UFBoot2: improving the ultrafast bootstrap approximation. *Mol. Biol. Evol.* 35, 518–522. doi: 10.1093/molbev/msx281

Holloway, A., Simmonds, M., Azad, A., Fox, J. L., and Storey, A. (2015). Resistance to UV-induced apoptosis by beta-HPV5 E6 involves targeting of activated BAK for proteolysis by recruitment of the HERC1 ubiquitin ligase. *Int. J. Cancer* 136, 2831–2843. doi: 10.1002/ijc.29350

Ibarrola-Villava, M., Fernandez, L. P., Pita, G., Bravo, J., Floristan, U., Sendagorta, E., et al. (2010). Genetic analysis of three important genes in pigmentation and melanoma susceptibility: CDKN2A, MC1R and HERC2/OCA2. *Exp. Dermatol.* 19, 836–844. doi: 10.1111/j.1600-0625.2010.01115.x

Imai, Y., Kobayashi, Y., Inoshita, T., Meng, H., Arano, T., Uemura, K., et al. (2015). The Parkinson's disease-associated protein kinase LRRK2 modulates notch signaling through the endosomal pathway. *PLoS Genet.* 11:e1005503. doi: 10.1371/journal.pgen.1005503

Izawa, N., Wu, W., Sato, K., Nishikawa, H., Kato, A., Boku, N., et al. (2011). HERC2 interacts with Claspin and regulates DNA origin firing and replication fork progression. *Cancer Res.* 71, 5621–5625. doi: 10.1158/0008-5472.CAN-11-0385

Jacquemet, G., and Humphries, M. J. (2013). IQGAP1 is a key node within the small GTPase network. *Small GTPases* 4, 199–207. doi: 10.4161/sgtp.27451

Ji, Y., Walkowicz, M. J., Buiting, K., Johnson, D. K., Tarvin, R. E., Rinchik, E. M., et al. (1999). The ancestral gene for transcribed, low-copy repeats in the Prader-Willi/Angelman region encodes a large protein implicated in protein trafficking, which is deficient in mice with neuromuscular and spermiogenic abnormalities. *Hum. Mol. Genet.* 8, 533–542. doi: 10.1093/hmg/8.3.533

Jin, Y., Birlea, S. A., Fain, P. R., Ferrara, T. M., Ben, S., Riccardi, S. L., et al. (2012). Genome-wide association analyses identify 13 new susceptibility loci for generalized vitiligo. *Nat. Genet.* 44, 676–680. doi: 10.1038/ng.2272

Johansson, P., Klein-Hitpass, L., Choidas, A., Habenberger, P., Mahboubi, B., Kim, B., et al. (2018). SAMHD1 is recurrently mutated in T-cell prolymphocytic leukemia. *Blood Cancer J.* 8:11. doi: 10.1038/s41408-017-0036-5

Kalyaanamoorthy, S., Minh, B. Q., Wong, T. K. F., von Haeseler, A., and Jermiin, L. S. (2017). ModelFinder: fast model selection for accurate phylogenetic estimates. *Nat. Methods* 14, 587–589. doi: 10.1038/nmeth.4285

Kang, T.-H., Lindsey-Boltz, L. A., Reardon, J. T., and Sancar, A. (2010). Circadian control of XPA and excision repair of cisplatin-DNA damage by cryptochrome and HERC2 ubiquitin ligase. *Proc. Natl. Acad. Sci. USA* 107, 4890–4895. doi: 10.1073/pnas.0915085107

Kang, T.-H., Reardon, J. T., and Sancar, A. (2011). Regulation of nucleotide excision repair activity by transcriptional and post-transcriptional control of the XPA protein. *Nucleic Acids Res.* 39, 3176–3187. doi: 10.1093/nar/gkq1318

Kannan, M., Bayam, E., Wagner, C., Rinaldi, B., Kretz, P. F., Tilly, P., et al. (2017). WD40-repeat 47, a microtubule-associated protein, is essential for brain development and autophagy. *Proc. Natl. Acad. Sci. USA* 114, E9308–E9317. doi: 10.1073/pnas.1713625114

Katoh, K. (2002). MAFFT: a novel method for rapid multiple sequence alignment based on fast Fourier transform. *Nucleic Acids Res.* 30, 3059–3066. doi: 10.1093/nar/gkf436

Kayser, M., Liu, F., Janssens, A. C. J. W., Rivadeneira, F., Lao, O., van Duijn, K., et al. (2008). Three genome-wide association studies and a linkage analysis identify HERC2 as a human iris color gene. *Am. J. Hum. Genet.* 82, 411–423. doi: 10.1016/j.ajhg.2007.10.003

Klein, B. E. K., Howard, K. P., Iyengar, S. K., Sivakumaran, T. A., Meyers, K. J., Cruickshanks, K. J., et al. (2014). Sunlight exposure, pigmentation, and incident age-related macular degeneration. *Invest. Ophthalmol. Vis. Sci.* 55, 5855–5861. doi: 10.1167/iovs.14-14602

Kosiniak-Kamysz, A., Marczakiewicz-Lustig, A., Marcinska, M., Skowron, M., Wojas-Pelc, A., Pospiech, E., et al. (2014). Increased risk of developing cutaneous malignant melanoma is associated with variation in pigmentation genes and VDR, and may involve epistatic effects. *Melanoma Res.* 24, 388–396. doi: 10.1097/CMR.0000000000000095

Kuhnle, S., Kogel, U., Glockzin, S., Marquardt, A., Ciechanover, A., Matentzoglu, K., et al. (2011). Physical and functional interaction of the HECT ubiquitin-protein ligases E6AP and HERC2. *J. Biol. Chem.* 286, 19410–19416. doi: 10.1074/jbc.M110.205211

Lee, T.-H., Park, J.-M., Leem, S.-H., and Kang, T.-H. (2014). Coordinated regulation of XPA stability by ATR and HERC2 during nucleotide excision repair. *Oncogene* 33, 19–25. doi: 10.1038/onc.2012.539

Lehman, A. L., Nakatsu, Y., Ching, A., Bronson, R. T., Oakey, R. J., Keiper-Hrynko, N., et al. (1998). A very large protein with diverse functional motifs is deficient in rjs (runty, jerky, sterile) mice. *Proc. Natl. Acad. Sci. USA* 95, 9436–9441. doi: 10.1073/pnas.95.16.9436

Letunic, I., and Bork, P. (2019). Interactive tree of life (iTOL) v4: recent updates and new developments. *Nucleic Acids Res.* 47, W256–W259. doi: 10.1093/nar/gkz239

Lim, J.-H., Song, M.-K., Cho, Y., Kim, W., Han, S. O., and Ryu, J.-C. (2017). Comparative analysis of microRNA and mRNA expression profiles in cells and exosomes under toluene exposure. *Toxicol. In Vitro* 41, 92–101. doi: 10.1016/j.tiv.2017.02.020

Mancias, J. D., Pontano Vaites, L., Nissim, S., Biancur, D. E., Kim, A. J., Wang, X., et al. (2015). Ferritinophagy via NCOA4 is required for erythropoiesis and is regulated by iron dependent HERC2-mediated proteolysis. *elife* 4:e10308. doi: 10.7554/eLife.10308

Marín, I. (2010). Animal HECT ubiquitin ligases: evolution and functional implications. *BMC Evol. Biol.* 10:56. doi: 10.1186/1471-2148-10-56

Mashimo, T., Hadjebi, O., Amair-Pinedo, F., Tsurumi, T., Langa, F., Serikawa, T., et al. (2009). Progressive Purkinje cell degeneration in tambaleante mutant mice is a consequence of a missense mutation in HERC1 E3 ubiquitin ligase. *PLoS Genet.* 5:e1000784. doi: 10.1371/journal.pgen.1000784

Mazurek, S. (2008). "Pyruvate kinase type M2: a key regulator within the tumour metabolome and a tool for metabolic profiling of tumours" in *Ernst Schering Foundation symposium proceedings* (Germany), 99–124.

Metzger, M. B., Hristova, V. A., and Weissman, A. M. (2012). HECT and RING finger families of E3 ubiquitin ligases at a glance. *J. Cell Sci.* 125, 531–537. doi: 10.1242/jcs.091777

Mohiuddin, Kobayashi, S., Keka, I. S., Guilbaud, G., Sale, J., Narita, T., et al. (2016). The role of HERC2 and RNF8 ubiquitin E3 ligases in the promotion of translesion DNA synthesis in the chicken DT40 cell line. *DNA Repair* 40, 67–76. doi: 10.1016/j.dnarep.2016.02.002

Morice-Picard, F., Benard, G., Rezvani, H. R., Lasseaux, E., Simon, D., Moutton, S., et al. (2016). Complete loss of function of the ubiquitin ligase HERC2 causes a severe neurodevelopmental phenotype. *Eur. J. Hum. Genet.* 25, 52–58. doi: 10.1038/ejhg.2016.139

Moroishi, T., Nishiyama, M., Takeda, Y., Iwai, K., and Nakayama, K. I. (2011). The FBXL5-IRP2 axis is integral to control of iron metabolism *in vivo*. *Cell Metab.* 14, 339–351. doi: 10.1016/j.cmet.2011.07.011

Moroishi, T., Yamauchi, T., Nishiyama, M., and Nakayama, K. I. (2014). HERC2 targets the iron regulator FBXL5 for degradation and modulates iron metabolism. *J. Biol. Chem.* 289, 16430–16441. doi: 10.1074/jbc.M113.541490

Nan, H., Kraft, P., Qureshi, A. A., Guo, Q., Chen, C., Hankinson, S. E., et al. (2009). Genome-wide association study of tanning phenotype in a population of European ancestry. *J. Invest. Dermatol.* 129, 2250–2257. doi: 10.1038/jid.2009.62

Neubert, G., von Au, K., Drossel, K., Tzschach, A., Horn, D., Nickel, R., et al. (2013). Angelman syndrome and severe infections in a patient with de novo 15q11.2-q13.1 deletion and maternally inherited 2q21.3 microdeletion. *Gene* 512, 453–455. doi: 10.1016/j.gene.2012.10.061

Neumann, M., Vosberg, S., Schlee, C., Heesch, S., Schwartz, S., Gokbuget, N., et al. (2015). Mutational spectrum of adult T-ALL. *Oncotarget* 6, 2754–2766. doi: 10.18632/oncotarget.2218

Nguyen, L.-T., Schmidt, H. A., von Haeseler, A., and Minh, B. Q. (2015). IQ-TREE: a fast and effective stochastic algorithm for estimating maximum-likelihood phylogenies. *Mol. Biol. Evol.* 32, 268–274. doi: 10.1093/molbev/msu300

Nguyen, L. S., Schneider, T., Rio, M., Moutton, S., Siquier-Pernet, K., Verny, F., et al. (2016). A nonsense variant in HERC1 is associated with intellectual disability, megalencephaly, thick corpus callosum and cerebellar atrophy. *Eur. J. Hum. Genet.* 24, 455–458. doi: 10.1038/ejhg.2015.140

Nishimoto, T., Eilen, E., and Basilico, C. (1978). Premature chromosome condensation in a ts DNA-mutant of BHK cells. *Cell* 15, 475–483. doi: 10.1016/0092-8674(78)90017-X

Oestergaard, V. H., Pentzold, C., Pedersen, R. T., Iosif, S., Alpi, A., Bekker-Jensen, S., et al. (2012). RNF8 and RNF168 but not HERC2 are required for DNA damage-induced ubiquitylation in chicken DT40 cells. *DNA Repair* 11, 892–905. doi: 10.1016/j.dnarep.2012.08.005

Ortega-Recalde, O., Beltran, O. I., Galvez, J. M., Palma-Montero, A., Restrepo, C. M., Mateus, H. E., et al. (2015). Biallelic HERC1 mutations in a syndromic form of overgrowth and intellectual disability. *Clin. Genet.* 88, e1–e3. doi: 10.1111/cge.12634

Peng, Y., Dai, H., Wang, E., Lin, C. C.-J., Mo, W., Peng, G., et al. (2015). TUSC4 functions as a tumor suppressor by regulating BRCA1 stability. *Cancer Res.* 75, 378–386. doi: 10.1158/0008-5472.CAN-14-2315

Perez-Villegas, E. M., Negrete-Diaz, J. V., Porras-Garcia, M. E., Ruiz, R., Carrion, A. M., Rodriguez-Moreno, A., et al. (2018). Mutation of the HERC 1 ubiquitin ligase impairs associative learning in the lateral amygdala. *Mol. Neurobiol.* 55, 1157–1168. doi: 10.1007/s12035-016-0371-8

Ping, Z., Siegal, G. P., Harada, S., Eltoum, I.-E., Youssef, M., Shen, T., et al. (2016). ERBB2 mutation is associated with a worse prognosis in patients with CDH1 altered invasive lobular cancer of the breast. *Oncotarget* 7, 80655–80663. doi: 10.18632/oncotarget.13019

Puffenberger, E. G., Jinks, R. N., Wang, H., Xin, B., Fiorentini, C., Sherman, E. A., et al. (2012). A homozygous missense mutation in HERC2 associated with global developmental delay and autism spectrum disorder. *Hum. Mutat.* 33, 1639–1646. doi: 10.1002/humu.22237

Roberts, J. L., Hovanes, K., Dasouki, M., Manzardo, A. M., and Butler, M. G. (2014). Chromosomal microarray analysis of consecutive individuals with autism spectrum disorders or learning disability presenting for genetic services. *Gene* 535, 70–78. doi: 10.1016/j.gene.2013.10.020

Rosa, J. L., and Barbacid, M. (1997). A giant protein that stimulates guanine nucleotide exchange on ARF1 and Rab proteins forms a cytosolic ternary complex with clathrin and Hsp70. *Oncogene* 15, 1–6. doi: 10.1038/sj.onc.1201170

Rosa, J. L., Casaroli-Marano, R. P., Buckler, A. J., Vilaró, S., and Barbacid, M. (1996). p619, a giant protein related to the chromosome condensation regulator RCC1, stimulates guanine nucleotide exchange on ARF1 and Rab proteins. *EMBO J.* 15, 4262–4273. doi: 10.1002/j.1460-2075.1996.tb00801.x

Ruiz, R., Perez-Villegas, E. M., Bachiller, S., Rosa, J. L., and Armengol, J. A. (2016). HERC 1 ubiquitin ligase mutation affects neocortical, CA3 hippocampal and spinal cord projection neurons: an ultrastructural study. *Front. Neuroanat.* 10:42. doi: 10.3389/fnana.2016.00042

Ryu, M.-S., Duck, K. A., and Philpott, C. C. (2018). Ferritin iron regulators, PCBP1 and NCOA4, respond to cellular iron status in developing red cells. *Blood Cells Mol. Dis.* 69, 75–81. doi: 10.1016/j.bcmd.2017.09.009

Sánchez-Tena, S., Cubillos-Rojas, M., Schneider, T., and Rosa, J. L. (2016). Functional and pathological relevance of HERC family proteins: a decade later. *Cell. Mol. Life Sci.* 73, 1955–1968. doi: 10.1007/s00018-016-2139-8

Schmelzer, C., and Doring, F. (2010). Identification of LPS-inducible genes downregulated by ubiquinone in human THP-1 monocytes. *Biofactors* 36, 222–228. doi: 10.1002/biof.93

Schneider, T., Martinez-Martinez, A., Cubillos-Rojas, M., Bartrons, R., Ventura, F., Rosa, J. L., et al. (2018). The E3 ubiquitin ligase HERC1 controls the ERK signaling pathway targeting C-RAF for degradation. *Oncotarget* 9, 31531–31548. doi: 10.18632/oncotarget.25847

Sigrist, C. J. A., de Castro, E., Cerutti, L., Cuche, B. A., Hulo, N., Bridge, A., et al. (2012). New and continuing developments at PROSITE. *Nucleic Acids Res.* 41, D344–D347. doi: 10.1093/nar/gks1067

Streich, F. C., and Lima, C. D. (2014). Structural and functional insights to ubiquitin-like protein conjugation. *Annu. Rev. Biophys.* 43, 357–379. doi: 10.1146/annurev-biophys-051013-022958

Sturm, R. A., Duffy, D. L., Zhao, Z. Z., Leite, F. P. N., Stark, M. S., Hayward, N. K., et al. (2008). A single SNP in an evolutionary conserved region within intron 86 of the HERC2 gene determines human blue-brown eye color. *Am. J. Hum. Genet.* 82, 424–431. doi: 10.1016/j.ajhg.2007.11.005

Sulovari, A., Kranzler, H. R., Farrer, L. A., Gelernter, J., and Li, D. (2015). Eye color: a potential indicator of alcohol dependence risk in European Americans. *Am. J. Med. Genet. B Neuropsychiatr. Genet.* 168B, 347–353. doi: 10.1002/ajmg.b.32316

Ulivi, S., Mezzavilla, M., and Gasparini, P. (2013). Genetics of eye colours in different rural populations on the Silk Road. *Eur. J. Hum. Genet.* 21, 1320–1323. doi: 10.1038/ejhg.2013.41

Utine, G. E., Taskiran, E. Z., Kosukcu, C., Karaosmanoglu, B., Guleray, N., Dogan, O. A., et al. (2017). HERC1 mutations in idiopathic intellectual disability. *Eur. J. Med. Genet.* 60, 279–283. doi: 10.1016/j.ejmg.2017.03.007

Valnegri, P., Huang, J., Yamada, T., Yang, Y., Mejia, L. A., Cho, H. Y., et al. (2017). RNF8/UBC13 ubiquitin signaling suppresses synapse formation in the mammalian brain. *Nat. Commun.* 8:1271. doi: 10.1038/s41467-017-01333-6

Walkowicz, M., Ji, Y., Ren, X., Horsthemke, B., Russell, L. B., Johnson, D., et al. (1999). Molecular characterization of radiation- and chemically induced mutations associated with neuromuscular tremors, runting, juvenile lethality, and sperm defects in jdf2 mice. *Mamm. Genome* 10, 870–878. doi: 10.1007/s003359901106

Walz, C., Grimwade, D., Saussele, S., Lengfelder, E., Haferlach, C., Schnittger, S., et al. (2010). Atypical mRNA fusions in PML-RARA positive, RARA-PML negative acute promyelocytic leukemia. *Genes Chromosomes Cancer* 49, 471–479. doi: 10.1002/gcc.20757

Wang, K., Baldassano, R., Zhang, H., Qu, H.-Q., Imielinski, M., Kugathasan, S., et al. (2010). Comparative genetic analysis of inflammatory bowel disease and type 1 diabetes implicates multiple loci with opposite effects. *Hum. Mol. Genet.* 19, 2059–2067. doi: 10.1093/hmg/ddq078

Waterhouse, A., Bertoni, M., Bienert, S., Studer, G., Tauriello, G., Gumienny, R., et al. (2018). SWISS-MODEL: homology modelling of protein structures and complexes. *Nucleic Acids Res.* 46, W296–W303. doi: 10.1093/nar/gky427

Weersma, R. K., Stokkers, P. C. F., Cleynen, I., Wolfkamp, S. C. S., Henckaerts, L., Schreiber, S., et al. (2009). Confirmation of multiple Crohn's disease susceptibility loci in a large Dutch-Belgian cohort. *Am. J. Gastroenterol.* 104, 630–638. doi: 10.1038/ajg.2008.112

Wilde, S., Timpson, A., Kirsanow, K., Kaiser, E., Kayser, M., Unterlander, M., et al. (2014). Direct evidence for positive selection of skin, hair, and eye pigmentation in Europeans during the last 5,000 y. *Proc. Natl. Acad. Sci. USA* 111, 4832–4837. doi: 10.1073/pnas.1316513111

Wu, W., Rokutanda, N., Takeuchi, J., Lai, Y., Maruyama, R., Togashi, Y., et al. (2018). HERC2 facilitates BLM and WRN helicase complex interaction with RPA to suppress G-Quadruplex DNA. *Cancer Res.* 78, 6371–6385. doi: 10.1158/0008-5472.CAN-18-1877

Wu, W., Sato, K., Koike, A., Nishikawa, H., Koizumi, H., Venkitaraman, A. R., et al. (2010). HERC2 is an E3 ligase that targets BRCA1 for degradation. *Cancer Res.* 70, 6384–6392. doi: 10.1158/0008-5472.CAN-10-1304

Xue, Y., Zhang, X., Huang, N., Daly, A., Gillson, C. J., Macarthur, D. G., et al. (2009). Population differentiation as an indicator of recent positive selection in humans: an empirical evaluation. *Genetics* 183, 1065–1077. doi: 10.1534/genetics.109.107722

Yoo, N. J., Park, S. W., and Lee, S. H. (2011). Frameshift mutations of ubiquitination-related genes HERC2, HERC3, TRIP12, UBE2Q1 and UBE4B in gastric and colorectal carcinomas with microsatellite instability. *Pathology* 43, 753–755. doi: 10.1097/PAT.0b013e32834c7e78

Yuan, J., Luo, K., Deng, M., Li, Y., Yin, P., Gao, B., et al. (2014). HERC2-USP20 axis regulates DNA damage checkpoint through Claspin. *Nucleic Acids Res.* 42, 13110–13121. doi: 10.1093/nar/gku1034

Yuasa, I., Umetsu, K., Nishimukai, H., Fukumori, Y., Harihara, S., Saitou, N., et al. (2009). HERC1 polymorphisms: population-specific variations in haplotype composition. *Cell Biochem. Funct.* 27, 402–405. doi: 10.1002/cbf.1582

Yucesoy, B., Kaufman, K. M., Lummus, Z. L., Weirauch, M. T., Zhang, G., Cartier, A., et al. (2015). Genome-wide association study identifies novel loci associated with diisocyanate-induced occupational asthma. *Toxicol. Sci.* 146, 192–201. doi: 10.1093/toxsci/kfv084

Zhang, Z., Yang, H., and Wang, H. (2014). The histone H2A deubiquitinase USP16 interacts with HERC2 and fine-tunes cellular response to DNA damage. *J. Biol. Chem.* 289, 32883–32894. doi: 10.1074/jbc.M114.599605

Zhu, D., Yang, D., Li, X., and Feng, F. (2018). Heterogeneous expression and biological function of SOX18 in osteosaroma. *J. Cell. Biochem.* 119, 4184–4192. doi: 10.1002/jcb.26635

Zhu, M., Zhao, H., Liao, J., and Xu, X. (2014). HERC2/USP20 coordinates CHK1 activation by modulating CLASPIN stability. *Nucleic Acids Res.* 42, 13074–13081. doi: 10.1093/nar/gku978

**Conflict of Interest Statement:** The authors declare that the research was conducted in the absence of any commercial or financial relationships that could be construed as a potential conflict of interest.

frontiers in Physiology

REVIEW
published: 01 October 2019
doi: 10.3389/fphys.2019.01144

# Cullin Ring Ubiquitin Ligases (CRLs) in Cancer: Responses to Ionizing Radiation (IR) Treatment

*Shahd Fouad[1], Owen S. Wells[2], Mark A. Hill[1] and Vincenzo D'Angiolella[1]**

*[1] Medical Research Council Institute for Radiation Oncology, Department of Oncology, University of Oxford, Oxford, United Kingdom, [2] Genome Damage and Stability Centre, School of Life Sciences, University of Sussex, Brighton, United Kingdom*

OPEN ACCESS

**Edited by:**
*Fumiyo Ikeda, Institute of Molecular Biotechnology (OAW), Austria*

**Reviewed by:**
*Sumit Sahni, Kolling Institute of Medical Research, Australia*
*Giovanna Calabrese, University of Catania, Italy*

***Correspondence:**
*Vincenzo D'Angiolella vincenzo.dangiolella@oncology.ox.ac.uk*

**Specialty section:**
*This article was submitted to Integrative Physiology, a section of the journal Frontiers in Physiology*

**Received:** *03 May 2019*
**Accepted:** *22 August 2019*
**Published:** *01 October 2019*

**Citation:**
*Fouad S, Wells OS, Hill MA and D'Angiolella V (2019) Cullin Ring Ubiquitin Ligases (CRLs) in Cancer: Responses to Ionizing Radiation (IR) Treatment. Front. Physiol. 10:1144. doi: 10.3389/fphys.2019.01144*

Treatment with ionizing radiation (IR) remains the cornerstone of therapy for multiple cancer types, including disseminated and aggressive diseases in the palliative setting. Radiotherapy efficacy could be improved in combination with drugs that regulate the ubiquitin-proteasome system (UPS), many of which are currently being tested in clinical trials. The UPS operates through the covalent attachment of ATP-activated ubiquitin molecules onto substrates following the transfer of ubiquitin from an E1, to an E2, and then to the substrate *via* an E3 enzyme. The specificity of ubiquitin ligation is dictated by E3 ligases, which select substrates to be ubiquitylated. Among the E3s, cullin ring ubiquitin ligases (CRLs) represent prototypical multi-subunit E3s, which use the cullin subunit as a central assembling scaffold. CRLs have crucial roles in controlling the cell cycle, hypoxia signaling, reactive oxygen species clearance and DNA repair; pivotal factors regulating the cancer and normal tissue response to IR. Here, we summarize the findings on the involvement of CRLs in the response of cancer cells to IR, and we discuss the therapeutic approaches to target the CRLs which could be exploited in the clinic.

**Keywords: cullins, ionizing radiation (IR), double-strand breaks (DSBs), DNA-damage, cullin ring ligases (CRLs), E3-ligases**

## INTRODUCTION: THE CULLIN RING UBIQUITIN LIGASES

Ubiquitylation is a versatile post-translational modification to control protein levels in cells and modulate cellular states to allow adaptation under stress. Indeed, this secondary modification is crucial for the cellular response to DNA damaging agents including (Ionizing Radiation) IR (Schwertman et al., 2016). The classical process of ubiquitylation is based on the activation of a ubiquitin molecule by ATP, followed by its covalent attachment to an E1 enzyme,

then its transfer from the E1 enzyme to an E2 enzyme, and finally its transfer from the E2 enzyme onto selected substrates (Hershko et al., 1983; Finley et al., 2004). Selection of substrates is operated by the E3 enzymes, which bridge substrates to the E2 enzyme for ubiquitin transfer. The human genome codes for 2 E1s, ∼35 E2s and more than 700 E3 ubiquitin ligases. The organization of the system is hierarchical which allows for substrate specificity and, at the same time, diversity in substrate modification.

Cullin ring ubiquitin ligases are multi-subunit E3 ubiquitin ligases which use a specific cullin as a central scaffold to bridge an E2 enzyme to the substrate. All the cullin complexes use a cullin C-terminal portion to recruit a RING-Box protein (Rbx1 or Rbx2), required for the interaction with an E2. The N-terminal portion of the cullin binds to a different adaptor protein containing a domain that interacts with a range of variable substrate recruitment subunits, specific to that culllin class. In general, an adaptor protein, different for each cullin, links the cullin N-terminus to the aforementioned variable substrate recruitment subunit (Sarikas et al., 2011). The specific complexes formed by Cul1, Cul2, Cul3, Cul4, Cul5, Cul7, and Cul9 are highlighted in **Figure 1** and are individually discussed below.

The prototypical multi-subunit E3s are Cullin1-based E3s, which assemble an SCF complex composed of Skp1, Cul1, and an F-box protein. In this particular E3 machinery, the Cul1 N-terminus binds to Skp1 (adaptor subunit), which in turn binds to a variable F-box protein (**Figure 1A**). F-box proteins derive their name from cyclin F in which the F-box domain, required for interaction with Skp1, was first discovered (Bai et al., 1996). After the discovery of cyclin F, about 69 F-box proteins were identified in the human genome based on their interaction with Skp1 and sequence homology within the F-box domain (Cenciarelli et al., 1999; Winston et al., 1999). F-box proteins were further sub-classified according to the protein domains they use to recruit substrates. Three F-box subfamilies exist; a subfamily that has a WD-40 domain (Fbxws), another that has a Leucine zipper (Fbxls) and finally one that has other variable domains (Fbxos) (Jin et al., 2004) (**Figure 1A**).

Work in the nematode *C. elegans* revealed the presence of cullin genes highly related and similar to Cul1. A search for EST in the human database identified Cul1, Cul2, Cul3, Cul4A, Cul4B, and Cul5 genes (Kipreos et al., 1996). Although the general organization of Cul2, Cul3, Cul4A, Cul4B, and Cul5 resemble the SCF assembly, structural studies have revealed substantial differences in the assembly and use of adaptors. These different features likely reflect different biochemical properties and mechanisms of action/ubiquitylation, however, studies on the kinetics of action comparing Cul1 to Cul2, Cul3, Cul4A, Cul4B, and Cul5 are lacking.

Cul2 and Cul5 are the most structurally related among the cullins and use elongins B and C as adaptors to engage a variable substrate recruitment protein. Among the most well-studied substrate recruitment proteins are the VHL tumor suppressor protein and VHL-like proteins, which use Cul2 as scaffold. Cul5 also recruits elongins B and C as adaptors but assembles with SOCS proteins to form a functional E3 (**Figure 1B**). The difference in specificity between Cul2 and Cul5 is related to the presence of a Cul2 and a Cul5 box, and these two distinct sequences mediate the interaction with the substrate recruitment subunits (Kamura et al., 2004).

In Cul3 complexes several BTB domain-containing proteins assemble directly with Cul3 and act as both an adaptor and a substrate recognition subunit. The BTB domain-containing proteins recognize substrates with their MATH (Meprin and TRAF homology) motif and Kelch beta-propeller repeats (Pintard et al., 2004; Genschik et al., 2013). A characteristic of these complexes is their intrinsic capacity for assembling homo-dimers through the BTB (**Figure 1C**). A quality control system regulating homo-heterodimerization of Kelch like proteins (Klhls) has recently been unveiled and depends on the activity of another E3 ubiquitin ligase of the F-box clade (Fbxl17) (Mena et al., 2018).

Cul4 machineries, which comprise Cul4A and Cul4B, use Ddb1 as an adapter. Ddb1 contains three WD40 propeller domains (BPA, BPB, and BPC) and assembles with a large family of DCAF (Ddb1 and Cul4 Associated Factor) proteins using a WDXR motif within the substrate recruitment factors (**Figure 1D**) (Jin et al., 2006).

Cul7 is similar to Cul1 in using Skp1 as an adaptor and recruiting Fbxw8 as a substrate receptor (Dias et al., 2002), but

**Abbreviations:** APOBEC3G, apolipoprotein B mRNA editing enzyme catalytic subunit 3G; ARE, antioxidant response element; ATF, activating transcription factor; ATM, ataxia telangiectasia-mutated; ATR, ataxia telangiectasia and Rad3-related; BACK, BTB and C-terminal kelch; BRCA, breast cancer susceptibility gene/protein; BTB, bric-a-brac/tramtrack/broad complex; β-TrCP, beta transduction repeat-containing protein; Cdc25, cell division cycle 25; Cdt, chromatin licensing and DNA replication factor; CDK, cyclin-dependent kinase; Chk, checkpoint kinase; CkIα, casein kinase Iα; CRBN, cereblon; CRL, cullin-RING ligase; Cul, cullin; DCAF, Ddb1 and Cul4-associated factor; Ddb1, UV-damaged DNA-binding protein 1; DDR, DNA damage response; dNTPs, deoxyribonucleotides; DSB, double-strand break; Emi1, early mitotic inhibitor 1; EST, expressed sequence tag; Exo1, exonuclease 1; FDA, US Food and Drug Administration; Gsk3β, glycogen synthase kinase 3 Beta; Hif, hypoxia-inducible factor; HIV, human immunodeficiency virus; HPV, human papilloma virus; HR, homologous recombination; IR, ionizing radiation; Jak2, Janus kinase 2; Jfk, just one F-box and kelch domain-containing protein; Kdm4A, lysine demethylase 4A; Keap1, kelch-like ECH-associated protein; Klhl, kelch-like protein; Ku, Ku70/Ku80 heterodimer; MAPK, mitogen-activated protein kinase; MATH, meprin and TRAF homology; MDM2, mouse double minute 2, human homolog of; P53-binding protein matrix extracellular; Mepe/Of, phosophoglycoprotein/osteoblast factor; MRN, Mre11-Rad50-Nbs1 complex; Nek11, NIMA (never in mitosis gene A)-related kinase 11; NF-κB, nuclear factor kappa-light-chain-enhancer of activated B cells; NHEJ, non-homologous end joining; NLS, nuclear localization signal; Nrf2, Nf-E2-related factor 2; ODD, oxygen-dependent degradation; PALB2, partner and localizer of BRCA2; PARP, poly-ADP-ribose polymerase; PCNA, proliferating cell nuclear antigen; Pd-1, programed cell death protein 1; PDGF, platelet-derived growth factor; Pd-L1, programed cell death 1 ligand 1; Plk1, polo like kinase 1; PML, promyelocytic leukemia; PROTAC, proteolysis-targeting chimera; Rbx, RING-box protein; Rnf, RING-finger protein; RNR, ribonucleotide reductase; ROS, reactive oxygen species; RRM, ribonucleotide reductase family member; SCCHN, squamous cell carcinoma of the head and neck; SCF, Skp1/Cul1/F-box protein; Skp1, S-phase kinase-associated protein 1; SOCS, suppressor of cytokine signaling; Spop, speckle-type poxvirus and zinc-finger protein; SRM, substrate recruitment motif; SSB, single-strand break; STAT, signal transducer and activator of transcription; Tip60, 60 kDa tat-interactive protein; TOP3, TAT-ODD-procaspase-3; UPS, ubiquitin-proteasome system; Usp11, ubiquitin specific peptidase 11; VEGF, vascular endothelial growth factor; VHL, von-Hippel-Lindau; Vif, viral infectivity factor; Wsb1, WD repeat and SOCS box-containing protein 1; Xrcc4, X-ray repair cross complementing 4.

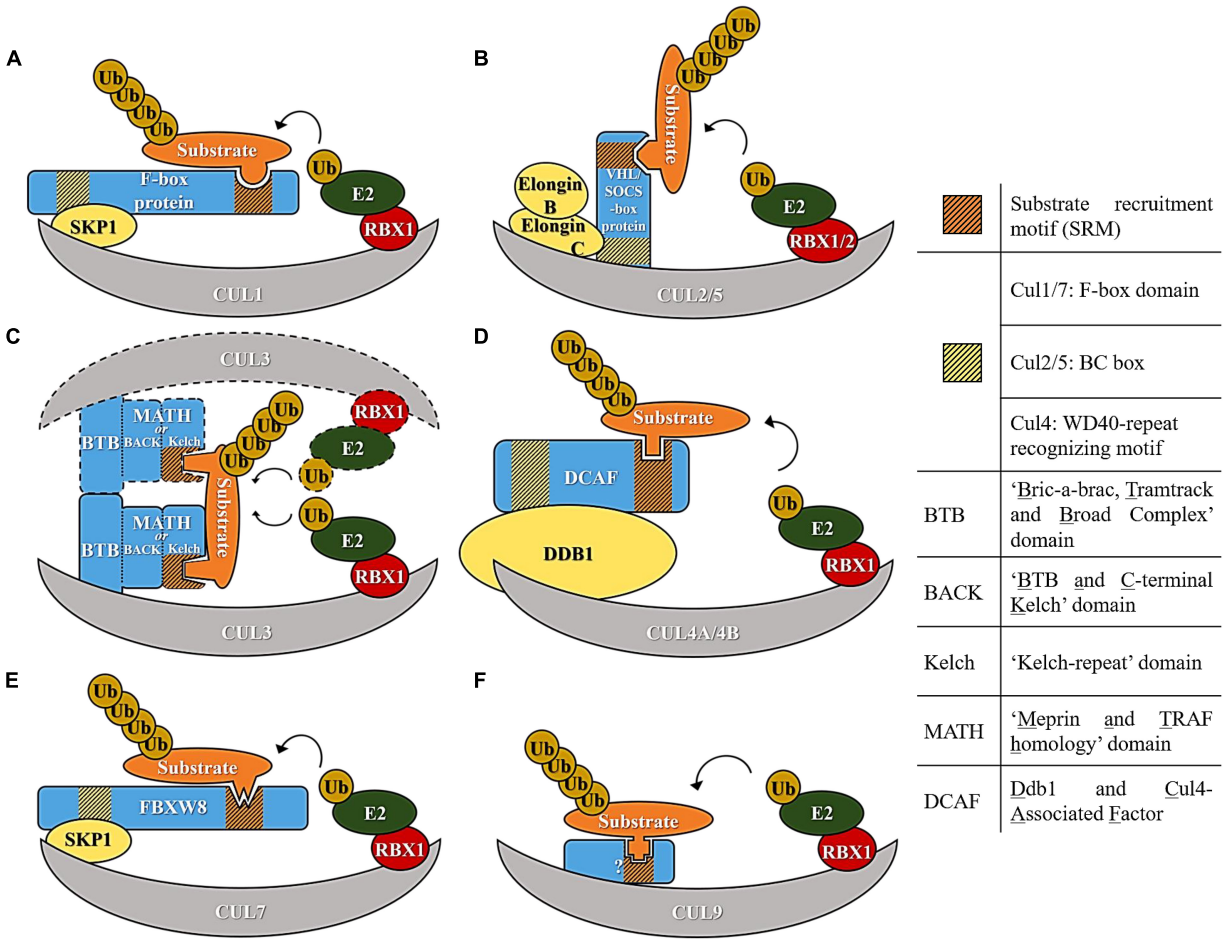


**FIGURE 1 |** Diagram representing E3 ubiquitin ligase complexes of the cullin family of E3 ligases. **(A)** Cul1-based E3 ligase. **(B)** Cul2/5-based E3 ligase. **(C)** Cul3-based E3 ligase. **(D)** Cul4-based E3 ligase. **(E)** Cul7-based E3 ligase. **(F)** Cul9-based E3 ligase.

it can only assemble with Fbxw8 and not other F-box proteins (**Figure 1E**). The last member of the family and the most recently identified is Cul9 for which features of a cullin assembly are less clear (**Figure 1F**).

An attribute of the majority of the substrate recruitment subunits of the CRLs is that they recognize modified or unmodified short and unique amino acid sequences in substrates to initiate substrate engagement and ubiquitylation. These are collectively termed "degrons," as they mark proteins for proteasomal degradation by the respective cullin machinery. Degrons are well-established but only for a small fraction of CRLs and novel insights have been recently made in deciphering the degron code at a system-wide level (Koren et al., 2018). Although the general organization of CRLs is conserved across different cullins there are substantial differences in complex assembly, which could dictate diverse modes of substrate engagement and modification. As more details of substrate engagement and ubiquitin chain specificity emerge, it will be important to compare the kinetics of action as well as the specificities of the different CRL complexes.

CRL complexes have been linked to many aspects of tumorigenesis as they participate in multiple biological processes. This review focuses specifically on the role of CRLs in the cellular response to IR covering also aspects of IR responses not related strictly to DSB repair.

## IONIZING RADIATION-INDUCED DAMAGE

IR can induce a wide variety of biological effects within the cells and tissues and there is strong evidence to suggest that DNA damage is a major consequence. Indeed, a typical 2 Gy X-ray fraction used in clinical radiotherapy will result in approximately 80 DSBs, 2,000 SSBs, and over 4,000 base damages (Shrieve and Loeffler, 2011). Interestingly, the number of DNA lesions produced is low in comparison to the background level of endogenous DNA damage which corresponds to the order of 50,000 DNA lesions per day as a result of Reactive Oxygen Species (ROS) and other reactive metabolites (De Bont and van Larebeke, 2004). A critical feature of all types of IR is the deposition of

energy in the form of highly structured tracks of ionization and excitation events and is therefore highly heterogeneous in space and time (Hill, 2018). This results in clusters of events not only on the nanometer scale, but in some cases on the micrometer scale, which could be responsible for the effectiveness of IR in treating cancers.

Damage to DNA is produced either by direct ionization of constituent atoms or indirectly as a result of free radicals produced close by in the surrounding water. This indirect damage is dominated by the hydroxyl (OH) radical which has a lifetime of $\sim$ 4 ns and a diffusion distance of $\sim$6 nm within the cell (Roots and Okada, 1975). As a result of clustering, these events not only produce simple isolated lesions such as base damage, abasic sites, SSBs, DNA-protein cross-links, but importantly are also efficient at producing combinations of these, including complex SSBs, DSBs, or complex DSBs. The increase in complexity of these DSBs results in an increase in the lifetime of these lesions and a decrease in overall repairability (Eccles et al., 2011). The relative proximity of these breaks can subsequently result in a wide range of chromosome aberrations including deletions, and for many cell types is an important driver of cell death as a result of a mitotic catastrophe.

While DNA damage produced is likely to dominate the response following clinical exposures, it is also known that IR can perturb existing intra- and inter-cellular signaling which may result in a change in the background level of ROS. These changes may be temporary but can often result in a persistent change in homeostasis of this signaling, and associated changes in oxidative stress can lead to a modulation of the background rate of endogenous DNA damage induction. Almost all solid tumors contain oxygen-deficient regions and as a result oxygen, or more specifically the absence of it, can play a significant role in the radiation response of tumors. The presence of oxygen at the time of irradiation results in an enhancement in the yield and complexity of the initial damage produced over that produced under hypoxia, as a result of the oxygen chemically "fixing" the damage thereby making it permanent (Rockwell et al., 2009). In addition to modulating the initial DNA damage produced by radiation, hypoxia results in the dysregulation of oxygen homeostasis and activates pathways which alter the phenotype of the cell, adapting the cell to the stress associated with low oxygen levels.

## ROLES OF Cul1 IN THE CELLULAR RESPONSE TO IR

### Cul1 and IR-Induced Cell Cycle Arrest

Cells entering the cell cycle duplicate their DNA in S phase and complete cell division in M phase. The presence of checkpoints allows fidelity of cell cycle transitions. For instance, when cells are exposed to IR, the DNA damage generated promotes the activation of a checkpoint response. Cell cycle progression restarts only when the DNA damage is repaired.

The progression from one cell cycle phase to the next is promoted by the periodic oscillations of cyclins that partner with CDKs to phosphorylate target substrates (Murray, 2004). The activity of CDKs is halted by phosphorylation of the CDK subunit on tyrosine 15 mediated by the tyrosine kinase Wee1 and reverted by the Cdc25A phosphatase. The presence of DNA damage induced by IR activates checkpoint kinases (Chk1 and Chk2) whose role is to prevent the activity of CDKs and arrest cell cycle progression to allow DNA repair. Chk1 performs this function by controlling the ubiquitylation and subsequent degradation of the Cdc25A phosphatase (Busino et al., 2003; Jin et al., 2003). Cdc25A activates CDKs by removing the Wee1-mediated inhibitory phosphorylation on Tyr15 of CDKs. Therefore, upon activation of Chk1, the degradation of Cdc25A prevents CDK activity which in turn restrains DNA replication and progression of the cell cycle (Bartek and Lukas, 2003).

Beta Transduction Repeat-Containing Proteins β-TrCP1/Fbxw1 and β-TrCP2/Fbxw11, jointly referred to as β-TrCP, are the two Cul1 E3 ubiquitin ligases promoting the degradation of Cdc25A (Busino et al., 2003; Jin et al., 2003). A feature of the $SCF^{\beta\text{-}TrCP}$ ubiquitin ligase is that it recognizes substrates containing the degron sequence DSGXXS in which both serines need to be phosphorylated (Guardavaccaro et al., 2003). Chk1 promotes the phosphorylation of Cdc25A and its subsequent degradation but the specific kinases responsible for Cdc25A degron phosphorylation are not completely clear. A number of kinases have been proposed to phosphorylate Cdc25A in addition to Chk1. Cdc25A, unlike the majority of other β-TrCP substrates that have the consensus degron DSGXXS, has the alternate degron $^{76}$SSESTDSG$^{83}$ with serines Ser76, Ser79, and Ser82 phosphorylated (Busino et al., 2003; Jin et al., 2003). CkIα was shown to phosphorylate Ser76 of Cdc25A (Honaker and Piwnica-Worms, 2010), while Nek11 was shown to phosphorylate Ser82 (Melixetian et al., 2009). Gsk3β can carry out the priming phosphorylation of Ser76 on the Cdc25A degron (Kang et al., 2008).

The choice of kinase could be influenced by the cell cycle phase, for example Nek11-phosphorylation of Cdc25A is most active in S and G2 phases and is required for the establishment of a G2/M checkpoint promoted by IR, whereas Gsk3β and Chk1 are active in G1 and S phases. The control of Cdc25A by β-TrCP following DNA damage is crucial for normal cell cycle progression and the checkpoint response. Therefore, it represents a node with multiple control points. The lack of β-TrCP and Cdc25A degradation forces cells to undergo DNA replication in the presence of DNA damage, giving rise to a subsequent mitotic catastrophe and cell death (Busino et al., 2003; Jin et al., 2003).

In addition to Cdc25A, β-TrCP regulates other crucial components of the checkpoint response: Claspin and Wee1. Wee1 counteracts the activity of Cdc25A on CDK1. It follows that since β-TrCP is simultaneously acting on Wee1 and Cdc25A, the net effect of blocking β-TrCP should have no overall impact on cell cycle progression. However, the consequences of β-TrCP knockdown are significant. The discrepancy could be explained by the different-timed action of β-TrCP on Cdc25A and Wee1 dictated by the kinases responsible for phosphorylating the respective degrons. The kinases phosphorylating Cdc25A are acting when the checkpoint is operating, whereas the kinases phosphorylating Wee1 are Polo Like Kinase 1 (Plk1) and CDK1

itself, whose activity marks mitotic entry and, thus, checkpoint resolution (Watanabe et al., 2004).

An important sensor of DNA damage functioning to sustain the checkpoint response is Claspin. Claspin is required for Chk1 activity prompted by the ATR kinase, which detects the presence of DNA damage. Claspin levels are also regulated by β-TrCP, and Plk1 kinase triggers Claspin degradation (Mailand et al., 2006; Peschiaroli et al., 2006). This β-TrCP-mediated degradation of Claspin prevents any further activation of Chk1 during recovery from genotoxic stress. The process facilitates the restart of the cell cycle once the DNA damage has been resolved. The leftover active Chk1 is targeted for degradation by the F-box protein Fbxo6. Fbxo6 regulates Chk1 degradation to terminate the checkpoint response in S phase (Zhang et al., 2005; Zhang Y.-W. et al., 2009). From the regulation of Cdc25A, Wee1, Claspin and Chk1 by β-TrCP and Fbxo6, a temporally-ordered picture of checkpoint activation and resolution emerges where the action of kinases is enforced and coordinated by E3 ubiquitin ligases to promote irreversible cell cycle phase transitions.

Interestingly, Liu and colleagues reported that Matrix Extracellular Phosphoglycoprotein/Osteoblast Factor 45 (Mepe/Of45) is a co-factor of Chk1. Upon knocking down Mepe/Of45 in transformed rat embryo fibroblasts, Chk1 levels decrease which sensitizes cells to IR and other DNA damaging agents. It is suggested that the way Mepe/Of45 achieves that is by competing with the E3 ubiquitin ligases binding to Chk1, therefore decreasing the degradation of Chk1 by the UPS (Liu et al., 2009). However, more detailed mechanistic insights are necessary to derive a clear picture of the role of Mepe/Of45.

Another Cul1 adaptor with important roles in the IR-induced checkpoint response is cyclin F (Fbxo1). It has been shown that cyclin F prevents mitotic entry after IR by enforcing a G2 checkpoint. The mechanism relies on the capacity of cyclin F to competitively inhibit B-Myb. B-Myb activates the transcription of a number of genes required for mitotic entry, therefore the inhibition of transcriptional activity of B-Myb by cyclin F enables cyclin F to control mitotic entry after IR (Klein et al., 2015). Our laboratory has shown that the levels of cyclin F are reduced by β-TrCP at mitotic entry to facilitate the transition from G2 to M phase of the cell cycle (Mavrommati et al., 2018). However, it is yet unclear whether the regulation of cyclin F by β-TrCP has a role in the checkpoint response induced by IR in G2 as well.

It is also important to note that cyclin F ubiquitylates Exo1 which is a 5′ to 3′ exonuclease with a significant role in DNA repair after IR (Elia et al., 2015). One of the major forms of DNA damage induced by IR is the formation of DSBs. DSBs could be repaired by two main pathways: (1) simply ligating the broken ends together by non-homologous end joining (NHEJ); (2) by using a second copy of DNA as a template to initiate homologous recombination (HR). HR includes a number of steps which enable the engagement of a second copy of DNA to use as a template. An important part of the process that commits the cells to repair through HR is the resection of the broken ends of DNA to facilitate strand invasion of the homologous template. Exo1 controls long-range resection at DSBs upon IR, a process that needs to be tightly regulated to avoid hyper or hypo activity of Exo1. Thus, Exo1 levels are regulated by both phosphorylation and ubiquitylation after IR (Tomimatsu et al., 2017). Cyclin F was shown to mediate ubiquitylation of Exo1 after cells were challenged with 4NQO, a radio-mimetic drug (Elia et al., 2015), however it is unclear whether cyclin F is participating in regulating Exo1 levels and activity (and therefore resection) after IR.

Exo1 is not the only substrate of cyclin F involved in maintaining genome stability; there is also RRM2. RRM2 assembles with the RRM1 subunit to form a functional RNR, an essential enzyme in the production of deoxyribonucleotides (dNTPs) which are the building blocks of DNA (Nordlund and Reichard, 2006). The activity of RNR must be regulated in accordance with the cell cycle to maintain balanced levels of dNTPs for optimal DNA replication and DNA repair (D'Angiolella et al., 2012).

Abnormal dNTP levels have a negative effect on genomic stability and are known to promote transformation as well as an increase in the frequency of spontaneous mutations (Kunz et al., 1994). Accordingly, the overexpression of RRM2 promotes the development of lung cancer in mice (Xu et al., 2008), and elevated levels of RRM2 are often linked to poor prognosis in different cancer types (Morikawa et al., 2010a,b; Jones et al., 2011). RRM2 is targeted for degradation by cyclin F after phosphorylation of RRM2 on Thr33 by cyclin A/CDK1. This phosphorylation of RRM2 by CDK1 represents a failsafe mechanism to destroy RRM2 only in G2/M when the bulk of DNA replication has been completed (D'Angiolella et al., 2012). RRM2 alterations have been shown to impact DSB repair by HR in yeast (Moss et al., 2010) and mammalian cells (Gustafsson et al., 2018), thus cyclin F could also impact IR response by regulating RRM2.

Two other F-box proteins involved in checkpoint activation in response to IR are Fbxo4 and Fbxo31. This is due to their ability to regulate cyclin D1 levels following IR. Cyclin D1 promotes entry into the cell cycle from G0, and the regulation of cyclin D levels is important after the genotoxic stress induced by IR to promote cell survival (Lukas et al., 1994; Pagano et al., 1994; Agami and Bernards, 2000). It has been shown that the phosphorylation of Thr286 of cyclin D1 promotes the degradation of cyclin D1 by Fbxo4 in a cell cycle-dependent manner both in the absence of genotoxic stress, and in response to DNA damage (Pontano et al., 2008). Cell cycle-linked degradation of cyclin D1 by Fbxo4 requires RAS/RAF as its upstream pathway, whereas the DNA damage-induced degradation of cyclin D1 requires the ATM pathway (Pontano et al., 2008). Similarly to Fbxo4, Fbxo31 targets cyclin D1 for degradation after phosphorylation of Thr286, but in this case the presence of DNA damage is central to promote its degradation. The levels of Fbxo31 increase after DNA damage, unlike the levels of Fbxo4. Evidence indeed suggests that Fbxo31-mediated degradation of cyclin D1 following DNA damage may explain the prompt implementation of G1 arrest for checkpoint control (Santra et al., 2009).

## Cul1 and p53-Mediated Checkpoint Response

Arguably, the most important regulator of cell fate upon checkpoint responses is the tumor suppressor and transcription factor p53. Upon IR, p53 is activated to promote the transcription of thousands of genes required for multiple cellular functions

that range from activation of cell death and immune responses to checkpoint control and DNA repair. The major E3 ubiquitin ligase for p53 is MDM2, which targets p53 for ubiquitylation to maintain it in an inactive state (Momand et al., 1992; Oliner et al., 1993). However, given its central role, p53 is regulated by a myriad of other mechanisms. Such complex regulation is necessary, because p53 represents a central hub for cell survival, thus, multiple diverse pathways converge to regulate its function. For instance, numerous studies uncovered links between p53 and NF-κB, a family of transcription regulators with roles in regulating proliferation, apoptosis, inflammation, and the DDR (Wang et al., 2017). Interestingly, one study showed that IκB Kinase 2 (IKK2/IKKβ) phosphorylates p53 on Ser362 and Ser366, and stimulates the $SCF^{\beta\text{-}TrCP}$-mediated degradation of p53 (Xia et al., 2009). This is required to enforce inactivation of p53 in addition to the role of MDM2, however, biological consequences of this regulation are not yet fully elucidated.

The literature is somewhat confusing with regards to the regulation of p53 as another study suggests that MDM2 can be targeted for degradation by β-TrCP. MDM2 is phosphorylated by CkIα on multiple putative β-TrCP degrons (Inuzuka et al., 2010). This mechanism of regulation of MDM2 could be relevant after repeated DNA damage insults to control the transcriptional activity of p53. It is important to note that other researchers pointed out that what seems to be the degradation of MDM2 could just be epitope-masking by phosphorylation which blocks the epitope for the most commonly used MDM2 western blotting antibodies (Cheng and Chen, 2011).

Besides β-TrCP and MDM2, several ubiquitin ligases also target p53 for degradation like the Kelch domain-containing F-box protein, Jfk (Fbxo42). Jfk was found to inhibit p53-dependent transcription, and the depletion of Jfk was found to stabilize p53 and hence sensitizes cells to IR-induced DNA damage (Sun et al., 2009).

Among the transcriptional targets of p53, p21 has the most significant function in promoting cell cycle arrest. p21 acts as a direct inhibitor of CDKs and is required to enforce checkpoint control. Fbxl1, more widely-recognized as Skp2, targets p21 and p27 (the two CDK inhibitors) for ubiquitin-mediated proteolysis (Carrano et al., 1999). Skp2 has been linked to the regulation of a p53-dependent checkpoint response in melanoma cells through the control of p27 (Hu and Aplin, 2008). It is less clear whether Skp2 has a role in controlling checkpoint resolution through p21 degradation in G2, although Cul4-mediated degradation of p21 could also play a role (the roles of Cul4 are discussed in more detail later in this review).

Some F-box proteins are direct transcriptional targets of p53 like Fbxo22 (Vrba et al., 2008), however, the function of Fbxo22 as a p53 transcriptional target is yet unclear. It has been shown that Fbxo22 targets KDM4A for degradation. KDM4A is a histone demethylase that regulates the demethylation of histone H3 at positions K9 and K36 (Tan et al., 2011). However, a different study pointed out that Fbxo22 ubiquitylates p53 by forming a complex with KDM4A. In this case Fbxo22 was shown to recognize a methylated form of p53 and to promote the degradation of methylated p53. The degradation of p53 operated by Fbxo22 is required for the induction of senescence after DNA damage induced by IR (Johmura et al., 2016). Overall, multiple F-box proteins have been shown to regulate p53, and diversity in p53 regulation could simply reflect redundancy. However, it is also plausible that the regulation of p53 by each ligase depends on the input DNA damage signal and could lead to different transcriptional outputs and consequences for cell survival.

## Cul1 and DSB Repair

Breast Cancer Type 1 Susceptibility Protein (BRCA1) is a tumor suppressor that has a significant role in HR following DNA DSBs. BRCA1, with its obligate binding partner BARD1, has been shown to act as a marker for sister chromatid availability (Nakamura et al., 2019) and to serve as a scaffold at DSB sites to recruit several proteins involved in the DNA damage repair pathway (Huen et al., 2009). BRCA1 forms a complex with BRCA2 which is facilitated by PALB2 (Sy et al., 2009; Zhang F. et al., 2009). This complex recruits the recombinase Rad51 to DSB sites and promotes the loading of Rad51 onto single-strand DNA, ultimately leading to the repair of DSBs by HR (Bhattacharyya et al., 2000; Zhang et al., 2012). The loss of BRCA2 and BRCA1 function is frequent in breast and ovarian cancers. Cancers bearing inactivating mutations in these genes are defective in the repair of DSBs by HR. It follows that forcing the use of HR by promoting the formation of unrepairable SSBs and DSBs triggers cell death. This principle is at the basis of the synthetic lethality observed between the loss of BRCA and the use of PARPi (Helleday, 2011). The striking sensitivity of tumors lacking BRCA1 and BRCA2 is exploited in the treatment of breast and ovarian cancers with PARPi.

The regulation of BRCA1 and BRCA2 is complex and far from being fully elucidated. Lu and colleagues proposed that the F-box protein Fbxo44 targets BRCA1 for its UPS-mediated degradation through the $SCF^{Fbxo44}$ E3 ligase complex (Lu et al., 2012). However, Fbxo44 did not localize= at damaged DNA sites and PARPi sensitivity was not tested after Fbxo44 depletion.

The F-box protein Emi1, also known as Fbxo5, has been recently discovered to be involved in controlling the BRCA1-BRCA2-Rad51 axis. In cell lines with inactivating BRCA1 mutations, $SCF^{Emi1}$ was found to target Rad51 for its ubiquitin-mediated degradation. However, under genotoxic stress Chk1 was found to inhibit Rad51 degradation by Emi1 through phosphorylation. The phosphorylation of Rad51 increases its affinity to BRCA2 and hence results in a surplus of Rad51, which restores HR in cells with faulty BRCA1 (Marzio et al., 2018). Given its role in regulating Rad51 proteolysis in cells lacking BRCA1, Emi1 was identified as a regulator of PARPi sensitivity in BRCA1-deficient triple-negative breast cancer (Marzio et al., 2018).

The Ku70/Ku80 heterodimer (Ku) is the initiating factor of the NHEJ pathway of DSB repair. Ku recognizes the ends of DSBs and recruits other components of the DNA damage repair pathway to the site of the break. After serving its role, Ku needs to be removed from the repaired DSB site but the mechanism of its removal is not clearly understood. Studying the egg extract of *Xenopus laevis* (African clawed frog), Postow et al. (2008) demonstrated that Ku80 is degraded in response

to DSBs in a ubiquitin-dependent manner, and postulated that an SCF complex is the E3 ligase responsible for this ubiquitylation. It was shown that the K48-linked ubiquitylation step, but not the proteasomal degradation step that follows it, is required for removing Ku80 from repaired DSB sites (Postow et al., 2008). Fbxl12 was found to be the F-box protein responsible for the recruitment of the Ku80-ubiquitylating SCF complex to sites of DSBs, resulting in the degradation of Ku80 (Postow and Funabiki, 2013).

In mammalian cells other E3 ubiquitin ligases, which are not members of the CRL clade of E3s, have been shown to contribute to Ku80 removal from DSB sites. RING-Finger Protein 8 (RNF8) (Feng and Chen, 2012) and RNF126 (Ishida et al., 2017) were shown to be essential for the ubiquitylation and degradation of Ku80. RNF138 also promotes the ubiquitylation but not the degradation of Ku80 (Ismail et al., 2015).

Another F-box protein involved in DNA repair through Ku is Fbxw7. Fbxw7 has been previously found responsible for the ubiquitylation and subsequent degradation of a set of oncoproteins such as cyclin E, c-Jun and c-Myc via K48 linkage, which earned Fbxw7 recognition as a tumor suppressor (Nakayama and Nakayama, 2006; Welcker and Clurman, 2008). Adding to the functions of Fbxw7, it was recently discovered to promote DNA repair through NHEJ. Following exposure to IR, the ATM kinase phosphorylates Fbxw7 at Ser26 allowing the recruitment of the F-box protein to the DSB sites. Once at the DSB sites, Fbxw7 proceeds to K63-ubiquitylate the protein Xrcc4 at Lys296, which enhances the association of Xrcc4 with Ku and in turn promotes NHEJ. Given the ability of Fbxw7 to regulate NHEJ, inactivation of Fbxw7 promotes increased sensitivity of cancer cells to IR (Zhang et al., 2016).

## ROLES OF Cul2 AND Cul5 IN THE CELLULAR RESPONSE TO IR

### Cul2: Crucial Regulator of Hypoxia Response

Hypoxia-inducible factor 1 is a transcriptional factor expressed in hypoxic tumor cells and transiently induced in tumors as a result of oxidative stress following radiation (Semenza, 1999). Hif-1 transactivates several hypoxia-responsive genes, which results in the tumor acquiring malignant properties such as apoptotic resistance, enhanced tumor growth, invasion and metastasis (Semenza, 2003). Additionally, Hif-1 activates VEGFs and PDGFs which promote resistance to radiotherapy in endothelial cells, and also promote cell proliferation and blood vessel growth around tumors (Gorski et al., 1999; Moeller et al., 2004). Hif-1 is a heterodimer that consists of α and β subunits, and oxygen is responsible for the regulation of the α subunit (Hif-1α) at a post-translational level (Huang et al., 1998). In normoxia, proline residues in the ODD domain of Hif-1α get hydroxylated by oxygen-dependent prolyl hydroxylases (Bruick and McKnight, 2001; Epstein et al., 2001). The hydroxylation of Hif-1 serves as a signal to initiate the binding of Hif-1α to VHL. VHL is a Cul2 E3 ligase that assembles with Cul2, elongins B and C, and Rbx1, resulting in the proteasomal degradation of Hif-1α subunits. Under hypoxic conditions, the prolyl hydroxylases are inhibited, hindering the recognition of Hif-1α by the VHL protein and resulting in Hif-1 accumulation and a transcriptional response to hypoxia (Maxwell et al., 1999).

Given the contribution of Hif-1α and hypoxia to malignant and radiotherapy-resistant phenotypes in cancer, researchers have been trying to eliminate Hif-1α-active cells using strategies that hijack E3 ubiquitin ligases. One strategy worth noting is the development of the fusion protein TOP3 (TAT-ODD-procaspase-3) (**Figure 2A**) (reproduced from Harada et al., 2002). In this three-domain protein, the first domain is constituted by the HIV-Tat protein-transduction domain, required for the efficient delivery of TOP3 to cells and tissues *in vitro* and *in vivo*. The second domain is ODD (the VHL-mediated protein destruction motif of human Hif-1α), which promotes the stabilization of the peptide in hypoxia and its degradation in normoxia. The last domain is the proenzyme form of the human caspase-3, which endows TOP3 with cytocidal activity. The caspase 3 domain is activated following accumulated-TOP3 cleavage by endogenous caspases and triggers apoptosis. TOP3 is actively eliminated by VHL in normoxic cells but is stable in hypoxic cells where it promotes cell death. Since this design enables TOP3 to target hypoxic cells for elimination while sparing normoxic cells, and IR effectively targets normoxic cells but is less effective against hypoxic cells (Brown, 1999; Vaupel, 2004), the group suggested that the combination of IR and TOP3 could be a valuable therapeutic strategy. They proceeded to test their hypothesis, and found that this combinatorial approach efficiently reduces the population of tumor cells with Hif-1α induced by both hypoxia and IR, resulting in long-term suppression of tumor growth and angiogenesis compared to treatment by either IR or TOP3 alone (Harada et al., 2002).

While additionally investigating the role of Hif-1 in the IR response, it was discovered that exposing cells to IR results in the p38 MAPK-mediated stabilization of Hif-1 under both hypoxic and normoxic conditions. It was found that upon IR, Hif-1α is stabilized by the decreased half-life of its E3 ligase subunit VHL and of its hydroxylating enzymes prolyl hydroxylases 2. Findings from this study suggest that, in combination with IR, targeting Hif-1α through its MAPK-mediated stabilization possibly has the potential to increase the efficacy of IR treatment in glioma (Kim et al., 2014). Hypoxic IR-resistant cells tend to spread, often resulting in relapse after treatment, therefore inactivation of Hif-1α could have a significant therapeutic response in glioma.

### Roles of SOCS Boxes in Signaling and as Viral Adaptors

In addition to VHL, Cul2 or Cul5 can assemble with SOCS-box and 'ankyrin repeat and SOCS box (ASB)' proteins to form E3 ubiquitin ligase complexes that target proteins for proteasomal degradation. In complex with Cul2, elongin BC subcomplex, and Rbx1, SOCS1 accelerates the UPS-mediated degradation of Jak2 (Kamizono et al., 2001), a STAT3-activating tyrosine kinase which when inhibited using a small-molecule inhibitor sensitizes lung cancer cells

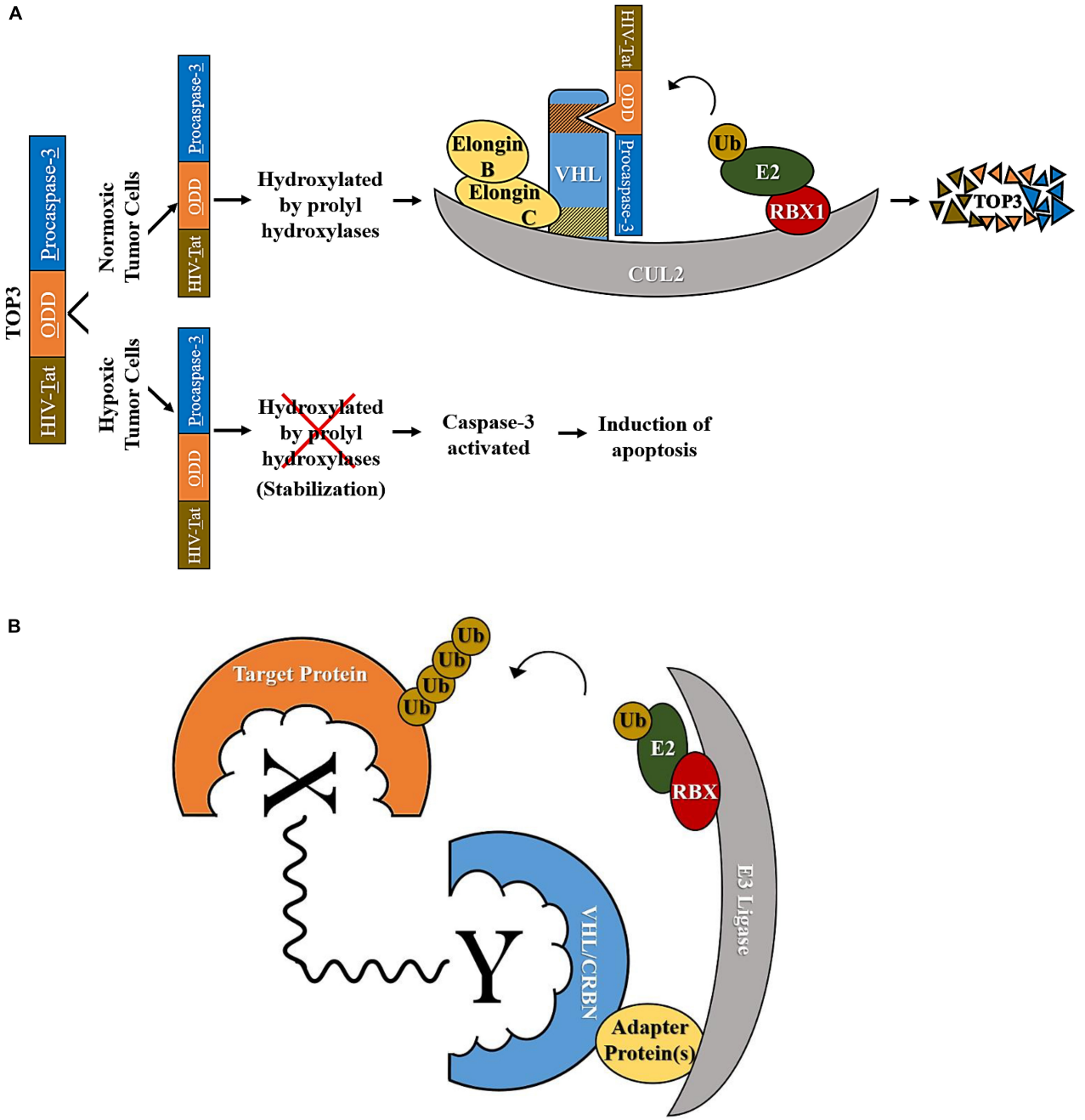


**FIGURE 2 |** Examples of therapeutic approaches that exploit CRL complexes. **(A)** TOP3 technology; in normoxic tumor cells $CRL2^{VHL}$ targets TOP3 for degradation while in hypoxic tumor cells TOP3 is stabilized, caspase-3 is activated, and apoptosis is induced (adapted from Harada et al., 2005). **(B)** Degradation of a target protein through bringing it in close proximity to an E3 ligase using a PROTAC (represented as X∼Y where X is the target-binding ligand, Y is the E3-binding ligand, and ∼ is the linker molecule).

to radiotherapy (Sun et al., 2011). Furthermore, SOCS1 has been shown to directly regulate the p53 response and apoptosis in T cells after IR by modulating STAT signaling (Calabrese et al., 2009). SOCS1 was also found to act as a substrate-binding motif targeting the HPV oncoprotein E7, inducing its ubiquitylation and subsequent degradation (Kamio et al., 2004). HPV is implicated in the formation of a subgroup of head and neck cancers that display high sensitivity to radiotherapy both *in vitro* and *in vivo* (Kimple et al., 2013; Dok et al., 2014; Sorensen et al., 2014). Therefore, the inhibition of SOCS1 could further enhance E7 levels to promote radiosensitivity.

Some SOCS-box-containing viral proteins such as the HIV-1 Vif have the capacity to hijack Cul5 E3 ubiquitin ligase complexes through which they acquire the ability to degrade host proteins (Yu et al., 2003). Acting as the substrate-specificity subunit of a CRL5 complex, the HIV-1 Vif protein targets the cellular intrinsic restriction factor APOBEC3G for proteasomal degradation (Yu et al., 2004). It has been reported that the inhibition of APOBEC3G activity using a Vif-derived peptide (Vif25-39) hinders DNA DSB repair in lymphoma cells, and hence sensitizes the cells to IR. The results from this study suggest that the peptide-mediated inhibition of APOBEC3G may be a potential radiosensitizing strategy (Prabhu et al., 2016), however, the mechanisms through which APOBEC3G affects DNA repair are not fully elucidated.

Another elongin BC-box protein is Wsb1. Kim et al. (2015) discovered that Wsb1 binds VHL and mediates its ubiquitylation and its subsequent proteasomal degradation. Hence, Wsb1 stabilizes Hif-1α by promoting the degradation of VHL under both hypoxic and normoxic conditions (Kim et al., 2015). Given that Hif-1 promotes resistance to radiotherapy, it is plausible that Wsb1 negatively influences the cellular response to IR by regulating Hif-1α, however, the role of Wsb1 in radiation sensitivity remains to be investigated.

Interestingly, it was found that in glioblastoma (GBM) cell lines, SOCS1 and SOCS3 are regulated reciprocally and SOCS3 is highly expressed in GBM, while SOCS1 is not. Expressing SOCS1 promotes radiosensitivity, while SOCS3 expression activates prosurvival signals in cancer cells through STAT-signaling, specifically STAT3 (Zhou et al., 2007; Sitko et al., 2008). Baek et al. (2016) evaluated the effect of the drug Resveratrol, a known suppressor of STAT3 signaling, on apoptosis induction and radiosensitization in SCCHN. They found that Resveratrol induces the expression of the SOCS1 protein and also its mRNA, which blocks the STAT3 signaling pathway, induces apoptosis and even enhances the rate of apoptosis when combined with IR (Baek et al., 2016). However, the functions of SOCS1 and SOCS3 in regulating STAT3 signaling in terms of their capacity to form Cul5 complexes are yet to be unraveled.

## ROLES OF Cul3 IN THE CELLULAR RESPONSE TO IR: DNA REPAIR AND ROS REGULATION

Bric-a-brac/tramtrack/broad complex -domain proteins serve as substrate-recruitment motifs of E3 ubiquitin ligase complexes and function as bridges to connect Cul3 and substrates. They have crucial roles in regulating two aspects of the IR response: DNA repair and ROS quenching.

An important aspect of DNA repair at DSBs is the choice between HR and NHEJ. While NHEJ is considered a fast and error prone repair mechanism, HR is considered error-free. However, while NHEJ can occur throughout the cell cycle, HR can only be carried out if a homologous template is present and thus is restricted to S and G2 phases of the cell cycle. Multiple mechanisms controlled by the ubiquitin system exist to control repair choice at specific phases of the cell cycle. For instance, Klhl15, a Cul3 adaptor, was found to accelerate the UPS-mediated degradation of the DNA endonuclease CtIP (Ferretti et al., 2016). CtIP together with the Mre11-Rad50-Nbs1 (MRN) complex control the choice of DNA DSB repair pathway by initiating DNA end-resection, which commits cells to HR by inhibiting NHEJ as processed DSB ends can no longer be targeted by the NHEJ pathway (Sartori et al., 2007; Chapman et al., 2012; Ceccaldi et al., 2016). Since IR induces DSBs, and CtIP is an essential factor of the DDR, the regulation of CtIP turnover by CRL3-Klhl15 is required to fine-tune the balance between HR and NHEJ in the cellular response to IR. Depletion of Klhl15 sensitizes cells to IR by disrupting the balance between these two repair pathways (Ferretti et al., 2016).

Another BTB protein that is crucial for responses to IR is Kelch-like ECH-Associated Protein 1 (Keap1). Keap1 has been directly implicated in the control of DSB repair; Keap1 ubiquitylates the BRCA1-interacting site of PALB2, preventing the interaction of PALB2 and BRCA1 and hence prohibits HR. The ubiquitylation by Keap1 does not lead to PALB2 proteolysis but restricts the interaction with BRCA1. The ubiquitylation of PALB2 is counteracted by USP11 during G2. This mechanism prevents the execution of HR in G1 (Orthwein et al., 2015).

The most well-studied function of CRL3-Keap1 is the regulation of the transcription factor Nf-E2-Related Factor 2 (Nrf2), a master mediator of the cellular defenses against ROS (Cullinan et al., 2004; Kobayashi et al., 2004; Zhang et al., 2004). Nrf2 binds to the ARE found within the promoters of several genes encoding proteins that have crucial roles in the anti-oxidation responses (Kensler et al., 2007). Under oxidative stress, several cysteine residues in Keap1 are covalently modified by thiol intermediates activated by the ROS radicals. The chemical modifications in Keap1 prevent the binding to Nrf2, which, as a consequence, is stabilized and can transcribe the genes required for the anti-oxidation response.

As oxidative stress is a key player in carcinogenesis, the Keap1-Nrf2 pathway serves a chemopreventive role and protects healthy cells from carcinogenesis. However, cancer cells have the ability to hijack this pathway to acquire survival advantages under high ROS, which are common events in cancer tissues (Chen and Chen, 2016). It was indeed found that Nrf2 overexpression in cancer cells decreases their sensitivity to IR and chemotherapy, while Nrf2 knockdown sensitizes the cells to such treatments (Shibata et al., 2008a; Wang et al., 2008; Solis et al., 2010; Zhang et al., 2010). Nrf2 is aberrantly overexpressed in many cancers, and one reason for this is the presence of mutations in Keap1, the ligase targeting Nrf2 (Shibata et al., 2008b; Yoo et al., 2012). Loss-of-function mutations in Keap1 were found in human lung carcinoma, NSCLC, gallbladder, ovarian, and liver cancers (Singh et al., 2006; Ohta et al., 2008; Shibata et al., 2008a; Konstantinopoulos et al., 2011; Yoo et al., 2012), whereas gain-of-function mutations in Nrf2 were

found in lung, head and neck, and esophageal carcinoma (Shibata et al., 2008a, 2011).

Mutations in Nrf2 prevent binding to Keap1, leading to an increase in protein stability and constitutively high levels of Nrf2 (Tong et al., 2006). The mutational status of Keap1 and of Nrf2 have been directly connected to the success of localized radiotherapy in lung cancer (Jeong et al., 2017), underscoring the crucial role of this E3 ubiquitin ligase-substrate axis in the cellular response to IR.

Another protein worth noting is the chromatin-modifying enzyme Tip60; it is essential for DNA repair and apoptosis after IR (Ikura et al., 2000), its inhibition abolishes IR-induced G1 cell-cycle arrest (Berns et al., 2004), and it was also found to activate ATM following genotoxic stress (Sun et al., 2005). The stability and activity of Tip60 is reportedly tightly regulated by the combined action of Activating Transcription Factor-2 (ATF2) and CRL3, however, since ATF2 lacks a BTB domain, it is speculated that an unidentified BTB domain-containing protein is part of this CRL3 complex (Bhoumik et al., 2008).

## ROLES OF Cul4A AND Cul4B IN THE CELLULAR RESPONSE TO IR: CONTROLLING DNA REPAIR AND DNA REPLICATION

Cul4 and Ddb1, the substrate adapter for CRL4 complexes (Bondar et al., 2006; Sugasawa, 2009), are conserved from yeast to humans (Holmberg et al., 2005; Bondar et al., 2006; Kim and Kipreos, 2007). In lower organisms, the Cul4 protein is encoded by a single gene, but in mammals Cul4A and Cul4B proteins are encoded by two highly homologous genes (Iovine et al., 2011). Cul4A and Cul4B are 82% identical, and the difference between the two proteins is highlighted at their N-terminals; Cul4B is 149 amino acids longer than Cul4A as it has an N-terminal extension that contains an NLS. The NLS in Cul4B is believed to mediate the nuclear localization of Cul4B whereas Cul4A is mostly located in the cytoplasm (Zou et al., 2009; Hannah and Zhou, 2015).

Cul4A is reportedly aberrantly expressed in a plethora of cancers including breast cancer, squamous cell carcinoma, pleural mesothelioma (Shinomiya et al., 1999; Yasui et al., 2002; Melchor et al., 2009; Hung et al., 2011), and lung cancer (Wang et al., 2014), and its overexpression contributes to tumor progression, metastasis and poor prognosis (Wang et al., 2014). Compared to Cul4A, findings linking Cul4B to cancer are less common, however it was still found to be overexpressed in colon cancer (Jiang et al., 2013), cervical cancer, lung cancer, esophageal cancer, and breast cancer (Hu et al., 2012), with its overexpression closely related to tumor stage, invasion and metastasis.

Again as a *leitmotiv* of all E3 ubiquitin ligases, it was reported that Cul4A associates with MDM2 to degrade p53 (Nag et al., 2004), however, dissecting the role of Cul4 from all its adaptors is quite difficult and the emerging picture is that the observed activation of p53 is likely indirect.

One role of Cul4 complexes is to recognize UV-induced pyrimidine photodimers in DNA. In this case, the Ddb1 is bound to Ddb2 and directly recognizes DNA lesions. The ubiquitylation events mediated by Ddb1-Ddb2 following recognition subsequently help recruit the required proteins for the repair of the DNA lesion. A detailed explanation of the role of Cul4 complexes in UV-irradiation is outside the scope of this review and there are excellent reviews on the topic (Scrima et al., 2011). However, it is important to mention other important Cul4 adaptors that regulate genome stability, in particular Cdt2. Cdt2 is a Cul4 substrate-recognition subunit that targets p21 (Abbas et al., 2008), p27 (Li et al., 2006), Cdt1 (Jin et al., 2006) and the histone methyl-transferase Set8 (Abbas et al., 2010) for degradation. The mode of substrate engagement that Cdt2 uses is unique: Cdt2 couples substrate degradation to DNA replication by interacting with a modified PCNA Interacting Peptide (PIP) box in the substrate.

Proliferating cell nuclear antigen is an essential DNA clamp which travels with the DNA replication fork and acts as a scaffold for the recruitment of proteins required for DNA replication completion and fidelity. Proteins that interact with PCNA have in common a PIP-box motif consisting of the following amino-acid residues: Qxxψxxϑϑ. Substrates of Cdt2 contain an equivalent PIP box, but with modifications that increase the affinity for PCNA and favor a concomitant interaction with Cdt2. Thus, the recognition of Cdt2 substrates is mediated through the PIP degron: QxxψTDϑϑxxxK/R (Havens and Walter, 2009; Michishita et al., 2011). This strategy is important to control degradation of substrates present on the chromatin and traveling with DNA replication. Indeed, Cdt2 targets chromatin-bound p21 for degradation (Abbas et al., 2008; Kim et al., 2008) whilst the soluble p21 is targeted for degradation by Skp2 (Fbxl1) (Carrano et al., 1999).

Cdt2 also targets Cdt1 for degradation during S phase. Cdt1 is an important component of the Pre-RC, which defines DNA replication origins in G1. The Cdt2-dependant degradation of Cdt1 in S phase is one of several redundant mechanisms that prevent the re-initiation of DNA replication from regions of the genome which have already been replicated (Ralph et al., 2006). Interestingly, it was previously reported that Cdt1 is degraded by a CRL4 complex upon IR. This may contribute to the inhibition of replication in response to IR, although the majority of DNA replication inhibition is ascribed to checkpoint activation (Higa et al., 2003). The turnover of Cdt2 itself is also UPS-dependent and is mediated by the E3 ligase $SCF^{Fbxo11}$. This hints at an interesting crosstalk between CRL1 and CRL4 ligases (Abbas et al., 2013; Rossi et al., 2013).

Literature linking CRL4 complexes to IR is limited, but evidence from lower eukaryotes suggests that Cul4 based machineries could play a significant role in processing DSBs (Moss et al., 2010). More recently, Zeng et al. (2016) identified WDR70, a conserved DCAF that is recruited to DNA DSBs. WDR70 is part of a Cul4-Ddb1 ubiquitin ligase complex and promotes HR by stimulating long range resection (Zeng et al., 2016). Interestingly, knockdown of WDR70

sensitizes HEK293T cells to IR and is comparable to the survival observed upon Ddb1 depletion.

Whilst the hijacking of cullin machinery has been previously discussed, about 50% of human hepatocellular carcinomas are associated with chronic hepatitis B infection, and risk of carcinogenesis increases with viral load (El-Serag, 2011). The hepatitis B virus encodes an oncoprotein, Hepatitis B x protein (HBx) that can hijack the Cul4-Ddb1 machinery by displacing WDR70 (and likely other DCAFs) to form viral $CRL4^{HBx}$. Disassembly of the $CRL4^{WDR70}$ complex by HBx compromises DNA end resection and results in HR deficiency (Ren et al., 2019). Understanding the target of the $CRL4^{WDR70}$ machinery may provide insights into new targets for sensitizing cancer cells to IR.

## TARGETING CRL COMPLEXES FOR CANCER THERAPY

Given the central role that CRLs have in regulating cancer pathogenesis and therapy responses, inhibitors of CRLs with limited specificity have been developed (Jang et al., 2018). MLN4924 (pevonedistat), a small-molecule inhibitor that selectively inhibits NEDD-8, was shown to inactivate CRL complexes and suppress tumor growth both *in vitro* and *in vivo* (Soucy et al., 2009). TAS4464 is another NEDDylation inhibitor, and most clinical trials involving either MLN4924 or TAS4464 are still restricted to phase I and II trials (Jang et al., 2018). The mechanism of action of MLN4924 is not selective as MLN4924 inhibits all the NEDDylation reactions in the cells. NEDDylation is essential for ubiquitylation operated by CRLs and thus NEDDylation inhibitors are effectively blocking the action of more than 400 enzymes in the cells. Despite the limited specificity, MLN4924 was shown to sensitize cancer cells to several chemotherapeutic drugs, so several of the ongoing trials are testing this small-molecule inhibitor in combination with DNA-damaging drugs such as carboplatin (Jang et al., 2018). MLN4924 was shown to act as a radiosensitizer in a mouse xenograft model of human pancreatic cancer (Wei et al., 2012), and in the human colorectal cancer cell lines HT-29 and HCT-116 (Wan et al., 2016). It was also found that MLN4924 radiosensitizes SCCHN in culture, and enhances IR-induced suppression of SCCHN xenografts in mice (Vanderdys et al., 2018).

It is possible to specifically inhibit individual CRLs or CRL-interacting proteins such as CRL substrates or CRL substrate-recruitment units, as opposed to global CRL- or proteasomal-inhibition, and this has in fact been attempted in a number of studies. For example, targeting CRL substrates that enhance the resistance of cells to radiotherapy, or targeting CRLs whose substrates sensitize cells to IR could potentially prove as an effective strategy to radiosensitize cancer cells. Substrates and substrate-recruitment members of CRLs that are involved in the cellular response to IR are summarized below in **Table 1**. An alternative emerging possibility to exploit CRL roles in cancer therapy is to use PROTACs (**Figure 2B**). PROTACs are heterobifunctional molecules made up of two different ligands and a linker; one of the two ligands binds to the target protein, and the other binds to an E3 ubiquitin ligase (An and Fu, 2018). Upon the formation of the E3 ligase-PROTAC-protein complex, E2 enzymes ubiquitylate the target protein marking it for proteasomal degradation (An and Fu, 2018). Thereby, a PROTAC molecule increases the proximity between the target protein and an E3 ligase, and acts catalytically to induce the proteolysis of this substrate.

**TABLE 1 |** Summary of the subunits of E3 ligase complexes of the cullin family that are involved in the IR response.

| Cullin family member | CRL substrate-recruitment subunit | Substrate(s) | References |
|---|---|---|---|
| Cul1 | β-TrCP (Fbxw1/11) | Cdc25A | Busino et al., 2003 |
| | | Claspin | Mailand et al., 2006; Peschiaroli et al., 2006 |
| | | p53 | Isoda et al., 2009 |
| | | Wee1 | Watanabe et al., 2004 |
| | Cyclin F (Fbxo1) | Exo1 | Elia et al., 2015 |
| | | RRM2 | D'Angiolella et al., 2012 |
| | Emi1 (Fbxo5) | Rad51 | Marzio et al., 2018 |
| | Fbxl12 | Ku80 | Postow and Funabiki, 2013 |
| | Fbxo4 and Fbxo31 | Cyclin D1 | Lin et al., 2006; Santra et al., 2009 |
| | Fbxo6 | Chk1 | Zhang F. et al., 2009 |
| | Fbxo11 | Cdt2 | Abbas et al., 2013 |
| | Fbxo22 | p53 | Vrba et al., 2008 |
| | Fbxo44 | BRCA1 | Lu et al., 2012 |
| | Fbxw7 | Xrcc4 | Zhang et al., 2016 |
| | Jfk (Fbxo42) | p53 | Uchida et al., 2009 |
| | Mepe/Of45 (co-factor of Chk1) | | Liu et al., 2009 |
| | Skp2 (Fbxl1) | p21 and p27 | Carrano et al., 1999 |
| Cul2 | SOCS1 | HPV-E7 | Kamio et al., 2004 |
| | | Jak2 | Kamizono et al., 2001 |
| | SOCS1, SOCS3 in GBM | | Zhou et al., 2007 |
| | VHL | Hif-1α | Maxwell et al., 1999 |
| Cul3 | Keap1 | Nrf2 | Zhang et al., 2004 |
| | | PALB2 | Orthwein et al., 2015 |
| | Klhl15 | CtIP | Ferretti et al., 2016 |
| | Klhl20 | PML (TRIM19) | Yuan et al., 2011 |
| | Spop | | Zhang et al., 2014 |
| | | Tip60 | Bhoumik et al., 2008 |
| Cul4 | Ddb1-Cdt2 | Cdt1 | Higa et al., 2003 |
| | | p21 | Stuart and Wang, 2009 |
| | Ddb1-WDR70 | | Zeng et al., 2016 |
| Cul5 | HIV-1 Vif | APOBEC3G | Yu et al., 2003 |
| | Wsb1 | VHL | Kim et al., 2015 |

Proteolysis-targeting chimeras were designed to overcome several of the limitations that face their predecessors, small-molecule inhibitors. Small-molecule inhibitors are the most common targeted treatment method for intracellular proteins, however, they have several shortcomings. One example of such shortcomings is that small-molecule inhibitors are mainly engineered to target proteins with active sites (ex., enzymes or receptors), whereas the majority of the proteome lacks active sites and is therefore not targetable using this method (Toure and Crews, 2016). Target protein-binding ligands in PROTACs overcome this through binding to crevices on the surface of target proteins as opposed to active sites, making a much wider range of proteins druggable (An and Fu, 2018).

Through this design, and due to the nature of PROTAC-substrate binding being transient and reversible, PROTACs are also less prone than small-molecule inhibitors to drug resistance arising from mutations at the active site of the target protein (An and Fu, 2018).

Additionally, in contrast to the relatively high concentration of small-molecule inhibitors required to reach therapeutic capacity which often leads to off-target effects, PROTACs are required at much lower concentrations for two reasons. The first is that PROTACs act sub-stoichiometrically so they are involved in multiple rounds of protein degradation as opposed to small-molecule inhibitors that act in a 1:1 ratio to the substrate (Bondeson et al., 2015; Lu et al., 2015; Olson et al., 2018). And the second reason is that the hook effect applies to PROTACs, which entails that at high PROTAC concentrations the protein degradation efficiency decreases due to the direct inhibition of the E3 target (An and Fu, 2018).

Another advantage of PROTACs over small-molecule inhibitors stems from the fact that PROTACs exploit the intracellular UPS to degrade target proteins so the whole protein is lysed, as opposed to only disrupting the activity of a single domain in a protein by small-molecule inhibitors, which leaves the other domains in a multi-domain protein fully functional.

The concept of PROTACs was first introduced in 2001 (Sakamoto et al., 2001), and the first cell-permeable PROTAC was designed a few years later in 2004 (Schneekloth et al., 2004). At their infancy, PROTACs were peptide-based but that soon changed due to the poor permeability as well as low potency of the high-molecular weight peptide ligands, and the first small-molecule PROTAC was reported in 2008 (Schneekloth et al., 2008; Lai and Crews, 2017). It was reported that immunomodulatory drugs thalidomide, lenalidomide, and pomalidomide have the ability to hijack the ubiquitin ligase $CRL4^{CRBN}$ so small-molecule PROTACs with thalidomide (and derivatives)-based CRBN binding ligands were developed (An and Fu, 2018). Since 2015, the number of small-molecule PROTACs reported is more than 30, most of them utilizing VHL and cereblon (CRBN, a substrate recognition subunit of CRL4) E3 ligases (An and Fu, 2018). Currently, several pharmaceutical companies have programs for developing PROTACs, such companies include Arvinas, C4 Therapeutics, Kymera Therapeutics, and Captor Therapeutics (An and Fu, 2018). A large expansion of small molecules targeting E3 ligases is predicted given the significant investment from both pharma companies and academia.

## CONCLUSION AND FUTURE RESEARCH DIRECTIONS

Given the specific roles of E3 ligase adaptors in regulating multiple aspects of the cellular responses to IR, it is possible to envision that alteration of the CRLs could be exploited to improve radiotherapy response in cancer cells. For instance, the development of PROTACs targeting CRL adaptors in the DNA damage could lead to drugs that are only activated upon IR or under a specific stimulus like hypoxia. In the future it will be important to dissect the roles of the diverse CRLs at a system-wide level. It is important to emphasize the fact that studies on some subfamilies of CRLs (like CRL4 and CRL3) and DNA damage are quite limited and require further investigations that take into consideration the role of the adaptor, the alteration in selected cancer types and the impact in therapy response with radiotherapy and other DNA damaging agents.

In the search for new approaches to improve patient response to radiotherapy, all possible ways IR affects the cell need to be considered. The effect of IR is not limited to DNA damage by DSBs and SSBs, it also affects the immune system. It was recently noted that IR treatment could facilitate the immune responses by activating a cGAS/STING pathway to initiate immune signaling (Harding et al., 2017). This observation is likely at the basis of a well-known phenomena in the clinic called the abscopal effect. The abscopal effect, first defined in 1953, is the ability of localized radiotherapy to induce off-target anti-tumor effects leading to tumor regression at non-irradiated metastatic sites (Mole, 1953). Following this discovery, researchers began looking into the mechanisms guiding such effect and only 50 years later were able to make the breakthrough proposition that it was immune-system mediated (Demaria et al., 2004). With a plethora of recent studies reporting successful oncological applications of immune checkpoint inhibitors in clinical trials, researchers are becoming increasingly interested in the effects of combining immunotherapy with localized radiotherapy to best exploit the abscopal effect (Ng and Dai, 2016; Liu et al., 2018). The cullin family of E3 ligases is involved in several pathways of immune responses (Kawaida et al., 2005; Bibeau-Poirier et al., 2006; Kuiken et al., 2012; Mathew et al., 2012; Saucedo-Cuevas et al., 2014), therefore they could also be exploited to modulate the abscopal effect and/or cGAS/STING activation in combination with radiotherapy. A recent example of the involvement of E3s in immune checkpoint responses is represented by the E3 ligase Spop. In its E3 ligase complex with Cul3, Spop targets the ligand of the immune checkpoint Pd-L1 for its ubiquitin-mediated degradation (Zhang et al., 2018). Based on this mechanism, inhibiting Spop was found to result in an abundance of Pd-L1, and in combination with anti-Pd-1 immunotherapy was found to improve tumor regression and overall survival rates in murine models (Zhang et al., 2018).

In the future, CRL adaptors could be targeted with PROTACs to enhance the response of tumors to radiotherapy and elicit

a systemic immune response. Given the large expansion of PROTAC- like-molecules in the last years, it is conceivable that further studies on CRLs might improve patient survival by changing the clinical approaches to cancer treatment with radiotherapy.

## AUTHOR CONTRIBUTIONS

SF worked on the main body of the review and collected the relevant literature. OW critically analyzed and reviewed the manuscript, and contributed to the description of the roles of Cul4 in IR responses. MH, as a radiation biophysics expert, wrote the paragraph on the biological effects of ionizing radiation. VD'A organized the literature, provided insightful comments, and revised the work on cullins.

## FUNDING

This study was possible thanks to the support of a Medical Research Council (MRC) grant (MC_UU_00001/7) to VD'A. Funding provided by the MRC Strategic Partnership Funding (MC_PC_12004) for the Cancer Research UK (CRUK)/MRC Oxford Institute for Radiation Oncology is also gratefully acknowledged. This work was additionally supported by a CRUK grant (C5255/A18085) through the CRUK Oxford Centre.

## REFERENCES

Abbas, T., Mueller, A. C., Shibata, E., Keaton, M., Rossi, M., and Dutta, A. (2013). Crl1-Fbxo11 promotes Cdt2 ubiquitylation and degradation and regulates Pr-Set7/Set8-mediated cellular migration. *Mol. Cell* 49, 1147–1158. doi: 10.1016/j.molcel.2013.02.003

Abbas, T., Shibata, E., Park, J., Jha, S., Karnani, N., and Dutta, A. (2010). Crl4(Cdt2) regulates cell proliferation and histone gene expression by targeting Pr-Set7/Set8 for degradation. *Mol. Cell* 40, 9–21. doi: 10.1016/j.molcel.2010.09.014

Abbas, T., Sivaprasad, U., Terai, K., Amador, V., Pagano, M., and Dutta, A. (2008). Pcna-dependent regulation of p21 ubiquitylation and degradation via the Crl4Cdt2 ubiquitin ligase complex. *Genes Dev.* 22, 2496–2506. doi: 10.1101/gad.1676108

Agami, R., and Bernards, R. (2000). Distinct initiation and maintenance mechanisms cooperate to induce G1 Cell cycle arrest in response to dna damage. *Cell* 102, 55–66. doi: 10.1016/s0092-8674(00)00010-6

An, S., and Fu, L. (2018). Small-molecule protacs: an emerging and promising approach for the development of targeted therapy drugs. *EBioMedicine* 36, 553–562. doi: 10.1016/j.ebiom.2018.09.005

Baek, S. H., Ko, J. H., Lee, H., Jung, J., Kong, M., Lee, J. W., et al. (2016). Resveratrol inhibits Stat3 signaling pathway through the induction of Socs-1: Role in apoptosis induction and radiosensitization in head and neck tumor cells. *Phytomedicine* 23, 566–577. doi: 10.1016/j.phymed.2016.02.011

Bai, C., Sen, P., Hofmann, K., Ma, L., Goebl, M., Harper, J. W., et al. (1996). Skp1 connects cell cycle regulators to the ubiquitin proteolysis machinery through a novel motif, the F-box. *Cell* 86, 263–274. doi: 10.1016/s0092-8674(00)80098-7

Bartek, J., and Lukas, J. (2003). Chk1 and Chk2 kinases in checkpoint control and cancer. *Cancer Cell* 3, 421–429. doi: 10.1016/s1535-6108(03)00110-7

Berns, K., Hijmans, E. M., Mullenders, J., Brummelkamp, T. R., Velds, A., Heimerikx, M., et al. (2004). A large-scale Rnai screen in human cells identifies new components of the p53 pathway. *Nature* 428, 431–437. doi: 10.1038/nature02371

Bhattacharyya, A., Ear, U. S., Koller, B. H., Weichselbaum, R. R., and Bishop, D. K. (2000). The breast cancer susceptibility gene Brca1 is required for subnuclear assembly of Rad51 and survival following treatment with the Dna cross-linking agent cisplatin. *J. Biol. Chem.* 275, 23899–23903. doi: 10.1074/jbc.c000276200

Bhoumik, A., Singha, N., O'connell, M. J., and Ronai, Z. A. (2008). Regulation of Tip60 by Atf2 modulates Atm activation. *J. Biol. Chem.* 283, 17605–17614. doi: 10.1074/jbc.M802030200

Bibeau-Poirier, A., Gravel, S. P., Clement, J. F., Rolland, S., Rodier, G., Coulombe, P., et al. (2006). Involvement of the IkappaB kinase (Ikk)-related kinases tank-binding kinase 1/Ikki and cullin-based ubiquitin ligases in Ifn regulatory factor-3 degradation. *J. Immunol.* 177, 5059–5067. doi: 10.4049/jimmunol.177.8.5059

Bondar, T., Kalinina, A., Khair, L., Kopanja, D., Nag, A., Bagchi, S., et al. (2006). Cul4A and Ddb1 associate with Skp2 to target p27Kip1 for proteolysis involving the Cop9 signalosome. *Mol. Cell Biol.* 26, 2531–2539. doi: 10.1128/mcb.26.7.2531-2539.2006

Bondeson, D. P., Mares, A., Smith, I. E., Ko, E., Campos, S., Miah, A. H., et al. (2015). Catalytic in vivo protein knockdown by small-molecule protacs. *Nat. Chem. Biol.* 11, 611–617. doi: 10.1038/nchembio.1858

Brown, J. M. (1999). The hypoxic cell. *Cancer Res.* 59, 5863–5870.

Bruick, R. K., and McKnight, S. L. (2001). A conserved family of prolyl-4-Hydroxylases that modify hif. *Science* 294, 1337–1340. doi: 10.1126/science.1066373

Busino, L., Donzelli, M., Chiesa, M., Guardavaccaro, D., Ganoth, D., Dorrello, N. V., et al. (2003). Degradation of Cdc25A by beta-Trcp during S phase and in response to Dna damage. *Nature* 426, 87–91. doi: 10.1038/nature02082

Calabrese, V., Mallette, F. A., Deschenes-Simard, X., Ramanathan, S., Gagnon, J., Moores, A., et al. (2009). Socs1 links cytokine signaling to p53 and senescence. *Mol. Cell.* 36, 754–767. doi: 10.1016/j.molcel.2009.09.044

Carrano, A. C., Eytan, E., Hershko, A., and Pagano, M. (1999). Skp2 is required for ubiquitin-mediated degradation of the Cdk inhibitor p27. *Nat. Cell Biol.* 1, 193–199. doi: 10.1038/12013

Ceccaldi, R., Rondinelli, B., and D'andrea, A. D. (2016). Repair pathway choices and consequences at the double-strand break. *Trends Cell Biol.* 26, 52–64. doi: 10.1016/j.tcb.2015.07.009

Cenciarelli, C., Chiaur, D. S., Guardavaccaro, D., Parks, W., Vidal, M., and Pagano, M. (1999). Identification of a family of human F-box proteins. *Curr. Biol.* 9, 1177–1179.

Chapman, J. R., Sossick, A. J., Boulton, S. J., and Jackson, S. P. (2012). Brca1-associated exclusion of 53bp1 from Dna damage sites underlies temporal control of Dna repair. *J. Cell Sci.* 125, 3529–3534. doi: 10.1242/jcs.105353

Chen, H. Y., and Chen, R. H. (2016). Cullin 3 ubiquitin ligases in cancer biology: functions and therapeutic implications. *Front. Oncol.* 6:113. doi: 10.3389/fonc.2016.00113

Cheng, Q., and Chen, J. (2011). The phenotype of Mdm2 auto-degradation after Dna damage is due to epitope masking by phosphorylation. *Cell Cycle* 10, 1162–1166. doi: 10.4161/cc.10.7.15249

Cullinan, S. B., Gordan, J. D., Jin, J., Harper, J. W., and Diehl, J. A. (2004). The Keap1-Btb protein is an adaptor that bridges Nrf2 to a Cul3-based E3 ligase: oxidative stress sensing by a Cul3-Keap1 ligase. *Mol. Cell Biol.* 24, 8477–8486. doi: 10.1128/mcb.24.19.8477-8486.2004

D'Angiolella, V., Donato, V., Forrester, F. M., Jeong, Y. T., Pellacani, C., Kudo, Y., et al. (2012). Cyclin F-mediated degradation of ribonucleotide reductase M2 controls genome integrity and Dna repair. *Cell* 149, 1023–1034. doi: 10.1016/j.cell.2012.03.043

De Bont, R., and van Larebeke, N. (2004). Endogenous Dna damage in humans: a review of quantitative data. *Mutagenesis* 19, 169–185. doi: 10.1093/mutage/geh025

Demaria, S., Ng, B., Devitt, M. L., Babb, J. S., Kawashima, N., Liebes, L. and Formenti, S. C. (2004). Ionizing radiation inhibition of distant untreated tumors (abscopal effect) is immune mediated. *Int. J. Radiat. Oncol. Biol. Phys.* 58, 862–870. doi: 10.1016/j.ijrobp.2003.09.012

Dias, D. C., Dolios, G., Wang, R., and Pan, Z. Q. (2002). Cul7: A Doc domain-containing cullin selectively binds Skp1.F*bx*29 to form an Scf-like complex. *Proc. Natl. Acad. Sci. U.S.A.* 99, 16601–16606. doi: 10.1073/pnas.252646399

Dok, R., Kalev, P., Van Limbergen, E. J., Asbagh, L. A., Vazquez, I., Hauben, E., et al. (2014). p16ink4a impairs homologous recombination-mediated Dna repair in human papillomavirus-positive head and neck tumors. *Cancer Res.* 74, 1739–1751. doi: 10.1158/0008-5472.CAN-13-2479

Eccles, L. J., O'neill, P., and Lomax, M. E. (2011). Delayed repair of radiation induced clustered Dna damage: friend or foe? *Mutat. Res.* 711, 134–141. doi: 10.1016/j.mrfmmm.2010.11.003

Elia, A. E., Boardman, A. P., Wang, D. C., Huttlin, E. L., Everley, R. A., Dephoure, N., et al. (2015). Quantitative proteomic atlas of ubiquitination and acetylation in the dna damage response. *Mol. Cell* 59, 867–881. doi: 10.1016/j.molcel.2015.05.006

El-Serag, H. B. (2011). Hepatocellular carcinoma. *N. Engl. J. Med.* 365, 1118–1127.

Epstein, A. C. R., Gleadle, J. M., Mcneill, L. A., Hewitson, K. S., O'rourke, J., Mole, D. R., et al. (2001). *C. elegans* Egl-9 and mammalian homologs define a family of dioxygenases that regulate hif by prolyl hydroxylation. *Cell* 107, 43–54. doi: 10.1016/s0092-8674(01)00507-4

Feng, L., and Chen, J. (2012). The E3 ligase Rnf8 regulates Ku80 removal and Nhej repair. *Nat. Struct. Mol. Biol.* 19, 201–206. doi: 10.1038/nsmb.2211

Ferretti, L. P., Himmels, S. F., Trenner, A., Walker, C., Von Aesch, C., Eggenschwiler, A., et al. (2016). Cullin3-Klhl15 ubiquitin ligase mediates Ctip protein turnover to fine-tune Dna-end resection. *Nat. Commun.* 7:12628. doi: 10.1038/ncomms12628

Finley, D., Ciechanover, A., and Varshavsky, A. (2004). Ubiquitin as a central cellular regulator. *Cell* 116, S29–S32.

Genschik, P., Sumara, I., and Lechner, E. (2013). The emerging family of Cullin3-Ring ubiquitin ligases (Crl3s): cellular functions and disease implications. *EMBO J.* 32, 2307–2320. doi: 10.1038/emboj.2013.173

Gorski, D. H., Beckett, M. A., Jaskowiak, N. T., Calvin, D. P., Mauceri, H. J., Salloum, R. M., et al. (1999). Blockade of the vascular endothelial growth factor stress response increases the antitumor effects of ionizing radiation. *Cancer Res.* 59, 3374–3378.

Guardavaccaro, D., Kudo, Y., Boulaire, J., Barchi, M., Busino, L., Donzelli, M., et al. (2003). Control of meiotic and mitotic progression by the F box protein beta-Trcp1 in vivo. *Dev. Cell* 4, 799–812. doi: 10.1016/s1534-5807(03)00154-0

Gustafsson, N. M. S., Farnegardh, K., Bonagas, N., Ninou, A. H., Groth, P., Wiita, E., et al. (2018). Targeting Pfkfb3 radiosensitizes cancer cells and suppresses homologous recombination. *Nat. Commun.* 9:3872. doi: 10.1038/s41467-018-06287-x

Hannah, J., and Zhou, P. (2015). Distinct and overlapping functions of the cullin E3 ligase scaffolding proteins Cul4A and Cul4B. *Gene* 573, 33–45. doi: 10.1016/j.gene.2015.08.064

Harada, H., Hiraoka, M., and Kizaka-Kondoh, S. (2002). Antitumor effect of tat-oxygen-dependent degradation-caspase-3 fusion protein specifically stabilized and activated in hypoxic tumor cells. *Cancer Res.* 62, 2013–2018.

Harada, H., Kizaka-Kondoh, S., and Hiraoka, M. (2005). Optical imaging of tumor hypoxia and evaluation of efficacy of a hypoxia-targeting drug in living animals. *Mol. Imaging* 4, 182–193.

Harding, S. M., Benci, J. L., Irianto, J., Discher, D. E., Minn, A. J., and Greenberg, R. A. (2017). Mitotic progression following Dna damage enables pattern recognition within micronuclei. *Nature* 548, 466–470. doi: 10.1038/nature23470

Havens, C. G., and Walter, J. C. (2009). Docking of a specialized Pip Box onto chromatin-bound Pcna creates a degron for the ubiquitin ligase Crl4Cdt2. *Mol. Cell* 35, 93–104. doi: 10.1016/j.molcel.2009.05.012

Helleday, T. (2011). The underlying mechanism for the Parp and Brca synthetic lethality: clearing up the misunderstandings. *Mol. Oncol.* 5, 387–393. doi: 10.1016/j.molonc.2011.07.001

Hershko, A., Heller, H., Elias, S., and Ciechanover, A. (1983). Components of ubiquitin-protein ligase system. Resolution, affinity purification, and role in protein breakdown. *J. Biol. Chem.* 258, 8206–8214.

Higa, L. A., Mihaylov, I. S., Banks, D. P., Zheng, J., and Zhang, H. (2003). Radiation-mediated proteolysis of Cdt1 by Cul4-Roc1 and Csn complexes constitutes a new checkpoint. *Nat. Cell Biol.* 5, 1008–1015. doi: 10.1038/ncb1061

Hill, M. A. (2018). Track to the future: historical perspective on the importance of radiation track structure and Dna as a radiobiological target. *Int. J. Radiat. Biol.* 94, 759–768. doi: 10.1080/09553002.2017.1387304

Holmberg, C., Fleck, O., Hansen, H. A., Liu, C., Slaaby, R., Carr, A. M., et al. (2005). Ddb1 controls genome stability and meiosis in fission yeast. *Genes Dev.* 19, 853–862. doi: 10.1101/gad.329905

Honaker, Y., and Piwnica-Worms, H. (2010). Casein kinase 1 functions as both penultimate and ultimate kinase in regulating Cdc25A destruction. *Oncogene* 29, 3324–3334. doi: 10.1038/onc.2010.96

Hu, H., Yang, Y., Ji, Q., Zhao, W., Jiang, B., Liu, R., et al. (2012). Crl4B catalyzes H2ak119 monoubiquitination and coordinates with Prc2 to promote tumorigenesis. *Cancer Cell* 22, 781–795. doi: 10.1016/j.ccr.2012.10.024

Hu, R., and Aplin, A. E. (2008). Skp2 regulates G2/M progression in a p53-dependent manner. *Mol. Biol. Cell.* 19, 4602–4610. doi: 10.1091/mbc.E07-11-1137

Huang, L. E., Gu, J., Schau, M., and Bunn, H. F. (1998). Regulation of hypoxia-inducible factor 1α is mediated by an O2-dependent degradation domain via the ubiquitin-proteasome pathway. *Proc. Natl. Acad. Sci. U.S.A.* 95, 7987–7992. doi: 10.1073/pnas.95.14.7987

Huen, M. S. Y., Sy, S. M. H., and Chen, J. (2009). Brca1 and its toolbox for the maintenance of genome integrity. *Nat. Rev. Mol. Cell Biol.* 11, 138–148. doi: 10.1038/nrm2831

Hung, M. S., Mao, J. H., Xu, Z., Yang, C. T., Yu, J. S., Harvard, C., et al. (2011). Cul4A is an oncogene in malignant pleural mesothelioma. *J. Cell Mol. Med.* 15, 350–358. doi: 10.1111/j.1582-4934.2009.00971.x

Ikura, T., Ogryzko, V. V., Grigoriev, M., Groisman, R., Wang, J., Horikoshi, M., et al. (2000). Involvement of the Tip60 histone acetylase complex in Dna repair and apoptosis. *Cell* 102, 463–473. doi: 10.1016/s0092-8674(00)00051-9

Inuzuka, H., Tseng, A., Gao, D., Zhai, B., Zhang, Q., Shaik, S., et al. (2010). Phosphorylation by casein kinase i promotes the turnover of the Mdm2 oncoprotein via the Scfβ-Trcp Ubiquitin ligase. *Cancer Cell* 18, 147–159. doi: 10.1016/j.ccr.2010.06.015

Iovine, B., Iannella, M. L., and Bevilacqua, M. A. (2011). Damage-specific Dna binding protein 1 (Ddb1): a protein with a wide range of functions. *Int. J. Biochem. Cell Biol.* 43, 1664–1667. doi: 10.1016/j.biocel.2011.09.001

Ishida, N., Nakagawa, T., Iemura, S. I., Yasui, A., Shima, H., Katoh, Y., et al. (2017). Ubiquitylation of Ku80 by Rnf126 promotes completion of nonhomologous end joining-mediated dna repair. *Mol. Cell Biol.* 37:e00347-16. doi: 10.1128/MCB.00347-16

Ismail, I. H., Gagne, J. P., Genois, M. M., Strickfaden, H., Mcdonald, D., Xu, Z., et al. (2015). The Rnf138 E3 ligase displaces Ku to promote Dna end resection and regulate Dna repair pathway choice. *Nat. Cell Biol.* 17, 1446–1457. doi: 10.1038/ncb3259

Isoda, M., Kanemori, Y., Nakajo, N., Uchida, S., Yamashita, K., Ueno, H., et al. (2009). The extracellular signal-regulated kinase–mitogen-activated protein kinase pathway phosphorylates and targets Cdc25A for Scfβ-Trcp-dependent degradation for cell cycle arrest. *Mol. Biol. Cell* 20, 2186–2195. doi: 10.1091/mbc.e09-01-0008

Jang, S. M., Redon, C. E., and Aladjem, M. I. (2018). Chromatin-bound cullin-ring ligases: regulatory roles in dna replication and potential targeting for cancer therapy. *Front. Mol. Biosci.* 5:19. doi: 10.3389/fmolb.2018.00019

Jeong, Y., Hoang, N. T., Lovejoy, A., Stehr, H., Newman, A. M., Gentles, A. J., et al. (2017). Role of Keap1/Nrf2 and Tp53 mutations in lung squamous cell carcinoma development and radiation resistance. *Cancer Discov.* 7, 86–101. doi: 10.1158/2159-8290.CD-16-0127

Jiang, T., Tang, H. M., Wu, Z. H., Chen, J., Lu, S., Zhou, C. Z., et al. (2013). Cullin 4B is a novel prognostic marker that correlates with colon cancer progression and pathogenesis. *Med. Oncol.* 30:534. doi: 10.1007/s12032-013-0534-7

Jin, J., Arias, E. E., Chen, J., Harper, J. W., and Walter, J. C. (2006). A family of diverse Cul4-Ddb1-interacting proteins includes Cdt2, which is required for S phase destruction of the replication factor Cdt1. *Mol. Cell* 23, 709–721. doi: 10.1016/j.molcel.2006.08.010

Jin, J., Cardozo, T., Lovering, R. C., Elledge, S. J., Pagano, M., and Harper, J. W. (2004). Systematic analysis and nomenclature of mammalian F-box proteins. *Genes Dev.* 18, 2573–2580. doi: 10.1101/gad.1255304

Jin, J., Shirogane, T., Xu, L., Nalepa, G., Qin, J., Elledge, S. J., et al. (2003). Scfbeta-Trcp links Chk1 signaling to degradation of the Cdc25A protein phosphatase. *Genes Dev.* 17, 3062–3074. doi: 10.1101/gad.1157503

Johmura, Y., Sun, J., Kitagawa, K., Nakanishi, K., Kuno, T., Naiki-Ito, A., et al. (2016). Scf(Fbxo22)-Kdm4A targets methylated p53 for degradation and regulates senescence. *Nat. Commun.* 7:10574. doi: 10.1038/ncomms10574

Jones, R. J., Baladandayuthapani, V., Neelapu, S., Fayad, L. E., Romaguera, J. E., Wang, M., et al. (2011). Hdm-2 inhibition suppresses expression of ribonucleotide reductase subunit M2, and synergistically enhances gemcitabine-induced cytotoxicity in mantle cell lymphoma. *Blood* 118, 4140–4149. doi: 10.1182/blood-2011-03-340323

Kamio, M., Yoshida, T., Ogata, H., Douchi, T., Nagata, Y., Inoue, M., et al. (2004). Socs1 inhibits Hpv-E7-mediated transformation by inducing degradation of E7 protein. *Oncogene* 23, 3107–3115. doi: 10.1038/sj.onc.1207453

Kamizono, S., Hanada, T., Yasukawa, H., Minoguchi, S., Kato, R., Minoguchi, M., et al. (2001). The Socs box of Socs-1 accelerates ubiquitin-dependent proteolysis of Tel-Jak2. *J. Biol. Chem.* 276, 12530–12538. doi: 10.1074/jbc.m010074200

Kamura, T., Maenaka, K., Kotoshiba, S., Matsumoto, M., Kohda, D., Conaway, R. C., et al. (2004). Vhl-box and Socs-box domains determine binding specificity for Cul2-Rbx1 and Cul5-Rbx2 modules of ubiquitin ligases. *Genes Dev.* 18, 3055–3065. doi: 10.1101/gad.1252404

Kang, T., Wei, Y., Honaker, Y., Yamaguchi, H., Appella, E., Hung, M. C., et al. (2008). Gsk-3 beta targets Cdc25A for ubiquitin-mediated proteolysis, and Gsk-3 beta inactivation correlates with Cdc25A overproduction in human cancers. *Cancer Cell* 13, 36–47. doi: 10.1016/j.ccr.2007.12.002

Kawaida, R., Yamada, R., Kobayashi, K., Tokuhiro, S., Suzuki, A., Kochi, Y., et al. (2005). Cul1, a component of E3 ubiquitin ligase, alters lymphocyte signal transduction with possible effect on rheumatoid arthritis. *Genes Immun.* 6, 194–202. doi: 10.1038/sj.gene.6364177

Kensler, T. W., Wakabayashi, N., and Biswal, S. (2007). Cell survival responses to environmental stresses via the Keap1-Nrf2-Are pathway. *Annu. Rev. Pharmacol. Toxicol* 47, 89–116. doi: 10.1146/annurev.pharmtox.46.120604.141046

Kim, J. J., Lee, S. B., Jang, J., Yi, S. Y., Kim, S. H., Han, S. A., et al. (2015). Wsb1 promotes tumor metastasis by inducing pvhl degradation. *Genes Dev*, 29, 2244–2257. doi: 10.1101/gad.268128.115

Kim, Y., and Kipreos, E. T. (2007). Cdt1 degradation to prevent Dna re-replication: conserved and non-conserved pathways. *Cell Div.* 2:18. doi: 10.1186/1747-1028-2-18

Kim, Y., Starostina, N. G., and Kipreos, E. T. (2008). The Crl4Cdt2 ubiquitin ligase targets the degradation of p21Cip1 to control replication licensing. *Genes Dev.* 22, 2507–2519. doi: 10.1101/gad.1703708

Kim, Y. H., Yoo, K. C., Cui, Y. H., Uddin, N., Lim, E. J., Kim, M. J., et al. (2014). Radiation promotes malignant progression of glioma cells through Hif-1alpha stabilization. *Cancer Lett.* 354, 132–141. doi: 10.1016/j.canlet.2014.07.048

Kimple, R. J., Smith, M. A., Blitzer, G. C., Torres, A. D., Martin, J. A., Yang, R. Z., et al. (2013). Enhanced radiation sensitivity in Hpv-positive head and neck cancer. *Cancer Res.* 73, 4791–4800. doi: 10.1158/0008-5472.CAN-13-0587

Kipreos, E. T., Lander, L. E., Wing, J. P., He, W. W., and Hedgecock, E. M. (1996). cul-1 is required for cell cycle exit in *C. elegans* and identifies a novel gene family. *Cell* 85, 829–839. doi: 10.1016/s0092-8674(00)81267-2

Klein, D. K., Hoffmann, S., Ahlskog, J. K., O'hanlon, K., Quaas, M., Larsen, B. D., et al. (2015). Cyclin F suppresses B-Myb activity to promote cell cycle checkpoint control. *Nat. Commun.* 6:5800. doi: 10.1038/ncomms6800

Kobayashi, A., Kang, M. I., Okawa, H., Ohtsuji, M., Zenke, Y., Chiba, T., et al. (2004). Oxidative stress sensor Keap1 functions as an adaptor for Cul3-based E3 ligase to regulate proteasomal degradation of Nrf2. *Mol. Cell Biol.* 24, 7130–7139. doi: 10.1128/mcb.24.16.7130-7139.2004

Konstantinopoulos, P. A., Spentzos, D., Fountzilas, E., Francoeur, N., Sanisetty, S., Grammatikos, A. P., et al. (2011). Keap1 mutations and Nrf2 pathway activation in epithelial ovarian cancer. *Cancer Res.* 71, 5081–5089. doi: 10.1158/0008-5472.CAN-10-4668

Koren, I., Timms, R. T., Kula, T., Xu, Q., Li, M. Z., and Elledge, S. J. (2018). The Eukaryotic Proteome Is Shaped by E3 Ubiquitin Ligases Targeting C-Terminal Degrons. *Cell* 173, 1622.e14–1635.e14. doi: 10.1016/j.cell.2018.04.028

Kuiken, H. J., Egan, D. A., Laman, H., Bernards, R., Beijersbergen, R. L., and Dirac, A. M. (2012). Identification of F-box only protein 7 as a negative regulator of Nf-kappaB signalling. *J. Cell Mol. Med.* 16, 2140–2149. doi: 10.1111/j.1582-4934.2012.01524.x

Kunz, B. A., Kohalmi, S. E., Kunkel, T. A., Mathews, C. K., Mcintosh, E. M., and Reidy, J. A. (1994). Deoxyribonucleoside triphosphate levels: A critical factor in the maintenance of genetic stability. *Mutat. Res.* 318, 1–64. doi: 10.1016/0165-1110(94)90006-x

Lai, A. C., and Crews, C. M. (2017). Induced protein degradation: an emerging drug discovery paradigm. *Nat. Rev. Drug Discov.* 16, 101–114. doi: 10.1038/nrd.2016.211

Li, B., Jia, N., Kapur, R., and Chun, K. T. (2006). Cul4A targets p27 for degradation and regulates proliferation, cell cycle exit, and differentiation during erythropoiesis. *Blood* 107, 4291–4299. doi: 10.1182/blood-2005-08-3349

Lin, D. I., Barbash, O., Kumar, K. G. S., Weber, J. D., Harper, J. W., Klein-Szanto, A J. P., et al. (2006). Phosphorylation-dependent ubiquitination of cyclin D1 by the Scffbx4-αB crystallin complex. *Mol. Cell* 24, 355–366. doi: 10.1016/j.molcel.2006.09.007

Liu, S., Wang, H., Wang, X., Lu, L., Gao, N., Rowe, P. S., et al. (2009). Mepe/Of45 protects cells from Dna damage induced killing via stabilizing Chk1. *Nucleic Acids Res.* 37, 7447–7454. doi: 10.1093/nar/gkp768

Liu, Y., Dong, Y., Kong, L., Shi, F., Zhu, H., and Yu, J. (2018). Abscopal effect of radiotherapy combined with immune checkpoint inhibitors. *J. Hematol. Oncol.* 11:104. doi: 10.1186/s13045-018-0647-8

Lu, J., Qian, Y., Altieri, M., Dong, H., Wang, J., Raina, K., et al. (2015). Hijacking the E3 ubiquitin ligase cereblon to efficiently target Brd4. *Chem. Biol.* 22, 755–763. doi: 10.1016/j.chembiol.2015.05.009

Lu, Y., Li, J., Cheng, D., Parameswaran, B., Zhang, S., Jiang, Z., et al. (2012). The F-box protein Fbxo44 mediates Brca1 ubiquitination and degradation. *J. Biol. Chem.* 287, 41014–41022. doi: 10.1074/jbc.M112.407106

Lukas, J., Pagano, M., Staskova, Z., Draetta, G., and Bartek, J. (1994). Cyclin D1 protein oscillates and is essential for cell cycle progression in human tumour cell lines. *Oncogene* 9, 707–718.

Mailand, N., Bekker-Jensen, S., Bartek, J., and Lukas, J. (2006). Destruction of claspin by ScfβTrcp restrains Chk1 activation and facilitates recovery from genotoxic stress. *Mol. Cell* 23, 307–318. doi: 10.1016/j.molcel.2006.06.016

Marzio, A., Puccini, J., Kwon, Y., Maverakis, N. K., Arbini, A., Sung, P., et al. (2018). The F-Box domain-dependent activity of emi1 regulates parpi sensitivity in triple-negative breast cancers. *Mol. Cell* 73, 224.e6–237.e6. doi: 10.1016/j.molcel.2018.11.003

Mathew, R., Seiler, M. P., Scanlon, S. T., Mao, A. P., Constantinides, M. G., Bertozzi-Villa, C., et al. (2012). Btb-Zf factors recruit the E3 ligase cullin 3 to regulate lymphoid effector programs. *Nature* 491, 618–621. doi: 10.1038/nature11548

Mavrommati, I., Faedda, R., Galasso, G., Li, J., Burdova, K., Fischer, R., et al. (2018). beta-Trcp- and casein kinase ii-mediated degradation of cyclin F controls timely mitotic progression. *Cell Rep.* 24, 3404–3412. doi: 10.1016/j.celrep.2018.08.076

Maxwell, P. H., Wiesener, M. S., Chang, G. W., Clifford, S. C., Vaux, E. C., Cockman, M. E., et al. (1999). The tumour suppressor protein Vhl targets hypoxia-inducible factors for oxygen-dependent proteolysis. *Nature* 399, 271–275. doi: 10.1038/20459

Melchor, L., Saucedo-Cuevas, L. P., Munoz-Repeto, I., Rodriguez-Pinilla, S. M., Honrado, E., Campoverde, A., et al. (2009). Comprehensive characterization of the Dna amplification at 13q34 in human breast cancer reveals Tfdp1 and Cul4A as likely candidate target genes. *Breast Cancer Res.* 11:R86. doi: 10.1186/bcr2456

Melixetian, M., Klein, D. K., Sørensen, C. S., and Helin, K. (2009). Nek11 regulates Cdc25A degradation and the Ir-induced G2/M checkpoint. *Nat. Cell Biol.* 11, 1247–1253. doi: 10.1038/ncb1969

Mena, E. L., Kjolby, R. A. S., Saxton, R. A., Werner, A., Lew, B. G., Boyle, J. M., et al. (2018). Dimerization quality control ensures neuronal development and survival. *Science* 362:eaa8236. doi: 10.1126/science.aap8236

Michishita, M., Morimoto, A., Ishii, T., Komori, H., Shiomi, Y., Higuchi, Y., et al. (2011). Positively charged residues located downstream of Pip box, together with Td amino acids within Pip box, are important for Crl4(Cdt2) -mediated proteolysis. *Genes Cells* 16, 12–22. doi: 10.1111/j.1365-2443.2010.01464.x

Moeller, B. J., Cao, Y., Li, C. Y., and Dewhirst, M. W. (2004). Radiation activates Hif-1 to regulate vascular radiosensitivity in tumors: role of reoxygenation, free radicals, and stress granules. *Cancer Cell* 5, 429–441. doi: 10.1016/s1535-6108(04)00115-1

Mole, R. H. (1953). Whole body irradiation; radiobiology or medicine? *Br. J. Radiol.* 26, 234–241.

Momand, J., Zambetti, G. P., Olson, D. C., George, D., and Levine, A. J. (1992). The mdm-2 oncogene product forms a complex with the p53 protein and inhibits p53-mediated transactivation. *Cell* 69, 1237–1245. doi: 10.1016/0092-8674(92)90644-r

Morikawa, T., Hino, R., Uozaki, H., Maeda, D., Ushiku, T., Shinozaki, A., et al. (2010a). Expression of ribonucleotide reductase M2 subunit in gastric cancer and effects of Rrm2 inhibition in vitro. *Hum. Pathol.* 41, 1742–1748. doi: 10.1016/j.humpath.2010.06.001

Morikawa, T., Maeda, D., Kume, H., Homma, Y., and Fukayama, M. (2010b). Ribonucleotide reductase M2 subunit is a novel diagnostic marker and a potential therapeutic target in bladder cancer. *Histopathology* 57, 885–892. doi: 10.1111/j.1365-2559.2010.03725.x

Moss, J., Tinline-Purvis, H., Walker, C. A., Folkes, L. K., Stratford, M. R., Hayles, J., et al. (2010). Break-induced Atr and Ddb1-Cul4(Cdt)(2) ubiquitin ligase-dependent nucleotide synthesis promotes homologous recombination repair in fission yeast. *Genes Dev.* 24, 2705–2716. doi: 10.1101/gad.1970810

Murray, A. W. (2004). Recycling the cell cycle: cyclins revisited. *Cell* 116, 221–234.

Nag, A., Bagchi, S., and Raychaudhuri, P. (2004). Cul4A physically associates with Mdm2 and participates in the proteolysis of p53. *Cancer Res.* 64, 8152–8155. doi: 10.1158/0008-5472.can-04-2598

Nakamura, K., Saredi, G., Becker, J. R., Foster, B. M., Nguyen, N. V., Beyer, T. E., et al. (2019). H4K20me0 recognition by Brca1-Bard1 directs homologous recombination to sister chromatids. *Nat. Cell Biol.* 21, 311–318. doi: 10.1038/s41556-019-0282-9

Nakayama, K. I., and Nakayama, K. (2006). Ubiquitin ligases: cell-cycle control and cancer. *Nat. Rev. Cancer* 6, 369–381. doi: 10.1038/nrc1881

Ng, J., and Dai, T. (2016). Radiation therapy and the abscopal effect: a concept comes of age. *Ann. Transl. Med.* 4:118. doi: 10.21037/atm.2016.01.32

Nordlund, P., and Reichard, P. (2006). Ribonucleotide reductases. *Annu. Rev. Biochem.* 75, 681–706.

Ohta, T., Iijima, K., Miyamoto, M., Nakahara, I., Tanaka, H., Ohtsuji, M., et al. (2008). Loss of Keap1 function activates Nrf2 and provides advantages for lung cancer cell growth. *Cancer Res.* 68, 1303–1309. doi: 10.1158/0008-5472.CAN-07-5003

Oliner, J. D., Pietenpol, J. A., Thiagalingam, S., Gyuris, J., Kinzler, K. W., and Vogelstein, B. (1993). Oncoprotein Mdm2 conceals the activation domain of tumour suppressor p53. *Nature* 362, 857–860. doi: 10.1038/362857a0

Olson, C. M., Jiang, B., Erb, M. A., Liang, Y., Doctor, Z. M., Zhang, Z., et al. (2018). Pharmacological perturbation of Cdk9 using selective Cdk9 inhibition or degradation. *Nat. Chem. Biol.* 14, 163–170. doi: 10.1038/nchembio.2538

Orthwein, A., Noordermeer, S. M., Wilson, M. D., Landry, S., Enchev, R. I., Sherker, A., et al. (2015). A mechanism for the suppression of homologous recombination in G1 cells. *Nature* 528, 422–426. doi: 10.1038/nature16142

Pagano, M., Theodoras, A. M., Tam, S. W., and Draetta, G. F. (1994). Cyclin D1-mediated inhibition of repair and replicative Dna synthesis in human fibroblasts. *Genes Dev.* 8, 1627–1639. doi: 10.1101/gad.8.14.1627

Peschiaroli, A., Dorrello, N. V., Guardavaccaro, D., Venere, M., Halazonetis, T., Sherman, N. E., et al. (2006). ScfβTrcp-mediated degradation of claspin regulates recovery from the dna replication checkpoint response. *Mol. Cell* 23, 319–329. doi: 10.1016/j.molcel.2006.06.013

Pintard, L., Willems, A., and Peter, M. (2004). Cullin-based ubiquitin ligases: Cul3-Btb complexes join the family. *EMBO J.* 23, 1681–1687. doi: 10.1038/sj.emboj.7600186

Pontano, L. L., Aggarwal, P., Barbash, O., Brown, E. J., Bassing, C. H., and Diehl, J. A. (2008). Genotoxic stress-induced cyclin D1 phosphorylation and proteolysis are required for genomic stability. *Mol. Cell Biol.* 28, 7245–7258. doi: 10.1128/MCB.01085-08

Postow, L., and Funabiki, H. (2013). An Scf complex containing Fbxl12 mediates Dna damage-induced Ku80 ubiquitylation. *Cell Cycle* 12, 587–595. doi: 10.4161/cc.23408

Postow, L., Ghenoiu, C., Woo, E. M., Krutchinsky, A. N., Chait, B. T., and Funabiki, H. (2008). Ku80 removal from Dna through double strand break-induced ubiquitylation. *J. Cell Biol.* 182, 467–479. doi: 10.1083/jcb.200802146

Prabhu, P., Shandilya, S. M., Britan-Rosich, E., Nagler, A., Schiffer, C. A., and Kotler, M. (2016). Inhibition of Apobec3G activity impedes double-stranded Dna repair. *FEBS J.* 283, 112–129. doi: 10.1111/febs.13556

Ralph, E., Boye, E., and Kearsey, S. E. (2006). Dna damage induces Cdt1 proteolysis in fission yeast through a pathway dependent on Cdt2 and Ddb1. *EMBO Rep.* 7, 1134–1139. doi: 10.1038/sj.embor.7400827

Ren, L., Zeng, M., Tang, Z., Li, M., Wang, X., Xu, Y., et al. (2019). The antiresection activity of the X protein encoded by hepatitis virus B. *Hepatology* 69, 2546–2561. doi: 10.1002/hep.30571

Rockwell, S., Dobrucki, I. T., Kim, E. Y., Marrison, S. T., and Vu, V. T. (2009). Hypoxia and radiation therapy: past history, ongoing research, and future promise. *Curr. Mol. Med.* 9, 442–458. doi: 10.2174/15665240978816 7087

Roots, R., and Okada, S. (1975). Estimation of life times and diffusion distances of radicals involved in x-ray-induced Dna strand breaks of killing of mammalian cells. *Radiat. Res.* 64, 306–320.

Rossi, M., Duan, S., Jeong, Y. T., Horn, M., Saraf, A., Florens, L., et al. (2013). Regulation of the Crl4(Cdt2) ubiquitin ligase and cell-cycle exit by the Scf(Fbxo11) ubiquitin ligase. *Mol. Cell* 49, 1159–1166. doi: 10.1016/j.molcel.2013.02.004

Sakamoto, K. M., Kim, K. B., Kumagai, A., Mercurio, F., Crews, C. M., and Deshaies, R. J. (2001). Protacs: chimeric molecules that target proteins to the Skp1-Cullin-F box complex for ubiquitination and degradation. *Proc. Natl. Acad. Sci. U.S.A.* 98, 8554–8559. doi: 10.1073/pnas.141230798

Santra, M. K., Wajapeyee, N., and Green, M. R. (2009). F-box protein Fbxo31 mediates cyclin D1 degradation to induce G1 arrest after Dna damage. *Nature* 459, 722–725. doi: 10.1038/nature08011

Sarikas, A., Hartmann, T., and Pan, Z. Q. (2011). The cullin protein family. *Genome Biol.* 12:220. doi: 10.1186/gb-2011-12-4-220

Sartori, A. A., Lukas, C., Coates, J., Mistrik, M., Fu, S., Bartek, J., et al. (2007). Human Ctip promotes Dna end resection. *Nature* 450, 509–514. doi: 10.1038/nature06337

Saucedo-Cuevas, L. P., Ruppen, I., Ximenez-Embun, P., Domingo, S., Gayarre, J., Munoz, J., et al. (2014). Cul4A contributes to the biology of basal-like breast tumors through modulation of cell growth and antitumor immune response. *Oncotarget* 5, 2330–2343.

Schneekloth, A. R., Pucheault, M., Tae, H. S., and Crews, C. M. (2008). Targeted intracellular protein degradation induced by a small molecule: en route to chemical proteomics. *Bioorg. Med. Chem. Lett.* 18, 5904–5908. doi: 10.1016/j.bmcl.2008.07.114

Schneekloth, J. S. Jr., Fonseca, F. N., Koldobskiy, M., Mandal, A., Deshaies, R., Sakamoto, K., et al. (2004). Chemical genetic control of protein levels: selective in vivo targeted degradation. *J. Am. Chem. Soc.* 126, 3748–3754. doi: 10.1021/ja039025z

Schwertman, P., Bekker-Jensen, S., and Mailand, N. (2016). Regulation of Dna double-strand break repair by ubiquitin and ubiquitin-like modifiers. *Nat. Rev. Mol. Cell Biol.* 17, 379–394. doi: 10.1038/nrm.2016.58

Scrima, A., Fischer, E. S., Lingaraju, G. M., Bohm, K., Cavadini, S., and Thoma, N. H. (2011). Detecting Uv-lesions in the genome: the modular Crl4 ubiquitin ligase does it best! *FEBS Lett.* 585, 2818–2825. doi: 10.1016/j.febslet.2011.04.064

Semenza, G. L. (1999). Regulation of mammalian O2 homeostasis by hypoxia-inducible factor 1. *Annu. Rev. Cell Dev. Biol.* 15, 551–578. doi: 10.1146/annurev.cellbio.15.1.551

Semenza, G. L. (2003). Targeting Hif-1 for cancer therapy. *Nat. Rev. Cancer* 3, 721–732. doi: 10.1038/nrc1187

Shibata, T., Kokubu, A., Gotoh, M., Ojima, H., Ohta, T., Yamamoto, M., et al. (2008a). Genetic alteration of Keap1 confers constitutive Nrf2 activation and resistance to chemotherapy in gallbladder cancer. *Gastroenterology* 135, 1358.e4–1368.e4. doi: 10.1053/j.gastro.2008.06.082

Shibata, T., Ohta, T., Tong, K. I., Kokubu, A., Odogawa, R., Tsuta, K., et al. (2008b). Cancer related mutations in Nrf2 impair its recognition by Keap1-Cul3 E3 ligase and promote malignancy. *Proc. Natl. Acad. Sci. U.S.A.* 105, 13568–13573. doi: 10.1073/pnas.0806268105

Shibata, T., Kokubu, A., Saito, S., Narisawa-Saito, M., Sasaki, H., Aoyagi, K., et al. (2011). Nrf2 mutation confers malignant potential and resistance to chemoradiation therapy in advanced esophageal squamous cancer. *Neoplasia* 13, 864–873.

Shinomiya, T., Mori, T., Ariyama, Y., Sakabe, T., Fukuda, Y., Murakami, Y., et al. (1999). Comparative genomic hybridization of squamous cell carcinoma of the esophagus: the possible involvement of the Dpi gene in the 13q34 amplicon.

*Genes Chromosomes Cancer* 24, 337–344. doi: 10.1002/(sici)1098-2264(199904)24:4<337::aid-gcc7>3.3.co;2-f

Shrieve, D. C., and Loeffler, J. S. (2011). *Human Radiation Injury*, 1st Edn. Philadelphia, PA: Lippincott Williams & Wilkins.

Singh, A., Misra, V., Thimmulappa, R. K., Lee, H., Ames, S., Hoque, M. O., et al. (2006). Dysfunctional Keap1-Nrf2 interaction in non-small-cell lung cancer. *PLoS Med.* 3:e420. doi: 10.1371/journal.pmed.0030420

Sitko, J. C., Yeh, B., Kim, M., Zhou, H., Takaesu, G., Yoshimura, A., et al. (2008). Socs3 regulates p21 expression and cell cycle arrest in response to Dna damage. *Cell Signal.* 20, 2221–2230. doi: 10.1016/j.cellsig.2008.08.011

Solis, L. M., Behrens, C., Dong, W., Suraokar, M., Ozburn, N. C., Moran, C. A., et al. (2010). Nrf2 and Keap1 abnormalities in non-small cell lung carcinoma and association with clinicopathologic features. *Clin. Cancer Res.* 16, 3743–3753. doi: 10.1158/1078-0432.CCR-09-3352

Sorensen, B. S., Busk, M., Horsman, M. R., Alsner, J., Overgaard, J., Kyle, A. H., et al. (2014). Effect of radiation on cell proliferation and tumor hypoxia in Hpv-positive head and neck cancer in vivo models. *Anticancer Res.* 34, 6297–6304.

Soucy, T. A., Smith, P. G., Milhollen, M. A., Berger, A. J., Gavin, J. M., Adhikari, S., et al. (2009). An inhibitor of Nedd8-activating enzyme as a new approach to treat cancer. *Nature* 458, 732–736. doi: 10.1038/nature07884

Stuart, S. A., and Wang, J. Y. (2009). Ionizing radiation induces Atm-independent degradation of p21Cip1 in transformed cells. *J. Biol. Chem.* 284, 15061–15070. doi: 10.1074/jbc.M808810200

Sugasawa, K. (2009). Uv-Ddb: a molecular machine linking Dna repair with ubiquitination. *DNA Repair* 8, 969–972. doi: 10.1016/j.dnarep.2009.05.001

Sun, L., Shi, L., Li, W., Yu, W., Liang, J., Zhang, H., et al. (2009). Jfk, a Kelch domain-containing F-box protein, links the Scf complex to p53 regulation. *Proc. Natl. Acad. Sci. U.S.A.* 106, 10195–10200. doi: 10.1073/pnas.0901864106

Sun, Y., Jiang, X., Chen, S., Fernandes, N., and Price, B. D. (2005). A role for the Tip60 histone acetyltransferase in the acetylation and activation of Atm. *Proc. Natl. Acad. Sci. U.S.A.* 102, 13182–13187. doi: 10.1073/pnas.0504211102

Sun, Y., Moretti, L., Giacalone, N. J., Schleicher, S., Speirs, C. K., Carbone, D. P., et al. (2011). Inhibition of Jak2 signaling by Tg101209 enhances radiotherapy in lung cancer models. *J. Thorac. Oncol.* 6, 699–706. doi: 10.1097/JTO.0b013e31820d9d11

Sy, S. M., Huen, M. S., and Chen, J. (2009). Palb2 is an integral component of the Brca complex required for homologous recombination repair. *Proc. Natl. Acad. Sci. U.S.A.* 106, 7155–7160. doi: 10.1073/pnas.0811159106

Tan, M. K., Lim, H. J., and Harper, J. W. (2011). Scf(Fbxo22) regulates histone H3 lysine 9 and 36 methylation levels by targeting histone demethylase Kdm4A for ubiquitin-mediated proteasomal degradation. *Mol. Cell Biol.* 31, 3687–3699. doi: 10.1128/MCB.05746-11

Tomimatsu, N., Mukherjee, B., Harris, J. L., Boffo, F. L., Hardebeck, M. C., Potts, P. R., et al. (2017). Dna-damage-induced degradation of Exo1 exonuclease limits Dna end resection to ensure accurate Dna repair. *J. Biol. Chem.* 292, 10779–10790. doi: 10.1074/jbc.M116.772475

Tong, K. I., Kobayashi, A., Katsuoka, F., and Yamamoto, M. (2006). Two-site substrate recognition model for the Keap1-Nrf2 system: a hinge and latch mechanism. *Biol. Chem.* 387, 1311–1320.

Toure, M., and Crews, C. M. (2016). Small-molecule protacs: new approaches to protein degradation. *Angew Chem. Int. Ed. Engl.* 55, 1966–1973. doi: 10.1002/anie.201507978

Uchida, S., Yoshioka, K., Kizu, R., Nakagama, H., Matsunaga, T., Ishizaka, Y., et al. (2009). Stress-activated mitogen-activated protein kinases c-Jun Nh2-terminal kinase and p38 target Cdc25B for degradation. *Cancer Res.* 69, 6438–6444. doi: 10.1158/0008-5472.CAN-09-0869

Vanderdys, V., Allak, A., Guessous, F., Benamar, M., Read, P. W., Jameson, M. J., et al. (2018). The neddylation inhibitor pevonedistat (Mln4924) suppresses and radiosensitizes head and neck squamous carcinoma cells and tumors. *Mol. Cancer Ther.* 17, 368–380. doi: 10.1158/1535-7163.MCT-17-0083

Vaupel, P. (2004). Tumor microenvironmental physiology and its implications for radiation oncology. *Semin. Radiat. Oncol.* 14, 198–206. doi: 10.1016/j.semradonc.2004.04.008

Vrba, L., Junk, D. J., Novak, P., and Futscher, B. W. (2008). p53 induces distinct epigenetic states at its direct target promoters. *BMC Genomics* 9:486. doi: 10.1186/1471-2164-9-486

Wan, J., Zhu, J., Li, G., and Zhang, Z. (2016). Radiosensitization of human colorectal cancer cells by Mln4924: an inhibitor of Nedd8-activating enzyme. *Technol. Cancer Res. Treat.* 15, 527–534. doi: 10.1177/1533034615588197

Wang, W., Mani, A. M., and Wu, Z. H. (2017). Dna damage-induced nuclear factor-kappa B activation and its roles in cancer progression. *J. Cancer Metastasis Treat.* 3, 45–59. doi: 10.20517/2394-4722.2017.03

Wang, X. J., Sun, Z., Villeneuve, N. F., Zhang, S., Zhao, F., Li, Y., et al. (2008). Nrf2 enhances resistance of cancer cells to chemotherapeutic drugs, the dark side of Nrf2. *Carcinogenesis* 29, 1235–1243. doi: 10.1093/carcin/bgn095

Wang, Y., Wen, M., Kwon, Y., Xu, Y., Liu, Y., Zhang, P., et al. (2014). Cul4A induces epithelial-mesenchymal transition and promotes cancer metastasis by regulating Zeb1 expression. *Cancer Res.* 74, 520–531. doi: 10.1158/0008-5472.CAN-13-2182

Watanabe, N., Arai, H., Nishihara, Y., Taniguchi, M., Watanabe, N., Hunter, T., et al. (2004). M-phase kinases induce phospho-dependent ubiquitination of somatic Wee1 by Scfβ-Trcp. *Proc. Natl. Acad. Sci. U.S.A.* 101, 4419–4424. doi: 10.1073/pnas.0307700101

Wei, D., Li, H., Yu, J., Sebolt, J. T., Zhao, L., Lawrence, T. S., et al. (2012). Radiosensitization of human pancreatic cancer cells by Mln4924, an investigational Nedd8-activating enzyme inhibitor. *Cancer Res.* 72, 282–293. doi: 10.1158/0008-5472.CAN-11-2866

Welcker, M., and Clurman, B. E. (2008). Fbw7 ubiquitin ligase: a tumour suppressor at the crossroads of cell division, growth and differentiation. *Nat. Rev. Cancer* 8, 83–93. doi: 10.1038/nrc2290

Winston, J. T., Koepp, D. M., Zhu, C., Elledge, S. J., and Harper, J. W. (1999). A family of mammalian F-box proteins. *Curr. Biol.* 9, 1180–1182.

Xia, Y., Padre, R. C., De Mendoza, T. H., Bottero, V., Tergaonkar, V. B., and Verma, I. M. (2009). Phosphorylation of p53 by IκB kinase 2 promotes its degradation by β-Trcp. *Proc. Natl. Acad. Sci. U.S.A.* 106, 2629–2634. doi: 10.1073/pnas.0812256106

Xu, X., Page, J. L., Surtees, J. A., Liu, H., Lagedrost, S., Lu, Y., et al. (2008). Broad overexpression of ribonucleotide reductase genes in mice specifically induces lung neoplasms. *Cancer Res.* 68, 2652–2660. doi: 10.1158/0008-5472.CAN-07-5873

Yasui, K., Arii, S., Zhao, C., Imoto, I., Ueda, M., Nagai, H., et al. (2002). Tfdp1, Cul4A, and Cdc16 identified as targets for amplification at 13q34 in hepatocellular carcinomas. *Hepatology* 35, 1476–1484. doi: 10.1053/jhep.2002.33683

Yoo, N. J., Kim, H. R., Kim, Y. R., An, C. H., and Lee, S. H. (2012). Somatic mutations of the Keap1 gene in common solid cancers. *Histopathology* 60, 943–952. doi: 10.1111/j.1365-2559.2012.04178.x

Yu, X., Yu, Y., Liu, B., Luo, K., Kong, W., Mao, P., et al. (2003). Induction of Apobec3G ubiquitination and degradation by an Hiv-1 Vif-Cul5-Scf complex. *Science* 302, 1056–1060. doi: 10.1126/science.1089591

Yu, Y., Xiao, Z., Ehrlich, E. S., Yu, X., and Yu, X. F. (2004). Selective assembly of Hiv-1 Vif-Cul5-ElonginB-ElonginC E3 ubiquitin ligase complex through a novel Socs box and upstream cysteines. *Genes Dev.* 18, 2867–2872. doi: 10.1101/gad.1250204

Yuan, W. C., Lee, Y. R., Huang, S. F., Lin, Y. M., Chen, T. Y., Chung, H. C., et al. (2011). A Cullin3-Klhl20 Ubiquitin ligase-dependent pathway targets Pml to potentiate Hif-1 signaling and prostate cancer progression. *Cancer Cell* 20, 214–228. doi: 10.1016/j.ccr.2011.07.008

Zeng, M., Ren, L., Mizuno, K., Nestoras, K., Wang, H., Tang, Z., et al. (2016). Crl4(Wdr70) regulates H2B monoubiquitination and facilitates Exo1-dependent resection. *Nat. Commun.* 7:11364. doi: 10.1038/ncomms11364

Zhang, D., Wang, H., Sun, M., Yang, J., Zhang, W., Han, S., et al. (2014). Speckle-type Poz protein, Spop, is involved in the DNA damage response. *Carcinogenesis* 35, 1691–1697. doi: 10.1093/carcin/bgu022

Zhang, D. D., Lo, S. C., Cross, J. V., Templeton, D. J., and Hannink, M. (2004). Keap1 is a redox-regulated substrate adaptor protein for a Cul3-dependent ubiquitin ligase complex. *Mol. Cell Biol.* 24, 10941–10953. doi: 10.1128/mcb.24.24.10941-10953.2004

Zhang, F., Bick, G., Park, J. Y., and Andreassen, P. R. (2012). Mdc1 and Rnf8 function in a pathway that directs Brca1-dependent localization of Palb2 required for homologous recombination. *J. Cell Sci.* 125, 6049–6057. doi: 10.1242/jcs.111872

Zhang, F., Ma, J., Wu, J., Ye, L., Cai, H., Xia, B., et al. (2009). Palb2 links Brca1 and Brca2 in the DNA-damage response. *Curr. Biol.* 19, 524–529. doi: 10.1016/j.cub.2009.02.018

Zhang, Y.-W., Brognard, J., Coughlin, C., You, Z., Dolled-Filhart, M., Aslanian, A., et al. (2009). The F box protein Fbx6 regulates Chk1 stability and cellular sensitivity to replication stress. *Mol. Cell* 35, 442–453. doi: 10.1016/j.molcel.2009.06.030

Zhang, J., Bu, X., Wang, H., Zhu, Y., Geng, Y., Nihira, N. T., et al. (2018). Cyclin D-Cdk4 kinase destabilizes Pd-L1 via cullin 3-Spop to control cancer immune surveillance. *Nature* 553, 91–95. doi: 10.1038/nature25015

Zhang, P., Singh, A., Yegnasubramanian, S., Esopi, D., Kombairaju, P., Bodas, M., et al. (2010). Loss of Kelch-like Ech-associated protein 1 function in prostate cancer cells causes chemoresistance and radioresistance and promotes tumor growth. *Mol. Cancer Ther.* 9, 336–346. doi: 10.1158/1535-7163.MCT-09-0589

Zhang, Q., Karnak, D., Tan, M., Lawrence, T. S., Morgan, M. A., and Sun, Y. (2016). Fbxw7 facilitates nonhomologous end-joining via K63-linked polyubiquitylation of Xrcc4. *Mol. Cell* 61, 419–433. doi: 10.1016/j.molcel.2015.12.010

Zhang, Y.-W., Otterness, D. M., Chiang, G. G., Xie, W., Liu, Y.-C., Mercurio, F., et al. (2005). Genotoxic stress targets human Chk1 for degradation by the ubiquitin-proteasome pathway. *Mol. Cell* 19, 607–618. doi: 10.1016/j.molcel.2005.07.019

Zhou, H., Miki, R., Eeva, M., Fike, F. M., Seligson, D., Yang, L., et al. (2007). Reciprocal regulation of Socs 1 and Socs3 enhances resistance to ionizing radiation in glioblastoma multiforme. *Clin. Cancer Res.* 13, 2344–2353. doi: 10.1158/1078-0432.ccr-06-2303

Zou, Y., Mi, J., Cui, J., Lu, D., Zhang, X., Guo, C., et al. (2009). Characterization of nuclear localization signal in the N terminus of Cul4B and its essential role in cyclin E degradation and cell cycle progression. *J. Biol. Chem.* 284, 33320–33332. doi: 10.1074/jbc.M109.050427

**Conflict of Interest Statement:** The authors declare that the research was conducted in the absence of any commercial or financial relationships that could be construed as a potential conflict of interest.

frontiers in Physiology

ORIGINAL RESEARCH
published: 10 October 2019
doi: 10.3389/fphys.2019.01278

# A Conserved Requirement for *Fbxo7* During Male Germ Cell Cytoplasmic Remodeling

*Claudia C. Rathje[1], Suzanne J. Randle[2], Sara Al Rawi[2], Benjamin M. Skinner[2†], David E. Nelson[2†], Antara Majumdar[2], Emma E. P. Johnson[2], Joanne Bacon[2], Myrto Vlazaki[2], Nabeel A. Affara[2], Peter J. Ellis[1‡] and Heike Laman[2*‡]*

[1] School of Biosciences, University of Kent, Canterbury, United Kingdom, [2] Department of Pathology, University of Cambridge, Cambridge, United Kingdom

OPEN ACCESS

**Edited by:**
Brian James Morris,
The University of Sydney, Australia

**Reviewed by:**
Hermann Steller,
The Rockefeller University, United States
Michael Mitchell,
Institut National de la Santé et de la Recherche Médicale (INSERM), France

***Correspondence:**
Heike Laman
hl316@cam.ac.uk

**†Present address:**
Benjamin M. Skinner,
School of Biological Sciences, University of Essex, Colchester, United Kingdom
David E. Nelson,
Middle Tennessee State University, Murfreesboro, TN, United States

‡These authors have contributed equally to this work

**Specialty section:**
This article was submitted to Integrative Physiology, a section of the journal Frontiers in Physiology

**Received:** 15 February 2019
**Accepted:** 23 September 2019
**Published:** 10 October 2019

**Citation:**
Rathje CC, Randle SJ, Al Rawi S, Skinner BM, Nelson DE, Majumdar A, Johnson EEP, Bacon J, Vlazaki M, Affara NA, Ellis PJ and Laman H (2019) A Conserved Requirement for Fbxo7 During Male Germ Cell Cytoplasmic Remodeling. Front. Physiol. 10:1278. doi: 10.3389/fphys.2019.01278

Fbxo7 is the substrate-recognition subunit of an SCF-type ubiquitin E3 ligase complex. It has physiologically important functions in regulating mitophagy, proteasome activity and the cell cycle in multiple cell types, like neurons, lymphocytes and erythrocytes. Here, we show that in addition to the previously known Parkinsonian and hematopoietic phenotypes, male mice with reduced Fbxo7 expression are sterile. In these males, despite successful meiosis, nuclear elongation and eviction of histones from chromatin, the developing spermatids are phagocytosed by Sertoli cells during late spermiogenesis, as the spermatids undergo cytoplasmic remodeling. Surprisingly, despite the loss of all germ cells, there was no evidence of the symplast formation and cell sloughing that is typically associated with spermatid death in other mouse sterility models, suggesting that novel cell death and/or cell disposal mechanisms may be engaged in Fbxo7 mutant males. Mutation of the *Drosophila* Fbxo7 ortholog, *nutcracker* (*ntc*) also leads to sterility with germ cell death during cytoplasmic remodeling, indicating that the requirement for Fbxo7 at this stage is conserved. The *ntc* phenotype was attributed to decreased levels of the proteasome regulator, DmPI31 and reduced proteasome activity. Consistent with the fly model, we observe a reduction in PI31 levels in mutant mice; however, there is no alteration in proteasome activity in whole mouse testes. Our results are consistent with findings that Fbxo7 regulates PI31 protein levels, and indicates that a defect at the late stages of spermiogenesis, possibly due to faulty spatial dynamics of proteasomes during cytoplasmic remodeling, may underlie the fertility phenotype in mice.

**Keywords: *Fbxo7*, PI31, proteasome, spermatogenesis, cell remodeling, germ cell**

## INTRODUCTION

During spermiogenesis, round haploid spermatids undergo terminal differentiation to form spermatozoa, developing specialized organelles – the acrosome and flagellum – necessary for fertility and motility, respectively. This involves a dramatic morphological transformation, including nuclear compaction via the eviction of histones and their replacement with protamines, and elimination of the bulk cytoplasmic content of the developing cells. Until late spermiogenesis, spermatids remain connected by intercellular bridges, through which cytoplasmic constituents are shared among haploid spermatids (Braun et al., 1989; Ventela et al., 2003). Cytoplasmic shedding

also removes these bridges and allows the individual sperm cells to separate in a process called individualization.

The disposal of excess cytoplasmic contents, including mitochondria and other organelles, is critical to many aspects of late spermatid differentiation (Sakai and Yamashina, 1989). In mammalian spermatogenesis, cytoplasmic processes from the supporting Sertoli cells invade the spermatid cytoplasm during late elongation to form the "mixed body." Concurrently, deep invaginations known as "crypts" form within the Sertoli cell cytoplasm. Active transport of the spermatids to the base of the crypts enables the development of extensive cell–cell contacts between the Sertoli and germ cells. As remodeling progresses, branches of the invading processes engulf and phagocytose portions of the spermatid cytoplasm, resulting in the loss of around 50% of spermatid cytoplasmic volume prior to spermiation. Finally, at spermiation, the spermatids are ejected from the crypts and actively transported back to the tubule lumen. There, they shed their remaining cytoplasm as residual bodies, which are then also phagocytosed by the Sertoli cells (Kerr and de Kretser, 1974; Sakai and Yamashina, 1989; Russell et al., 1989). In mice, crypt entry initiates at spermatid step 14 (epithelial stage II), and the spermatids are most deeply invaginated at step 15 (epithelial stages IV–VI), before migrating back to the lumen during step 16 (epithelial stages VI–VIII). Processing of spermatid cytoplasm in preparation for phagocytosis by the Sertoli cells includes caspase activation (Blanco-Rodriguez and Martinez-Garcia, 1999; Arama et al., 2003; Cagan, 2003) and the degradation of cellular components by specialized variants of the proteasome (Zhong and Belote, 2007; Qian et al., 2013; Bose et al., 2014). The 20S catalytic core of a proteasome is a barrel-shaped assembly, comprised of α and β subunits. Three of the β subunits, β1, β2 and β5, have peptidase activity, while access of substrates into the core is controlled by α subunits, which recruit proteasome activators (PAs). The constitutively expressed proteasome consists of a regulatory 19S "lid" associated with a 20S core particle (Bochtler et al., 1999; Voges et al., 1999), but in particular cell types, including sperm, or under stress conditions, alternate proteasome configurations come into play (Kniepert and Groettrup, 2014).

*Drosophila* spermatogenesis differs from mammalian spermatogenesis in several ways. In particular, *Drosophila* germ cells develop in cysts containing synchronously developing germ cells, rather than in tubules with multiple generations of germ cells contacting a single Sertoli cell. Nevertheless, many aspects of spermiogenesis are conserved, including the involvement of proteasomes and caspases in cytoplasmic remodeling of spermatids into mature sperm. In *Drosophila*, each cell assembles an actin-based "individualization complex" at the base of the nucleus following nuclear elongation. These complexes then slide caudally along the flagella of a group of 64 interconnected spermatids, promoting their separation and the removal of most of their cytoplasm and organelles into a membrane-bound sack, the cystic bulge, eventually discarded as a waste bag – the equivalent of the mammalian residual body (Fabian and Brill, 2012). During individualization, proteasomes migrate ahead of the individualization complex.

In *Drosophila*, Nutcracker (*ntc*) protein is essential for spermatid individualization, and homozygous *ntc* null mutant flies are sterile. Spermatids in flies with a null mutation in *ntc* undergo apoptosis in late spermiogenesis at the point when individualization would normally occur. The spermatid apoptosis is associated with failure to form individualization complexes, failure to activate spermiogenesis-related caspases, and reduced proteasome activity. These defects have been ascribed to an interaction between Nutcracker and proteasome binding protein PI31 (Arama et al., 2007; Bader et al., 2010, 2011). PI31 was discovered as an *in vitro* inhibitor of proteasome activity (McCutchen-Maloney et al., 2000; Zaiss et al., 2002), which distinguished it from other proteasome regulators, like PA200, PA28, and 19S, which all activate the 20S proteasome. However, within intact cells, multiple studies on the effects of PI31 homologs on proteasome activity in different species including yeast, flies, plants and mammals suggest that PI31 regulation of the proteasome may be contextually and spatially regulated. Its effects range from subtle or no effect in some cell types to functioning as an inhibitor of immunoproteasome maturation, a proteasome activator and a proteasome transporter in others (Chu-Ping et al., 1992, 1994; Zaiss et al., 1999; McCutchen-Maloney et al., 2000; Zaiss et al., 2002; Kirk et al., 2008; Li et al., 2014; Shang et al., 2015; Yang et al., 2016; Merzetti et al., 2017; Corridoni et al., 2019; Liu et al., 2019). In flies, DmPI31 activation of the 26S proteasome is essential for sperm differentiation, and DmPI31 levels are greatly reduced in *ntc* mutant testes, indicating that DmPI31 requires a stabilizing interaction with *ntc* to achieve sufficiently high expression levels (Arama et al., 2007; Bader et al., 2010, 2011). However, while transgenic overexpression of DmPI31 in *ntc* mutant testes promoted caspase activation in germ cells, it did not restore the ability to form individualization complexes, and the flies remained sterile (Bader et al., 2011).

A mammalian ortholog of Nutcracker is Fbxo7, although there are likely to be functional differences between them given the inability of human Fbxo7 to rescue the sterility of *ntc* flies (Burchell et al., 2013). Fbxo7 is a multifunctional, F-box protein with distinct activities in different cell types. In human health Fbxo7 impacts on numerous pathologies, including Parkinson's disease, cancer and anaemia (Laman, 2006; Soranzo et al., 2009; Di Fonzo et al., 2009; Ganesh et al., 2009; Paisan-Ruiz et al., 2010; Lomonosov et al., 2011; Ding et al., 2012; van der et al., 2012; Lohmann et al., 2015). At a molecular level, Fbxo7 functions as a receptor for SCF-type E3 ubiquitin ligases and also non-canonically, as a scaffolding chaperone for other regulatory proteins. Its effects are observable in NF-κB signaling, via cIAP and TRAF2 interactions (Kuiken et al., 2012), and in cell cycle regulation via Cdk6 activation and p27 stabilisation (Laman, 2006; Meziane et al., 2011; Randle et al., 2015; Patel et al., 2016). Fbxo7 has also been shown to interact with and ubiquitinate proteasome subunits, like PSMA2 (Bousquet-Dubouch et al., 2009; Fabre et al., 2015; Teixeira et al., 2016; Vingill et al., 2016). Because of its multi-functional nature affecting numerous cell types, several different mouse models of Fbxo7, including conditional and KO, have been engineered to study its effects in different cell types (Randle et al., 2015; Vingill et al., 2016; Patel et al., 2016; Stott et al., 2019; Joseph et al., 2019).

The hypomorphic LacZ insertion mouse is anemic, shows thymic hypoplasia and T cell deficiencies, while conditional loss in different neuronal populations causes neurodegeneration. The KO mouse shows a pre-weaning lethality.

We report here that, like *ntc* flies, male mice with a reduced expression of Fbxo7 are infertile, and characterize the novel histology exhibited by this mutant. Given that the interactions of Fbxo7 and PI31 with each other and with the proteasome are known to be conserved between *Drosophila* and mammals (Kirk et al., 2008; Bader et al., 2011; Shang et al., 2015), we also investigated PI31 levels and localisation during testicular development. We show that Fbxo7 mutant mice have reduced PI31 levels in adult testes, but normal levels of constitutive proteasome activity in spermatids. This indicates that in mouse the fertility effects of Fbxo7 mutation are unlikely to be due to an overall deficiency in proteasome activity but may be due to a cell stage- or location-specific requirement for proteasome function.

# RESULTS

## Fbxo7$^{LacZ/LacZ}$ Mice Are Sterile Due to Azoospermia

In the course of our investigations into the physiological functions of mammalian Fbxo7, we generated mice that are either heterozygous or homozygous for an allele of Fbxo7 containing a *LacZ* insertion between exons 3 and 4 of Fbxo7 (Randle et al., 2015; Patel et al., 2016). This insertion severely disrupts expression of all Fbxo7 isoforms but does not completely abolish it (Randle et al., 2015), and thus the phenotype(s) of the hetero- and homozygous animals can, respectively, be ascribed to moderate or severe under-expression of Fbxo7. In maintaining the colony of LacZ-transgenic animals, we observed that homozygous Fbxo7$^{LacZ/LacZ}$ males never sired any offspring, while heterozygous males and all genotypes of female were able to produce litters. In heterozygous crosses, there was a mild deficit of homozygous offspring (**Figure 1A**), suggestive of a small degree of embryonic lethality in this genotype.

Initial characterization showed a significant reduction in mean testis weight for the Fbxo7$^{LacZ/LacZ}$ compared to heterozygous and WT males (92.4 mg vs 108.2 and 107.7 mg; **Figure 1B**), indicative of abnormal testis development. Strikingly, there were virtually no mature sperm in the lumen of the epididymis of the Fbxo7$^{LacZ/LacZ}$ males (**Figures 1C–F**), demonstrating that these males are sterile due to azoospermia. A very few residual sperm were retrieved from dissected epididymides of Fbxo7$^{LacZ/LacZ}$ males, with a total yield of fewer than 1,000 cells per cauda epididymis, compared to a normal count of around $10^8$ sperm cells per cauda. The residual sperm were all grossly misshapen, and a high proportion of cells showed abnormal compression of the rear of the sperm head. Heterozygous Fbxo7$^{LacZ/+}$ males also showed a slight increase in the frequency of abnormally shaped sperm, with the most severely deformed sperm resembling the homozygous phenotype (**Figure 1G**). Using a newly developed image analysis program for sperm morphometry (Skinner et al., 2019), we determined that the remaining sperm from Fbxo7$^{LacZ/LacZ}$ males showed an average 14% reduction in cross-sectional area, with high morphological variability (**Supplementary Figures S1**, **S2**).

## Developing Fbxo7$^{LacZ/LacZ}$ Spermatids Are Lost During Late Spermiogenesis

The relatively small magnitude of the change in testis weight suggested that any germ cell abnormality was likely to only affect later stages of germ cell development. To characterize the stage of germ cell loss in Fbxo7$^{LacZ/LacZ}$ males, we carried out an initial assessment by FACS to see if there was any gross defect in meiotic progression (**Figure 1H**). There was no significant alteration in the ratio of cells containing 1C, 2C or 4C DNA content, respectively, representing haploid round spermatids, spermatogonia and primary spermatocytes, indicating no cell loss prior to the onset of spermatid elongation. Elongating and condensing spermatids/spermatozoa often appear as lower than 1C DNA content in FACS staining, but cannot be reliably quantified due to their high variability in staining parameters (Simard et al., 2015).

Histological examination of adult testes using hematoxylin and eosin staining (H&E) showed limited gross changes in testis structure (**Figure 2** and **Supplementary Figure S2**). In both Fbxo7$^{LacZ/LacZ}$ males and wild type (WT) males, pre-meiotic, meiotic and post-meiotic stages of germ cell development were all present in the testis parenchyma (**Figures 2A,B**). However, in Fbxo7$^{LacZ/LacZ}$ testes, very few tubules showed sperm heads adjacent to the lumen (**Figures 2B,C**), suggesting that germ cells are lost prior to spermiation. Instead, testes from these males contained tubules with no (or virtually no) elongating cells, but where the first layer of spermatids was still round. These are tubules in the first half of the seminiferous cycle but where the late elongating cells have been lost. In these tubules, sperm heads were observed lying deep within the Sertoli cell cytoplasm near to the basement membrane, often in quite dramatic "graveyards" containing multiple cells in advanced stages of karyolysis (**Figures 2D–F**). Strikingly, however, we did not observe any formation of multinucleate symplasts or any sloughing of degenerating cells into the lumen (note also the lack of sloughed cells in the epididymis in **Figure 1F**).

## "Graveyards" of Phagocytosed Fbxo7$^{LacZ/LacZ}$ Condensing Spermatids at Tubule Stage VI Are Positive for Caspase-2

Since the normal fate of arrested germ cells is apoptosis followed by either phagocytosis or cell sloughing, we used fluorescent immunohistochemical staining for caspase-2 and LAMP2 (Lysosome-associated membrane protein 2) to trace these processes. Caspase 2 is an apical caspase implicated in stress-mediated germ cell death (Zheng et al., 2006; Lysiak et al., 2007; Johnson et al., 2008), while LAMP2 labels late stage phagolysosomes. In this experiment, we also used fluorescently labelled peanut agglutinin (PNA) to label the acrosomes, allowing for more detailed tubule staging (**Figures 2G–K**). This showed that the cells in the "graveyards" were most prominent at tubule stage VI, and were positive for both LAMP2 and caspase-2.

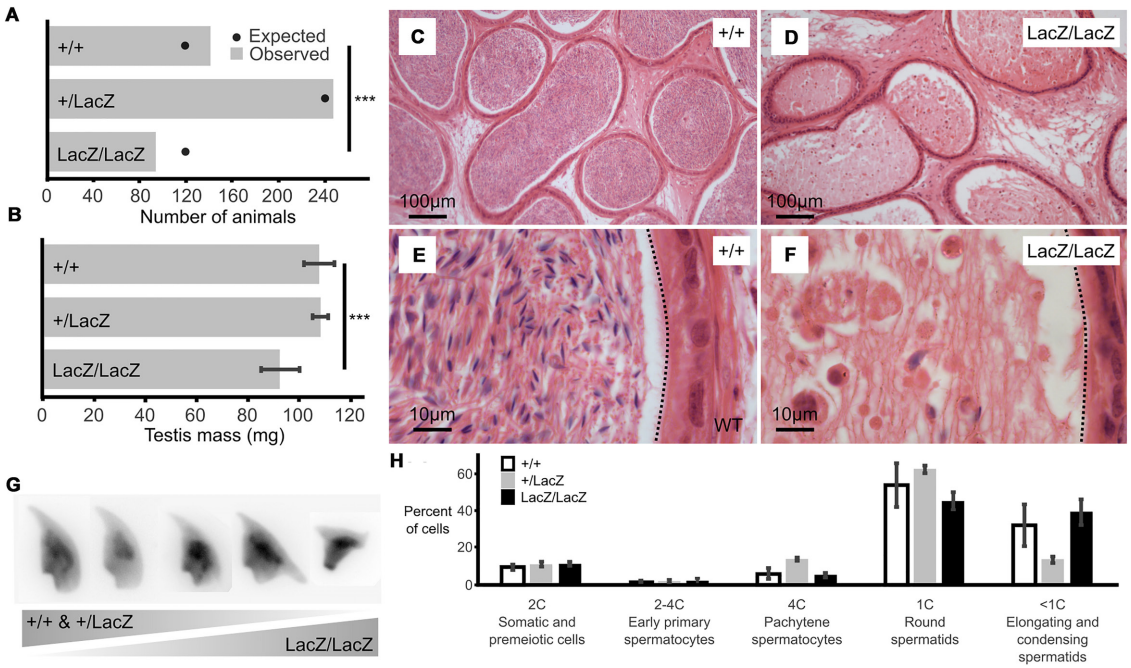


**FIGURE 1 |** Male mice with reduced expression of Fbxo7 are sterile. **(A)** Colony data showing the genotypes of animals ($n$ = 481) born from matings between heterozygous parents. All three potential genotypes are observed in the offspring, but the proportion of homozygous Fbxo7LacZ/LacZ offspring is lower than expected (*** chi-squared goodness-of fit test $p$ = 0.007 vs. Mendelian 1:2:1 expectation). **(B)** Average testis weight for each genotype ($n$ = 6; WT and homozygous; $n$ = 4, heterozygous LacZ; One-way ANOVA, ***$p$ = 0.001067). **(C)** Wild type cauda epididymis showing large numbers of stored sperm. **(D)** Fbxo7LacZ/LacZ cauda epididymis showing very few degenerating sperm. **(E,F)** High resolution zoom of sections **(C,D)**. Dotted line indicates the border of the tubule lumen in each view. **(G)** Montage of DAPI-stained sperm nuclei showing the spectrum of sperm morphologies present (see also **Supplementary Figure S1**). **(H)** FACS quantitation of testis cells according to DNA content as measured by propidium iodide staining (note that highly condensed spermatids and mature sperm were not quantitated); $n$ = 4 WT, 2 heterozygous, 2 homozygous LacZ mice.

Lower-level caspase-2 staining was sometimes visible at this stage in spermatids located further from the basement membrane. We hypothesize these latter cells to be in the process of engulfment. The few remaining condensing spermatids near the lumen were still caspase-2 negative. Thus, the spermatids in the "graveyards" are apoptotic cells that have been phagocytosed by the Sertoli cells. We attempted to distinguish cells in later stages of apoptosis by immunohistochemical staining for caspase 3; however, this gave negative results in WT and mutant samples (data not shown). Activation of apical caspases independently of effector caspases is a known alternative cell death pathway in *Drosophila* germ cells, but has not yet to our knowledge been described in mammalian germ cells (Yacobi-Sharon et al., 2013).

In this experiment, we also noted occasional spermatids at earlier tubule stages (e.g., stage IV, **Figure 2L**) that appeared to be mis-localized, appearing next to the basement membrane, outside the peripheral ring of spermatogonia. Sperm heads are very rarely seen in this location in wild type testes unless they have been phagocytosed; however, these cells were generally negative for both caspase-2 and LAMP2, indicating that they were not yet apoptotic. Since LAMP2 only labels later stages of phagocytosis, we cannot exclude the possibility that these cells were in early stages of phagocytosis, and that phagocytosis in Fbxo7$^{LacZ/LacZ}$ testes may precede the induction of apoptosis.

## Aberrant Localisation of Fbxo7$^{LacZ/LacZ}$ Condensing Spermatids Initiates at the Onset of Cytoplasmic Remodeling, From Stages I-II Onward

We used periodic acid/Schiff/Hematoxylin (PAS-H) staging to quantify the onset of aberrant localisation of the condensing spermatids in the Fbxo7$^{LacZ/LacZ}$ testes (**Figures 3A–H**). Here, the PAS staining labels the acrosome, allowing detection of spermatid location and staging. Only very light hematoxylin counterstaining was used to avoid obscuring the PAS signal. For maximal sensitivity in detecting the earliest stages of disorganization of the seminiferous epithelium, we scored any tubule with even a single spermatid observed at the basement membrane (i.e., appearing to be outside the Sertoli cell tight junctions) as positive.

We observed that mis-localization of late stage spermatids in the Fbxo7$^{LacZ/LacZ}$ testes initiated as early as spermatid step 13–14 (tubule stage I–II), with the proportion of affected tubules apparently peaking at spermatid step 15 (tubule stage IV). From tubule stage VI onward, the phagocytosed spermatid heads were barely visible by PAS-H, most likely due to digestion of the epitopes detected by the PAS stain, and thus the apparent drop-off after stage

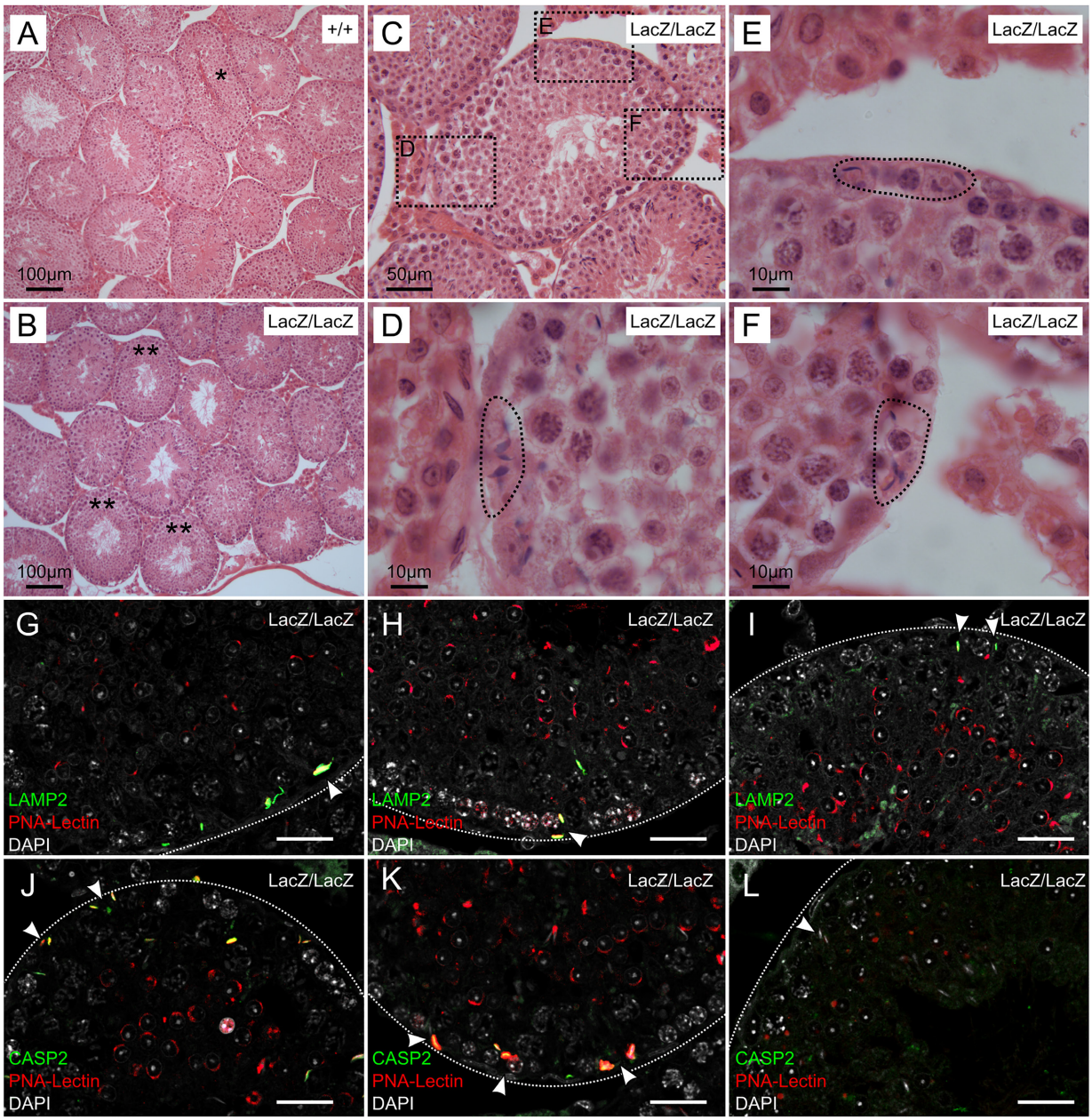


**FIGURE 2 |** Immunochemical staining of caspase 2 and LAMP2 in Fbxo7LacZ/LacZ testis sections. **(A–B)** Low magnification view of H&E sections from wild type **(A)** and Fbxo7LacZ/LacZ testes **(B)**. * In panel **(A)** indicates a tubule at stage VII-VIII with sperm heads lined up at the lumen awaiting release. These were never observed in Fbxo7LacZ/LacZ testes. ** In panel **(B)** indicates tubules with a layer of round spermatids but which lack elongating spermatids. **(C)** High magnification view of a Fbxo7LacZ/LacZ tubule lacking elongating spermatids: **(D–F)** Close up zoom from panel **C** at the indicated locations. The dotted outlines indicate "graveyards" containing multiple phagocytosed spermatid heads. **(G–I)** Immunofluorescent stains in Fbxo7LacZ/LacZ tubules for LAMP2 (green) with PNA-lectin (red) to stage the tubules and DAPI counterstain (gray). Phagocytosed cells marked by LAMP2 were visible at tubule stage VI as indicated by the extent of the lectin-stained acrosomal cap. **(J–L)** Immunofluorescent stains in Fbxo7LacZ/LacZ tubules for CASP2 (green) with PNA-lectin (red) to stage the tubules and DAPI counterstain (gray). Apoptotic cells marked by CASP2 were visible at tubule stage VI as indicated by the extent of the lectin-stained acrosomal cap. At tubule stage IV **(L)**, occasional mis-localised elongating spermatids were seen next to the basement membrane. These cells were not marked with CASP2 at this stage. For quantitation of spermatid mis-localisation, see **Figure 3**.

IV is a technical artifact (note that dead cells at this stage remained visible via H&E and immunostaining; see **Figures 1**, **2**). This contrasts with the immunostaining data where the mis-localized cells prior to stage VI were LAMP2 and CASP2-negative, but the phagocytosed cells at stages VI-VIII were strongly LAMP2 and CASP2 positive. The two experiments thus probe different aspects of the phenotype: mis-localization followed by apoptosis.

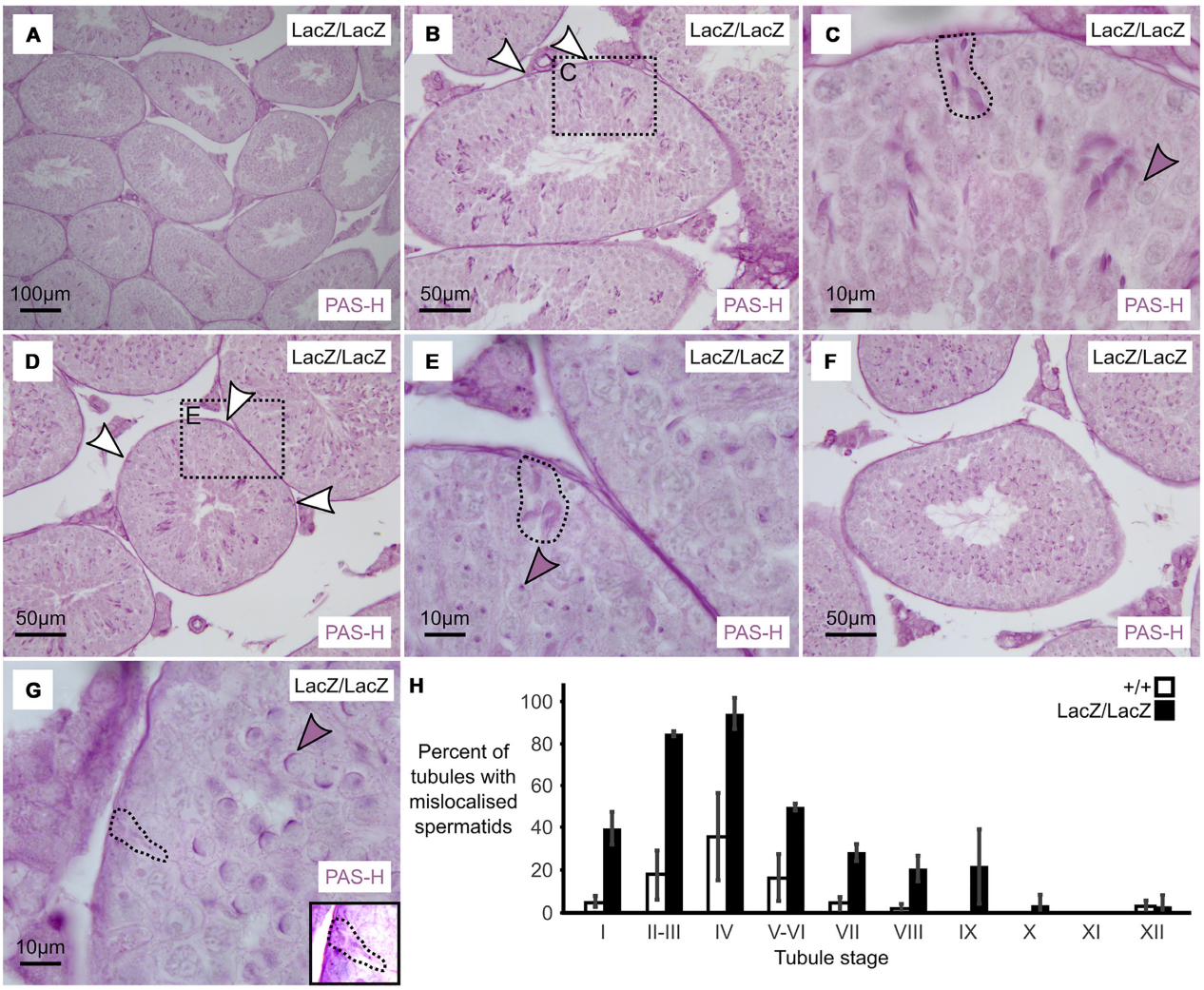


**FIGURE 3 |** Massive loss of maturing sperm in Fbxo7 mutant males. **(A–G)** PAS-H staining of Fbxo7LacZ/LacZ testis sections used to quantitate spermatid mis-localisation. PAS marks the developing acrosome in purple, allowing both identification of the mis-localised elongating spermatids and also tubule staging. Panel **(A)** shows a low magnification view indicating general testis architecture. Panel **(B,D,F)** show complete tubules at stage II, IV, and VI, respectively, and white arrowheads indicate mislocalised elongating spermatids apposed to the basement membrane of the tubules – these are rarely visible at stage VI. Panel **(C,E,G)** show high magnification images at tubule stages II, IV and VI. Dotted outlines highlight mislocalised elongating spermatids, while shaded arrowheads indicate the developing acrosomes in the round spermatid layer, used to stage the tubules. Mislocalised spermatids were readily detected up to stage IV. After stage IV, the mislocalised cells were still present but began to lose their PAS staining were thus harder to detect. Panel **(G)** inset shows a rare example of a mislocalised cell remaining visible by PAS staining at stage VI. **(H)** Proportion of tubules containing at least one mis-localised cell at each tubule stage in wild type and Fbxo7LacZ/LacZ testes. Error bars indicate standard deviation across replicates ($n$ = 3 animals per genotype).

Complete data from the PAS-H cell counting are supplied as **Supplementary Table S2**.

## PI31 Expression Is Reduced in Fbxo7$^{LacZ/LacZ}$ Testes, but Proteasome Activity Is Unaltered

The basis for sterility in *ntc*-mutant null flies is proposed to be the loss of a stabilizing interaction with DmPI31, leading to reduced proteasome activity (Bader et al., 2011). To address whether this relationship is conserved in spermatogenesis in mice, we tested the expression of Fbxo7 and PI31 in lysates made from testes of mature males (**Figure 4A**). As expected, the presence of the Fbxo7$^{LacZ}$ allele caused dose-dependent decreases in Fbxo7 expression, as seen by both Western blot and qRT-PCR (**Figures 4A,B**). We note that for homozygous Fbxo7$^{LacZ/LacZ}$ mice, expression of both mRNA and protein for Fbxo7 was reduced by approximately 94%. This is partial effect on Fbxo7 mRNA expression in testes is comparable to the that seen in liver (93%), cerebellum (80%), bone marrow (78%), and spleen (60%) (Randle et al., 2015).

PI31 protein levels were significantly reduced by 39% in adult Fbxo7$^{LacZ/LacZ}$ testes (**Figure 4A**), while a 23% reduction in mRNA levels was not statistically significant (**Figure 4C**).

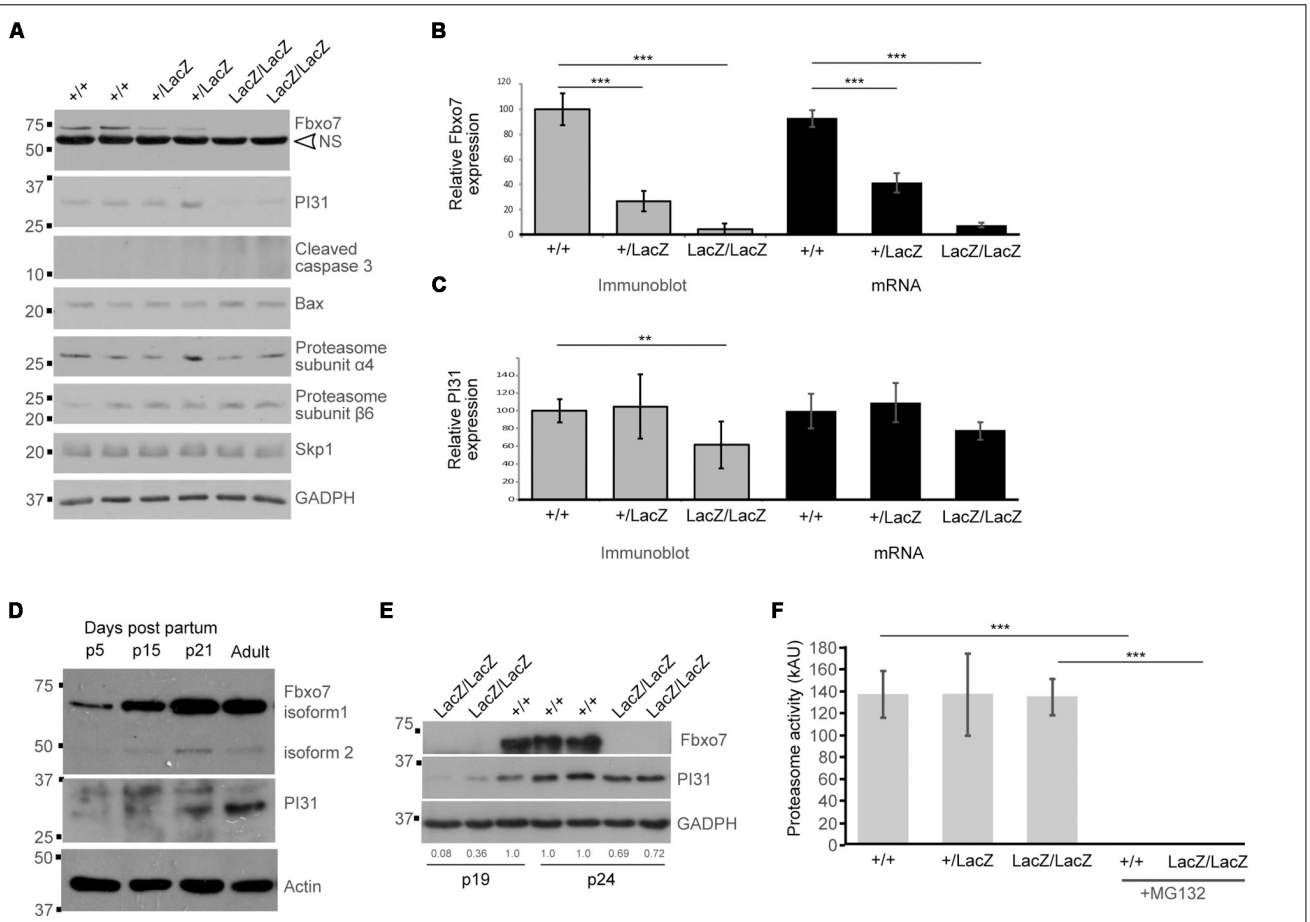


**FIGURE 4 |** Decreased PI31 levels but normal proteasome activity in Fbxo7LacZ/LacZ testis. **(A)** Immunoblot analysis for various proteins in whole testes lysates from WT, heterozygous, and homozygous LacZ mice at 8.1 weeks of age, as indicated. NS = non-specific band in Fbxo7 (Santa Cruz Biotechnology, sc-271763) Western blot. **(B)** Quantitation of Fbxo7 expression from immunoblots, relative to GADPH loading control; gray bars; $n$ = 10 WT, 8 heterozygous, 7 homozygous LacZ mice. RT-qPCR of Fbxo7 relative to three housekeeping genes (cyclophilin, GAPDH, and actin); black bars; $n$ = 4 for each genotype). Images were analyzed in ImageJ. $^{***}p < 0.001$ One-way ANOVA with Dunnett's multiple comparisons test. **(C)** Quantitation of PI31 expression from immunoblots, relative to GADPH loading control; gray bars; $n$ = 10 WT, 8 heterozygous, 7 homozygous LacZ mice. RT-qPCR of Psmf1/PI31 relative to three housekeeping genes (cyclophilin, GAPDH, and actin); black bars; $n$ = 4 for each genotype). Images were analyzed in ImageJ. $^{**}p < 0.01$ One-way ANOVA with Dunnett's multiple comparisons test. **(D)** Immunoblot analysis for Fbxo7 (Laman Lab polyclonal antibody) and PI31 protein in whole testes lysates from mice harvested at the indicated days post-partum (p). **(E)** Immunoblot analysis for Fbxo7 (Santa Cruz Biotechnology, sc-271763) and PI31 protein in whole testes lysates from mice harvested at 19 and 24 days post-partum. Quantification of PI31 protein levels relative to WT GADPH levels for each sample is indicated. **(F)** Proteasome activity measured in whole testis extract for each genotype. Treatment with MG132 abolished the signal, confirming the specificity of the assay. $n$ = 3 WT, 2 heterozygous, and 4 homozygous LacZ mice, each performed in triplicate $^{***}p < 0.0001$.

The fact that PI31 protein levels show a more pronounced decline than mRNA levels suggests that Fbxo7 has a role in stabilizing PI31 protein levels in adult testes. We therefore characterized the developmental profile of both proteins in normally developing wild type testes. Both Fbxo7 and PI31 were weakly detected at all ages by Western blot, indicating widespread low-level expression in the testis. Both, however, also showed strong upregulation between postnatal day 15 and day 21, concurrent with the first appearance of haploid spermatids in the testis (**Figure 4D**). PI31 was further upregulated between day 21 and adult testes, consistent with increased expression in later stage elongating/condensing spermatids. Finally, we examined Fbxo7 and PI31 levels in Fbxo7$^{LacZ/LacZ}$ testes at days 19 and 24, i.e., at time points before the onset of germ cell mis-localization and loss. At 19 days of age, mutant testes showed a 64–92% reduction, while at 24 days, there was a ∼30% reduction in PI31 protein levels compared to wild type testes (**Figure 4E**). We conclude that Fbxo7 is required for PI31 stability in earlier stage germ cells.

To test whether the observed reduction in PI31 levels in adult testes led to decreases in proteasome activity, we conducted proteasome activity assays on whole testes from WT, heterozygous and homozygous *Fbxo7*$^{LacZ}$ males. However, no reduction in proteasome activity was detected (**Figure 4F**). Consistent with these data, we observed no changes in the levels of core proteasome subunits α4 or β6 among the different adult WT and mutant testes by Western blot analysis (**Figure 4A**), indicating stable overall levels of proteasomes. Our attempts to

measure PI31 levels and to conduct similar proteasome activity assays on elutriated cell populations were inconclusive due to the poor recovery of later stage spermatids from mutant testes (data not shown). These data indicated there were no major alterations in the overall levels of proteasome activity in testes from Fbxo7 mutant males.

Since Fbxo7 can form part of an E3 ubiquitin ligase, we also assayed for the levels of Skp1, the adaptor protein which recruits F-box proteins into SCF-type E3 ubiquitin ligases. Skp1 levels were unchanged, indicating that other SCF-type E3 ubiquitin ligases would be unaffected in mutant testes. Finally, we also examined levels of cleaved caspase 3 and the pro-apoptotic mediator Bax, both of which are implicated in germ cell death during the first wave of spermatogenesis (Russell et al., 2002; Said et al., 2004). We observed no changes in Bax levels between genotypes, and no expression of cleaved caspase 3, which was consistent with our inability to detect cleaved caspase 3 by IHC staining (data not shown). These data suggest that classical apoptotic pathways were not engaged during germ cell death in Fbxo7 mutant testes.

### Spermatoproteasome Localisation and Histone Removal From Spermatid Chromatin Are Unaltered in Fbxo7$^{LacZ/LacZ}$ Testes

During spermatogenesis, in addition to the constitutive proteasome, alternative proteasomes are co-expressed. PA200-capped spermatoproteasomes promote the degradation of acetylated histones, which enables their removal from DNA and replacement with protamines, for enhanced nuclear compaction into the spermatid head (Gaucher et al., 2010; Qian et al., 2013). They contain an alternative α4-type proteasome subunit, α4s/PSMA8, a testis-specific subunit, which replaces its 20S counterpart, and enables the recruitment of an alternate lid, PA200. A second proteasome, known as the immunoproteasome, is also expressed and has alternate β-subunits, β1i, β2i and β5i, and a different regulatory 11S lid (Qian et al., 2013). As sperm differentiation requires major cellular remodeling and volume reduction, these alternate proteasomes are thought to play crucial roles in fashioning this specialized cell form (Zhong and Belote, 2007; Kniepert and Groettrup, 2014; Rathke et al., 2014).

Although spermatoproteasome activity cannot be directly assayed independently of total proteasome activity, the spermatoproteasome has a key role in histone degradation during nuclear elongation (Kniepert and Groettrup, 2014). We therefore stained WT and mutant testes for LMP7 (β5i), a component of the immunoproteasome and spermatoproteasome which is not present in normal proteasomes, to determine whether this was altered by Fbxo7 deficiency (**Figure 5A**), and for histone H3 to determine whether the dynamics of histone removal was perturbed in the knockout males (**Figure 5B**). This showed no alteration in LMP7 localization in the mutant, with nuclear LMP7 signal being specific to stage IX-XII spermatids in both genotypes. There was also no delay in histone removal in the mutant, with all histone H3 signal being removed from the nucleus by the end of stage XII in both wild type and Fbxo7$^{LacZ/LacZ}$ testes. Taken together with the overall proteasome assay data shown above, we conclude that both LMP7-containing proteasomes and normal proteasome activity are apparently unaffected by Fbxo7 deficiency in mouse testes.

Finally, while unfortunately, the available Fbxo7 antibodies do not work for immunohistochemical (IHC) staining in mouse testes, we investigated the spatial distribution of PI31 to determine whether this was consistent with a role in nuclear or cytoplasmic remodeling of spermatids. In wild type testes, PI31 was present in the cytoplasm of most cell types, becoming significantly stronger in the cytoplasm of late condensing spermatids from stage V onward and being retained into the residual bodies shed at stage VIII. In addition to the stage-specific cytoplasmic signal, PI31 also showed nuclear staining specifically in wild type elongating spermatids from stages IX through to XII (**Figure 6**). Thus, there is the potential for Fbxo7 and/or PI31 to regulate proteasomes during spermatid nuclear and/or cytoplasmic remodeling.

## DISCUSSION

### The Mammalian Phenotype Associated With Fbxo7 Deficiency

Spermiogenesis is a multi-step process that transforms morphologically simple round spermatids into highly specialized mature sperm. It occurs in four successive phases, namely; (a) nuclear elongation and replacement of histones by transition proteins in tubule stages IX to XII, spermatid step 9–12), (b) migration of condensing spermatids into Sertoli cell crypts, protamination of sperm chromatin and cytoplasmic reduction by ∼50% in tubule stages I to VI, spermatid steps 13–15, (c) migration of the mature spermatids to the tubule lumen in tubule stage VII, spermatid early step 16, (d) spermiation, the release of fully formed sperm at tubule stage VIII, spermatid late step 16. In Fbxo7$^{LacZ/LacZ}$ males, we observe a peculiar and very specific phenotype consisting of mass phagocytosis of condensing spermatids, occurring after nuclear elongation and prior to migration of spermatids back to the tubule lumen. This coincides with the cytoplasmic remodeling of the spermatids during steps 13–15, equivalent to the individualization stage of *Drosophila* sperm development. The requirement for Fbxo7 at this stage thus appears to be conserved from fruit flies to mammals.

The nature of the sterility phenotype in Fbxo7$^{LacZ/LacZ}$ males is to our knowledge unprecedented in a mammalian system. Various null mutants with defects in cytoplasmic remodeling have previously been described, including Sept4, Spem1, Capza3, and Ube2j1 mutants. These all show either no phagocytosis or only limited phagocytosis of elongating spermatids during the first half of the cycle, followed by spermiation failure and spermatid retention at the lumen into stage IX and beyond (Kissel et al., 2005; Zheng et al., 2007; Geyer et al., 2009; Koenig et al., 2014). Further mutants have been described that show a step 13 block

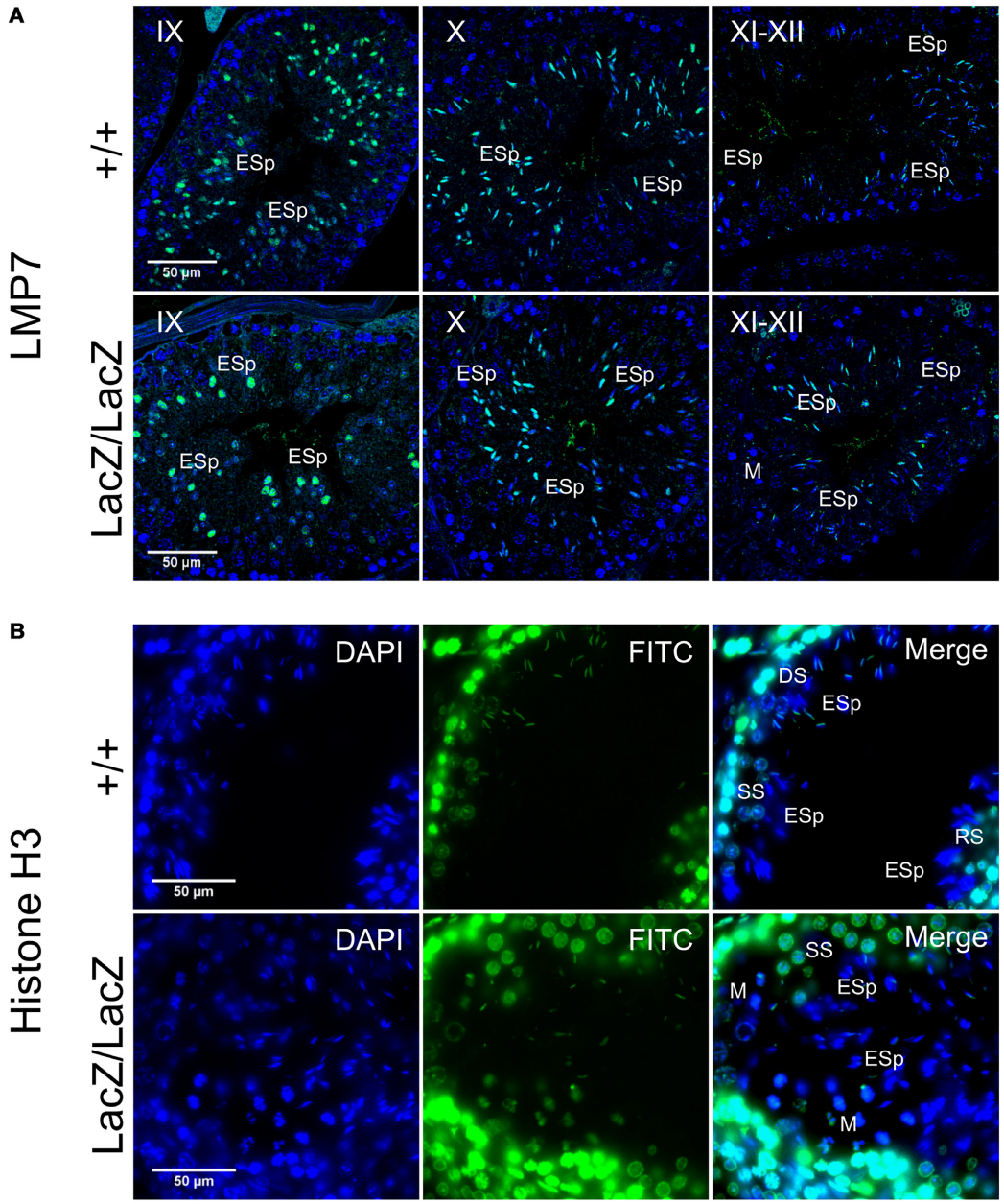


**FIGURE 5 |** Immunochemical staining of LMP7 and histone H3 in Fbxo7LacZ/LacZ testis sections. **(A)** Immunochemical staining of LMP7 (FITC, green) in wild type and Fbxo7LacZ/LacZ testes with DAPI (blue) nuclear counterstain. Roman numerals indicate tubule stage. In both genotypes, nuclear LMP7 expression is first seen in early ES at mid-stage IX as the nuclei begin to elongate. This nuclear expression is highest at stage X, and then is lost during stage XI-XII as nuclei complete elongation. **(B)** Immunochemical staining of histone H3 (FITC, green) in wild type and Fbxo7LacZ/LacZ testes with DAPI (blue) nuclear counterstain. The wild type tubule shown is in transition between stages, with early stage XII (DS next to ESp) at upper left, mid stage XII (SS next to ESp) at lower left and stage XII/I border (M and RS next to ESp) at lower right. Nuclear H3 signal in ESp is still present at early stage XII, is restricted to the posterior of the nucleus in mid stage XII, and entirely lost by stage I. The Fbxo7LacZ/LacZ tubule shown is in mid stage XII, and the H3 signal in the ESp is absent or restricted to the posterior extremity of the nucleus, confirming the kinetics and spatial pattern of H3 removal are indistinguishable between genotypes. Key: DS = diplotene spermatocytes, SS = secondary spermatocytes, M = metaphase figures, RSp = round spermatids, ESp = elongating spermatids.

to spermatid development without defects in cytoplasmic remodeling, including the Bclw and Brd7 null mutants. In these mice, the arrested step 13 spermatids degenerate while still near the tubule lumen, followed by phagocytosis of large symplasts and other cell debris (Russell et al., 2001; Wang et al., 2016). In stark contrast to both of the above types of mutant, the Fbxo7$^{LacZ/LacZ}$ males showed complete phagocytosis of all developing spermatids with no detectable symplast formation, sloughing of degenerating cells into the lumen, or spermiation failure.

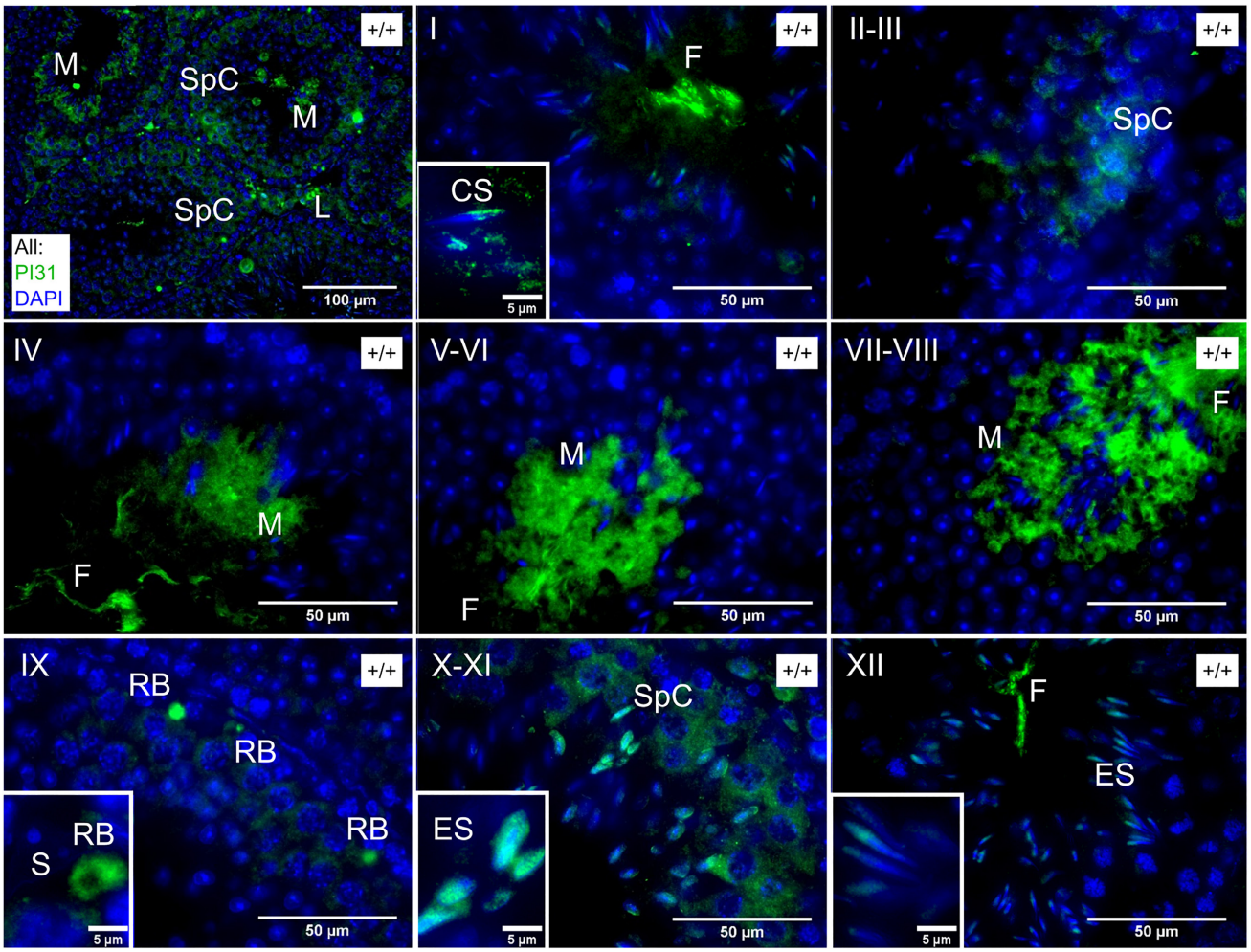


**FIGURE 6 |** Immunochemical staining of PI31 localisation in wild type testes. Roman numerals indicate tubule stage. PI31 signal is cytoplasmic in Spc/M/RB/L but nuclear in ES and early CS. Key: SpC = spermatocyte, ES = elongating spermatid, CS = early condensing spermatid, M = mature or late condensing spermatid, RB = residual body, L = Leydig cell, S = Sertoli cell, F = flagellum of mature sperm.

## How Are the Germ Cells Eliminated in Fbxo7$^{LacZ/LacZ}$ Testes?

In Fbxo7$^{LacZ/LacZ}$ testes, mis-localized condensing spermatids are visible by PAS-H staining at the basement membrane from tubule stage ∼I-II onward, and by stage IV almost 100% of tubules have mis-localized cells. At these early stages, however, mis-localized spermatids are negative for caspase-2 and LAMP-2, and retain their acrosomes (i.e., they are stainable by PAS), suggesting that they are not yet apoptotic and/or that phagocytic degradation has not yet initiated. By stage VI, however, the cells have lost their normal orientation, become positive for caspase 2 and LAMP-2, and karyolysis has initiated.

One possible scenario is that the early stages of mis-localization represent an abnormal deepening of the Sertoli cell crypts in mutant testes, and that the condensing spermatids have not yet been phagocytosed at this point. The trafficking of spermatids into and out of Sertoli cell crypts is governed by dynein-coupled motion of a specialized adherens junction complex between germ cell and Sertoli cell, known as the apical ectoplasmic specialisation (AES). If the AES is dissolved prematurely, the Sertoli cell may be unable to eject the spermatids from the crypts, leading ultimately to their death and phagocytosis.

An alternative scenario is that the phagocytosis initiates at stage I-II due to defects in germ cell remodeling, but that the engulfed cells remain alive and non-apoptotic for a short period after being phagocytosed. That is, the developing spermatids are "eaten alive" some time before finally dying. In this case, this would represent death by primary phagocytosis or "phagoptosis," a relatively newly identified manner of cell elimination (Brown and Neher, 2012). Phagoptosis of elongating spermatids in Fbxo7$^{LacZ/LacZ}$ testes would explain the absence of symplasts and the lack of sloughing of dead cells into the lumen, since in the case of phagoptosis, the eliminated cells would remain alive until they have already become trapped inside phagocytic vacuoles. Future studies to distinguish between these models using electron

microscopy, in conjunction with immuno-labeling to resolve the intracellular machinery, are planned.

## Are the Consequences of Fbxo7 Deficiency Mediated by PI31/Proteasome Regulation?

In flies, *ntc* has been shown to be important for caspase activation and sperm individualization through enhancing DmPI31 stability, which acts as a proteasome activator. However, transgenic restoration of PI31 levels in *ntc* testes restored caspase activity but did not restore individualization complex assembly, suggesting that nutcracker and DmPI31 may both be necessary for sperm production (Bader et al., 2011). We and others have previously shown that the stabilising interaction between Fbxo7 and PI31 is conserved in many different cell types (Kirk et al., 2008; Bader et al., 2011; Shang et al., 2015; Merzetti et al., 2017). Consistent with this, we show here that PI31 protein levels are reduced in adult Fbxo7$^{LacZ/LacZ}$ testes. Importantly, PI31 protein levels are more strongly reduced than mRNA levels, indicating that this is a stabilizing effect of Fbxo7 on PI31 at the protein level.

The reduction in PI31 levels in Fbxo7$^{LacZ/LacZ}$ testes is also seen in juvenile testes at days 19 and 24 days post-partum. At postnatal day 19, the most advanced germ cells are at the early round spermatid stage, while at day 24, the most advanced germ cells are early elongating (not condensing) spermatids. Thus, the reduction in PI31 precedes the appearance of condensing spermatids in the testis and is not simply a secondary consequence of the loss of late stage condensing spermatids in mutant testes.

In wild type testes, we show that PI31 and LMP7 are both present in the nucleus of step 10–12 spermatids, indicating that alternate proteasomes play a role in nuclear elongation. PI31 then shifts to the cytoplasm of step 13–16 spermatids at tubule stages I-VIII. The loss of germ cells in the knockout is thus coincident with this shift in PI31 localization from the nucleus to the cytoplasm. This is especially intriguing in the light of recent work showing that PI31 acts as an adaptor to facilitate proteasome transport in axons (Liu et al., 2019). One could imagine a role for PI31 in the re-localization of proteasomes in the remodeling cytoplasm. The spermiogenesis phenotypes could arise due to insufficient levels of PI31 causing deficiencies in localized requirements for proteasomes during remodeling but leaving overall proteasome activity intact.

Although we could not directly measure spermatoproteasome activity, whole-testis proteasome activity showed no changes in Fbxo7$^{LacZ/LacZ}$ testes. Other proteasome-related knockout males (PA200, PA28γ) have defects in multiple stages of germ cell development, both pre- and post-meiotic. The post-meiotic phenotypes of these knockout models include delayed histone replacement during nuclear remodeling and delayed spermiation, neither of which was seen in Fbxo7$^{LacZ/LacZ}$ testes (Qian et al., 2013; Huang et al., 2016). Moreover, unlike Fbxo7$^{LacZ/LacZ}$ males, even the PA200/PA28γ double knockout males were able to produce substantial numbers of morphologically normal sperm in their epididymis (Huang et al., 2016). A knockout of the spermatoproteasome-specific subunit PSMA8 has recently been shown to lead to meiotic abnormalities and early spermatid arrest [Gómez Hernández et al., unpublished data, preprint[1]], unlike the late stage spermatid loss described in the present study.

Taken together, our data shows that the Fbxo7$^{LacZ/LacZ}$ male sterility phenotype differs from all other existing mouse knockouts related to proteasome function at both the histological and molecular levels. Hence, the Fbxo7 sterility phenotype appears not to be due to a generalized insufficiency of proteasome activity, although it is plausible that localized proteasome function in the cytoplasm is necessary during spermiogenesis, and our experiments have not addressed this.

## Potential Non-proteasomal Pathways Regulated by Fbxo7 That May Lead to Male Sterility

Fbxo7 is required for PINK1/Parkin-mediated mitophagy, a process that requires the fragmentation and engulfment of depolarized regions of the mitochondrial network (Burchell et al., 2013), and interestingly, both the *nutcracker* and *parkin* null flies show male sterility, with a specific defect during sperm individualization (Greene et al., 2003; Bader et al., 2010). In the *parkin* null mutant in *Drosophila*, a specialized mitochondrial aggregate present in insect sperm, known as the Nebenkern, failed to form, and spermatids failed to individualize suggesting that rearrangement of mitochondria is necessary for individualization. However, the mouse parkin null mutant is fertile with no known effects on germ cell development (Itier et al., 2003), and thus the sterility of Fbxo7 mutant males is unlikely to relate directly to its interaction with Parkin.

One possible explanation is that Fbxo7 is more generally involved with specialized cytoplasmic remodeling. In a similar vein to the sperm maturation defects, Fbxo7 has also been shown to be required during the final maturation steps of erythrocytes. We previously reported Fbxo7$^{LacZ/LacZ}$ mice are anemic due to delayed mitophagy and defects in exiting cell cycle (Randle and Laman, 2016). Importantly, during this maturation step, macrophages in erythroblast islands phagocytose the shed organelles from maturing reticulocytes (Geminard et al., 2002; Zhang et al., 2015; Ovchynnikova et al., 2018), a process requiring the coupling of the autophagy and exocytosis pathways (Mankelow et al., 2015). Could this coupling be coordinated by Fbxo7? If so, then in a testis context, Fbxo7 may enable the fragmentation and isolation of portions of the spermatid cytoplasm to allow phagocytosis by Sertoli cells. In the absence of Fbxo7, failure to correctly package spermatid cytoplasm for elimination could instead lead to wrongful engulfment of complete cells and phagoptotic cell death.

As a third alternative but non-exclusive possibility, we note that the dead cells at tubule stage VI were strongly positive for caspase 2. TRAF2, a target of Fbxo7 ubiquitination

[1]https://www.biorxiv.org/content/early/2018/08/03/384354

(Kuiken et al., 2012), has recently been shown to bind to active caspase 2 dimers and ubiquitinate it to stabilize the activated complex (Robeson et al., 2018). Consequently, Fbxo7 deficiency could lead to over-activity of TRAF2 and subsequently signal the activation of caspase 2 precipitating germ cell death. Identifying the substrates of Fbxo7 underlying the unique phenotypes reported here is an area of future research.

# CONCLUSION

*Fbxo7* mutant mice exhibit a novel sterility phenotype unlike any previously described, in that total death and phagocytosis of all condensing spermatids occurs in the absence of typical hallmarks of spermatid apoptosis such as symplast formation and cell sloughing. The mis-localization of elongating spermatids initiates substantially before the appearance of markers of apoptosis and phagocytosis, indicating that aspects of spermatid trafficking into and out of Sertoli cell crypts may also be perturbed in these males. These males thus provide a new model of late spermiogenic failure, and an exciting new avenue to investigate cell remodeling, tissue remodeling and apoptosis in germ cell development.

# MATERIALS AND METHODS

## Mice

Mice used in this study are *Fbxo7*$^{LacZ}$ mice (*Fbxo7*$^{tm1a(EUCOMM)Hmgu}$ on a C57BL/6J background) and experiments involving them were performed in accordance with the United Kingdom Animals (Scientific Procedures) Act 1986 and ARRIVE guidelines. Mice were housed in individually ventilated cages with unrestricted access to food and water, and 12-h day-night cycle. Animal licenses were approved by the Home Office and the University of Cambridge's Animal Welfare and Ethical Review Body Standing Committee. Experiments were performed under the Home Office licenses PPL 80/2474 and 70/9001 (HL).

## Tissue Processing and Immunohistochemistry

Testes were fixed in Bouin's fixative at 4°C overnight and embedded in paraffin. Sections were subjected to standard methods of hematoxylin/eos/in or periodic acid/Schiff/hematoxylin staining for histological examination. For immunohistochemical studies, sections were de-paraffinised in xylene and rehydrated through a graded ethanol series prior to blocking and antibody staining steps. Details of primary and secondary antibody concentrations are given in **Supplementary Table S1**. Antibody-stained sections were counterstained with DAPI and visualized via epifluorescence (PI31, Histone H3) or confocal fluorescence microscopy (Caspase 2, Lamp-2, LMP7). In some experiments, fluorescently conjugated peanut agglutinin from *Arachis hypogaea* (PNA-lectin) was included during the secondary antibody incubation step to visualize acrosomal morphology and facilitate staging of seminiferous tubules. Antibody validation and negative controls are shown in **Supplementary Figure S3**.

## Sperm Morphometric Analysis

Sperm were collected from two Fbxo7$^{LacZ/LacZ}$, three Fbxo7$^{LacZ/+}$, and two wild type males. The vasa deferentia and caudae epididymides were dissected from each animal, and the contents extracted into 1 mL PBS. Sperm were transferred to a microfuge tube, and tissue clumps were allowed to settle. Then sperm were transferred to a new tube and pelleted at 500 × *g* for 5 mins. The supernatant was removed, and the sperm fixed dropwise with 3:1 methanol-acetic acid. Sperm were again pelleted at 500 × *g* for 5 mins, and washed in fixative twice more. Samples were stored at −20°C. Fixed sperm nuclei were stained with DAPI and imaged using a 100× objective on a Nikon Microphot SA epifluorescence microscope equipped with a cooled CCD camera and appropriate filters. Images were captured using SmartCapture 2, exported in 8-bit tiff format and analyzed using the automated morphometric software Nuclear Morphology Analysis v1.13.7[2] (Skinner et al., 2019). Hierarchical clustering was performed on nuclear shapes to group them into morphological categories, and the proportion of cells from each genotype in each category was calculated. The total numbers of nuclei analyzed for each genotype were 453 for Fbxo7LacZ/LacZ, 1225 for Fbxo7$^{LacZ/+}$ and 756 for wild type.

## Flow Cytometry

Single-cell suspensions from whole testis tissue were pelleted by centrifugation, and resuspended in 1 mL of ice cold 80% ethanol/PBS while vortexing to disperse clumps. The suspended cells were fixed for at least 1 hr at 4$^{o}$C. After fixation, cells were collected by centrifugation and washed once in PBS. The washed cell pellet was resuspended in 1 mL of a solution of 50 μg/mL propidium iodide (PI) staining and 10 μg/mL DNase-free RNase, and incubated for 10 min at 37°C, prior to analysis by flow cytometry (Beckman-Coulter, Inc.).

## Lysis and Immunoblotting

Whole testis tissue were lysed in RIPA buffer (50 mM Tris–HCl pH 7.6, 150 mM NaCl, 1% NP-40, 0.1% SDS, 0.1% Na deoxycholate, 1x protease inhibitors, 1 mM PMSF, 10 mM sodium fluoride, 1 mM sodium orthovanadate) (all from Sigma-Aldrich), and incubated on ice for 30 min with occasional vortexing. Cell debris was pelleted by centrifugation at 16,000 × *g* for 10 min at 4°C, and the supernatant retained. Protein concentration was determined via 96-well BCA assay (Pierce). Sample concentrations were standardized by dilution with lysis buffer. For Western blot, samples were mixed with equal volumes of 2x Laemmli buffer, denatured (95°C, 5 min), separated via SDS polyacrylamide gel electrophoresis (SDS-PAGE), and transferred onto polyvinylidenefluoride (PVDF) membrane (Millipore) using a semi-dry transfer system (Biorad). Membranes were blocked for 1 h with 5% non-fat, milk powder/PBS-Tween 20 (0.05%) (PBS-T), and then probed with primary antibody overnight at 4°C in 5% non-fat, milk powder/PBS-T. Membranes

[2]https://bitbucket.org/bmskinner/nuclear_morphology/wiki/Home

were washed in PBS-T and incubated with the appropriate HRP-conjugated secondary antibody in 5% non-fat, milk powder/PBS-T followed by further washes, and detection of HRP bound protein using enhanced chemiluminescence (ECL, GE Healthcare) and exposure onto X-ray film (Konica Minolta). Signal was quantified with background correction and normalized using ImageJ software (NIH, Maryland). Antibodies used in this study are provided in **Supplementary Table S1**.

## mRNA Isolation and RT-qPCR

Tissue was homogenised in 350 μL RLT buffer with β-mercaptoethanol and RNA isolated using RNeasy Plus kit (Qiagen) as per the manufacturer's recommendations. One μg of mRNA was converted to cDNA using Quantitect reverse transcriptase (Qiagen), and then diluted 1:10 for subsequent RT-qPCR analysis using SYBR Green JumpStart Taq (Sigma) on a CFX Connect Real-Time PCR machine (Biorad). The following primers for *Fbxo7* (5′-CGCAGCCAAAGTGTACAAAG; 3′-AGGTTCAGTACTTGCCGTGTG) and *Psmf1*(PI31) (5′-CAATCATGCCACCTCTCTGA; 3′-CCGTCCTCATACTAG CAGGC) were used. RT-qPCR reactions were as follows: 95°C for 5 min then 45 cycles of 95°C for 30 s, 60°C for 30 s, 72°C for 30 s, followed by melt curve analysis to confirm a single PCR product was made. Relative gene expression was determined using relative standard curve method, data was normalized to three housekeeping genes (*Ppai, Gapdh, Actb*) as previously described [see (Birkenfeld et al., 2011; Meziane et al., 2011) for primer sequences], and expressed relative to WT levels.

## Counting of Mis-Localised Cells at Different Tubule Stages

Tubules were staged using periodic acid/Schiff staining to visualize the stages of acrosomal development (Oakberg, 1956; Russell et al., 1993). Every tubule in a complete testis cross-section was staged for three replicate males per genotype, by an observer blinded to the sample identity. Tubules were scored as positive if there were any mis-located elongating spermatid heads detected beyond the Sertoli cell tight junctions, within the outermost layer of nuclei in the tubule, and negative if there were no elongating spermatid heads within this layer. Tubules were also scored for the presence of "graveyards" defined as 2 or more mis-localized elongated spermatids enveloped by a single Sertoli cell. These definitions were chosen to maintain consistency across the seminiferous cycle, and their sensitivity is discussed in the main text.

## Measurement of Proteasome Activity

Assays for proteasome activity were performed using the Proteasome-Glo$^{TM}$ Chymotrypsin-Like Cell-Based Assay Kit (Promega) according to the manufacturer's protocol. Briefly, testes from 10 wk old mice were harvested and lysed in buffer (20 mM Hepes pH 7.6, 150 mM NaCl, 10% glycerol, 1% Triton X-100, 2 mM EDTA, 1 mM DTT) using a Dounce homogenizer in 10X the volume/weight of tissue. Protein concentration was measured, and lysates were diluted so that 100 μg of protein in 100 μL volume/well was loaded into a 96-well plate, and samples were plated in triplicate. Where applicable, samples were pre-incubated with MG-132 for 30 min prior to the addition of reagents, with protease inhibitors ($Na_2VO_4$, NaF, PSMF), or without inhibitors. Samples were equilibrated to RT for 15 min and then 100 μL of assay reagent was added. After a 10 min incubation, luminescence was measured in triplicate.

# DATA AVAILABILITY STATEMENT

All datasets generated for this study are included in the manuscript/**Supplementary Files**.

# ETHICS STATEMENT

Mice used in this study are *Fbxo7*$^{LacZ}$ mice (*Fbxo7*$^{tm1a(EUCOMM)Hmgu}$ on a C57BL/6J background) and experiments involving them were performed in accordance with the United Kingdom Animals (Scientific Procedures) Act 1986 and ARRIVE guidelines. Animal licenses were approved by the Home Office and the University of Cambridge's Animal Welfare and Ethical Review Body Standing Committee. Experiments were performed under the Home Office licenses PPL 80/2474 and PPL 70/9001 (HL).

# AUTHOR CONTRIBUTIONS

HL and PE: conceptualization, methodology, and supervision. BS: software. CR, SA, SR, BS, DN, AM, EJ, JB, and MV: investigation. PE, HL, CR, SA, and BS: writing – original draft. BS, CR, PE, and HL: visualization. HL, PE, and NA: funding acquisition.

# FUNDING

This work was supported by the BBSRC (BB/J007846/1 to HL, BB/N000463/1 to PE, and BB/N000129/1 to NA).

# SUPPLEMENTARY MATERIAL

The Supplementary Material for this article can be found online at: https://www.frontiersin.org/articles/10.3389/fphys.2019.01278/full#supplementary-material

**FIGURE S1 |** Sperm shape abnormalities are overrepresented in Fbxo7LacZ/LacZ animals compared to wild type and heterozygous animals. Sperm from all genotypes were clustered according to shape into three categories of normal, somewhat abnormal and severely deformed. Upper panel; representative DAPI-stained sperm nuclei from each cluster; middle panel; consensus shape of the cluster; lower panel; percent of each genotype within the cluster. The majority of the Fbxo7LacZ/LacZ sperm have severe abnormalities, compared with less than 10% of wild type or heterozygote sperm.

**FIGURE S2 |** Sperm from Fbxo7LacZ/LacZ animals are mostly smaller than sperm from wild type and heterozygous animals, with higher variability (measured as the difference between each nucleus' shape and the median shape).

**FIGURE S3 | (A)** Immunoblotting using the antibody against human Fbxo7 (made in house) of duplicate samples of whole cell lysates made from SHSY5Y cells stably expressing with an empty vector or a short hairpin RNA targeting Fbxo7 expression. **(B)** Immunoblotting of samples of whole cell lysates made from U2OS cells stably expressing with an empty vector or three independent short hairpin RNAs targeting PI31 expression. **(C)** Representative examples of negative control immunohistochemical staining on wild type and homozygous LacZ testes, omitting the various primary antibodies, relating to images shown in **Figures 2G–L, 5A,B**. Arrows indicate mis-localised spermatid nuclei in the "graveyards." **(D)** Representative examples of negative control immunohistochemical staining on wild type testes, omitting the PI31 primary antibody, relating to images shown in **Figure 6**. There was no specific germ cell staining, only residual auto-fluorescence in interstitial tissue between the seminiferous tubules, which is highlighted in these images due to the long exposure time. In particular, at stage X-XI the negative control showed no signal in elongating spermatid nuclei and minimal staining in spermatocyte cytoplasm (compare to **Figure 6** lower middle panel). Similarly, at stage V-VI, there was no signal in the condensing spermatid cytoplasm (compare to **Figure 6**, central panel).

**TABLE S1 |** Details of antibodies used in this study.

**TABLE S2 |** All tubules were examined for a complete testis cross section for three males from each genotype. sgl, tubules with one or more singleton spermatid heads located at the basement membrane. gy, tubules with one or more "graveyards" consisting of 2 or more mislocalised spermatids lying within the same Sertoli cell.

# REFERENCES


Arama, E., Agapite, J., and Steller, H. (2003). Caspase activity and a specific cytochrome C are required for sperm differentiation in *Drosophila*. *Dev. Cell* 4, 687–697. doi: 10.1016/s1534-5807(03)00120-5

Arama, E., Bader, M., Rieckhof, G. E., and Steller, H. (2007). A ubiquitin ligase complex regulates caspase activation during sperm differentiation in *Drosophila*. *PLoS Biol.* 5:e251. doi: 10.1371/journal.pbio.0050251

Bader, M., Arama, E., and Steller, H. (2010). A novel F-box protein is required for caspase activation during cellular remodeling in *Drosophila*. *Development* 137, 1679–1688. doi: 10.1242/dev.050088

Bader, M., Benjamin, S., Wapinski, O. L., Smith, D. M., Goldberg, A. L., and Steller, H. (2011). A conserved F box regulatory complex controls proteasome activity in *Drosophila*. *Cell* 145, 371–382. doi: 10.1016/j.cell.2011.03.021

Birkenfeld, A. L., Lee, H. Y., Guebre-Egziabher, F., Alves, T. C., Jurczak, M. J., and Jornayvaz, F. R. (2011). Deletion of the mammalian INDY homolog mimics aspects of dietary restriction and protects against adiposity and insulin resistance in mice. *Cell Metab.* 14, 184–195. doi: 10.1016/j.cmet.2011.06.009

Blanco-Rodriguez, J., and Martinez-Garcia, C. (1999). Apoptosis is physiologically restricted to a specialized cytoplasmic compartment in rat spermatids. *Biol. Reprod.* 61, 1541–1547. doi: 10.1095/biolreprod61.6.1541

Bochtler, M., Ditzel, L., Groll, M., Hartmann, C., and Huber, R. (1999). The proteasome. *Annu. Rev. Biophys. Biomol. Struct.* 28, 295–317.

Bose, R., Manku, G., Culty, M., and Wing, S. S. (2014). Ubiquitin-proteasome system in spermatogenesis. *Adv. Exp. Med. Biol.* 759, 181–213. doi: 10.1007/978-1-4939-0817-2_9

Bousquet-Dubouch, M. P., Baudelet, E., Guerin, F., Matondo, M., Uttenweiler-Joseph, S., Burlet-Schiltz, O., et al. (2009). Affinity purification strategy to capture human endogenous proteasome complexes diversity and to identify proteasome-interacting proteins. *Mol. Cell Proteomics* 8, 1150–1164. doi: 10.1074/mcp.M800193-MCP200

Braun, R. E., Behringer, R. R., Peschon, J. J., Brinster, R. L., and Palmiter, R. D. (1989). Genetically haploid spermatids are phenotypically diploid. *Nature* 337, 373–376. doi: 10.1038/337373a0

Brown, G. C., and Neher, J. J. (2012). Eaten alive! Cell death by primary phagocytosis: 'phagoptosis'. *Trends Biochem. Sci.* 37, 325–332. doi: 10.1016/j.tibs.2012.05.002

Burchell, V. S., Nelson, D. E., Sanchez-Martinez, A., Delgado-Camprubi, M., Ivatt, R. M., and Pogson, J. H. (2013). The Parkinson's disease-linked proteins Fbxo7 and Parkin interact to mediate mitophagy. *Nat. Neurosci.* 16, 1257–1265. doi: 10.1038/nn.3489

Cagan, R. L. (2003). Spermatogenesis: borrowing the apoptotic machinery. *Curr. Biol.* 13, R600–R602.

Chu-Ping, M., Slaughter, C. A., and DeMartino, G. N. (1992). Purification and characterization of a protein inhibitor of the 20S proteasome (macropain). *Biochim. Biophys. Acta* 1119, 303–311. doi: 10.1016/0167-4838(92)90218-3

Chu-Ping, M., Vu, J. H., Proske, R. J., Slaughter, C. A., and DeMartino, G. N. (1994). Identification, purification, and characterization of a high molecular weight, ATP-dependent activator (PA700) of the 20 S proteasome. *J. Biol. Chem.* 269, 3539–3547.

Corridoni, D., Shiraishi, S., Chapman, T., Steevels, T., Muraro, D., and Thezenas, M. L. (2019). NOD2 and TLR2 Signal via TBK1 and PI31 to Direct Cross-Presentation and CD8 T Cell Responses. *Front. Immunol.* 10:958. doi: 10.3389/fimmu.2019.00958

Di Fonzo, A., Dekker, M. C., Montagna, P., Baruzzi, A., Yonova, E. H., and Correia, G. L. (2009). FBXO7 mutations cause autosomal recessive, early-onset parkinsonian-pyramidal syndrome. *Neurology* 72, 240–245. doi: 10.1212/01.wnl.0000338144.10967.2b

Ding, K., Shameer, K., Jouni, H., Masys, D. R., Jarvik, G. P., Kho, A. N., et al. (2012). Genetic loci implicated in erythroid differentiation and cell cycle regulation are associated with red blood cell traits. *Mayo Clin. Proc.* 87, 461–474. doi: 10.1016/j.mayocp.2012.01.016

Fabian, L., and Brill, J. A. (2012). *Drosophila* spermiogenesis: big things come from little packages. *Spermatogenesis* 2, 197–212. doi: 10.4161/spmg.21798

Fabre, B., Lambour, T., Garrigues, L., Amalric, F., Vigneron, N., Menneteau, T., et al. (2015). Deciphering preferential interactions within supramolecular protein complexes: the proteasome case. *Mol. Syst. Biol.* 11:771. doi: 10.15252/msb.20145497

Ganesh, S. K., Zakai, N. A., van Rooij, F. J., Soranzo, N., Smith, A. V., and Nalls, M. A. (2009). Multiple loci influence erythrocyte phenotypes in the CHARGE Consortium. *Nat. Genet.* 41, 1191–1198. doi: 10.1038/ng.466

Gaucher, J., Reynoird, N., Montellier, E., Boussouar, F., Rousseaux, S., and Khochbin, S. (2010). From meiosis to postmeiotic events: the secrets of histone disappearance. *FEBS J.* 277, 599–604. doi: 10.1111/j.1742-4658.2009.07504.x

Geminard, C., de Gassart, A., and Vidal, M. (2002). Reticulocyte maturation: mitoptosis and exosome release. *Biocell* 26, 205–215.

Geyer, C. B., Inselman, A. L., Sunman, J. A., Bornstein, S., Handel, M. A., and Eddy, E. M. (2009). A missense mutation in the Capza3 gene and disruption of F-actin organization in spermatids of repro32 infertile male mice. *Dev. Biol.* 330, 142–152. doi: 10.1016/j.ydbio.2009.03.020

Greene, J. C., Whitworth, A. J., Kuo, I., Andrews, L. A., Feany, M. B., and Pallanck, L. J. (2003). Mitochondrial pathology and apoptotic muscle degeneration in *Drosophila* parkin mutants. *Proc. Natl. Acad. Sci. U.S.A.* 100, 4078–4083. doi: 10.1073/pnas.0737556100

Huang, L., Haratake, K., Miyahara, H., and Chiba, T. (2016). Proteasome activators, PA28gamma and PA200, play indispensable roles in male fertility. *Sci. Rep.* 6:23171. doi: 10.1038/srep23171

Itier, J. M., Ibanez, P., Mena, M. A., Abbas, N., Cohen-Salmon, C., and Bohme, G. A. (2003). Parkin gene inactivation alters behaviour and dopamine neurotransmission in the mouse. *Hum. Mol. Genet.* 12, 2277–2291. doi: 10.1093/hmg/ddg239

Johnson, C., Jia, Y., Wang, C., Lue, Y. H., Swerdloff, R. S., Zhang, X. S., et al. (2008). Role of caspase 2 in apoptotic signaling in primate and murine germ cells. *Biol. Reprod.* 79, 806–814. doi: 10.1095/biolreprod.108.068833

Joseph, S., Vingill, S., Jahn, O., Fledrich, R., Werner, H. B., and Katona, I. (2019). Myelinating glia-specific deletion of Fbxo7 in mice triggers axonal degeneration in the central nervous system together with peripheral neuropathy. *J. Neurosci.* 39, 5606–5626. doi: 10.1523/JNEUROSCI.3094-18.2019

Kerr, J. B., and de Kretser, D. M. (1974). Proceedings: the role of the Sertoli cell in phagocytosis of the residual bodies of spermatids. *J. Reprod. Fertil.* 36, 439–440. doi: 10.1530/jrf.0.0360439

Kirk, R., Laman, H., Knowles, P. P., Murray-Rust, J., Lomonosov, M., Meziane, E. K., et al. (2008). Structure of a conserved dimerization domain within the F-box protein Fbxo7 and the PI31 proteasome inhibitor. *J. Biol. Chem.* 283, 22325–22335. doi: 10.1074/jbc.M709900200

Kissel, H., Georgescu, M. M., Larisch, S., Manova, K., Hunnicutt, G. R., and Steller, H. (2005). The Sept4 septin locus is required for sperm terminal differentiation in mice. *Dev. Cell* 8, 353–364. doi: 10.1016/j.devcel.2005.01.021

Kniepert, A., and Groettrup, M. (2014). The unique functions of tissue-specific proteasomes. *Trends Biochem. Sci.* 39, 17–24. doi: 10.1016/j.tibs.2013.10.004

Koenig, P. A., Nicholls, P. K., Schmidt, F. I., Hagiwara, M., Maruyama, T., Frydman, G. H., et al. (2014). The E2 ubiquitin-conjugating enzyme UBE2J1 is required for spermiogenesis in mice. *J. Biol. Chem.* 289, 34490–34502. doi: 10.1074/jbc.M114.604132

Kuiken, H. J., Egan, D. A., Laman, H., Bernards, R., Beijersbergen, R. L., and Dirac, A. M. (2012). Identification of F-box only protein 7 as a negative regulator of NF-kappaB signalling. *J. Cell Mol. Med.* 16, 2140–2149. doi: 10.1111/j.1582-4934.2012.01524.x

Laman, H. (2006). Fbxo7 gets proactive with cyclin D/cdk6. *Cell Cycle* 5, 279–282. doi: 10.4161/cc.5.3.2403

Li, X., Thompson, D., Kumar, B., and DeMartino, G. N. (2014). Molecular and cellular roles of PI31 (PSMF1) protein in regulation of proteasome function. *J. Biol. Chem.* 289, 17392–17405. doi: 10.1074/jbc.M114.561183

Liu, K., Jones, S., Minis, A., Rodriguez, J., Molina, H., and Steller, H. (2019). PI31 is an adaptor protein for proteasome transport in axons and required for synaptic development. *Dev. Cell.* 50, 509.e10–524.e10. doi: 10.1016/j.devcel.2019.06.009

Lohmann, E., Coquel, A. S., Honore, A., Gurvit, H., Hanagasi, H., and Emre, M. (2015). A new F-box protein 7 gene mutation causing typical Parkinson's disease. *Mov Disord.* 30, 1130–1133. doi: 10.1002/mds.26266

Lomonosov, M., Meziane, E. K., Ye, H., Nelson, D. E., Randle, S. J., and Laman, H. (2011). Expression of Fbxo7 in haematopoietic progenitor cells cooperates with p53 loss to promote lymphomagenesis. *PLoS One* 6:e21165. doi: 10.1371/journal.pone.0021165

Lysiak, J. J., Zheng, S., Woodson, R., and Turner, T. T. (2007). Caspase-9-dependent pathway to murine germ cell apoptosis: mediation by oxidative stress. BAX, and caspase 2. *Cell Tissue Res.* 328, 411–419. doi: 10.1007/s00441-006-0341-y

Mankelow, T. J., Griffiths, R. E., Trompeter, S., Flatt, J. F., Cogan, N. M., Massey, E. J., et al. (2015). Autophagic vesicles on mature human reticulocytes explain phosphatidylserine-positive red cells in sickle cell disease. *Blood* 126, 1831–1834. doi: 10.1182/blood-2015-04-637702

McCutchen-Maloney, S. L., Matsuda, K., Shimbara, N., Binns, D. D., Tanaka, K., Slaughter, C. A., et al. (2000). cDNA cloning, expression, and functional characterization of PI31, a proline-rich inhibitor of the proteasome. *J. Biol. Chem.* 275, 18557–18565. doi: 10.1074/jbc.m001697200

Merzetti, E. M., Dolomount, L. A., and Staveley, B. E. (2017). The FBXO7 homologue nutcracker and binding partner PI31 in *Drosophila melanogaster* models of Parkinson's disease. *Genome* 60, 46–54. doi: 10.1139/gen-2016-0087

Meziane, E. K., Randle, S. J., Nelson, D. E., Lomonosov, M., and Laman, H. (2011). Knockdown of Fbxo7 reveals its regulatory role in proliferation and differentiation of haematopoietic precursor cells. *J. Cell Sci.* 124, 2175–2186. doi: 10.1242/jcs.080465

Oakberg, E. F. (1956). A description of spermiogenesis in the mouse and its use in analysis of the cycle of the seminiferous epithelium and germ cell renewal. *Am. J. Anat.* 99, 391–413. doi: 10.1002/aja.1000990303

Ovchynnikova, E., Aglialoro, F., von Lindern, M., and van den, A. E. (2018). The shape shifting story of reticulocyte maturation. *Front. Physiol.* 9:829. doi: 10.3389/fphys.2018.00829

Paisan-Ruiz, C., Guevara, R., Federoff, M., Hanagasi, H., Sina, F., and Elahi, E. (2010). Early-onset L-dopa-responsive parkinsonism with pyramidal signs due to ATP13A2, PLA2G6, FBXO7 and spatacsin mutations. *Mov. Disord.* 25, 1791–1800. doi: 10.1002/mds.23221

Patel, S. P., Randle, S. J., Gibbs, S., Cooke, A., and Laman, H. (2016). Opposing effects on the cell cycle of T lymphocytes by Fbxo7 via Cdk6 and p27. *Cell. Mol. Life Sci.* 74, 1553–1566. doi: 10.1007/s00018-016-2427-3

Qian, M. X., Pang, Y., Liu, C. H., Haratake, K., Du, B. Y., and Ji, D. Y. (2013). Acetylation-mediated proteasomal degradation of core histones during DNA repair and spermatogenesis. *Cell* 153, 1012–1024. doi: 10.1016/j.cell.2013.04.032

Randle, S. J., and Laman, H. (2016). Structure and function of Fbxo7/PARK15 in Parkinson's disease. *Curr. Protein Pept. Sci.* 18, 715–724. doi: 10.2174/1389203717666160311121433

Randle, S. J., Nelson, D. E., Patel, S. P., and Laman, H. (2015). Defective erythropoiesis in a mouse model of reduced Fbxo7 expression due to decreased p27 expression. *J. Pathol.* 237, 263–272. doi: 10.1002/path.4571

Rathke, C., Baarends, W. M., Awe, S., and Renkawitz-Pohl, R. (2014). Chromatin dynamics during spermiogenesis. *Biochim. Biophys. Acta* 1839, 155–168. doi: 10.1016/j.bbagrm.2013.08.004

Robeson, A. C., Lindblom, K. R., Wojton, J., Kornbluth, S., and Matsuura, K. (2018). Dimer-specific immunoprecipitation of active caspase-2 identifies TRAF proteins as novel activators. *EMBO J.* 37:e97072. doi: 10.15252/embj.201797072

Russell, L. D., Chiarini-Garcia, H., Korsmeyer, S. J., and Knudson, C. M. (2002). Bax-dependent spermatogonia apoptosis is required for testicular development and spermatogenesis. *Biol. Reprod.* 66, 950–958. doi: 10.1095/biolreprod66.4.950

Russell, L. D., Ettlin, R. A., Sinha Hikim, A. P., and Clegg, E. D. (1993). Histological and histopathological evaluation of the testis. *Int. J. Androl.* 16, 120–161.

Russell, L. D., Saxena, N. K., and Turner, T. T. (1989). Cytoskeletal involvement in spermiation and sperm transport. *Tissue Cell* 21, 361–379. doi: 10.1016/0040-8166(89)90051-7

Russell, L. D., Warren, J., Debeljuk, L., Richardson, L. L., Mahar, P. L., and Waymire, K. G. (2001). Spermatogenesis in Bclw-deficient mice. *Biol. Reprod.* 65, 318–332. doi: 10.1095/biolreprod65.1.318

Said, T. M., Paasch, U., Glander, H. J., and Agarwal, A. (2004). Role of caspases in male infertility. *Hum. Reprod. Update* 10, 39–51. doi: 10.1093/humupd/dmh003

Sakai, Y., and Yamashina, S. (1989). Mechanism for the removal of residual cytoplasm from spermatids during mouse spermiogenesis. *Anat. Rec.* 223, 43–48. doi: 10.1002/ar.1092230107

Shang, J., Huang, X., and Du, Z. (2015). The FP domains of PI31 and Fbxo7 have the same protein fold but very different modes of protein-protein interaction. *J. Biomol. Struct. Dyn.* 33, 1528–1538. doi: 10.1080/07391102.2014.963675

Simard, O., Leduc, F., Acteau, G., Arguin, M., Gregoire, M. C., Brazeau, M. A., et al. (2015). Step-specific sorting of mouse spermatids by flow cytometry. *J. Vis. Exp.* 106:e53379. doi: 10.3791/53379

Skinner, B. M., Rathje, C. C., Bacon, J., Johnson, E. E. P., Larson, E. L., and Kopania, E. E. K. (2019). A high-throughput method for unbiased quantitation and categorisation of nuclear morphology. *Biol. Reprod.* 100, 1250–1260. doi: 10.1093/biolre/ioz013

Soranzo, N., Spector, T. D., Mangino, M., Kuhnel, B., Rendon, A., and Teumer, A. (2009). A genome-wide meta-analysis identifies 22 loci associated with eight hematological parameters in the HaemGen consortium. *Nat. Genet.* 41, 1182–1190. doi: 10.1038/ng.467

Stott, S. R., Randle, S. J., Al Rawi, S., Rowicka, P. A., Harris, R., Mason, B., et al. (2019). Loss of FBXO7 results in a Parkinson's-like dopaminergic degeneration via an RPL23-MDM2-TP53 pathway. *J. Pathol.* doi: 10.1002/path.5312 [Epub ahead of print].

Teixeira, F. R., Randle, S. J., Patel, S. P., Mevissen, T. E., Zenkeviciute, G., Koide, T., et al. (2016). Gsk3beta and Tomm20 are substrates of the SCFFbxo7/PARK15 ubiquitin ligase associated with Parkinson's disease. *Biochem. J.* 473, 3563–3580. doi: 10.1042/bcj20160387

van der, H. P., Zhang, W., Mateo, L. I., Rendon, A., Verweij, N., and Sehmi, J. (2012). Seventy-five genetic loci influencing the human red blood cell. *Nature* 492, 369–375. doi: 10.1038/nature11677

Ventela, S., Toppari, J., and Parvinen, M. (2003). Intercellular organelle traffic through cytoplasmic bridges in early spermatids of the rat: mechanisms of haploid gene product sharing. *Mol. Biol. Cell* 14, 2768–2780. doi: 10.1091/mbc.e02-10-0647

Vingill, S., Brockelt, D., Lancelin, C., Tatenhorst, L., Dontcheva, G., Preisinger, C., et al. (2016). Loss of FBXO7 (PARK15) results in reduced proteasome activity and models a parkinsonism-like phenotype in mice. *EMBO J.* 35, 2008–2025. doi: 10.15252/embj.201593585

Voges, D., Zwickl, P., and Baumeister, W. (1999). The 26S proteasome: a molecular machine designed for controlled proteolysis. *Annu. Rev. Biochem.* 68, 1015–1068. doi: 10.1146/annurev.biochem.68.1.1015

Wang, H., Zhao, R., Guo, C., Jiang, S., Yang, J., and Xu, Y. (2016). Knockout of BRD7 results in impaired spermatogenesis and male infertility. *Sci. Rep.* 6:21776. doi: 10.1038/srep21776

Yacobi-Sharon, K., Namdar, Y., and Arama, E. (2013). Alternative germ cell death pathway in *Drosophila* involves HtrA2/Omi, lysosomes, and a caspase-9 counterpart. *Dev. Cell* 25, 29–42. doi: 10.1016/j.devcel.2013.02.002

Yang, B. J., Han, X. X., Yin, L. L., Xing, M. Q., Xu, Z. H., and Xue, H. W. (2016). Arabidopsis PROTEASOME REGULATOR1 is required for auxin-mediated suppression of proteasome activity and regulates auxin signalling. *Nat. Commun.* 7:11388. doi: 10.1038/ncomms11388

Zaiss, D. M., Standera, S., Holzhutter, H., Kloetzel, P., and Sijts, A. J. (1999). The proteasome inhibitor PI31 competes with PA28 for binding to 20S proteasomes. *FEBS Lett.* 457, 333–338. doi: 10.1016/s0014-5793(99)01072-8

Zaiss, D. M., Standera, S., Kloetzel, P. M., and Sijts, A. J. (2002). PI31 is a modulator of proteasome formation and antigen processing. *Proc. Natl. Acad. Sci. U.S.A.* 99, 14344–14349. doi: 10.1073/pnas.212257299

Zhang, J., Wu, K., Xiao, X., Liao, J., Hu, Q., Chen, H., et al. (2015). Autophagy as a regulatory component of erythropoiesis. *Int. J. Mol. Sci.* 16, 4083–4094. doi: 10.3390/ijms16024083

Zheng, H., Stratton, C. J., Morozumi, K., Jin, J., Yanagimachi, R., and Yan, W. (2007). Lack of Spem1 causes aberrant cytoplasm removal, sperm deformation, and male infertility. *Proc. Natl. Acad. Sci. U.S.A.* 104, 6852–6857. doi: 10.1073/pnas.0701669104

Zheng, S., Turner, T. T., and Lysiak, J. J. (2006). Caspase 2 activity contributes to the initial wave of germ cell apoptosis during the first round of spermatogenesis. *Biol. Reprod.* 74, 1026–1033. doi: 10.1095/biolreprod.105.044610

Zhong, L., and Belote, J. M. (2007). The testis-specific proteasome subunit Prosalpha6T of *D. melanogaster* is required for individualization and nuclear maturation during spermatogenesis. *Development* 134, 3517–3525. doi: 10.1242/dev.004770

**Conflict of Interest:** The authors declare that the research was conducted in the absence of any commercial or financial relationships that could be construed as a potential conflict of interest.

frontiers in Physiology

REVIEW
published: 22 October 2020
doi: 10.3389/fphys.2020.01022

# E3 Ubiquitin Ligases in Neurological Diseases: Focus on Gigaxonin and Autophagy

*Léa Lescouzères and Pascale Bomont**

*ATIP-Avenir Team, INM, INSERM, University of Montpellier, Montpellier, France*

Ubiquitination is a dynamic post-translational modification that regulates the fate of proteins and therefore modulates a myriad of cellular functions. At the last step of this sophisticated enzymatic cascade, E3 ubiquitin ligases selectively direct ubiquitin attachment to specific substrates. Altogether, the ∼800 distinct E3 ligases, combined to the exquisite variety of ubiquitin chains and types that can be formed at multiple sites on thousands of different substrates confer to ubiquitination versatility and infinite possibilities to control biological functions. E3 ubiquitin ligases have been shown to regulate behaviors of proteins, from their activation, trafficking, subcellular distribution, interaction with other proteins, to their final degradation. Largely known for tagging proteins for their degradation by the proteasome, E3 ligases also direct ubiquitinated proteins and more largely cellular content (organelles, ribosomes, etc.) to destruction by autophagy. This multi-step machinery involves the creation of double membrane autophagosomes in which engulfed material is degraded after fusion with lysosomes. Cooperating in sustaining homeostasis, actors of ubiquitination, proteasome and autophagy pathways are impaired or mutated in wide range of human diseases. From initial discovery of pathogenic mutations in the E3 ligase encoding for E6-AP in Angelman syndrome and Parkin in juvenile forms of Parkinson disease, the number of E3 ligases identified as causal gene for neurological diseases has considerably increased within the last years. In this review, we provide an overview of these diseases, by classifying the E3 ubiquitin ligase types and categorizing the neurological signs. We focus on the Gigaxonin-E3 ligase, mutated in giant axonal neuropathy and present a comprehensive analysis of the spectrum of mutations and the recent biological models that permitted to uncover novel mechanisms of action. Then, we discuss the common functions shared by Gigaxonin and the other E3 ligases in cytoskeleton architecture, cell signaling and autophagy. In particular, we emphasize their pivotal roles in controlling multiple steps of the autophagy pathway. In light of the various targets and extending functions sustained by a single E3 ligase, we finally discuss the challenge in understanding the complex pathological cascade underlying disease and in designing therapeutic approaches that can apprehend this complexity.

**Keywords: Gigaxonin, E3 ligase, ubiquitin, neurodevelopmental disease, neurodegenerative disease, cytoskeleton, cell signaling, autophagy**

OPEN ACCESS

***Edited by:***
*Julien Licchesi,*
*University of Bath, United Kingdom*

***Reviewed by:***
*George K. Tofaris,*
*University of Oxford, United Kingdom*
*Dhanendra Tomar,*
*Temple University, United States*

***Correspondence:**
*Pascale Bomont*
*pascale.bomont@inserm.fr*

***Specialty section:***
*This article was submitted to Integrative Physiology, a section of the journal Frontiers in Physiology*

***Received:*** *01 June 2020*
***Accepted:*** *27 July 2020*
***Published:*** *22 October 2020*

***Citation:***
*Lescouzères L and Bomont P (2020) E3 Ubiquitin Ligases in Neurological Diseases: Focus on Gigaxonin and Autophagy. Front. Physiol. 11:1022. doi: 10.3389/fphys.2020.01022*

## INTRODUCTION: E3 UBIQUITIN LIGASES IDENTIFIED AS CAUSAL GENE PRODUCTS IN NEUROLOGICAL DISEASES

E3 ubiquitin ligases constitute a large family of enzymes that play pivotal roles in protein ubiquitination, a major posttranslational modification regulating various cellular functions, as diverse as DNA repair, proliferation, apoptosis, transcription, circadian clock, endocytosis, cell signaling, immunity, and protein quality control (Swatek and Komander, 2016). Ubiquitination involves a cascade of enzymatic reactions, driven by ubiquitin-activating enzymes (E1), ubiquitin-conjugating enzymes (E2) and ubiquitin-ligases (E3) that ultimately transfer the ubiquitin moieties to specific targets (Komander and Rape, 2012; **Figure 1A**). Represented by ∼800 distinct genes, E3 ligases provide an exquisite precise and diverse mode of control of cellular processes, through the spatial, temporal and substrate specificity of the E3 ligases, and the variety of ubiquitination types (mono, multi, and poly) and ubiquitin chains (on the 7 Lys residues or the N-terminal Met of ubiquitin) (Kwon and Ciechanover, 2017). This diversity underlies the multiples roles of ubiquitination in regulating the fate of proteins, from their activity, interaction, trafficking, subcellular distribution, and degradation. Ubiquitinated substrates can be degraded by the proteasome and/or autophagy, two pathways that cooperate to maintain cellular and tissue homeostasis but that bear distinct properties (Kocaturk and Gozuacik, 2018). Proteasome is a multi-catalytic protease complex essential to degrade short-lived proteins or misfolded/damaged proteins, whereas autophagy preferentially eliminates long-lived proteins, insoluble protein aggregates and also organelles and parasites (Rousseau and Bertolotti, 2018). The (macro)autophagy machinery is a multistep process leading to the engulfment of material in a double membrane vesicle called autophagosomes, that subsequently fuse to lysosomes for degradation of content by lysosomal enzyme (Klionsky and Emr, 2000; Galluzzi et al., 2017). While degradation can be independent of ubiquitination (called bulk autophagy), ubiquitin signaling triggers a specific response (called selective autophagy), to clear identified material. Cooperating with proteasome to clear damaged or old cellular compounds in basal conditions, autophagy is upregulated upon stress (nutritional, hypoxia, and chemical) to recycle material and therefore provide nutrients essential for adaptation and survival. Thus, the ubiquitin proteasome system (UPS) and autophagy are crucial for physiology and alterations of these machineries underlie a wide range of human diseases, including cancer, immune and neurodegenerative diseases (Menzies et al., 2017; Rousseau and Bertolotti, 2018; Levine and Kroemer, 2019).

Conferring substrate specificity for ubiquitination, E3 ligases are key in regulating protein activation, function, and degradation. There are classified into three major groups: the HECT (homologous to E6-AP carboxyl terminus), the RING (really interesting new gene) and the RING-HECT hybrid E3s (Zheng and Shabek, 2017; **Figure 1B**). The HECT domain E3 ligases catalyze the attachment of ubiquitin to the substrate, while the RING finger E3 ligases do not have a catalytic role and act as scaffold to bridge E2 and substrate for the transfer of ubiquitin from the E2 to the substrate. RING E3s constitute a large family, which is formed of monomeric RINGs, dimeric RINGs or multi-subunit RINGs assembled around Cullin subunits. Hybrid E3s, the RING-HECT ligases interact with E2 as the RING enzymes but transfer ubiquitin with HECT-like mechanism. The last years have seen a rise in the identification of E3 ligase encoding genes as the cause of neurological diseases in human. Since the identification of the first HECT (E6-AP in Angelman syndrome; AS) and RING (Parkin in juvenile form of Parkinson disease) E3 ligases (Kishino et al., 1997; Matsuura et al., 1997; Kitada et al., 1998), 42 additional players are shaping the diversified landscape of E3 types in the origin of neurological diseases (**Figure 1B**). These diseases, mostly inherited by a recessive mode for a general loss-of-function mechanism of the respective E3 ligases are extremely diverse. The spectrum spreads from neurodevelopmental to adult neurodegenerative pathologies, including various forms of intellectual disability, encephalopathy, epilepsy, retinitis pigmentosa, ataxia, and Parkinson's disease (**Figure 2**). These clinical features can be mixed in various neurodevelopmental conditions like AS, or represent one component of broader multisystemic diseases, like Opitz G/BBB and Bardet–Biedl syndromes. E3 ligases mutated in peripheral neuropathies are exemplified by several forms of Charcot-Marie-Tooth (CMT) diseases and distal hereditary motor neuropathy. While rare cases of peripheral neuropathies exhibit some central signs [TRIM2 with vocal cord paralysis (Pehlivan et al., 2015) and LRSAM1 with Parkinson features (Aerts et al., 2016)], Giant Axonal Neuropathy (GAN), caused by a CRL3 adaptor named Gigaxonin stands for the spreading of symptoms across neuronal tissues in both peripheral nervous system (PNS) and central nervous system (CNS). In this review, we present the genetic underlying GAN, the generation of novel biological models and the recent advances into the key functions of Gigaxonin. With this focus on Gigaxonin, we then provide a comprehensive analysis of common functional themes shared with other E3 ligases in controlling pivotal cellular pathways: cytoskeleton organization, cell signaling, and autophagy. Expanding on the later, we discuss how E3 ligases mutated in neurological diseases directly modulate multiple steps of the autophagy pathway, hence providing novel opportunities for the identification of specific spots for therapeutic intervention in neurological diseases, and more largely for the use of these E3 ligases in developing novel tools for the benefit of many other diseases.

## GIGAXONIN ENCODING GENE, GENETIC CAUSE OF GIANT AXONAL NEUROPATHY

### Giant Axonal Neuropathy

Giant axonal neuropathy (GAN, MIM#256850) is a rare neurodegenerative disease with an autosomic and recessive mode of inheritance (Asbury et al., 1972; Berg et al., 1972). This review will not provide an exhaustive presentation

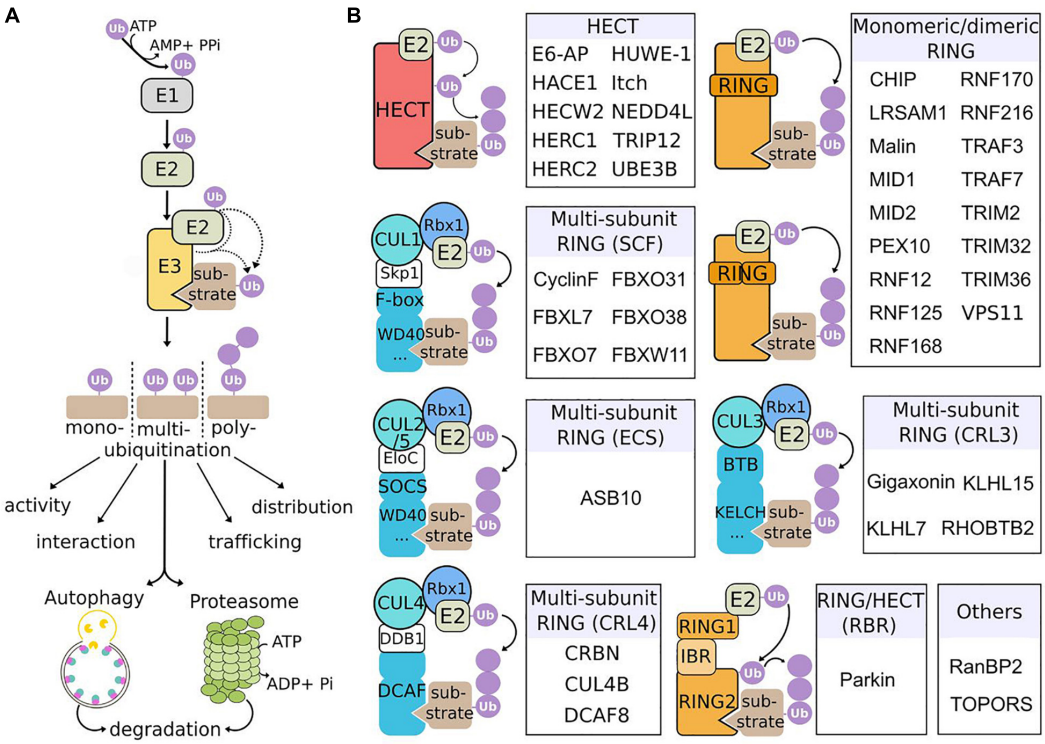


**FIGURE 1 |** Mechanism of action and classification of E3 ubiquitin ligases causing neurological diseases in human. **(A)** Ubiquitination cascade. E1 enzymes activate ubiquitin (Ub) in an ATP-dependent manner, forming a thioester bound with Ub. Activated-Ub is then transferred to Ub-conjugating enzymes (E2). Finally, E3 ubiquitin ligases assist or directly catalyze the transfer of Ub to substrates. Substrates can be mono-, multi- or poly-ubiquitinated, with different types of Ub chains, to modulate various processes, including protein activation, interaction, trafficking, subcellular localization, and degradation through the 26S proteasome or the autophagy pathway. **(B)** E3 ligases underlying neurological diseases and their classification. The three classes of E3 (HECT, RING, and RING-HECT hybrid) are represented. E3 ligases identified as the genetic cause of neurodevelopmental and neurodegenerative diseases in human are classified within each category (sub-classes with no disease representative are not shown). The HECT and RING E3 ligases differ in the way they transfer Ub to the substrate. The HECT E3s receive Ub from E2 enzymes, form a thioester intermediate with Ub, and catalyze the transfer to the substrate. RING E3s associate with E2 enzymes and substrates and mediate the transfer of Ub from E2 to the substrate. RING E3s can function as monomers, dimers or multi-subunit RING E3s. The latter class is subdivided in different groups, among which the Cullin-RING Ligases (CRLs) are the largest E3 ligase family. SCF, ECS, CRL3 and CRL4 ligases are composed of a modular E3 core containing specific Cullins (respectively CUL1, CUL2/5, CUL3, CUL4) and RBX1 (RING-box1 proteins), and a substrate specificity module composed of an adaptor (Skp1, EloC, and DDB1) and a substrate receptor. The RING-HECT hybrid ligases (RBR for RING-between-RING) interact with E2 as the RING E3 but transfer Ub with HECT-like mechanism. Finally, particular E3 are represented ("Others"): RanBP2 does not transfer Ub but Sumo (small ubiquitin-related modifier) and is neither an HECT, nor a RING E3 ligase; TOPORS has a RING domain and is a dual E3 Ub and Sumo ligase.

of clinical symptoms, which has been described elsewhere (Kuhlenbaumer et al., 1993; Johnson-Kerner et al., 2014) but will highlight key features. Giant axonal neuropathy is unique, for its wide alteration of the nervous system and its severity (**Figure 3A**). In the classical severe form, GAN starts in infancy, touches both sensory and motor modalities of the PNS, evolves toward a loss complete of ambulation and sensitivity during adolescence, and subsequently spreads to the CNS during adulthood. The outcome is fatale in young adult, usually before the third decade. Few milder cases have been described, varying in disease onset and presenting slow progression with, in certain cases no overt alteration of the CNS (see **Supplementary Table 1**). Underlying this massive deterioration of nervous functions are the decreased axonal density and presence of enlarged "giant" axons throughout the nervous system (**Figure 3B**). Giant axons are filled with abnormally packed neurofilaments, the neuronal Intermediate Filaments (IFs) that constitute the most abundant cytoskeletal component of the nervous system. Notably, IF aggregation extends beyond the nervous system, touching other IF types as keratin, desmin, and vimentin (**Figure 3C**), hence placing GAN as a disease of the cytoskeletal IFs. Extremely severe, GAN still shares at early stage features with several forms of CMT diseases, that present similar sensory-motor deficits, giant axons, and NF aggregation (Fabrizi et al., 2004; Azzedine et al., 2006; Ylikallio et al., 2013; Klein et al., 2014).

## The *GAN* Gene: Transmission and Mutations

While gene identification can be achieved through direct sequencing of the human genome nowadays, the *GAN* gene was discovery through a two steps process, comprising genetic

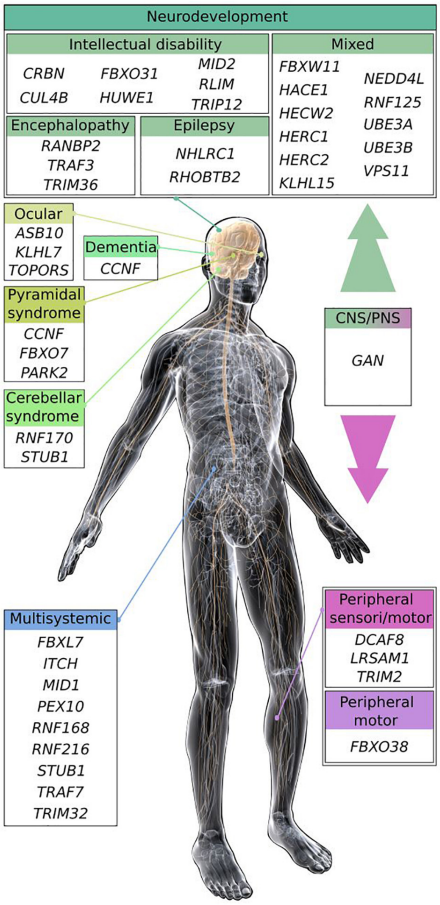


**FIGURE 2 |** Scheme of the main clinical features shared by E3 ligase encoding genes causing neurodevelopmental and neurodegenerative diseases. Most of the E3 ligase genes, when mutated cause neurodevelopmental diseases (intellectual disability, encephalopathy, and epilepsy), or regionalized neuropathies (cerebellar, ocular, and pyramidal syndrome) within the CNS. Some pathologies exhibit mixed symptoms that can be part of broader multisystemic disorders. E3 ligase genes inducing peripheral neuropathies are represented by Charcot-Marie-Tooth diseases (CMT), and distal hereditary motor neuropathy (HMN). The GAN E3 ligase gene causes a disease affecting broadly the nervous system, leading to a myriad of symptoms within the peripheral and the CNS. Illustration: © www.gograph.com/ Eraxion. Genes (protein if different), names of diseases and references (in alphabetical order): *ASB10,* Glaucoma (Pasutto et al., 2012); *CCNF* (cyclinF), Amyotrophic Lateral Sclerosis and Frontotemporal dementia (Williams et al., 2016); *CRBN,* mental retardation (MRT2A; Higgins et al., 2004); *CUL4B*, mental retardation (MRXS15; Zou et al., 2007); *DCAF8,* Charcot-Marie-Tooth disease (CMT2; Klein et al., 2014); *FBXL7,* Hennekam syndrome (Boone et al., 2020); *FBXO7,* Parkinson syndrome (PARK15; Shojaee et al., 2008); *FBXO31*, mental retardation (MRT45; Mir et al., 2014); *FBXO38,* distal hereditary motor neuropathy (HMN2D; Sumner et al., 2013); *FBXW11,* neurodevelopmental syndrome (Holt et al., 2019); *GAN* (Gigaxonin), Giant Axonal Neuropathy (Bomont et al., 2000); *HACE1,* neurodevelopmental syndrome (SPPRS; Hollstein et al., 2015); *HECW2,* neurodevelopmental syndrome (NDHSAL; Berko et al., 2017); *HERC1,* neurodevelopmental syndrome (MDFPMR; Nguyen et al., 2016); *HERC2,* mixed with mental retardation (MRT38; Puffenberger et al., 2012); *HUWE1,* mental retardation (MRXST; Froyen et al., 2008); *ITCH* (Itch), multi-system autoimmune disease with neurodevelopmental defects (Lohr et al., 2010); *KLHL7,* retinitis pigmentosa (RP42; Friedman et al., 2009); *KLHL15,* mixed with mental

*(Continued)*

**FIGURE 2 |** Continued
retardation (MRX103; Mignon-Ravix et al., 2014); *LRSAM1*, CMT2P (Guernsey et al., 2010); *MID1,* Opitz G/BBB syndrome 1 (GBBB1; Quaderi et al., 1997); *MID2*, mental retardation (MRX101; Geetha et al., 2014); *NEDD4L,* Periventricular nodular heterotopia 7 (PVNH7; Broix et al., 2016); *NHLRC1* (Malin), Lafora disease (Chan et al., 2003); *PARK2* (Parkin), Parkinson disease 2 (PARK2; Kitada et al., 1998); *PEX10,* Zellweger syndrome (Okumoto et al., 1998; Warren et al., 1998); *RANBP2** (RanBP2), acute necrotizing encephalopathy (Neilson et al., 2009); *RHOBTB2,* epileptic encephalopathy (EIEE64; Belal et al., 2018); *RLIM* (RNF12) intellectual disability (Tonne et al., 2015); *RNF125,* overgrowth syndrome (Tenorio et al., 2014); *RNF168*, RIDDLE syndrome (Stewart et al., 2009); *RNF170*, sensory ataxia (SNAX1; Valdmanis et al., 2011); *RNF216,* Gordon Holmes syndrome (GHS; Margolin et al., 2013); *STUB1* (CHIP), Spinocerebellar ataxia (SCAR16, SCA48, and GHS; Shi et al., 2013, 2014; Genis et al., 2018); *TOPORS,* retinitis pigmentosa (RP31; Chakarova et al., 2007); *TRAF3**, encephalopathy (Perez de Diego et al., 2010); *TRAF7*, multisystem disorder with neurodevelopmental delay (Tokita et al., 2018); *TRIM2,* CMT2R (Ylikallio et al., 2013); *TRIM32,* Bardet-Biedl syndrome (BBS11; Chiang et al., 2006); *TRIM36,* anencephaly (Singh et al., 2017); *TRIP12,* intellectual disability with or without autism (O'Roak et al., 2014; Lelieveld et al., 2016); *UBE3A* (E6-AP), Angelman syndrome (Kishino et al., 1997; Matsuura et al., 1997); *UBE3B,* Kaufman oculocerebrofacial syndrome (KOS; Flex et al., 2013); *VPS11*, neurodevelopmental and leukoencephalopathy (Edvardson et al., 2015; Zhang et al., 2016). Asterisk (*) are susceptibility genes for viral-induced neuropathies.

mapping and screening of potential coding sequences within the interval co-segregating with the disease. As for many rare recessively inherited-disease, the genetic localization of the *GAN* gene was made possible thanks to homozygosity mapping, in consanguineous families that present a higher risk of transmitting mutated alleles. Thus, the GAN locus was delineated within the cytogenetic portion of chromosome 16 in 16q24.1 (Ben Hamida et al., 1997; Flanigan et al., 1998) with borders being further reduced thanks to the concomitant identification of novel polymorphic markers and other families (Cavalier et al., 2000). Subsequently, a bioinformatic methodology was developed to make profit of the partial and fragmented genomic sequences released by the ongoing Human Genome sequencing initiative. This pioneer in silico approach (as acknowledged in Lander et al., 2001) led to the discovery of the *GAN* gene subsequently to identification, extension of novel coding portions within the GAN interval and screening for mutations in patients (Bomont et al., 2000). With the first genetic variant identified in the short ESTaa306952, the full 1791 bp coding sequence was cloned and shown to encompass 11 exons. The novel protein, named Gigaxonin was shown to contain a BTB domain at its N-terminus and a Kelch domain, composed of 6 Kelch repetitions at its C-terminal end (Bomont et al., 2000; **Figure 4A**).

In the initial study, a total of 14 distinct pathogenic variants were identified in 12 families, including 2 homozygous truncating mutations, hence unambiguously defining Gigaxonin as the GAN causing gene product. This original publication, which highlighted a large spectrum of mutation types and a scattering along the entire gene has been expanded by various laboratories worldwide. Today, 75 distinct mutations have been

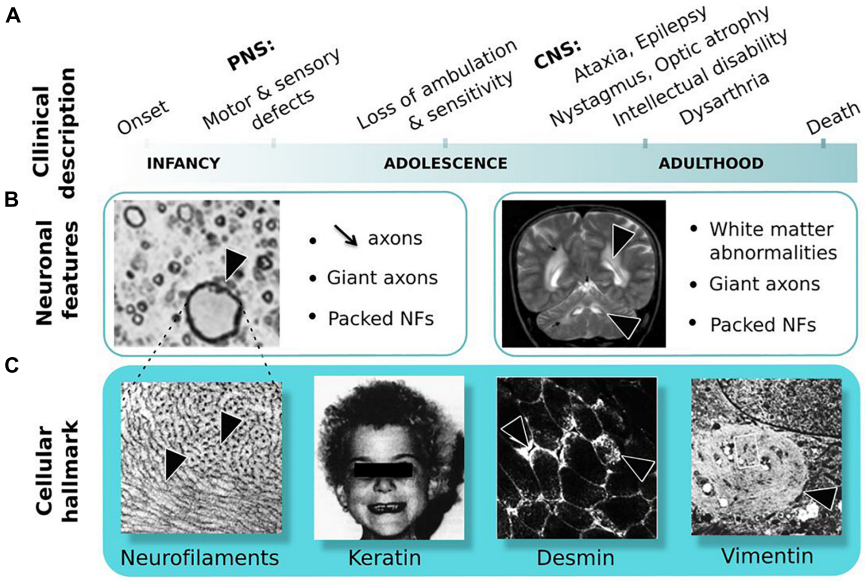


**FIGURE 3 |** Giant Axonal Neuropathy. **(A)** Symptoms are shown in order of occurrence: from onset in childhood in the peripheral nervous system (PNS) to adulthood in the central nervous system (CNS). **(B)** Neuronal features: (left) nerve cross-section in the PNS shows reduced axonal content and giant axon; (right) magnetic resonance imaging of the brain reveals white matter abnormalities. Giant axons of CNS are not represented here. **(C)** Cellular hallmark: (from left to right) accumulation and altered distribution of neurofilaments (NFs) in giant axons, curled hair, desmin bundles in muscles and aggregates of vimentin in skin-derived fibroblasts. Copyright with permission from BioMed Central, Springer and Elsevier.

identified in 75 families from various geographic origins, at homozygous and heterozygous state (**Supplementary Table 1**). The major genetic alterations are missense mutations (60%), the remaining causing truncation of Gigaxonin, due to nonsense mutations (17.4%), deletions/insertions (from small amino acids to the entire gene) (16%), and mutations at donor/accepting splicing sites (6.6%).

While most mutations are unique (81.3%), others are enriched in given populations (R293X and IVS9+1G > T in Turkey, R477X in Algeria), probably as a result of the spreading of common alleles through consanguinity. Several mutations are shared by different countries, that could indicate an ancestral funder effect but could also represent independent mutational "spots": S79L, R162X, R242X, R269W, P315L, G368R, G474R, E486K, E493K, R545H, R477X, A576E, as well as V7Fs-ins/del, A49E/T, S52G/N, and R545C/H/L. Altogether, these genetic studies have revealed that no major hot spot is found in GAN and that no exon is left intact. As a result, genetic diagnosis for GAN requires the full sequencing of the gene, complemented by cytogenetic analysis for large deletions. In regard to the various phenotypic expression of GAN, which is extremely severe in the vast majority of cases but can exhibit milder forms, assumption is often made to correlate mutation type and position with severity. This is very hazardous, and certainly neither missense, nor position outside the BTB or Kelch domains is synonymous of mild. They are many examples and counter-examples in GAN to show that this is not that simple. Moreover, inter and intra-familial clinical heterogeneity has been evidenced for patients bearing the same mutation (Tazir et al., 2009), hence suggesting that genetic alteration might not be the only determinant of clinical expression. While speculation on the effect of individual mutation is difficult to make, the global analysis of data can permit to point out general features (**Figure 4B**). First, the majority (67%) of missense mutations are associated to severe forms of GAN, the remaining contributing to 88% of the mild forms. Indeed, except for two truncating mutations (compound heterozygous V7Fs/Y299C and Q44X/G474R), all mutations associated with mild forms are composed of missense mutations (homozygous or heterozygous). Second, with the exceptions of V7Fs and Q44X cited above, all truncating mutations are associated with severe forms of GAN. Third, the analysis of shared mutations between families of various origins is very informative. Indeed, in four cases, families sharing one common mutation (R269W, G474R, R545H, or A576E) in association with distinct ones show different severity (see example in **Figure 4B**). Thus, with the caution that mutation may not be the only determinant of severity, this might tell us that mutation can affect one another to modulate Gigaxonin functionality, at the protein and possibly mRNA level. Another characteristic of GAN was suggested as a potential predictive marker of the mild cases: the hair. Indeed, while all GAN patients present giant axons filled with abnormally bundled NFs at the nerve biopsy, few mild cases were associated to normal hair among patients with kinky hairs (**Figure 3C** and **Supplementary Table 1**). Here, the analysis of both criteria reveals that "normal hair" is equally found in mildly or severely affected patients but that most of mild cases have normal hair. This implies that the criteria "normal hair" can't be

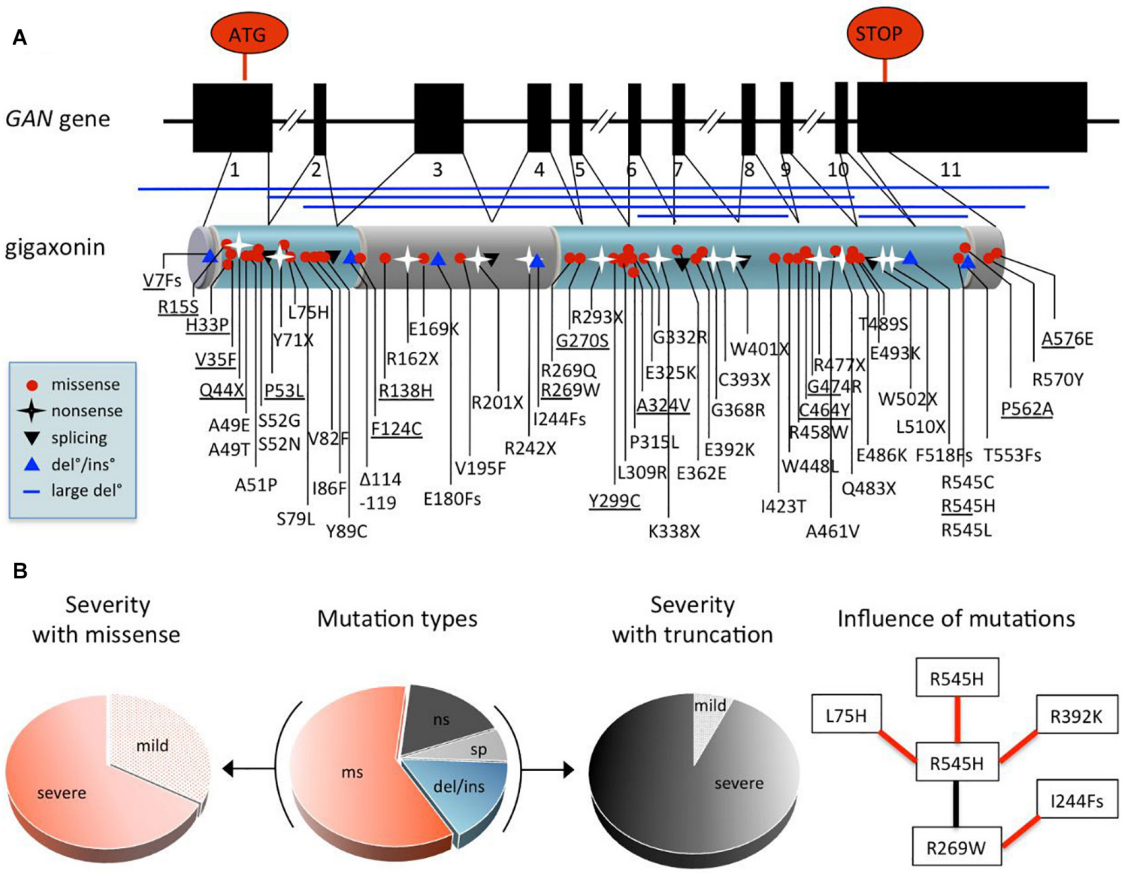


**FIGURE 4 |** Comprehensive analysis of *GAN* mutations. **(A)** Exon-intron structure of the *GAN* gene and domain organization of the encoded protein Gigaxonin, with a N-terminal BTB domain and a C-terminal Kelch domain (depicted in blue, linker is called BACK domain). Mapping of the 75 mutations (see also **Supplementary Table 1** for details): missense mutation (red circle), nonsense mutations (black star), mutations at splicing sites (black triangle), deletions/insertion (blue triangle) and large deletion (blue line). **(B)** Pie charts depicting the effects of GAN mutations. Distribution of mutation types in patients (middle): 60% are missense mutations "ms," 17.4% of nonsense mutations "ns," 16% of deletions/insertions "del/ins," and 6.6% mutations at donor/accepting splicing sites "sp." Other pie charts indicate the predominance of severe forms associated with missense mutations (left) and truncations [(right), including "ns," "sp," "del/ins"], representing 67.7 and 93.3% of cases, respectively. On (right), flow chart showing the influence of mutations on severity. Black and red lines indicate, respectively that the patient bearing both mutations has a mild or severe form of the disease. As example, the R545H mutation leads to a severe phenotype when found homozygous, while it is attenuated by combination with R269W, which is severe when associated to I244Fs.

used as a predictive marker of disease severity, at least in correlation with general clinical presentation that can vary between laboratories.

## GIGAXONIN, SUBSTRATE ADAPTOR OF CUL3-E3 LIGASE

### Novel BTB-Kelch Protein and Structure

Gigaxonin is a 597 amino acid long BTB-Kelch protein (GenBank ID: mRNA AF291673, protein protein_id = AAG35311) belonging to the Cullin 3-RING (CRL3) subgroup of E3 ubiquitin ligases (**Figures 1**, **5C**). This link is mediated by the BTB domain, and was established by the key findings of the (i) structural similarity of the BTB domain-fold with Skp1/elonginC (Schulman et al., 2000) and (ii) specific interaction of BTB containing proteins with Cul3 (Furukawa et al., 2003; Pintard et al., 2003; Xu et al., 2003). This central work demonstrated that BTB family members are the substrate-specific adaptors of Cul3 E3 ligases, and that Gigaxonin indeed interacts with Cul3 (Furukawa et al., 2003). As known for transcription factors bearing a BTB domain, Gigaxonin BTB domain was shown to homodimerize (Cullen et al., 2004), a process that is predicted to be of functional importance for E3 ligase activity. Thus, the C-terminal Kelch domain of Gigaxonin, which is composed of 6 Kelch motifs, would serve as a binding domain for substrates. The x-ray crystal structure of another BTB-Kelch protein (Keap1) revealed that the Kelch domain forms a ß-propeller structure in which individual repeats constitute the blades (Li X. et al., 2004). This tri-dimensional structure generates multiple surfaces for protein–protein interaction. The structure of Gigaxonin was solved by crystallography for its BTB portion (Zhuang et al., 2009) and modelized for its interface with Cul3 and its Kelch domain (Boizot et al., 2014) (**Figures 5A,B**). This model represents

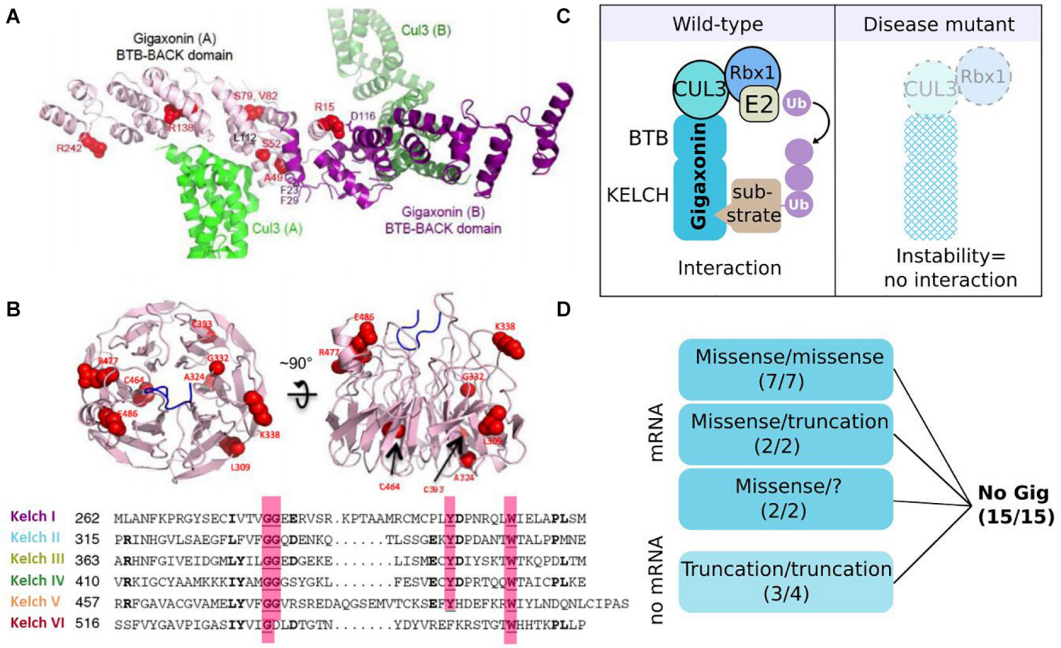


**FIGURE 5 |** Gigaxonin-E3 ligase: protein structure and instability as a general effect of mutations. **(A)** Structural model of the BTB-BACK homodimer of Gigaxonin (purple), in complex with Cul3 (green). Some mutations are represented in red (Boizot et al., 2014). **(B)** Representation of the top and side views of a structural model for the β-propeller Kelch domain of Gigaxonin, whose 6-blades are shown in sequence alignment below. Some mutations are represented in red. **(C)** In wild-type condition (left) Gigaxonin interacts with Cul3 through its N-terminal BTB domain and binds to substrates through its C-terminal Kelch domain, hence catalyzing the transfer of ubiquitin chain from the E2 to the recognized substrate. In disease (right), *GAN* mutations induce a general instability of Gigaxonin, by affecting the proper folding of the BTB or Kelch domain, or impairing homodimerization and interaction with Cul3. **(D)** Dramatic reduction of Gigaxonin levels in patient's cells: due to instability of the mutated protein, or degradation of the corresponding mRNA, depending on the mutation type and combination. "?": compound heterozygous mutations await to be discovered. Copyright with permission from BioMed Central.

the dimers of Gigaxonin in interaction with Cul3 and the ß-propeller structure formed by the six Kelch repetitions, exposing interacting surfaces at the top, the bottom, and the circumference. In this three-dimensional organization, the interaction motif for a given substrate may involve amino acids spatially close (intra Kelch) or very distant (inter Kelch). This, combined to the low identity between individual Kelch repeats hampers the prediction of putative partners for Kelch proteins by sequence alignment but surely generates a high diversity of interaction amongst Kelch proteins. So far, seven substrates have been identified for Gigaxonin and their identity and functions will be detailed in the "Gigaxonin functions" part.

## General Effects of Mutations on mRNA/Protein Stability

Giant axonal neuropathy is a recessive disease and so far, Gigaxonin abundance is found systematically reduced in patients (**Figure 5D**), as seen on immunoblots with the specific monoclonal antibodies $Gig^A$ on various immortalized lymphoblast cells (Cleveland et al., 2009). This method has been challenged and validated as a powerful research tool for the differential diagnosis of GAN (Boizot et al., 2014), whose clinical and histopathological features are overlapping with several forms of CMT diseases. Pulse-chase labeling of Gigaxonin overexpressing mutants demonstrated that regardless of the mutation type and the associated severity of the pathology, Gigaxonin mutants exhibit a shorter half-life (1–3 h) in comparison to the wild-type protein (10 h), suggesting a general mechanism of protein instability. It is important to note that while overexpression studies are useful to characterize the protein and its interaction with substrates for example, it certainly can't be used to conclude on the physiology, nor on the functional roles of specific mutants. Indeed, reduced Gigaxonin amount (as seen in patients) is not equal to a massive expression of a mutant, whose shorter half-life is masked by continuous expression. Moreover, pulse-chase experiments revealed that mutant levels exhibit a high variation at 0 h, hence pointing out that results on different mutant/wild-type proteins can't be compared without adjusting their expression levels. To investigate the causes of the generalized instability of Gigaxonin mutants, 19 mutations from 15 families (with mild or severe GAN) were mapped onto the structural model. With two exceptions for which hypothesis was challenging, this analysis predicted a general instability of the three-dimensional structure of the mutated proteins. Mainly, mutations would affect the proper folding of the BTB or Kelch domain, and could also impair interaction with the BTB domain or Cul3, all conditions expected to induce the degradation of mutated Gigaxonin. Additional examination of mRNA levels from patient

cells revealed that truncating mutations have barely detectable mRNA (**Figure 5D**), probably as a result of a mechanism of mRNA quality control called non-sense mediated mRNA decay. Interestingly, when combined to a missense mutation (in two heterozygous compound mutants), truncating mutation present with normal amount of mRNA level, indicating that the missense mRNA may either be increasingly transcribed or exhibit a dominant positive effect on the truncated one. As discussed above in the genetic part, this also suggests that mutation can affect one another, here to modulate Gigaxonin level.

Altogether, our current knowledge points to a general effect of *GAN* mutations on instability, hence disrupting the global interactome of Gigaxonin in all patients (**Figure 5C**). This indicates that continuous overload of overexpressed mutants (which maintain a high level of protein despite the instability of the mutants) should not be used to demonstrate disease specificity, as mutants most probably conserve their interaction with partners.

### Gigaxonin Localization and Expression Pattern

Determining tissular, cellular and subcellular localization of a protein contributes tremendously to the investigation of its function(s). For Gigaxonin, 20 years of research have not quite answered the question. Over 50 monoclonal and polyclonal antibodies have been produced by several laboratories or from commercial sources. With the caution that should be made towards overexpression system, ectopic Gigaxonin produces a wide range of granular staining depending on the cell type (Bomont and Koenig, 2003), and its putative localization to the Golgi apparatus (Cullen et al., 2004) has not been reproduced (Bomont, 2016). For subcellular localization of the endogenous Gigaxonin, the outcome is that no one demonstrated specificity: not only the publications reporting subcellular localization of Gigaxonin in neuronal tissues (Ding et al., 2002; Cullen et al., 2004) did not provide internal controls but the comparison of immunostaining using many antibodies (including the ones cited above) with patient cells and tissues/cells from the GAN knock-out mice evidenced aspecific detection (Bomont, 2016). Incorrect statements on the localization of Gigaxonin are due to the detection of major aspecific band(s) by many (non)-commercial antibodies, as revealed by immunoblotting method (Bomont, 2016). The systematic analysis using samples from patients and 2 independent GAN mice shows that the endogenous Gigaxonin is a 65kDa predicted protein that migrates between 55 and 62 kDa (Dequen et al., 2008; Cleveland et al., 2009; Ganay et al., 2011; Boizot et al., 2014). To our knowledge, only the $Gig^A$ monoclonal antibody detects endogenous Gigaxonin with a unique band (Cleveland et al., 2009), and still, this valuable reagent was not able to reveal the subcellular localization of Gigaxonin. This is most certainly attributed to the low level of expression of this E3 ligase adaptor, hence constituting an intracellular limiting factor to regulate the activity of this multi-subunit Cul3-E3 complex. Indeed, Gigaxonin was shown to account for 1.25 $10^{-3}$% of total proteins in tissues (detergent soluble lysates of mouse brain) and 7500 molecules per cell (human lymphoblast cells) (Cleveland et al., 2009). Moreover, Gigaxonin was shown to be equally expressed in neuronal tissues, with higher degree in prenatal stages, but was also detected to a lower extend in non-neuronal adult tissues (Ganay et al., 2011).

## BIOLOGICAL MODELS TO STUDY THE GAN PATHOLOGY

Several complementary biological models have been generated for GAN, to study the disease mechanisms but also to provide robust systems for therapeutic development. Thus, tracers of the pathology have been very useful to validate or invalidate these novel tools. As discussed earlier, the most manifest cellular hallmark of the GAN pathology is the wide bundling of the IF cytoskeletal network throughout tissues. At the physiological level, alterations of the sensory and motor systems, leading to loss of sensitivity and motility in patients during adolescence are the common peripheral pathological signs that have been used to evaluate the robustness of animal models. Here, we describe the different GAN systems, present their advantages and limitations (**Figure 6**) and how they were instrumental in providing crucial insights into Gigaxonin functions.

The first cellular model developed for GAN is the primary fibroblasts derived from skin biopsies of patients (Pena, 1981). Abnormal bundling of vimentin IF was evidenced in patient's cells, while actin and microtubule networks seem unaltered. After the discovery of the *GAN* gene, analysis of several patients with identified mutations revealed that the ovoid perinuclear bundles, highly resistant to detergent is partial, conditional and dynamic (illustration no. 1 in **Figure 6B**) (Bomont and Koenig, 2003). First, in normal culture conditions, aggregates coexist with well-formed vimentin network and are detected in only 3–15% of total cells. Second, this proportion can considerably vary between laboratories for the same patient (Pena et al., 1983; Klymkowsky and Plummer, 1985), which seems to depend on culture conditions. The most striking demonstration was the quantitative and qualitative changes using low serum and confluency. Indeed, in these conditions (and independently of cell cycle stage), not only the proportion of aggregates increased by 5–20 fold, but aggregation forms a perinuclear ring cage that recruits all vimentin (Bomont and Koenig, 2003). This cytoskeletal alteration is specific for IF, as actin and microtubules are intact in GAN cells. In fact, microtubules have been shown to preserve cells from a total collapse of vimentin in GAN fibroblasts (Bomont and Koenig, 2003; Cleveland et al., 2009). Third, vimentin alteration in GAN cells is a dynamic process that can be exacerbated or reversed within day(s). While this cellular model is not valid to study neuronal alterations and exhibits a high interclonal variability, it represents the only naïve source from patient. The GAN fibroblast model was very crucial in identifying the role of Gigaxonin in controlling IF degradation (details on mechanistic in the next section).

The skin fibroblasts were also used to produce neurons, through differentiation of induced pluripotent stem cells (iPSCs) from patients. Thus, iPSC-derived motor neurons from distinct

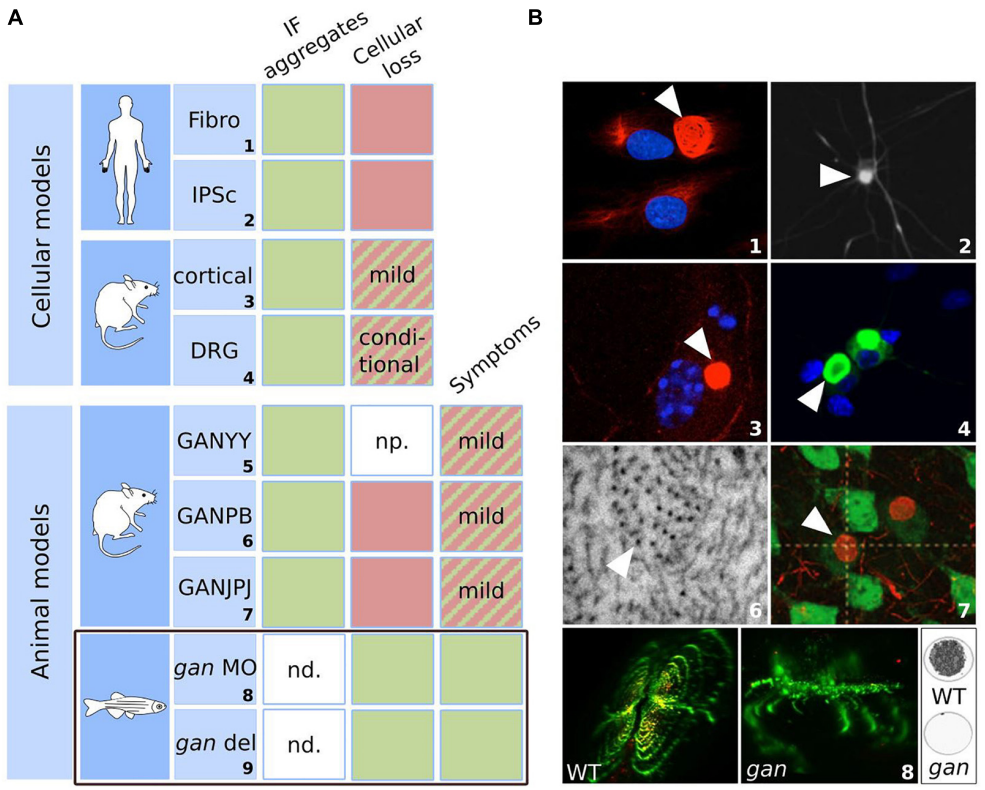


**FIGURE 6 |** Biological models for GAN: strengths and weaknesses. Summary table **(A)** and illustrations **(B)** of the cellular and animal models developed for GAN. The table highlights their ability to reproduce the cellular marker and symptoms of the pathology. Green: the model satisfies the criteria; red: the model does not meet the criteria; hatched: the model partially satisfies the criteria. IF aggregation is evidenced in all cellular and animal models. Cellular loss was observed in aging GAN cortical neurons and upon specific conditions in DRG neurons. While GAN mice exhibit only modest symptoms, the *gan* zebrafish stands out as the first robust animal model for GAN, reproducing both neuronal loss and loss of motility, as in patients. np. not provided; nd: not determined. *gan* MO: transient repression using morpholino antisense oligonucleotide; *gan* del: genetic deletion mutant of *gan*. Numbers correspond to original publications: **1**: patient fibroblasts with bundling of vimentin (Pena, 1981; Bomont and Koenig, 2003); **2**: iPSC-derived motor neurons from GAN patients exhibiting peripherin aggregation (Johnson-Kerner et al., 2015a); **3**: GAN$^{-/-}$ cortical neurons showing NF aggregate (Bomont: personal data). **4**: GAN DRG neurons with accumulations of α-internexin (Israeli et al., 2016); **5**: GAN1$^{\Delta ex3-5}$ (Ding et al., 2006); **6**: Electron micrograph of the axoplasm of GAN2$^{\Delta ex3-5}$ nerves (Ganay et al., 2011), showing abnormal packing and orientation of NFs; **7**: NF inclusions in GAN$^{\Delta ex1}$ brain neurons (Dequen et al., 2008); **8**: *gan* zebrafish exhibit abnormal spinal cord architecture, abolished neuromuscular junctions (left) and impaired locomotion (right: cumulative movement of larvae in a well during 1 h). Copyright with permission from Oxford University Press, BioMed Central (John Wiley & Sons) and J Clin Invest.

patients exhibit 3–4 fold increased in the abundance of the light-neurofilament protein (NFL), and more modestly peripherin, which still aggregates in motor neurons (illustration no. 2 in **Figure 6B**) (Johnson-Kerner et al., 2015a). The iPSCs are the only neuronal source derived from patients and were useful to confirm the aggregation of neuronal IFs in human. Nevertheless, as for human fibroblasts, there was no report of cell death in iPSC-motor neurons (MNs), limiting the relevance of these models for the investigation of the cytoskeleton deficits in patients.

Neurodegeneration has been investigated in primary neurons derived from independent GAN knock-out mouse (see next paragraph). An initial study, performed on GAN$^{-/-}$ cortical neurons reported a massive degeneration (90%) at 15 days in culture (Allen et al., 2005), which would have been extremely robust if the same group did not contradict himself. Thus, similar pictures (showing DAPI staining with decreased tubulin staining) were simultaneously considered as dead cells (Allen et al., 2005), and alive cells with decreased tubulin content (Wang et al., 2005), to fit with a statement on microtubules. Independently, quantification of cell number over time revealed the modest degeneration of GAN$^{-/-}$ cortical neurons from 15 days, a time where wild-type cells also exhibit some degeneration (Scrivo et al., 2019).

Neurons from the dorsal root ganglia (DRG) of another GAN model were characterized (Israeli et al., 2016). While they do not exhibit cell death in normal culture conditions, degeneration occurs when metabolic stress is applied (galactose and inhibitor of mitochondrial functions), hence revealing a susceptibility of GAN neurons towards degeneration. Giant Axonal Neuropathy DRG neurons also induce aggregation of all neuronal IFs, including neurofilament light (NFL), medium (NFM), heavy (NFH) subunits, peripherin and α-internexin (illustration no. 4 in **Figure 6B**). Similarly, GAN cortical and motor neurons exhibit aggregation of neuronal IF proteins (illustration no. 3 in

**Figure 6B**) (Bomont, personal data). Altogether, these studies place these diverse primary neuronal cells as valuable tools to study IF biology and the specific process underlying susceptibility to neurodegeneration. An interesting avenue is mitochondria, as motility and bioenergetic defects have been evidenced in primary fibroblasts of patients and in GAN DRG neurons (Israeli et al., 2016; Lowery et al., 2016). The role of the metabolic balance in GAN pathogenicity is an exciting area to pursue, and recent work indicates the importance of glycosylation sites on Gigaxonin to modulate its activity on IFs (Chen et al., 2020). Identifying the metabolic conditions that directly control Gigaxonin activity and modulate GAN phenotypes would be particularly important to precise the mode of regulation of this ubiquitous E3 ligase and may explain why, among others, neuronal tissues are most severely affected.

Study of the recessive GAN pathology has been conducted in three independent mouse models, though the deletion of the promotor-exon1 ($GAN^{\Delta ex1}$, called GANJPJ in illustration no. 7 in **Figure 6B**) and early exons ($GAN1^{\Delta ex3-5}$ for GANYY and $GAN2^{\Delta ex3-5}$ for GANPB) leading to a premature stop codon. The first mouse to be described, the $GAN1^{\Delta ex3-5}$ was presented as recapitulating the human pathology (Ding et al., 2006), with a deterioration of motor functions from 6 months of age accompanied by axonal loss and densely packed neurofilaments. Unfortunately, the reported defects were not quantified in the original publication and appropriate behavioral tests, performed independently did not confirm the neurological symptoms in this mouse (Ganay et al., 2011). The two other GAN mice ($GAN^{\Delta ex1}$ and $GAN2^{\Delta ex3-5}$) presented both a mild phenotype with no overt neurodegeneration (Dequen et al., 2008; Ganay et al., 2011). In the $GAN^{\Delta ex1}$ mouse, the 10% increase of muscle denervation and 27% decrease in axon caliber, observed from 6 months of age did not induce spinal motor neuron degeneration nor affected motor performance over a 15 month-period (Dequen et al., 2008). Analyzed over a longer period (18 months) and with a large set of motor and sensory behavioral tests, the $GAN2^{\Delta ex3-5}$ mouse was shown to develop a late onset phenotype, with no axonal and motor neuron loss (Ganay et al., 2011). Interestingly, $GAN2^{\Delta ex3-5}$ were backcrossed in two different pure backgrounds and revealed an exclusive penetrance of the phenotype, with alterations of (i) motor performances solely in 129/SvJ mice from 15 months of age, and (ii) sensitivity from 12 months of age in C57BL/6 mice. These findings reveal the existence of modifiers genes for GAN that modulate specific functions of Gigaxonin in the motor and sensory systems. In addition to a late onset, the phenotype was quite mild, in comparison to the total loss of sensitivity and motility seen in patients during adolescence. Nonetheless, both $GAN^{\Delta ex1}$ and $GAN2^{\Delta ex3-5}$ mice exhibit the characteristic aggregation of IFs throughout the nervous system. Starting at the early age of 3 months, the steady levels of IF proteins (NFL, NFM, NFH, α-internexin, and vimentin) are increased in the brain, cerebellum and spinal cord of the $GAN^{\Delta ex1}$ mice (Dequen et al., 2008). A consistent increase in the abundance of NF proteins has been evidenced in the three mouse models in the brain, spinal cord and sciatic nerves, escalating to a seven fold increase for NFL in brain at 12 months (Ganay et al., 2011). At this age, ultrastructural analysis revealed an abnormal spatial distribution of the NF network, together with an increase in NF diameter, although not as severe as what is described in patients (illustration no. 6 in **Figure 6B**). In particular, none of the models revealed the characteristic presence of giant axons filled with densely packed NFs. In the brain, neuronal IF inclusions have been identified in the cerebral cortex and thalamus (NFH and α-internexin) of $GAN^{\Delta ex1}$ mice (illustration no. 7 in **Figure 6B**) (Dequen et al., 2008). These data show that detection of NF abnormalities (from 3 months) occurs prior to expression of mild symptoms (12 months), leading to the hypothesis that NF may not be a causal factor for neurological deficits, unless NF defects might be too mild to induce neurodegeneration in the present mouse models.

Thus, it is now established that the strategy of knocking-out the murine *GAN* gene does not phenocopy the severity of the human pathology. This phenomenon observed for numerous diseases is recognized as a genetic compensation response (GCR) in which upregulation of related genes contribute in maintaining functions in the context of deleterious mutations. This mechanism has been recently elucidated in both mouse and zebrafish species. Thus, in the presence of a premature stop codon on the mRNA (as expected in the $GAN^{\Delta ex3-5}$ mice), the machinery leading to its degradation (called nonsense-mediated mRNA decay) triggers a specific signaling response to upregulate the transcription of related genes (El-Brolosy et al., 2019; Ma et al., 2019). This novel mechanism, called nonsense-induced transcriptional compensation (NITC) may be gene-dependent but explains why many knock-out strategies fail in mouse.

Considering the challenges in modeling the GAN pathology in mouse, a novel strategy was initiated on an alternative vertebrate model, the zebrafish or *Danio rerio*. This species presents many advantages to study the nervous system at a physiological level. First, zebrafish presents a high conservation of the nervous system and genes (>70%) with human. Second, the fertilized eggs are produced *ex vivo*. This allows various manipulations from one cell-stage, including gene knock-down (for recessive diseases), mRNA overexpression (for dominant diseases or rescue experiment) using microinjection and screening of libraries of chemicals by simple dilution in the water. Third, the high number of eggs generated per clutch provides substantial statistical power to experimental outcome. Fourth, the optic transparency of embryos permits to investigate neuronal and neuromuscular integrity at the physiological level, within tissues. Thus, the *GAN* orthologous gene, identified at one copy on the zebrafish genome was cloned and characterized. The zebrafish Gigaxonin (z-Gigaxonin) shows a 78% identity with the human Gigaxonin and shares the same domain organization with the BTB motif in N-terminus and six Kelch repeats at the C-terminus (Arribat et al., 2019). The spatial and temporal analysis of the *gan* mRNA transcripts revealed ubiquitous expression and distribution, in agreement with the data gathered on the human Gigaxonin (Bomont et al., 2000). Repression of z-Gigaxonin was first performed in a transient set-up, by injecting *gan* antisense morpholino oligonucleotides (MO) in fertilized eggs to generate *gan* morphants. In the zebrafish community, this methodology, which impairs pre-mRNA splicing and blocks translation is widely used to silence gene expression. The

discovery of the CRISPR technology, enabling the creation of stable KO lines evidenced that several mutants failed to reproduce the phenotypes described in the corresponding morphants (Kok et al., 2015). This poor correlation between morpholino-induced and mutant phenotypes in zebrafish questioned the specificity of the MO approach and suggested off-targets effects. Reciprocally, the comparison of the transcriptome and proteome between MO and KO lines altering the same gene revealed a specific genetic compensation in the knock-out line (Rossi et al., 2015), which constituted the basis of the discovery of the NITC pathway that can be triggered in KO design (El-Brolosy et al., 2019; Ma et al., 2019). In this respect, the MO approach is more relevant to study gene functions. For GAN, the specificity of action of *gan* morphants was demonstrated by the analysis of oligonucleotides targeting two independent regions of the *gan* mRNA, dose-dependent curves, use of mismatch counterparts and rescue using the human *GAN* mRNA. Thus, repression of z-Gigaxonin induces severe neurological phenotypes, including the shortening/absence of axons of primary spinal motor neurons [pMNs, first born around 1dpf (day postfertilization)], their abnormal protrusion from the spinal cord, and a global abolishment of neuromuscular junctions (illustration no. 8 in **Figure 6B**). Intriguingly, this was also accompanied by a loss of secondary motor neurons (sMNs, born around 2dpf), which was not resulting from cell death but from incapacity to generate novel neurons. The mechanism underlying this unexpected outcome is discussed in the next section. Altogether, these neurological alterations induce a severe locomotor defect, which is also significant in the genetic line created through the knocking-out of the entire gene, yet less penetrant. Thus, swimming defects upon touch stimuli are observed in 72.4% of the morphants (49% of mutants) at 72 hpf (hours postfertilization) and persist latter on freely moving assay, with 80% of immobile morphants/mutants at 5 dpf. Considering the design of the mutant, which generates premature stop codon within exon 1, this modest discrepancy is most probably due to the activation of the NITC pathway in the genetic line. For GAN, both methodologies of gene inactivation demonstrate that absence of Gigaxonin causes severe neuronal alterations resulting in locomotor impairment.

In conclusion, several cellular and mouse animal models have been generated for GAN. There were very valuable and complementary to study of IF aggregation within and outside the nervous system and to decipher the pivotal role of Gigaxonin in IF biology. On the other hand, the neurodegenerative traits of GAN could not be reproduced. Neuronal loss was only evidenced in vitro on aging GAN neurons or upon stress, and motor and sensory deficits are mild and of late onset in the GAN mouse. Mimicking the loss of motility seen in young GAN patients, the *gan* zebrafish represents the first robust animal model for the pathology.

## GIGAXONIN FUNCTIONS

So far, seven substrates or family of substrates (IF family) have been identified for Gigaxonin (**Figure 7A**). They include proteins involved in cytoskeleton architecture (MAP1B, MAP8, TBCB, and IFs), neuronal specification (Ptch) and autophagy (ATG16L1). While we will focus here on the pathways implicated in neurological physiology, Gigaxonin was also shown to modulate chemosensitivity of cancer, through ubiquitination of NFκB (Veena et al., 2014).

### Gigaxonin Is a Universal Regulator of the Intermediate Filament Cytoskeleton

Intermediate Filament regulation is the best-known function of Gigaxonin. Evidenced 2 years after the discovery of the GAN pathology (Pena, 1981), the aggregation of vimentin in patient-derived fibroblasts constitutes a key cellular tracer that paved the avenue for functional studies, in spite of the fact that it is non-neuronal. From a cell biology point of view, vimentin and fibroblasts are relevant to study Gigaxonin functions, considering the wide impact of GAN on IF architecture beyond neuronal tissues. As discussed earlier, the detection of densely packed NFs within giant axons in the nervous system has been extended to various classes of IFs in patient tissues (**Figure 3**). The development of cellular and animal models for GAN (**Figure 6**) has further completed the picture of a general and massive collapse of cytoplasmic IFs that constitute the nervous system, hair, muscle, blood vessel/mesenchyme and skin (**Figure 7B**). In the nervous system, Gigaxonin depletion affects neuronal IFs in their spatial orientation, distribution and abundance (see previous section for details). Thus, besides nestin, which has not been investigated yet, all neuronal IF proteins are abnormally bundled in absence of Gigaxonin: NFL, NFM, NFH, α-internexin, and peripherin. While this aggregation could results from a qualitative effect on distribution, several studies have shown an increase of neuronal IF levels in GAN iPSc-derived neurons, DRG neurons and mouse tissues (Dequen et al., 2008; Ganay et al., 2011; Johnson-Kerner et al., 2015a; Israeli et al., 2016). Interestingly, no overt change in vimentin level could be evidenced in human fibroblasts, MEFs and iPS-derived motor neurons (Mahammad et al., 2013; Johnson-Kerner et al., 2015a). Still, vimentin abundance is regulated by Gigaxonin, as its prolonged overexpression is sufficient to induce complete destruction in control cells after 72 h (**Figure 7B**). This effect is so robust that it also enables the clearance of vimentin bundles in fibroblasts from patients and GAN mouse embryonic fibroblasts (Mahammad et al., 2013). From this initial key findings, the potent effect of Gigaxonin has been extended to various IFs of the nervous system, and is now confirmed in normal cells [neurons in Mahammad et al. (2013), Israeli et al. (2016) and astrocytes in Lin et al. (2016)], but also in disease context [GAN iPSC-derived neurons in Johnson-Kerner et al. (2015a), and GAN DRG in Israeli et al. (2016)]. To understand this unique action on multiple IFs proteins, that constitute the cytoskeleton of tissues throughout the body, it is important to introduce the structure of IF proteins. IF proteins have a tripartite organization, with a central α-helical rod domain flanked by non-α-helical domains at the extremities, also called the head and a tail domains (**Figure 7B**). While the extremities show variation in sequence and length, the central rod domain is highly conserved

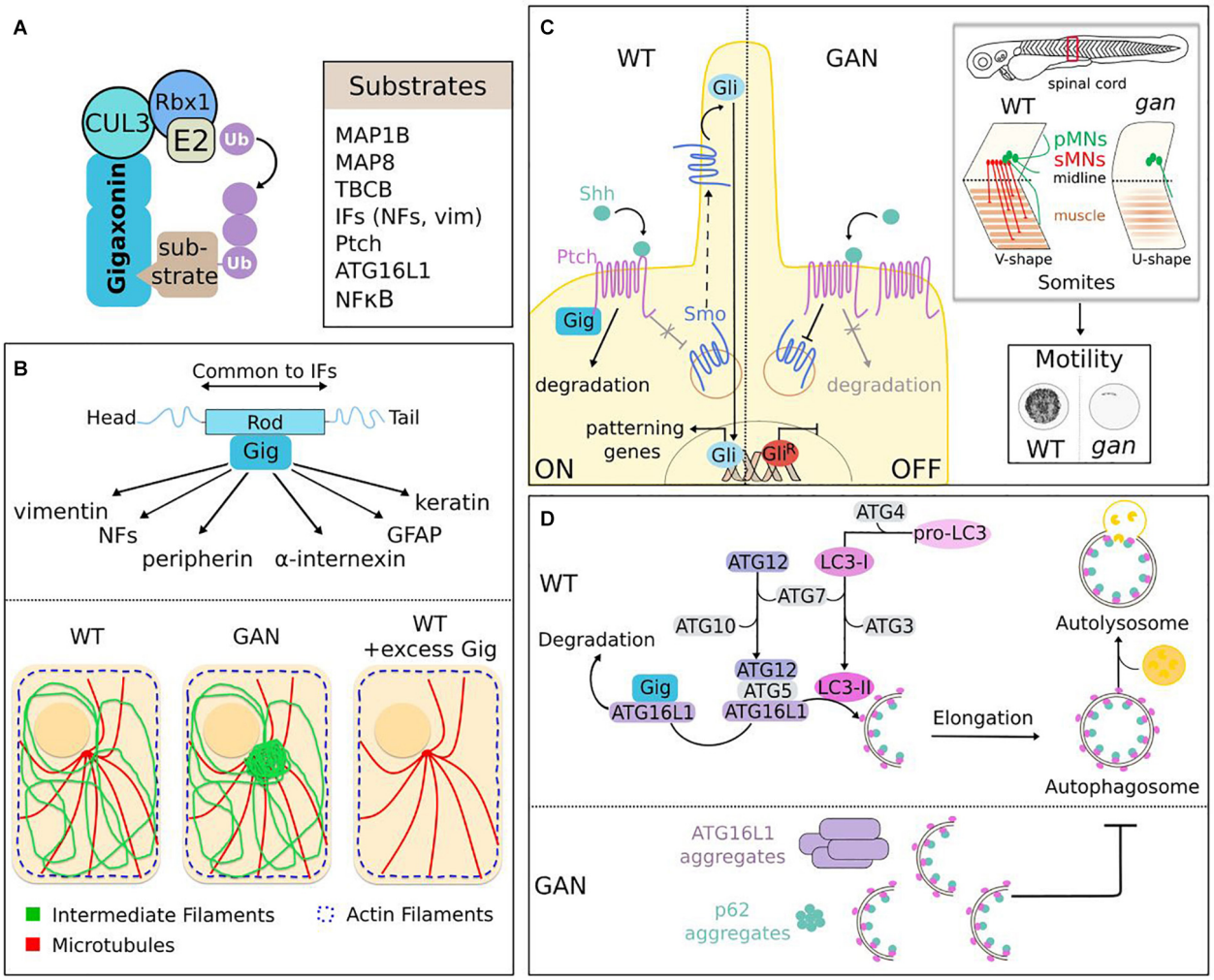


**FIGURE 7 |** Functions of the Gigaxonin-E3 ligase. **(A)** Identified substrates for Gigaxonin include cytoskeletal components (MAPs, TBCB, IFs), Shh receptor (Ptch), autophagy core protein (ATG16L1) and transcriptional factor ($NF_KB$). **(B)** Gigaxonin controls the turn-over of the IF family. Through interaction with the central α-helical rod domain, a common domain of IF proteins, Gigaxonin controls the steady-level of IF family, including neuronal (NFs, peripherin, and α-internexin) and non-neuronal (vimentin, GFAP, and keratin) IF types. This is mediated by Gigaxonin-dependent ubiquitination (as revealed for peripherin). In absence of Gigaxonin (patients and GAN models), IF proteins bundle at perinuclear region, while actin and microtubules do not show overt alteration. Excess of Gigaxonin completely destroys IFs, including bundles in GAN samples. **(C)** Control of the initiation of Shh signaling by Gigaxonin is essential for locomotion. In normal condition (left), Gigaxonin initiates signal transduction by degrading Shh-bound Ptch receptor, hence suppressing its constitutive inhibition on the signal transducer Smo, allowing its translocation to the primary cilium, and leading to the transcriptional activation of Gli. In absence of Gigaxonin (right), the repression of Smo is maintained by accumulated Ptch receptor, which hampers the initiation of Shh signaling and favors the generation of a repressor form of Gli. In zebrafish, this defective Shh signaling impairs motility of *gan* larvae (cumulative representation of the spontaneous locomotion of larvae for 1 h). This severe motility defect is caused by a dramatic remodeling of spinal cord architecture, [shortening of pMNs axons (primary motor neurons, green), defective production of sMNs (secondary motor neurons, red)], and failure to generate proper neuromuscular junctions (NMJ). This phenotype is accompanied by a muscular defect (neuronal-independent or dependent), characterized by "U-shape" myofibers instead of the normal "V-shape." **(D)** Gigaxonin regulates autophagosome production. Elongation of phagophore membrane involves two ubiquitin-like conjugation systems: ATG12 and LC3 undergo transfer from E1 (ATG7) to E2 (ATG10 and ATG3) enzymes. ATG12-ATG5 subsequently forms a complex with ATG16L1, which addresses it to the nascent membrane to act as an E3 ligase for the lipidation of LC3, to generate LC3-II. Gigaxonin induces the ubiquitin-dependent degradation of ATG16L1, and its absence in GAN neurons causes a failure to generate productive autophagosomes upon autophagy induction. As a result, ATG16L1 bundles in GAN neurons, the autophagy receptor P62 accumulates and autophagosome-lysosome fusion is impaired, hence blocking autophagy flux.

across IF proteins. This is of particular importance, as this central domain constitutes the structural backbone enabling the sequential steps necessary to assemble mature IFs across IF types (Herrmann and Aebi, 2016). In agreement with the structure of IFs, and the control of multiple IF types by Gigaxonin, the later has been shown to specifically interact with the rod domain of vimentin (Mahammad et al., 2013). This interaction seems to be direct, as assessed by ELISA assay using recombinant vimentin proteins. Accordingly, additional studies showed that other IF types can be found in Gigaxonin immunocomplexes

in HEK cells and astrocytes (Johnson-Kerner et al., 2015b; Lin et al., 2016). Interestingly, the potent action of Gigaxonin has been confirmed for keratin and GFAP, mutated and aggregating, respectively in the skin disease EBS and Alexander disease (Lin et al., 2016; Buchau et al., 2018). Gigaxonin was shown to clear GFAP network in swi13 stably expressing various mutants but resistance was conferred to some GFAP mutants, which exhibit reduced binding capacity to Gigaxonin. While these mutations lies within the rod domain, the screening of additional mutants in Alexander diseases will be important to ascertain this hypothesis and map the interaction motif with Gigaxonin. While the interaction of Gigaxonin with IF proteins has been repeatedly confirmed, there was challenges in demonstrating its mode of action on IFs. Indeed, only a partial recovery of both vimentin and GFAP levels upon Gigaxonin overexpression was seen with proteasome inhibitor, and laddering of vimentin could not be evidenced with in vivo and in vitro assays, and very low with GFAP (Mahammad et al., 2013; Lin et al., 2016). One study was able to show a Gigaxonin-dependent ubiquitin laddering of peripherin in GAN DRG neurons (Israeli et al., 2016). Interestingly, authors also showed that DRG neurons depleted in Cul3 exhibit increased levels and aggregation of all neuronal IF proteins, similarly to GAN. Now, more work is needed to further define the interacting motifs on IFs, the identity of the ubiquitin chains, and mode of regulation of Gigaxonin on this stable but dynamic cytoskeletal network.

Altogether, the complementarity of several laboratories, and the focus on non-neuronal primary fibroblasts have established that Gigaxonin is the first factor controlling the degradation of the IF family (Bomont, 2016). This has a major impact on cell biology as no drug or compound exists to clear IFs (as it is largely developed for microtubules and actin). Moreover, considering the >80 different diseases caused by mutations in many IF types, Gigaxonin represents one exciting candidate for therapeutic perspectives for human health.

## What About Microtubules?

Two microtubule-associated proteins and one chaperone of tubulin have been identified as interacting partners for Gigaxonin: MAP1B (Allen et al., 2005), MAP8 (Ding et al., 2006), and TBCB (Wang et al., 2005) (see **Box 1**). The abundance of MAP1B, MAP8, and TBCB is decreased upon Gigaxonin overexpression. While this degradation is fully restored upon proteasome inhibition, the Gigaxonin-dependent ubiquitination has only been firmly evidenced for TBCB. Interestingly, two Gigaxonin disease mutants were shown to interact with TBCB, and one was equally promoting TBCB ubiquitination, as efficiently as the wild-type Gigaxonin. This emphasizes what we discussed earlier regarding the cautiousness in the interpretation using Gigaxonin mutants in overexpression system, as they can retain activity. Nevertheless, TBCB level was shown to be unaffected between control and patient fibroblasts, and by overexpression of Gigaxonin (Cleveland et al., 2009; Mahammad et al., 2013); and MAP1B was shown to be equally abundant in control and GAN iPSC-derived motor neurons (Johnson-Kerner et al., 2015a).

In light of the microtubule-binding capacities of the substrates, claims have been made to link microtubules (MTs) to GAN deficits and to convince on their relevance for the pathology, but these suffered from lack of reproducibility in independent studies and incomplete assessment (see **Box 1**).

MAP8 overexpression was shown to cause abnormal MT organization ranging from wavy pattern to aggregation, trapping dynein motor proteins (Ding et al., 2006). TBCB overexpression was found to clear MTs, and Gigaxonin addition to reverse this, but no quantification was provided (Wang et al., 2005). Instead, in another study, the effect of TBCB on MTs was shown to be modest, with only 36% of cells presenting, at most a slight reduction in MT intensity (Cleveland et al., 2009). With this partial knowledge, concluding that these substrates recapitulate the GAN pathology is highly hypothetical. Particularly, examination of MTs or tubulin levels has not revealed overt alterations in none of the patient derived cells (Bomont and Koenig, 2003; Cleveland et al., 2009; Mahammad et al., 2013; Johnson-Kerner et al., 2015a). In contrary to what is proposed, the fact that MTs have been found sparser in peripheral GAN nerves (Ganay et al., 2011) doesn't imply a direct action by MTs. First, tubulin levels are equal in WT and KO tissues (Dequen et al., 2008; Ganay et al., 2011). Second, data coming from patients suggest a change in the distribution of MTs along the nerves. Indeed, in GAN axons, MTs are excluded from densely packed NFs and form clusters, and many axons devoid of NFs are filled by MTs (Donaghy et al., 1988; Treiber-Held et al., 1994). This dependence towards NF density has been evidenced in several animal models and is mediated by the ability of specific motifs in NF (and IF) proteins to bind to soluble tubulin, hence modulating the local assembly of MTs (Bocquet et al., 2009). In this regard, MT disorganization could be caused by NF aggregation. Third, the alteration of the motility of vesicles (Ding et al., 2006), and mitochondria in GAN DRG neurons and patient fibroblasts (Israeli et al., 2016; Lowery et al., 2016) is not necessarily caused by MT putative dysfunction. As MTs, IFs are major regulators of vesicle trafficking by tethering to organelles and may be at play in GAN, as proposed by the alignment of mitochondria along

**What we know:**

- MAP1B, MAP8 and TBCB are substrates of Gigaxonin
- MAP8/TBCB overexpression causes alteration of MTs
- Distribution of MTs is modified in GAN nerves
- Motility of organelles is affected in GAN cells

**But :**

- Substrates are not altered in patient-derived cells
- Tubulin and MTs are normal in patient cells
- MTs are protective in GAN cells
- NFs are known to control local assembly of MTs
- IFs are known to control organelle motility
- Organelles decorate IF bunddles in patients

**BOX 1 |** Role of microtubules in GAN? Caution.

bundled vimentin in GAN fibroblasts (Lowery et al., 2016). Fourth, the suggestion of the causal role of MT alteration in IF aggregation is not supported in GAN primary fibroblasts. Indeed, not only TBCB abundance is not altered in patient cells, MTs clearance (upon overexpression of TBCB or the potent MT destabilizing agent TBCE, or nocodazole) does not produce vimentin aggregation in control fibroblasts. Instead, MTs was found to be protective in patients cells, from a greater collapse of vimentin upon nocodazole treatment (Cleveland et al., 2009). While a contribution of MT is not excluded, its demonstration requires further work.

Another concern is the relevance of MT-related substrates for neurodegeneration in GAN. Individually, MAP1B and MAP8 were shown to be sufficient to cause death when overexpressed in wild-type neurons, and to substantially improve survival rate when silenced in GAN neurons (Allen et al., 2005; Ding et al., 2006). These conclusions can be questioned, considering that, as mentioned in the previous section, measure of cell death was based on tubulin staining and that no wild-type controls were added to estimate the magnitude of the rescue of cell death in silencing experiment. Moreover, the 1.5–3 fold increase in the levels of MAP1B, MAP8, and TBCB in KO tissues does not constitute by itself an argument for their role in neurodegeneration.

In conclusion, Gigaxonin controls important players of MT dynamics but the statement of their causal role, and of MT implication in the pathogenesis of GAN is an incorrect shortcut with our current knowledge. Additional work should definitively be performed to deepen this and identify possible roles of MTs in GAN.

While the discovery of the pivotal role of Gigaxonin in controlling IF cytoskeleton was directed by its aggregation in patients, novel roles have recently unexpectedly emerged from exploration of the biological models of GAN.

## Gigaxonin Controls Shh Signaling Pathway to Sustain Locomotor Activity

As discussed in the previous section, the *gan* zebrafish constitutes the first robust animal model for the pathology (Arribat et al., 2019). Indeed, inactivation of the z-Gigaxonin was shown to abolish motility in 80% of both morphants and mutants, hence mimicking the loss of motility seen in patients (**Figure 6**). Alteration of the motor system was further detailed in three-dimensional imaging to reveal a dramatic remodeling of spinal cord architecture, with absence of many axons, the remaining being shortened and abnormally protruding from the spinal axis, and with lack of neuromuscular junctions. The deciphering of the underlying mechanisms (**Figure 7C**) was guided by interesting observation on the alteration of muscle architecture. Indeed, in absence of z-Gigaxonin, the structure of somites is damaged and presents abnormal sarcomeric organization. Myofibers are less dense and somite boundaries define a "U-shape" instead of the normal "V-shape." Specifically, this characteristic is observed in mutants of the Sonic Hedgehog (Shh) pathway (Chen et al., 2001; Varga et al., 2001), one of the key developmental machinery that assigns neuronal (Jessell, 2000) and muscle (Te and Reggiani, 2002) fate in vertebrates. Implicated during embryogenesis but also in homeostasis in adults, Shh impairment causes a wide range of human diseases, ranging from malformations of the nervous system, of the axial skeleton and limbs to cancer (Bale, 2002). Shh signaling is triggered by the active fragment of the morphogen Shh, whose binding to the Ptch receptor in progenitor cells alleviates the repression of another receptor Smo, therefore inducing a cascade of events leading to the transcriptional activation of specifying genes (Lee et al., 2016) (**Figure 7C**). Thus, concomitantly to neurodegeneration, birth of MNs was investigated in the *gan* zebrafish model. While cell death was not evidenced within spinal motor neurons, an overt reduction in their production was shown in both morphants and mutants. In zebrafish, spinal motor neurons are generated in two successive waves (around 24 and 48 hpf), and only the second is impaired in *gan* zebrafish, leading to a total absence of secondary axons. On the contrary, primary MNs are generated but they project truncated and misguided axons, as mentioned above in three-dimensional imaging. Thus, these data revealed a differential and temporal effect, causing axonal abnormalities in the first wave, and an improper specification of MNs in the second wave, as further demonstrated by the down-regulation of Shh-responsive genes. Altogether, the different neuronal defects (and possibly muscle alterations) in *gan* zebrafish impede nerve conductivity through loss of neuromuscular junctions that is sufficient to abolish locomotion. Considering the known roles of Shh signaling in neuromuscular specification, but also in axonal guidance (Aviles et al., 2013), and the data presented above, its implication in *gan* phenotypes has been investigated using drugs that modulate its activity. Thus, inhibition of Shh signaling (using cyclopamine) during the second wave in control embryos reproduces the *gan* phenotype, with "U-shape" somites and absence of secondary MNs. Conversely, increase of Shh activity (using purmorphamine) restores "V-shape" somites in 24% of morphants. The recovery of MN specification was obtained in *gan* treated embryos, but penetrance increases from 17.5 to 70% when drug was applied earlier (during the first wave), suggesting a Shh-dependent requirement of early event for sMN specification. Analysis of distinct biological models in zebrafish, mouse, and human demonstrated that Gigaxonin acts as a positive regulator of Shh. Thus, in situ hybridization revealed a decrease of Shh-responsive gene expression in *gan* morphants and mutants. In addition, repression of Gigaxonin in the Shh Light-2 reporter line impairs its responsiveness to the morphogen. Finally, translocation of Smo to the cilium, which represents an important readout of Shh activation is severely impaired in two independent GAN fibroblasts exposed to Shh, hence evidencing a decrease responsiveness to Shh in human cells. Deciphering the molecular mechanisms by which Gigaxonin controls Shh signaling would have been ideal in drosophila species, a powerful genetic system that is widely used in this field. Nevertheless, Gigaxonin is not conserved in fly, which may suggest that Gigaxonin participates in the evolution of the system in vertebrates (Briscoe and Therond, 2013). Thus, the underlying molecular mechanism by which Gigaxonin positively regulates Shh signaling has

been deciphered in cell lines. It was shown that Gigaxonin interacts with the receptor Ptch and induces its degradation in a Shh-dependent manner, which suggests that the E3 ligase controls the entry point of Shh signaling, and not the basal recycling of the receptor, as reported for other E3 ligases Itchy and Smurf (Huang et al., 2013; Chen et al., 2014). Interestingly, ubiquitination of Ptch was not detected in presence of Gigaxonin but was considerably enriched in Gig-immunocomplexes, suggesting that a small pool of Ptch is modified by Gigaxonin within a cell. Certainly, further work is needed to deepen this ubiquitination aspect and the regulation of Gigaxonin interaction. Monitoring simultaneously Ptch activation and Gigaxonin interaction upon Shh stimulation would help understanding the temporal and spatial mode of action of the E3 ligase in physiology.

Importantly, this work provides the first hints for a developmental origin in GAN, and adds to relevant findings of a developmental contribution in the setting of post-natal neurological diseases. Indeed, emerging evidence from patients and animal models suggests that abnormal neurodevelopment is a component of the pathophysiology of adult neurological diseases, including Alzheimer's and Huntington's diseases. The most striking demonstration is that mice expressing mutant huntingtin solely during developmental stage recapitulate symptoms of the human pathology (Molero et al., 2016). For human GAN, this hypothesis is supported by atrophies in various regions of the nervous system using MRI (magnetic resonance imaging), and the presence of a morphological marker of developmental deficits in patients (Demir et al., 2005). Demonstrating the role of Gigaxonin-mediated Shh activity in sustaining motility in zebrafish, this initial study opens a novel avenue for understanding the origin of GAN pathophysiology. Future work will determine whether inhibition of Shh signaling contributes or is sufficient to induce neuronal loss and neurological deficits in patients. Finally, considering the role of the impaired Shh signaling in various diseases, Gigaxonin may represent one interesting target to modulate Shh response as potential therapy for other conditions.

## Gigaxonin Regulates Autophagosome Production

As many neurodegenerative diseases, autophagy is altered in GAN but deeper exploration revealed that Gigaxonin controls an essential step of the pathway, by driving membrane expansion of the phagophore to produce mature autophagosomes that can fuse to lysosomes (Scrivo et al., 2019) (**Figure 7D**). This key process was evidenced in GAN primary cortical neurons in which lipidation of the LC3 protein (LC3-II), occurring at the site of membrane elongation was monitored under basal and experimental conditions. Using conventional drugs to boost autophagy and block fusion of autophagosomes with lysosomes, a specific defect in the net production of LC3-II (presumably autophagosomes) was shown in GAN neurons. More precisely, GAN neurons generate autophagosomes but are in incapacity of increasing production over prolonged induction of autophagy. Studies of additional markers of autophagy flux converged towards an inhibition of the elongation step, leading to an accumulation of the main autophagy receptor p62, and decrease detection of autophagosome-lysosome events. LC3 lipidation is a tightly regulated process that involves two conserved ubiquitin-like conjugation systems. Structurally related to ubiquitin, the ATG12 and LC3 proteins are transferred by E1- and E2-like enzymes to their substrates ATG5 and ATG3 (**Figure 7D**). Subsequently, ATG12–ATG5 acts as the E3 ligase enabling lipidation of LC3. In this complex hierarchical process, Gigaxonin was shown to regulate the ATG16 protein (Scrivo et al., 2019), which binds ATG12–ATG5 and addresses it onto nascent membrane (Fujita et al., 2008), hence specifying the site of lipidation. Crucial for autophagosome formation, ATG16L1 is essential for survival and ATG16L1 KO mouse is lethal 1 day after birth (Saitoh et al., 2008). Gigaxonin binds to the C-terminal WD40 domain of ATG16L1 and induces its degradation. As for IF proteins, the clearance of ATG16L1 by ectopic Gigaxonin is extremely robust and is only modestly rescued upon proteasome or autophagy inhibition. This constituted an obstacle to investigate ATG16L1 ubiquitination, but was solved by evidencing its decrease using Gig siRNA. Single-cell analysis completed the picture and demonstrated co-labeling of K48-ubiquitin chains onto ATG16L1 when Gigaxonin was present. The abnormal bundling of ATG16L1 in the soma of GAN neurons further confirmed its regulation by Gigaxonin, and specificity towards ATG16L1 was provided by rescue experiment using lentiviral expression of the E3 ligase. Equally efficient, Gigaxonin clears aggregates in GAN neurons and leads to the destruction of ATG16L1 in control neurons. Altogether, this initial study unveils a key regulatory mechanism that drives the dynamic of autophagosome production. In absence of Gigaxonin, accumulated ATG16L1 would impair membrane elongation and cause the stacking of phagophores/incomplete autophagosomes, as shown upon overexpression, or deletion of ATG16 (Fujita et al., 2008; Saitoh et al., 2008). An important perspective would be to determine whether Gigaxonin regulates autophagosome production in basal or specific physiological conditions. Indeed, limitation of the study concerns the investigation of LC3 lipidation and ATG12-ATG5 docking to membrane in basal condition, which was challenged by the low expression level of LC3 and high density of dots in primary neurons. Thus, while the later represents the ideal system to investigate endogenous mechanisms, other systems using fluorescently labeled LC3 overexpression in cell lines may be preferred for some aspects. Another attractive perspective is to use the GAN model to investigate the spatial control of autophagy within neurons (Bomont, 2019). In polarized cells, the best-described process is distal: biogenesis occurs at axonal tip, phagophores elongate and autophagosomes mature and fuse to lysosomes while undergoing retrograde transport towards the soma. Still, autophagosome biogenesis has also been evidenced in the soma (Maday and Holzbaur, 2016; Stavoe and Holzbaur, 2019) and GAN might constitute a powerful biological system to study its process and function. Finally, the novel avenue of the control of ATG16L1 by Gigaxonin may offer therapeutic perspective for GAN but also for other diseases, for which

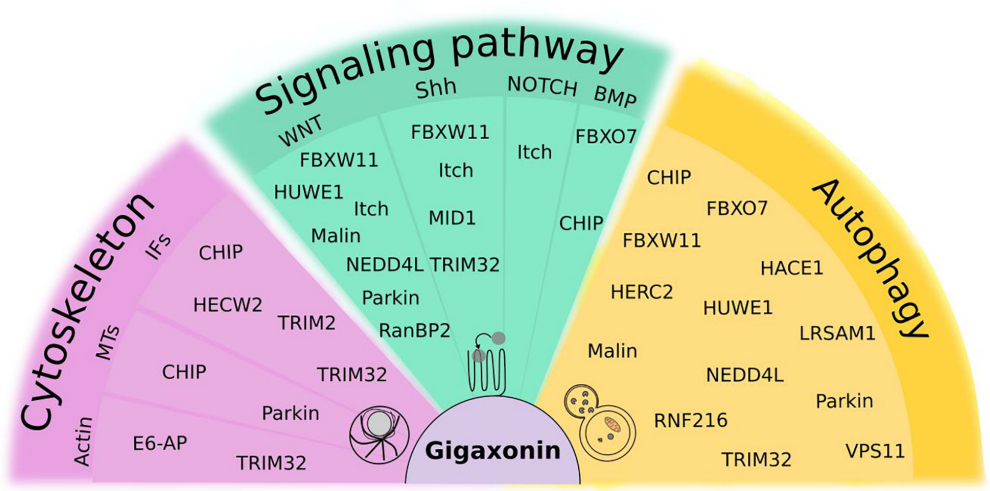


**FIGURE 8 |** Focus on ubiquitin(like)-dependent regulation of cellular mechanisms shared by Gigaxonin and other E3 ligases. Cytoskeleton comprises actin, microtubules (MTs) and Intermediate Filaments (IFs). Signaling pathways, selected from their roles in spinal cord development and maintenance include WNT, Sonic Hedgehog (Shh), NOTCH and Bone Morphogenetic Protein (BMP). For Fibroblast Growth Factor (FGF) and Retinoic acid (RA), no function of E3 ligases was reported to our knowledge. As substantial proportion of E3 ligases (30%) control the autophagy pathway. Some E3 ligases act at multiple levels within the same pathways (like Itch, NEDD4L), and 23% of them exhibit functions in different pathways, with Gigaxonin, TRIM32, and CHIP crossing all pathways.

the E3 ligase may represent a molecular switch to diminish autophagy activity.

## COMMON MECHANISMS AMONGST E3 LIGASES: EMERGING ROLES IN AUTOPHAGY

Beyond the nervous system, E3 ligases mutated in neurological diseases exhibit numerous biological functions, such as DNA repair, cell division and immunity and can be implicated in the pathophysiology of other human diseases among which cancer is the most important class. Here, we will present the common cellular mechanisms shared by Gigaxonin and the other E3 ligases (**Figure 8**), and will focus on their role in autophagy (**Figure 9**). Noteworthy, we will restrict our window to pathways for which substrates have been identified, and ubiquitin(like)-dependent mode of regulation (at least partially) demonstrated, therefore excluding other functions such as some transcriptional activation types.

### Control of Cytoskeleton by E3 Ligases

Very little is known regarding the control of cytoskeleton by E3 ubiquitin ligases (those selected in this review) (**Figure 8**). E6-AP controls the degradation of the Ephexin5, a RhoA guanine nucleotide exchange factor that remodels actin cytoskeleton to promote excitatory synapse development (Margolis et al., 2010). TRIM32 controls the ubiquitin-dependent degradation of actin filament to sustain muscle remodeling and function (Kudryashova et al., 2005). Microtubule dynamic is modulated by Parkin, in part through degradation of α and ß tubulin (Ren et al., 2003), while CHIP regulates microtubule severing through control of katanin (Yang et al., 2013) and Gigaxonin regulates the turn-over of MAPs and TBCB. Regarding IFs, the far most recognized E3 ligase is Gigaxonin, which controls the steady-state of the entire family in multiple tissues, as discussed in this review. Other E3 ligases have shown specificity towards particular IF types, including TRIM2 for Neurofilaments (Balastik et al., 2008), CHIP for keratin (Loffek et al., 2010), TRIM32 for desmin (Cohen et al., 2012), and HECW2 for laminB1 (Krishnamoorthy et al., 2018).

### Regulation of Signal Transduction by E3 Ligases

Here, we will present E3 ligases that act as Gigaxonin on Shh signaling, expanding on other main pathways for spinal cord development and maintenance (**Figure 8**): Wnt, FGF (Fibroblast Growth Factor), and RA (Retinoic Acid), whose signal gradients establish the antero-posterior axis of the CNS, and Shh, Wnt and BMP (Bone Morphogenetic Protein) patterning the dorso-ventral axis of the neural tube, assisted by Notch signaling. Depending on the target (receptor, mediator/regulator or effector), E3 ligases can act as a positive or negative regulator of cell signaling.

As Gigaxonin, the Itch ligase regulates the turn-over of the Ptch receptor. Nevertheless, Ptch acts in absence of Shh, showing that Itch is not dispensable for canonical Hh signaling but essential to limit the proapoptotic activity of unliganded Ptch in non-canonical forms (Chen et al., 2014). The findings of the requirement of Shh for Ptch degradation by Gigaxonin unveil the identity of the first E3 ligase controlling the entry point of Shh signaling (Arribat et al., 2019). Consistently, Itch has also been shown to regulate the degradation of Notch in a ligand-independent manner (Chastagner et al.,

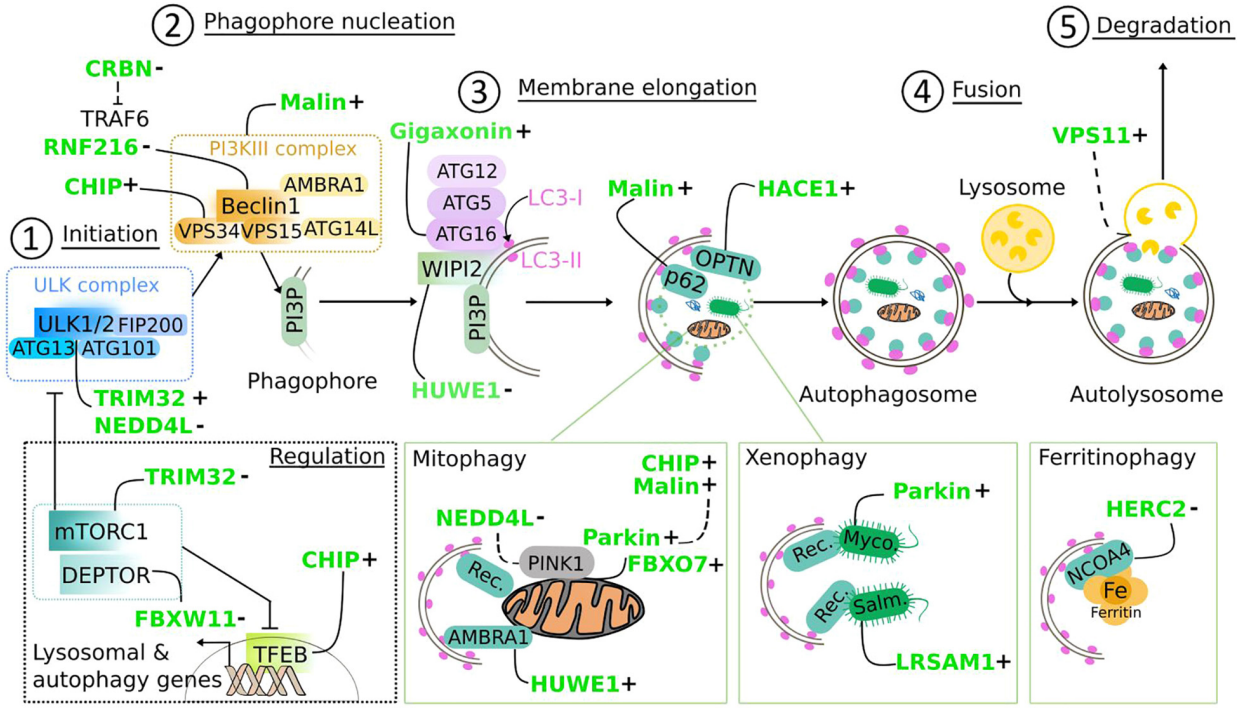


**FIGURE 9 |** Regulation of the autophagy pathway by E3 ubiquitin ligases. E3 ligases mutated in neurodegenerative diseases (in green) target core components of the autophagy machinery, from the initiation **(1)** to the fusion of the autophagosome to lysosomes **(4)** to positively (+) or negatively (–) regulate autophagic flux. Following (macro)autophagy induction, the inhibitory effect of mTORC1 on the ULK complex is lifted, allowing the activation of the ULK1/2 kinases **(1)**, leading to a cascade of phosphorylation events that contribute to the activation of the PI3KIII complex via Beclin1, to promote PI3P synthesis on nascent phagophore **(2)**. Interacting with PI3P, WIPI2 subsequently recruits ATG16L1 in complex with ATG12-ATG5, the E3 ligase that catalyzes the lipidation of LC3 at membranes, a step **(3)** required for membrane elongation and autophagosome formation. Fusion with lysosome **(4)** leads to the degradation of sequestered material, which can be non-specific (called bulk autophagy) or specific (called selective autophagy). Selectivity is triggered by ubiquitination of substrates [**(bottom panels)** mitochondria, pathogens, and Ferritin], and mediated by adaptor proteins that direct them to autophagosomes thanks to LC3-interacting region (LIR domain) and ubiquitin-associated domain (UBA) domain. "Rec" for mitophagy: p62, OPTN, NDP52, TAX1BP1, NBR1, or AMBRA1; of note, some mitochondrial proteins have a LIR domain and contribute to mitophagy. "Rec" for xenophagy: p62, NDP52, NBR1. Myco., *Mycobacterium* tuberculosis; Salm., *Salmonella* Typhimurium. mTOR signaling, which is an upstream inhibitor of autophagy induction is also regulated by E3 ligases: through action on mTOR inhibitors (DEPTOR) and transcriptional control of autophagy genes (TFEB). Dashed line: partial demonstration of mechanistic. E3 ligase-dependent ubiquitination can trigger degradative or non-degradative routes. Several E3 ligases act at multiple steps of the autophagy pathway and can have antagonized actions.

2008). Regarding Wnt pathway, Itch and NEDD4L regulate, respectively LRP6 and LGR5 receptors that potentiate Wnt signaling (Vijayakumar et al., 2017; Novellasdemunt et al., 2020). Downstream the receptors, central modulators of signaling are targeted by E3 ligases. The best know is Dishevelled (Dvl) which activates Wnt cascade upon binding of Wnt to the receptor Frizzled. Thus, Dvl turn-over is regulated by Itch, Malin and NEDD4L (Sharma et al., 2012; Wei et al., 2012; Ding et al., 2013). E3 ligases are also modulating pathways through the effectors of signal transduction. Gli1 and Gli2, two transcriptional mediators of Hh response are degraded, respectively by TRIM32, Itch, and FBXW11 (also known as ß-TRCP2; Bhatia et al., 2006; Di Marcotullio et al., 2011; Wang et al., 2020); and Smad transcription factors are degraded by CHIP to modulate BMP signaling (Li L. et al., 2004). Transcription of Wnt target genes is ensured by the nuclear translocation of ß-catenin, which binds to the TCF factor. Both are targeted by E3 ligases: FBXW11 and Parkin regulates ß-catenin (Fuchs et al., 1999; Rawal et al., 2009), while RanBP2 modify TCF (by sumoylation) to promote its interaction with ß-catenin and strengthen Wnt signaling, by increasing their nuclear import and transcriptional activity (Shitashige et al., 2008). Other examples of a non-degradative regulation of cell signaling are coming with HUWE1 (de Groot et al., 2014), Itch (Infante et al., 2018), MID1 (Schweiger et al., 2014), and FBXO7 (Kang and Chung, 2015), whose ubiquitinating action on Dvl, SuFu and Fu (two regulators in Shh signaling) and RNAGE (modulator of non-canonical BMP pathway) regulates multimerization, cleavage and complex formation, which is essential for signal transduction.

Thus, E3 ligases mutated in neurological disorders control essential players of cell signaling, and they can act at multiple levels in the same pathway (like NEDD4L) and even multiples pathways (Wnt, Shh, Notch for Itch). Future investigations will probably increase this picture and further detail the elaborate mechanistic actions E3 ligases have on cell signaling. Considering that pathways also communicate between each other, mutation in a given E3 ligase may affect the equilibrium in many direct and

indirect ways, hence representing a challenge when it comes to understand and treat pathophysiology in disease.

## Emerging Roles of E3 Ligases in the Control of Autophagy

Proteolysis, and in particular autophagy has been shown to be impaired in most neurodegenerative diseases. While this alteration can be indirect as a result of dysfunction of the neuron, we will discuss here the growing evidence culminating the last 2 years of the direct role of E3 ligases in regulating the autophagy pathway.

As shown in **Figure 9**, the E3 ligases mutated in neurological diseases target core components of the autophagy machinery, from the initiation to the fusion of the autophagosome to lysosomes. Autophagy is initiated by the activation of the ULK1/2 kinase within the ULK complex, which subsequently contributes to the activation of the PI3KIII complex (though Beclin1) that drives the formation of the phagophore, via the synthesis of a specific pool of PI3P on the primary membrane. In the initiation step, ULK1 activity is either promoted by TRIM32 through K63 chain ubiquitination (Di Rienzo et al., 2019), or silenced by NEDD4L through unusual K27/29 ubiquitin-dependent degradation following few hours of induction, as a regulatory mechanism to avoid damages from overactivity (Nazio et al., 2016). Promoting phagophore formation, Malin (in complex with Laforin) and CHN-1 (the *Caenorhabditis elegans* homologous of CHIP) activates the PI3KC3 complex, trough K63-ubiquitination of Beclin1 and several regulators (Sanchez-Martin et al., 2020) and VPS34 (Liu et al., 2018), respectively. On the contrary, RNF216 acts as a negative regulator of autophagy by targeting Beclin1 to degradation (Xu et al., 2014). Indirectly, autophagy can be down-regulated by CRBN which inhibits the ubiquitination of Beclin1 by the E3 ligase TRAF6 (Kim et al., 2019), but the mechanisms remains to be identified. Following the early steps of autophagy induction, which is largely coordinated by a myriad of phosphorylation events by core autophagy proteins (Botti-Millet et al., 2016), autophagosome is formed thanks to coordinated rounds of lipidation. Indeed, membrane elongation is powered by two ubiquitin-like conjugation systems (ATG12 and LC3) that generate the ATG12–ATG5 ligase activity responsible for the lipidation of LC3. Specifying the site of lipidation at the nascent membrane, the core proteins WIPI2 and ATG16L1 are pivotal in autophagosome elongation. Thus, WIPI2 binds first to membrane-bound PIP3 and then recruits the ATG12-ATG5-ATG16L1 complex which acts as an E3 ligase for the lipidation of LC3 [conjugation of phosphatidylethanolamine (PE)] that allow the growing of the phagophore. These two critical core proteins are targeted by E3 ligases mutated in neurological diseases. As discussed previously, Gigaxonin is a positive regulator of neuronal autophagy by fine-tuning ATG16L1 levels (Scrivo et al., 2019), while HUWE1 inhibits autophagy by degrading WIP2, a process under the direct control of mTORC1 (Wan et al., 2018). Before closure of the autophagosome, cytoplasmic material can be either engulfed in bulk autophagy, or selected through a process involving ubiquitination and recognition by autophagic receptors that contain both a LIR (LC3-interacting region) and an UBD (ubiquitin binding domain) motifs in selective autophagy. Mitophagy is the most extensively studied type of selective autophagy. Following the identification of the role of Parkin in the elimination of damaged mitochondria by autophagy (Narendra et al., 2008), concomitant publications revealed its mode of action: recruited by the kinase PINK1 onto altered organelles, Parkin gets activated and ubiquitinates several outer membrane components including mitofusin1/2, hence leading to the recognition of depolarized mitochondria by autophagy receptors (Gegg et al., 2010; Geisler et al., 2010; Poole et al., 2010; Ziviani et al., 2010). Interestingly, the FBXO7 E3 ligase, which is involved in Parkin-mediated mitophagy can promote mitophagy in similar way and compensate for parkin deficiency (Burchell et al., 2013). This general model may be enriched by other modulators, such as Malin and CHIP which interact with Parkin to enhance its stability and activity (Imai et al., 2002; Upadhyay et al., 2017), and NEDD4L which controls the ubiquitin-dependent degradation of Pink1 and negatively regulates autophagy (Huang et al., 2020), but their role in mitophagy remains to be demonstrated. Mitophagy can also be triggered independently of Parkin/Pink. In this context, HUWE1 is an inducer of AMBRA-mediated mitophagy, which does not require the main receptors as damaged organelles are addressed to autophagosomes by AMBRA, after activation of its LIR domain (Di Rita et al., 2018).

E3 ligases involved in neurological diseases control other types of selective autophagy. In xenophagy, Parkin and LRSAM1 mediate resistance to pathogens, by promoting ubiquitin coating of bacteria and their targeting to autophagosomes by receptors (Huett et al., 2012; Manzanillo et al., 2013). The HERC2 ligase was shown to negatively regulate ferritinophagy, the process that permits the release of iron through the breaking-down of ferritin by autophagy. Here, the action of HERC2 differs from the other types of selective autophagy, as the E3 ligase targets the ferritin receptor NCOA4 to ubiquitin-dependent degradation to prevent iron release (Mancias et al., 2015). Other studies show that E3 ligases can also act on receptors to potentiate selective autophagy. Indeed, HACE1 ubiquitinates the receptor OPTN, increasing its association with another receptor p62/SQSTM1 leading to enhanced autophagy, presumably by the creation of an autophagy receptor complex (Liu et al., 2014). Interaction of p62 with Malin (and Laforin) increases the activity of the E3 ligase, causing p62 ubiquitination (Sanchez-Martin et al., 2015).

Finally, future lines of investigations concern the last step of autophagy and upstream events of autophagy induction. Fusion of autophagosome to lysosome is powered by HOPS, a tethering complex which interacts with the autophagosomal syntaxin17. While all six subunits constituting the complex are required for fusion (Takats et al., 2014), VPS11 has been identified as an E3 ligase (Segala et al., 2019) but its mode of action and cooperation with other subunits remains to be determined. At the opposite side of the pathway, the pivotal kinase mTOR is a sensor of metabolic and nutrient stress regulating many cellular processes, including the repression of autophagy in normal conditions. Amongst the numerous E3 ligases that modulate mTOR signaling, two were investigated for autophagy readout: FBXW11 and TRIM32

maintain the repressive activity of mTOR on autophagy by degrading inhibitors of mTOR, respectively DEPTOR (Duan et al., 2011; Gao et al., 2011; Zhao et al., 2011) and RGS10 (Zhu et al., 2020). Directly under the control of mTOR, TFEB, a pivotal transcriptional regulator of autophagy genes is positively modulated by CHIP, which degrades preferentially its phosphorylated inactive forms and induces autophagy (Sha et al., 2017).

## CONCLUSION

E3 ubiquitin ligases are the genetic causes of a large number of neurological diseases. Mutations in these genes underlie a wide panel of neurological dysfunctions within the CNS and/or the PNS. While the study of the functions of mutated proteins is expanding, their E3 ligase nature brings substantial challenge for the deciphering of the complex pathological cascade at stake in disease. As the final enzyme delivering the ubiquitin moiety to specific targets, E3 ligases can tag hundreds of different substrates. Proteomic-driven or candidate approaches have been successfully used to unravel key functions but certainly, we have only a partial view of the global picture. Focusing on a rare recessive disease called giant axonal neuropathy (GAN), for its wide alteration of both the PNS and CNS, we discuss here 20 years of research on the genetic and functions of the Gigaxonin-E3 ligase. This led to an essential breakthrough in cell biology, where Gigaxonin is the 1st factor to date to control the degradation of the IF family, in and outside the nervous system. Exemplified by the massive aggregation of IF proteins throughout the body of patients, this pivotal cellular function is a signature for Gigaxonin across all experimental tools developed for GAN. The creation of mouse and, recently zebrafish models of the pathology led to major advance in the mechanisms underlying neuronal dysfunctions in disease. Thus, the recapitulation of the severe motor deficits of patients in zebrafish uncovered an unexpected role of Gigaxonin in controlling motor neuron birth and axonal outgrowth, through the regulation of Shh signaling. The *gan* zebrafish represents the first robust animal model for GAN, which enables the demonstration of the physiological relevance of Gigaxonin function in cell signaling and opens exciting perspective of a developmental origin in the settings of GAN. While the GAN knock-out mouse has a mild phenotype, the study of GAN neurons permitted to discover a pivotal role of Gigaxonin in autophagy, more specifically in the production of autophagosomes, through the control of steady-level of the ATG16L1 protein.

As discussed in this review, other E3 ligases causing neurological diseases act in similar pathways. Among those, autophagy is the most prevalent, with third of E3s controlling multiple steps of the autophagic machinery. While this depends largely on the focus given by research groups, this review highlights that 23% of the E3 ligases bear functions in multiples pathways, with numerous ones acting at multiple levels within the same pathway. In this context, Gigaxonin, TRIM32 and CHIP are crossing all categories, by targeting substrates in cytoskeleton, cell signaling and autophagy. This current view is undoubtedly going to expand in the future, but it already highlights the big challenge we are facing when thinking about therapy.

## PERSPECTIVES FOR THERAPY

How can we integrate these various functions in therapeutic design, when working on reversing a single dysfunction is already a concern? Can one function be more biologically important than the others and be sufficient to alleviate neurological symptoms? Shall we reduce the complexity by targeting individual pathways or, on contrary embrace it by focusing on the E3 ligase, or on the physiological end point? To date, ongoing clinical trials for the neurological diseases discussed here concern symptomatic treatments for AS, or actions on the E3 ligases for AS and GAN. For AS, a phase I/II clinical trial strategy is based on silencing (by antisense oligonucleotide) a repressor transcript of the paternal *UBE3A* gene, to restore endogenous level of E6-AP [(Meng et al., 2015) and ClinicalTrials.gov Identifier: NCT04259281)], while GAN benefits from a phase I gene therapy approach (ClinicalTrials.gov Identifier: NCT02362438). Reintroducing Gigaxonin expression is in principle a promising approach, if appropriate level of the E3 ligase versus endogenous protein was determined. While we are assured that too much expression will generate serious deleterious effects, just mentioning the complete destruction of cytoskeleton, the risk of too little Gigaxonin is no impact on neurological signs. In absence of a robust GAN mouse and lack of demonstration that IF aggregation plays role in neurodegeneration, the benefit of this strategy (using a weak promotor) remains uncertain. To circumvent this, stabilizing the mutated E3 ligases (as it is the case for Gigaxonin) or modulating its activity (for dominant mode of inheritance) in disease constitutes an interesting approach, but knowledge on crystal structure are necessary for the latter. Another direction relies on the creation of powerful model systems to perform pharmacological screening, hence providing physiological relevance to candidate drugs. When it comes to mechanistic-driven approach, the pathologies discussed here may benefit from decades of pharmaceutical efforts done in other field, in particular cancer to potentiate or repress cell signaling, among which autophagy is certainly one prolific area of investigation (Dikic and Elazar, 2018). Thus, actual efforts in clinic favor strategies independent of mTOR, which exhibits deleterious side-effects due to its wide functions in other critical cellular processes, and search for more specificity, by targeting downstream regulators at every step of autophagy maturation, as well as selective autophagy (Boland et al., 2018).

As we are expanding our understanding of the functions of E3 ubiquitin ligases, there is a need to integrate them in a common ground in the future, to apprehend the complexity and the potential cross-talk between pathways in the settings of neurological symptoms. This constitutes a challenge, but the

impact will be extremely high, by enriching our comprehension of cellular functions, and helping defining the best therapeutic strategies that can benefit multiples neurological diseases. Moreover, modulating activity of the wild-type E3 ligases is extremely relevant for many other diseases, if we consider their known roles in various functions such as DNA repair, cell division, apoptosis and immunity. Extensively studied in that respect, Itch represents a valuable therapeutic target for cancer, skin and immune diseases (Yin et al., 2020). Finally, methodologies exploiting the ubiquitination properties of E3 ligases, amongst which CRBN stands out propose now toolboxes (Schapira et al., 2019) allowing degrading, in principle any protein, including the undruggable.

## AUTHOR CONTRIBUTIONS

PB wrote the manuscript, generated the table, and designed figures. LL executed complete drawing of figures and provided critical inputs into manuscript and figures. Both authors performed the bibliography search and reviewed the manuscript.

## FUNDING

PB is supported by the Institut National de la Santé et de la Recherche Médicale (INSERM), and LL is the recipient of a Ph.D. fellowship from Fondation pour la Recherche Medicale (FRM) (Fellowship Number: PLP20170939065).

## ACKNOWLEDGMENTS

We thank the funding agencies ATIP-Avenir program (INSERM), the Association Française contre les Myopathies (AFM), the FRM, the Fondation Maladies Rares (FMR), Région Languedoc-Roussillon, and Hannah's Hope Fund association.

## SUPPLEMENTARY MATERIAL

The Supplementary Material for this article can be found online at: https://www.frontiersin.org/articles/10.3389/fphys.2020.01022/full#supplementary-material

## REFERENCES

Aerts, M. B., Weterman, M. A., Quadri, M., Schelhaas, H. J., Bloem, B. R., Esselink, R. A., et al. (2016). A LRSAM1 mutation links Charcot-Marie-Tooth type 2 to Parkinson's disease. *Ann. Clin. Transl. neurol.* 3, 146–149. doi: 10.1002/acn3.281

Allen, E., Ding, J., Wang, W., Pramanik, S., Chou, J., Yau, V., et al. (2005). Gigaxonin-controlled degradation of MAP1B light chain is critical to neuronal survival. *Nature* 438, 224–228. doi: 10.1038/nature04256

Arribat, Y., Mysiak, K. S., Lescouzeres, L., Boizot, A., Ruiz, M., Rossel, M., et al. (2019). Sonic hedgehog repression underlies gigaxonin mutation-induced motor deficits in giant axonal neuropathy. *J. Clin. Invest.* 129, 5312–5326. doi: 10.1172/JCI129788

Asbury, A. K., Gale, M. K., Cox, S. C., Baringer, J. R., and Berg, B. O. (1972). Giant axonal neuropathy–a unique case with segmental neurofilamentous masses. *Acta Neuropathol.* 20, 237–247. doi: 10.1007/BF00686905

Aviles, E. C., Wilson, N. H., and Stoeckli, E. T. (2013). Sonic hedgehog and Wnt: antagonists in morphogenesis but collaborators in axon guidance. *Fron. Cell. Neurosci.* 7, 86. doi: 10.3389/fncel.2013.00086

Azzedine, H., Ravise, N., Verny, C., Gabreels-Festen, A., Lammens, M., Grid, D., et al. (2006). Spine deformities in Charcot-Marie-Tooth 4C caused by SH3TC2 gene mutations. *Neurology* 67, 602–606. doi: 10.1212/01.wnl.0000230225.19797.93

Balastik, M., Ferraguti, F., Pires-da Silva, A., Lee, T. H., Alvarez-Bolado, G., Lu, K. P., et al. (2008). Deficiency in ubiquitin ligase TRIM2 causes accumulation of neurofilament light chain and neurodegeneration. *Proc. Natl. Acad. Sci. U.S.A.* 105, 12016–12021. doi: 10.1073/pnas.0802261105

Bale, A. E. (2002). Hedgehog signaling and human disease. *Annu. Rev. Genomics Hum. Genet.* 3, 47–65. doi: 10.1146/annurev.genom.3.022502.103031

Belal, H., Nakashima, M., Matsumoto, H., Yokochi, K., Taniguchi-Ikeda, M., Aoto, K., et al. (2018). De novo variants in RHOBTB2, an atypical Rho GTPase gene, cause epileptic encephalopathy. *Hum. Mutat.* 39, 1070–1075. doi: 10.1002/humu.23550

Ben Hamida, C., Cavalier, L., Belal, S., Sanhaji, H., Nadal, N., Barhoumi, C., et al. (1997). Homozygosity mapping of giant axonal neuropathy gene to chromosome 16q24.1. *Neurogenetics* 1, 129–133. doi: 10.1007/s100480050019

Berg, B. O., Rosenberg, S. H., and Asbury, A. K. (1972). Giant axonal neuropathy. *Pediatrics* 49, 894–899.

Berko, E. R., Cho, M. T., Eng, C., Shao, Y., Sweetser, D. A., Waxler, J., et al. (2017). De novo missense variants in HECW2 are associated with neurodevelopmental delay and hypotonia. *J. Med. Genet.* 54, 84–86. doi: 10.1136/jmedgenet-2016-103943

Bhatia, N., Thiyagarajan, S., Elcheva, I., Saleem, M., Dlugosz, A., Mukhtar, H., et al. (2006). Gli2 is targeted for ubiquitination and degradation by beta-TrCP ubiquitin ligase. *J. Biol. Chem.* 281, 19320–19326. doi: 10.1074/jbc.M513203200

Bocquet, A., Berges, R., Frank, R., Robert, P., Peterson, A. C., and Eyer, J. (2009). Neurofilaments bind tubulin and modulate its polymerization. *J. Neurosci.* 29, 11043–11054. doi: 10.1523/JNEUROSCI.1924-09.2009

Boizot, A., Talmat-Amar, Y., Morrogh, D., Kuntz, N. L., Halbert, C., Chabrol, B., et al. (2014). The instability of the BTB-KELCH protein Gigaxonin causes Giant Axonal Neuropathy and constitutes a new penetrant and specific diagnostic test. *Acta neuropathol. Commun.* 2:47. doi: 10.1186/2051-5960-2-47

Boland, B., Yu, W. H., Corti, O., Mollereau, B., Henriques, A., Bezard, E., et al. (2018). Promoting the clearance of neurotoxic proteins in neurodegenerative disorders of ageing. *Nat. Rev. Drug Discov.* 17, 660–688. doi: 10.1038/nrd.2018.109

Bomont, P. (2016). Degradation of the intermediate filament family by gigaxonin. *Methods Enzymol.* 569, 215–231. doi: 10.1016/bs.mie.2015.07.009

Bomont, P. (2019). GAN (gigaxonin) E3 ligase and ATG16L1: master and commander of autophagosome production. *Autophagy* 15, 1650–1652. doi: 10.1080/15548627.2019.1628546

Bomont, P., Cavalier, L., Blondeau, F., Ben Hamida, C., Belal, S., Tazir, M., et al. (2000). The gene encoding gigaxonin, a new member of the cytoskeletal BTB/kelch repeat family, is mutated in giant axonal neuropathy. *Nat. Genet.* 26, 370–374. doi: 10.1038/81701

Bomont, P., and Koenig, M. (2003). Intermediate filament aggregation in fibroblasts of giant axonal neuropathy patients is aggravated in non dividing cells and by microtubule destabilization. *Hum. Mol. Genet.* 12, 813–822. doi: 10.1093/hmg/ddg092

Boone, P. M., Paterson, S., Mohajeri, K., Zhu, W., Genetti, C. A., Tai, D. J. C., et al. (2020). Biallelic mutation of FBXL7 suggests a novel form of hennekam syndrome. *Am. J. Med. Genet. A* 182, 189–194. doi: 10.1002/ajmg.a.61392

Botti-Millet, J., Nascimbeni, A. C., Dupont, N., Morel, E., and Codogno, P. (2016). Fine-tuning autophagy: from transcriptional to post-translational regulation. *Am. J. Physiol. Cell physiol.* 311, C351–C362. doi: 10.1152/ajpcell.00129.2016

Briscoe, J., and Therond, P. P. (2013). The mechanisms of hedgehog signalling and its roles in development and disease. *Nat. Rev. Mol. Cell Biol.* 14, 416–429. doi: 10.1038/nrm3598

Broix, L., Jagline, H., Ivanova, E., Schmucker, S., Drouot, N., Clayton-Smith, J., et al. (2016). Mutations in the HECT domain of NEDD4L lead to AKT-mTOR pathway deregulation and cause periventricular nodular heterotopia. *Nat. Genet.* 48, 1349–1358. doi: 10.1038/ng.3676

Buchau, F., Munz, C., Has, C., Lehmann, R., and Magin, T. M. (2018). KLHL16 degrades epidermal keratins. *J. Investig. Dermatol.* 138, 1871–1873. doi: 10.1016/j.jid.2018.02.017

Burchell, V. S., Nelson, D. E., Sanchez-Martinez, A., Delgado-Camprubi, M., Ivatt, R. M., Pogson, J. H., et al. (2013). The Parkinson's disease-linked proteins Fbxo7 and Parkin interact to mediate mitophagy. *Nat. Neurosci.* 16, 1257–1265. doi: 10.1038/nn.3489

Cavalier, L., BenHamida, C., Amouri, R., Belal, S., Bomont, P., Lagarde, N., et al. (2000). Giant axonal neuropathy locus refinement to a < 590 kb critical interval. *Eur. J. Hum. Genet.* 8, 527–534. doi: 10.1038/sj.ejhg.5200476

Chakarova, C. F., Papaioannou, M. G., Khanna, H., Lopez, I., Waseem, N., Shah, A., et al. (2007). Mutations in TOPORS cause autosomal dominant retinitis pigmentosa with perivascular retinal pigment epithelium atrophy. *Am. J. Hum. Genet.* 81, 1098–1103. doi: 10.1086/521953

Chan, E. M., Young, E. J., Ianzano, L., Munteanu, I., Zhao, X., Christopoulos, C. C., et al. (2003). Mutations in NHLRC1 cause progressive myoclonus epilepsy. *Nat. Genet.* 35, 125–127. doi: 10.1038/ng1238

Chastagner, P., Israel, A., and Brou, C. (2008). AIP4/Itch regulates Notch receptor degradation in the absence of ligand. *PLoS One* 3:e2735. doi: 10.1371/journal.pone.0002735

Chen, P. H., Hu, J., Wu, J., Huynh, D. T., Smith, T. J., Pan, S., et al. (2020). Gigaxonin glycosylation regulates intermediate filament turnover and may impact giant axonal neuropathy etiology or treatment. *JCI Insight* 5, e127751. doi: 10.1172/jci.insight.127751

Chen, W., Burgess, S., and Hopkins, N. (2001). Analysis of the zebrafish smoothened mutant reveals conserved and divergent functions of hedgehog activity. *Development* 128, 2385–2396.

Chen, X. L., Chinchilla, P., Fombonne, J., Ho, L., Guix, C., Keen, J. H., et al. (2014). Patched-1 proapoptotic activity is downregulated by modification of K1413 by the E3 ubiquitin-protein ligase Itchy homolog. *Mol. Cell Biol.* 34, 3855–3866. doi: 10.1128/MCB.00960-14

Chiang, A. P., Beck, J. S., Yen, H. J., Tayeh, M. K., Scheetz, T. E., Swiderski, R. E., et al. (2006). Homozygosity mapping with SNP arrays identifies TRIM32, an E3 ubiquitin ligase, as a bardet-biedl syndrome gene (BBS11). *Proc. Natl. Acad. Sci. U.S.A.* 103, 6287–6292. doi: 10.1073/pnas.0600158103

Cleveland, D. W., Yamanaka, K., and Bomont, P. (2009). Gigaxonin controls vimentin organization through a tubulin chaperone-independent pathway. *Hum. Mol. Genet.* 18, 1384–1394. doi: 10.1093/hmg/ddp044

Cohen, S., Zhai, B., Gygi, S. P., and Goldberg, A. L. (2012). Ubiquitylation by Trim32 causes coupled loss of desmin, Z-bands, and thin filaments in muscle atrophy. *J. Cell Biol.* 198, 575–589. doi: 10.1083/jcb.201110067

Cullen, V. C., Brownlees, J., Banner, S., Anderton, B. H., Leigh, P. N., Shaw, C. E., et al. (2004). Gigaxonin is associated with the Golgi and dimerises via its BTB domain. *Neuroreport* 15, 873–876. doi: 10.1097/00001756-200404090-00028

de Groot, R. E., Ganji, R. S., Bernatik, O., Lloyd-Lewis, B., Seipel, K., Sedova, K., et al. (2014). Huwe1-mediated ubiquitylation of dishevelled defines a negative feedback loop in the Wnt signaling pathway. *Sci. Signal.* 7:ra26. doi: 10.1126/scisignal.2004985

Demir, E., Bomont, P., Erdem, S., Cavalier, L., Demirci, M., Kose, G., et al. (2005). Giant axonal neuropathy: clinical and genetic study in six cases. *J. Neurol. Neurosurg Psychiatry* 76, 825–832. doi: 10.1136/jnnp.2003.035162

Dequen, F., Bomont, P., Gowing, G., Cleveland, D. W., and Julien, J. P. (2008). Modest loss of peripheral axons, muscle atrophy and formation of brain inclusions in mice with targeted deletion of gigaxonin exon 1. *J. Neurochem.* 107, 253–264. doi: 10.1111/j.1471-4159.2008.05601.x

Di Marcotullio, L., Greco, A., Mazza, D., Canettieri, G., Pietrosanti, L., Infante, P., et al. (2011). Numb activates the E3 ligase Itch to control Gli1 function through a novel degradation signal. *Oncogene* 30, 65–76. doi: 10.1038/onc.2010.394

Di Rienzo, M., Antonioli, M., Fusco, C., Liu, Y., Mari, M., Orhon, I., et al. (2019). Autophagy induction in atrophic muscle cells requires ULK1 activation by TRIM32 through unanchored K63-linked polyubiquitin chains. *Sci. Adv.* 5:eaau8857. doi: 10.1126/sciadv.aau8857

Di Rita, A., Peschiaroli, A., Acunzo, P. D., Strobbe, D., Hu, Z., Gruber, J., et al. (2018). HUWE1 E3 ligase promotes PINK1/PARKIN-independent mitophagy by regulating AMBRA1 activation via IKKalpha. *Nat. Commun.* 9:3755. doi: 10.1038/s41467-018-05722-3

Dikic, I., and Elazar, Z. (2018). Mechanism and medical implications of mammalian autophagy. *Nat. Rev. Mol. Cell Biol.* 19, 349–364. doi: 10.1038/s41580-018-0003-4

Ding, J., Allen, E., Wang, W., Valle, A., Wu, C., Nardine, T., et al. (2006). Gene targeting of GAN in mouse causes a toxic accumulation of microtubule-associated protein 8 and impaired retrograde axonal transport. *Hum. Mol. Genet.* 15, 1451–1463. doi: 10.1093/hmg/ddl069

Ding, J., Liu, J. J., Kowal, A. S., Nardine, T., Bhattacharya, P., Lee, A., et al. (2002). Microtubule-associated protein 1B: a neuronal binding partner for gigaxonin. *J. Cell Biol.* 158, 427–433. doi: 10.1083/jcb.200202055

Ding, Y., Zhang, Y., Xu, C., Tao, Q. H., and Chen, Y. G. (2013). HECT domain-containing E3 ubiquitin ligase NEDD4L negatively regulates Wnt signaling by targeting dishevelled for proteasomal degradation. *J. Biol. Chem.* 288, 8289–8298. doi: 10.1074/jbc.M112.433185

Donaghy, M., King, R. H., Thomas, P. K., and Workman, J. M. (1988). Abnormalities of the axonal cytoskeleton in giant axonal neuropathy. *J. Neurocytol.* 17, 197–208. doi: 10.1007/BF01674207

Duan, S., Skaar, J. R., Kuchay, S., Toschi, A., Kanarek, N., Ben-Neriah, Y., et al. (2011). mTOR generates an auto-amplification loop by triggering the betaTrCP- and CK1alpha-dependent degradation of DEPTOR. *Mol. Cell* 44, 317–324. doi: 10.1016/j.molcel.2011.09.005

Edvardson, S., Gerhard, F., Jalas, C., Lachmann, J., Golan, D., Saada, A., et al. (2015). Hypomyelination and developmental delay associated with VPS11 mutation in Ashkenazi-Jewish patients. *J. Med. Genet.* 52, 749–753. doi: 10.1136/jmedgenet-2015-103239

El-Brolosy, M. A., Kontarakis, Z., Rossi, A., Kuenne, C., Gunther, S., Fukuda, N., et al. (2019). Genetic compensation triggered by mutant mRNA degradation. *Nature* 568, 193–197. doi: 10.1038/s41586-019-1064-z

Fabrizi, G. M., Cavallaro, T., Angiari, C., Bertolasi, L., Cabrini, I., Ferrarini, M., et al. (2004). Giant axon and neurofilament accumulation in Charcot-Marie-Tooth disease type 2E. *Neurology* 62, 1429–1431. doi: 10.1212/01.WNL.0000120664.07186.3C

Flanigan, K. M., Crawford, T. O., Griffin, J. W., Goebel, H. H., Kohlschutter, A., Ranells, J., et al. (1998). Localization of the giant axonal neuropathy gene to chromosome 16q24. *Ann. Neurol.* 43, 143–148. doi: 10.1002/ana.410430126

Flex, E., Ciolfi, A., Caputo, V., Fodale, V., Leoni, C., Melis, D., et al. (2013). Loss of function of the E3 ubiquitin-protein ligase UBE3B causes Kaufman oculocerebrofacial syndrome. *J. Med. Genet.* 50, 493–499. doi: 10.1136/jmedgenet-2012-101405

Friedman, J. S., Ray, J. W., Waseem, N., Johnson, K., Brooks, M. J., Hugosson, T., et al. (2009). Mutations in a BTB-Kelch protein, KLHL7, cause autosomal-dominant retinitis pigmentosa. *Am. J. Hum. Genet.* 84, 792–800. doi: 10.1016/j.ajhg.2009.05.007

Froyen, G., Corbett, M., Vandewalle, J., Jarvela, I., Lawrence, O., Meldrum, C., et al. (2008). Submicroscopic duplications of the hydroxysteroid dehydrogenase HSD17B10 and the E3 ubiquitin ligase HUWE1 are associated with mental retardation. *Am. J. Hum. Genet.* 82, 432–443. doi: 10.1016/j.ajhg.2007.11.002

Fuchs, S. Y., Chen, A., Xiong, Y., Pan, Z. Q., and Ronai, Z. (1999). HOS, a human homolog of Slimb, forms an SCF complex with Skp1 and Cullin1 and targets the phosphorylation-dependent degradation of IkappaB and beta-catenin. *Oncogene* 18, 2039–2046. doi: 10.1038/sj.onc.1202760

Fujita, N., Itoh, T., Omori, H., Fukuda, M., Noda, T., and Yoshimori, T. (2008). The Atg16L complex specifies the site of LC3 lipidation for membrane biogenesis in autophagy. *Mol. Biol. Cell* 19, 2092–2100. doi: 10.1091/mbc.e07-12-1257

Furukawa, M., He, Y. J., Borchers, C., and Xiong, Y. (2003). Targeting of protein ubiquitination by BTB-Cullin 3-Roc1 ubiquitin ligases. *Nat. Cell Biol.* 5, 1001–1007. doi: 10.1038/ncb1056

Galluzzi, L., Baehrecke, E. H., Ballabio, A., Boya, P., Bravo-San Pedro, J. M., Cecconi, F., et al. (2017). Molecular definitions of autophagy and related processes. *EMBO J.* 36, 1811–1836. doi: 10.15252/embj.201796697

Ganay, T., Boizot, A., Burrer, R., Chauvin, J. P., and Bomont, P. (2011). Sensory-motor deficits and neurofilament disorganization in gigaxonin-null mice. *Mol. Neurodegener.* 6:25. doi: 10.1186/1750-1326-6-25

Gao, D., Inuzuka, H., Tan, M. K., Fukushima, H., Locasale, J. W., Liu, P., et al. (2011). mTOR drives its own activation via SCF(betaTrCP)-dependent degradation of the mTOR inhibitor DEPTOR. *Mol. Cell* 44, 290–303. doi: 10.1016/j.molcel.2011.08.030

Geetha, T. S., Michealraj, K. A., Kabra, M., Kaur, G., Juyal, R. C., and Thelma, B. K. (2014). Targeted deep resequencing identifies MID2 mutation for X-linked intellectual disability with varied disease severity in a large kindred from India. *Hum. Mutat.* 35, 41–44. doi: 10.1002/humu.22453

Gegg, M. E., Cooper, J. M., Chau, K. Y., Rojo, M., Schapira, A. H., and Taanman, J. W. (2010). Mitofusin 1 and mitofusin 2 are ubiquitinated in a PINK1/parkin-dependent manner upon induction of mitophagy. *Hum. Mol. Genet.* 19, 4861–4870. doi: 10.1093/hmg/ddq419

Geisler, S., Holmstrom, K. M., Skujat, D., Fiesel, F. C., Rothfuss, O. C., Kahle, P. J., et al. (2010). PINK1/Parkin-mediated mitophagy is dependent on VDAC1 and p62/SQSTM1. *Nat. Cell Biol.* 12, 119–131. doi: 10.1038/ncb2012

Genis, D., Ortega-Cubero, S., San Nicolas, H., Corral, J., Gardenyes, J., de Jorge, L., et al. (2018). Heterozygous STUB1 mutation causes familial ataxia with cognitive affective syndrome (SCA48). *Neurology* 91, e1988–e1998. doi: 10.1212/WNL.0000000000006550

Guernsey, D. L., Jiang, H., Bedard, K., Evans, S. C., Ferguson, M., Matsuoka, M., et al. (2010). Mutation in the gene encoding ubiquitin ligase LRSAM1 in patients with Charcot-Marie-Tooth disease. *PLoS Genet.* 6:e1001081. doi: 10.1371/journal.pgen.1001081

Herrmann, H., and Aebi, U. (2016). Intermediate filaments: structure and assembly. *Cold Spring Harb. Perspect. Biol.* 8:a018242. doi: 10.1101/cshperspect.a018242

Higgins, J. J., Pucilowska, J., Lombardi, R. Q., and Rooney, J. P. (2004). A mutation in a novel ATP-dependent lon protease gene in a kindred with mild mental retardation. *Neurology* 63, 1927–1931. doi: 10.1212/01.WNL.0000146196.01316.A2

Hollstein, R., Parry, D. A., Nalbach, L., Logan, C. V., Strom, T. M., Hartill, V. L., et al. (2015). HACE1 deficiency causes an autosomal recessive neurodevelopmental syndrome. *J. Med. Genet.* 52, 797–803. doi: 10.1136/jmedgenet-2015-103344

Holt, R. J., Young, R. M., Crespo, B., Ceroni, F., Curry, C. J., Bellacchio, E., et al. (2019). De novo missense variants in FBXW11 cause diverse developmental phenotypes including brain, eye, and digit anomalies. *Am. J. Hum. Genet.* 105, 640–657. doi: 10.1016/j.ajhg.2019.07.005

Huang, S., Zhang, Z., Zhang, C., Lv, X., Zheng, X., Chen, Z., et al. (2013). Activation of Smurf E3 ligase promoted by smoothened regulates hedgehog signaling through targeting patched turnover. *PLoS Biol.* 11:e1001721. doi: 10.1371/journal.pbio.1001721

Huang, Z., Zhao, J., Wang, W., Zhou, J., and Zhang, J. (2020). Depletion of LncRNA NEAT1 rescues mitochondrial dysfunction through NEDD4L-dependent PINK1 degradation in animal models of Alzheimer's Disease. *Front. Cell. Neurosci.* 14:28. doi: 10.3389/fncel.2020.00028

Huett, A., Heath, R. J., Begun, J., Sassi, S. O., Baxt, L. A., Vyas, J. M., et al. (2012). The LRR and RING domain protein LRSAM1 is an E3 ligase crucial for ubiquitin-dependent autophagy of intracellular *Salmonella* Typhimurium. *Cell Host Microbe* 12, 778–790. doi: 10.1016/j.chom.2012.10.019

Imai, Y., Soda, M., Hatakeyama, S., Akagi, T., Hashikawa, T., Nakayama, K. I., et al. (2002). CHIP is associated with Parkin, a gene responsible for familial Parkinson's disease, and enhances its ubiquitin ligase activity. *Mol. Cell* 10, 55–67. doi: 10.1016/S1097-2765(02)00583-X

Infante, P., Faedda, R., Bernardi, F., Bufalieri, F., Lospinoso Severini, L., Alfonsi, R., et al. (2018). Itch/beta-arrestin2-dependent non-proteolytic ubiquitylation of SuFu controls Hedgehog signalling and medulloblastoma tumorigenesis. *Nat. Commun.* 9:976. doi: 10.1038/s41467-018-03339-0

Israeli, E., Dryanovski, D. I., Schumacker, P. T., Chandel, N. S., Singer, J. D., Julien, J. P., et al. (2016). Intermediate filament aggregates cause mitochondrial dysmotility and increase energy demands in giant axonal neuropathy. *Hum. Mol. Genet.* 25, 2143–2157. doi: 10.1093/hmg/ddw081

Jessell, T. M. (2000). Neuronal specification in the spinal cord: inductive signals and transcriptional codes. *Nat. Rev. Genet.* 1, 20–29. doi: 10.1038/35049541

Johnson-Kerner, B. L., Ahmad, F. S., Diaz, A. G., Greene, J. P., Gray, S. J., Samulski, R. J., et al. (2015a). Intermediate filament protein accumulation in motor neurons derived from giant axonal neuropathy iPSCs rescued by restoration of gigaxonin. *Hum. Mol. Genet.* 24, 1420–1431. doi: 10.1093/hmg/ddu556

Johnson-Kerner, B. L., Garcia Diaz, A., Ekins, S., and Wichterle, H. (2015b). Kelch Domain of gigaxonin Interacts with Intermediate Filament Proteins Affected in Giant Axonal Neuropathy. *PLoS One* 10:e0140157. doi: 10.1371/journal.pone.0140157

Johnson-Kerner, B. L., Roth, L., Greene, J. P., Wichterle, H., and Sproule, D. M. (2014). Giant axonal neuropathy: An updated perspective on its pathology and pathogenesis. *Muscle Nerve* 50, 467–476. doi: 10.1002/mus.24321

Kang, J., and Chung, K. C. (2015). The F-box protein FBXO7 positively regulates bone morphogenetic protein-mediated signaling through Lys-63-specific ubiquitination of neurotrophin receptor-interacting MAGE (NRAGE). *Cell Mol. Life Sci.* 72, 181–195. doi: 10.1007/s00018-014-1665-5

Kim, M. J., Min, Y., Shim, J. H., Chun, E., and Lee, K. Y. (2019). CRBN Is a Negative Regulator of Bactericidal Activity and Autophagy Activation Through Inhibiting the Ubiquitination of ECSIT and BECN1. *Front. Immunol.* 10:2203. doi: 10.3389/fimmu.2019.02203

Kishino, T., Lalande, M., and Wagstaff, J. (1997). UBE3A/E6-AP mutations cause angelman syndrome. *Nat. Genet.* 15, 70–73. doi: 10.1038/ng0197-70

Kitada, T., Asakawa, S., Hattori, N., Matsumine, H., Yamamura, Y., Minoshima, S., et al. (1998). Mutations in the parkin gene cause autosomal recessive juvenile parkinsonism. *Nature* 392, 605–608. doi: 10.1038/33416

Klein, C. J., Wu, Y., Vogel, P., Goebel, H. H., Bonnemann, C., Zukosky, K., et al. (2014). Ubiquitin ligase defect by DCAF8 mutation causes HMSN2 with giant axons. *Neurology* 82, 873–878. doi: 10.1212/WNL.0000000000000206

Klionsky, D. J., and Emr, S. D. (2000). Autophagy as a regulated pathway of cellular degradation. *Science* 290, 1717–1721. doi: 10.1126/science.290.5497.1717

Klymkowsky, M. W., and Plummer, D. J. (1985). Giant axonal neuropathy: a conditional mutation affecting cytoskeletal organization. *J. Cell Biol.* 100, 245–250. doi: 10.1083/jcb.100.1.245

Kocaturk, N. M., and Gozuacik, D. (2018). Crosstalk between mammalian autophagy and the ubiquitin-proteasome system. *Front. Cell Dev. Biol.* 6:128. doi: 10.3389/fcell.2018.00128

Kok, F. O., Shin, M., Ni, C. W., Gupta, A., Grosse, A. S., van Impel, A., et al. (2015). Reverse genetic screening reveals poor correlation between morpholino-induced and mutant phenotypes in zebrafish. *Dev. Cell* 32, 97–108. doi: 10.1016/j.devcel.2014.11.018

Komander, D., and Rape, M. (2012). The ubiquitin code. *Annu. Rev. Biochem.* 81, 203–229. doi: 10.1146/annurev-biochem-060310-170328

Krishnamoorthy, V., Khanna, R., and Parnaik, V. K. (2018). E3 ubiquitin ligase HECW2 targets PCNA and lamin B1. *Biochim. Biophys. Acta Mol. Cell Res.* 1865, 1088–1104. doi: 10.1016/j.bbamcr.2018.05.008

Kudryashova, E., Kudryashov, D., Kramerova, I., and Spencer, M. J. (2005). Trim32 is a ubiquitin ligase mutated in limb girdle muscular dystrophy type 2H that binds to skeletal muscle myosin and ubiquitinates actin. *J. Mol. Biol.* 354, 413–424. doi: 10.1016/j.jmb.2005.09.068

Kuhlenbaumer, G., Timmerman, V., and Bomont, P. (1993). "Giant axonal neuropathy," in *GeneReviews(R)*, eds R. A. Pagon, M. P. Adam, H. H. Ardinger, S. E. Wallace, A. Amemiya, L. J. H. Bean, et al. (Seattle, WA: University of Washington).

Kwon, Y. T., and Ciechanover, A. (2017). The ubiquitin code in the ubiquitin-proteasome system and autophagy. *Trends Biochem. Sci.* 42, 873–886. doi: 10.1016/j.tibs.2017.09.002

Lander, E. S., Linton, L. M., Birren, B., Nusbaum, C., Zody, M. C., Baldwin, J., et al. (2001). Initial sequencing and analysis of the human genome. *Nature* 409, 860–921. doi: 10.1038/35057062

Lee, R. T., Zhao, Z., and Ingham, P. W. (2016). Hedgehog signalling. *Development* 143, 367–372. doi: 10.1242/dev.120154

Lelieveld, S. H., Reijnders, M. R., Pfundt, R., Yntema, H. G., Kamsteeg, E. J., de Vries, P., et al. (2016). Meta-analysis of 2,104 trios provides support for 10 new genes for intellectual disability. *Nat. Neurosci.* 19, 1194–1196. doi: 10.1038/nn.4352

Levine, B., and Kroemer, G. (2019). Biological functions of autophagy genes: a disease perspective. *Cell* 176, 11–42. doi: 10.1016/j.cell.2018.09.048

Li, L., Xin, H., Xu, X., Huang, M., Zhang, X., Chen, Y., et al. (2004). CHIP mediates degradation of Smad proteins and potentially regulates smad-induced transcription. *Mol. Cell Biol.* 24, 856–864. doi: 10.1128/MCB.24.2.856-864.2004

Li, X., Zhang, D., Hannink, M., and Beamer, L. J. (2004). Crystal structure of the kelch domain of human Keap1. *J. Biol. Chem.* 279, 54750–54758. doi: 10.1074/jbc.M410073200

Lin, N. H., Huang, Y. S., Opal, P., Goldman, R. D., Messing, A., and Perng, M. D. (2016). The role of gigaxonin in the degradation of the glial-specific intermediate filament protein GFAP. *Mol. Biol. Cell* 27, 3980–3990. doi: 10.1091/mbc.E16-06-0362

Liu, J., Li, M., Li, L., Chen, S., and Wang, X. (2018). Ubiquitination of the PI3-kinase VPS-34 promotes VPS-34 stability and phagosome maturation. *J. Cell Biol.* 217, 347–360. doi: 10.1083/jcb.201705116

Liu, Z., Chen, P., Gao, H., Gu, Y., Yang, J., Peng, H., et al. (2014). Ubiquitylation of autophagy receptor Optineurin by HACE1 activates selective autophagy for tumor suppression. *Cancer Cell* 26, 106–120. doi: 10.1016/j.ccr.2014.05.015

Loffek, S., Woll, S., Hohfeld, J., Leube, R. E., Has, C., Bruckner-Tuderman, L., et al. (2010). The ubiquitin ligase CHIP/STUB1 targets mutant keratins for degradation. *Hum. Mutat.* 31, 466–476. doi: 10.1002/humu.21222

Lohr, N. J., Molleston, J. P., Strauss, K. A., Torres-Martinez, W., Sherman, E. A., Squires, R. H., et al. (2010). Human ITCH E3 ubiquitin ligase deficiency causes syndromic multisystem autoimmune disease. *Am. J. Hum. Genet.* 86, 447–453. doi: 10.1016/j.ajhg.2010.01.028

Lowery, J., Jain, N., Kuczmarski, E. R., Mahammad, S., Goldman, A., Gelfand, V. I., et al. (2016). Abnormal intermediate filament organization alters mitochondrial motility in giant axonal neuropathy fibroblasts. *Mol. Biol. Cell* 27, 608–616. doi: 10.1091/mbc.E15-09-0627

Ma, Z., Zhu, P., Shi, H., Guo, L., Zhang, Q., Chen, Y., et al. (2019). PTC-bearing mRNA elicits a genetic compensation response via Upf3a and COMPASS components. *Nature* 568, 259–263. doi: 10.1038/s41586-019-1057-y

Maday, S., and Holzbaur, E. L. (2016). Compartment-specific regulation of autophagy in primary neurons. *J. Neurosci.* 36, 5933–5945. doi: 10.1523/JNEUROSCI.4401-15.2016

Mahammad, S., Murthy, S. N., Didonna, A., Grin, B., Israeli, E., Perrot, R., et al. (2013). Giant axonal neuropathy-associated gigaxonin mutations impair intermediate filament protein degradation. *J. Clin. Invest.* 123, 1964–1975. doi: 10.1172/JCI66387

Mancias, J. D., Pontano Vaites, L., Nissim, S., Biancur, D. E., Kim, A. J., Wang, X., et al. (2015). Ferritinophagy via NCOA4 is required for erythropoiesis and is regulated by iron dependent HERC2-mediated proteolysis. *eLife* 4:e10308. doi: 10.7554/eLife.10308.014

Manzanillo, P. S., Ayres, J. S., Watson, R. O., Collins, A. C., Souza, G., Rae, C. S., et al. (2013). The ubiquitin ligase parkin mediates resistance to intracellular pathogens. *Nature* 501, 512–516. doi: 10.1038/nature12566

Margolin, D. H., Kousi, M., Chan, Y. M., Lim, E. T., Schmahmann, J. D., Hadjivassiliou, M., et al. (2013). Ataxia, dementia, and hypogonadotropism caused by disordered ubiquitination. *New Eng. J. Med.* 368, 1992–2003. doi: 10.1056/NEJMoa1215993

Margolis, S. S., Salogiannis, J., Lipton, D. M., Mandel-Brehm, C., Wills, Z. P., Mardinly, A. R., et al. (2010). EphB-mediated degradation of the RhoA GEF Ephexin5 relieves a developmental brake on excitatory synapse formation. *Cell* 143, 442–455. doi: 10.1016/j.cell.2010.09.038

Matsuura, T., Sutcliffe, J. S., Fang, P., Galjaard, R. J., Jiang, Y. H., Benton, C. S., et al. (1997). De novo truncating mutations in E6-AP ubiquitin-protein ligase gene (UBE3A) in Angelman syndrome. *Nat. Genet.* 15, 74–77. doi: 10.1038/ng0197-74

Meng, L., Ward, A. J., Chun, S., Bennett, C. F., Beaudet, A. L., and Rigo, F. (2015). Towards a therapy for angelman syndrome by targeting a long non-coding RNA. *Nature* 518, 409–412. doi: 10.1038/nature13975

Menzies, F. M., Fleming, A., Caricasole, A., Bento, C. F., Andrews, S. P., Ashkenazi, A., et al. (2017). Autophagy and neurodegeneration: pathogenic mechanisms and therapeutic opportunities. *Neuron* 93, 1015–1034. doi: 10.1016/j.neuron.2017.01.022

Mignon-Ravix, C., Cacciagli, P., Choucair, N., Popovici, C., Missirian, C., Milh, M., et al. (2014). Intragenic rearrangements in X-linked intellectual deficiency: results of a-CGH in a series of 54 patients and identification of TRPC5 and KLHL15 as potential XLID genes. *Am. J. Med. Genet. A* 164A, 1991–1997. doi: 10.1002/ajmg.a.36602

Mir, A., Sritharan, K., Mittal, K., Vasli, N., Araujo, C., Jamil, T., et al. (2014). Truncation of the E3 ubiquitin ligase component FBXO31 causes non-syndromic autosomal recessive intellectual disability in a Pakistani family. *Hum. Genet.* 133, 975–984. doi: 10.1007/s00439-014-1438-0

Molero, A. E., Arteaga-Bracho, E. E., Chen, C. H., Gulinello, M., Winchester, M. L., Pichamoorthy, N., et al. (2016). Selective expression of mutant huntingtin during development recapitulates characteristic features of Huntington's disease. *Proc. Natl. Acad. Sci. U.S.A.* 113, 5736–5741. doi: 10.1073/pnas.1603871113

Narendra, D., Tanaka, A., Suen, D. F., and Youle, R. J. (2008). Parkin is recruited selectively to impaired mitochondria and promotes their autophagy. *J. Cell Biol.* 183, 795–803. doi: 10.1083/jcb.200809125

Nazio, F., Carinci, M., Valacca, C., Bielli, P., Strappazzon, F., Antonioli, M., et al. (2016). Fine-tuning of ULK1 mRNA and protein levels is required for autophagy oscillation. *J. Cell Biol.* 215, 841–856. doi: 10.1083/jcb.201605089

Neilson, D. E., Adams, M. D., Orr, C. M., Schelling, D. K., Eiben, R. M., Kerr, D. S., et al. (2009). Infection-triggered familial or recurrent cases of acute necrotizing encephalopathy caused by mutations in a component of the nuclear pore. RANBP2. *Am. J. Hum. Genet.* 84, 44–51. doi: 10.1016/j.ajhg.2008.12.009

Nguyen, L. S., Schneider, T., Rio, M., Moutton, S., Siquier-Pernet, K., Verny, F., et al. (2016). A nonsense variant in HERC1 is associated with intellectual disability, megalencephaly, thick corpus callosum and cerebellar atrophy. *Eur. J. Hum. Genet.* 24, 455–458. doi: 10.1038/ejhg.2015.140

Novellasdemunt, L., Kucharska, A., Jamieson, C., Prange-Barczynska, M., Baulies, A., Antas, P., et al. (2020). NEDD4 and NEDD4L regulate Wnt signalling and intestinal stem cell priming by degrading LGR5 receptor. *EMBO J.* 39:e102771. doi: 10.15252/embj.2019102771

Okumoto, K., Itoh, R., Shimozawa, N., Suzuki, Y., Tamura, S., Kondo, N., et al. (1998). Mutations in PEX10 is the cause of Zellweger peroxisome deficiency syndrome of complementation group B. *Hum. Mol. Genet.* 7, 1399–1405. doi: 10.1093/hmg/7.9.1399

O'Roak, B. J., Stessman, H. A., Boyle, E. A., Witherspoon, K. T., Martin, B., Lee, C., et al. (2014). Recurrent de novo mutations implicate novel genes underlying simplex autism risk. *Nat. Commun.* 5:5595. doi: 10.1038/ncomms6595

Pasutto, F., Keller, K. E., Weisschuh, N., Sticht, H., Samples, J. R., Yang, Y. F., et al. (2012). Variants in ASB10 are associated with open-angle glaucoma. *Hum. Mol. Genet.* 21, 1336–1349. doi: 10.1093/hmg/ddr572

Pehlivan, D., Coban Akdemir, Z., Karaca, E., Bayram, Y., Jhangiani, S., Yildiz, E. P., et al. (2015). Exome sequencing reveals homozygous TRIM2 mutation in a patient with early onset CMT and bilateral vocal cord paralysis. *Hum. Genet.* 134, 671–673. doi: 10.1007/s00439-015-1548-3

Pena, S. D. (1981). Giant axonal neuropathy: intermediate filament aggregates in cultured skin fibroblasts. *Neurology* 31, 1470–1473. doi: 10.1212/WNL.31.11.1470

Pena, S. D., Opas, M., Turksen, K., Kalnins, V. I., and Carpenter, S. (1983). Immunocytochemical studies of intermediate filament aggregates and their relationship to microtubules in cultured skin fibroblasts from patients with giant axonal neuropathy. *Eur. J. Cell Biol.* 31, 227–234.

Perez de Diego, R., Sancho-Shimizu, V., Lorenzo, L., Puel, A., Plancoulaine, S., Picard, C., et al. (2010). Human TRAF3 adaptor molecule deficiency leads to impaired Toll-like receptor 3 response and susceptibility to herpes simplex encephalitis. *Immunity* 33, 400–411. doi: 10.1016/j.immuni.2010.08.014

Pintard, L., Willis, J. H., Willems, A., Johnson, J. L., Srayko, M., Kurz, T., et al. (2003). The BTB protein MEL-26 is a substrate-specific adaptor of the CUL-3 ubiquitin-ligase. *Nature* 425, 311–316. doi: 10.1038/nature01959

Poole, A. C., Thomas, R. E., Yu, S., Vincow, E. S., and Pallanck, L. (2010). The mitochondrial fusion-promoting factor mitofusin is a substrate of the PINK1/parkin pathway. *PLoS One* 5:e10054. doi: 10.1371/journal.pone.0010054

Puffenberger, E. G., Jinks, R. N., Wang, H., Xin, B., Fiorentini, C., Sherman, E. A., et al. (2012). A homozygous missense mutation in HERC2 associated with global developmental delay and autism spectrum disorder. *Hum. Mutat.* 33, 1639–1646. doi: 10.1002/humu.22237

Quaderi, N. A., Schweiger, S., Gaudenz, K., Franco, B., Rugarli, E. I., Berger, W., et al. (1997). Opitz G/BBB syndrome, a defect of midline development, is due to mutations in a new RING finger gene on Xp22. *Nat. Genet.* 17, 285–291. doi: 10.1038/ng1197-285

Rawal, N., Corti, O., Sacchetti, P., Ardilla-Osorio, H., Sehat, B., Brice, A., et al. (2009). Parkin protects dopaminergic neurons from excessive Wnt/beta-catenin signaling. *Biochem. Biophys. Res. Commun.* 388, 473–478. doi: 10.1016/j.bbrc.2009.07.014

Ren, Y., Zhao, J., and Feng, J. (2003). Parkin binds to alpha/beta tubulin and increases their ubiquitination and degradation. *J. Neurosci.* 23, 3316–3324. doi: 10.1523/JNEUROSCI.23-08-03316.2003

Rossi, A., Kontarakis, Z., Gerri, C., Nolte, H., Holper, S., Kruger, M., et al. (2015). Genetic compensation induced by deleterious mutations but not gene knockdowns. *Nature* 524, 230–233. doi: 10.1038/nature14580

Rousseau, A., and Bertolotti, A. (2018). Regulation of proteasome assembly and activity in health and disease. *Nat. Rev. Mol. Cell Biol.* 19, 697–712. doi: 10.1038/s41580-018-0040-z

Saitoh, T., Fujita, N., Jang, M. H., Uematsu, S., Yang, B. G., Satoh, T., et al. (2008). Loss of the autophagy protein Atg16L1 enhances endotoxin-induced IL-1beta production. *Nature* 456, 264–268. doi: 10.1038/nature07383

Sanchez-Martin, P., Lahuerta, M., Viana, R., Knecht, E., and Sanz, P. (2020). Regulation of the autophagic PI3KC3 complex by laforin/malin E3-ubiquitin ligase, two proteins involved in Lafora disease. *Biochim. Biophys. Acta Mol. Cell Res.* 1867:118613. doi: 10.1016/j.bbamcr.2019.118613

Sanchez-Martin, P., Roma-Mateo, C., Viana, R., and Sanz, P. (2015). Ubiquitin conjugating enzyme E2-N and sequestosome-1 (p62) are components of the ubiquitination process mediated by the malin-laforin E3-ubiquitin ligase complex. *Int. J. Biochem. Cell Biol.* 69, 204–214. doi: 10.1016/j.biocel.2015.10.030

Schapira, M., Calabrese, M. F., Bullock, A. N., and Crews, C. M. (2019). Targeted protein degradation: expanding the toolbox. *Nat. Rev. Drug. Discov.* 18, 949–963. doi: 10.1038/s41573-019-0047-y

Schulman, B. A., Carrano, A. C., Jeffrey, P. D., Bowen, Z., Kinnucan, E. R., Finnin, M. S., et al. (2000). Insights into SCF ubiquitin ligases from the structure of the Skp1-Skp2 complex. *Nature* 408, 381–386. doi: 10.1038/35042620

Schweiger, S., Dorn, S., Fuchs, M., Kohler, A., Matthes, F., Muller, E. C., et al. (2014). The E3 ubiquitin ligase MID1 catalyzes ubiquitination and cleavage of Fu. *J. Biol. Chem.* 289, 31805–31817. doi: 10.1074/jbc.M113.541219

Scrivo, A., Codogno, P., and Bomont, P. (2019). Gigaxonin E3 ligase governs ATG16L1 turnover to control autophagosome production. *Nat. Commun.* 10:780. doi: 10.1038/s41467-019-08331-w

Segala, G., Bennesch, M. A., Ghahhari, N. M., Pandey, D. P., Echeverria, P. C., Karch, F., et al. (2019). Vps11 and Vps18 of Vps-C membrane traffic complexes are E3 ubiquitin ligases and fine-tune signalling. *Nat. Commun.* 10:1833. doi: 10.1038/s41467-019-09800-y

Sha, Y., Rao, L., Settembre, C., Ballabio, A., and Eissa, N. T. (2017). STUB1 regulates TFEB-induced autophagy-lysosome pathway. *EMBO J.* 36, 2544–2552. doi: 10.15252/embj.201796699

Sharma, J., Mulherkar, S., Mukherjee, D., and Jana, N. R. (2012). Malin regulates Wnt signaling pathway through degradation of dishevelled2. *J. Biol. Chem.* 287, 6830–6839. doi: 10.1074/jbc.M111.315135

Shi, C. H., Schisler, J. C., Rubel, C. E., Tan, S., Song, B., McDonough, H., et al. (2014). Ataxia and hypogonadism caused by the loss of ubiquitin ligase activity of the U box protein CHIP. *Hum. Mol. Genet.* 23, 1013–1024. doi: 10.1093/hmg/ddt497

Shi, Y., Wang, J., Li, J. D., Ren, H., Guan, W., He, M., et al. (2013). Identification of CHIP as a novel causative gene for autosomal recessive cerebellar ataxia. *PLoS One* 8:e81884. doi: 10.1371/journal.pone.0081884

Shitashige, M., Satow, R., Honda, K., Ono, M., Hirohashi, S., and Yamada, T. (2008). Regulation of Wnt signaling by the nuclear pore complex. *Gastroenterology* 134, 1961–1971, 1971.e1–1974.e1. doi: 10.1053/j.gastro.2008.03.010

Shojaee, S., Sina, F., Banihosseini, S. S., Kazemi, M. H., Kalhor, R., Shahidi, G. A., et al. (2008). Genome-wide linkage analysis of a Parkinsonian-pyramidal syndrome pedigree by 500 K SNP arrays. *Am. J. Hum. Genet.* 82, 1375–1384. doi: 10.1016/j.ajhg.2008.05.005

Singh, N., Kumble Bhat, V., Tiwari, A., Kodaganur, S. G., Tontanahal, S. J., Sarda, A., et al. (2017). A homozygous mutation in TRIM36 causes autosomal recessive anencephaly in an Indian family. *Hum. Mol. Genet.* 26, 1104–1114. doi: 10.1093/hmg/ddx020

Stavoe, A. K. H., and Holzbaur, E. L. F. (2019). Autophagy in Neurons. *Annu. Rev. Cell Dev. Biol.* 35, 477–500. doi: 10.1146/annurev-cellbio-100818-125242

Stewart, G. S., Panier, S., Townsend, K., Al-Hakim, A. K., Kolas, N. K., Miller, E. S., et al. (2009). The RIDDLE syndrome protein mediates a ubiquitin-dependent signaling cascade at sites of DNA damage. *Cell* 136, 420–434. doi: 10.1016/j.cell.2008.12.042

Sumner, C. J., d'Ydewalle, C., Wooley, J., Fawcett, K. A., Hernandez, D., Gardiner, A. R., et al. (2013). A dominant mutation in FBXO38 causes distal spinal muscular atrophy with calf predominance. *Am. J. Hum. Genet.* 93, 976–983. doi: 10.1016/j.ajhg.2013.10.006

Swatek, K. N., and Komander, D. (2016). Ubiquitin modifications. *Cell Res.* 26, 399–422. doi: 10.1038/cr.2016.39

Takats, S., Pircs, K., Nagy, P., Varga, A., Karpati, M., Hegedus, K., et al. (2014). Interaction of the HOPS complex with syntaxin 17 mediates autophagosome clearance in Drosophila. *Mol. Biol. Cell* 25, 1338–1354. doi: 10.1091/mbc.e13-08-0449

Tazir, M., Nouioua, S., Magy, L., Huehne, K., Assami, S., Urtizberea, A., et al. (2009). Phenotypic variability in giant axonal neuropathy. *Neuromuscul. Disord.* 19, 270–274. doi: 10.1016/j.nmd.2009.01.011

Te, K. G., and Reggiani, C. (2002). Skeletal muscle fibre type specification during embryonic development. *J. Muscle Res. Cell motil.* 23, 65–69. doi: 10.1023/A:1019940932275

Tenorio, J., Mansilla, A., Valencia, M., Martinez-Glez, V., Romanelli, V., Arias, P., et al. (2014). A new overgrowth syndrome is due to mutations in RNF125. *Hum. Mutat.* 35, 1436–1441. doi: 10.1002/humu.22689

Tokita, M. J., Chen, C. A., Chitayat, D., Macnamara, E., Rosenfeld, J. A., Hanchard, N., et al. (2018). De novo missense variants in TRAF7 cause developmental delay, congenital anomalies, and dysmorphic features. *Am. J. Hum. Genet.* 103, 154–162. doi: 10.1016/j.ajhg.2018.06.005

Tonne, E., Holdhus, R., Stansberg, C., Stray-Pedersen, A., Petersen, K., Brunner, H. G., et al. (2015). Syndromic X-linked intellectual disability segregating with a missense variant in RLIM. *Eur. J. Hum. Genet.* 23, 1652–1656. doi: 10.1038/ejhg.2015.30

Treiber-Held, S., Budjarjo-Welim, H., Reimann, D., Richter, J., Kretzschmar, H. A., and Hanefeld, F. (1994). Giant axonal neuropathy: a generalized disorder of intermediate filaments with longitudinal grooves in the hair. *Neuropediatrics* 25, 89–93. doi: 10.1055/s-2008-1071592

Upadhyay, M., Agarwal, S., Bhadauriya, P., and Ganesh, S. (2017). Loss of laforin or malin results in increased Drp1 level and concomitant mitochondrial fragmentation in Lafora disease mouse models. *Neurobiol. Dis.* 100, 39–51. doi: 10.1016/j.nbd.2017.01.002

Valdmanis, P. N., Dupre, N., Lachance, M., Stochmanski, S. J., Belzil, V. V., Dion, P. A., et al. (2011). A mutation in the RNF170 gene causes autosomal dominant sensory ataxia. *Brain* 134, 602–607. doi: 10.1093/brain/awq329

Varga, Z. M., Amores, A., Lewis, K. E., Yan, Y. L., Postlethwait, J. H., Eisen, J. S., et al. (2001). Zebrafish smoothened functions in ventral neural tube specification and axon tract formation. *Development* 128, 3497–3509.

Veena, M. S., Wilken, R., Zheng, J. Y., Gholkar, A., Venkatesan, N., Vira, D., et al. (2014). p16 Protein and gigaxonin are associated with the ubiquitination of NFkappaB in cisplatin-induced senescence of cancer cells. *J. Biol. Chem.* 289, 34921–34937. doi: 10.1074/jbc.M114.568543

Vijayakumar, S., Liu, G., Wen, H. C., Abu, Y., Chong, R., Nastri, H., et al. (2017). Extracellular LDLR repeats modulate Wnt signaling activity by promoting LRP6 receptor endocytosis mediated by the Itch E3 ubiquitin ligase. *Genes Cancer* 8, 613–627. doi: 10.18632/genesandcancer.146

Wan, W., You, Z., Zhou, L., Xu, Y., Peng, C., Zhou, T., et al. (2018). mTORC1-Regulated and HUWE1-Mediated WIPI2 degradation controls autophagy flux. *Mol. Cell* 72, 303.e6–315.e6. doi: 10.1016/j.molcel.2018.09.017

Wang, M., Luo, W., Zhang, Y., Yang, R., Li, X., Guo, Y., et al. (2020). Trim32 suppresses cerebellar development and tumorigenesis by degrading Gli1/sonic hedgehog signaling. *Cell Death Differ.* 27, 1286–1299. doi: 10.1038/s41418-019-0415-5

Wang, W., Ding, J., Allen, E., Zhu, P., Zhang, L., Vogel, H., et al. (2005). Gigaxonin interacts with tubulin folding cofactor B and controls its degradation through the ubiquitin-proteasome pathway. *Curr. Biol.* 15, 2050–2055. doi: 10.1016/j.cub.2005.10.052

Warren, D. S., Morrell, J. C., Moser, H. W., Valle, D., and Gould, S. J. (1998). Identification of PEX10, the gene defective in complementation group 7 of the peroxisome-biogenesis disorders. *Am. J. Hum. Genet.* 63, 347–359. doi: 10.1086/301963

Wei, W., Li, M., Wang, J., Nie, F., and Li, L. (2012). The E3 ubiquitin ligase ITCH negatively regulates canonical Wnt signaling by targeting dishevelled protein. *Mol. Cell Biol.* 32, 3903–3912. doi: 10.1128/MCB.00251-12

Williams, K. L., Topp, S., Yang, S., Smith, B., Fifita, J. A., Warraich, S. T., et al. (2016). CCNF mutations in amyotrophic lateral sclerosis and frontotemporal dementia. *Nat. Commun.* 7:11253. doi: 10.1038/ncomms11253

Xu, C., Feng, K., Zhao, X., Huang, S., Cheng, Y., Qian, L., et al. (2014). Regulation of autophagy by E3 ubiquitin ligase RNF216 through BECN1 ubiquitination. *Autophagy* 10, 2239–2250. doi: 10.4161/15548627.2014.981792

Xu, L., Wei, Y., Reboul, J., Vaglio, P., Shin, T. H., Vidal, M., et al. (2003). BTB proteins are substrate-specific adaptors in an SCF-like modular ubiquitin ligase containing CUL-3. *Nature* 425, 316–321. doi: 10.1038/nature01985

Yang, S. W., Oh, K. H., Park, E., Chang, H. M., Park, J. M., Seong, M. W., et al. (2013). USP47 and C terminus of Hsp70-interacting protein (CHIP) antagonistically regulate katanin-p60-mediated axonal growth. *J. Neurosci.* 33, 12728–12738. doi: 10.1523/JNEUROSCI.0698-13.2013

Yin, Q., Wyatt, C. J., Han, T., Smalley, K. S. M., and Wan, L. (2020). ITCH as a potential therapeutic target in human cancers. *Semin. Cancer Biol.* doi: 10.1016/j.semcancer.2020.03.003 [Epub ahead of print].

Ylikallio, E., Poyhonen, R., Zimon, M., De Vriendt, E., Hilander, T., Paetau, A., et al. (2013). Deficiency of the E3 ubiquitin ligase TRIM2 in early-onset axonal neuropathy. *Hum. Mol. Genet.* 22, 2975–2983. doi: 10.1093/hmg/ddt149

Zhang, J., Lachance, V., Schaffner, A., Li, X., Fedick, A., Kaye, L. E., et al. (2016). A founder mutation in vps11 causes an autosomal recessive leukoencephalopathy linked to autophagic defects. *PLoS Genet.* 12:e1005848. doi: 10.1371/journal.pgen.1005848

Zhao, Y., Xiong, X., and Sun, Y. (2011). DEPTOR, an mTOR inhibitor, is a physiological substrate of SCF(betaTrCP) E3 ubiquitin ligase and regulates survival and autophagy. *Mol. Cell* 44, 304–316. doi: 10.1016/j.molcel.2011.08.029

Zheng, N., and Shabek, N. (2017). Ubiquitin ligases: structure, function, and regulation. *Annu. Rev. Biochem.* 86, 129–157. doi: 10.1146/annurev-biochem-060815-014922

Zhu, J. W., Zou, M. M., Li, Y. F., Chen, W. J., Liu, J. C., Chen, H., et al. (2020). Absence of TRIM32 leads to reduced GABAergic interneuron generation and autism-like behaviors in mice via suppressing mTOR signaling. *Cereb. Cortex* 30, 3240–3258. doi: 10.1093/cercor/bhz306

Zhuang, M., Calabrese, M. F., Liu, J., Waddell, M. B., Nourse, A., Hammel, M., et al. (2009). Structures of SPOP-substrate complexes: insights into molecular architectures of BTB-Cul3 ubiquitin ligases. *Mol. Cell* 36, 39–50. doi: 10.1016/j.molcel.2009.09.022

Ziviani, E., Tao, R. N., and Whitworth, A. J. (2010). Drosophila parkin requires PINK1 for mitochondrial translocation and ubiquitinates mitofusin. *Proc. Natl. Acad. Sci. U.S.A.* 107, 5018–5023. doi: 10.1073/pnas.0913485107

Zou, Y., Liu, Q., Chen, B., Zhang, X., Guo, C., Zhou, H., et al. (2007). Mutation in CUL4B, which encodes a member of cullin-RING ubiquitin ligase complex, causes X-linked mental retardation. *Am. J. Hum. Genet.* 80, 561–566. doi: 10.1086/512489

**Conflict of Interest:** The authors declare that the research was conducted in the absence of any commercial or financial relationships that could be construed as a potential conflict of interest.

frontiers in Physiology

REVIEW
published: 29 October 2020
doi: 10.3389/fphys.2020.573372

# Natural Killer Lytic-Associated Molecule (NKLAM): An E3 Ubiquitin Ligase With an Integral Role in Innate Immunity

*Donald W. Lawrence[1], Paul A. Willard[1], Allyson M. Cochran[1], Emily C. Matchett[1] and Jacki Kornbluth[1,2]**

*[1] Department of Pathology, Saint Louis University School of Medicine, St. Louis, MO, United States, [2] St. Louis VA Health Care System, St. Louis, MO, United States*

Natural Killer Lytic-Associated Molecule (NKLAM), also designated RNF19B, is a unique member of a small family of E3 ubiquitin ligases. This 14-member group of ligases has a characteristic cysteine-rich RING-IBR-RING (RBR) domain that mediates the ubiquitination of multiple substrates. The consequence of substrate ubiquitination varies, depending on the type of ubiquitin linkages formed. The most widely studied effect of ubiquitination of proteins is proteasome-mediated substrate degradation; however, ubiquitination can also alter protein localization and function. Since its discovery in 1999, much has been deciphered about the role of NKLAM in innate immune responses. We have discerned that NKLAM has an integral function in both natural killer (NK) cells and macrophages *in vitro* and *in vivo*. NKLAM expression is required for each of these cell types to mediate maximal killing activity and cytokine production. However, much remains to be determined. In this review, we summarize what has been learned about NKLAM expression, structure and function, and discuss new directions for investigation. We hope that this will stimulate interest in further exploration of NKLAM.

**Keywords: NKLAM, ubiquitin ligase, innate immunity, natural killer, macrophage, phagocytosis, cytotoxicity, RNF19B**

OPEN ACCESS

***Edited by:***
*Fumiyo Ikeda,*
*Kyushu University, Japan*

***Reviewed by:***
*Yenniffer Ávalos,*
*University of Santiago, Chile*
*Magdalena Paolino,*
*Karolinska Institutet (KI), Sweden*

***Correspondence:**
*Jacki Kornbluth*
*jacki.kornbluth@health.slu.edu*

***Specialty section:***
*This article was submitted to Integrative Physiology, a section of the journal Frontiers in Physiology*

***Received:*** *16 June 2020*
***Accepted:*** *05 October 2020*
***Published:*** *29 October 2020*

***Citation:***
*Lawrence DW, Willard PA, Cochran AM, Matchett EC and Kornbluth J (2020) Natural Killer Lytic-Associated Molecule (NKLAM): An E3 Ubiquitin Ligase With an Integral Role in Innate Immunity. Front. Physiol. 11:573372. doi: 10.3389/fphys.2020.573372*

## INTRODUCTION TO NKLAM

### Discovery of NKLAM

Studies were initiated to identify new genes and gene products associated with cytokine-enhanced natural killer (NK) anti-tumor cytotoxic activity. For these experiments, we used the human NK clone NK3.3, which had been generated previously (Kornbluth et al., 1982). This cell line was cloned from the peripheral blood of a healthy individual, and has all the characteristics of an NK cell. Most importantly, the cytotoxic activity of NK3.3 can be upregulated by cytokine stimulation (Kornbluth and Hoover, 1988). A cDNA library from interferon beta (IFNβ) stimulated NK3.3 cells was made and differential screening was performed to compare expression in unstimulated cells. From this analysis, 56 IFNβ-upregulated genes were identified; 46 were novel at the time. We named one of those novel cDNA clones Natural Killer Lytic-Associated Molecule (NKLAM) (Kozlowski et al., 1999).

Kinetic analysis determined that NKLAM mRNA levels peak 4–6 h after IFNβ stimulation of NK cells; additionally, NKLAM levels are strongly induced by interleukin (IL)-2, peaking

6–12 h after IL-2 stimulation. These expression levels strongly correlate with both IFNβ and IL-2-enhanced NK3.3 anti-tumor cytolytic activity. NKLAM mRNA is short lived, with a half-life of 2.5 h (Kozlowski et al., 1999).

Peripheral blood subsets from healthy donors were isolated and examined for NKLAM mRNA expression. Levels were found to be relatively high in monocytes and upregulated by IFNβ. NKLAM mRNA levels were also high in NK cells and further upregulated by IL-2 and IFNβ. NKLAM mRNA was not found in resting T cells and not induced by IL-2 or the mitogen phytohemagglutinin (PHA). NKLAM was, however, expressed in a $CD8^+$ cytotoxic T lymphocyte (CTL) clone and further upregulated by exposure to its target antigen (Kozlowski et al., 1999).

## NKLAM Gene Structure

We cloned both full-length human and mouse NKLAM (Portis et al., 2000). NKLAM is highly conserved throughout evolution. There is 89% nucleotide and 94% amino acid homology between human and mouse NKLAM. The human NKLAM gene is composed of 9 exons and is found on chromosome 1 (**Figure 1**). Mouse NKLAM has an almost identical genetic structure of 9 exons and maps to chromosome 4. A major difference is that in humans, there are two forms of NKLAM protein: one is 732 amino acids and the other is 587 amino acids. These arise by alternative splicing in exon 9, resulting in two mRNA transcripts that differ at the 3′ end. Mice (and rats) only produce one mRNA transcript, encoding the longer form of NKLAM protein (Portis et al., 2000). One unresolved question is the functional difference between the two forms of human NKLAM. Both transcripts and proteins are similarly up-regulated and expressed upon activation of human NK cells and macrophages.

## NKLAM Protein Structure and Homology to RING-In Between RING-RING (RBR) Ubiquitin Ligases

When we first described NKLAM, computer analysis predicted it to be a transmembrane protein. It also identified three cysteine-rich clusters, with homology to proteins found in *Caenorhabditis elegans*, mosquitos and in the mouse ovary. This cysteine-rich domain is 99% identical between mouse and human NKLAM. Subsequent cloning and characterization of additional proteins with this signature domain placed NKLAM within the E3 RBR ubiquitin ligase family of proteins. Ubiquitination is one of the most important post-translational modifications, regulating both the stability, function and localization of proteins. Ubiquitin ligases modify proteins by adding either a single ubiquitin or polyubiquitin chains (Swatek and Komander, 2016). Over 800 ubiquitin ligases are known; only 14 have this RBR structure (Smit and Sixma, 2014; Spratt et al., 2014; Lechtenberg et al., 2016; Dove and Klevit, 2017). In addition, only 4 of these are transmembrane proteins like NKLAM. All the RBR E3 ubiquitin ligases are highly conserved and important in cellular physiology. The most studied RBR ligase is Parkin; mutations in Parkin are associated with autosomal recessive juvenile Parkinson's disease (Kitada et al., 1998). By their ability to control expression of key regulatory proteins involved in cell growth and death signaling, ubiquitin ligases also have a role in development of autoimmunity and cancer (Sun, 2006).

Ubiquitination is a three-step process that involves an E1 activating enzyme that uses ATP and a catalytic cysteine to activate ubiquitin, an E2 conjugating enzyme that accepts the activated ubiquitin from the E1, and an E3 ligase that coordinates the ligation of the E2-bound active ubiquitin onto the target protein (Hochstrasser, 1996). There are three families of E3 ubiquitin ligases: HECT-type, RING-type, and RBR-type ligases. HECT ligases contain the HECT (homologous to the E6-AP carboxyl terminus) domain which provides a catalytic cysteine to accept active ubiquitin from the E2 and form an intermediate E3-ubiquitin prior to ligation onto the substrate (Weber et al., 2019). This frees the E2 and enables the HECT E3 ligase to dictate whether the ubiquitin is added singly to a target substrate or ligated to create a ubiquitin chain. RING ligases are identified by the presence of a RING (Really Interesting New Gene) domain of the canonical C3HC4 structure. RING ligases do not have a catalytic cysteine, but function as a scaffold, facilitating the direct transfer of the active ubiquitin from the E2 to the substrate (Metzger et al., 2014). It is, therefore, the E2 that determines the ubiquitin linkage that is created. RBR ligases are composed of a C3HC4 RING domain (RING1), identical to RING-type ligases, followed by an In-Between RING (IBR), and another RING (RING2) domain. RING2 contains a conserved catalytic cysteine for accepting active ubiquitin to form an intermediate E3-ubiquitin, similar to HECT-type ligases (Spratt et al., 2014; Walden and Rittinger, 2018). RBR ligases control ubiquitin linkage type in a manner similar to HECT ligases.

The conserved catalytic cysteine in the RING2 domain of RBR E3 ubiquitin ligases, including Parkin and Dorfin (RNF19A), is considered a defining feature of this ligase family. NKLAM also has a comparable cysteine (C302) that we predict is critical for its ligase activity (Lechtenberg et al., 2016; Dove and Klevit, 2017).

RING-IBR-RING ubiquitin ligases also have preference for the E2s that they interact with. We identified the ubiquitin conjugating enzymes UbcH7 and UbcH8 interacting with NKLAM. There is a level of E2 specificity; UbcH10 is unable to bind NKLAM (Fortier and Kornbluth, 2006). Upon stimulation of NK cells with IFNβ, both NKLAM and UbcH8 are upregulated and can be co-immunoprecipitated. These ubiquitin conjugates bind to the RING domain of NKLAM. Most E2-conjugating enzymes transfer ubiquitins onto both lysine and cysteine residues and therefore function with multiple types of ubiquitin ligases. However, UbcH7 is unique in being strictly cysteine-reactive and works predominantly with RBR E3 ligases like NKLAM (Martino et al., 2018).

The first 100 amino acids of NKLAM consist primarily of alanine, arginine, glutamate, glycine, and proline. Bioinformatic analysis using the DEPICTER server identifies this amino acid stretch as an intrinsically disordered region (IDR) of the protein (Barik et al., 2020; **Figure 2**). This combination and arrangement of amino acids is predicted to give NKLAM the capability to bind RNA, DNA, and protein. Following the N-terminal IDR is the RBR ligase domain of NKLAM. There are two transmembrane domains that anchor the protein, and a second larger IDR at the

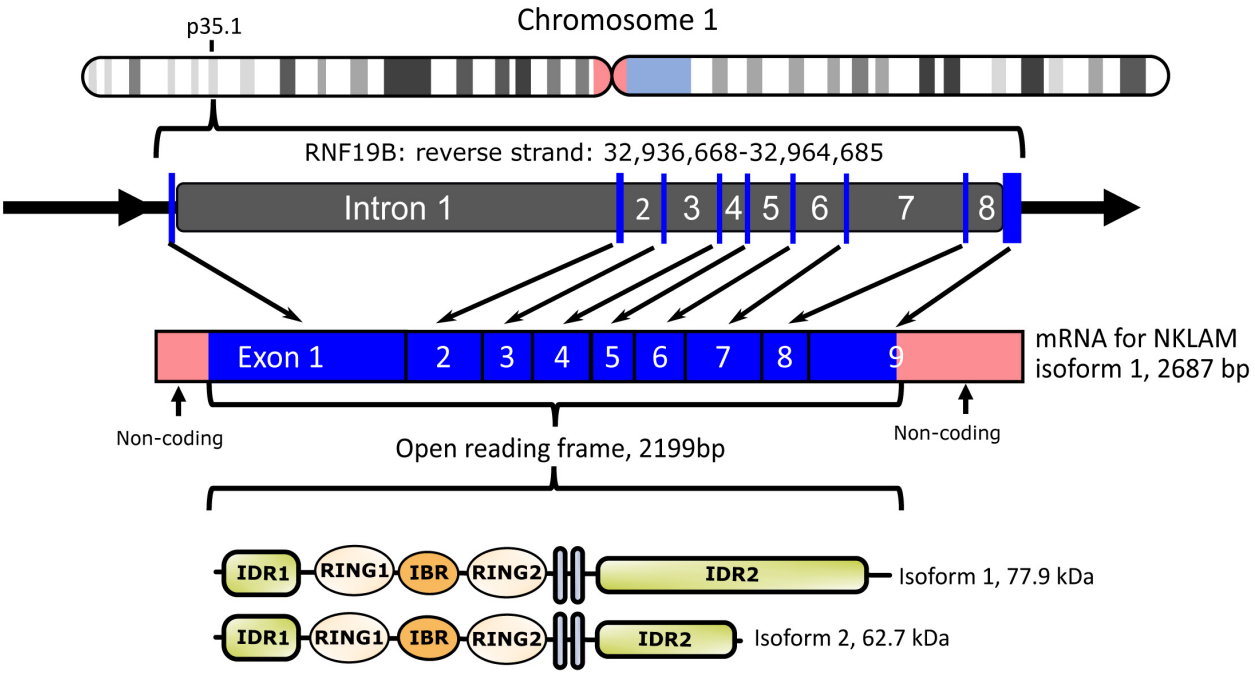


**FIGURE 1 |** Diagram of human NKLAM (RNF19B) gene organization. NKLAM is encoded by 9 exons (depicted as blue bars) spanning 28 kb in the reverse strand of chromosome 1. Exons 1–3 encode intrinsically disordered region 1 (IDR1) and the three RINGS of the ligase domain. Exons 4 and 5 encode the two transmembrane domains (gray bars), while IDR 2 is encoded across the remaining exons 6–9. Mouse NKLAM, located on chromosome 4, has the same genomic structure. Human NKLAM mRNA isoform 1 encodes a protein with a predicted molecular weight of 77.9 kDa. Alternative splicing of exon 9 results in a shorter mRNA isoform 2 encoding a protein with a predicted molecular weight of 62.7 kDa. Mice only express the long form of NKLAM protein.

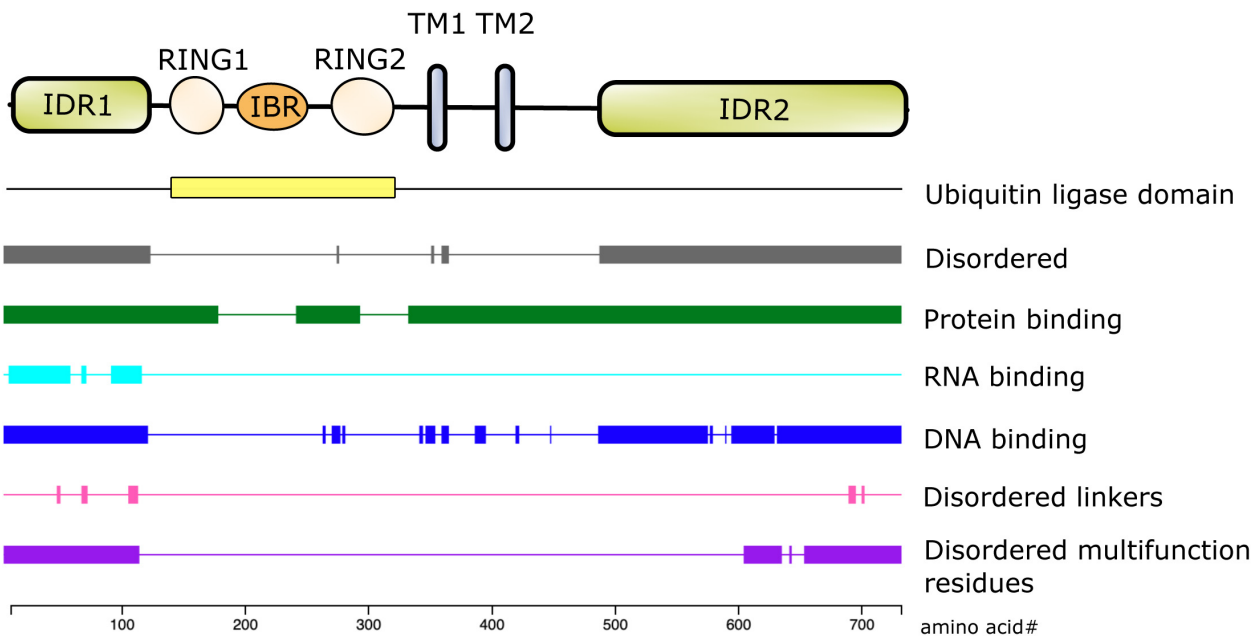


**FIGURE 2 |** Structure/function of NKLAM protein. The RING1-IBR-RING2 (RBR) domain has the ubiquitin ligase activity. RING2 contains the highly conserved, active site catalytic cysteine (C302), which is the defining feature of this family of RBR ligases. In addition to the two transmembrane (TM) domains, the N- and C-terminal ends of NKLAM are intrinsically disordered regions (IDR). Bioinformatic analysis using the DEPICTER server indicate the possible roles of the IDR in protein, DNA, and RNA binding.

C-terminal end of NKLAM that is also predicted to interact with DNA and proteins.

Intrinsically disordered regions are typically rich in charged or polar residues, enabling interactions with proteins or nucleic acids (Wright and Dyson, 2015; Dyson, 2016). These regions are often flexible enough to either conform to the surface of an interacting protein, thereby stabilizing the interaction, or to adopt a different conformation to allow interactions with additional ligands (Dunker et al., 2005). Post-translational modifications of these regions can induce changes in conformation, thereby changing the accessibility of binding sites or altering the activity of the protein (Darling and Uversky, 2018; Owen and Shewmaker, 2019).

## Regulation of NKLAM Expression

Natural killer lytic-associated molecule is expressed by a variety of hematopoietic cells, including NK cells, $CD8^+$ cytotoxic T cells and murine bone marrow-derived macrophages (BMDM). Our earliest studies of NKLAM demonstrated its expression in freshly isolated human peripheral blood monocytes and upregulation by IFNβ. Similar results were obtained using macrophages from the spleen and peritoneal cavity of mice (Portis et al., 2000). There is limited experimental data on NKLAM expression in non-immune cells; however, NKLAM was found to be associated with ppp1cc in testes (Fardilha et al., 2011). Our laboratory found that NKLAM is expressed in mouse tracheal epithelial cells treated with IFNγ (Lawrence et al., 2019). The experimental data on NKLAM expression is largely derived from NK cell and macrophage studies.

Natural killer lytic-associated molecule expression is induced by both IFNγ and IFNβ; thus, NKLAM is an interferon-stimulated gene (ISG). Resting NK cells have low levels of NKLAM; treatment with IFNβ rapidly induces transcription and translation of NKLAM, where it localizes to lytic granule membranes (Kozlowski et al., 1999). In addition to IFNβ, IL-2, IL-12, IL-15, and IL-21 also promote transcription of NKLAM in NK cells. Similarly, under baseline conditions, macrophages express minimal amounts of NKLAM. Treatment with IFNγ induces NKLAM expression in a time dependent manner with maximal levels reached at 12 h (Portis et al., 2000; Lawrence and Kornbluth, 2012). Using transcription factor binding site prediction software PROMO[1], the promoter region of NKLAM contains a binding site for STAT1. The signal transduction pathway for IFNγ, a type II interferon, results in STAT1 binding a gamma-activated sequence (GAS) within an ISG promoter region. Additionally, there are STAT4 and STAT5 binding sites in the NKLAM promoter. STAT4 and STAT5 are involved in signal transduction from various cytokine receptors for IL-2, IL-12, and IL-15. The NKLAM promoter also contains binding sites for members of the interferon-regulatory factor (IRF) family of transcription factors. IRF proteins are regulators of the type I interferon system. The expression of NKLAM in mouse immune cells is the same as seen in human cells and its regulation is also mediated by the same activation signals.

[1]http://alggen.lsi.upc.es/cgi-bin/promo_v3/promo/promoinit.cgi?dirDB=TF_8.3/

Natural killer lytic-associated molecule expression can also be induced by Toll-like receptor (TLR) agonists. Mouse macrophage cell lines RAW 264.7 and J774A.1 were stimulated with TLR4 agonist lipopolysaccharide (LPS), the combination of LPS plus IFNγ, *Escherichia coli,* or *Staphylococcus aureus* and NKLAM protein expression was assessed over time. In both RAW 264.7 and J774 cells, peak NKLAM expression is seen 16 h after stimulation with all treatments (Lawrence and Kornbluth, 2012). Stimulation with LPS plus IFNγ leads to the largest increase in NKLAM levels (Portis et al., 2000). Poly (I:C), a mimetic of double stranded RNA and a TLR3 agonist, was also found to induce NKLAM expression in BMDM (Lawrence et al., 2019). TLR stimulation culminates in the activation of transcription factors NFκB, IRFs, and MAP kinases to regulate gene expression (Kawasaki and Kawai, 2014). In addition to binding sites for IRF-1 and IRF-2, the NKLAM promoter contains binding sites for NFκB proteins p50 and p65/RelA.

# NKLAM FUNCTION

## NKLAM Function in Cytotoxic Cells

Natural killer lytic-associated molecule mRNA expression strongly correlates with cytotoxic activity. To determine whether NKLAM is necessary for NK killing, NK cells were treated with NKLAM antisense (AS) oligonucleotides (ODN) or control ODN. There is a significant and specific downregulation of NKLAM expression and cytotoxic function of NK cells after treatment with NKLAM AS ODN. Granule exocytosis-mediated killing is diminished after NKLAM AS ODN treatment; however, Fas-mediated killing appears to be NKLAM-independent. In 4 h killing assays, the cytotoxic activity of CTL against its specific target is reduced by 60% after treatment with NKLAM AS ODN (Kozlowski et al., 1999). This suggests that NKLAM function is associated with killing mediated by lymphocyte granule exocytosis.

We generated a panel of monoclonal antibodies to NKLAM. Resting peripheral blood NK cells express little to no NKLAM; upon cytokine activation, NKLAM protein levels increase. Subcellular fractionation experiments localized NKLAM to the membranes of the cytolytic granules in NK cells. Unlike other granule proteins, NKLAM is not pre-formed; it is rapidly transcribed, translated and embedded in granule membranes upon NK activation (Kozlowski et al., 1999).

To further investigate the function of NKLAM in NK cytotoxic activity, we generated NKLAM-deficient ($NKLAM^{-/-}$) mice (Hoover et al., 2009). This was accomplished by genomic deletion of exons 2–5, which removes the 2nd and 3rd RING domains and both transmembrane domains. These mice are completely NKLAM deficient. By both RT-PCR and protein analysis, there is no detectable full length or fragments of NKLAM in these mice. Mice were backcrossed to C57BL/6 mice for 11 generations. $NKLAM^{-/-}$ mice appear normal and are fertile. The lymphoid and myeloid subpopulations in the spleen are comparable to wild type (WT) mice in numbers and distribution. They also have normal numbers of NK cells in the spleen; these NK cells have similar amounts of cytotoxic proteins perforin and granzyme B in

their granules as WT NK cells. Granule release is comparable in both NKLAM$^{-/-}$ and WT NK cells. However, NKLAM$^{-/-}$ NK cells have 60% less tumor killing activity *in vitro* and secrete less IFNγ after target or cytokine stimulation (Hoover et al., 2009).

## NKLAM-Mediated Ubiquitination of Uridine-Cytidine Kinase Like-1 (UCKL-1)

We employed the yeast-two-hybrid system to identify potential substrate proteins that bind to and are ubiquitinated by NKLAM. The RING domain of NKLAM was used as bait to trap binding proteins from a human spleen cell cDNA library in yeast. Using high stringency binding conditions, we identified uridine-cytidine kinase-like 1 (UCKL-1, previously called URKL-1) interacting with NKLAM. Co-transfection studies in HEK293 cells confirmed the interaction between NKLAM and UCKL-1, leading to UCKL-1 ubiquitination and degradation (Fortier and Kornbluth, 2006). NKLAM constructs containing one or more of the RING domains were designed and analyzed for their ability to bind UCKL-1 and ubiquitin conjugates. We demonstrated that the entire RBR domain, without the N-terminal and C-terminal regions of NKLAM, is capable of binding UCKL-1, and ubiquitin conjugates UbcH7 and UbcH8. Although UCKL-1 co-immunoprecipitates with multiple combinations of two of the three RING domains, it is maximally ubiquitinated and degraded by full length NKLAM or the entire RBR domain (Fortier and Kornbluth, 2006). Since the highly conserved catalytic cysteine (C302) in the RING2 domain is considered required for its ubiquitin ligase activity, we generated NKLAM constructs with a cysteine to alanine (C-A) mutation of C302 (C302A). A comparison of WT and mutant NKLAM will determine the role of ubiquitination in NKLAM functions.

Uridine kinases are involved in the pyrimidine salvage pathway. UCKL-1 is often upregulated in cancers and is proposed as a biomarker for several cancer types (Geiger et al., 2012; Cheng et al., 2014). Since uridine kinase expression is associated with cancer growth, we hypothesized that upon NK-tumor cell interaction, during the process of granule exocytosis, NKLAM may be able to interact with tumor-associated proteins, like UCKL-1. This would result in loss of UCKL-1 expression in the tumor cell, thereby impacting its survival.

To model the potential effect of NKLAM on reduction of UCKL-1 expression in tumor cells, we performed siRNA experiments. Downregulation of UCKL-1 in tumor cells by siRNA slows their proliferation, induces apoptosis and enhances their susceptibility to NK-mediated lysis (Ambrose and Kornbluth, 2009). Conversely, over-expression of UCKL-1 protects tumor cells from NK killing and enhances tumor survival *in vitro* and *in vivo* (Gullickson et al., 2016). These data suggest a model where, upon NK-tumor interaction and release of lytic granules, NKLAM enters the tumor cell, ubiquitinates and degrades UCKL-1, thereby promoting cell death.

The cytotoxic granules in NK cells are heterogeneous, varying in size and in the amount of electron-dense material in their core. They are called hybrid organelles, with the properties of both lysosomes and secretory granules. This heterogeneity may reflect a continuum of maturation (Burkhardt et al., 1990; De Saint Basile et al., 2010). Some of the granules contain multi-vesicular bodies, where smaller membrane-bound intragranular vesicles, exosomes, are generated. It has been demonstrated that exosomes derived from NK cells contain the cytolytic molecules perforin, granzymes A and B and granulysin, as well as the membrane proteins FasL and CD63, and have anti-tumor cytotoxic activity (Lugini et al., 2012; Jong et al., 2017). During NK-tumor cell interaction and degranulation, exosomes and other extracellular vesicles (EVs) are released, and may participate in tumor killing (Wu et al., 2019). This would provide a mechanism for delivery of the granule membrane protein NKLAM from the NK cell to the target cell, where it would ubiquitinate and degrade UCKL-1, ultimately resulting in cell death. A model of tumor killing is depicted in **Figure 3**.

## Role of NKLAM in Anti-Tumor Activity *in vivo*

The B16 melanoma model of experimental lung metastasis was used to evaluate NK function in NKLAM$^{-/-}$ mice *in vivo*. This model is widely used in studies of NK function *in vivo* because B16 melanoma cells express low amounts of MHC class I molecules, are poorly immunogenic so they do not generate a significant adaptive immune response, and are readily killed by NK cells (Hanna and Burton, 1981; Gorelik et al., 1982; Warner and Dennert, 1982). NKLAM$^{-/-}$ and WT mice were injected intravenously with B16 melanoma cells; tumor colonies in the lungs were counted 15 days later. NKLAM$^{-/-}$ mice have substantially higher numbers and larger lung melanoma nodules than WT mice. These results indicate the importance of NKLAM in controlling tumor metastasis, likely by enhancing NK anti-tumor function (Hoover et al., 2009).

The role of NKLAM in NK-mediated tumor immunity *in vivo* was further investigated by employing additional tumor models to compare tumor development, progression and metastasis in NKLAM$^{-/-}$ and WT mice. We injected mice with RMA-S, a mouse T cell lymphoma, and well-characterized NK-susceptible hematopoietic tumor. These cells are MHC class I negative and are killed exclusively by NK cells (Kim et al., 2000; Cerwenka et al., 2001; Diefenbach et al., 2001). Using a sensitive real-time quantitative PCR assay for tumor burden, we found greater dissemination of RMA-S tumor cells to the lungs, lymph nodes, bone marrow and blood of NKLAM$^{-/-}$ mice compared to WT mice (Hoover et al., 2012). These results indicate that NKLAM$^{-/-}$ mice are less capable of controlling lymphoma dissemination than WT mice.

The potential role of NKLAM in controlling breast cancer growth and metastasis was evaluated by injecting syngeneic EO771 breast cancer cells into the mammary fat pads of NKLAM$^{-/-}$ and WT mice. EO771 is poorly immunogenic, incapable of generating a primary cytotoxic T cell response *in vivo*. It is also estrogen receptor positive, highly aggressive, and prone to metastasis (Ewens et al., 2005; Zhou et al., 2005; Gu et al., 2009). Primary tumor growth is similar between NKLAM$^{-/-}$ and WT mice. However, there are much higher levels of disseminated tumor cells in the bloodstream and more metastatic EO771 breast cancer cells in the lungs of NKLAM$^{-/-}$

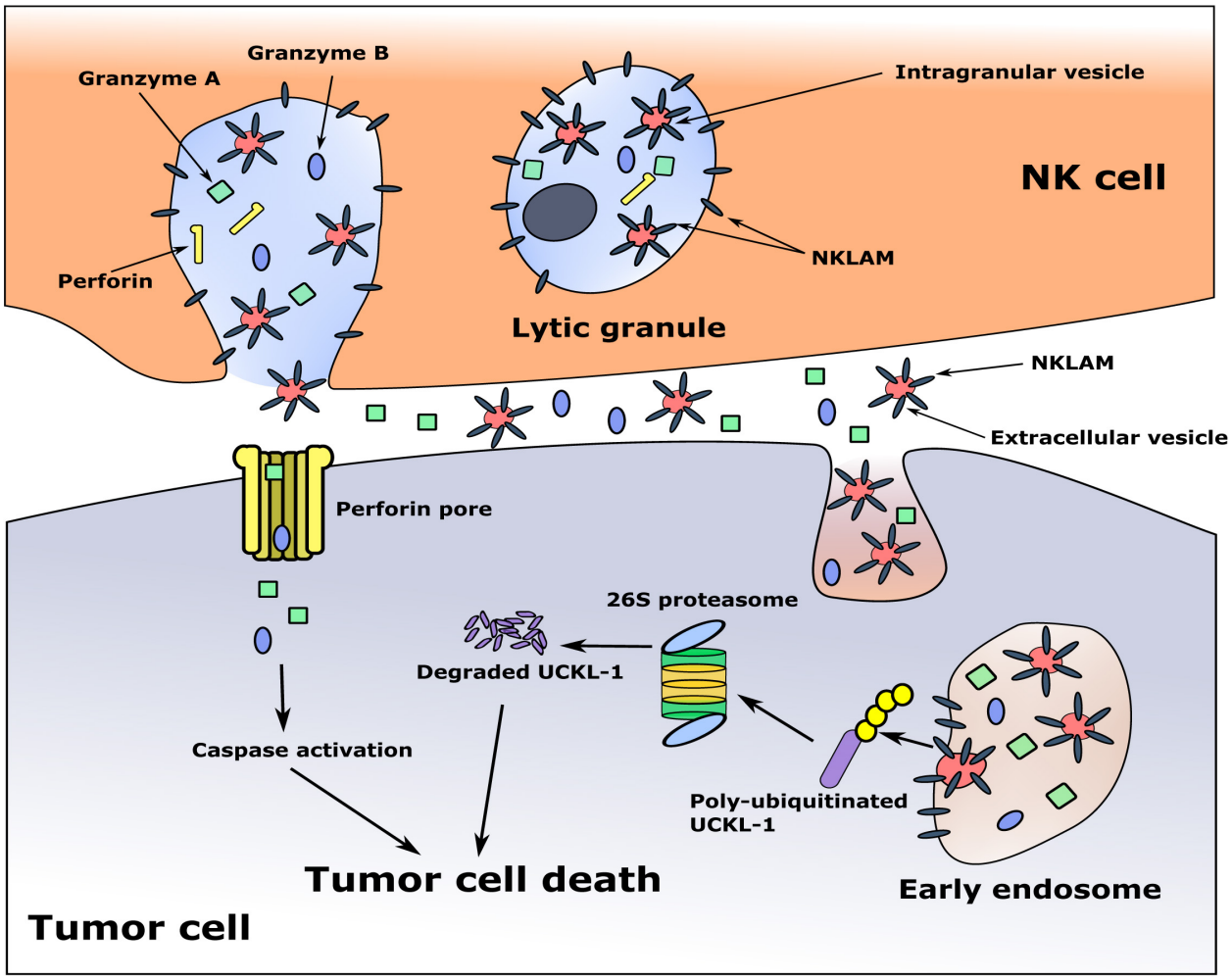


**FIGURE 3 |** Proposed model of NKLAM function in NK cells. The cytolytic granules of resting NK cells contain little to no NKLAM. Upon cytokine exposure or target stimulation, activated NK cells rapidly transcribe and translate NKLAM, which is embedded in cytolytic granule membranes. Smaller, intragranular vesicles also have NKLAM in their membranes. NK-tumor interaction releases granule contents (perforin, granzymes) into the tumor cell at the immunological synapse. Intragranular vesicles are also released; these now called extracellular vesicles (EVs) contain NKLAM, as well as perforin and granzymes, and enter the tumor cell by endocytosis. Granzymes induce caspase activation; NKLAM ubiquitinates and degrades the tumor survival protein UCKL-1. This combination of perforin, granzymes, and NKLAM ensures death of the tumor cell. Red circles: EVs; gray bars: NKLAM; green squares, blue ovals: cytolytic proteins granzymes A and B; yellow bars: perforin; purple bar: UCKL-1; yellow circles: ubiquitin.

than WT mice (Hoover et al., 2012). These results suggest that NKLAM-expressing NK cells play a key role in controlling tumor dissemination and metastasis *in vivo*. Reversal of these effects by reconstitution of NKLAM$^{-/-}$ mice with WT bone marrow would confirm the role of NKLAM$^{+}$ hematopoietic cells in anti-tumor immunity; adoptive transfer of WT NK cells into NKLAM$^{-/-}$ mice would confirm the role of NKLAM$^{+}$ NK cells in controlling tumor spread.

## NKLAM Function in Macrophages

Macrophages are an important cellular component of the innate and adaptive immune systems and represent a first line of defense against invading pathogens. Macrophages employ oxidative and non-oxidative killing mechanisms to rid the host of pathogens. Since NKLAM is highly expressed in macrophages, we performed macrophage bacterial killing studies to determine whether NKLAM plays a role in macrophage bactericidal activity.

Transient transfection of J774 cells with NKLAM results in increased intracellular killing of *E. coli* compared with control-transfected cells. These results suggest that NKLAM enhances macrophage-mediated bacterial degradation. These data were confirmed in experiments using WT and NKLAM$^{-/-}$ BMDM and peritoneal macrophages isolated from WT and NKLAM$^{-/-}$ mice; WT macrophages have greater bacterial killing activity than NKLAM$^{-/-}$ macrophages (Lawrence and Kornbluth, 2012).

We evaluated each of the steps associated with macrophage bactericidal activity. We measured phagocytosis of fluorescently labeled *E. coli* by flow cytometry and found no significant difference in uptake of bacteria between WT and NKLAM$^{-/-}$ macrophages. We also assayed pH reduction during phagosome

maturation by incubating macrophages with *E. coli* labeled with a pH sensitive fluorescent dye (pHrodo). There were no significant differences in phagosome pH between WT and NKLAM$^{-/-}$ macrophages. Additionally, cleavage of cathepsin D, that occurs during phagosome maturation, is also similar between WT and NKLAM$^{-/-}$ macrophages (Lawrence and Kornbluth, 2012).

Phagosome maturation is a highly dynamic process. The number of proteins associated with the phagosome range from hundreds (Garin et al., 2001) to thousands (Trost et al., 2009). These proteins are involved in phagosome trafficking, protein degradation, phagosome acidification, and antigen presentation (Kinchen and Ravichandran, 2008). We isolated phagosomes from WT and NKLAM$^{-/-}$ macrophages and found that NKLAM is a component of macrophage phagosomes and co-localizes with phagosome proteins EEA-1 and LAMP-1 (Lawrence and Kornbluth, 2012). Using immunofluorescence, we localized NKLAM to the phagosome membrane surrounding ingested fluorescently labeled bacteria (Lawrence and Kornbluth, 2012). NKLAM expression in the phagosome is maximal at ∼35 min post-ingestion and this correlates with increased ubiquitination of phagosome proteins; however, the identity of NKLAM phagosome targets is unknown. Ubiquitinated proteins on the phagosome membrane have been shown to interact with ESCRT (endosomal sorting complex required for transport) machinery and are necessary for protein sorting and phagosome maturation (Migliano and Teis, 2018). A recent study by Dean et al. (2019) suggests that post-translational modification of phagosome proteins (e.g., phosphorylation and ubiquitination) may transform the phagosome into a subcellular signaling platform. In support of this concept, a mass spectrometry (MS)-based analysis of macrophage phagosome proteins revealed the presence of ubiquitin conjugation machinery including E1, E2, and E3 enzymes (Guo et al., 2015).

Since NKLAM is a membrane-bound protein, investigation of the orientation of the catalytic RING domain will determine whether NKLAM has access to phagosome cargo or cytosolic targets. If NKLAM is embedded in the phagosome membrane with its catalytic RING domains and C-terminal tail orientated into the cytoplasm, it would have access to phagosome membrane and cytoplasmic targets (**Figure 4**). In such an orientation, NKLAM would have access to bacteria that have evolved phagosomal escape mechanisms (e.g., *Mycobacterium tuberculosis* and *Listeria monocytogenes*). Another RBR ligase, Parkin, has been shown to ubiquitinate cytosolic *M. tuberculosis,* reducing its replication via destruction in the autophagolysosome (Manzanillo et al., 2013). Identification of NKLAM targets will be critical for determining the role of NKLAM in macrophage bactericidal function.

The processes of phagocytosis and autophagy have overlapping roles and mechanisms. LC3-associated phagocytosis (LAP) is a process in which some components of the autophagy pathway are recruited to the phagosome to lipidate LC3 molecules on a single membrane. Despite some overlap, LAP and canonical autophagy are distinct at the molecular, cellular, and functional levels. After phagocytic cargo uptake and phagosome formation, the class 3 PI-3-kinase complex (PI3KC3) is the first to be recruited to the membrane (Heckmann et al., 2017; Herb et al., 2020). This process is shared between LAP and canonical autophagy. Affinity purification MS has identified numerous proteins that interact with NKLAM (Huttlin et al., 2015, 2017). The BioGRID[2] database lists 56 interacting proteins; of these, three are members of the PI-3 kinase complex. This would place NKLAM not only in the phagosome membrane, but also in the membrane of the LAPosome. Our recent studies using a Sendai virus pneumonia model show that the lack of NKLAM negatively affects not only the conversion of LC3I to LC3II but the overall expression of LC3 (Lawrence et al., 2019). This observation implicates NKLAM as a potential regulator of LAP through its regulation of LC3 protein expression. Further studies are needed to determine whether NKLAM acts locally at the level of the LAPosome or more systemically at the transcriptional level.

## NKLAM Regulation of Immune-Associated Transcription Factor Activity

Transcription factors that are crucial to the immune response are proteins of the STAT and NFκB families. Studies from our laboratory have shown that NKLAM plays an important role in regulating the activity of key members of both groups of transcription factors.

Using a transfection-based approach in HEK293 cells, we observed that NKLAM and STAT1 are associated in a protein complex (Lawrence and Kornbluth, 2016). Similar results were obtained using RAW 264.7 macrophages. *In vitro*, NKLAM is transiently localized to the interferon gamma receptor (IFNGR) during BMDM stimulation with IFNγ (Lawrence and Kornbluth, 2016). STAT1 immunoprecipitated from WT and NKLAM$^{-/-}$ BMDM during IFNγ stimulation shows evidence of increased transient K63-linked polyubiquitination in WT but not in NKLAM$^{-/-}$ cells. Total STAT1 levels are not significantly altered during the time course, suggesting that polyubiquitination does not induce large-scale STAT1 degradation (Lawrence and Kornbluth, 2016).

The observation that NKLAM associates with STAT1 and has a positive effect on its K63-linked polyubiquitination prompted us to determine if STAT1 DNA binding and/or transcriptional activity are affected by NKLAM. To that end, we performed oligonucleotide pull down assays. Our results demonstrated that the lack of NKLAM negatively affects STAT1 binding to an oligonucleotide containing a GAS (Lawrence and Kornbluth, 2016). In support of this observation, transfection studies using a GAS luciferase reporter plasmid demonstrated that STAT1-mediated transcriptional activity is lower in NKLAM$^{-/-}$ than in WT cells (Lawrence and Kornbluth, 2016). Precisely which lysines of STAT1 serve as potential NKLAM ubiquitination targets and how ubiquitination affects STAT1 activity remain to be determined. Interestingly, a study by Huntelmann et al. (2014) determined that lysine 567 in STAT1 is required for GAS recognition; however, it has not been determined if that particular lysine is ubiquitinated. Recently, Guo et al. (2020) demonstrated

[2]https://thebiogrid.org/

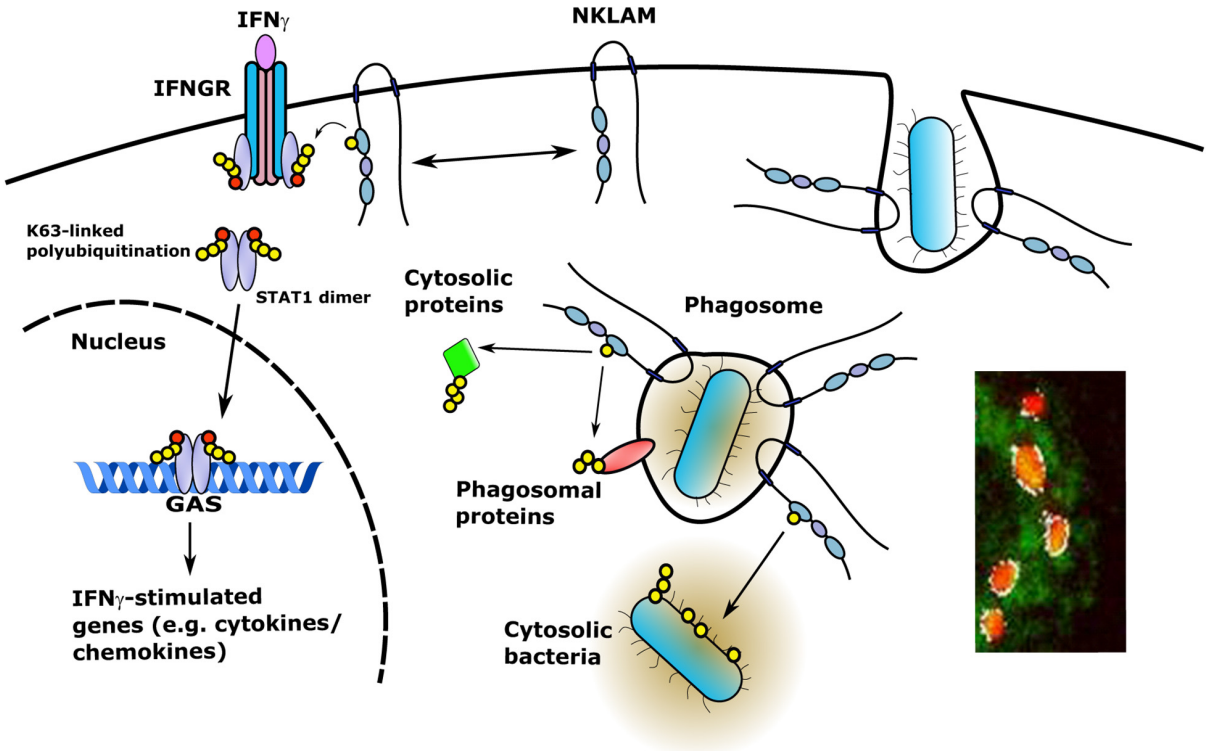


**FIGURE 4 |** NKLAM in macrophage immune function. Upon exposure to IFNγ, STAT1 is phosphorylated and NKLAM is transiently associated with the IFNγ-IFNGR complex at the plasma membrane. In this location, NKLAM is in close proximity to STAT1, which would allow NKLAM to ubiquitinate STAT1 or other proteins to promote STAT1 transcriptional activity. After ingestion of bacterial targets, NKLAM is localized to the phagosome membrane with the catalytic RING2 domain and C-terminal tail facing the cytoplasm. This would provide NKLAM with access to phagosome membrane proteins and cytosolic target proteins, as well as bacteria that escape the phagosome. Red circles; phosphotyrosine, yellow circles; ubiquitin. Immunomicrograph insert: Macrophage phagosomes after ingestion of fluorescent-labeled *E. coli* (red). NKLAM staining: green; Image J-defined co-localization of *E. coli* and NKLAM: white. Adapted from Lawrence, D.W., and Kornbluth, J. E3 ubiquitin ligase NKLAM is a macrophage phagosome protein and plays a role in bacterial killing. Copyright 2012, with permission from Elsevier and Lawrence D.W., and Kornbluth, J. E3 ubiquitin ligase NKLAM ubiquitinates STAT1 and positively regulates STAT1-mediated transcriptional activity. Copyright 2016, with permission from Elsevier.

that E3 ligase RNF220 mediated K63-linked ubiquitination of STAT1 at lysine 110 promotes the interaction between STAT1 and JAK1. Similar to our studies, the authors showed that RNF220 expression was induced by IFNγ signaling and importantly, K63-linked ubiquitination of STAT1 promoted cytokine induction (Guo et al., 2020). Additionally, others have shown that K63-linked poly-ubiquitination of transcription factors is a positive regulator of transcriptional activity (Adhikary et al., 2005; Yao et al., 2018).

STAT1 phosphorylation precedes translocation into the nucleus and transcriptional activation. NKLAM affects the phosphorylation state of both STAT1 and STAT3 during active pulmonary infection. In a model of bacterial pneumonia, STAT1 and STAT3 phosphorylation in the lungs of mice infected with *Streptococcus pneumoniae* is significantly lower in NKLAM$^{-/-}$ mice than in WT mice (Lawrence and Kornbluth, 2018). In support of this novel observation, we observed that phosphatase activity is significantly higher in NKLAM$^{-/-}$ mouse lungs infected with *S. pneumoniae* (Lawrence and Kornbluth, 2018). In a parallel study, using a model of viral pneumonia, STAT1 phosphorylation is also lower in lungs from NKLAM$^{-/-}$ mice than from WT mice infected with Sendai virus (SeV) (Lawrence et al., 2019).

The NFκB pathway is considered the prototypical proinflammatory signaling cascade. NFκB regulates the expression of proinflammatory cytokines and chemokines crucial to the immune response. We found that nuclear translocation of the NFκB protein p65 is significantly delayed in NKLAM$^{-/-}$ BMDM compared to WT macrophages after stimulation with LPS (Lawrence et al., 2015). The classical consensus nuclear localization signal (NLS) contains lysine and arginine residues (K-K/R-X-K/R), and is thus a potential target for ubiquitin ligases; however, data demonstrating that E3 ubiquitin ligases can positively regulate nuclear import via NLS ubiquitination is lacking.

Studies in macrophages treated with LPS have also shown that p65 phosphorylation at serine 536 is significantly attenuated in NKLAM$^{-/-}$ macrophages (Lawrence et al., 2015). Phosphorylation at serine 536 is associated with NFκB transcriptional activity (Giridharan and Srinivasan, 2018). In agreement with the above studies, NKLAM$^{-/-}$ macrophages have attenuated NFκB transcriptional activity as determined by

a luciferase reporter assay, as well as lower expression of iNOS, a protein regulated by NFκB. Similarly, p65 phosphorylation in the lung is lower in NKLAM$^{-/-}$ mice than in WT mice infected with SeV (Lawrence et al., 2019).

Collectively, these data suggest that NKLAM is involved in regulating the phosphorylation state of two immunologically important transcription factors, and in doing so, positively modulates their transcriptional activity. An attractive hypothesis is that NKLAM promotes the ubiquitin-dependent degradation of key phosphatases, resulting in maintenance of the phosphorylated state of the transcription factor, thus sustaining its activation of gene expression. Studies are ongoing to test this hypothesis.

## Regulation of Cytokine and Chemokine Expression by NKLAM

Cytokines and chemokines are immune regulators that control cell activation, migration, and differentiation. Many of the target genes of the STAT and NFκB family of transcription factors are cytokines and chemokines. This fact prompted our investigation into the regulation of cytokine and chemokine expression by NKLAM.

Early analyses of NK cells from NKLAM$^{-/-}$ mice found that they secrete significantly less IFNγ than WT NK cells after target cell stimulation (Hoover et al., 2009). Initial *in vitro* studies demonstrated that BMDM and resident splenic macrophages from NKLAM$^{-/-}$ mice produce significantly less IFNβ than WT macrophages following treatment with LPS (Lawrence et al., 2015). Additionally, NKLAM$^{-/-}$ macrophages produce less IL-6, IFNγ, and MCP-1 than WT macrophages when treated with poly (I:C) (Lawrence et al., 2019). Tracheal epithelial cells isolated from NKLAM$^{-/-}$ mice produce significantly less IL-6 and IFNγ than WT cells when infected with SeV (Lawrence et al., 2019). Importantly, this observation demonstrates that the regulation of proinflammatory cytokine production by NKLAM is not limited to immune cells. *In vivo* infection studies confirm a role for NKLAM in regulating proinflammatory cytokine expression. Both viral (SeV) and bacterial (*S. pneumoniae*) pneumonia models demonstrate that the lack of NKLAM results in significantly lower cytokine/chemokine levels in the lungs and plasma of infected mice (Lawrence and Kornbluth, 2018; Lawrence et al., 2019).

There are several chemokines among the list of cytokines tested in our animal infection studies, including MCP-1, MIP-1α, RANTES, and KC (**Table 1**). These chemokines serve to recruit leukocytes to sites of inflammation. In infected NKLAM$^{-/-}$ mice, chemokine expression is significantly lower than in WT mice. This corresponds to significantly fewer leukocytes recruited into the lungs of infected mice, as determined by both flow cytometric and histologic studies (Lawrence and Kornbluth, 2018; Lawrence et al., 2019). NKLAM$^{-/-}$ mice are not able to mount an immune response to *S. pneumoniae* and SeV comparable to WT mice.

Decreased cytokine and chemokine production in response to infection would suggest that NKLAM$^{-/-}$ mice are immunocompromised. Indeed, we found this to be the case when

**TABLE 1 |** Proinflammatory cytokines and chemokines were measured in NKLAM$^{-/-}$ and WT cells treated with LPS or IFNγ *in vitro* and in biological tissues and organs from NKLAM$^{-/-}$ and WT mice exposed to live pathogens or TLR agonists *in vivo*.

| Cytokine/ Chemokine: | Stimulus: | Cell Type/Tissue: | References |
|---|---|---|---|
| IL-1 | SeV | Lung | Lawrence et al., 2019 |
| IL-2 | SeV | Lung | Lawrence et al., 2019 |
| IL-6 | SeV, Poly (I:C) | Lung, Tracheal epithelial cells, Macrophages (BMDM) | Lawrence et al., 2019 |
| IL-12 | SeV, *S. pneumoniae* | Lung | Lawrence et al., 2019; Lawrence and Kornbluth, 2018 |
| IL-17 | SeV | Lung | Lawrence et al., 2019 |
| IFNγ | Tumor cell stimulation, SeV, *S. pneumoniae*, Poly (I:C) | NK cells, Lung, Plasma, Macrophages (BMDM) | Hoover et al., 2009; Lawrence and Kornbluth, 2018; Lawrence et al., 2019 |
| IFNβ | LPS, SeV | Macrophages (BMDM), Macrophages (spleen), Tracheal epithelial cells | Lawrence et al., 2015; Lawrence et al., 2019 |
| TNFα | SeV, *S. pneumoniae* | Lung | Lawrence et al., 2019; Lawrence and Kornbluth, 2018 |
| KC | SeV | Lung | Lawrence et al., 2019 |
| MCP-1 | SeV, *S. pneumoniae*, Poly (I:C) | Lung, Plasma, Macrophages (BMDM) | Lawrence and Kornbluth, 2018; Lawrence et al., 2019 |
| RANTES | IFNγ, SeV | Macrophages (BMDM), Lung | Lawrence and Kornbluth, 2016; Lawrence et al., 2019 |
| MIP-1α | SeV | Lung | Lawrence et al., 2019 |
| MIP-1β | SeV | Lung | Lawrence et al., 2019 |
| MIP-2 | SeV | Lung | Lawrence et al., 2019 |
| GM-CSF | SeV | Lung | Lawrence et al., 2019 |
| G-CSF | SeV | Lung | Lawrence et al., 2019 |
| IP-10 | SeV | Lung | Lawrence et al., 2019 |
| Eotaxin-1 | SeV | Lung | Lawrence et al., 2019 |
| AXL | SeV | Lung | Lawrence et al., 2019 |

we infected mice with a large dose of Sendai virus. Eighty percent of NKLAM$^{-/-}$ mice died 8 days post-infection compared to only 20% of WT mice. A large, pathogenic challenge overwhelms NKLAM$^{-/-}$ mice and leads to rapid mortality. The lack of a robust immune response by NKLAM$^{-/-}$ mice in this instance is detrimental. However, when smaller doses of infectious agents (either SeV or *S. pneumoniae*) are given, NKLAM$^{-/-}$ mice are afforded a slight survival benefit. This is likely due to less inflammatory leukocytes in the lungs of NKLAM$^{-/-}$ mice, which would correspond to less host-mediated tissue destruction during inflammation.

These data suggest a model for a role of NKLAM in STAT1-mediated transcriptional activity in macrophages, in cytokine and chemokine production and in their phagosome-mediated pathogen destruction (**Figure 4**)[3]. Overall, these studies are defining NKLAM as a key component of the innate immune system. Further research into NKLAM substrates and potential immune signaling pathways is warranted to identify novel control points for the therapeutic modulation of inflammation.

## Links Between RBR Family Members and Immune Functions

There is very limited published data from other investigators regarding the expression/function of NKLAM. However, they collectively point to a role of NKLAM in innate immunity and response to infectious agents. One report showed that NKLAM expression is increased in chickens infected with pathogenic avian influenza virus; this increase is associated with survivability (Uchida et al., 2012). Another study documented upregulation of NKLAM expression in salmon exposed to infectious salmon anemia virus (Li et al., 2011). NKLAM levels are also significantly increased in grass carp infected with grass carp reovirus (Luo et al., 2019). The precise function of NKLAM in these infection models was not determined, but implicates NKLAM as an important component of innate immunity.

A study comparing gene expression in monocytes from adults with low versus high peak bone mass was performed to identify potential genes associated with osteoclast differentiation (Xiao et al., 2012). One of the candidate genes was NKLAM, suggesting that it plays a role in osteoporosis. NKLAM (RNF19B) gene expression was also upregulated, along with other pro-inflammatory genes, in the peripheral blood of Chinese patients with acute myocardial infarction compared to healthy controls (Su et al., 2018). Survey of the Gene Expression Omnibus (GEO)[4] of microarray analyses identified elevation of NKLAM mRNA expression in monocytes and macrophages exposed to LPS, *Borrelia burgdorferi* (the spirochete responsible for Lyme disease), *Chlamydia pneumoniae*, *Francisella tularensis* (the causative agent for tularemia), *Porphyromonas gingivalis* (the pathogenic bacterium associated with periodontitis), *M. tuberculosis*, as well as upon infection with several adenoviruses and rhinoviruses that cause respiratory infections.

Other RBR family members have also been implicated in innate immune function. Alterations in the Parkin gene (*PARK2*) have been associated with increased susceptibility to *Salmonella typhi*, *Salmonella paratyphi* (Ali et al., 2006), and *Mycobacterium leprae* (Mira et al., 2004; Malhotra et al., 2006). Additionally, Parkin-deficient mice and *Drosophila melanogaster* are highly susceptible to infection with *M. tuberculosis* (Manzanillo et al., 2013). In a recent study, Aalto et al. (2019) found that RBR family member HOIP (HOIL-1L interacting protein) ortholog LUBEL was required for *D. melanogaster* to survive oral challenge with Gram-negative bacteria.

## Role of NKLAM in Non-Immune Functions

Hematopoietic cell activation is not the only circumstance that elicits NKLAM expression. In searching for ubiquitin ligases that may be involved in protein degradation within the endoplasmic reticulum (ER), Kaneko et al. (2016) found that HeLa cells undergoing ER stress, caused by exposure to thapsigargin or tunicamycin, upregulated NKLAM mRNA expression. In another study, it was found that MCF7 breast cancer cells upregulate NKLAM expression when exposed to oxyphenisatin acetate, a drug that was being tested as a potential cancer therapeutic (Morrison et al., 2013). This drug is known to have antiproliferative activity, but the investigators learned that treatment with this drug is also associated with autophagy, mitochondrial dysfunction, and generation of reactive oxygen species.

NKLAM mRNA expression is induced in mouse tracheal epithelial cells infected with SeV (Lawrence et al., 2019). However, these levels are extremely low compared to that seen in NK cells and macrophages. The role of non-hematopoietic cells in the phenotype we observe in NKLAM$^{-/-}$ mice is uncertain. Reconstitution of these mice with WT bone marrow will help answer this question.

Protein ubiquitination is a critical regulatory mechanism of autophagy, controlling its initiation, execution, and termination (Chen et al., 2019). One of our recent studies suggests that NKLAM may play a role in autophagic flux. Upon induction of autophagy by treatment with rapamycin, NKLAM$^{-/-}$ macrophages convert less LC3I to LC3II and translocate less LC3 to autophagosomes than WT macrophages. These indicators of autophagy suggest that NKLAM is associated with autophagic flux and expression of key autophagy-related proteins (Lawrence et al., 2019). Further studies are underway to analyze the role of NKLAM in autophagy.

# FUTURE DIRECTIONS

Identification of the role of the ubiquitin ligase activity of NKLAM *in vitro* and *in vivo* is of paramount importance. The derivation of an NKLAM$^{-/-}$ NK3.3 cell line is in development to further delineate the role NKLAM plays in human NK cell effector function. This cell line, in combination with fluorescently

[3] Adapted from Lawrence, D.W., and Kornbluth, J. E3 ubiquitin ligase NKLAM is a macrophage phagosome protein and plays a role in bacterial killing. Copyright 2012, with permission from Elsevier and Lawrence D.W., and Kornbluth, J. E3 ubiquitin ligase NKLAM ubiquitinates STAT1 and positively regulates STAT1-mediated transcriptional activity. Copyright 2016, with permission from Elsevier.

[4] https://www.ncbi.nlm.nih.gov/geo/

tagged NKLAM WT and ligase-inactive constructs, will provide the ability to monitor and measure differences between WT and NKLAM$^{-/-}$ NK cells during activation, effector function, and target cell death. Similarly, these NKLAM constructs will allow us to track NKLAM in macrophages during the process of phagocytosis and pathogen destruction and facilitate identification of NKLAM-interacting proteins during this event. Comparison of cells expressing WT and NKLAM constructs with mutations in the RBR domain (C302A) will be critical for establishing the role of ubiquitination in the function of NKLAM. Similarly, introduction of WT and catalytically inactive NKLAM into NKLAM$^{-/-}$ mice would allow for studies of the ubiquitination function of NKLAM *in vivo*.

Experimental evidence that defines specific targets of RBR ligases is limited. The exception is RBR ligase Parkin, which has been shown to ubiquitinate dozens of proteins (Sarraf et al., 2013). The identification of NKLAM substrates would provide insight into the cellular mechanisms regulated by NKLAM-mediated ubiquitination. To this end, the use of diGly capture and MS detection methodologies followed by bioinformatic comparison of WT and NKLAM$^{-/-}$ ubiquitomes will allow us to define specific NKLAM target proteins. Identification of NKLAM substrates, as well as the specific lysines targeted by NKLAM, will allow for the development of reagents that can be used to modulate NKLAM function in the context of innate immunity.

Several proteins that interact with NKLAM have been identified by affinity purification MS; 56 in the BioGRID database and 71 in IntAct[5]. The biological/functional validity and significance of these protein associations remains to be determined.

The prediction that intrinsically disordered domains may bind RNA or DNA provides an interesting direction for research on NKLAM. RNA-protein interactions can be divided into two categories: (1) RNA acting on the RNA binding protein (RBP) (Lunde et al., 2007) or (2) the RBP acting on the RNA (Oliveira et al., 2017). When RNA acts on the RBP, it can lead to changes in RBP function, localization, stability, or interactions. An RBP acting on the RNA can change RNA stability, processing or modification. DNA binding proteins would be localized to the nucleus and likely play a role in gene transcription, replication, repair or the regulation of those processes.

The potential for these disordered regions to interact with a variety of proteins and for these interactions to be controlled by post-translational modifications will make studying these interactions inherently difficult. NKLAM expression is tightly regulated and induced under specific activation conditions. These conditions may alter the post-translational modifications of NKLAM, thereby exposing it to different combinations of interactors (protein, DNA, and RNA). It will be necessary to not just identify which region an interacting protein binds to but also under what conditions it interacts with NKLAM, as well as differentiate between interacting proteins and ubiquitinated substrates.

Studies to date have shown that NKLAM is a unique and important ubiquitin ligase that participates in multiple regulatory pathways essential for immune function. A greater understanding of its role in controlling infection, inflammation and anti-tumor activity will hopefully lead to the development of new strategies for treating bacterial and viral infections, sepsis, autoimmunity, and cancer.

## AUTHOR CONTRIBUTIONS

DL, PW, AC, EM, and JK contributed to the writing and editing of this review article. DL prepared the figures and table. The research performed by the Kornbluth laboratory was funded by grants obtained by JK. All authors are accountable for the content of this review article.

## FUNDING

This research by the Kornbluth laboratory described in this review article was funded by Merit Awards (I01 BX000705) provided to JK by the United States Department of Veterans Affairs, Biomedical Laboratory Research and Development Service[6]. The funders had no role in study design, data collection and analysis, decision to publish, or preparation of the manuscript. Additional funding was provided by the Department of Pathology and Saint Louis University.

## ACKNOWLEDGMENTS

The authors thank the students, fellows and staff who contributed to the studies of NKLAM over the past 20 years. The authors also thank the Research Microscopy Core, Flow Cytometry Core, and Comparative Medicine staff at Saint Louis University for their expertise and support.

[5] https://www.ebi.ac.uk/intact/

[6] https://www.va.gov/

## REFERENCES

Aalto, A. L., Mohan, A. K., Schwintzer, L., Kupka, S., Kietz, C., Walczak, H., et al. (2019). M1-linked ubiquitination by LUBEL is required for inflammatory responses to oral infection in *Drosophila*. *Cell Death Differ.* 26, 860–876. doi: 10.1038/s41418-018-0164-x

Adhikary, S., Marinoni, F., Hock, A., Hulleman, E., Popov, N., Beier, R., et al. (2005). The ubiquitin ligase HectH9 regulates transcriptional activation by Myc and is essential for tumor cell proliferation. *Cell* 123, 409–421. doi: 10.1016/j.cell.2005.08.016

Ali, S., Vollaard, A. M., Widjaja, S., Surjadi, C., Van De Vosse, E., and Van Dissel, J. T. (2006). PARK2/PACRG polymorphisms and susceptibility to typhoid and paratyphoid fever. *Clin. Exp. Immunol.* 144, 425–431. doi: 10.1111/j.1365-2249.2006.03087.x

Ambrose, E. C., and Kornbluth, J. (2009). Downregulation of uridine-cytidine kinase like-1 decreases proliferation and enhances tumor susceptibility to lysis

by apoptotic agents and natural killer cells. *Apoptosis* 14, 1227–1236. doi: 10.1007/s10495-009-0385-z

Barik, A., Katuwawala, A., Hanson, J., Paliwal, K., Zhou, Y., and Kurgan, L. (2020). DEPICTER: intrinsic disorder and disorder function prediction server. *J. Mol. Biol.* 432, 3379–3387. doi: 10.1016/j.jmb.2019.12.030

Burkhardt, J. K., Hester, S., Lapham, C. K., and Argon, Y. (1990). The lytic granules of natural killer cells are dual-function organelles combining secretory and pre-lysosomal compartments. *J. Cell Biol.* 111, 2327–2340. doi: 10.1083/jcb.111.6.2327

Cerwenka, A., Baron, J. L., and Lanier, L. L. (2001). Ectopic expression of retinoic acid early inducible-1 gene (RAE-1) permits natural killer cell-mediated rejection of a MHC class I-bearing tumor in vivo. *Proc. Natl. Acad. Sci. U.S.A.* 98, 11521–11526. doi: 10.1073/pnas.201238598

Chen, R. H., Chen, Y. H., and Huang, T. Y. (2019). Ubiquitin-mediated regulation of autophagy. *J. Biomed. Sci.* 26:80. doi: 10.1186/s12929-019-0569-y

Cheng, W. S., Tao, H., Hu, E. P., Liu, S., Cai, H. R., Tao, X. L., et al. (2014). Both genes and lncRNAs can be used as biomarkers of prostate cancer by using high throughput sequencing data. *Eur. Rev. Med. Pharmacol. Sci.* 18, 3504–3510.

Darling, A. L., and Uversky, V. N. (2018). Intrinsic disorder and posttranslational modifications: the darker side of the biological dark matter. *Front. Genet.* 9:158. doi: 10.3389/fgene.2018.00158

De Saint Basile, G., Menasche, G., and Fischer, A. (2010). Molecular mechanisms of biogenesis and exocytosis of cytotoxic granules. *Nat. Rev. Immunol.* 10, 568–579. doi: 10.1038/nri2803

Dean, P., Heunis, T., Hartlova, A., and Trost, M. (2019). Regulation of phagosome functions by post-translational modifications: a new paradigm. *Curr. Opin. Chem. Biol.* 48, 73–80. doi: 10.1016/j.cbpa.2018.11.001

Diefenbach, A., Jensen, E. R., Jamieson, A. M., and Raulet, D. H. (2001). Rae1 and H60 ligands of the NKG2D receptor stimulate tumour immunity. *Nature* 413, 165–171. doi: 10.1038/35093109

Dove, K. K., and Klevit, R. E. (2017). RING-between-RING E3 ligases: emerging themes amid the variations. *J. Mol. Biol.* 429, 3363–3375. doi: 10.1016/j.jmb.2017.08.008

Dunker, A. K., Cortese, M. S., Romero, P., Iakoucheva, L. M., and Uversky, V. N. (2005). Flexible nets. The roles of intrinsic disorder in protein interaction networks. *FEBS J.* 272, 5129–5148. doi: 10.1111/j.1742-4658.2005.04948.x

Dyson, H. J. (2016). Making sense of intrinsically disordered proteins. *Biophys. J.* 110, 1013–1016. doi: 10.1016/j.bpj.2016.01.030

Ewens, A., Mihich, E., and Ehrke, M. J. (2005). Distant metastasis from subcutaneously grown E0771 medullary breast adenocarcinoma. *Anticancer Res.* 25, 3905–3915.

Fardilha, M., Esteves, S. L., Korrodi-Gregorio, L., Vintem, A. P., Domingues, S. C., Rebelo, S., et al. (2011). Identification of the human testis protein phosphatase 1 interactome. *Biochem. Pharmacol.* 82, 1403–1415. doi: 10.1016/j.bcp.2011.02.018

Fortier, J. M., and Kornbluth, J. (2006). NK lytic-associated molecule, involved in NK cytotoxic function, is an E3 ligase. *J. Immunol.* 176, 6454–6463. doi: 10.4049/jimmunol.176.11.6454

Garin, J., Diez, R., Kieffer, S., Dermine, J. F., Duclos, S., Gagnon, E., et al. (2001). The phagosome proteome: insight into phagosome functions. *J. Cell Biol.* 152, 165–180. doi: 10.1083/jcb.152.1.165

Geiger, T., Madden, S. F., Gallagher, W. M., Cox, J., and Mann, M. (2012). Proteomic portrait of human breast cancer progression identifies novel prognostic markers. *Cancer Res.* 72, 2428–2439. doi: 10.1158/0008-5472.CAN-11-3711

Giridharan, S., and Srinivasan, M. (2018). Mechanisms of NF-kappaB p65 and strategies for therapeutic manipulation. *J. Inflamm. Res.* 11, 407–419. doi: 10.2147/JIR.S140188

Gorelik, E., Wiltrout, R. H., Okumura, K., Habu, S., and Herberman, R. B. (1982). Role of NK cells in the control of metastatic spread and growth of tumor cells in mice. *Int. J. Cancer* 30, 107–112. doi: 10.1002/ijc.2910300118

Gu, J. W., Young, E., Busby, B., Covington, J., and Johnson, J. W. (2009). Oral administration of pyrrolidine dithiocarbamate (PDTC) inhibits VEGF expression, tumor angiogenesis, and growth of breast cancer in female mice. *Cancer Biol. Ther.* 8, 514–521. doi: 10.4161/cbt.8.6.7689

Gullickson, G., Ambrose, E. C., Hoover, R. G., and Kornbluth, J. (2016). Uridine cytidine kinase like-1 enhances tumor cell proliferation and mediates protection from natural killer-mediated killing. *Int. J. Immunol. Immunother.* 3. doi: 10.23937/2378-3672/1410018

Guo, M., Hartlova, A., Dill, B. D., Prescott, A. R., Gierlinski, M., and Trost, M. (2015). High-resolution quantitative proteome analysis reveals substantial differences between phagosomes of RAW 264.7 and bone marrow derived macrophages. *Proteomics* 15, 3169–3174. doi: 10.1002/pmic.201400431

Guo, X., Ma, P., Li, Y., Yang, Y., Wang, C., Xu, T., et al. (2020). RNF220 mediates K63-linked polyubiquitination of STAT1 and promotes host defense. *Cell Death Differ.* doi: 10.1038/s41418-020-00609-7 [Epub ahead of print].

Hanna, N., and Burton, R. C. (1981). Definitive evidence that natural killer (NK) cells inhibit experimental tumor metastases in vivo. *J. Immunol.* 127, 1754–1758.

Heckmann, B. L., Boada-Romero, E., Cunha, L. D., Magne, J., and Green, D. R. (2017). LC3-associated phagocytosis and inflammation. *J. Mol. Biol.* 429, 3561–3576. doi: 10.1016/j.jmb.2017.08.012

Herb, M., Gluschko, A., and Schramm, M. (2020). LC3-associated phagocytosis - the highway to hell for phagocytosed microbes. *Semin. Cell Dev. Biol.* 101, 68–76. doi: 10.1016/j.semcdb.2019.04.016

Hochstrasser, M. (1996). Ubiquitin-dependent protein degradation. *Annu. Rev. Genet.* 30, 405–439. doi: 10.1146/annurev.genet.30.1.405

Hoover, R. G., Gullickson, G., and Kornbluth, J. (2009). Impaired NK cytolytic activity and enhanced tumor growth in NK lytic-associated molecule-deficient mice. *J. Immunol.* 183, 6913–6921. doi: 10.4049/jimmunol.0901679

Hoover, R. G., Gullickson, G., and Kornbluth, J. (2012). Natural killer lytic-associated molecule plays a role in controlling tumor dissemination and metastasis. *Front. Immunol.* 3:393. doi: 10.3389/fimmu.2012.00393

Huntelmann, B., Staab, J., Herrmann-Lingen, C., and Meyer, T. (2014). A conserved motif in the linker domain of STAT1 transcription factor is required for both recognition and release from high-affinity DNA-binding sites. *PLoS One* 9:e97633. doi: 10.1371/journal.pone.0097633

Huttlin, E. L., Bruckner, R. J., Paulo, J. A., Cannon, J. R., Ting, L., Baltier, K., et al. (2017). Architecture of the human interactome defines protein communities and disease networks. *Nature* 545, 505–509. doi: 10.1038/nature22366

Huttlin, E. L., Ting, L., Bruckner, R. J., Gebreab, F., Gygi, M. P., Szpyt, J., et al. (2015). The BioPlex network: a systematic exploration of the human interactome. *Cell* 162, 425–440. doi: 10.1016/j.cell.2015.06.043

Jong, A. Y., Wu, C. H., Li, J., Sun, J., Fabbri, M., Wayne, A. S., et al. (2017). Large-scale isolation and cytotoxicity of extracellular vesicles derived from activated human natural killer cells. *J. Extracell. Vesicles* 6:1294368. doi: 10.1080/20013078.2017.1294368

Kaneko, M., Iwase, I., Yamasaki, Y., Takai, T., Wu, Y., Kanemoto, S., et al. (2016). Genome-wide identification and gene expression profiling of ubiquitin ligases for endoplasmic reticulum protein degradation. *Sci. Rep.* 6:30955. doi: 10.1038/srep30955

Kawasaki, T., and Kawai, T. (2014). Toll-like receptor signaling pathways. *Front. Immunol.* 5:461. doi: 10.3389/fimmu.2014.00461

Kim, S., Iizuka, K., Aguila, H. L., Weissman, I. L., and Yokoyama, W. M. (2000). In vivo natural killer cell activities revealed by natural killer cell-deficient mice. *Proc. Natl. Acad. Sci. U.S.A.* 97, 2731–2736. doi: 10.1073/pnas.050588297

Kinchen, J. M., and Ravichandran, K. S. (2008). Phagosome maturation: going through the acid test. *Nat. Rev. Mol. Cell Biol.* 9, 781–795. doi: 10.1038/nrm2515

Kitada, T., Asakawa, S., Hattori, N., Matsumine, H., Yamamura, Y., Minoshima, S., et al. (1998). Mutations in the parkin gene cause autosomal recessive juvenile parkinsonism. *Nature* 392, 605–608. doi: 10.1038/33416

Kornbluth, J., Flomenberg, N., and Dupont, B. (1982). Cell surface phenotype of a cloned line of human natural killer cells. *J. Immunol.* 129, 2831–2837.

Kornbluth, J., and Hoover, R. G. (1988). Changes in gene expression associated with IFN-beta and IL-2-induced augmentation of human natural killer cell function. *J. Immunol.* 141, 3234–3240.

Kozlowski, M., Schorey, J., Portis, T., Grigoriev, V., and Kornbluth, J. (1999). NK lytic-associated molecule: a novel gene selectively expressed in cells with cytolytic function. *J. Immunol.* 163, 1775–1785.

Lawrence, D. W., Gullickson, G., and Kornbluth, J. (2015). E3 ubiquitin ligase NKLAM positively regulates macrophage inducible nitric oxide synthase expression. *Immunobiology* 220, 83–92. doi: 10.1016/j.imbio.2014.08.016

Lawrence, D. W., and Kornbluth, J. (2012). E3 ubiquitin ligase NKLAM is a macrophage phagosome protein and plays a role in bacterial killing. *Cell. Immunol.* 279, 46–52. doi: 10.1016/j.cellimm.2012.09.004

Lawrence, D. W., and Kornbluth, J. (2016). E3 ubiquitin ligase NKLAM ubiquitinates STAT1 and positively regulates STAT1-mediated transcriptional activity. *Cell. Signal.* 28, 1833–1841. doi: 10.1016/j.cellsig.2016.08.014

Lawrence, D. W., and Kornbluth, J. (2018). Reduced inflammation and cytokine production in NKLAM deficient mice during *Streptococcus pneumoniae* infection. *PLoS One* 13:e0194202. doi: 10.1371/journal.pone.0194202

Lawrence, D. W., Shornick, L. P., and Kornbluth, J. (2019). Mice deficient in NKLAM have attenuated inflammatory cytokine production in a Sendai virus pneumonia model. *PLoS One* 14:e0222802. doi: 10.1371/journal.pone.0222802

Lechtenberg, B. C., Rajput, A., Sanishvili, R., Dobaczewska, M. K., Ware, C. F., Mace, P. D., et al. (2016). Structure of a HOIP/E2˜ubiquitin complex reveals RBR E3 ligase mechanism and regulation. *Nature* 529, 546–550. doi: 10.1038/nature16511

Li, J., Boroevich, K. A., Koop, B. F., and Davidson, W. S. (2011). Comparative genomics identifies candidate genes for infectious salmon anemia (ISA) resistance in Atlantic salmon (*Salmo salar*). *Mar. Biotechnol.* 13, 232–241. doi: 10.1007/s10126-010-9284-0

Lugini, L., Cecchetti, S., Huber, V., Luciani, F., Macchia, G., Spadaro, F., et al. (2012). Immune surveillance properties of human NK cell-derived exosomes. *J. Immunol.* 189, 2833–2842. doi: 10.4049/jimmunol.1101988

Lunde, B. M., Moore, C., and Varani, G. (2007). RNA-binding proteins: modular design for efficient function. *Nat. Rev. Mol. Cell Biol.* 8, 479–490. doi: 10.1038/nrm2178

Luo, L., Zhu, D., Huang, R., Xiong, L., Mehjabin, R., He, L., et al. (2019). Molecular cloning and preliminary functional analysis of six RING-between-ring (RBR) genes in grass carp (*Ctenopharyngodon idellus*). *Fish Shellfish Immunol.* 87, 62–72. doi: 10.1016/j.fsi.2018.12.078

Malhotra, D., Darvishi, K., Lohra, M., Kumar, H., Grover, C., Sood, S., et al. (2006). Association study of major risk single nucleotide polymorphisms in the common regulatory region of PARK2 and PACRG genes with leprosy in an Indian population. *Eur. J. Hum. Genet.* 14, 438–442. doi: 10.1038/sj.ejhg.5201563

Manzanillo, P. S., Ayres, J. S., Watson, R. O., Collins, A. C., Souza, G., Rae, C. S., et al. (2013). The ubiquitin ligase parkin mediates resistance to intracellular pathogens. *Nature* 501, 512–516. doi: 10.1038/nature12566

Martino, L., Brown, N. R., Masino, L., Esposito, D., and Rittinger, K. (2018). Determinants of E2-ubiquitin conjugate recognition by RBR E3 ligases. *Sci. Rep.* 8:68. doi: 10.1038/s41598-017-18513-5

Metzger, M. B., Pruneda, J. N., Klevit, R. E., and Weissman, A. M. (2014). RING-type E3 ligases: master manipulators of E2 ubiquitin-conjugating enzymes and ubiquitination. *Biochim. Biophys. Acta* 1843, 47–60. doi: 10.1016/j.bbamcr.2013.05.026

Migliano, S. M., and Teis, D. (2018). ESCRT and membrane protein ubiquitination. *Prog. Mol. Subcell. Biol.* 57, 107–135. doi: 10.1007/978-3-319-96704-2_4

Mira, M. T., Alcais, A., Nguyen, V. T., Moraes, M. O., Di Flumeri, C., Vu, H. T., et al. (2004). Susceptibility to leprosy is associated with PARK2 and PACRG. *Nature* 427, 636–640. doi: 10.1038/nature02326

Morrison, B. L., Mullendore, M. E., Stockwin, L. H., Borgel, S., Hollingshead, M. G., and Newton, D. L. (2013). Oxyphenisatin acetate (NSC 59687) triggers a cell starvation response leading to autophagy, mitochondrial dysfunction, and autocrine TNFalpha-mediated apoptosis. *Cancer Med.* 2, 687–700. doi: 10.1002/cam4.107

Oliveira, C., Faoro, H., Alves, L. R., and Goldenberg, S. (2017). RNA-binding proteins and their role in the regulation of gene expression in *Trypanosoma cruzi* and *Saccharomyces cerevisiae*. *Genet. Mol. Biol.* 40, 22–30. doi: 10.1590/1678-4685-gmb-2016-0258

Owen, I., and Shewmaker, F. (2019). The role of post-translational modifications in the phase transitions of intrinsically disordered proteins. *Int. J. Mol. Sci.* 20:5501. doi: 10.3390/ijms20215501

Portis, T., Anderson, J., Esposito, A., and Kornbluth, J. (2000). Gene structure of human and mouse NKLAM, a gene associated with cellular cytotoxicity. *Immunogenetics* 51, 546–555. doi: 10.1007/s002510000182

Sarraf, S. A., Raman, M., Guarani-Pereira, V., Sowa, M. E., Huttlin, E. L., Gygi, S. P., et al. (2013). Landscape of the PARKIN-dependent ubiquitylome in response to mitochondrial depolarization. *Nature* 496, 372–376. doi: 10.1038/nature12043

Smit, J. J., and Sixma, T. K. (2014). RBR E3-ligases at work. *EMBO Rep.* 15, 142–154. doi: 10.1002/embr.201338166

Spratt, D. E., Walden, H., and Shaw, G. S. (2014). RBR E3 ubiquitin ligases: new structures, new insights, new questions. *Biochem. J.* 458, 421–437. doi: 10.1042/BJ20140006

Su, J., Gao, C., Wang, R., Xiao, C., and Yang, M. (2018). Genes associated with inflammation and the cell cycle may serve as biomarkers for the diagnosis and prognosis of acute myocardial infarction in a Chinese population. *Mol. Med. Rep.* 18, 1311–1322. doi: 10.3892/mmr.2018.9077

Sun, Y. (2006). E3 ubiquitin ligases as cancer targets and biomarkers. *Neoplasia* 8, 645–654. doi: 10.1593/neo.06376

Swatek, K. N., and Komander, D. (2016). Ubiquitin modifications. *Cell Res.* 26, 399–422. doi: 10.1038/cr.2016.39

Trost, M., English, L., Lemieux, S., Courcelles, M., Desjardins, M., and Thibault, P. (2009). The phagosomal proteome in interferon-gamma-activated macrophages. *Immunity* 30, 143–154. doi: 10.1016/j.immuni.2008.11.006

Uchida, Y., Watanabe, C., Takemae, N., Hayashi, T., Oka, T., Ito, T., et al. (2012). Identification of host genes linked with the survivability of chickens infected with recombinant viruses possessing H5N1 surface antigens from a highly pathogenic avian influenza virus. *J. Virol.* 86, 2686–2695. doi: 10.1128/JVI.06374-11

Walden, H., and Rittinger, K. (2018). RBR ligase-mediated ubiquitin transfer: a tale with many twists and turns. *Nat. Struct. Mol. Biol.* 25, 440–445. doi: 10.1038/s41594-018-0063-3

Warner, J. F., and Dennert, G. (1982). Effects of a cloned cell line with NK activity on bone marrow transplants, tumour development and metastasis in vivo. *Nature* 300, 31–34. doi: 10.1038/300031a0

Weber, J., Polo, S., and Maspero, E. (2019). HECT E3 ligases: a tale with multiple facets. *Front. Physiol.* 10:370. doi: 10.3389/fphys.2019.00370

Wright, P. E., and Dyson, H. J. (2015). Intrinsically disordered proteins in cellular signalling and regulation. *Nat. Rev. Mol. Cell Biol.* 16, 18–29. doi: 10.1038/nrm3920

Wu, C. H., Li, J., Li, L., Sun, J., Fabbri, M., Wayne, A. S., et al. (2019). Extracellular vesicles derived from natural killer cells use multiple cytotoxic proteins and killing mechanisms to target cancer cells. *J. Extracell. Vesicles* 8:1588538. doi: 10.1080/20013078.2019.1588538

Xiao, H., Shan, L., Zhu, H., and Xue, F. (2012). Detection of significant pathways in osteoporosis based on graph clustering. *Mol. Med. Rep.* 6, 1325–1332. doi: 10.3892/mmr.2012.1082

Yao, F., Zhou, Z., Kim, J., Hang, Q., Xiao, Z., Ton, B. N., et al. (2018). SKP2- and OTUD1-regulated non-proteolytic ubiquitination of YAP promotes YAP nuclear localization and activity. *Nat. Commun.* 9:2269. doi: 10.1038/s41467-018-04620-y

Zhou, H., Luo, Y., Mizutani, M., Mizutani, N., Reisfeld, R. A., and Xiang, R. (2005). T cell-mediated suppression of angiogenesis results in tumor protective immunity. *Blood* 106, 2026–2032. doi: 10.1182/blood-2005-03-0969

**Conflict of Interest:** The authors declare that the research was conducted in the absence of any commercial or financial relationships that could be construed as a potential conflict of interest.

# Advantages of publishing in Frontiers

**OPEN ACCESS**
Articles are free to read for greatest visibility and readership

**FAST PUBLICATION**
Around 90 days from submission to decision

**HIGH QUALITY PEER-REVIEW**
Rigorous, collaborative, and constructive peer-review

**TRANSPARENT PEER-REVIEW**
Editors and reviewers acknowledged by name on published articles

**Frontiers**
Avenue du Tribunal-Fédéral 34
1005 Lausanne | Switzerland

**Visit us:** www.frontiersin.org
**Contact us:** info@frontiersin.org | +41 21 510 17 00

**REPRODUCIBILITY OF RESEARCH**
Support open data and methods to enhance research reproducibility

**DIGITAL PUBLISHING**
Articles designed for optimal readership across devices

**FOLLOW US**
@frontiersin

**IMPACT METRICS**
Advanced article metrics track visibility across digital media

**EXTENSIVE PROMOTION**
Marketing and promotion of impactful research

**LOOP RESEARCH NETWORK**
Our network increases your article's readership